JPL Document Review Clearance # CL 04-3503

Mars Exploration Rover (MER) Project

Microscopic Imager Calibration Report
Rev B (Initial)

Ken Herkenhoff, Randy Kirk, Mark Rosiek, Larry Soderblom, Bob Sucharski, Jim Torson
USGS Astrogeology Team

Jim Bell, Heather Arneson, Alex Hayes, Miles Johnson, Jascha Sohl-Dickstein
Cornell University

David Brown, Andy Collins, Arsham Dingizian, Tom Elliott, Justin Maki, Larry Scherr, Mark Schwochert, Dave Thiessen, Mary White
Caltech Jet Propulsion Laboratory

Approved:

Steve Squyres Athena PI	Joy Crisp MER Project Scientist
Ken Herkenhoff MI Payload Element Lead	John Callas MER Science Manager

28 July 2004

Jet Propulsion Laboratory
California Institute of Technology

CHANGE LOG

DATE	SECTIONS CHANGED	REASON FOR CHANGE	REVISION
01/21/04	Initial version		
01/24/04	3.2.7, 3.2.8, Appendix L	Analysis completed	A
07/28/04	Minor changes throughout	W. Calvin review	Rev. B (Initial)

TABLE OF CONTENTS

1 INTRODUCTION

The Athena Microscopic Imager (MI) acquires images of natural surfaces with a resolution of about 30 µm/pixel (Herkenhoff *et al*., 2003). It is mounted on the Instrument Deployment Device (IDD), allowing it to be placed near surfaces that can also be examined by other Rover instruments (Squyres *et al*., 2003). The optics employ a fixed focus Cooke triplet design that provides over 6 mm depth-of-field at 30-µm/pixel sampling (Fig. 1.0.1). The Microscopic Imager acquires images using only solar or skylight illumination of the target surface. Stereoscopic observations are obtained by moving the Microscopic Imager between two adjacent positions at the same height above the target. The spectral bandpass of the Microscopic Imager is restricted to 400-700 nm by the addition of a single 2 mm thick Schott BG-40 filter.

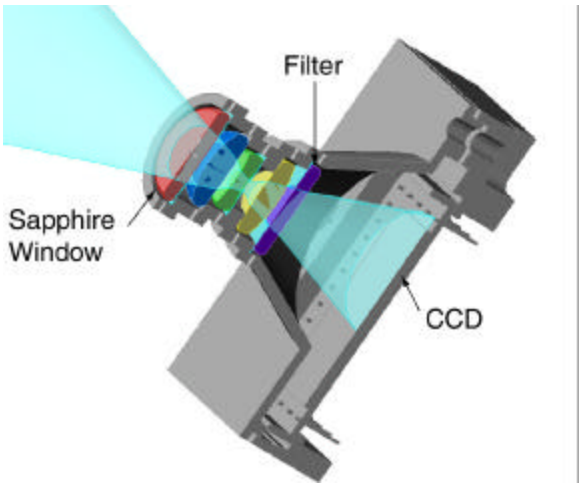

Figure 1.0.1. Cutaway diagram of MI optics barrel, showing sapphire window, lenses, and filter.

Coarse (~2 mm precision) focusing is achieved by moving the IDD away from a target after the contact sensor (Fig. 1.0.2) is activated. Multiple images taken at various distances are acquired to ensure good focus on all parts of rough surfaces. Position and orientation data for each acquired image is stored in the rover computer and returned to Earth with the image data. The Microscopic Imager optics are protected from the Martian environment by a dust cover (Fig. 1.0.2). When closed, the cover prevents dust that is falling vertically from the Martian atmosphere from settling onto MI optical surfaces in any IDD configuration, and minimizes accumulation of dust produced by the Rock Abrasion Tool (RAT) operation on MI optical surfaces.

To reduce complexity and cost, all MER cameras share the same electronics design. Some aspects of the MER camera design were inherited from the cameras built for the Athena Precursor Experiment (APEX; Squyres *et al*., 1999). The MER cameras include a Mitel front-side illuminated, frame-transfer charge-coupled device (CCD) with 1024×2048 pixels. Half of the array is covered by aluminum and is used for image storage during readout. Immediately following image integration of 0 to 335.5 seconds, the image is transferred into the storage area in 5.2 msec. Readout of a full image then requires 5.2 seconds, after which another integration may begin. The serial register has 16 extra “reference” pixels on each end that are read out along with each line of data. The value of the last reference pixel is always replaced with the camera serial number. Within the operating temperature range of -55°C to +5°C, the MI has a full well

depth in excess of 150,000 electrons. The gain of the MER science cameras (~50 e^-/DN) was designed to optimize the 12-bit digitization over the expected full well of the CCDs. The video offset can be set by command to bias the dynamic range of the CCD analog output relative to the range of the analog-to-digital converter. After conversion, 12-bit digital image data are sent to the rover computer. Further details of the MER camera electronics design are included in Bell *et al*. (2003). The non-operating (survival) temperature range of the cameras is -110°C to +55°C. The CCDs can safely operate between -110°C and +45°C, but is not formally be within calibrated specifications outside of -55°C to +5°C. The electronics can safely operate between -60°C and +55°C. The temperature of the MI CCD and electronics can not be controlled during flight, so variations in performance with temperature were carefully measured. Temperature sensors on the MI CCDs and electronics return data for each image obtained, allowing temperature calibration of dark current and linearity to be applied.

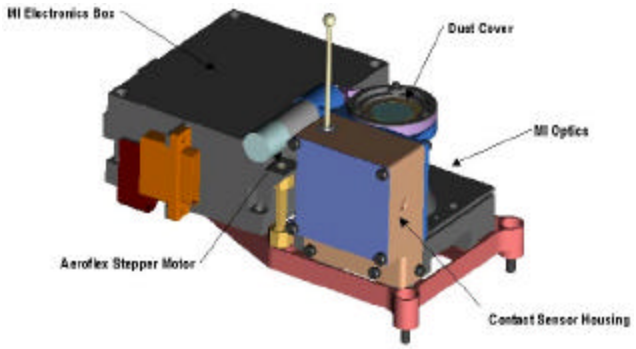

Figure 1.0.2. Schematic diagram of MI, dust cover, and contact sensor. Dust cover is rotated open by stepper motor. Ball at end of contact sensor was removed in final design.

Two MI flight units were fully tested and calibrated (serial numbers 105 and 110), one for each rover (Table 1.0.1). Both MI flight units were assembled, tested, and calibrated in JPL Building 168 in 2002. After each MI was integrated onto the IDD and MER flight system, they underwent testing at the MER system level. Test and calibration results are reported for both flight units below, in three major parts: component-level tests, stand-alone camera test and calibration, and system level test and calibration. The camera calibration was a subset of the flight acceptance testing program, summarized in Appendix A. Staffing for calibration activities included JPL engineering, science, and calibration team support plus Athena science team support from the PEL, Athena Co-Is, Athena team collaborators, and other graduate and undergraduate student assistants.

Table 1.0.1. MI serial number vs. spacecraft

	MI serial # 105	**MI serial # 110**
Spacecraft:	MER-A (“Spirit”)	MER-B (“Opportunity”)

1.1 Purpose

The purpose of this document is to report the methods used to acquire, reduce, and analyze the MI calibration data, and to compare the radiometric, geometric, thermal, optical, and mechanical performance to the functional requirements outlined in the Camera Functional

Requirements Document (FRD) (JPL Doc. # D-19702, MER 420-2-409) and other MER project requirements. The results described in this report define the accuracy, precision, and limitations of MI calibration.

1.2 Requirements

The MI utilizes a 1024 × 2048 Mitel frame transfer CCD detector array with 1024 × 1024 imaging pixels. The array is combined with optics and a single filter to yield images of surfaces approximating the view through a hand lens. The required operating temperature range for performance of the MI within specifications is -55°C to 5°C, and for survival is from -105°C to +50°C. Signal-to-noise ratio (SNR) is required to be =100 for nominal observing conditions (=20% full well within operating temperature range).

The primary goal of calibration and testing of the MI is to verify that the instrument will meet or exceed all of the MER Project requirements relevant to close-up imaging on Mars. Meeting these requirements and achieving the levels of calibration accuracy described below will ensure that the MI returns images, possibly taken under a wide variety of illumination conditions, that will yield useful new information about Mars. The spectral bandpass was chosen to mimic the photopic response of the human eye, simplifying interpretability and testing. The IFOV and f/# were selected after considerations of tradeoffs among overall FOV, diffraction blurring, operational complexity, and the expected size of natural features of interest. The relevant requirements are compiled in the MER Project System Level 2 Requirements Document (JPL D-19650), MER Flight System Level 3 Requirements Document (JPL D-19692), MER Science Requirements Document (JPL D-19638; MER 420-2-128), MER Cameras Level 3 Requirements (ECR 100497), and the MER Camera Functional Requirements Document (MER 420-2-409; JPL D-19702). The requirements in these documents that are relevant to MI calibration and testing are summarized in Tables 1.2.1 and 4.1.1. Note that Level 3 requirement #1188 applies to the optics only, not the MI camera system. As detailed below, all of these requirements have been met, with the following caveat: The “effective depth of field” Level 3 requirement (#1187) is not specified in terms of defocus or MTF degradation limits, so cannot be quantitatively compared with test results. Degradation of the MTF is insignificant within 1.5 mm of best focus (see section 3.2.8).

Table 1.2.1: MER Requirements Relevant to MI Component Level and Standalone Calibration and Testing

Level	ID #	Requirement
2	921	The Project System shall be capable of coregistering images from the Microscopic Imager with images and panoramas from the Pancam, Hazcam, Navcam observations of Mars.
2	922	The Project System shall ensure that the quality of the calibration of the science instruments be sufficient to satisfy the requirements and objectives in the Science Requirements Document and the Level 1 science requirements.
2	923	It shall be possible to produce radiometrically calibrated images from the Microscopic Imager, Hazcam, and Navcam observations on Mars, using pre-launch calibration data.
3	1184	The Microscopic Imager shall have an Instantaneous Field of View (IFOV) of 30 ± 1.5 micrometers/pixel on-axis.
3	1185	The Microscopic Imager shall have a Field of View (FOV) of 1024 x 1024 square pixels.
3	1186	The Microscopic Imager shall have a spectral bandpass of 400-680 nanometers.
3	1187	The Microscopic Imager shall have an effective depth of field of = ±3 millimeters.
3	1188	The Microscopic Imager shall have an MTF of =0.35 @ 30 lp/mm over spectral bandpass at best focus.
3	1189	The Microscopic Imager optical design shall minimize the contributions of stray and scattered light onto the CCD.
3	1190	Radiometric calibration of the Microscopic Imager shall be performed with an absolute accuracy of =20%.
3	1191	Radiometric calibration of the Microscopic Imager shall be performed with a relative (pixel-to-pixel) accuracy of =5%.
3	1192	The Microscopic Imager Signal to Noise Ratio (SNR) shall be =100 for exposures of =20% full well over the spectral bandpass and within the calibrated operating temperature range.
3	1193	The Microscopic Imager shall have a temperature sensor, accurate to ± 2 deg. Celsius, on the CCD package that can be read-out and associated with the image data in telemetry.
3	1194	The Microscopic Imager shall be able to have the sun in its field of view (powered and unpowered) and not sustain permanent damage.
4		Working f/# = 15 ± 0.75
4		Maximum RMS wavefront error over full field shall be =0.12 waves at 633 nm.
4		Operating temperature within calibrated specifications = -55±2°C to +5±2°C.

1.3 Scope

This report constitutes the MI "Deliverables" described in the MER Science Implementation Plan (MER 420-1-201, JPL D-20458).

1.4 Applicable Documents

- MER Project Level 1 Requirements Document (MER 420-2-005)
- MER Science Requirements Document (JPL D-19638; MER 420-2-128)
- MER Project System Level 2 Requirements Document (JPL D-19650; MER 420-2-120)
- MER Flight System Level 3 Requirements Document (JPL D-19692; MER 420-2-401)
- MER Mission Assurance Plan PD 7924-013
- MER Science and Engineering Cameras IICD JPL D-20257, MER 420-3-480.i
- MER Pancam Filter Wheels (PFW) IICD JPL D-20265, MER 420-3-480.q
- MER Engineering Camera Calibration Report, MER 420-6-786 (JPL D-25540)
- MER Planetary Protection Plan (JPL D-19534)
- MER Pancam Calibration Plan (MER 420-1-438, JPL D-19696)
- MER Camera Stereo Alignment Results (MER 420-6-0777, JPL D-25519)
- MER Project Implementation Plan (JPL D-19620; MER 420-1-101)
- MER Rover S/N 1 System Level EMC Self-Compatibility Test Report, JPL Interoffice Memorandum 5132-2003-045, March 18, 2003
- MER Rover S/N 2 System Level EMC Self-Compatibility Test Report, JPL Interoffice Memorandum 5132-2003-061, April 4, 2003
- MER Configuration Management Plan (MER 420-1-102, JPL D-19641)
- MER Camera Functional Requirements Document (MER 420-2-409, JPL D-19702)
- MI Calibration Plan (MER 420-1-437, JPL D-19695)
- MER Environmental Requirements Document (JPL D-19272)
- MER CCD Test Plan (MER 420-1-485, JPL D-20247)
- MER Camera CCD Specification Document (MER 420-7-495, JPL D-20365)
- MER Archive Generation, Validation, & Transfer Plan (MER 420-1-200; JPL D-19658)
- MER Pointing, Positioning, Phasing, and Coordinate Systems (MER 420-2-431; JPL D-20514)
- IDD/Instruments Functional Test Procedure (MER 420-5-4218)
- IDD/Instruments Baseline Functional Test (MER 420-5-4219)

2 COMPONENT-LEVEL TESTING AND CALIBRATION

Many of the MI components were tested before they were built into the cameras, primarily to verify performance. Many component-level tests are important to overall camera calibration, including spectral transmission of the optics, filters, and dust cover windows, calibration of temperature sensors, and performance of the CCDs. The spectral transmission of the optical barrel assemblies was tested by the optics vendor, Kaiser Electro-Optics. The spectral transmission of the MI filters was measured at JPL, and the dust cover window spectral transmission was measured at the NASA Johnson Space Center. The temperature sensors were calibrated at the vendor, Rosemount Aerospace.

Details of the design and operation of the MER CCDs can be found in the Mars Exploration Rover Camera CCD Specification Document (MER 420-7-495, JPL D-20365). The CCDs are 1024×2048 frame-transfer devices with a 1024×1024 imaging region. The storage region is architecturally equivalent to the imaging region, but utilizes an aluminum shield to block incident light. The pixels are 12 micrometers square, with 100% fill factor (no anti-blooming gates). The MER CCD assembly consists of a silicon CCD die that is epoxy-mounted into a metal package with glass feed-throughs and wire bond interconnects from die metallization to package leads. The component level tests are listed in Table 2.0.1 and described in more detail below.

Table 2.0.1. MI Component Level Calibration and Testing

Test	*Brief Description*
CCD Component Level Testing	
Electrical tests	Pre- and post-burn-in; see JPL D-20247
Operating voltage windows	See JPL D-20247
Photon transfer/linearity	Determine CCD linearity, read noise, full well, gain, bias, and dark current in both full resolution and summation modes
Dark current	See JPL D-20247
Flat field	See JPL D-20247
Pinholes	See JPL D-20247
Image	Record images in both full-resolution and summation modes
Temperature cycling	See JPL D-20247
Impedance	See JPL D-20247
Spectral quantum efficiency	Calibration; see JPL D-20247
Full well map	Calibration; see JPL D-20247
Charge transfer efficiency	Calibration; see JPL D-20247
Radiation tolerance (qualification test)	See JPL D-20247
Life testing (qualification test)	See JPL D-20247
Residual bulk image	Only significant below -70°C
Other Component Level Tests	
Optical barrel transmission	Determine throughput of each flight and flight spare optics barrel from 400 to 700 nm
Filter blocking and transmission	Determine throughput of filter in bandpass and integrated rejection band
Dust cover spectral transmission	Determine throughput of dust cover (or material from same batch)

2.1 Stand-alone CCD test and calibration

Each Mitel CCD was tested individually before installation into the cameras. In the process of testing, each CCD was cycled between room temperature and –55°C at least three times, so no additional temperature cycling was performed. The results of these tests were reviewed by the Athena science team and the various CCDs prioritized accordingly. The top 6 CCDs were selected for the flight science cameras (4 Pancams, 2 MIs) and subjected to further calibration at JPL. The results of these tests are summarized below, along with additional tests that were not included in the CCD test plan (edge response, blooming). CCD serial # 409 was used in MI serial # 105, and CCD serial # 360 was used in MI serial # 110.

2.1.1 Edge response

In response to the science team's desire to measure the point spread function (PSF) of the CCD, Tom Elliott (JPL) thought of a straightforward way to measure one quarter of the PSF. He illuminated a bare MER CCD with reasonably collimated light and measured the sharpness of the edge of the light shield that overlies half of the CCD. The light shield is deposited as part of the CCD wafer fabrication and, as such, it is aligned with an accuracy of better than a micron. Thus it provides an excellent step function with which to measure the leading edge of the PSF in the column direction.

The results of this test are shown in Figure 2.1.1a. Measured edge response curves are shown for six wavelengths, ranging from 405 nm to 1000 nm. As expected, the response is sharpest for the shortest wavelengths. Each curve is an average of data for 900 columns in the CCD, the illumination level was ~4500 e^- and the operating temperature was -55°C.

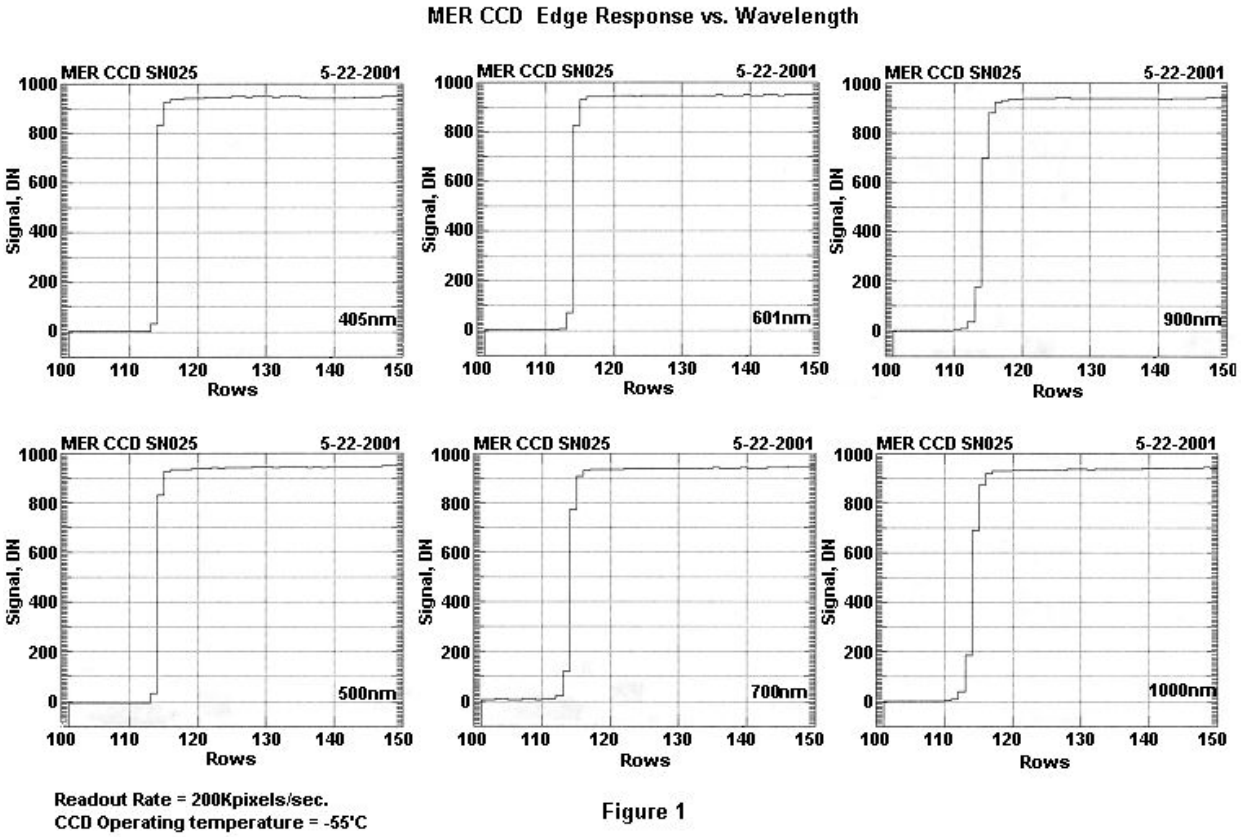

Figure 2.1.1a. Edge response of CCD serial # 25 (not used in flight cameras) at various wavelengths.

2.1.2 Blooming

Figure 2.1.2a shows the results of the MER CCD vertical blooming test at three different operating temperatures. The test consisted of focusing a spot of light on the CCD's imaging region at a flux rate of 3.3×10^6 interacting photons/pixel/second. The baseline condition is 1× full well at an exposure time of 6 msec. The exposure time is then increased to yield signal levels of 2×, 5× and 10× full well. Column traces were taken through the illuminated spot at each exposure level to measure the amount of vertical blooming charge. The same test was conducted at +5°C, -55°C and -85°C. The data indicate that there is not much difference in the vertical blooming characteristics between the three temperature levels tested.

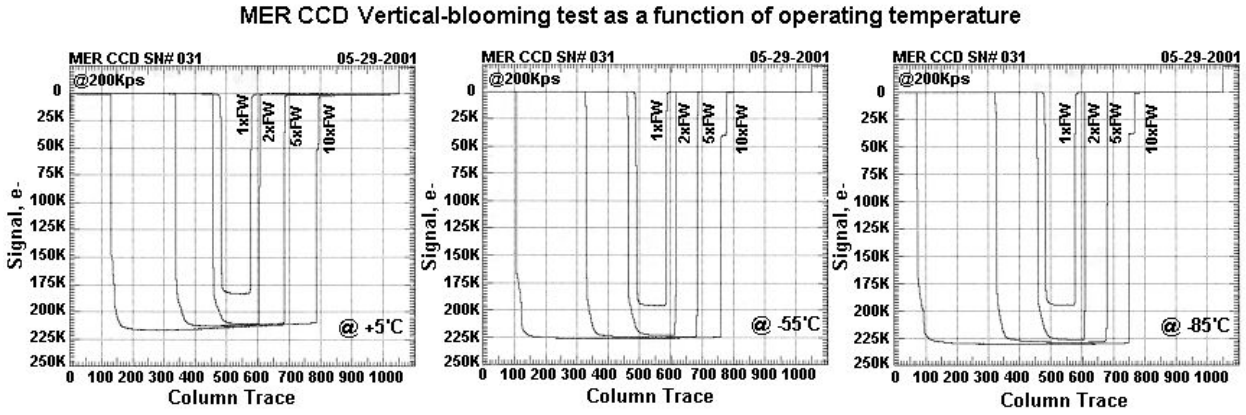

Figure 2.1.2a. Signal vs. row number plots for blooming tests at three temperatures. "FW" stands for full well.

2.1.3 Electrical tests

Functional tests were performed on each CCD before and after 72-hour burn-in at 125°C, and were used to identify changes in performance, if any; see MER CCD Test Plan (MER 420-1-485, JPL D-20247). For these tests, the CCDs were not exposed to light; the measured signals represent dark current. Pre-burn-in tests were performed at room temperature, and post-burn-in tests were performed at room temperature, 0°C, and –55°C. Video line plots for the pre-burn-in tests of the flight MI CCDs are shown in Figure 2.1.3a. Similar plots for the post-burn-in electrical tests are shown in Figures 2.1.3b (room temperature), 2.1.3c (0°C), and 2.1.3d (–55°C). In all cases, signal in DN is plotted increasing downward. Because the CCD temperature was not controlled for the room temperature tests, variations in dark current may be due to variations in CCD temperature. The increased dark current at the edges of the CCD is caused by diffusion into the array of thermal electrons generated in the Si outside of the active part of the CCD.

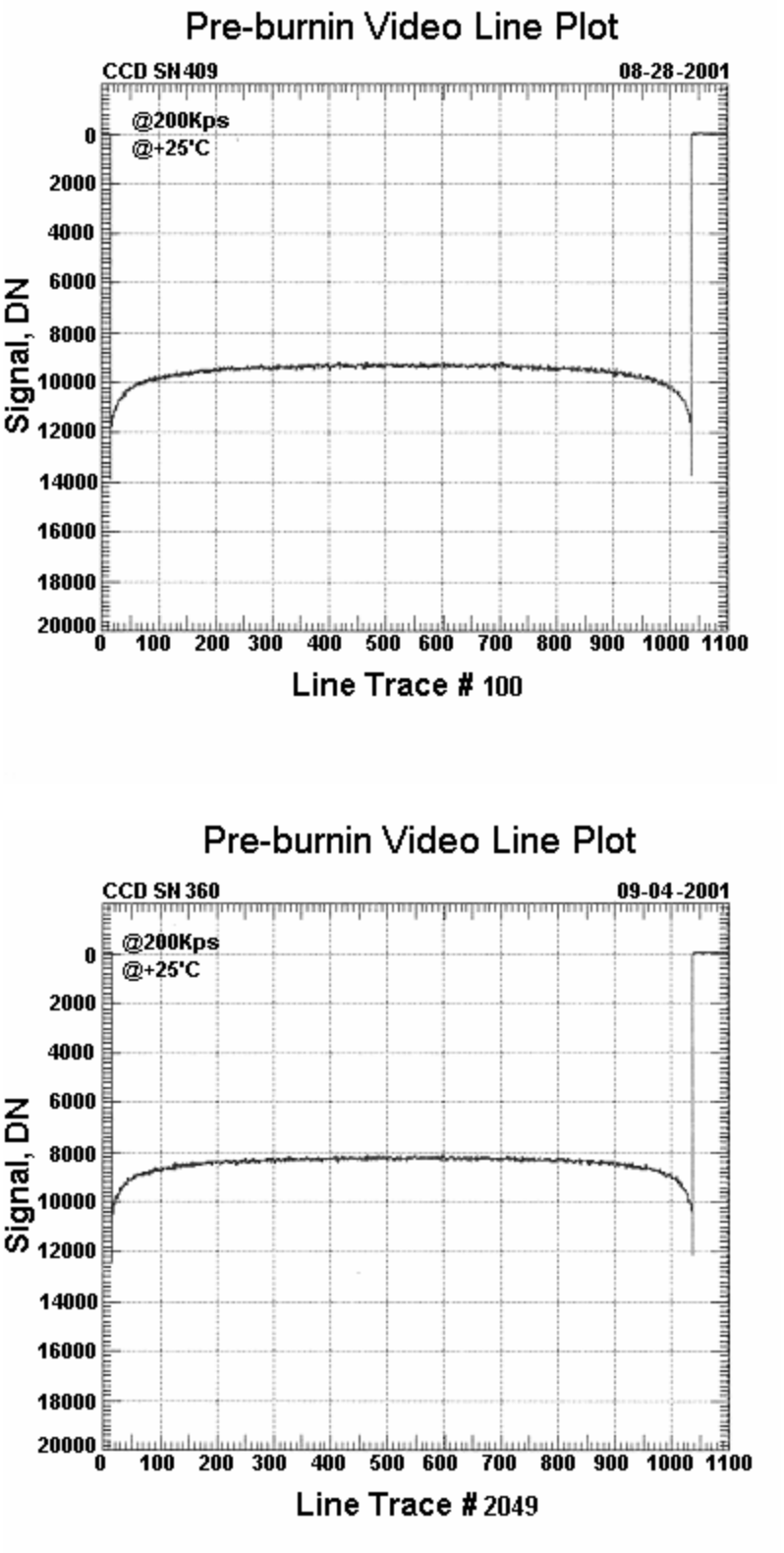

Figure 2.1.3a. Pre-burn-in video line plots for MI flight CCDs at room temperature. (top) CCD serial # 409, used in MI serial # 105. (bottom) CCD serial # 360, used in MI serial # 110.

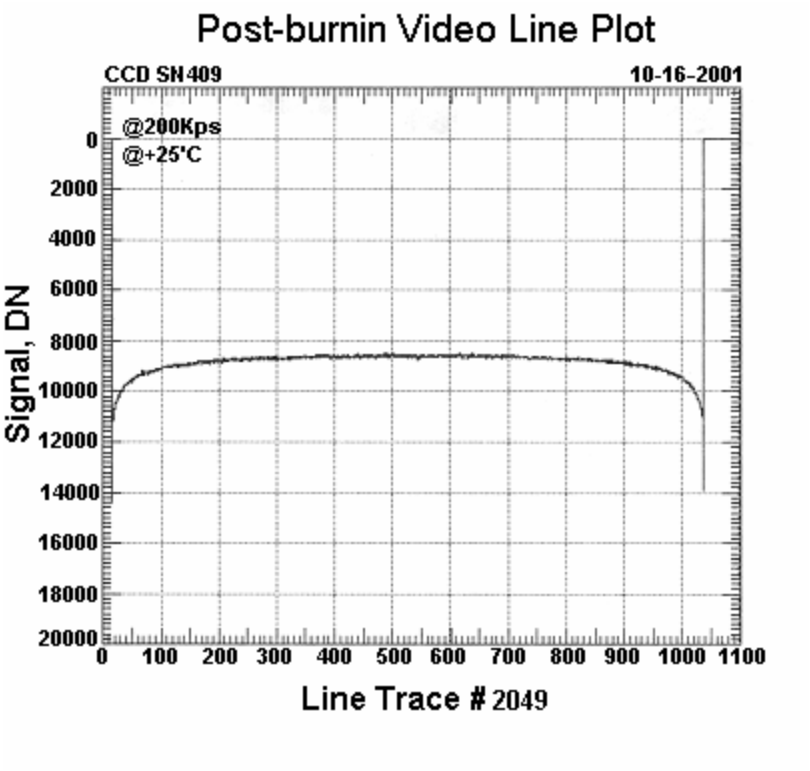

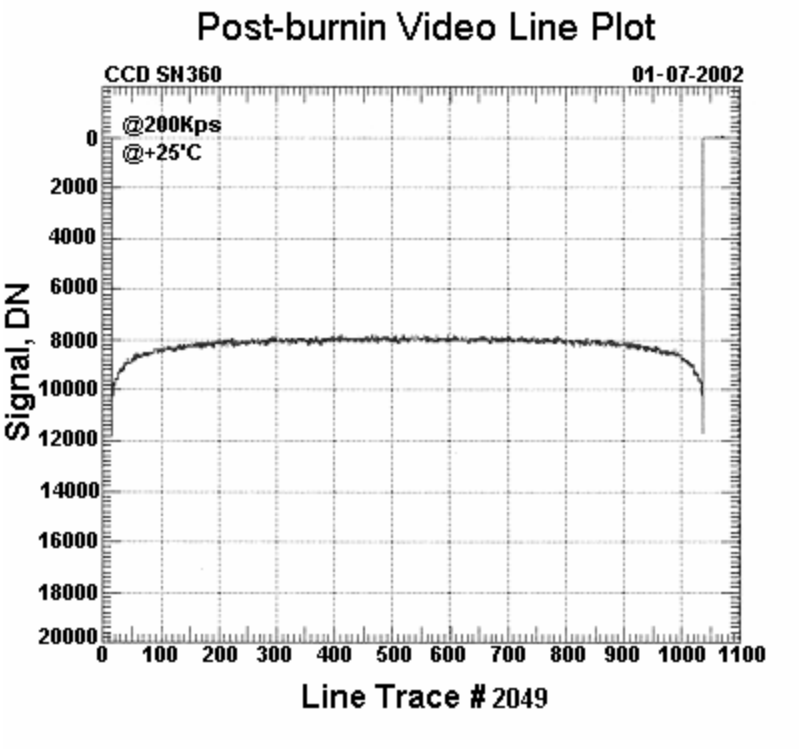

Figure 2.1.3b. Post-burn-in video line plots for MI flight CCDs at room temperature. (top) CCD serial # 409, used in MI serial # 105. (bottom) CCD serial # 360, used in MI serial # 110.

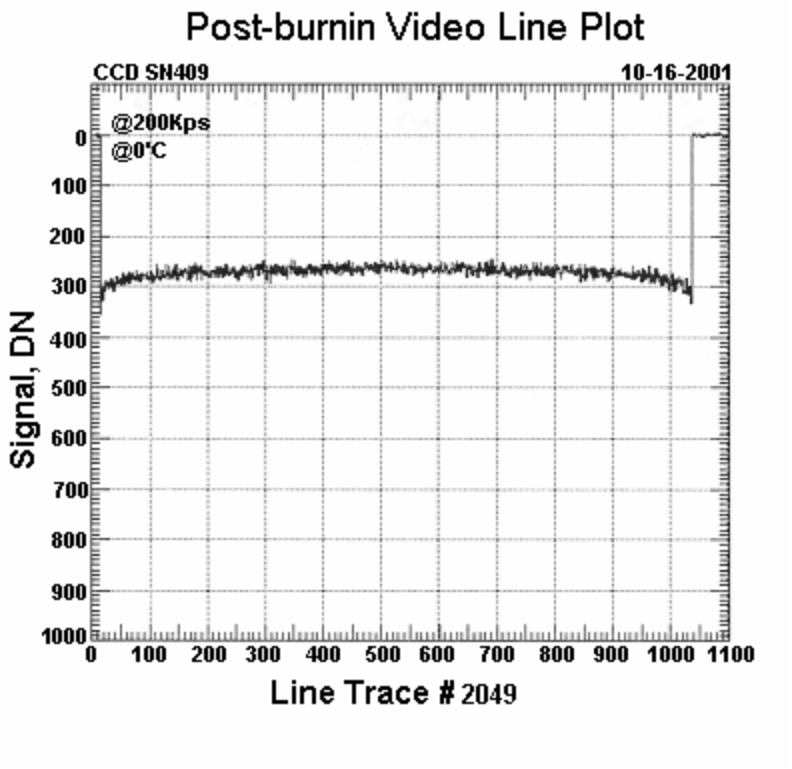

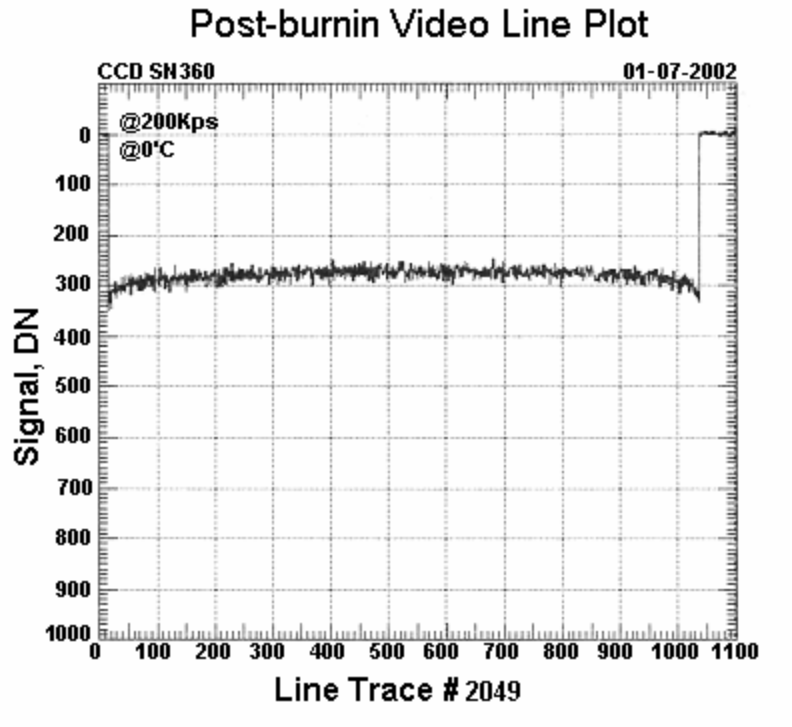

Figure 2.1.3c. Post-burn-in video line plots for MI flight CCDs at 0°C. (top) CCD serial # 409, used in MI serial # 105. (bottom) CCD serial # 360, used in MI serial # 110.

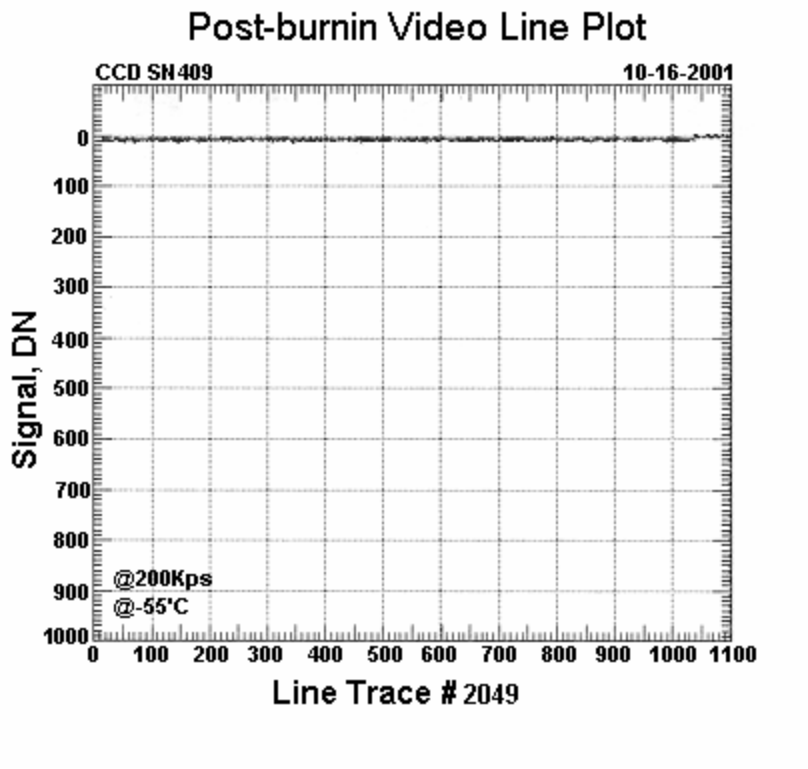

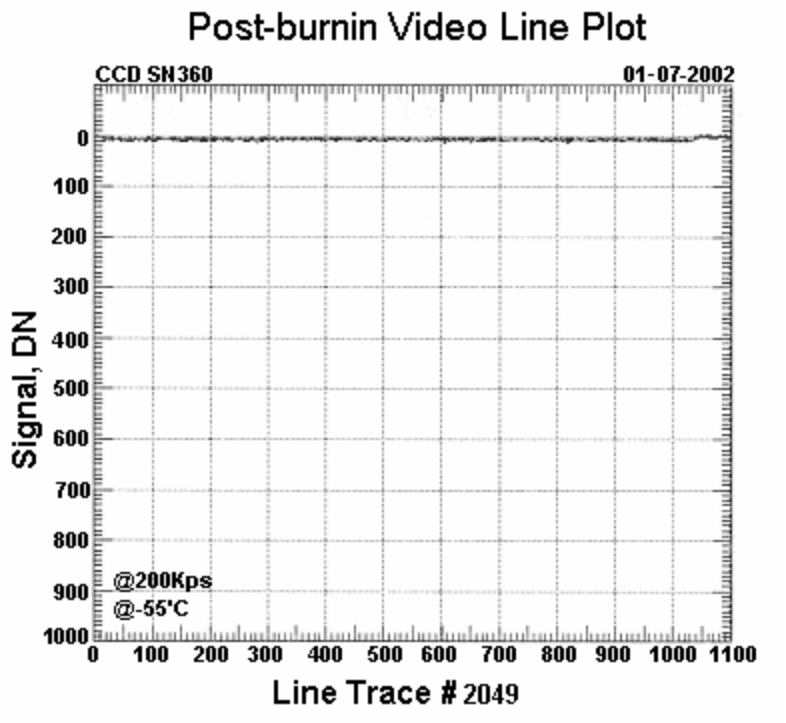

Figure 2.1.3d Post-burn-in video line plots for MI flight CCDs at -55°C. (top) CCD serial # 409, used in MI serial # 105. (bottom) CCD serial # 360, used in MI serial # 110.

2.1.4 Photon transfer/linearity

Photon transfer and linearity data were acquired at –20°C by exposing the CCDs to a constant illumination and increasing exposure time until saturation (full well) was reached. Data analysis followed the procedures described by Janesick *et al*. (1987). The results are summarized in Figures 2.1.4a and 2.1.4b below.

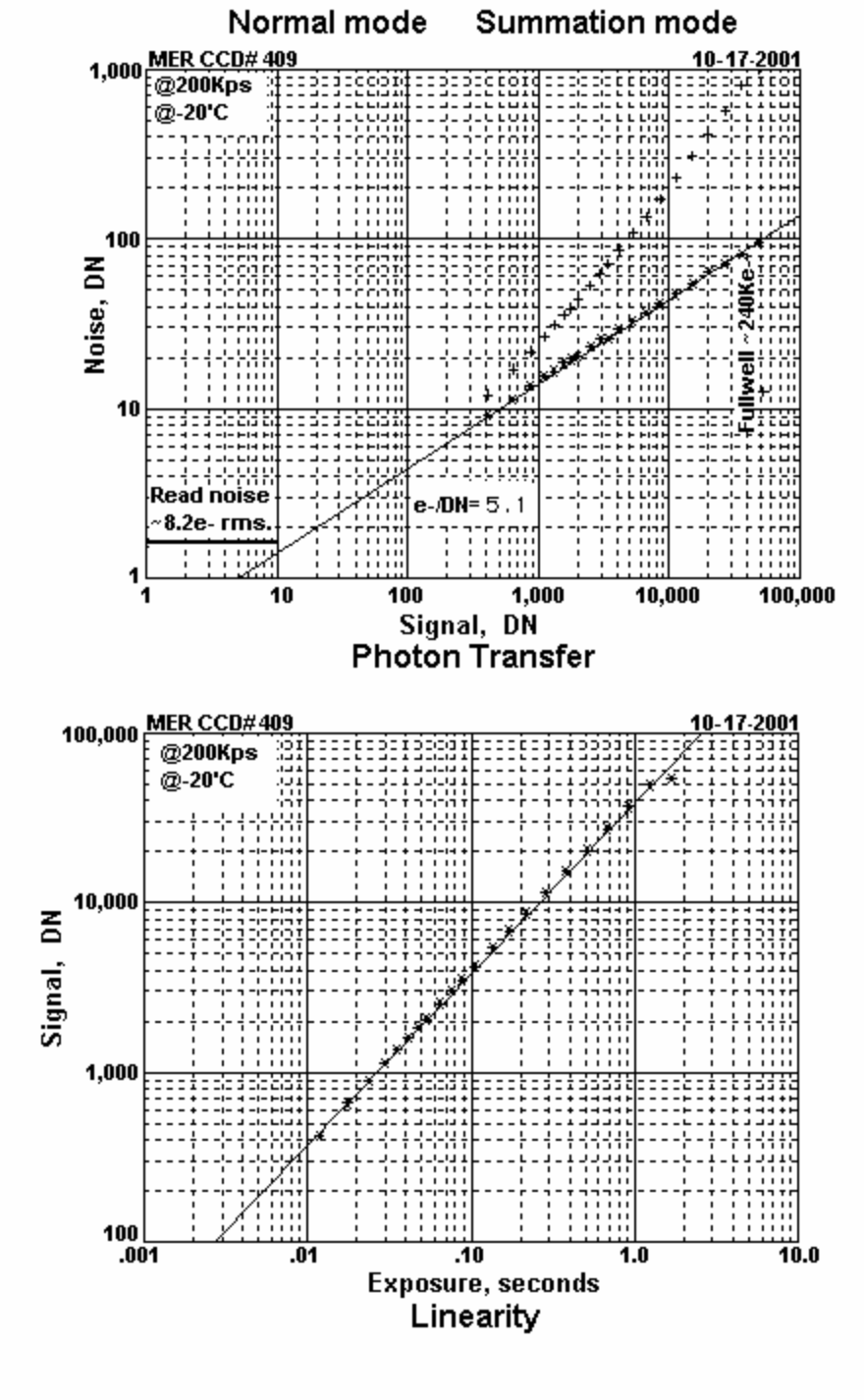

Figure 2.1.4a. CCD serial # 409 (MI serial # 105) full-frame (normal) mode. (top) Photon transfer plot with derived parameters. (bottom) Linearity plot.

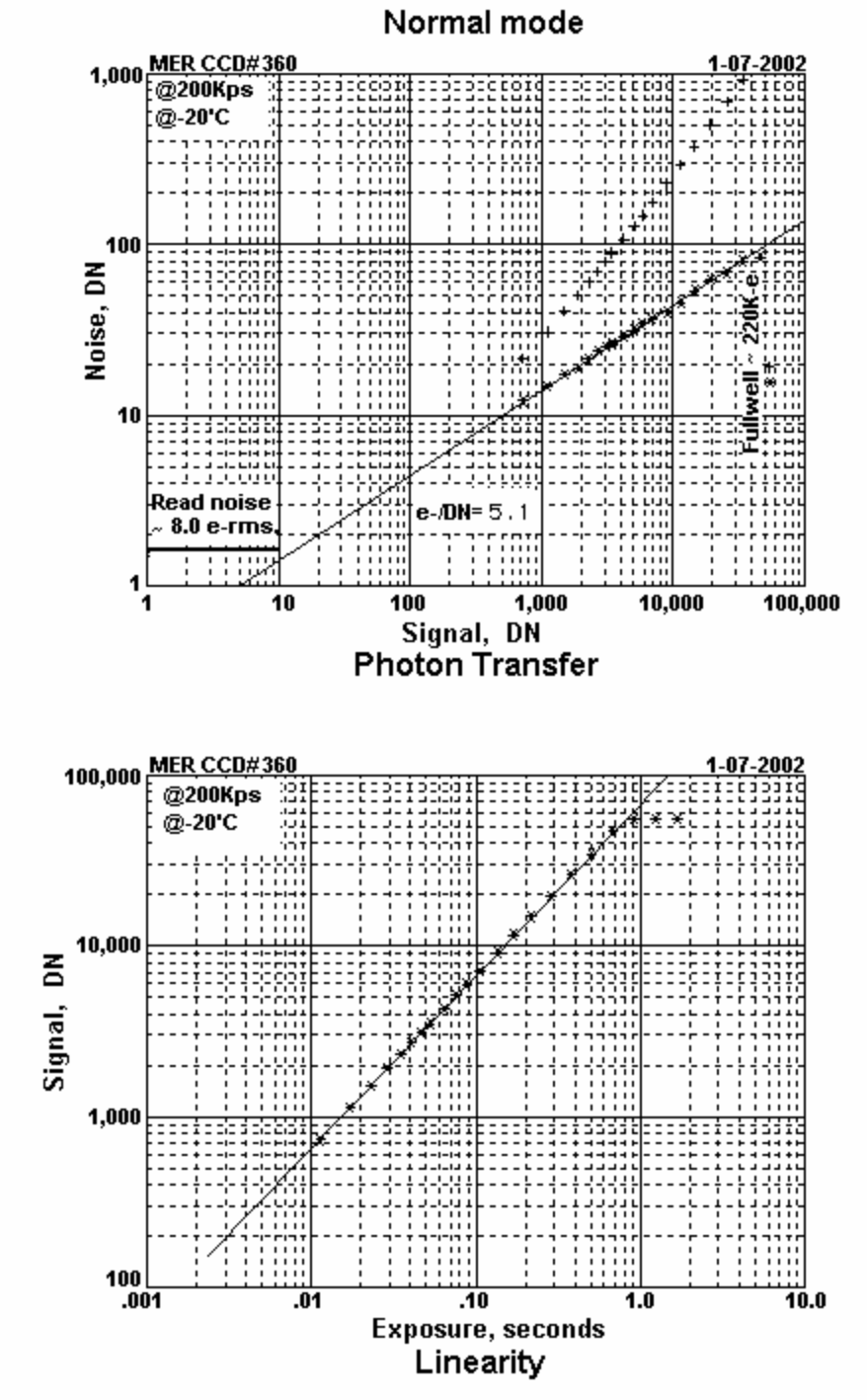

Figure 2.1.4b. CCD serial # 360 (MI serial # 110) full-frame (normal) mode. (top) Photon transfer plot with derived parameters. (bottom) Linearity plot.

Photon transfer and linearity data were also taken in the summation mode, in which 4 lines at a time are added together on the CCD during readout. The data were analyzed as described above, and the results are summarized in Figures 2.1.4c and 2.1.4d below.

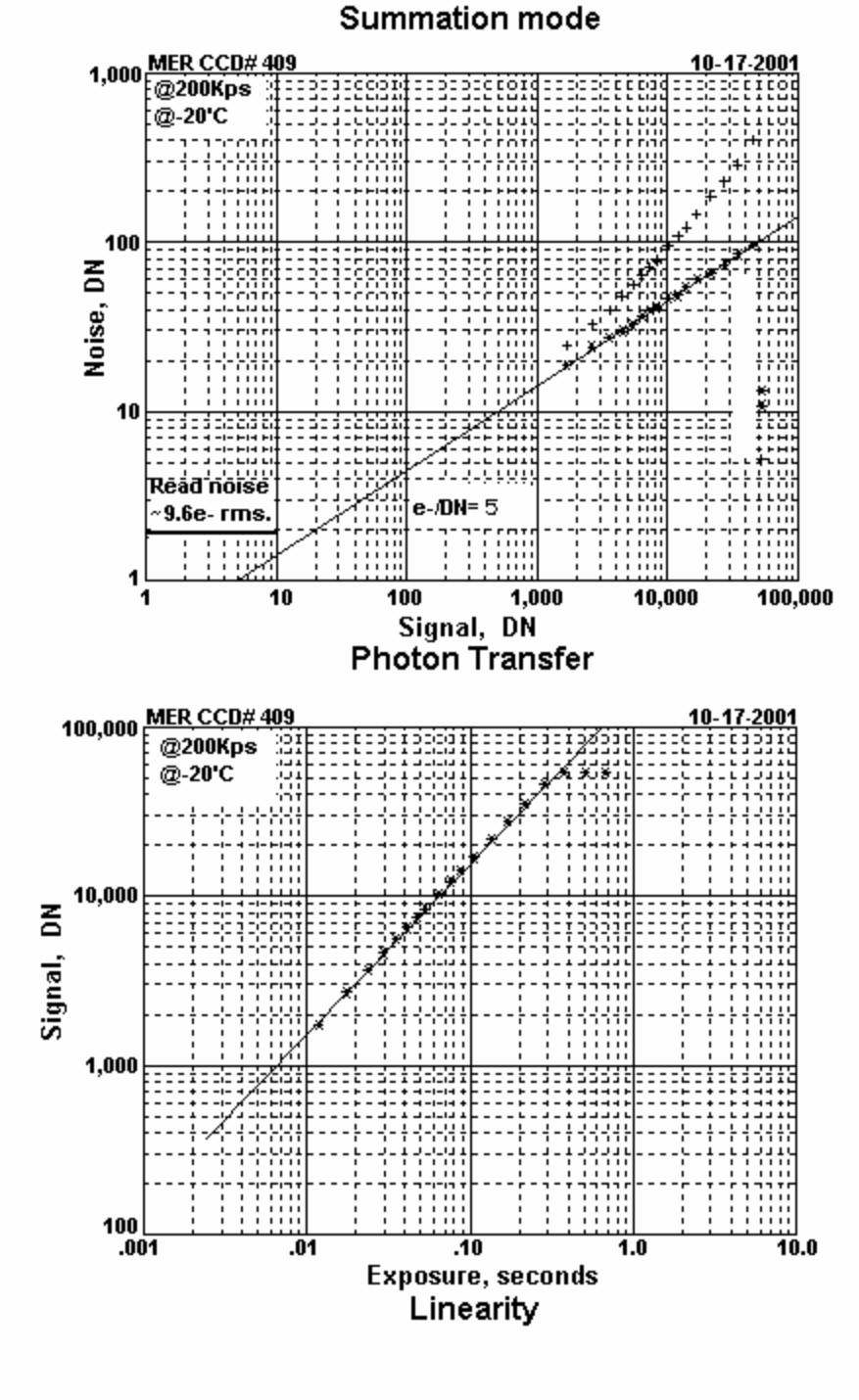

Figure 2.1.4c. CCD serial # 409 (MI serial # 105) summation (4×1) mode. (top) Photon transfer plot with derived parameters. (bottom) Linearity plot.

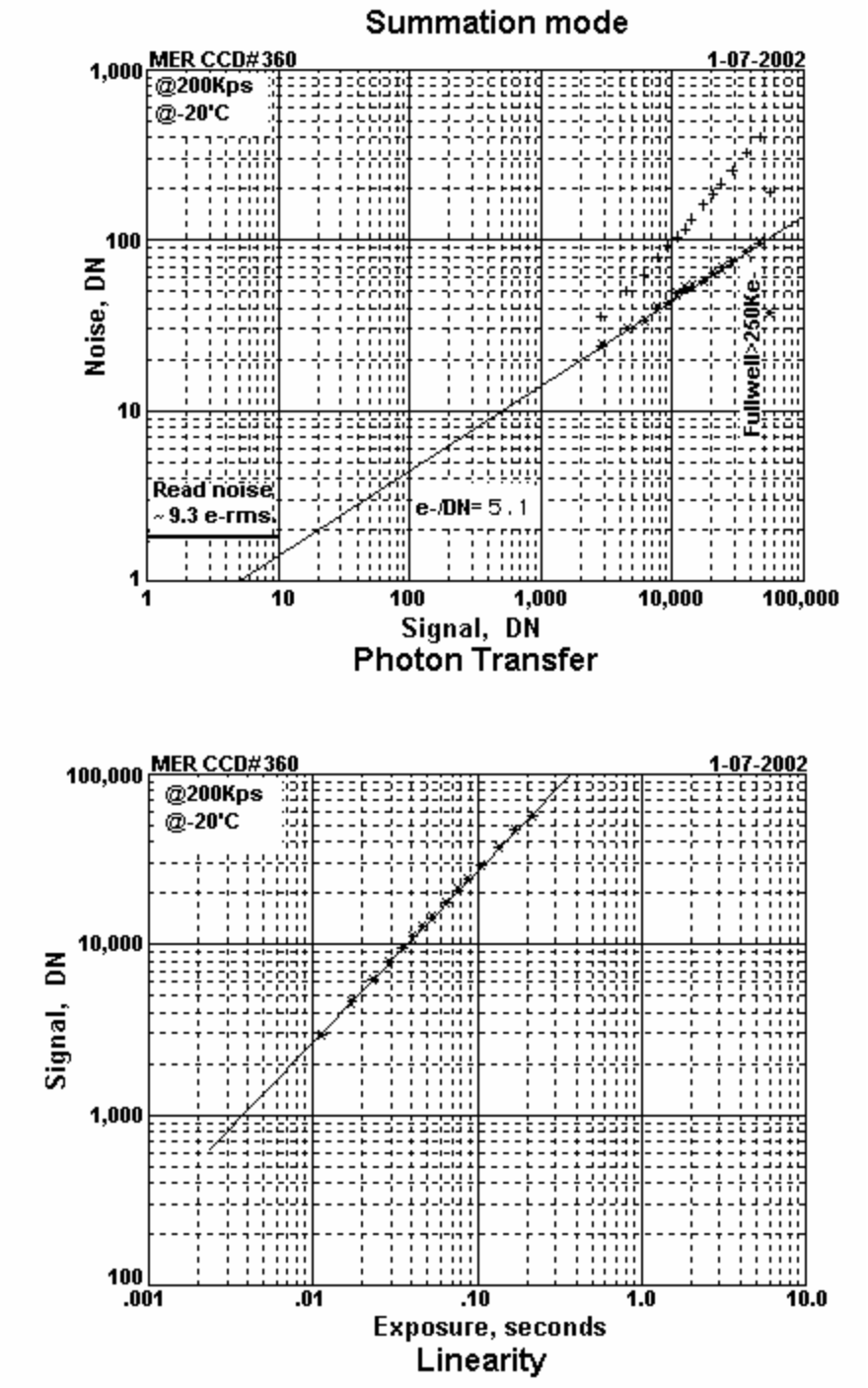

Figure 2.1.4d CCD serial # 360 (MI serial # 110) summation (4×1) mode. (top) Photon transfer plot with derived parameters. (bottom) Linearity plot.

2.1.5 Dark current

Dark current images were also recorded at –20°C. Histograms of the dark current are shown in Figures 2.1.5a and 2.1.5b.

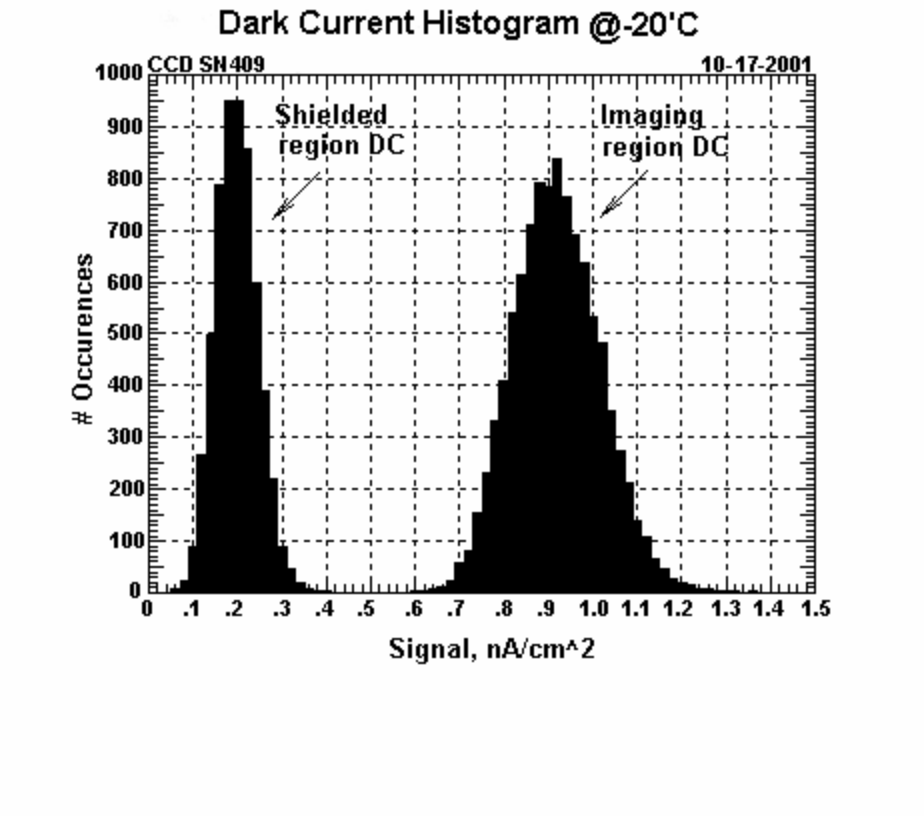

Figure 2.1.5a. Dark current (DC) histograms for CCD serial # 409 (used in MI serial # 105).

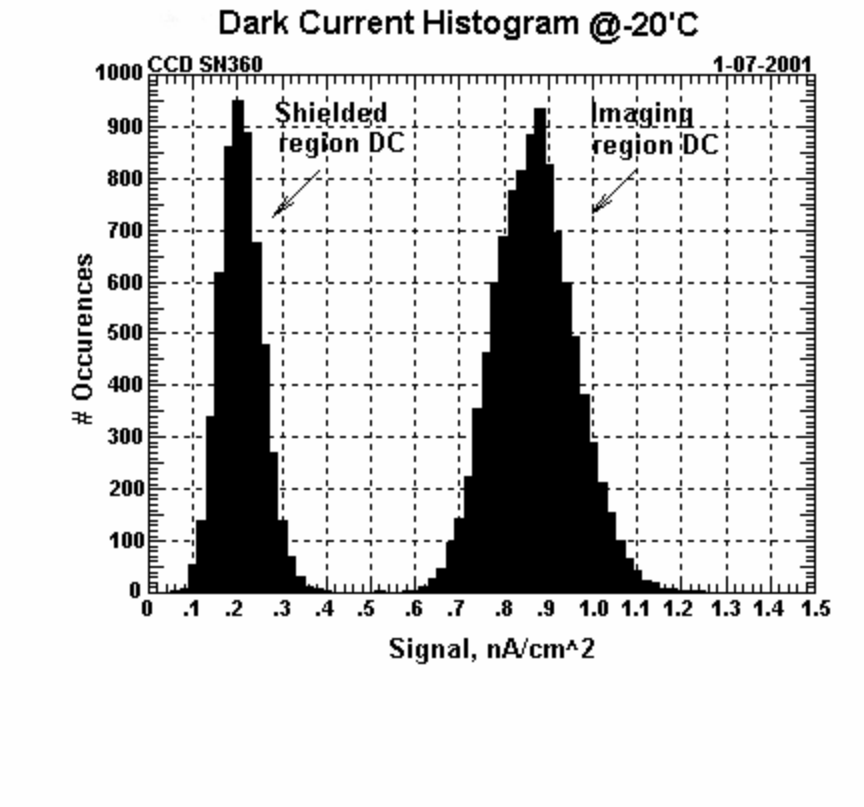

Figure 2.1.5b. Dark current (DC) histograms for CCD serial # 360 (used in MI serial # 110).

2.1.6 Flat field and other images

Flat fields were acquired for all of the CCDs and analyzed at Cornell University (see http://marswatch.astro.cornell.edu/pancam/ccd_anomalies.html). An example of the artifacts seen in several of the CCDs is shown in Figure 2.1.6. Images of other targets were also taken, in both full-resolution and summing modes.

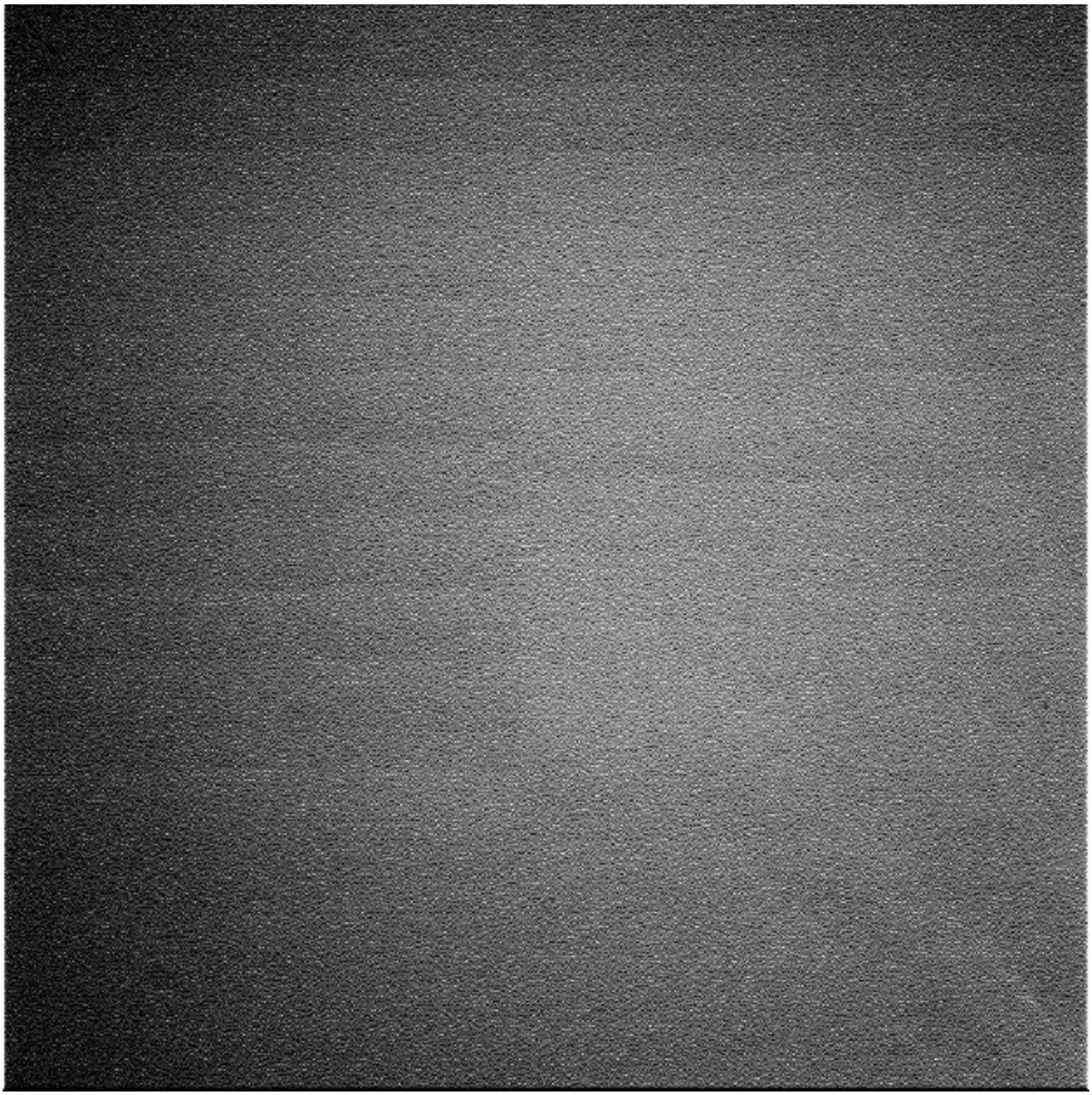

Figure 2.1.6. Contrast-enhanced flat field for CCD serial # 360 (used in MI serial # 110), taken at 5°C, 1000 nm illumination. High frequency features only a few DN in amplitude, less than 1% of average signal level.

2.1.7 Pinholes

The CCDs used in the MI flight units were not subjected to tests specifically designed to detect and measure the transmission of pinholes in the transfer region shield. The results of pinhole testing on CCD serial # 31 are shown in Appendix B.

2.1.8 Spectral quantum efficiency

The absolute quantum efficiency of the CCDs to be used in the science cameras was measured at several wavelengths, as shown in Figures 2.1.8a and 2.1.8b. Quantum efficiency (QE) is the ratio of output photoelectrons to input photons. The results show that the QE decreases with temperature in visible light and increases with temperature in infrared light, as expected.

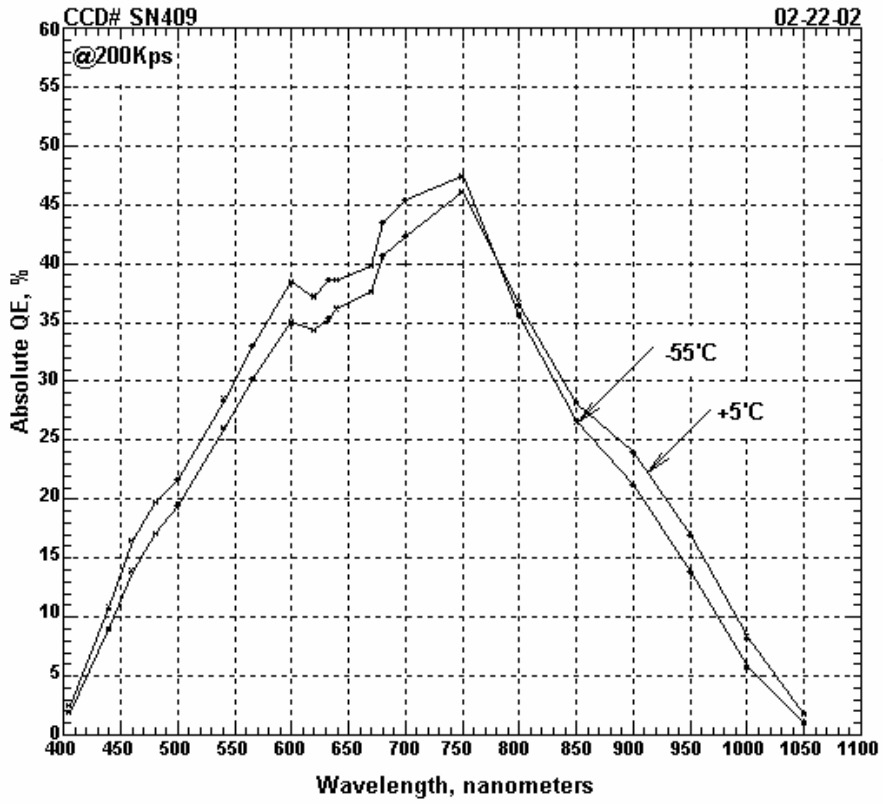

Nanometers	%QE +5'C	-55'C
405	1.9	2.5
440	9	10.8
460	13.9	16.5
481	17.1	19.7
500	19.5	21.7
541	26.1	28.5
566	30.2	33
600	35	38.5
620	34.3	37.2
633	35.3	38.6
640	36.2	38.6
670	37.6	39.8
680	40.6	43.5
700	42.3	45.4
750	46.1	47.4
800	36.6	35.7
850	28.1	26.6
900	24	21.2
950	17	13.9
1000	8.3	5.7
1050	1.8	1

Figure 2.1.8a. Spectral quantum efficiency of CCD serial # 409 (used in MI serial # 105).

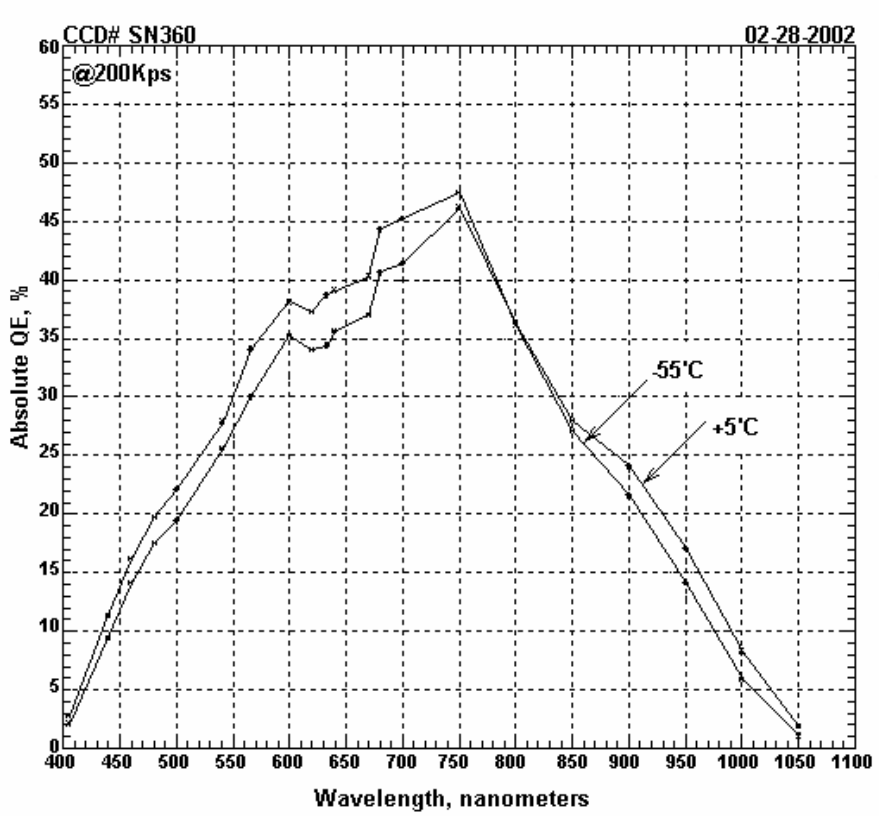

Nanometers	%QE +5'C	-55'C
405	2.1	2.8
440	9.4	11.3
468	14.1	16.2
481	17.5	19.7
500	19.4	22.1
541	25.6	27.9
566	30	34.1
600	35.2	38.1
628	34	37.3
633	34.4	38.7
640	35.7	39.1
670	37	40.3
680	40.6	44.3
700	41.4	45.2
750	46.2	47.5
800	36.4	36.2
850	28	27.1
900	24.1	21.6
950	17.1	14.1
1000	8.3	5.9
1050	1.9	1.1

Figure 2.1.8b. Spectral quantum efficiency of CCD serial # 360 (used in MI serial # 110).

2.1.9 Charge transfer efficiency

This test made use of an ^{55}Fe source, which produces mostly Mn Kα X-rays with energies of 5.9 keV, and a few Mn Kβ X-rays with energies of 6.4 keV. Each 5.9 keV photon produces 1620 electrons (e^-) in silicon, with a very narrow distribution about this number. 1620 e^- is very small compared to the MER CCD full well capacity (~200,000 e^-), so this test accurately shows how well a known, small quantity of charge is transferred through the array. Due to relatively high dark current, the +5°C data set is not very useful (Figures 2.1.9a and 2.1.9c). The -55°C data show a well-defined band of x-ray events (black dots) centered at a level of ~1620 e^- (Figures 2.1.9b and 2.1.9d). Any tilt in this band indicates a loss in signal amplitude as a charge packet is transferred across the array. Charge at the end of the serial register adjacent to the amplifier undergoes only a few transfers. Charge from the opposite, far end of the serial register undergoes ~1000 transfers. If the far-end signal equals the near-end signal, *i.e.*, if the line is horizontal, then no charge has been lost during the ~1000 transfers. Therefore, the figure of merit is how horizontal each line is. A tilt can first be detected when the charge transfer efficiency (CTE) drops to ~0.99998. A drop of 20 e^- would imply an ensemble efficiency of 0.988 for ~1000 transfers. The per-transfer CTE in this case would be the 1000th root of 0.988 or 0.999988. This test is far more demanding than other CTE measurements because it accurately measures CTE for very low signal levels, the regime where small charge losses are most important. The results of this test indicate that the CTE for these CCDs is excellent.

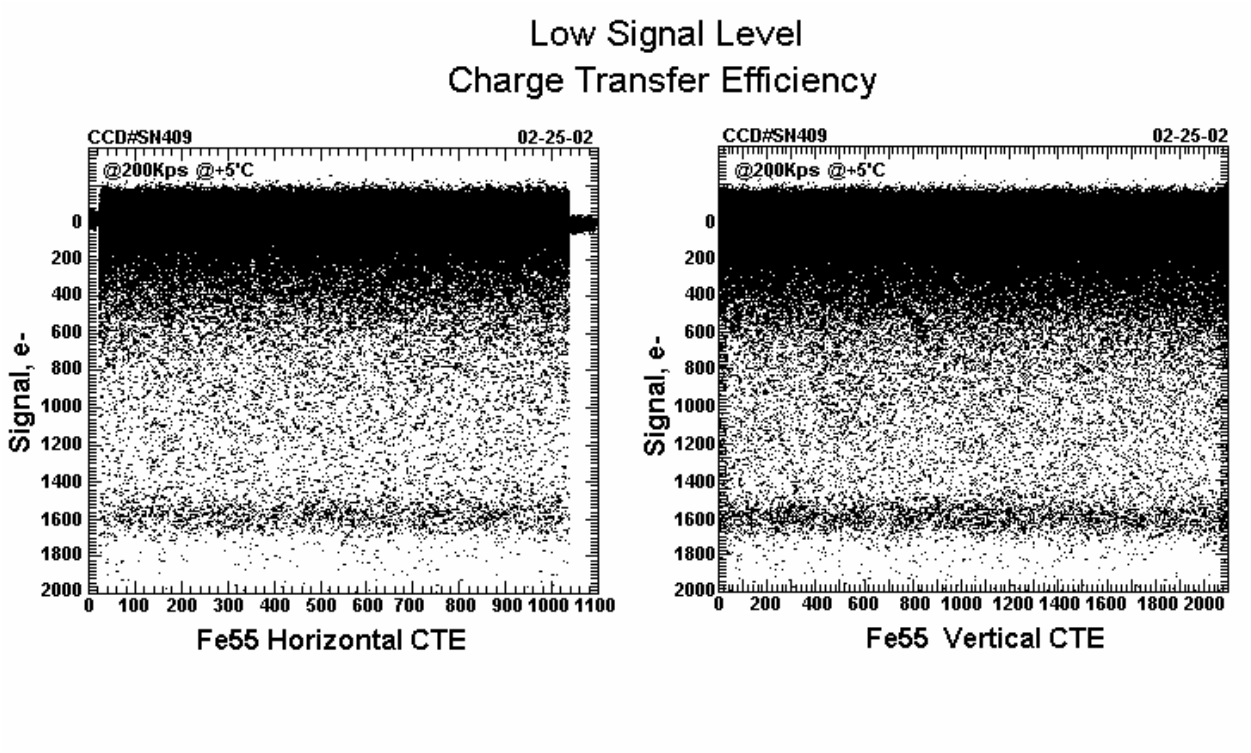

Figure 2.1.9a. Signal vs. pixel number for CCD serial # 409 (used in MI serial # 105) at +5°C. Note that signal increases downward.

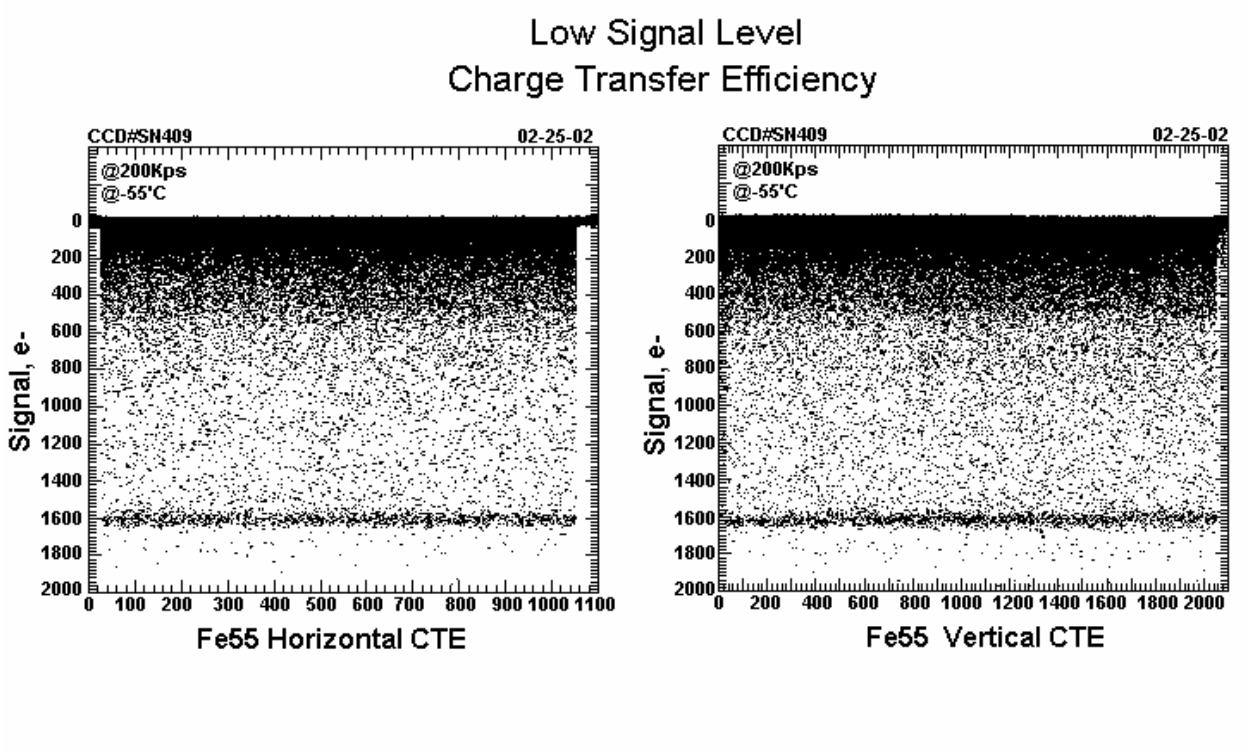

Figure 2.1.9b Signal vs. pixel number for CCD serial # 409 (used in MI serial # 105) at –55°C. Note that signal increases downward.

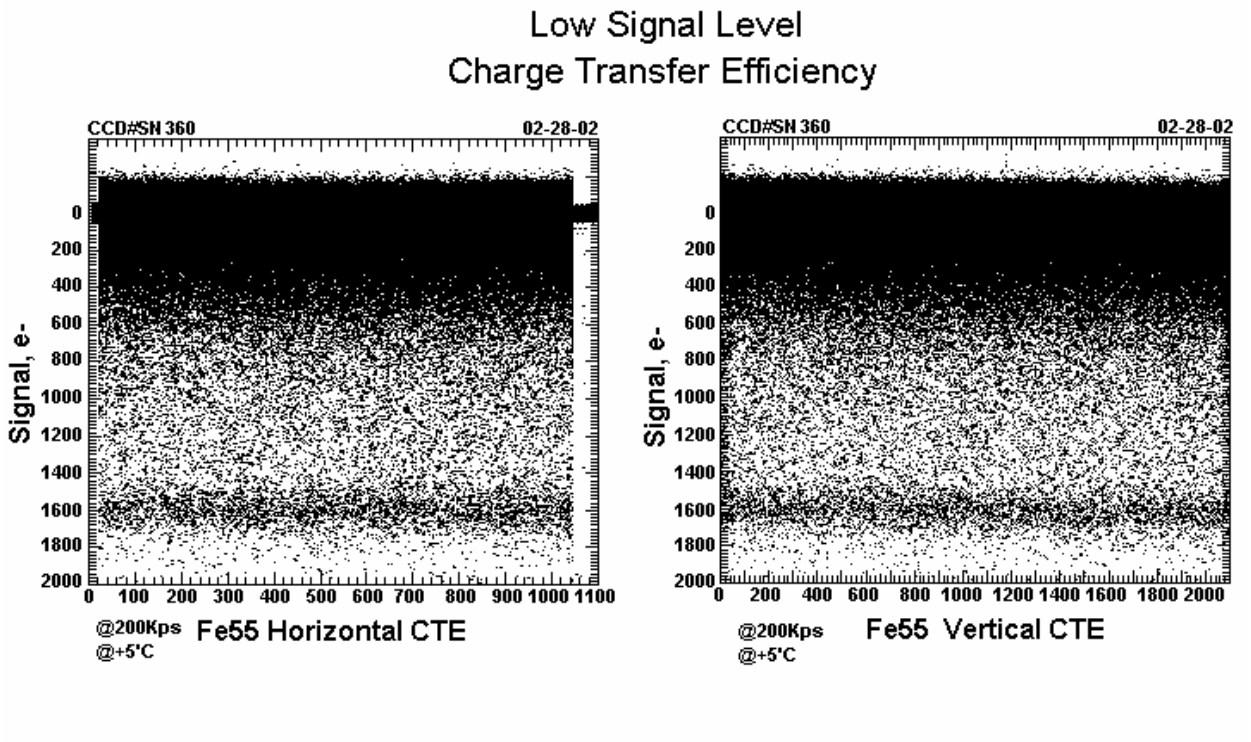

Figure 2.1.9c. Signal vs. pixel number for CCD serial # 360 (used in MI serial # 110) at +5°C. Note that signal increases downward.

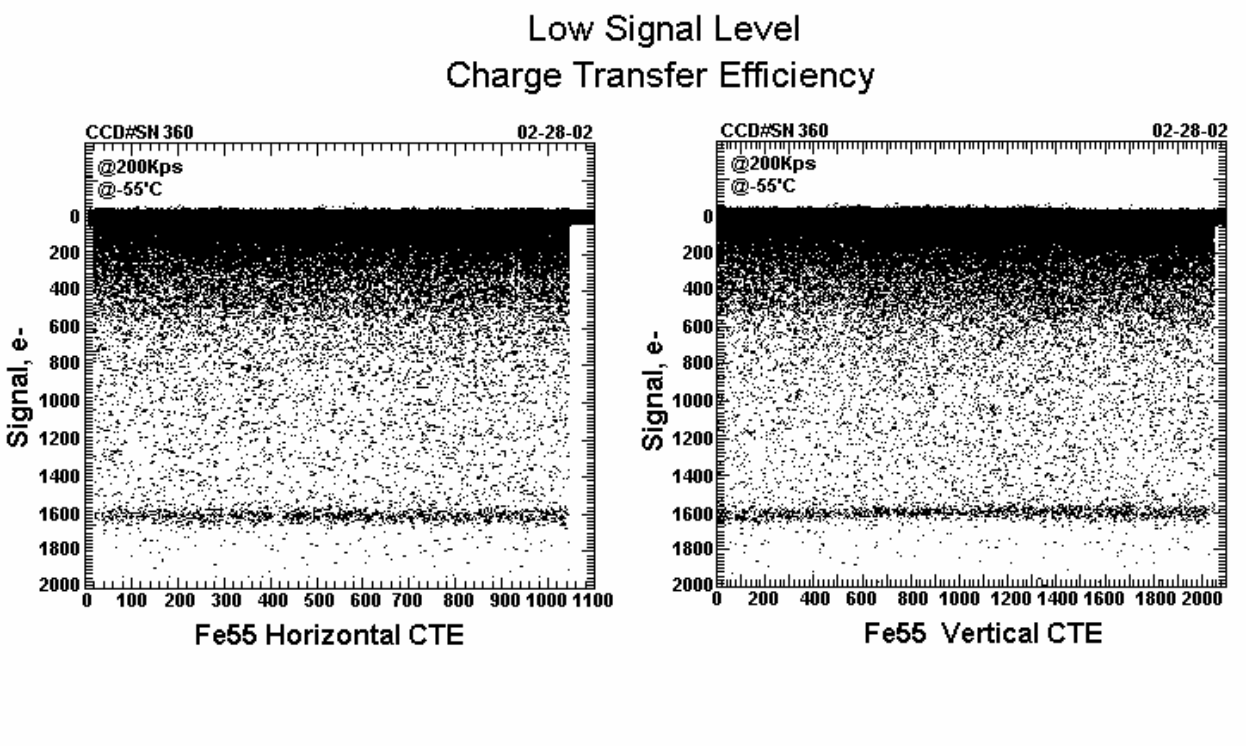

Figure 2.1.9d Signal vs. pixel number for CCD serial # 360 (used in MI serial # 110) at –55°C. Note that signal increases downward.

2.1.10 Residual bulk image and residual surface image

Residual bulk image (RBI) refers to long-wavelength signal charge that is temporarily trapped in the low-resistivity silicon layer that underlies the high-resistivity silicon layer in which most of the photon-to-charge conversion and all of the pixel-to-pixel charge transport takes place. Tom Elliott initially subjected a MER CCD to a 100× overexposure at -55°C. The resulting residual image (Figure 2.1.10a) had an amplitude of less than 10 electrons. He then conducted a series of tests at -55°C and -85°C. He exposed and read out a series of ten long-wavelength images (850 nm and 950 nm) and measured the small increase in signal that occurred during the sequence. This increase reflects the gradual filling of traps in the underlying low-resistivity silicon. In the worst case (-85°C, 950 nm) the signal increased by 0.6% during the sequence.

A related problem is that of residual surface image (RSI). In this instance, charge is temporarily trapped between the high-resistivity layer described above and the insulating oxide layer that overlies it. The charge-trapping and dark current characteristics of this interface vary somewhat as a function of the bias potential that is placed on the electrode that overlies the insulator. Concern arose over the electronic component that was initially selected to provide this bias and consideration was given to operating with a less negative bias, potentially increasing both dark current and residual surface image. Again, Tom characterized the implications of this possibility (see Appendix C). His measurements show that dark current will increase by ~20% and that at -85°C, surface residual image will be ~80 electrons for a 4x overexposure and a 1 volt change in operating bias. Radiation effects may worsen this impact.

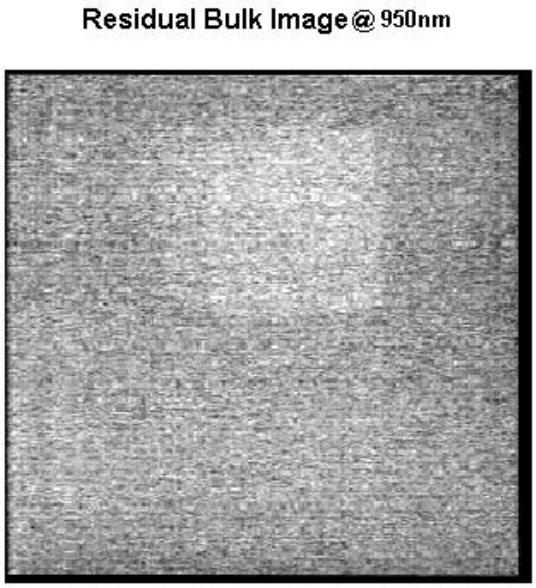

MER CCD 1024 x 1024 Residual Bulk Image taken at an operating temperature of -55'C and at a wavelength of 950 nm. The test consisted of exposing a focused image on the CCD to 100X fullwell then fast erasing the CCD and immediately integrating for ~10 second under dark conditions(shutter closed.)

Figure 2.1.10a. RBI test image.

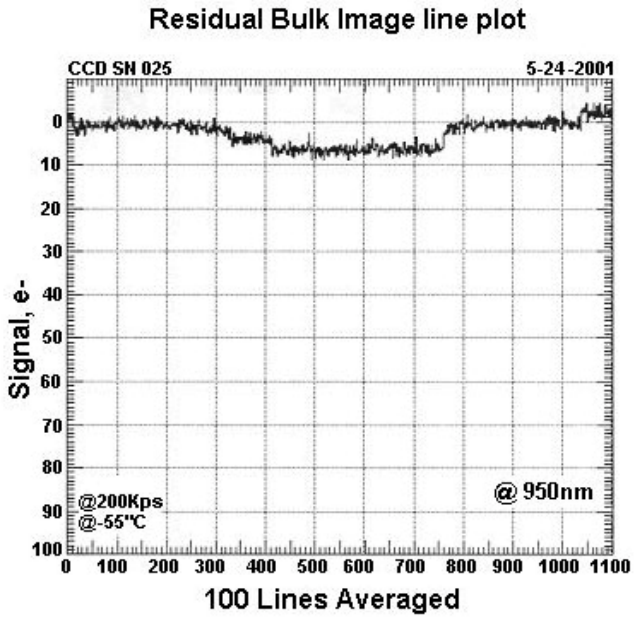

Figure 2.1.10b RBI line plot.

The RBI test conditions were: operating temperatures of -55°C and -85°C, the use of 850 and 950 nm wavelength light and a CCD readout rate of 200 Kpixels/second. Figure 2.1.10a shows an RBI image taken at -55°C after exposing the CCD to a 950 nm light level of 100 times full well, fast erasing the CCD and integrating under dark conditions for ten seconds. Figure 2.1.10b is an averaged line trace of 100 lines showing the signal level in electrons of the RBI image (note that signal increases downward).

Figure 2.1.10c is a comparison of residual bulk image quantum efficiency hysteresis (RBI QEH) at -55°C and -85°C and at wavelengths of 850 nm and 950 nm. The data were obtained by taking 10 flat-field frames and then taking 10 dark frames. The 10 exposed and dark frames were read out with no waiting in between. The exposed frames fill in the bulk traps found at the epitaxial/substrate interface and therefore change the QE response of the CCD and the dark frame allows the traps to discharge and bring the QE back to an equilibrium condition. From the data obtained at -55°C it appears that RBI QEH is only a concern for wavelengths >850 nm. When the operating temperature of the CCD is -85°C it appears there will be some RBI QEH at 850 nm wavelengths and greater. The largest amount of RBI QEH shown is approximately 0.6% at 950 nm and -85°C. Because the MI optics include a filter that restricts the bandpass to wavelengths <700 nm, RBI QEH is not an issue for the MI.

RBI QEH Test Sequence

1. Stabilize the CCD at desired operating temperature.

2. Allow the CCD to remain under dark conditions for ~10 frames.
3. Expose the CCD to 950nm light for 10 frames. Plot data point after each frame.
4. Allow the CCD to remain under dark conditions for 10 frames. Plot data point after each frame.
5. Repeat steps 3 and 4.

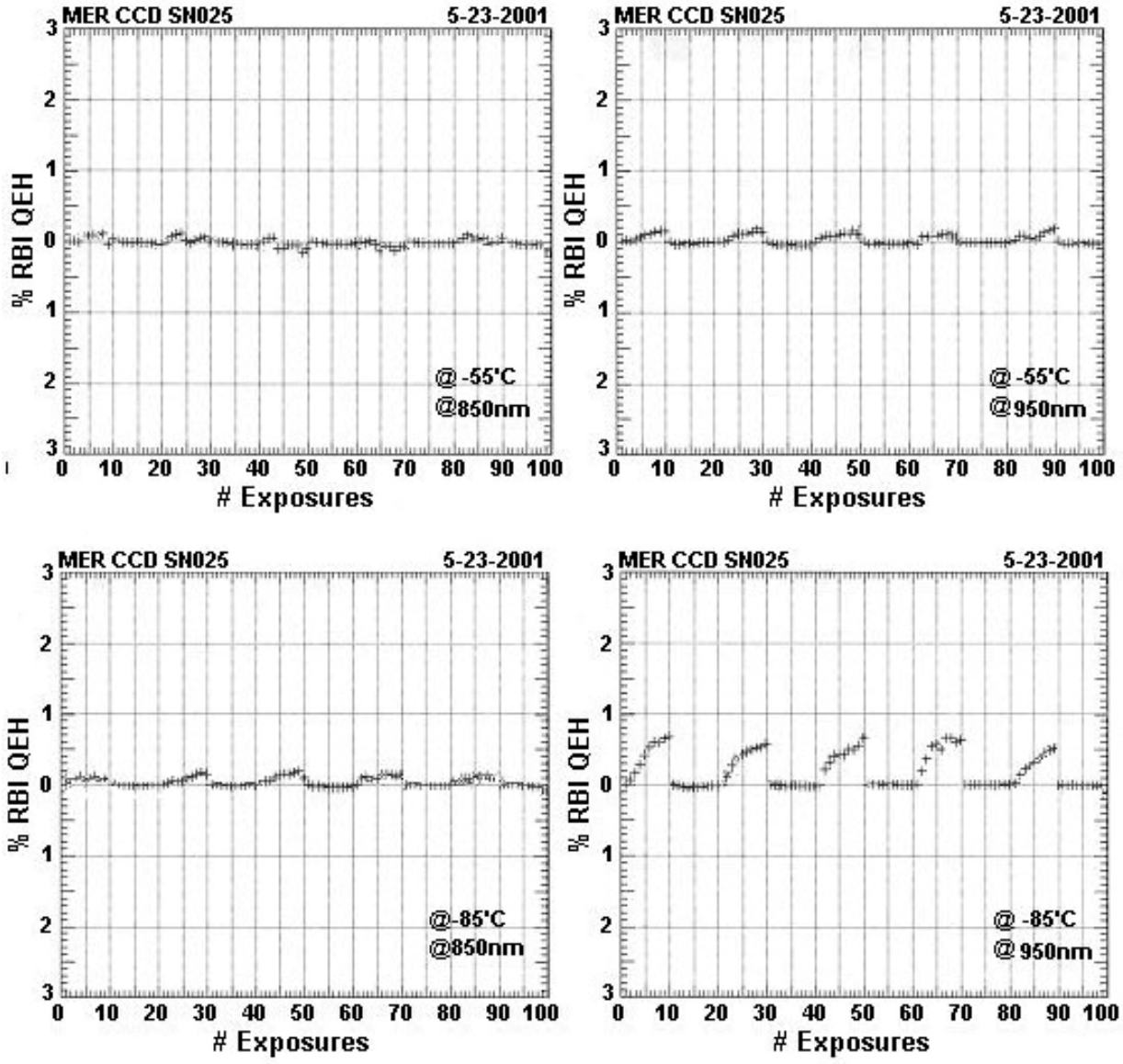

Figure 2.1.10c. Comparison of RBI quantum efficiency hysteresis at various temperatures and wavelengths.

In conclusion, the MER CCDs experience RBI and RBI QEH at low temperatures. The solution, if necessary, will be to allow time between images for the bulk traps to discharge. At -55°C this should be relatively quick but for colder operating temperatures it will be considerably longer. Because the MI will take images of Mars only in daylight and will be heated to the minimum operating temperature (-55°C), RBI is unlikely to be an issue during landed operations.

2.2 Optical barrel transmission and MTF

2.2.1 Purpose and Description

Transmission of each MI optics barrels was measured at Kaiser Electro-Optics (KEO) before integration of the optics into the camera. These data were acquired to determine the spectral radiometric response of the camera in the event that the monochromator calibration (section 3.2.3) was unsuccessful. The modulation transfer function (MTF), focal length, and distortion of the optics were also measured at KEO. The results of these tests also served as acceptance criteria for the optical barrel assemblies. Optical barrel assembly serial # 004 was used in MI flight unit 105 (Spirit), and optical barrel assembly serial # 005 was used in MI flight unit 110 (Opportunity).

2.2.2 Test Procedure

The procedures for the MI optics tests are documented in the KEO MER camera Acceptance Test Procedure (PR-511).

2.2.3 Data Processing and Products

The results of these tests are presented in Appendix D. The MTF, distortion, and focal length data are shown in Table 2.2.1. Spectral transmission data for the MI serial # 105 optical barrel assembly are listed in Table 2.2.2.

2.2.4 Accuracy and Relationship to Requirements

The accuracy of the KEO measurements is not available, but it is clear that the lens barrel assemblies meet the MER specifications (Level 3 requirement #1188, Level 4 requirements). Filter spectral transmission and CCD spectral quantum efficiency measurement uncertainties also contribute to overall radiometric calibration uncertainty.

2.3 Filter blocking and transmission

2.3.1 Purpose and Description

Transmission of each Schott BG-40 filter from 200 to 1100 nm was measured before integration of the filter into the optical assembly. These data will be used to check the camera-level absolute and spectral radiometric response calibration results. The results of this test also served as acceptance criteria for the Schott filters.

2.3.2 Test Procedure

Equipment used: Varian Cary Spectrophotometer 5e
MER filter holding adapter
X,Y Translation Stage (WF/PC III Configuration)

The Cary Spectrophotometer had recently been highly modified to accommodate WF/PC III filter testing, calibration and qualification, so it was very important not to change the set up in

any fashion. A special filter holding adapter was made to simulate WF/PC filter dimensions that would allow MER filters to be mounted in the center of the beam.

Basic Transmission Measurement Procedure: The spectrophotometer parameters (wavelength range, band-pass width, slit height, data interval and detector cross over) were configured to ensure that the results would satisfy the requirements. Once the parameters were set then a baseline measurement was run to establish the spectrophotometer optical path characteristics, one of which is the slit height. It is very important that the amount of energy that reaches the detector in the sample path, between baseline and throughput measurements, not change due to slit height truncation (the actual aperture used to hold the filter must be used for the baseline run).

MER Filter Measurements: Spectrophotometer parameters were set up. The adapter and filter was then placed into the x, y stage in the sample compartment and the stage driven to its center position. The spectrophotometer was then driven to 530 nm and the slits opened to their fullest position. A visual examination of the slit image on the MER filter was performed to ensure that the measurements would be made at the center of the filter. The filter was then removed from the adapter, the adapter installed back into the optical path, and a baseline measurement was made. Following the baseline measurement, a 100% transmission measurement (no filter in path) was made to verify the amplitude range. The empty filter adapter was removed, the filter installed, the adapter and filter replaced, and the transmission measurements made. The data file was then labeled according to filter serial number and was and stored in a folder. The spectral transmittance of each filter was measured 3 times from 200 to 1100 nm in 1 nm steps at room temperature and pressure.

2.3.3 Data Processing and Products

The 3 sets of measurements for each filter were averaged, and the 100% transmission measurements subtracted at each wavelength. The results are shown in Table 2.3.2 in Appendix E. These data show that the filter transmission in the near infrared is negligible. As shown in Fig. 2.3.1, the spectral transmissions of the 3 filters are essentially identical.

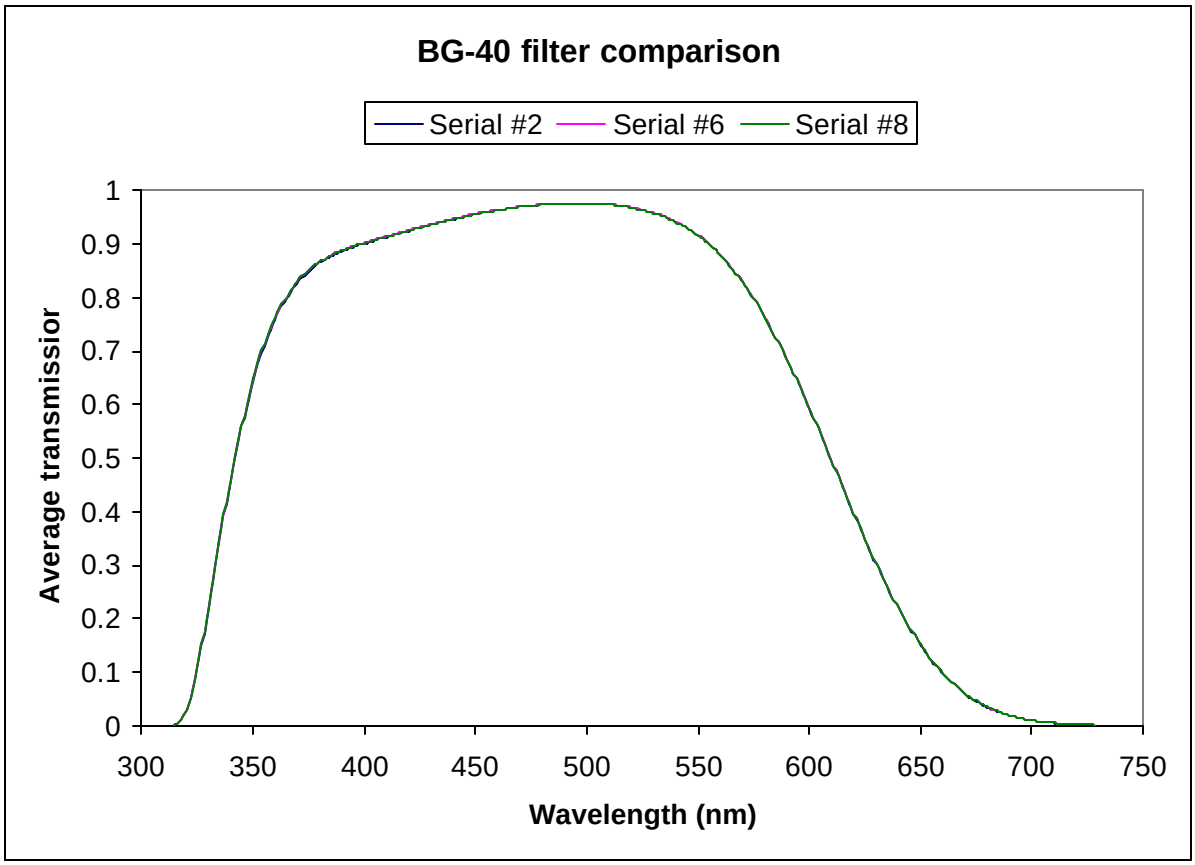

Figure 2.3.1. Average of 3 transmission measurements for 3 Schott BG-40 filters.

2.3.4 Accuracy and Relationship to Requirements

The standard deviation from the mean of the 100% transmission measurements was 0.056%, and is a measure of the accuracy of the transmission data. The standard deviation of the 3 sets of transmission measurements for each filter never exceeded 0.001%, and was typically less than 0.0001%. This level of accuracy is easily consistent with Level 3 requirement #1190 (absolute radiometric calibration accuracy). Optics spectral transmission and CCD spectral quantum efficiency measurement uncertainties also contribute to overall radiometric calibration uncertainty.

2.4 Dust Cover Spectral Transmission

2.4.1 Purpose and Description

Determine the spectral transmission of the flight dust cover windows or material from the same batch using a spectrophotometer. A sample of the Kapton polyimide film that was used for the flight dust covers was provided to Dick Morris (NASA Johnson Space Center) for spectrophotometric analysis. The spectral transmission of the Roscolux film that was originally planned to be used for the dust covers was also measured, but is not included here because it was not used on the flight MIs.

2.4.2 Test Procedure

The spectral transmittance of the dust cover window material was measured from 350 to 1200 nm in 4 nm steps at JSC. The sample was from both sides to evaluate possible differences in transmission.

2.4.3 Data Processing and Products

The transmittance data for the Kapton film that was used in the MI dust covers is shown in Figure 2.4.1. The average transmittance values at each wavelength are listed in Table 2.4 in Appendix F. No significant difference in transmission front/back is observed.

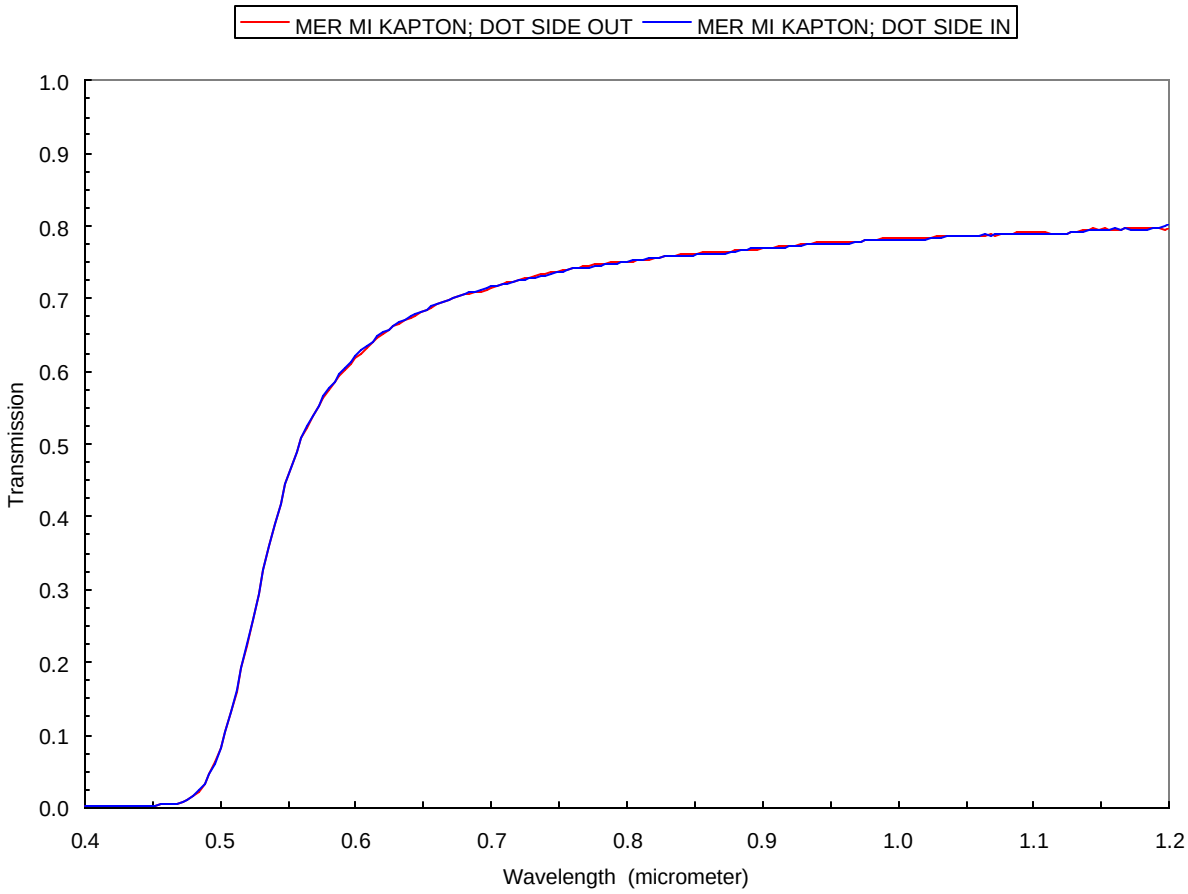

Figure 2.4.1. Spectral transmittance of MI dust cover window material.

2.4.4 Accuracy and Relationship to Requirements

The observed transmittance accuracy of ±2% easily meets Level 3 requirement #1190 (absolute radiometric accuracy). Filter spectral transmission and CCD spectral quantum efficiency measurement uncertainties also contribute to overall radiometric calibration uncertainty.

3 STAND-ALONE CAMERA TESTING AND CALIBRATION

3.1 Overview

The MER science cameras were assembled, tested, and calibrated in D. Thiessen's clean laboratory environment at JPL. The laboratory configuration and equipment were customized for MER testing and calibration. Most of the science camera testing and calibration was done in two labs, one for ambient testing (the "Askania" lab, named after one of the optical benches used in MER camera testing) and another for thermal/vacuum testing. The geometric and other tests that were unaffected by temperature were performed at room temperature and pressure on optical benches with electrostatic discharge protection. The lab configuration for MI ambient calibration is shown in Figure 3.1.1.

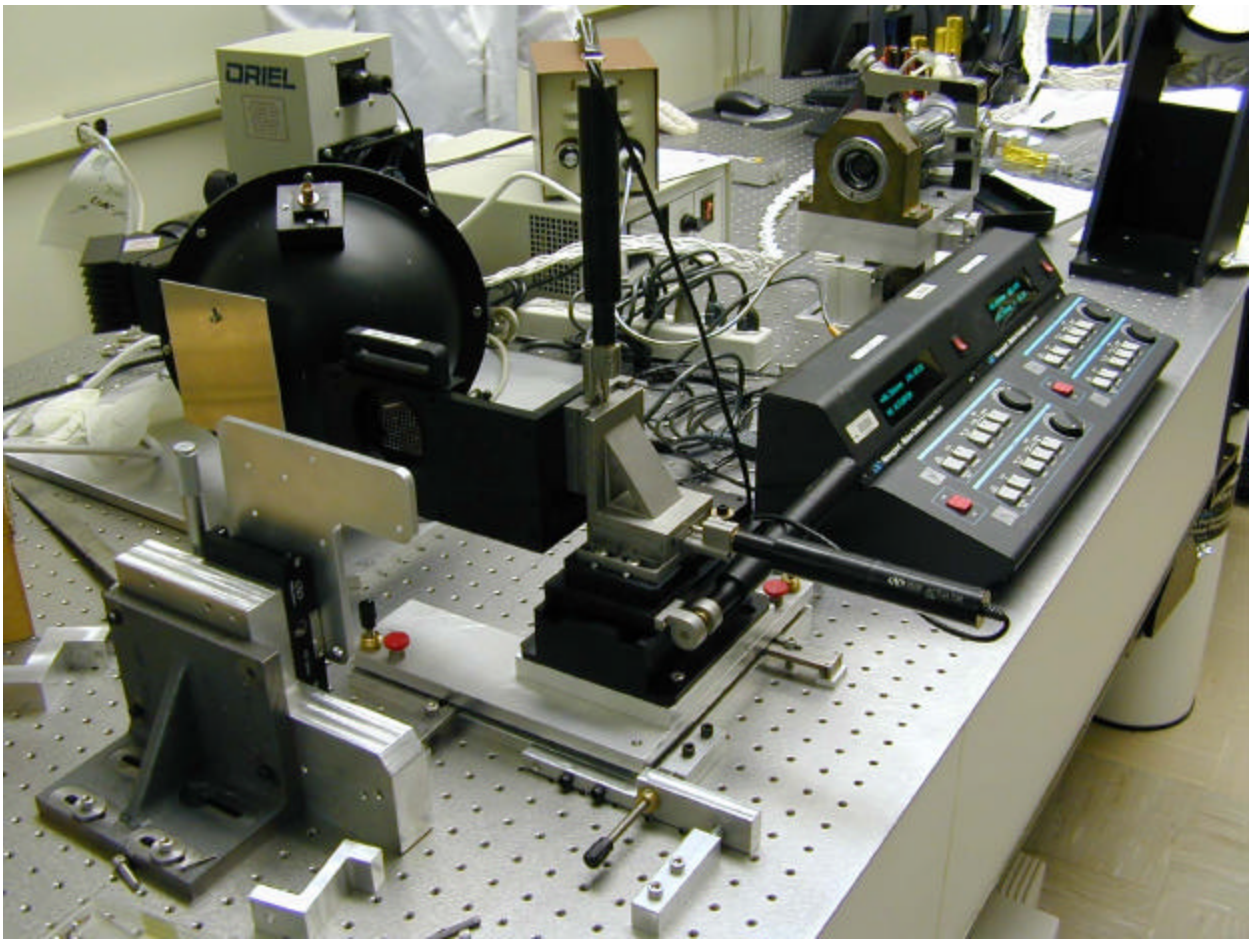

Figure 3.1.1. MI ambient test equipment. Camera (not shown) mounted on L-shaped bracket at left, viewing targets in holder mounted on 3-axis stage at center. Camera and targets aligned using telescope at top right, targets illuminated from behind by sliding small black integrating sphere to right.

Three science cameras (2 Pancams, 1 MI; see Figure 3.1.2) were tested together in the thermal/vacuum chamber, all three viewing external targets and sources through an optical-grade quartz window (Figures 3.1.3 and 3.1.4).

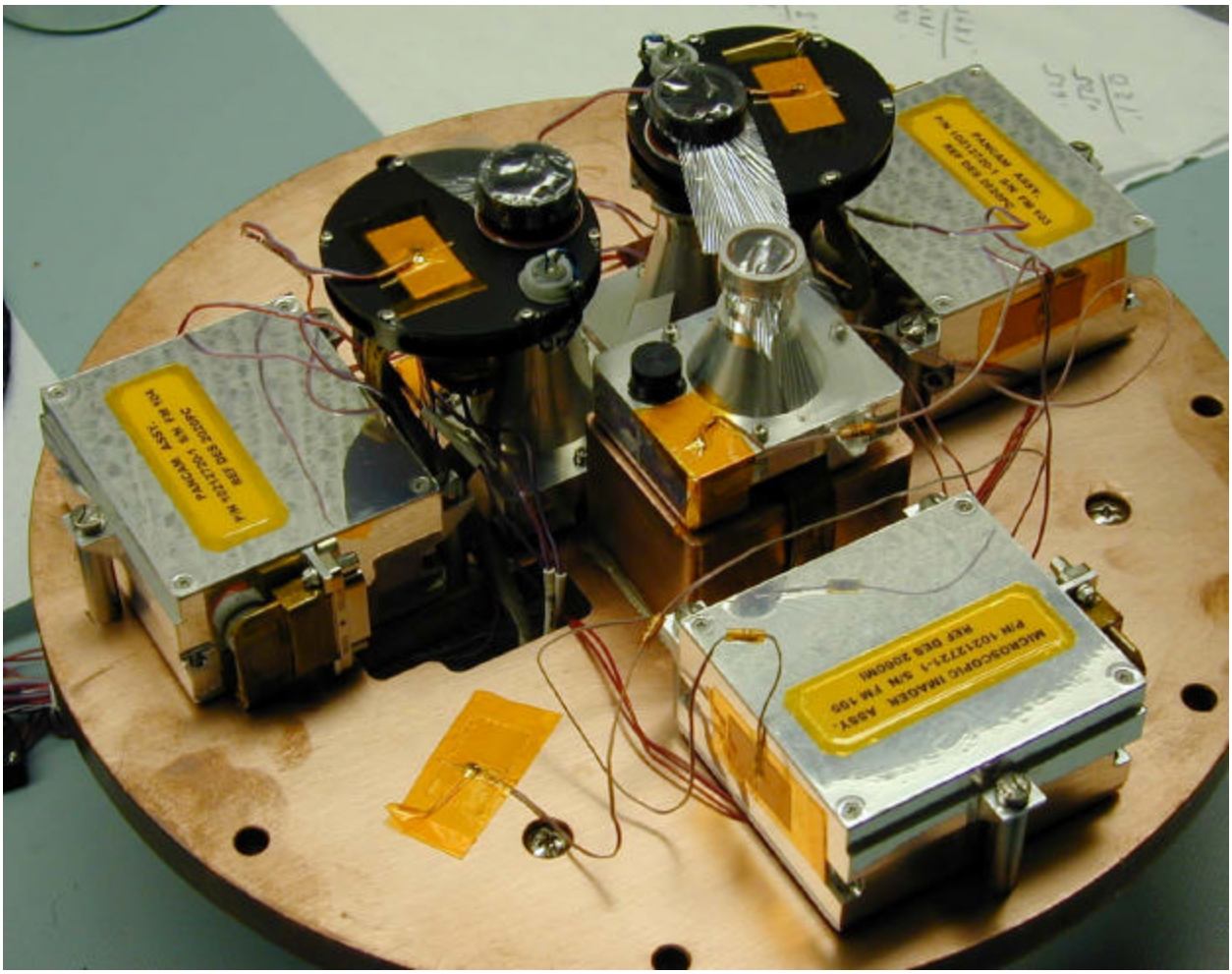

Figure 3.1.2. First set of flight science cameras mounted on cold plate for standalone thermal/vacuum testing. MI serial # 105 at lower right.

The thermal tests and calibration were performed under high vacuum (<10^{-6} torr) at a variety of temperatures spanning the expected temperature range on the surface of Mars. Flight-acceptance thermal cycling was performed before camera calibration, and some calibration data were acquired during the acceptance tests. At very low temperature (-110°C), the optimum video offset for each camera was determined by measuring the dark current in zero-exposure images and avoiding clipping the signal to zero DN. Most of the MI calibration was done at the extremes of the operating temperature range (-55°C and +5°C) and at one intermediate temperature (-10°C). The full suite of MI tests, the required accuracy of measurements, and environments are summarized in Table 3.1.1. All tests were successfully performed during the period July-September, 2002; 18.4 Gbytes of MI calibration data were generated and copied to the USGS for reduction and analysis.

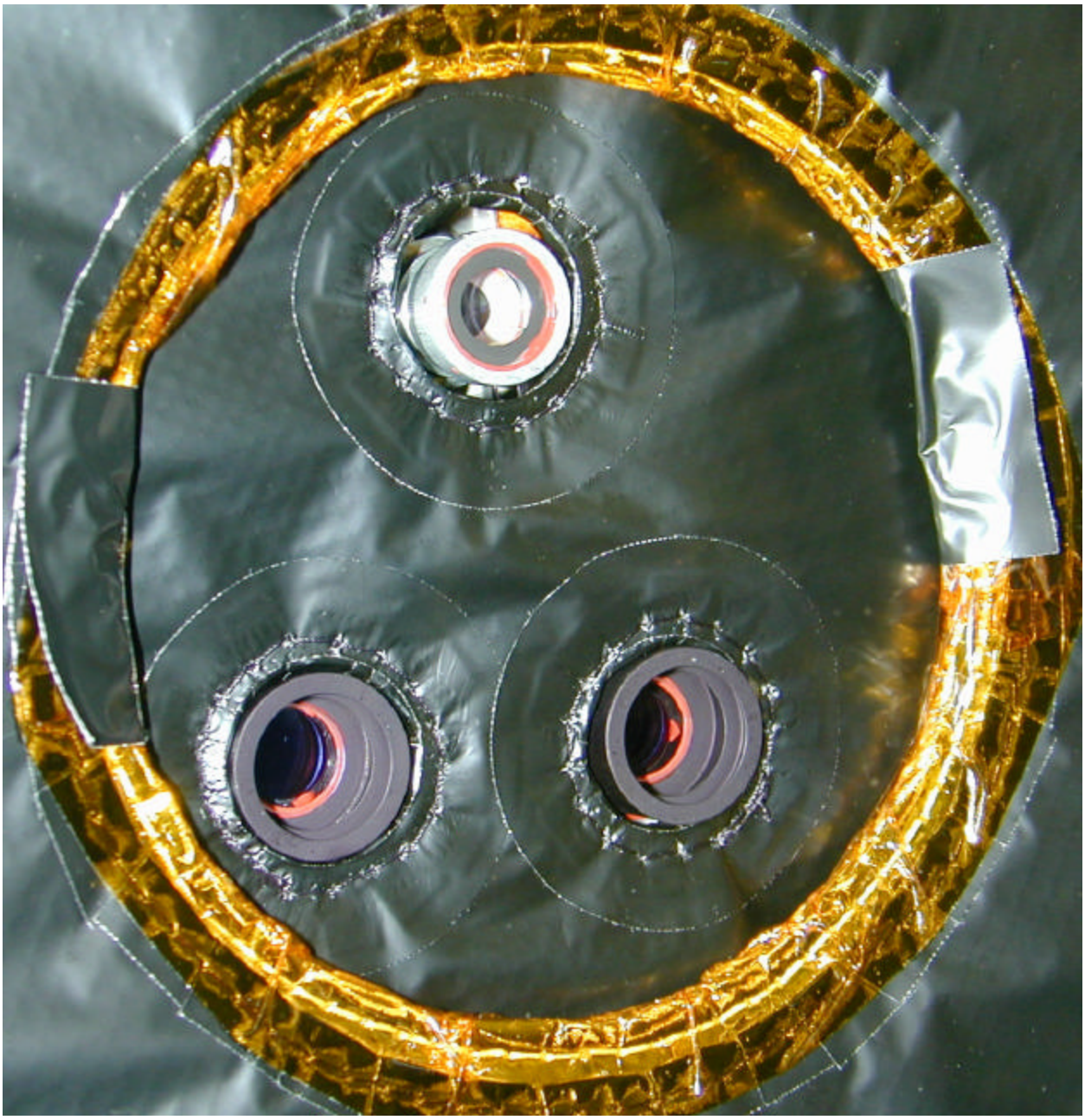

Figure 3.1.3. Configuration of MI serial # 105 (top) and Pancams 103 and 104 for thermal/vacuum testing. Thermal blanketing surrounds optical barrels.

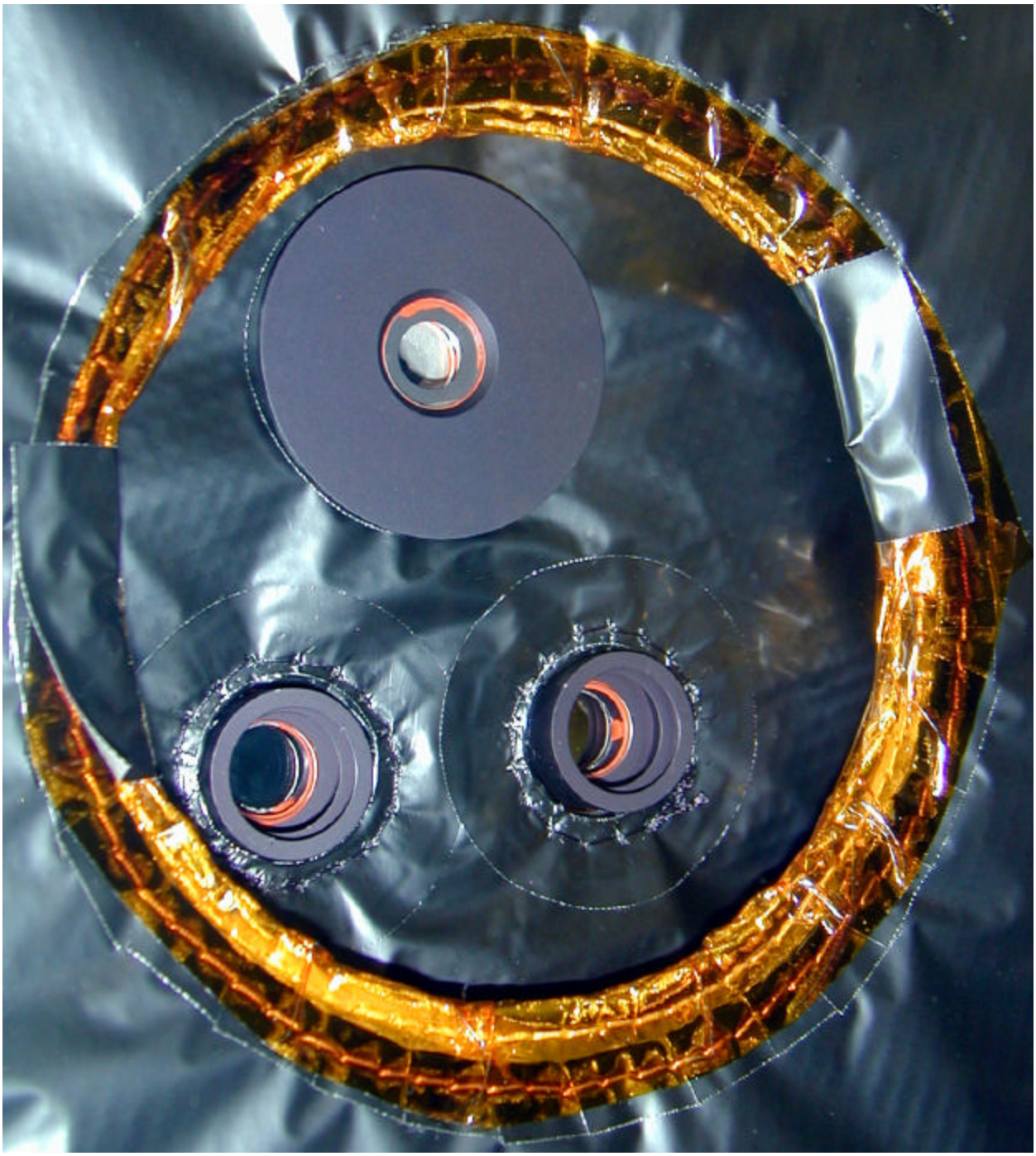

Figure 3.1.4. Configuration of MI serial # 110 (top) and Pancams 114 and 115 for thermal/vacuum testing. Thermal blanketing surrounds optical barrels. Black ring added to MI optical barrel assembly to reduce magnitude of reflections from chamber window.

Table 3.1.1. MI standalone calibration and testing

Test name	Subtest	Accuracy	Priority	Environmental Conditions
1. Light Transfer			High	
	system linearity	± 1%, from 10 to 90% full well		-55°C, -10°C and +5°C; pressure ≤ 10^{-6} torr
	read noise	± 2 e-		-55°C, -10°C and +5°C; pressure ≤ 10^{-6} torr
	full well	± 5% e-		-55°C, -10°C and +5°C; pressure ≤ 10^{-6} torr
	gain	± 2% e-/DN		-55°C, -10°C and +5°C; pressure ≤ 10^{-6} torr
	bias (offset)	± 1 DN		-55°C, -10°C and +5°C; pressure ≤ 10^{-6} torr
	dark current and noise	±0.1 e-, RMS noise		-55°C, -10°C and +5°C; pressure ≤ 10^{-6} torr
2. Absolute and Relative Radiometry		≤ 20% absolute; ≤ 5% relative	High	-55°C, -10°C and +5°C; pressure ≤ 10^{-6} torr
3. System Spectral Response		wavelength, ± 0.2 nm; flux, ±7%	High	-55°C, -10°C and +5°C; pressure ≤ 10^{-6} torr
4. CCD Blooming Behavior		±5%, adjacent pixels	Low	Ambient
5. Observation of Rock Targets		± 1 mm focus control	Medium	Ambient
6. CCD Transfer Smear		± 1% pixel response	Low	Ambient
7. Grid Target Imaging			High	Ambient
	Effective Focal Length	± 2% of EFL		
	Field of View	± 0.2°		
	Geometric Distortion	± 0.3%		
8. Bar Target Imaging			High	Ambient
	Depth of Field	± 1 mm		
	MTF	± 10 % at 30 lp/mm		
9. Scattered and Stray Light		Factor of 2 to 10	Medium	Ambient

3.2 Test Procedures and Results

The preflight calibration data were gathered using ground support equipment (GSE) in various laboratory settings. Temperature sensors on the CCD package and printed circuit board in the MI electronics box, accurate to ±0.5°C, were used to monitor camera temperature during the thermal/vacuum tests (they were not connected during ambient tests). Typically, full frames were acquired along with reference pixels and stored as 16-bit integers (no compression). The GSE generated image files in PDS format, with the PDS label composed of a subset of the keywords to be used for flight data. The filenaming scheme and overview of the ambient calibration data are given in Appendix G. Similar information for the thermal/vacuum calibration data is given in Appendix H.

The MI ambient and science camera thermal/vacuum test procedures are documented separately (JPL TP-518811 and TP-518863). Detailed descriptions of both ambient and thermal/vacuum tests are given below.

3.2.1 Light Transfer (linearity, noise, full well, gain, bias)

3.2.1.1 Purpose and Description

Light transfer sequences were designed to make use of the photon transfer technique (Janesick *et al*., 1987) to measure linearity, read noise, full well, and gain. During ambient tests, the dark current rate was high enough that "light transfer" sequences were obtained by taking dark frames at various integration times. During thermal/vacuum tests, an integrating sphere was adjusted to yield Mars-like radiance levels, and light transfer sequences were obtained by varying integration time. Typically, 21 integration times were used to produce light transfer data; at least 2 frames were acquired at each level. These data were also used to measure the linearity of the camera response with respect to input radiance.

Dark current images (no light source) were acquired along with CCD and electronics temperatures in the thermal/vacuum chamber at temperatures spanning the flight acceptance range. Dark current data were also acquired at ambient temperature and pressure in the Askania lab; during these tests data from the camera temperature sensors were not recorded.

The effect of changing the video offset on bias was evaluated at various temperatures, because the bias is affected primarily by the camera electronics temperature. The video offset is a commandable parameter that can be updated during flight, so test data were needed to determine the optimum video offset for each camera. By design, decreasing the video offset by N causes the bias to decrease by $N/2$. The goal was to adjust the video offset so that the full dynamic range of the ADC is utilized, without clipping low data values to zero. Light transfer and dark current images were taken at various video offsets for this purpose.

3.2.1.2 Test Procedure

To simplify acquisition of light transfer data, the GSE software included a program to take a series of exposures using a default or user-defined table of exposure times. During MI thermal/vacuum testing, the integrating sphere was used as a light source, with the following procedure:

- Set sphere shutter positions to 15 mm
- Position sphere close to window and align "D" markers along slide rail
- Set video offset to value determined above

- Create subdirectory below MI light transfer directory: Ltf#. Set directories on GSE to write images to this directory
- Using 1 sec. image acquired in part A at optimum video offset, calculate exposure needed to produce 1.1*4095 = 4505 DN. Divide this maximum exposure time by 20 and build LTF table with exposure times from 0 to maximum in steps of this value
- Turn off room lights
- Once electrometer is stable, run light transfer test ***twice*** using above table. Record electrometer output during tests
- Press "quit" on GSE and save log file
- Analyze results (quick look) using mer_ltf.pro with the following parameters:
  MIN_GAIN=6, MAX_GAIN=8, FULL_WELL=14

Dark current data were obtained separately during thermal/vacuum tests:

- Cover chamber window, room lights off
- Set directories to "Dark Current", video offset to value determined above
- Take 3 exposures each at: 0, 100, 200, 336 seconds
- Record CCD temperature for each exposure
- Press "quit" on GSE and save log file

3.2.1.3 Environmental Conditions

Temperature = -55°C, -10°C, and +5°C; pressure ≤ 10^{-6} torr. Additional dark current and noise data were acquired at other temperatures during transitions and at ambient temperature and pressure.

3.2.1.4 Data Processing and Products

The light transfer data processing and results are described in the following subsections: 1) Bias and Video Offset; 2) Dark Current; 3) Linearity, Read Noise, Full Well, and Gain.

3.2.1.4.1 Bias and Video Offset

The light transfer sequences taken on 8 August 2002 were used to characterize the effect of video offset on bias for MI serial # 105. The CCD temperature for this test was –114°C and the electronics temperature was about –60°C. An example of the results is shown in Figure 3.2.1a. Flat-field data (at a single intensity level) were taken on 11 September 2002 at various video offsets using MI serial # 110. The data show that changes in bias are approximately linearly related to changes in video offset for both cameras:

$$\Delta(Bias) = \frac{\Delta(Offset)}{2}, \text{ where } \Delta(Offset) = 4095 - \text{Video Offset}$$

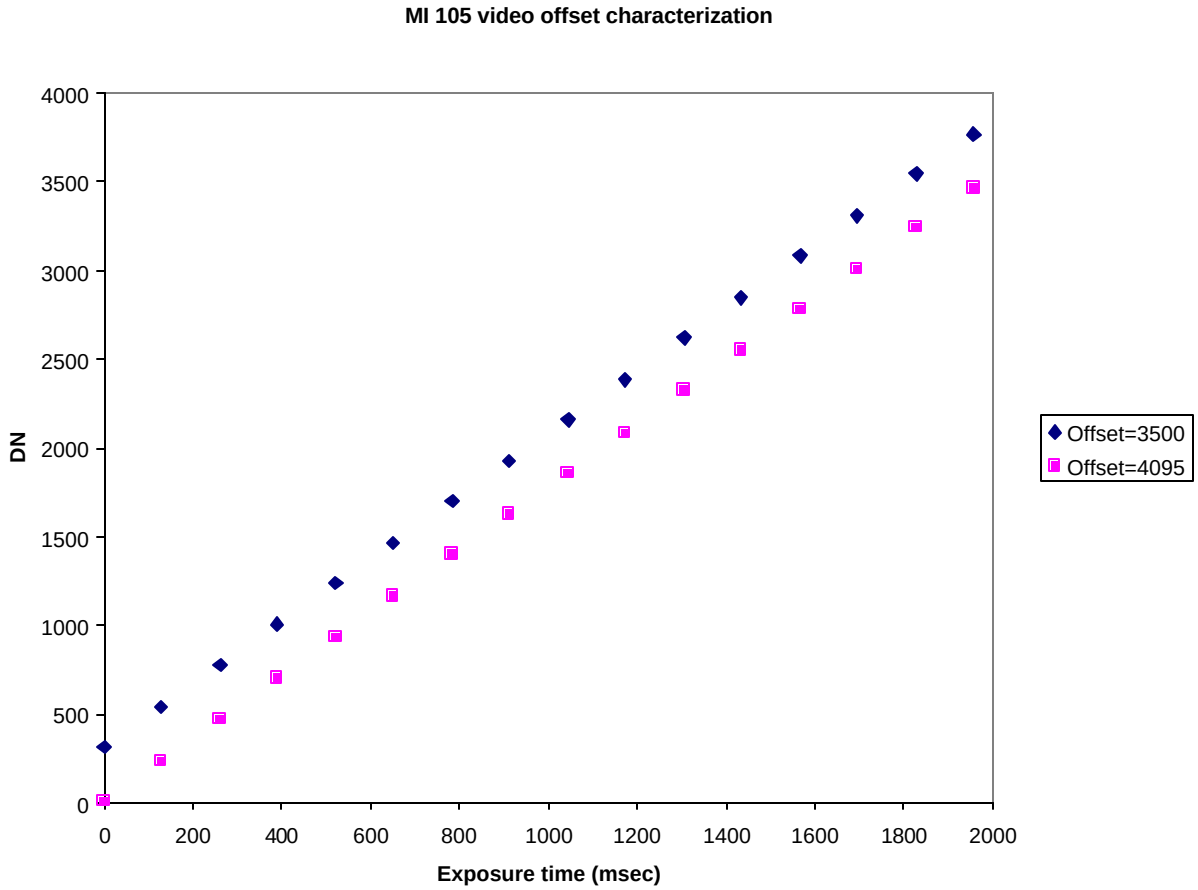

Figure 3.2.1a. Light transfer data for MI serial # 105 at 2 video offsets. Note difference in bias level is half of difference in video offset.

The cameras were tested for zero clipping by taking zero-second dark frames at various temperatures and video offsets during standalone calibration. For MI serial # 105, these data show that zero clipping does not occur at any temperature within the operating range, regardless of video offset. Zero clipping occurred only at very low temperature (CCD at –114.6°C, electronics at –62.9°C) with a maximum video offset of 4095. However, one dark frame taken during system thermal/vacuum testing does show zero clipping within the operating temperature range. This image (2M126571157EDR0007P0506M0M1) was a 10-second exposure taken when the CCD temperature was –53.8°C and the electronics temperature was –54.5°C. It is not clear why this image includes pixels at 0 DN while a zero-second image taken at lower temperature does not (Fig. 3.2.1b), but possible causes are the difference in temperature recording between standalone camera calibration and system testing, different thermal gradients (cameras mounted directly to cold plate during standalone testing as shown in Fig. 3.1.2), or different temperature sensor cabling resistance. Temperature data were manually entered into image labels and history logs during standalone calibration, and temperature records are therefore incomplete in some cases. To avoid zero clipping, the recommended video offset for MI 105 images taken within the operating temperature range (electronics temperature > –60°C) is 4090.

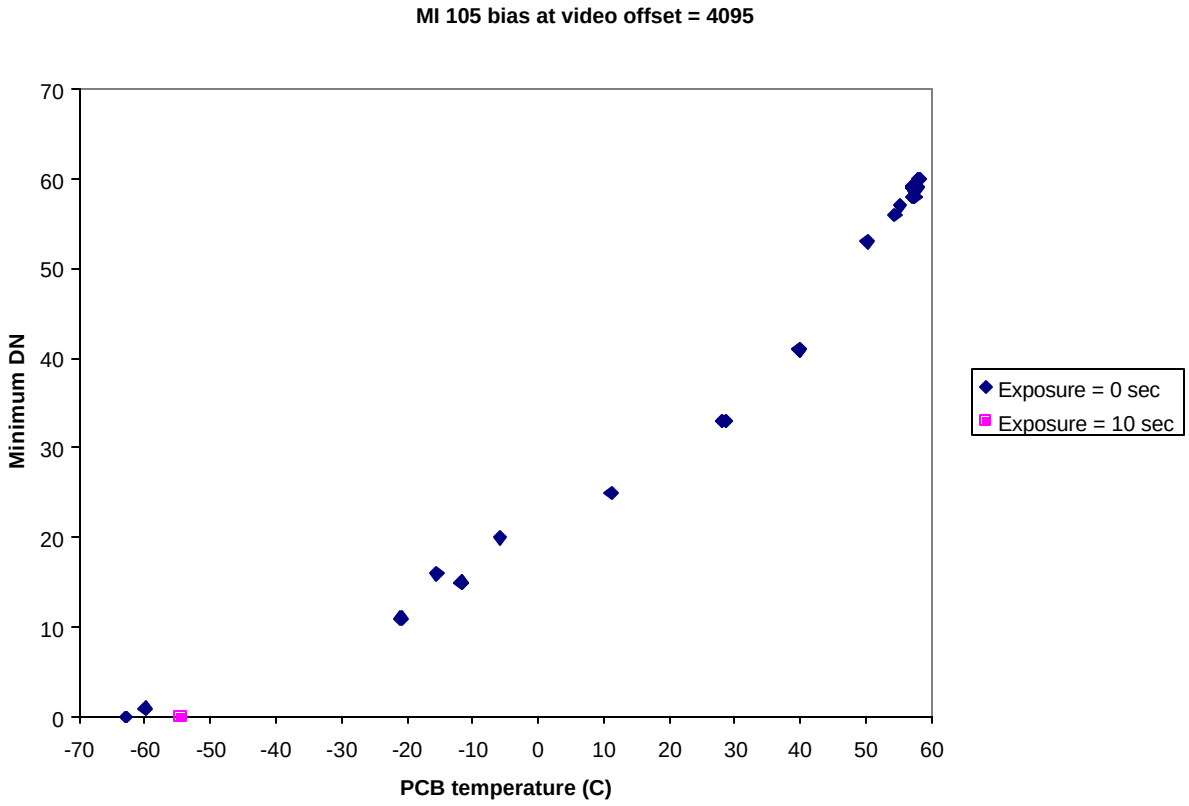

Figure 3.2.1b. Bias data for MI serial # 105 as a function of printed circuit board (electronics) temperature. Zero-second exposures taken during standalone camera calibration, 10-second exposure taken during system thermal testing.

MI serial # 110 shows zero clipping within the operating temperature range for video offsets of 4085 or more (Fig. 3.2.1c). An image taken during system thermal/vacuum testing with the electronics at –55.2°C and video offset of 4095 also shows zero clipping, consistent with the standalone camera calibration data. Therefore, the recommended video offset for MI 110 images taken within the operating temperature range (electronics temperature > –60°C) is 4080.

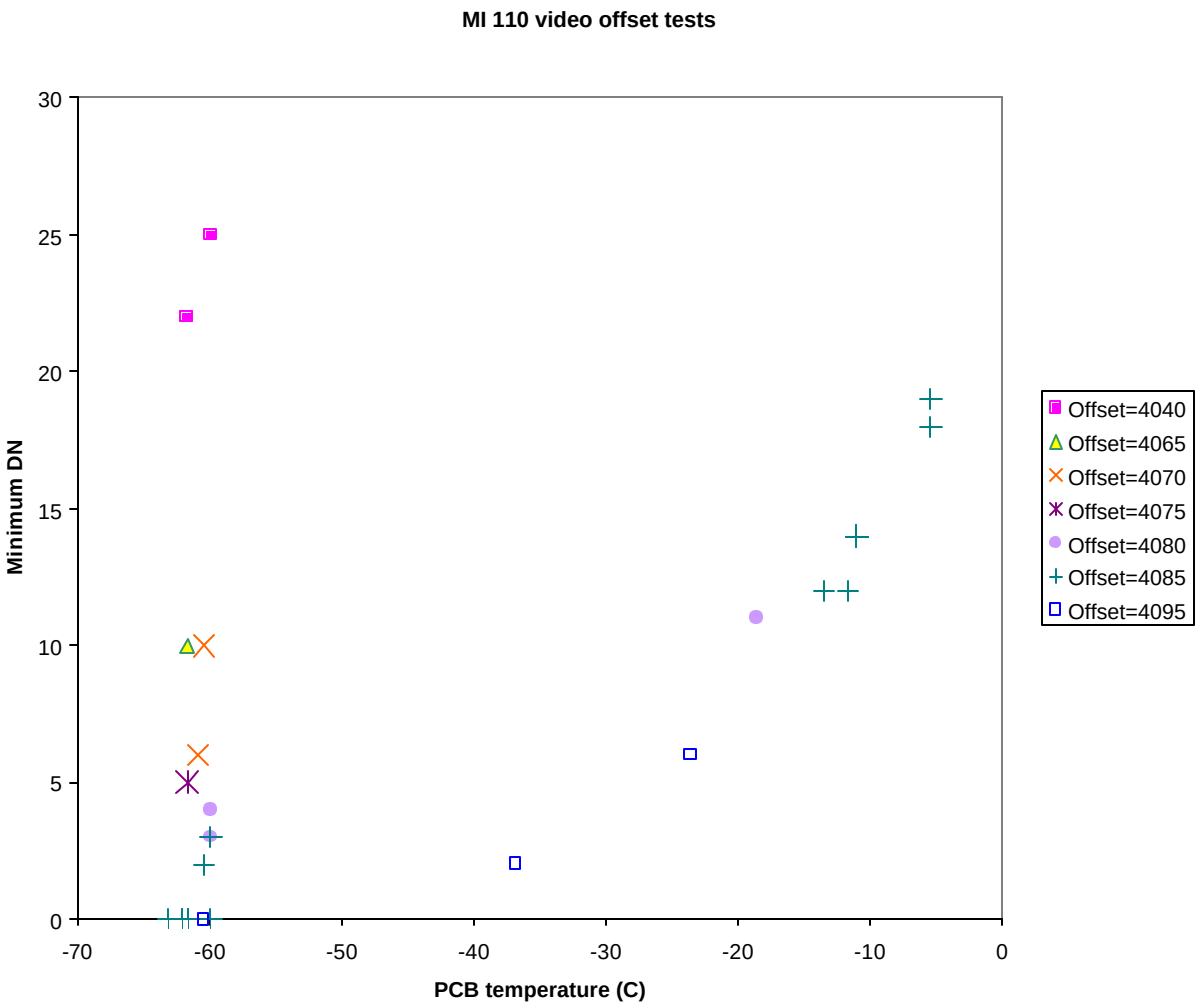

Figure 3.2.1c. Bias data (zero-exposure darks) for MI serial # 110 at various video offsets, as a function of printed circuit board (PCB) temperature.

3.2.1.4.2 Dark Current

Overview: Dark current generation leads to one of the largest uncertainties in generating accurate radiometrically calibrated images. During surface operations the CCD temperature could range up to ~10°C. A very dark target (low albedo, in shadow) might require an exposure of up to ~10 sec. Under these (worst-case) conditions the dark current would be 300 to 400 DN. Because the radiant flux of the scene is continually incident on the MI detectors (*i.e.*, the cameras are electronically shuttered and have no filters or other mechanical devices to block the incoming radiance), the dark current cannot be measured directly during Mars surface operations. (It could be measured at night but the temperatures would be much colder and not representative of the daytime conditions.) Hence it is important to carefully model the dark current and to understand the physical causes of its variance.

Dark current images (no light source) were acquired in the thermal/vacuum chamber at CCD and electronics temperatures spanning the flight acceptance range. We use these data to model three separable components of dark current (thermally-generated electrons) using a modular approach. These elements are referred to as: 1) the reference-pixel component, 2) zero-

exposure component, and 3) active-area component. In the event the dark current behavior changes after launch, this approach allows flexibility to adjust components of the model individually depending on the physics of the situation.

Reference-Pixel Component: The reference-pixel component, so named because it is measured directly by dummy pixels outside the active area of the detector (16 preceding and 15 trailing on each line; the last reference pixel value is replaced by the camera serial number). This component is first subtracted (on a line-by-line basis) before other dark current modeling and corrections are applied. The reference pixel values are principally a function of camera electronics (printed circuit board or "PCB") temperature and the applied video offset, and ranges up to ~50 DN. It is primarily due to thermal noise in the detector electronics although it has small dependencies (≤5 DN) on exposure time and CCD temperature as well. During surface operations, reference-pixel data may be optionally returned only occasionally in order to save downlink resources; in this case we must be able to model and predict this component, checking the model with occasional reference pixel data in the downlink. The reference-pixel image files (EFR) consist of a 32-pixel-wide strip, 1024 lines long.

In both sampling and in modeling, the reference pixel data samples 4-14 from the left-side reference pixel data strip were used because of their uniformity and repeatability. The model for the reference-pixel component is broken into two elements: 1) the average observed in the area including samples 4-14 and lines 412-612, and 2) the deviation from this average as a function of line. The deviation is quite small, ±1 DN (Fig. 3.2.1d), and remains very nearly constant (in DN) over a wide range of other parameters (PCB temperature, CCD temperature, exposure time).

The model for the average value (observed in the area including samples 4-14 and lines 412-612) is:

$$\begin{aligned} \text{REFPIXAVG} = {} & (\text{VOFFa} - \text{Video\_offset}) * \text{VOFFb} \\ & + (\text{PCBTa} + \text{PDBTb} * \text{Exposure\_time}) * e^{(\text{PCBTc} \times \text{PCB\_temperature})} \\ & + (\text{CCDTa} + \text{CCDTb} * \text{Exposure\_time}) * e^{(\text{CCDTc} \times \text{CCD\_temperature})} \end{aligned} \qquad (3.2.1a)$$

where Exposure_time is in msec and CCD_temperature and PCB_temperature are in centigrade. Derived coefficients (*a, *b, *c) are provided in Table 3.2.1a. The exponential form of the model was chosen because CCD dark current typically depends exponentially on CCD temperature. The reference pixel values were found to depend on PCB temperature as well.

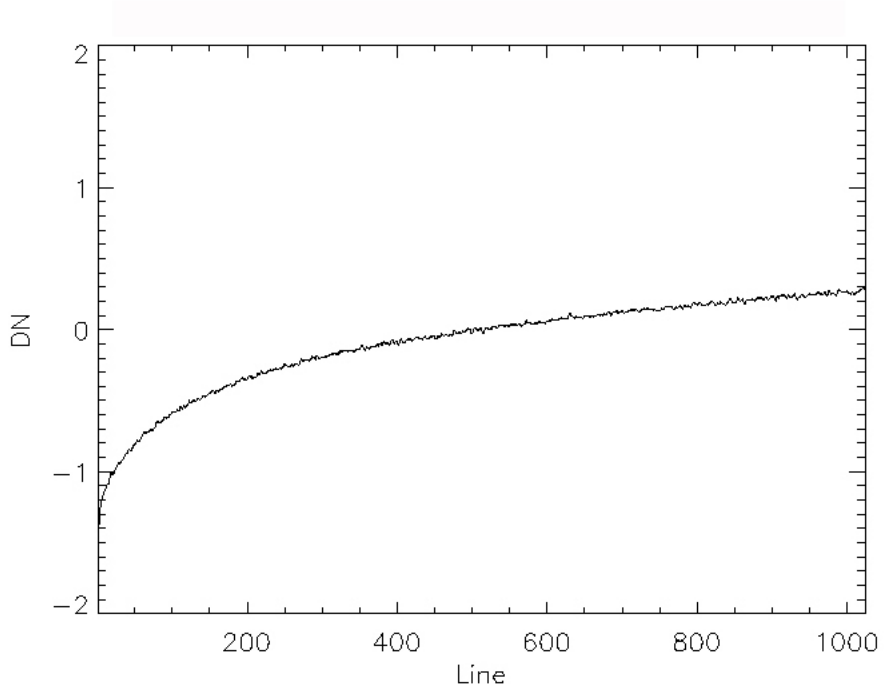

Figure 3.2.1d. Observed variation in reference pixel values. Normalized average of MI 110 reference pixel data. The pattern of this variation is constant in DN.

Table 3.2.1a. REFPIXAVG Model Coefficients

Coefficient	**MI_105**	**MI_110**
VOFFa	4070	4070
VOFFb	0.5	0.5
PCBTa	35.0	26.3
PCBTb	1.2×10^{-5}	6.8×10^{-6}
PCBTc	0.012	0.0143
CCDTa	0.32	0.32
CCDTb	1.54×10^{-5}	1.54×10^{-5}
CCDTc	0.11	0.11

The above model for the average reference pixel data is purely empirical, although the thermal vacuum data show that most of the dependence is on the video offset and PCB temperatures. Figure 3.2.1e shows the data set used for MI 110 before and after the video offset was normalized over the image set.

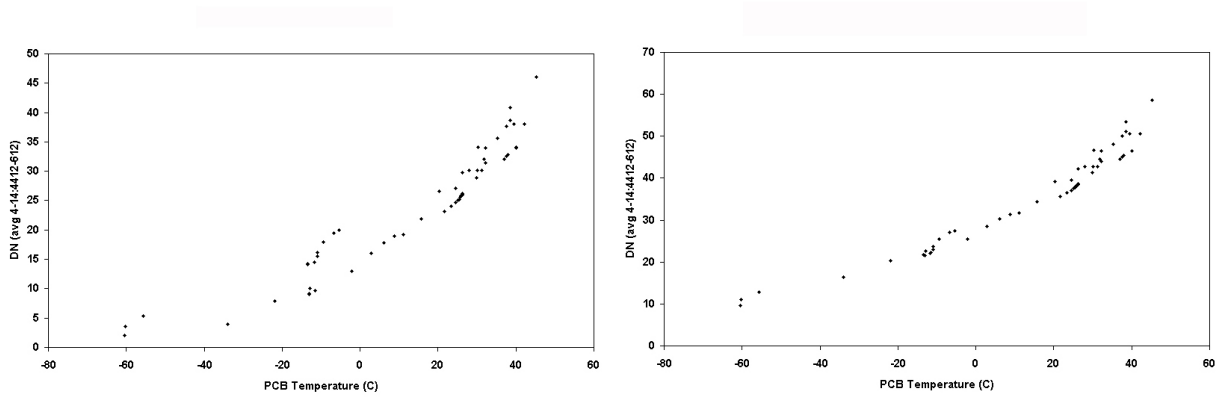

Figure 3.2.1e. (left) Original reference pixel average data set collected for MI 110 in thermal vacuum. No corrections have been applied. (right) Differences in video offset have been removed by normalizing the full set of observations to an equivalent video offset of 4070. The primary functional dependence is on the PCB temperature although small dependencies on exposure time and CCD temperature, amounting to ≤10 DN, are also evident.

After the video offset normalization, the combined PCB temperature and exposure time dependence (contained in the second term of the equation 3.2.1a) was fitted to the data set shown on the right side of Figure 3.2.1e. Figure 3.2.1f shows the residuals after that fit for a set of 100-sec exposures; these then represent the combined dependence on CCD temperature (contained in the last term of the equation 3.2.1a) for that exposure time.

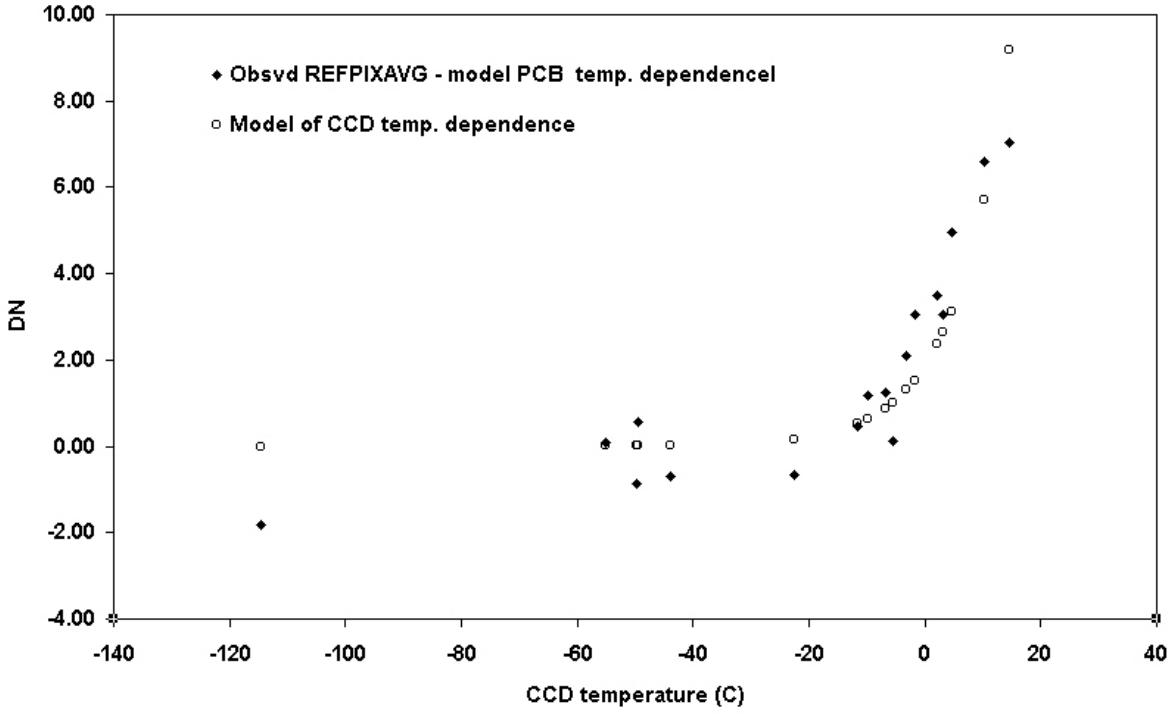

Figure 3.2.1f. Fitting the CCD temperature dependence to a set of 100-sec exposures. The residuals after video offset (first term in equation 3.2.1a) and combined PCB temperature and exposure time dependence (second term in equation 3.2.1a) are shown as diamonds. These were then fitted by the third term in equation 3.2.1a (open circles).

Finally, Figure 3.2.1g shows the residuals after the full model for the REFPIXAVG as defined by equation 3.2.1a was fitted to the MI 110 data set. The residuals are quite small, of order ±1 DN RMS.

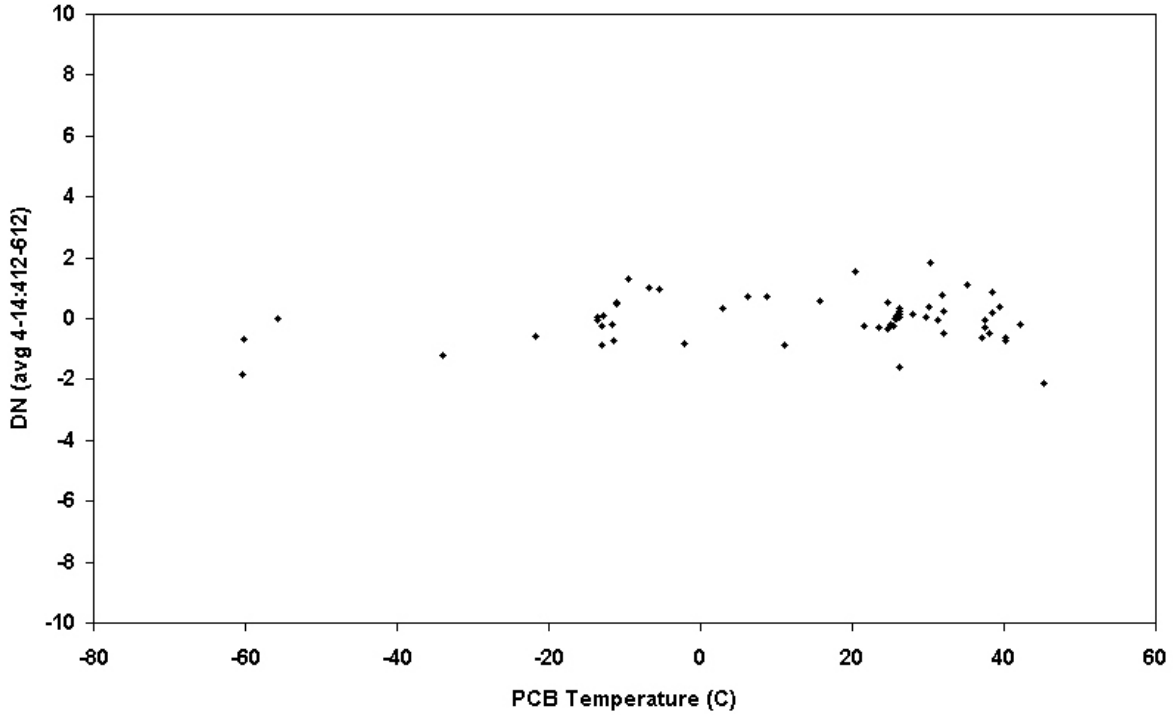

Figure 3.2.1g. Residuals after fit of REFPIXAVG model (with full set of dependencies) to MI 110 reference pixel data. The residual errors are very small compared to other uncertainties discussed in subsequent section for the active-area component.

Zero-Exposure Component: The zero-exposure component displays a common, fixed spatial modulation across the detector for all frames with zero exposure duration. In this fixed modulation the left and right edges of the frame are up to ~3× brighter than the center. The modulation is probably caused by fixed thermal gradients of a few degrees near the edges of the detector, generated by power dissipation in electronic components. All frames contain this relative spatial pattern and its absolute amplitude grows exponentially with increasing CCD temperature, ranging up to about 100 DN at the highest expected operating temperatures. This component can be obviously and easily be monitored directly during cruise and surface operations and is our best check of camera behavior.

The zero-exposure component is modeled as two elements: 1) the average observed in the central area (samples 412-612, lines 412-612), and 2) the variation from this average across the detector. When expressed as a modulation in terms of the ratio normalized to the average of the central pixels, the variation is observed to be extremely constant with CCD temperature. In fact it was found that the spatial patterns for this component for MI 105 and MI 110 are nearly identical, differing by ≤1% across the field. Figure 3.2.1h shows this pattern in a full frame and

a plot of the modulation across the central line; the modulation in the lower left and right corners reaches ~3.

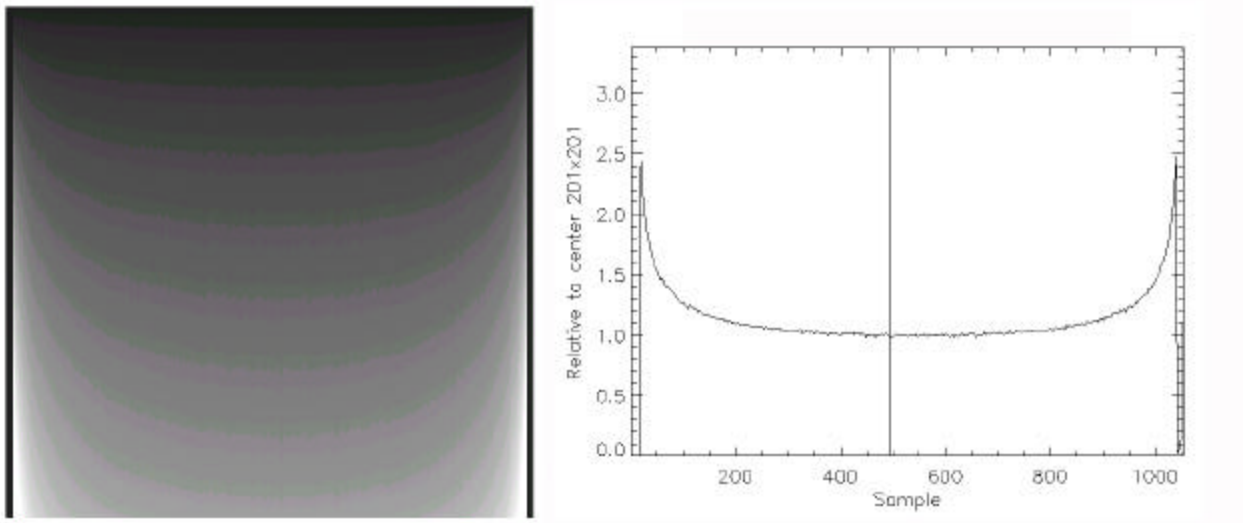

Figure 3.2.1h. Variation in dark current across the MI serial # 110 detector for zero exposures. (left) Zero-second exposure, showing dark current accumulated in transfer region during readout. Readout direction from bottom to top; reference pixels at right and left edges. (right) Normalized plot for line 511 showing modulation relative to central average. Modulation found to be very constant with CCD temperature and extremely similar between two MI flight units.

The CCD temperature dependence of the average central region in zero-second darks follows the simple exponential:

$$\text{ZEROEXPAVG} = \text{ZEXPa} * e^{(\text{ZEXPb} \times \text{CCD\_temperature})} \qquad (3.2.1b)$$

where CCD temperature is again in centigrade. Table 3.2.1b provides coefficients for the two MI cameras. Figure 3.2.1i shows the model fit to the observed data for MI 110.

Table 3.2.1b. ZEROEXPAVG Model Coefficients

Coefficient	**MI 105**	**MI 110**
ZEXPa	5.5	5.1
ZEXPb	0.11	0.11

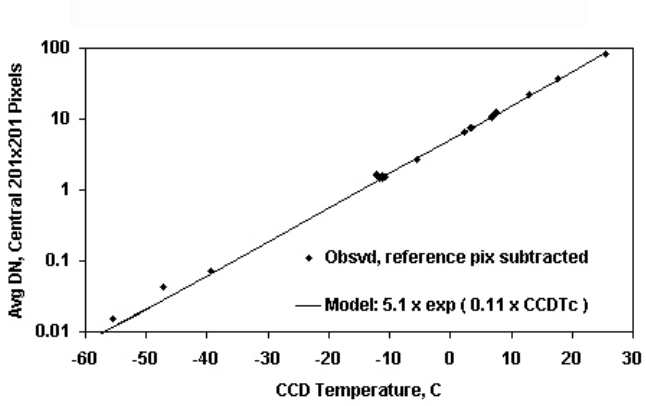

Figure 3.2.1i. Average MI serial # 110 zero-exposure dark current (for central 201×201 pixels) compared with exponential model.

Active-Area Dark Current Component: The last component is the most important and has been the most difficult to accurately predict. We refer to this as the active-area dark current component. Once the reference-pixel and zero-exposure components have been subtracted, this component is manifested as flat, granular image whose average DN increases linearly with exposure time and with exponentially with CCD temperature. This dark current component would saturate the image for an exposure >100 sec for a CCD temperature of >10°C. Fortunately these ranges are well beyond the expected operating conditions; colder CCD temperatures and shorter exposure times are anticipated.

The active-area dark current component is quite flat exhibiting low-frequency variations typically less than a percent. However, the peak-to-peak variance (granularity) has a standard deviation equal to ~10% of the average value (*cf*. Figure 3.2.1j). Most of this variance has a fixed pattern that is included in the dark current model correction and is thus largely removed. We have noted that the fixed pattern changed somewhat between the thermal vacuum laboratory calibration and the first inflight check of the cameras (ICO-1). We intend to generate new models of this granular pattern from inflight and surface data.

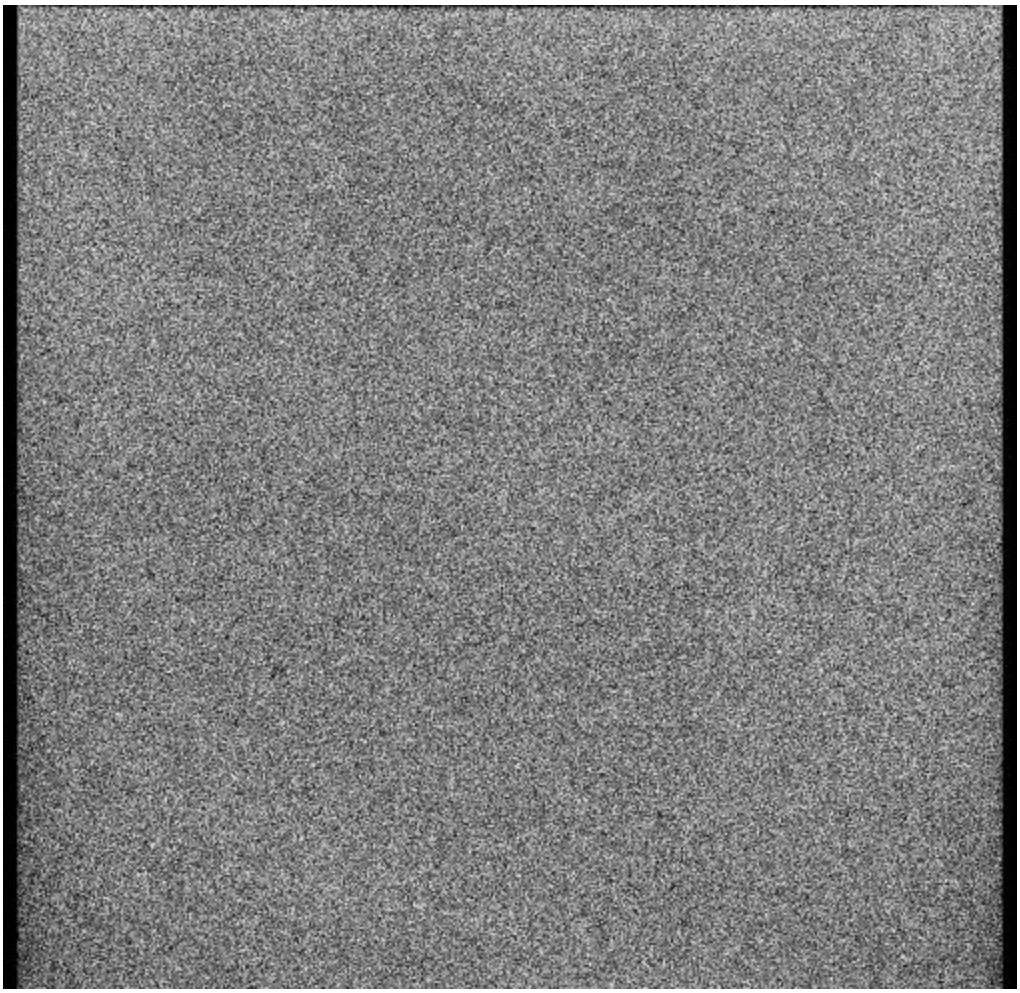

Figure 3.2.1j. Active-area dark current component for thermal vacuum laboratory calibration image 020823205505_0120013_MI105 (exposure time ~12 sec, CCD temperature ~21°C). The reference-pixel and zero-exposure components have been subtracted. The image has been contrast-stretched about its mean of 1400 DN (min=1250, max=1550). The standard deviation from the granular pattern is ~121 DN or roughly 8% of the mean. Dark bars on left and right are reference pixel data.

In modeling the active-area dark current, the procedure is to first subtract the reference-pixel and zero-exposure components to yield the nearly constant, spatially uniform component. Dividing this constant by the exposure time yields the active-area dark current generation rate in DN/s; this is plotted in Figure 3.2.1k for MI 110.

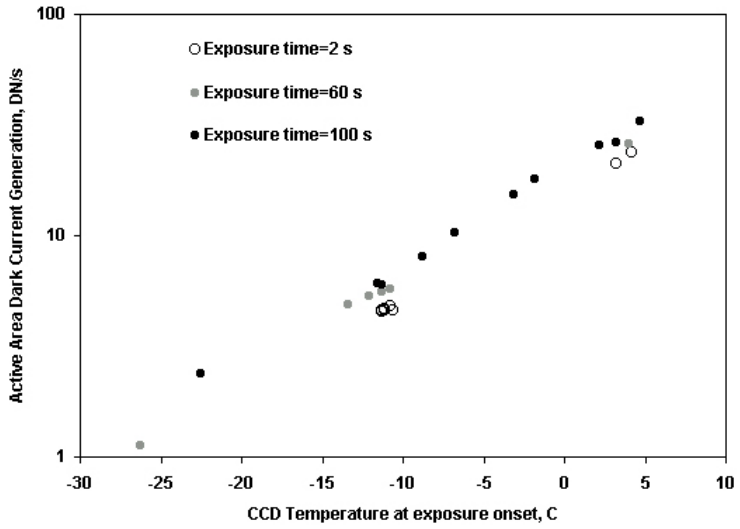

Figure 3.2.1k. Observed active-area dark current (constant across FOV) for MI 110 plotted against recorded CCD temperature measured at exposure start. Data normalized to exposure time to yield rate in DN/sec.

Because the dark current generation rate should increase as a simple exponential function in temperature, one would expect these results to fall on a single straight line in the coordinates plotted in Figure 3.2.1k. We hypothesize that the exposure-time dependence shown in Figure 3.2.1k is due to heating of the CCD detector during the course of exposure; CCD temperature increases were noted during long exposures. Power dissipation in the CCD during the exposure evidently causes the temperature to gradually shift from the pre-exposure rest state to a roughly constant offset. Because the CCD temperature shift should be independent of the initial temperature (a function only of the power dissipation and heat capacity) this would cause of linear shift of temperatures at longer exposures in Figure 3.2.1k to higher temperatures. Figure 3.2.1l shows the data and fitted model we use to adjust the CCD temperature as a function of exposure time.

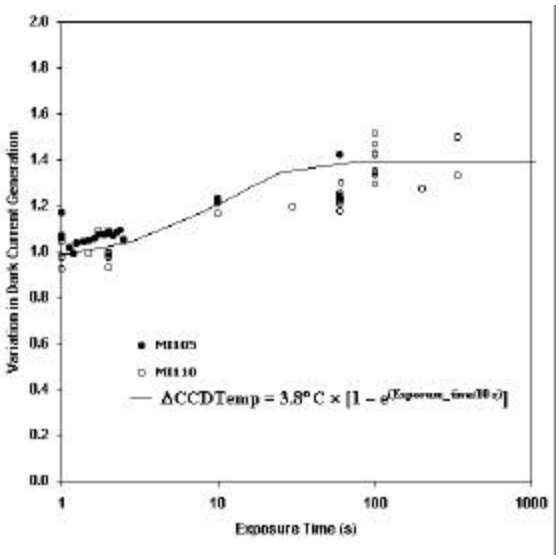

Figure 3.2.1l. Model for exposure-dependent shift in CCD temperature. Data represent observed deviation from a simple model in which dark current generation rate increases exponentially with CCD temperature.

Notice that the fitted model (we use a single common model for both cameras due to the crudeness of the fit) has a 1/e time constant of roughly 10 sec. Using this we next adjust the CCD temperatures for the data set shown in Figure 3.2.1k to account for this increase during exposures and arrive at a simple model for the active area dark current generation as shown in Figure 3.2.1m.

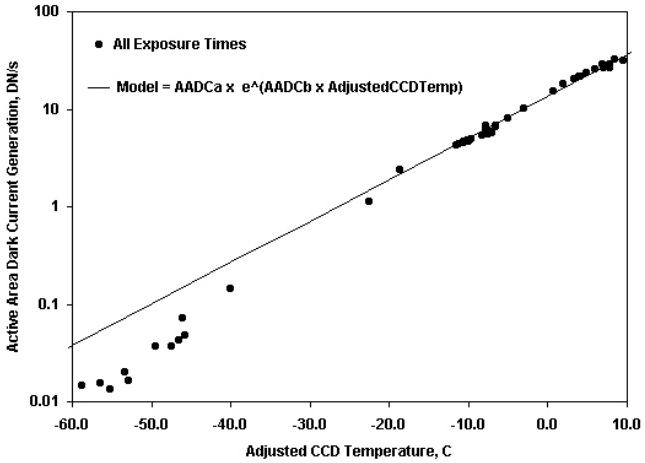

Figure 3.2.1m. Active-area dark current generation model for MI 110. CCD temperatures for the data of Fig. 3.2.1k were adjusted in using the model shown. Coefficients for the models for each camera are provided in Table 3.2.1c.

The model for the active area dark current generation rate is

$$\text{ACTIVE\_AREA\_DC (DN/sec)} = \text{AADCa} * e^{(\text{AADCb} \times \text{AdjustedCCD\_temperature})} \qquad (3.2.1c)$$

where parameters for each camera are supplied in Table 3.2.1c and the adjusted CCD temperature is derived as shown above.

Table 3.2.1c. ACTIVE_AREA_DC Model Coefficients

Coefficient	**MI 105**	**MI 110**
AADCa	13.5	13.5
AADCb	0.092	0.098

The small departures in Figure 3.2.1m of the model from the data for cold temperatures and very low dark current generation rates are not understood and could arise from any number of subtle non-linear effects. In any case the departures are negligible and will never be an issue for expected MI images acquired during daytime surface operations. Only for extremely long exposures at nighttime might this effect even become noticeable.

Both the reference pixel behavior and dark current variations along rows have been well modeled and are not a significant source of uncertainty. The principal dark current component is constant along rows and varies approximately linearly with exposure time and exponentially with CCD temperature. Because of the exponential growth with CCD temperature, the active-area dark current component is difficult to accurately model at high CCD

temperatures (> 0°C) and long exposures (>10 sec) and therefore could become a significant source of uncertainty. However, the MI is not expected to operate at these conditions, so uncertainties in dark current correction will be acceptably low for most MI data. Figure 3.2.1n shows the application of the complete dark current model (applied to the same image as in Figure 3.2.1j and shown with the same relative stretch).

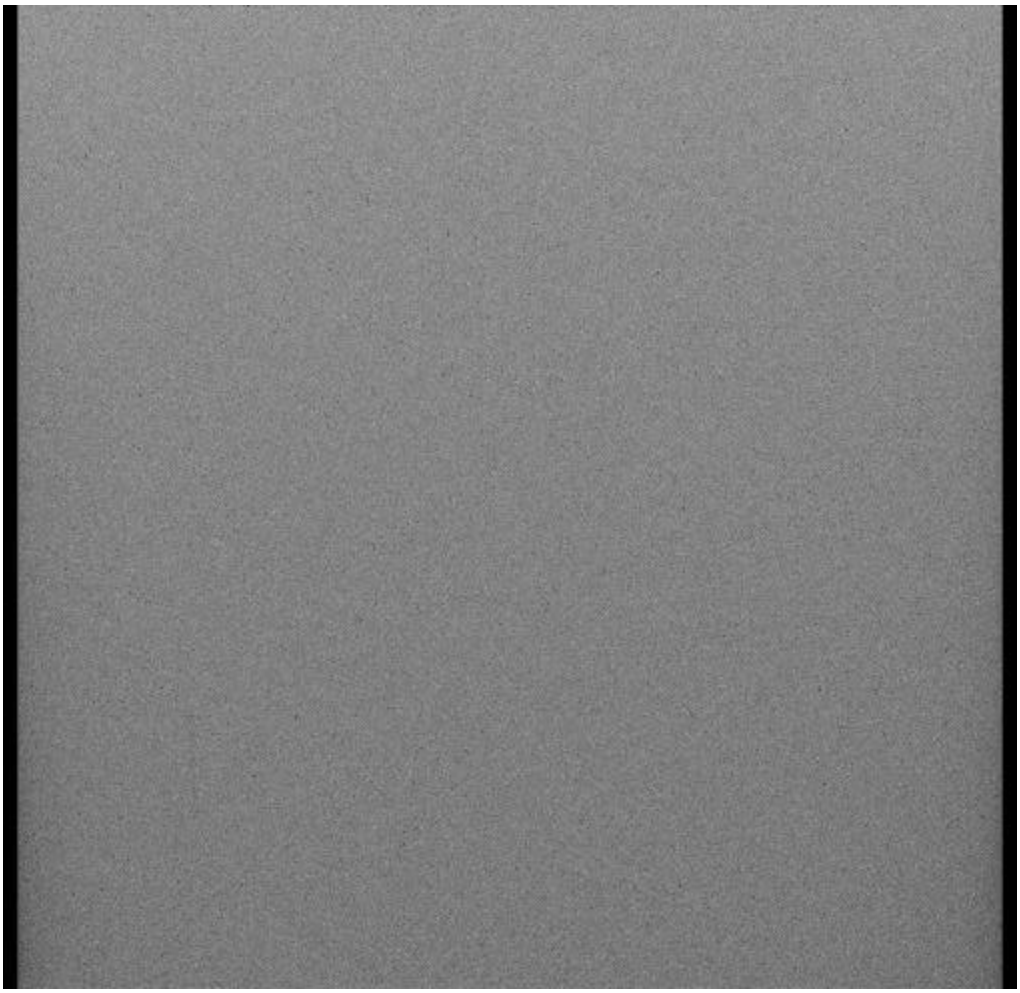

Figure 3.2.1n. Dark-current-corrected image (same image as Fig. 3.2.1j). The complete set of model dark-current components (Reference Pixel Variation, Zero-Exposure Variation, and Active-Area Variation) has been subtracted. The residual mean for this image is ~20 DN compared to the original raw mean of ~1500 DN. The standard deviation has been reduced from ~121 DN to ~22 DN.

3.2.1.4.3 Linearity, Read Noise, Full Well, Gain

Light transfer calibration was performed at ambient conditions and in the thermal/vacuum chamber. Light transfer sequences were designed to make use of the photon transfer technique (Janesick *et al*., 1987) to derive read noise, full well, and gain. Light transfer and dark current data were acquired at the CCD component level and at the camera level. During ambient tests, the dark current rate was high enough that "light transfer" sequences were obtained by taking dark frames at various integration times. During thermal/vacuum tests, an integrating sphere was adjusted to yield Mars-like radiance levels, and light transfer sequences

were obtained by varying integration time. Typically, 21 integration times were used to produce light transfer data. These data were also used to measure the linearity of the camera response with respect to input radiance.

For linearity, the response of a 50×50 pixel region in the center of each image was measured. An example image is shown in Figure 3.2.1l. Sampling of the images for analysis avoided the reflections of the front of the optics barrel and surrounding thermal blanketing (see Figure 3.1.3). These reflections were reduced for MI serial # 110 calibration by covering the front of the optical barrel assembly with black-anodized aluminum (Fig. 3.1.4). Jim Bell's "mer_ltf" software (Bell *et al*., 2004) was used to perform a linear least squares fit to the average signal between 0.1 and 0.9 times full well and determine the nonlinear residuals and goodness of fit. Read noise is a constant offset (at zero exposure) in a plot of pixel signal variance vs. signal level. Full well depth was estimated by picking the exposure just before saturation occurred. The full well was then calculated as the average value between this point and the next (saturated) image. Gain is the inverse of the slope of the linear least squares fit of pixel signal variance vs. signal level. Coherent noise was not observed in the images.

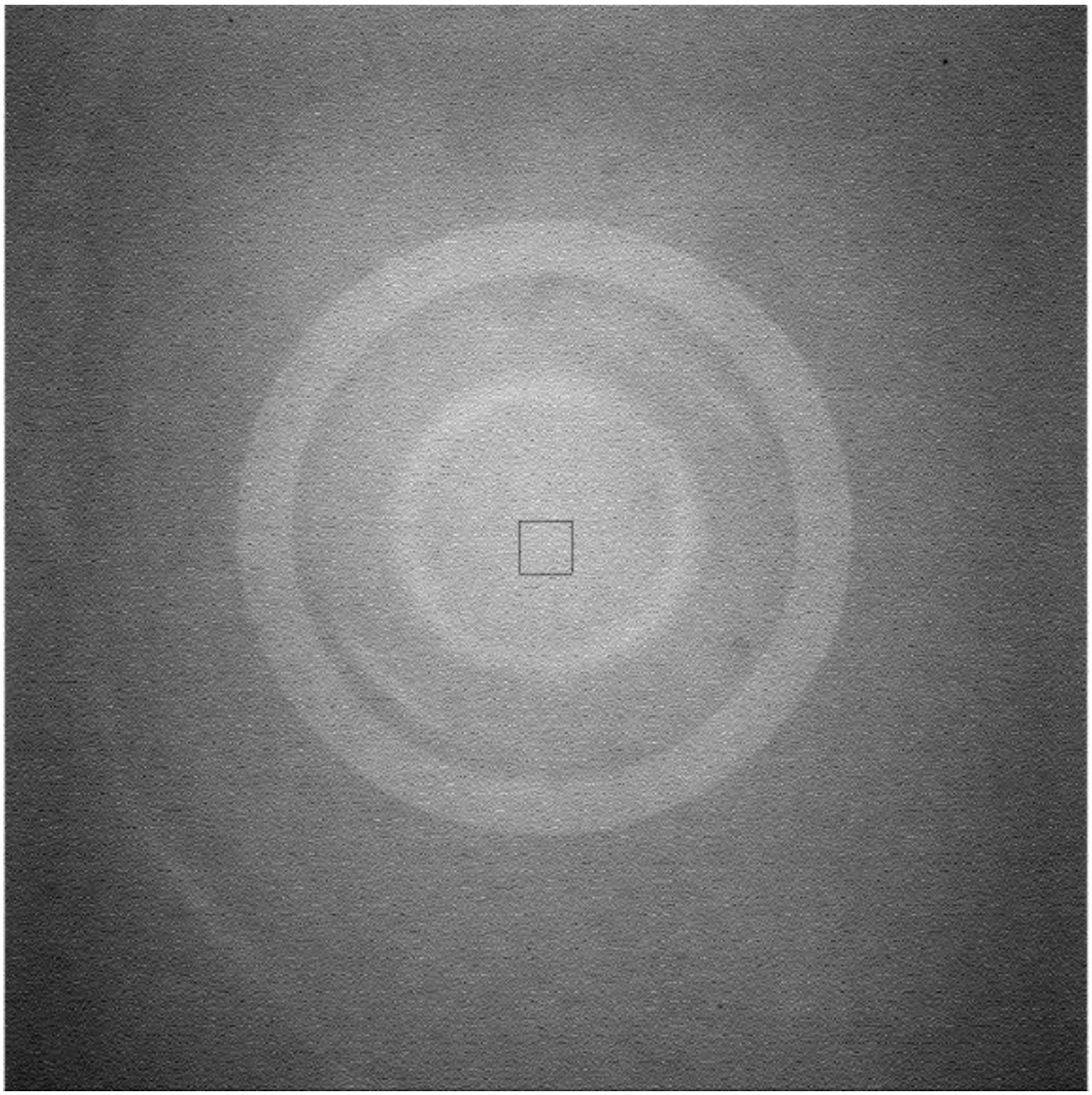

Figure 3.2.1l. MI serial # 105 image from light transfer sequence taken at approximately -55°C, showing reflections of camera optics barrel and thermal blanketing off of chamber window. Location of 50 × 50 pixel area sampled for analyses shown by black square.

Results of the analysis of light transfer data for MI serial # 105 are summarized in Table 3.2.1d. MI 105 light transfer sequences 4 through 9 were video offset characterization tests (see Fig. 3.2.1a), and are not included here. The CCD temperature was not recorded for light transfer sequences 1a, 2, and 3, so these data are not included either. Light transfer results for MI serial # 110 are summarized in Table 3.2.1e. The second column in both tables shows the r^2 goodness of a linear fit to the light transfer data. The accuracy of the full well measurements is limited by the spacing of exposure times near saturation: the mer_ltf program estimates the full well as the average between the last data point before saturation (selected by the user) and the next (saturated) data point. Therefore, the uncertainty in the estimated full well is half the difference between the data points, typically 100 DN or about 5000 electrons. The full well estimates have been adjusted for changes in video offset as necessary.

Table 3.2.1d. MI serial # 105 light transfer results

LTF #	CCD temperature, °C	r^2 linearity	Read Noise	Full Well	Gain
1b	3.5	1.000000	36.53	165883	49.80
1c	3.7	1.000000	37.32	160420	49.53
1d	-10.3	1.000000	30.14	173883	47.53
1e	-10.3	1.000000	27.85	165859	48.10
10	-117.7	0.999457	30.24	175441	44.10
11	-60.8	1.000000	28.20	169669	44.30
12	-61.0	1.000000	30.74	175555	45.85
13	-61.0	1.000000	28.50	170309	44.51
14	-61.0	0.999999	27.84	174407	45.52
15	-55.4	0.999999	28.98	175100	46.19
16	-55.9	0.999999	31.42	174681	46.03

The MI 105 response is very linear: $r^2 > 0.999$ overall and $r^2 \geq 0.999999$ within the operating temperature range (-57°C < CCD temperature < +7°C; see Table 1.2.1). The reason for the greater deviation from linearity in LTF10 is unknown: Inspection of the images shows no obvious problems with the data. The linearity plot for LTF10 is shown in Fig. 3.2.1m; the corresponding plots for other light transfer sequences show more linear trends. The read noise for MI 105 is 32.0 ± 4.0 electrons within the operating temperature range and increases with temperature as expected. The full well is 169304 ± 6099 electrons within the operating temperature range. The gain is 47.9 ± 1.6 electrons/DN within the operating temperature range, with a slight apparent increase with temperature that is not understood, but may be caused by increasing dark current during the light transfer sequences taken at higher temperatures.

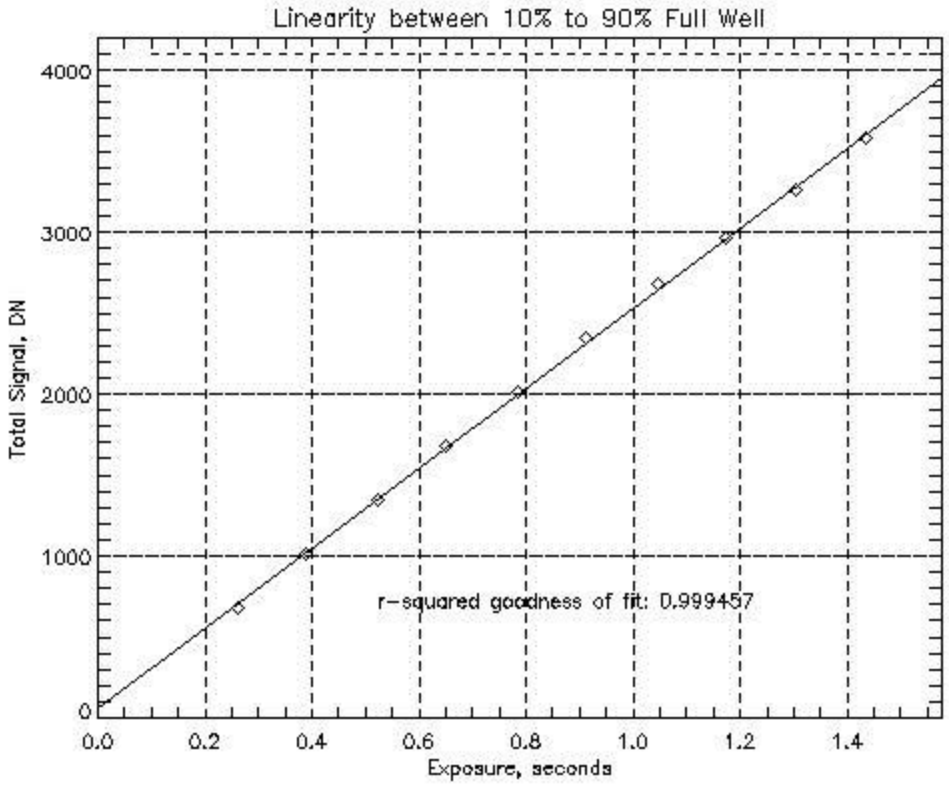

Figure 3.2.1m. Linearity plot for MI serial # 105 light transfer sequence 10.

Table 3.2.1e. MI serial # 110 light transfer results

LTF #	CCD temperature, °C	r^2 linearity	Read Noise	Full Well	Gain
2	-115.5	0.999999	27.71	171719	43.36
3	-116.3	1.000000	27.12	168282	42.46
5	3.2	0.999948	33.61	144486	47.21
6	3.2	0.999934	34.88	147980	48.33
7	-10.6	0.999997	29.34	157766	48.79
8	-10.8	0.999997	29.02	156289	48.33
9	-57.1	1.000000	26.83	177907	45.26
10	-56.9	1.000000	24.39	175688	44.71

The MI 110 response is also very linear: $r^2 > 0.9999$ overall. Figure 3.2.1n shows that linearity is excellent even for the worst-case result. The read noise for MI 110 is 29.7 ± 4.0 electrons within the operating temperature range (-57°C < CCD temperature < +7°C; see Table 1.2.1) and increases with temperature as expected. The full well is 160019 ± 13933 electrons within the operating temperature range. The gain is 47.1 ± 1.7 electrons/DN within the operating temperature range, with a slight apparent increase with temperature that is not understood. The apparent gain increase with temperature may be caused by increasing dark current during the light transfer sequences taken at higher temperatures. Both electronics and CCD temperatures were observed to increase during acquisition of light transfer sequences for both cameras.

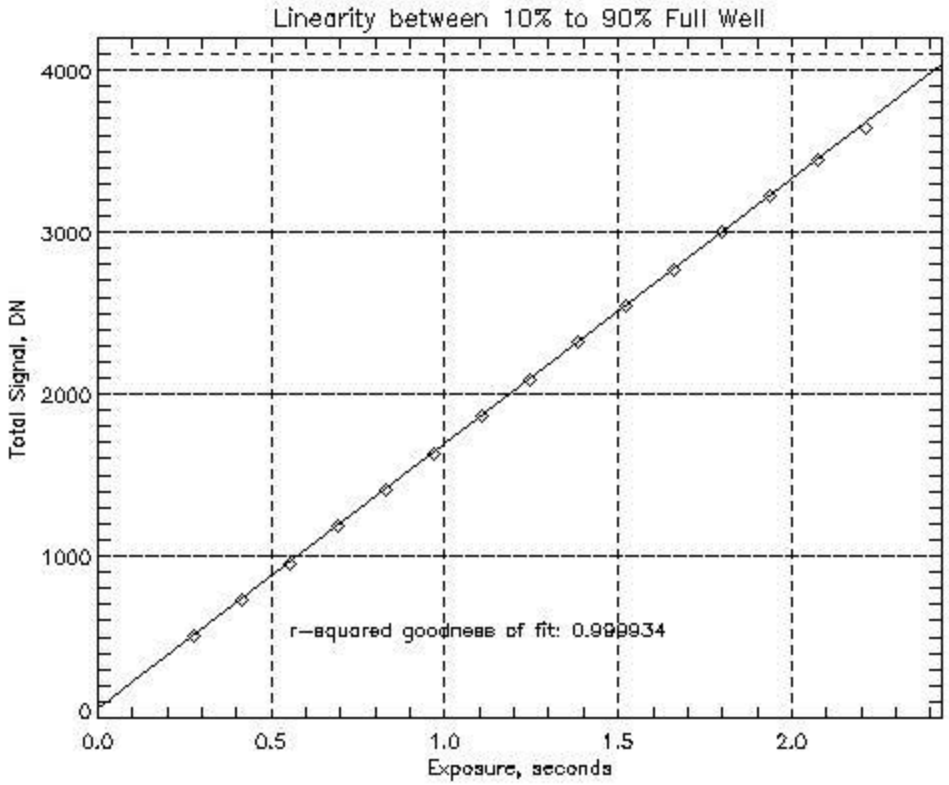

Figure 3.2.1n. Linearity plot for MI serial # 110 light transfer sequence 6.

3.2.1.5 Accuracy and Relationship to Requirements

The accuracy of the dark current model is best at low temperatures; uncertainty increases with temperature. At the highest operating temperature expected during flight (10°C) and the longest likely exposure time (10 seconds), the uncertainty in the dark current model is 50 DN. This uncertainty is due primarily to the uncertainty in temperatures recorded during thermal/vacuum testing. For a well exposed (2000 DN) image, dark current modeling errors are therefore less than 2.5%. Errors due to dark current are less than 10% for DN > 500 under worst-case conditions. For typical MI images (lower temperatures, shorter exposure times), errors in dark current modeling will be much less. Within the operating temperature range, response of the cameras is linear to better than 1%. The read noise is about 30 electrons and the full well exceeds 140,000 electrons. These results are consistent with Level 3 requirements #1191 (absolute radiometric accuracy) and #1192 (signal/noise > 100).

3.2.2 Absolute and Relative Radiometry

3.2.2.1 Purpose and Description

Determine the quantitative response of the MI to light so that image data in DN can be converted to absolute radiance. Measure pixel-to-pixel (relative) radiometric sensitivity variations so that they can be removed.

3.2.2.2 Test Procedure

We presented an absolutely-calibrated, uniform (± 1%) light source (1 m integrating sphere) to the cameras and acquired "flat field" images. The output of the sphere was monitored using a radiometer, whose output was recorded in the header of each image taken. Before each test, the spectral output of the sphere was measured by placing filters in the radiometer port and measuring the radiometer output at each wavelength (50 nm steps). The spectral transmission of the chamber window was measured separately. The radiometer, window and sphere calibration data are included in Appendix I. A 600 nm filter was then placed in front of the radiometer for MI calibration. Diffusing plates made from identical glass flats were placed over both the exit aperture and the radiometer port of the integrating sphere. In this configuration, we obtained 30 identical images at the half well level and 3 zero-second exposures before and after the half-wells. The test setup was adjusted so that integration times were in the range expected during flight (0.1 to 2 sec). Immediately after the images were obtained, a cover was placed over the chamber window and dark current images were acquired at the same exposure times used for the radiometry images.

3.2.2.3 Environmental Conditions

Temperature = -55°C, -10°C, and +5°C; pressure $\leq 10^{-6}$ torr for absolute radiometry. Ambient temperature and pressure for relative (flat field) radiometry.

3.2.2.4 Data Processing and Products

The dark current images associated with each radiometric data set were examined and images showing cosmic ray hits and other anomalies were noted. The average DN level of the dark current images was observed to increase due to CCD and electronics temperature increases during acquisition of a series of images. The temperature increases rapidly at first, then

approaches a steady-state after a few minutes (see section 3.2.1.4.2). Therefore, we selected a few good dark current images taken late in the dark sequence and averaged them together. The average darks for each test were subtracted from each of the flat field images taken during that test, as described below.

Dark current data were not acquired uniformly along with all of the absolute radiometry data. Therefore we used the dark current model described above to correct these images. Subsequent processing steps are summarized below.

3.2.2.4.1 Absolute Radiometry

Response Model: The spectral response of each MI camera system was modeled using data measured at the component level or from design parameters. These data included the 1) the measured spectral transmittance of each integrated optical system, 2) the measured quantum efficiencies of the Mitel CCDs used in the cameras (measured at -55°C and +5°C, recorded at ~20nm intervals; see section 2.1.8), 3) the full-well capacity of the CCDs and digitization (in electrons/Dn), and 4) the Aω of the system (IFOV × effective_aperture_area or $\pi/4 \times$ [pixel-pitch/F#]^2). Results are shown in Figures 3.2.2a and 3.2.2b.

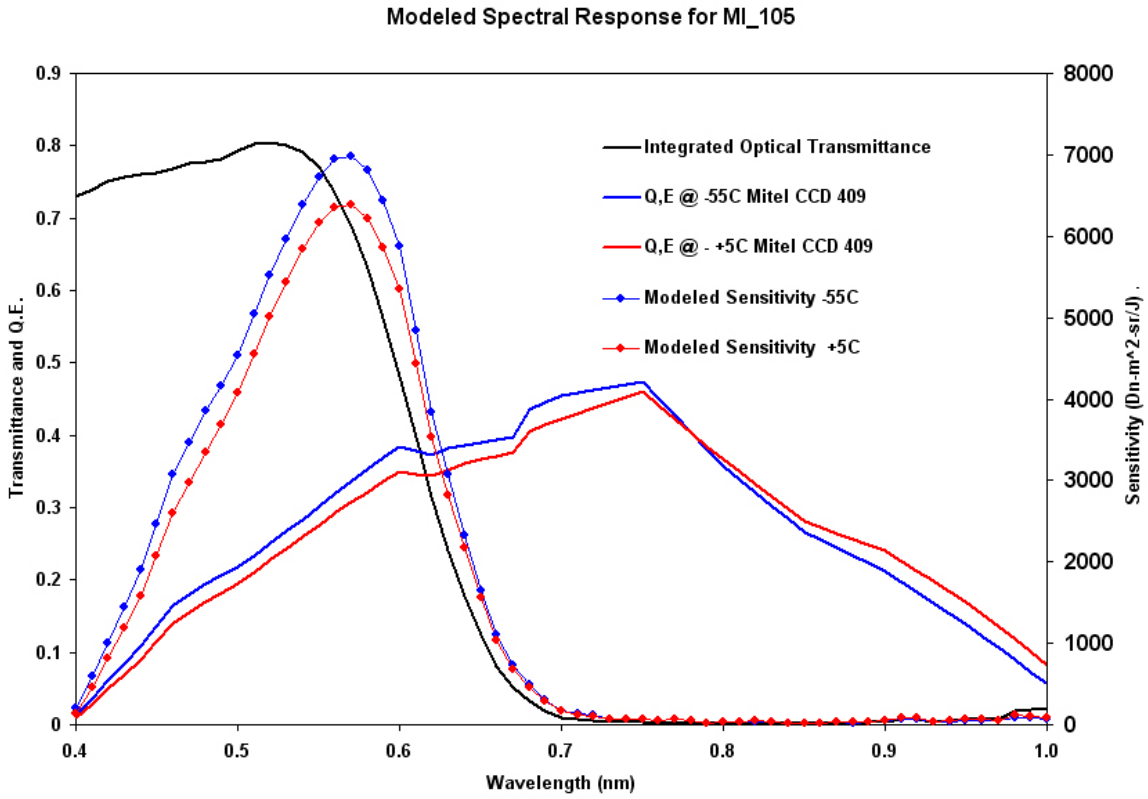

Figure 3.2.2.a. MI 105 response model. In addition to the transmittance and QE curves shown, the following values were used: Gain = 47.9 e^-/DN and Aω = 5.03 x 10^{13} m^2.

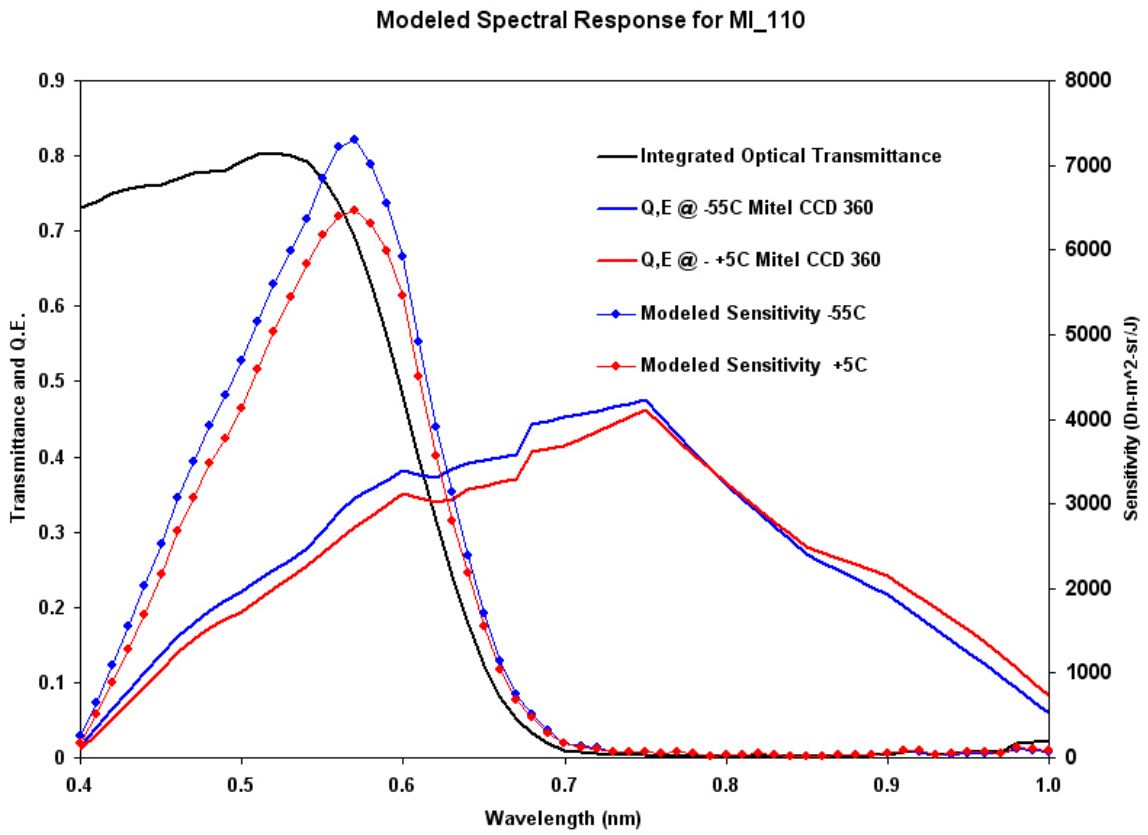

Figure 3.2.2.b. MI 110 response model. In addition to the transmittance and QE curves shown, the following values were used: Gain = 47.1 e^-/DN and $A\omega = 5.03 \times 10^{13} m^2$.

Measured Response and Comparison with Models: The spectral response was measured at the system level using a calibrated monochrometer source during thermal vacuum calibration (see section 3.2.3). This system-level measurement provided only *relative* spectral response owing to the difficulty of establishing the absolute radiance delivered to the MI focal plane by the monochromatic source. The measured relative spectral response and modeled absolute spectral responses (from previous subsection) are compared in Figures 3.2.2c and 3.2.2d. The normalized measured spectral responses, at 50 nm resolution as a function of CCD temperature are provided in Table 3.2.2a.

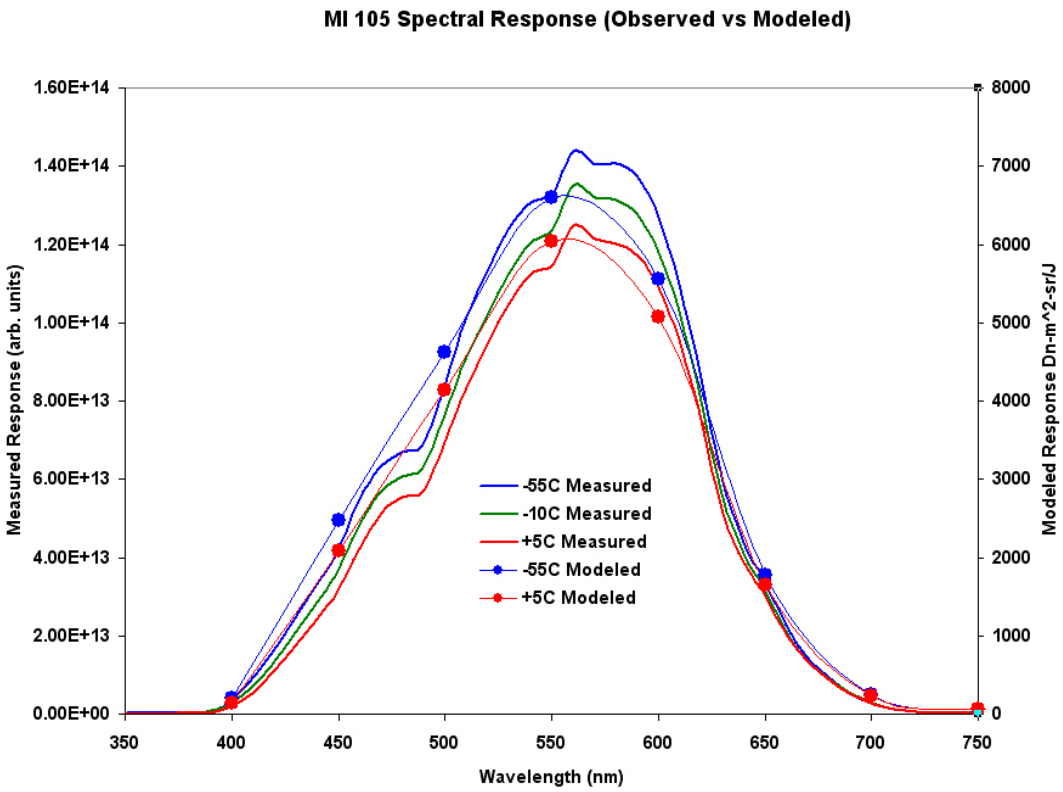

Figure 3.2.2c. MI 105 measured relative spectral response (left ordinate) and modeled absolute spectral response (right ordinate).

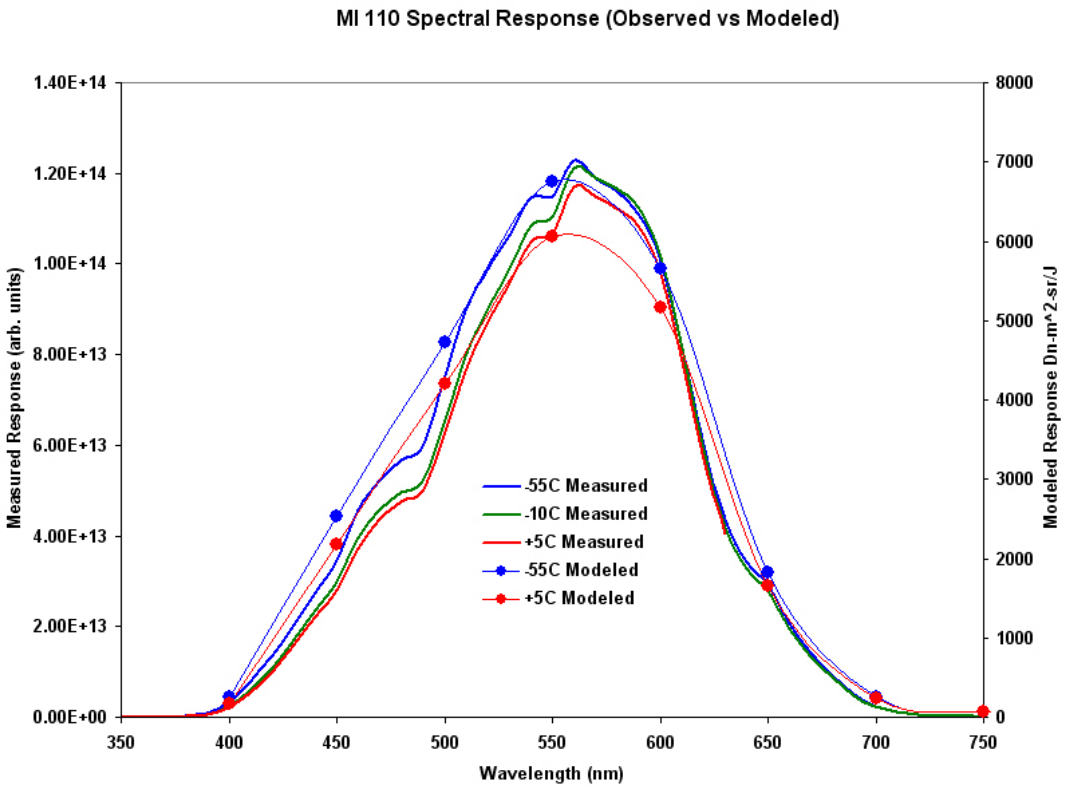

Figure 3.2.2d. MI 105 measured relative spectral response (left ordinate) and modeled absolute spectral response (right ordinate).

Table 3.2.2a. MI System Spectral Response Measured at Various Temperatures

Wavlength (nm)	MI 105 Normalized Spectral Response			MI 110 Normalized Spectral Response		
	-55° C	-10° C	+5° C	-55° C	-10° C	+5° C
400	3.476E-02	2.833E-02	2.292E-02	3.332E-02	2.654E-02	2.498E-02
450	3.199E-01	3.008E-01	2.803E-01	3.055E-01	2.734E-01	2.667E-01
500	6.248E-01	6.084E-01	5.965E-01	6.354E-01	5.777E-01	5.739E-01
550	1.000E+00	1.000E+00	1.000E+00	1.000E+00	1.000E+00	1.000E+00
600	9.209E-01	9.227E-01	9.129E-01	8.366E-01	8.731E-01	8.706E-01
650	2.469E-01	2.477E-01	2.563E-01	2.388E-01	2.349E-01	2.349E-01
700	2.378E-02	2.475E-02	2.703E-02	2.428E-02	2.471E-02	2.504E-02
750	7.866E-04	8.244E-04	8.321E-04	6.808E-04	7.876E-04	7.932E-04
800	3.382E-05	-5.608E-05	-1.479E-04	2.748E-06	1.302E-06	-5.256E-05
850	6.869E-06	-7.277E-05	-1.891E-04	1.882E-07	-4.912E-06	6.057E-02
900	3.251E-05	-7.525E-05	-2.082E-04	2.309E-06	-1.973E-05	-1.061E-04
950	2.821E-05	-1.240E-04	-3.161E-04	-6.987E-06	-5.023E-07	-1.319E-04
1000	-4.808E-05	-1.460E-04	-3.776E-04	-2.240E-05	-4.285E-05	-1.689E-04

System-Level Absolute Radiometric Response: The absolute radiometric response of the MI camera system was measured using the configuration shown in Figure 3.2.2e. The spectral irradiance of the lamp source and integrating sphere was measured with a calibrated radiometer. The radiometer measured the spectral radiance of the flux from the diffuser plate at the exit of the integrating sphere. An identical diffuser port was placed at the entrance to the thermal vacuum chamber. The spectral transmittance of the chamber window was known from independent measurement (see Appendix I).

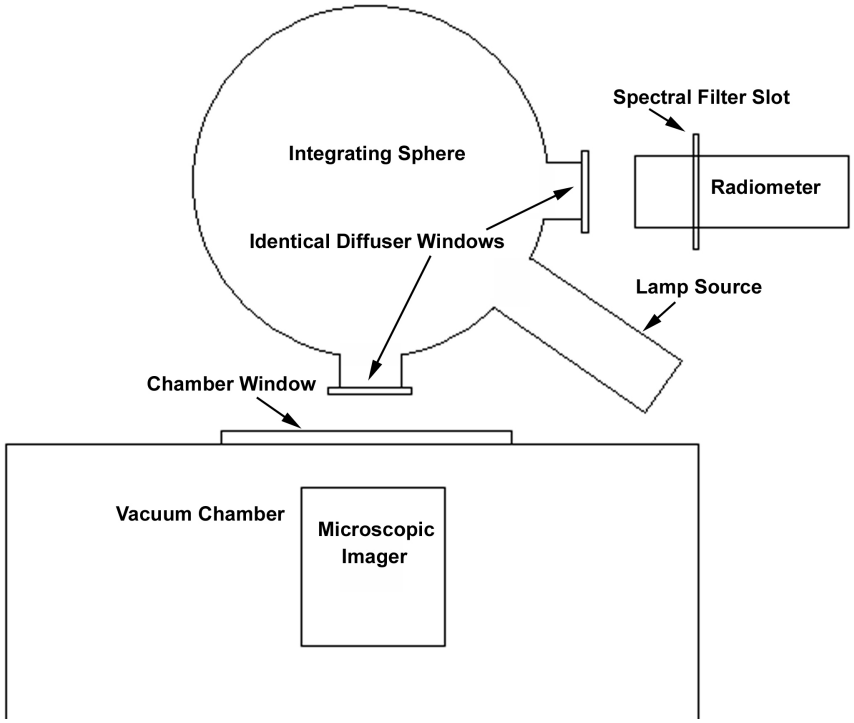

Figure 3.2.2e. Schematic diagram of laboratory setup used to measure absolute response of the integrated MI camera systems.

Calibration of the Radiometer: The first step in the procedure was to calibrate the radiometer (designated RED 1). Four sets of calibration data were collected at the JPL optical standards laboratory. In these calibrations a well-documented source was used to illuminate a white diffusing reflecting target (also of very well known reflective properties) at a distance of 0.50 m (see Appendix I). The data of Table 3.2.2b show the reduction of these data to derive an average calibrated response of the radiometer along with standard error.

Table 3.2.2b. Calibration of Radiometer (RED 1) Used to Monitor Output of Integrating Sphere

Filter nm	Original Detector Measurements nAmps				Mean (dark) nAmps	Stan. Dev. of Mean	Source Irradiance at 0.5m W/m²/nm	Reflec-tance of Surface at 0.5m	Radiance of Surface at 0.5m W/m²/nm/sr	Radiom eter Calibration: W/m²/nm/sr /Amp	Radiometer Cal.: StDev W/m²/nm/sr /Amp
	1/1998	12/2001	7/2002	10/2002							
Dark	0.011	0.0017	0.0035	0.001	n/a	n/a	n/a	n/a	n/a	n/a	n/a
350	0.271	0.2692	0.2583	0.263	0.258	0.005	2.361E-11	0.983	7.387E-04	2.859E+06	6.068E+04
400	0.676	0.677	0.662	0.688	0.669	0.014	5.965E-11	0.986	1.872E-03	2.800E+06	5.746E+04
450	1.758	1.780	1.745	1.812	1.767	0.034	1.157E-10	0.987	3.635E-03	2.057E+06	3.920E+04
500	4.910	5.012	4.936	5.097	4.982	0.090	1.863E-10	0.988	5.859E-03	1.176E+06	2.121E+04
550	6.392	6.437	6.351	6.551	6.426	0.090	2.638E-10	0.988	8.298E-03	1.291E+06	1.811E+04
600	9.494	9.512	9.413	9.686	9.519	0.118	3.389E-10	0.988	1.066E-02	1.120E+06	1.386E+04
650	13.231	13.340	13.203	13.605	13.338	0.188	4.052E-10	0.987	1.273E-02	9.545E+05	1.343E+04
700	13.081	13.172	13.015	13.405	13.161	0.174	4.596E-10	0.987	1.444E-02	1.097E+06	1.453E+04
750	16.130	16.050	15.888	16.309	16.087	0.176	5.009E-10	0.987	1.574E-02	9.783E+05	1.068E+04
800	18.875	18.420	18.313	18.767	18.587	0.266	5.289E-10	0.986	1.660E-02	8.931E+05	1.277E+04
850	14.630	14.320	14.256	14.575	14.438	0.181	5.440E-10	0.985	1.705E-02	1.181E+06	1.483E+04
900	12.395	12.050	12.025	12.276	12.179	0.175	5.485E-10	0.987	1.723E-02	1.415E+06	2.028E+04
950	6.810	6.610	6.596	6.754	6.685	0.102	5.452E-10	0.988	1.714E-02	2.564E+06	3.910E+04
1000	2.765	2.632	2.620	2.681	2.667	0.060	5.355E-10	0.986	1.681E-02	6.301E+06	1.417E+05
1050	1.192	1.1020	1.0923	1.113	1.118	0.039	5.205E-10	0.988	1.637E-02	1.464E+07	5.083E+05
1100	0.326	0.2980	0.2928	0.296	0.296	0.008	5.004E-10	0.988	1.574E-02	5.313E+07	1.500E+06
Dark	0.025	0.0086	0.0046	0.001	n/a	n/a	n/a	n/a	n/a	n/a	n/a

Measurement and Derivation of Absolute Response and w_0: Absolute responses were measured in thermal vacuum for MI 105 and MI 110 at three temperatures using the test setup shown in Figure 3.2.2e. Several sets of MI images were acquired at each temperature with exposure times near 1 sec. The images used to measure the absolute response of MI 105 are listed in Table 18.9 and the images used to measure the absolute response of MI 110 are listed in Table 18.10 (both in Appendix I). Sphere radiance calibration was not performed with the same light level as used for the MI 105 radiometry images at 5°C, so these data could not be analyzed. The spectral radiance of the integrating sphere output at the diffuser window (Fig. 3.2.2e) was measured near the time of each image set.

The formulation of the calibration data reduction is described here. We begin with the simple definition:

$$DN_{generation\_rate}(\lambda,T) = \int S(\lambda,T)\ R(\lambda)\ d\lambda,$$

where the measured $DN_{generation\_rate}(\lambda,T)$ is in units of DN/s; $S(\lambda,T)$ is the spectral sensitivity of the MI camera system in units of $DN/m^2/sr/W$; and $R(\lambda)$ is the radiance of the target in units of $W/m^2/sr/nm$. Although we do not yet know the absolute value of $S(\lambda,T)$, we do know its normalized value $S_{normalized}(\lambda,T)$ (*cf*. Table 3.2.2a) and will solve for the scalar $\Im(T)$ as shown below. We write three additional equations:

$$DN_{generation\_rate}(\lambda,T) = (DN_{observed} - DN_{dark\_current}) / ExposureTime$$

$$S(\lambda,T) = \Im(T)\ S_{normalized}(\lambda,T)$$

$$R(\lambda) = A(\lambda)\ M(\lambda)\ W(\lambda),$$

where $A(\lambda)$ is the calibration of the radiometer (in $W/m^2/nm/sr$ /Amp from Table 3.2.2b), $M(\lambda)$ is the observed radiometer signal in Amps, and $W(\lambda)$ the measured transmittance of the chamber window. Substitution and solving for the unknown sensitivity scalar yields:

$$\Im(T) = [DN_{observed} - DN_{dark\_current}] / [ExposureTime \times \int S_{normalized}(\lambda,T)\ A(\lambda)\ M(\lambda)\ W(\lambda)\ d\lambda]$$

Once the value of the scalar $\Im(T)$ has been determined, the absolute sensitivity $S(\lambda,T)$ is determined as well. Given the absolute sensitivity we can derive an estimate of $\omega_0(T)$, defined as camera signal (in DN/s) expected for a white 100% reflecting Lambertian target at 1 A.U. from the Sun and illuminated and viewed normal to its surface. This is derived by the expression:

$$\omega_0(T) = \Im(T) \int S_{normalized}(\lambda,T)\ R_{Lambert\_1AU}(\lambda)\ d\lambda$$

where $R_{Lambert\_1AU}(\lambda)$ is radiance of the hypothetical white target at 1 A.U. (in $W/m^2/sr/nm$). Table 3.2.2e shows the application of this approach to solve for the unknown scalar $\Im(T)$ and $\omega_0(T)$ for one case (MI 110 with CCD temperature of -10°C).

Table 3.2.2e. Example: Absolute Spectral Sensitivity and ω_0 for MI 110 for CCD Temperature of -10°C						
Wavelength nm	$S_{normalized}(\lambda,T)$	$A(\lambda)$	$M(\lambda)$	$W(\lambda)$		$R_{Lambert\_AU}(\lambda)$
400	2.65E-02	2.800E+06	7.375E-11	0.930		0.513
450	2.73E-01	2.057E+06	2.280E-10	0.932		0.654
500	5.78E-01	1.176E+06	7.030E-10	0.934		0.603
550	1.00E+00	1.291E+06	9.370E-10	0.935		0.595
600	8.73E-01	1.120E+06	1.375E-09	0.935		0.560
650	2.35E-01	9.545E+05	1.860E-09	0.936		0.505
700	2.47E-02	1.097E+06	1.794E-09	0.936		0.448
750	7.88E-04	9.783E+05	2.111E-09	0.936		0.404
800	1.30E-06	8.931E+05	2.326E-09	0.937		0.363
850	-4.91E-06	1.181E+06	1.718E-09	0.938		0.315
900	-1.97E-05	1.415E+06	1.347E-09	0.938		0.290
950	-5.02E-07	2.564E+06	6.890E-10	0.927		0.248
1000	-4.28E-05	6.301E+06	2.860E-10	0.938		0.237
			$\int S_n A M W d\lambda =$	0.1693	ω_0 (-10°C)=	8.54E+05
			$Dn_{observed} =$	2185		
			ExposureTime =	1.326		
			$\Im(T) =$	9.734E+03		

In order to derive I/F the following relation can be used (note that this does not take into account the attenuation/scattering of incoming solar irradiance by the atmosphere).

$$I/F = SolarRange(A.U)^2 \times [DN_{observed} - DN_{dark\_current}] / [ExposureTime \times \omega_0(T)]$$

Using the procedures described above, values of $\omega_0(T)$ were derived for each of the two MI flight cameras for CCD temperatures that were available in the thermal vacuum calibration data. Those data are summarized in Figure 3.2.2f.

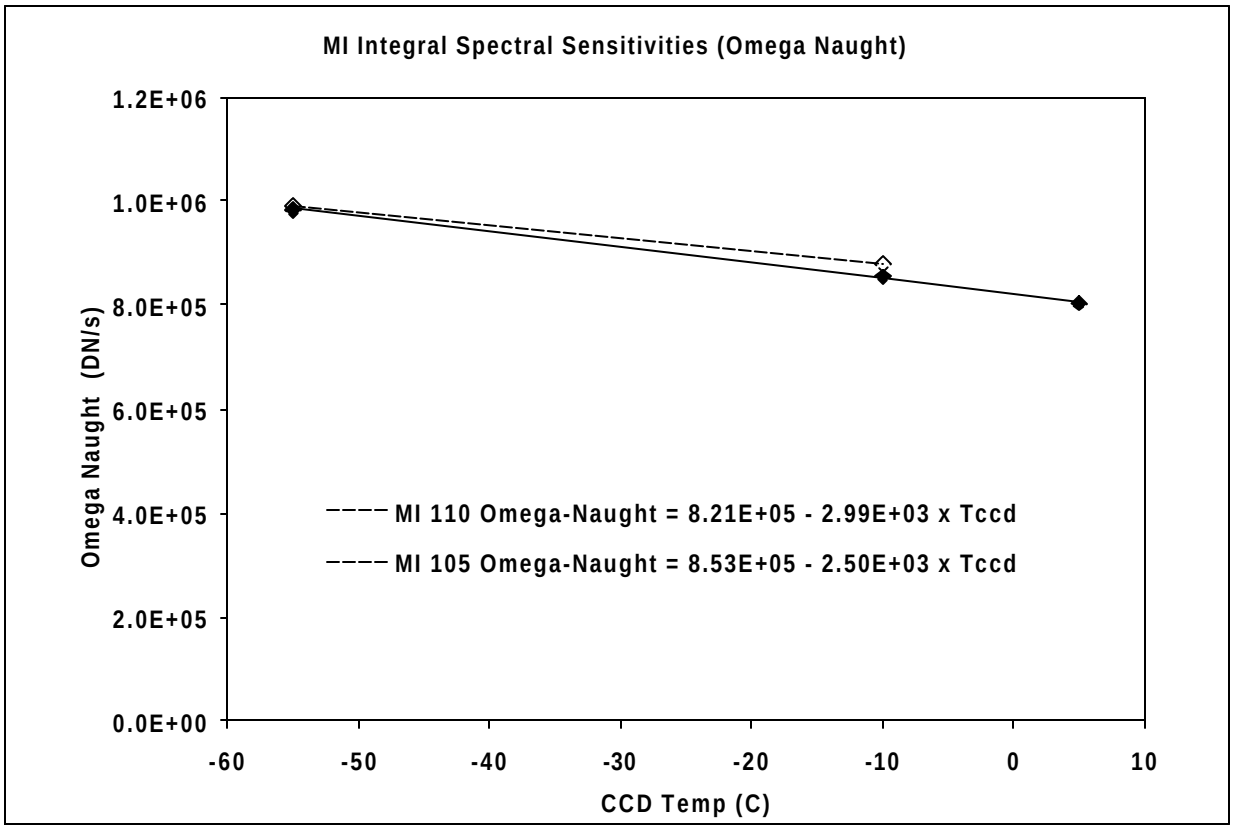

Figure 3.2.2f. Dependence of ω_0 on CCD temperature (°C) for both MI cameras: ω_0 is in units of DN/s and is defined as the expected signal for a 100% diffusely reflecting target at 1 A.U. from the Sun (see text).

3.2.2.4.2 Relative Radiometry (Flat Fields)

Because the images of the integrating sphere taken through the chamber window showed significant reflections (see Fig. 3.2.1l), they could not be used to determine the pixel-to-pixel (relative) variations in radiometric sensitivity of the MI flight units. While the flat fields taken with the CCDs before integration into the flight cameras show high-frequency variations in sensitivity (see Fig. 2.1.6), they do not include response variations caused by the MI optics. Therefore, flight unit images of the integrating sphere were taken with the chamber window removed (at ambient temperature and pressure). Dark current images were taken in the same configuration. The last 3-4 dark frames were averaged together and subtracted from each of the flat field images. The average of the central 101 x 101 pixels in each dark-corrected flat field is shown in Table 3.2.2.f for MI 105. A value of 2184 was subtracted from each mean and the results are shown in the "difference" column of Table 3.2.2f. Note that the mean values increase during the imaging sequence, due to increases in CCD and electronics temperatures that cause increased dark current. In cases where the difference exceeded 1 DN, the amount shown in the "Add (DN)" column was added to the entire image. The resulting images were averaged, along with the rest of the dark-corrected flat fields, to produce the flat field image shown in Fig. 3.2.2f. This average flat was corrected for transfer smear and normalized to the average value at the center of the image and stored in floating-point format to enable flattening of MI 105 images.

Table 3.2.2f. MI serial # 105 flat field statistics

Image	mean	std dev	difference	Add (DN)
020828171859_0009984_MI_105	2171.103	62.2973	-12.8975	13
020828172018_0009984_MI_105	2170.476	62.3816	-13.5244	13
020828172049_0009984_MI_105	2176.872	62.3252	-7.1282	7
020828172219_0009984_MI_105	2172.381	62.2363	-11.6194	12
020828172235_0009984_MI_105	2177.348	62.3308	-6.6523	7
020828172250_0009984_MI_105	2179.22	62.2082	-4.7805	5
020828172305_0009984_MI_105	2174.713	62.1563	-9.2866	9
020828172321_0009984_MI_105	2181.292	62.3491	-2.7078	3
020828172336_0009984_MI_105	2182.029	62.2791	-1.9714	2
020828172352_0009984_MI_105	2182.265	62.1954	-1.7346	2
020828172407_0009984_MI_105	2182.796	62.3449	-1.2043	
020828172422_0009984_MI_105	2183.188	62.2839	-0.8123	
020828172438_0009984_MI_105	2182.546	62.2497	-1.4543	
020828172453_0009984_MI_105	2183.217	62.2964	-0.783	
020828172509_0009984_MI_105	2183.462	62.1421	-0.5378	
020828172524_0009984_MI_105	2183.411	62.2403	-0.5894	
020828172540_0009984_MI_105	2183.739	62.2217	-0.2612	
020828172555_0009984_MI_105	2183.661	62.0815	-0.3394	
020828172610_0009984_MI_105	2183.445	62.1595	-0.5549	
020828172628_0009984_MI_105	2182.618	62.2504	-1.3823	
020828172643_0009984_MI_105	2183.704	62.2082	-0.2957	
020828172658_0009984_MI_105	2182.494	62.1859	-1.5056	
020828172714_0009984_MI_105	2184.236	62.2025	0.2363	
020828172729_0009984_MI_105	2183.335	62.2517	-0.6648	
020828172744_0009984_MI_105	2184.506	62.2971	0.5056	
020828172800_0009984_MI_105	2183.884	62.2507	-0.1157	
020828172815_0009984_MI_105	2184.22	62.2794	0.22	
020828172831_0009984_MI_105	2184.085	62.2488	0.0847	
020828172846_0009984_MI_105	2183.586	62.4101	-0.4138	
020828172901_0009984_MI_105	2184.531	62.3851	0.531	
020828172917_0009984_MI_105	2184.267	62.357	0.2673	
020828172932_0009984_MI_105	2184.302	62.0749	0.302	
020828172948_0009984_MI_105	2184.502	62.2613	0.5015	

Flat fields for MI 110 were processed in the same way, except that a value of 1792 was subtracted from each image in Table 3.2.2g.

Table 3.2.2g. MI serial # 110 flat field statistics

Image	mean	std dev	difference	Add (DN)
020924190848_0009984_MI_110	1780.57	50.0867	-11.4303	11
020924190903_0009984_MI_110	1784.581	49.7602	-7.4189	7
020924190919_0009984_MI_110	1787.077	49.9747	-4.9233	5
020924190934_0009984_MI_110	1788.479	49.8292	-3.5211	3
020924190950_0009984_MI_110	1788.986	49.8403	-3.0145	3
020924191006_0009984_MI_110	1789.823	49.9098	-2.1771	2
020924191021_0009984_MI_110	1790.251	49.7784	-1.749	2
020924191037_0009984_MI_110	1790.446	49.7587	-1.5544	1
020924191052_0009984_MI_110	1790.749	49.993	-1.2506	1
020924191107_0009984_MI_110	1790.608	49.8882	-1.3916	1
020924191123_0009984_MI_110	1791.26	49.8055	-0.7405	
020924191138_0009984_MI_110	1791.703	50.0023	-0.2974	
020924191154_0009984_MI_110	1791.416	49.8018	-0.5841	
020924191209_0009984_MI_110	1791.302	49.8725	-0.6981	
020924191225_0009984_MI_110	1791.295	49.8946	-0.7047	
020924191240_0009984_MI_110	1791.421	49.923	-0.5786	
020924191256_0009984_MI_110	1792.007	49.8758	0.0072	
020924191311_0009984_MI_110	1792.087	49.8514	0.087	
020924191326_0009984_MI_110	1791.642	49.8715	-0.3579	
020924191342_0009984_MI_110	1791.539	49.8217	-0.4606	
020924191357_0009984_MI_110	1791.479	49.8172	-0.5214	
020924191413_0009984_MI_110	1791.657	49.8638	-0.3427	
020924191428_0009984_MI_110	1791.725	49.8221	-0.2747	
020924191444_0009984_MI_110	1791.91	49.7817	-0.0905	
020924191459_0009984_MI_110	1791.656	49.7468	-0.344	
020924191514_0009984_MI_110	1791.258	49.8773	-0.7421	
020924191530_0009984_MI_110	1791.799	49.8248	-0.2015	
020924191545_0009984_MI_110	1792.438	49.8759	0.4382	
020924191601_0009984_MI_110	1792.295	49.866	0.295	
020924191616_0009984_MI_110	1792.208	49.8876	0.2078	

3.2.2.5 Accuracy and Relationship to Requirements

The accuracy of MI absolute radiometric calibration is TBD, but is likely to be better than 20%. Because of the relatively high noise levels in the flat fields taken at room temperature, there was a concern that the 5% relative radiometric calibration accuracy requirement could be met. However, the standard deviation of the pixel values in the MI 110 average flat field is 96 DN, or 4.8% of the average DN value. In summary, the ± 20% absolute, ± 5% relative radiometric accuracy requirements (Level 3 requirements #53 and #54) have been met.

3.2.3 System Spectral Response

3.2.3.1 Purpose and Description

To measure the camera system relative spectral response directly rather than calculating spectral response by combining optics and filter spectral transmission and CCD spectral QE. A monochromatic flux bundle was fed into each MI, with the image of the monochromator slit entirely contained within each image frame.

3.2.3.2 Test Procedure

The spectral response of the cameras was measured under vacuum at the three temperatures (-55°C, -10°C, and +5°C). An Acton VM505 0.5 monochromator was positioned in front of the chamber window, allowing an f/9 monochromatic beam to be fed into each camera. The monochromator light source was a 50 W tungsten lamp with a blackbody temperature of 3200 K. The monochromator was spectrally calibrated before and after the tests using a Neon I lamp, with the 8 nm/minute spectral "sweep" performed after all the tests being the most accurate (Appendix J). The spectral calibration data obtained during the tests were used to generate tables of wavelength data that were used to command the monochromator. Because these data were less accurate than the final "sweep" calibration data, they were not used in the reduction of the MI spectral calibration data except to determine the commanded wavelength for each image. The wavelength calibration data files used for MI 105 spectral data acquisition are listed in Table 3.2.3a; the wavelength calibration data files used for MI 110 spectral data acquisition are listed in Table 3.2.3b.

The monochromator output (light source spectral output) was monitored during the tests using a photodiode fed by a pick-off mirror. This diode was cross-calibrated to another photodiode that was periodically mounted over the exit slit of the monochromator. The diode cross-calibration data files used to reduce the MI 105 data are listed in Table 3.2.3a. The diode cross-calibration data files used to reduce the MI 110 data are listed in Table 3.2.3b. All of these data files are included in Appendix J. The spectral transmission of the chamber window was also measured (see Appendix I, table 18.1). Images of the (out of focus) monochromator beam were taken at 10 nm intervals from 350 to 800 nm and at 25 nm intervals at wavelengths between 800 and 1100 nm. Two or three images of the beam were taken at each wavelength, each followed by zero-second images at the same wavelength. This procedure was followed except for the longest wavelengths (>630 nm) for MI 110 at +5C, where 3 images of the beam were taken without any zero-second images.

Table 3.2.3a. MI serial # 105 spectral calibration data files

Temperature	Wavelength	Diode
-55°C	off_020814112912.prn	diode_020814161300.prn
-10°C	off_020814112912.prn	diode_020814191800.prn
+5°C	off_020816053000.prn	diode_020816200000.prn

Table 3.2.3b. MI serial # 110 spectral calibration data files

Temperature	Wavelength	Diode
-55°C	off_020913000000.prn	diode_020914044800.prn
-10°C	off_020913000000.prn	diode_020916081200.prn
+5°C	off_020913000000.prn	diode_020916131000.prn

3.2.3.3 Environmental Conditions

Temperature = -55°C, -10°C, and +5°C; pressure ≤ 10^{-6} torr.

3.2.3.4 Data Processing and Products

A typical image of the monochromator beam is shown in Figure 3.2.3a. The software used to reduce the MI spectral calibration data was based on the Pancam IDL software developed at Cornell University (Bell *et al.*, 2004). The zero following each image of the beam was subtracted from the image. This process removed the bias and zero-second component of the dark current, but not the active area dark current. The pixel values in a 121× 121 pixel box centered on the beam image were extracted from the resulting image. The average and standard deviation of the pixel values in 121× 121 pixel boxes to the left and right of the box centered on the beam image were also calculated. The average DN of the background pixels (left and right of the image) was subtracted from each of the pixel values in the central box. This removed the active area dark current and any scattered light in the images. The sum of the dark-corrected pixels in the central box was divided by the exposure time of the image. The desired monochromator wavelength was taken from the image labels, and the off_[mapping date].prn files were used to determine the wavelength that the monochromator was commanded to for each image. The multiple observations at each wavelength were averaged together. The longest wavelength (>630 nm) data for MI 110 at +5C were processed somewhat differently: A single zero-second dark frame, taken at approximately the same temperature as the monochromator images, was subtracted from each image. Transfer smear was then removed using the model described in section 3.2.6.4. The resulting images were then processed as described above.

The resulting spectral response data were divided by the spectral output of the light source using the diode_[mapping date].prn files. The monochromator "sweep" calibration data were then used to determine the actual wavelength of the monochromatic beam. The effects of the spectral response of the diode and the spectral transmission of the chamber window were then removed. The resulting spectral response files include total flux (arbitrary units) from the beam at each adjusted wavelength, as well as background level statistics.

Early runs of the data reduction software showed unexpected increases in MI response at the shortest wavelengths (350-370 nm). After examining the raw image data and ancillary calibration files, it was recognized that small errors in the diode_*.prn files (monochromator radiance calibration; see Appendix J) at these wavelengths would have large effects on the derived camera response. Specifically, the monochromator output at these wavelengths was very low, and these values appear in the denominator of the data correction equation. Because we seek only the relative spectral response (absolute radiometric response is derived separately), we added a constant value of 1.0 nA to the data in the diode_*.prn files. This removed the UV spike without affecting the results at other wavelengths.

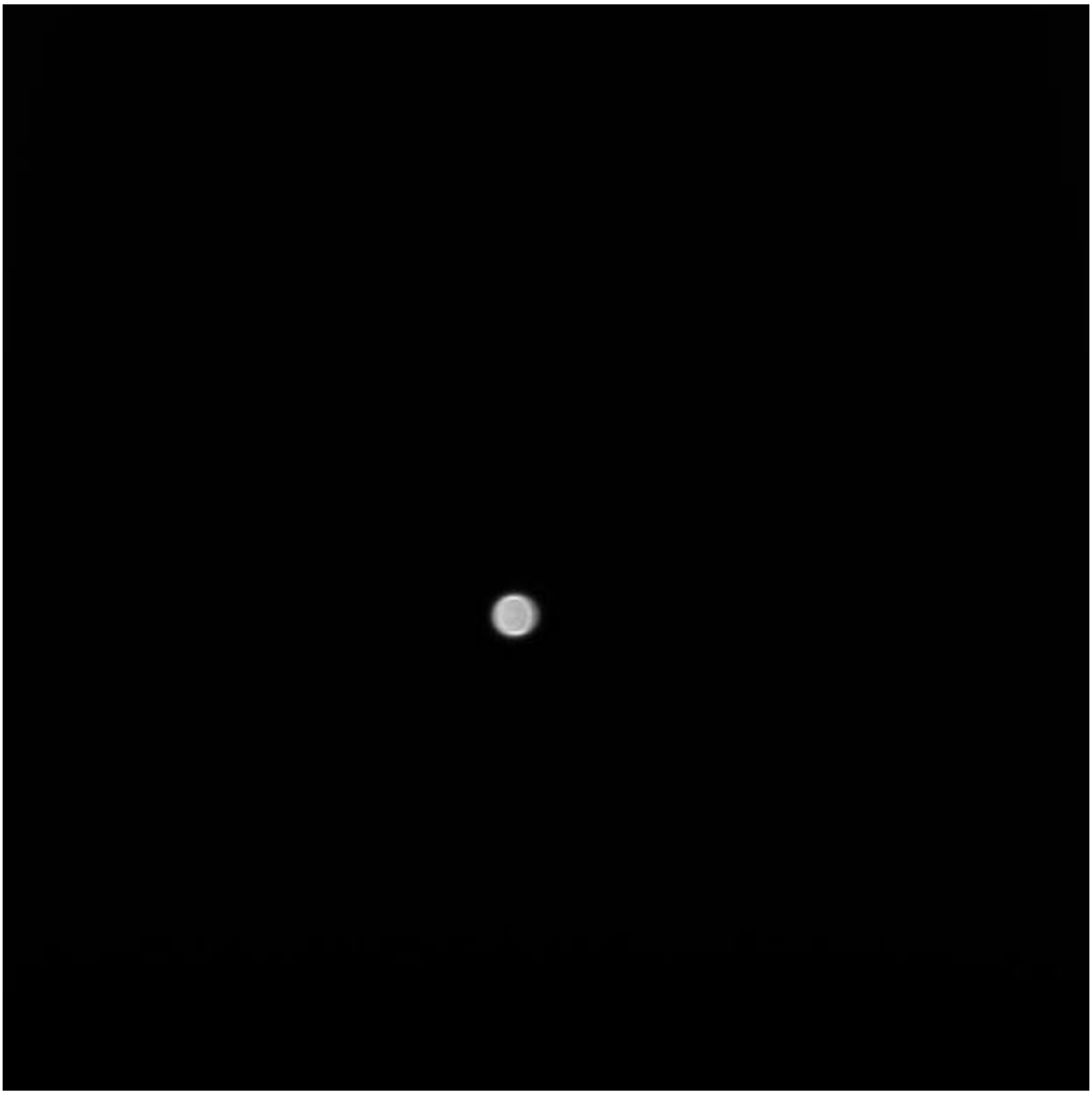

Figure 3.2.3a. MI 110 image of monochromator beam.

An example of the spectral response at various temperatures across the entire measurement range is shown in Figure 3.2.3b. Plots of spectral response within the visible bandpass at various temperatures, normalized to the value at 550 nm, are presented in Figures 3.2.3c (MI 105) and 3.2.3d (MI 110). As designed, the spectral response is similar to that of the human eye. The response outside of the visible band is not measurable above the noise. Note that the temperature-dependence of the spectral response is consistent with the measured variations in CCD spectral quantum efficiency (see section 2.1.8). The structure in the spectral response (*e.g.*, around 470 and 550 nm) is likely due to variations in spectral QE that were not fully resolved in component-level tests (see Figs. 2.1.8a and 2.1.8b).

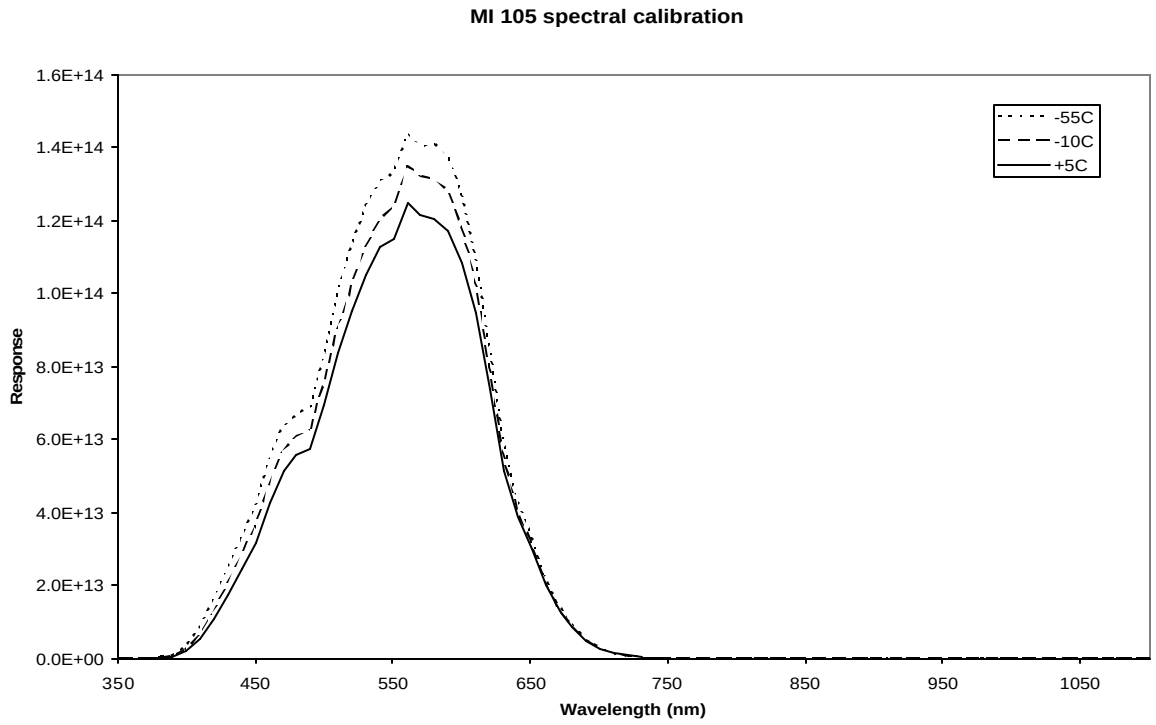

Figure 3.2.3 b. MI 105 spectral response at various temperatures, in arbitrary units.

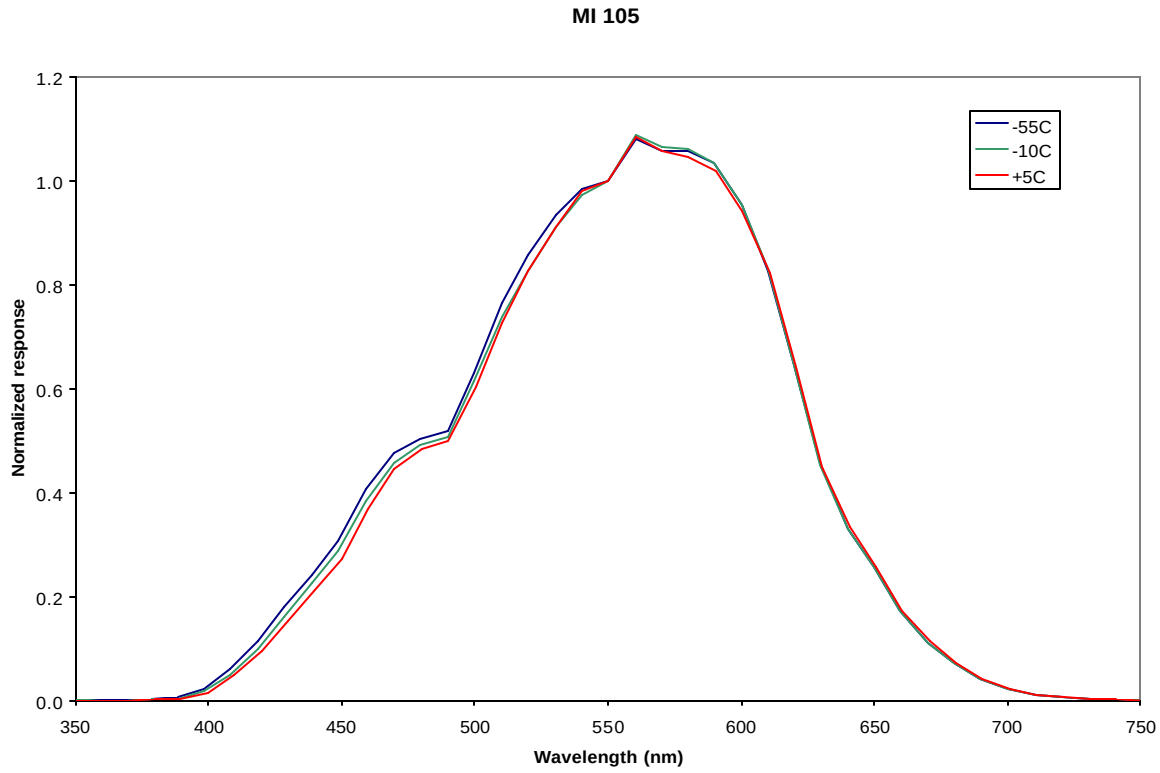

Figure 3.2.3c. MI 105 spectral response at various temperatures, normalized at 550 nm.

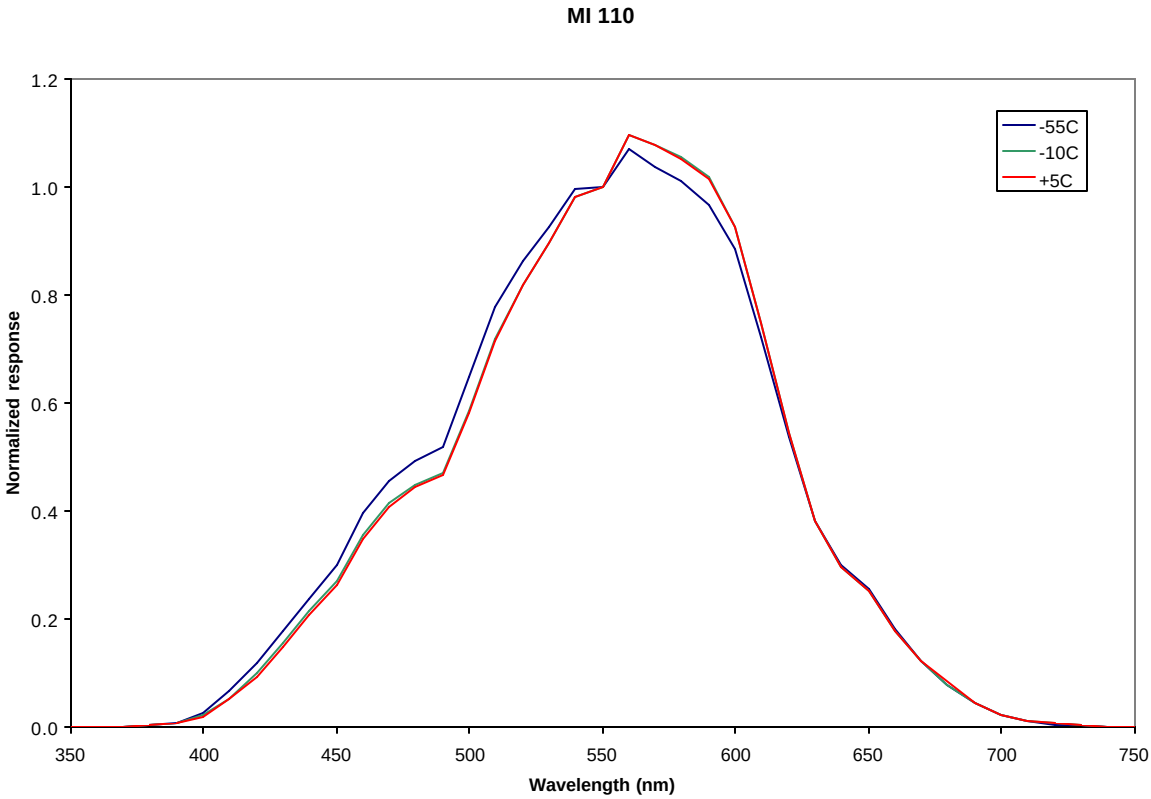

Figure 3.2.3d. MI 110 spectral response at various temperatures, normalized at 550 nm.

MI spectral calibration results are summarized in Table 3.2.3c. The temperature dependence of the CCD spectral QE causes a slight shift in MI bandpass to longer wavelengths with increasing temperature. The spectral response of the MI cameras at various temperatures is tabulated in Appendix J (section 19.3).

Table 3.2.3c. MI spectral calibration results

Camera:	**MI 105**			**MI 110**		
Temperature:	-55°C	-10°C	+5°C	-55°C	-10°C	+5°C
Effective wavelength:	551.0	552.4	553.6	550.0	552.8	552.5
Blue 50% edge:	492.0	493.5	494.3	491.2	496.7	497.0
Red 50% edge:	625.4	625.1	625.6	619.9	619.7	619.7
Full Width Half Max:	133.4	131.6	131.3	128.7	123.0	122.7
Blue 1% cutoff:	391.8	393.7	395.4	391.5	393.1	393.5
Red 1% cutoff:	709.9	710.5	712.2	709.9	710.2	710.6

3.2.3.5 Accuracy and Relationship to Requirements

These results verify compliance with Level 2 requirement #922 (calibration quality) and Level 3 requirement #48 (spectral bandpass).

3.2.4 CCD Blooming Behavior

3.2.4.1 Purpose and Description

Characterize CCD performance when signal exceeds the full well capacity. Take images at lower signal level (shorter integration or reduced illumination) immediately following bloomed image to evaluate residual effects, if any. Results will aid in design of autoexposure algorithm.

3.2.4.2 Test Procedure

A fiber illuminator was placed at the nominal best focus position of the MI in the Askania lab. The brightness of the fiber and the MI exposure time were adjusted to yield an image of the fiber that was well exposed (not saturated). The fiber brightness and exposure time was then increased to yield various amounts of blooming. Immediately following the bloomed image, a card was used to block the light from the camera and another image immediately acquired. The fiber was in the same location for all imaging during this test.

Blooming tests were also performed on MI serial # 105 at –110°C in the thermal/vacuum chamber on 8 August 2002, but the light source was not turned off or blocked to evaluate residual effects of blooming. The zero-second exposures that followed the bloomed images show frame transfer smear, as expected, but no residual effects of blooming.

3.2.4.3 Environmental Conditions

Ambient temperature and pressure.

3.2.4.4 Data Processing and Products

Zero-second dark frames taken in the same test configuration were subtracted from each image. The position of the fiber in the MI serial #105 images is shown in Figure 3.2.4a. The brightness of the fiber illuminator was measured at various input power levels (Appendix K), including those used for the blooming tests. These data were weighted by the MI spectral response (see section 3.2.3) in order to determine the ratio of intensities at the fiber settings used for the blooming tests.

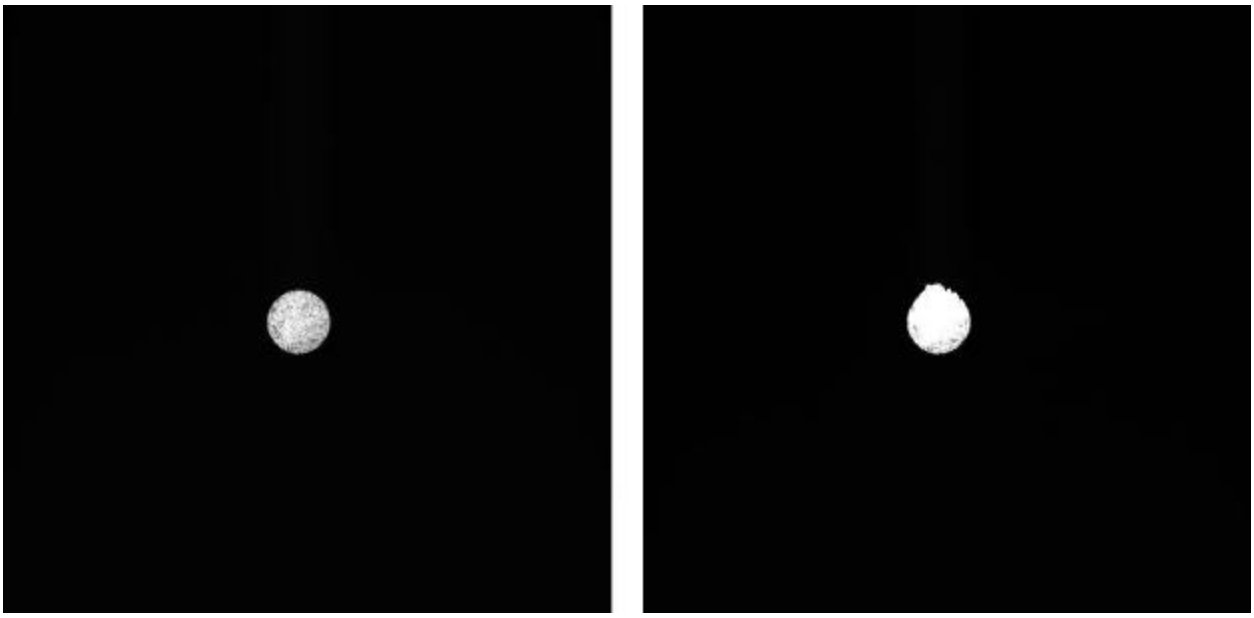

Figure 3.2.4a. MI serial # 105 images of fiber source used for blooming tests. (left) Unsaturated image (70 msec exposure). (right) Saturated image (150 msec exposure) showing slight blooming.

MI serial # 105 images taken at the same exposure time with the fiber brightness increased by a factor of 1106 show blooming (left image in Fig. 3.2.4b). Images were taken immediately after the bloomed image, with the source blocked. As shown in the right image of Fig. 3.2.4b, no residual effects of the blooming were observed.

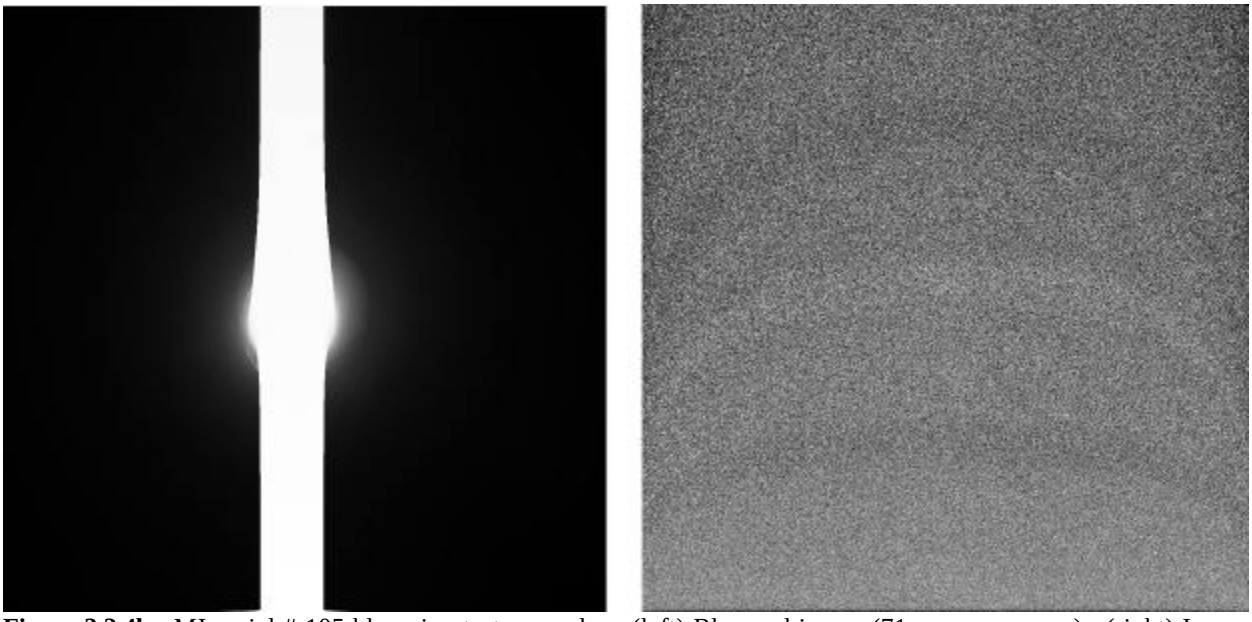

Figure 3.2.4b. MI serial # 105 blooming test examples. (left) Bloomed image (71 msec exposure). (right) Image taken immediately after bloomed image (71 msec exposure), with source blocked.

Similar tests were performed on MI serial # 110. As shown in Figure 3.2.4c, no residual effects of blooming were observed in MI serial # 110.

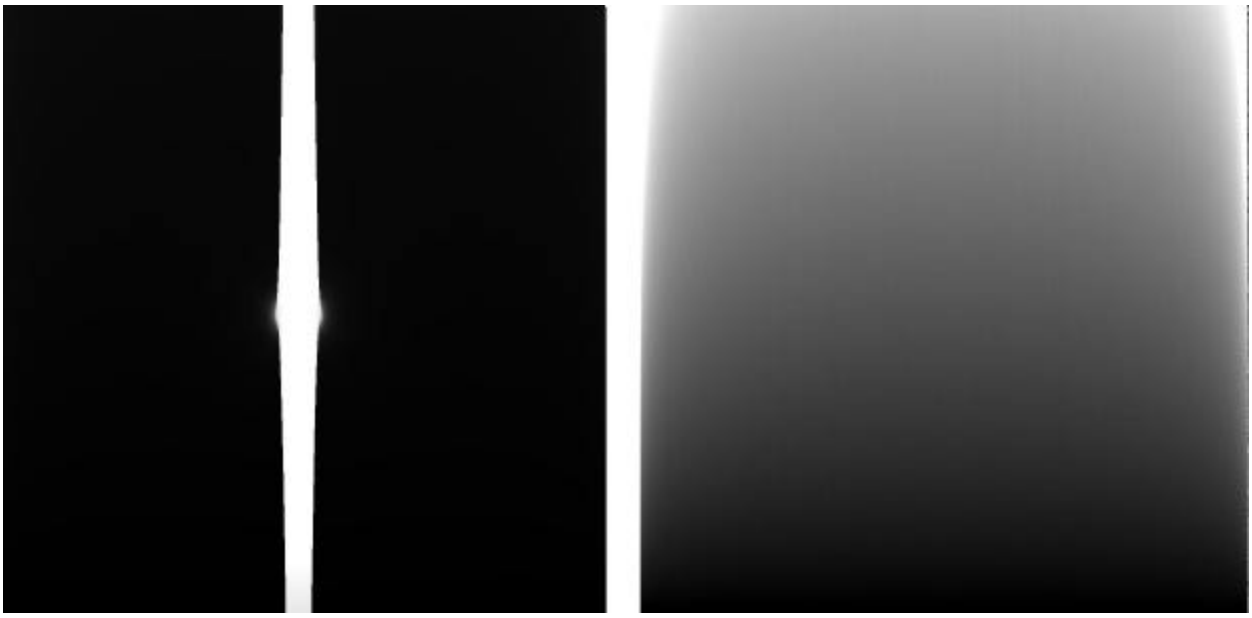

Figure 3.2.4c. MI serial # 110 blooming test examples. (left) Bloomed image (71 msec exposure). (right) Image taken immediately after bloomed image (0 msec exposure), with source blocked.

3.2.4.5 Accuracy and Relationship to Requirements

Blooming in the MI flight units is well behaved; no residual effects of blooming were observed. There is no specific blooming requirement for the MER cameras, but it is clear that residual effects of blooming do not affect the MI calibration accuracy. Blooming is evident when signal levels exceed 2 times full well.

3.2.5 Observations of Rock Targets

3.2.5.1 Purpose and Description

Take images of rock targets in good focus to provide data for software testing and calibration pipeline verification. The same targets will be observed by the other Athena flight instruments for comparison.

3.2.5.2 Test Procedure

A series of images was acquired at target distances up to 10 mm either side of nominal best focus. Image series were taken of both the rough and smooth (abraded) sides of many rock samples. The distance from target to camera was controlled to sub-micrometer accuracy for each position. The test setup was adjusted so that integration times were similar to those expected during flight (0.1 to 2 sec). We confirmed acquisition of well-focused images and out of focus images on either side.

3.2.5.3 Environmental Conditions

Ambient temperature and pressure.

3.2.5.4 Data Processing and Products

The table below summarizes images taken of rock targets during ambient calibration of the MI flight units. MI serial # 110 took images of rock targets with AREF IDs 174 and 222 (Squyres *et al*., 2003). MI serial # 105 took images of rock targets with AREF IDs 107, 178, 182, 183, 184, and 198.

Table 3.2.5a. MI observations of rock targets

Target distance	Rock sample AREF ID							
	107	174	178	182	183	184	198	222
49 mm						R	R	
52 mm					R	R	R	
55 mm	R	R		R, S	R	R	R	
58 mm	R	R	R	R, S	R	R	R	R, Rw
61 mm	R	R	R	R, S	R	R, S	R, S	R, Rw
64 mm	R, S	R, S	R, S		Rw	R	R, Sw	R
67 mm		R, S		R, S	R, Rw		R	R, S, Sw
70 mm		R, S		R, S	R, Rw		R	R
73 mm		R, S		R, S	R		R	R

Key: R = rough side of sample, S = smooth side of sample, “w” added if dust cover window material placed in front of target.

Examples of images taken by the MI engineering model of both sides of a rock target are shown in Figures 3.2.5a and 3.2.5b.

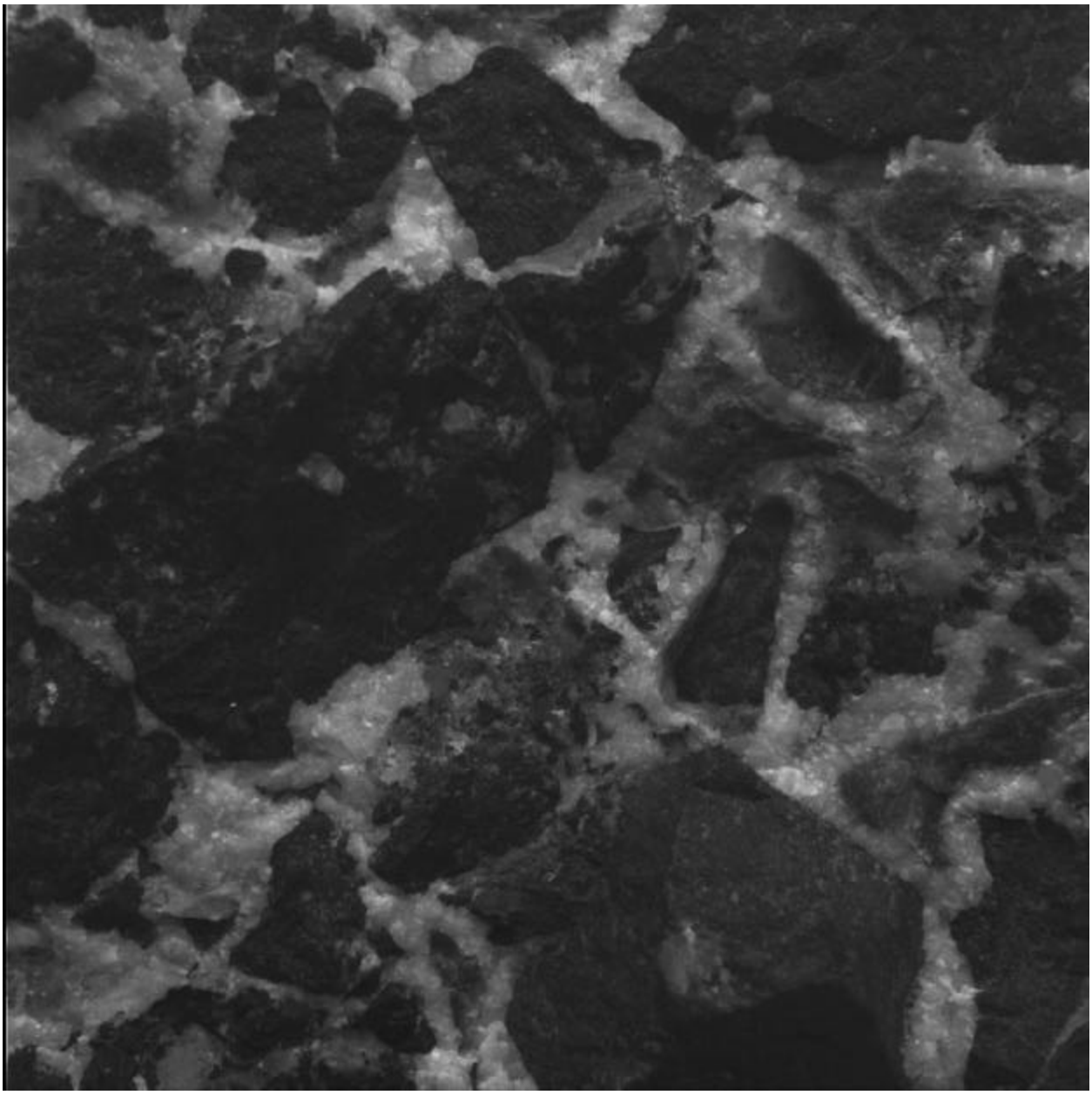

Figure 3.2.5a. Raw MI image of rough side of rock target AREF146, taken under room lighting.

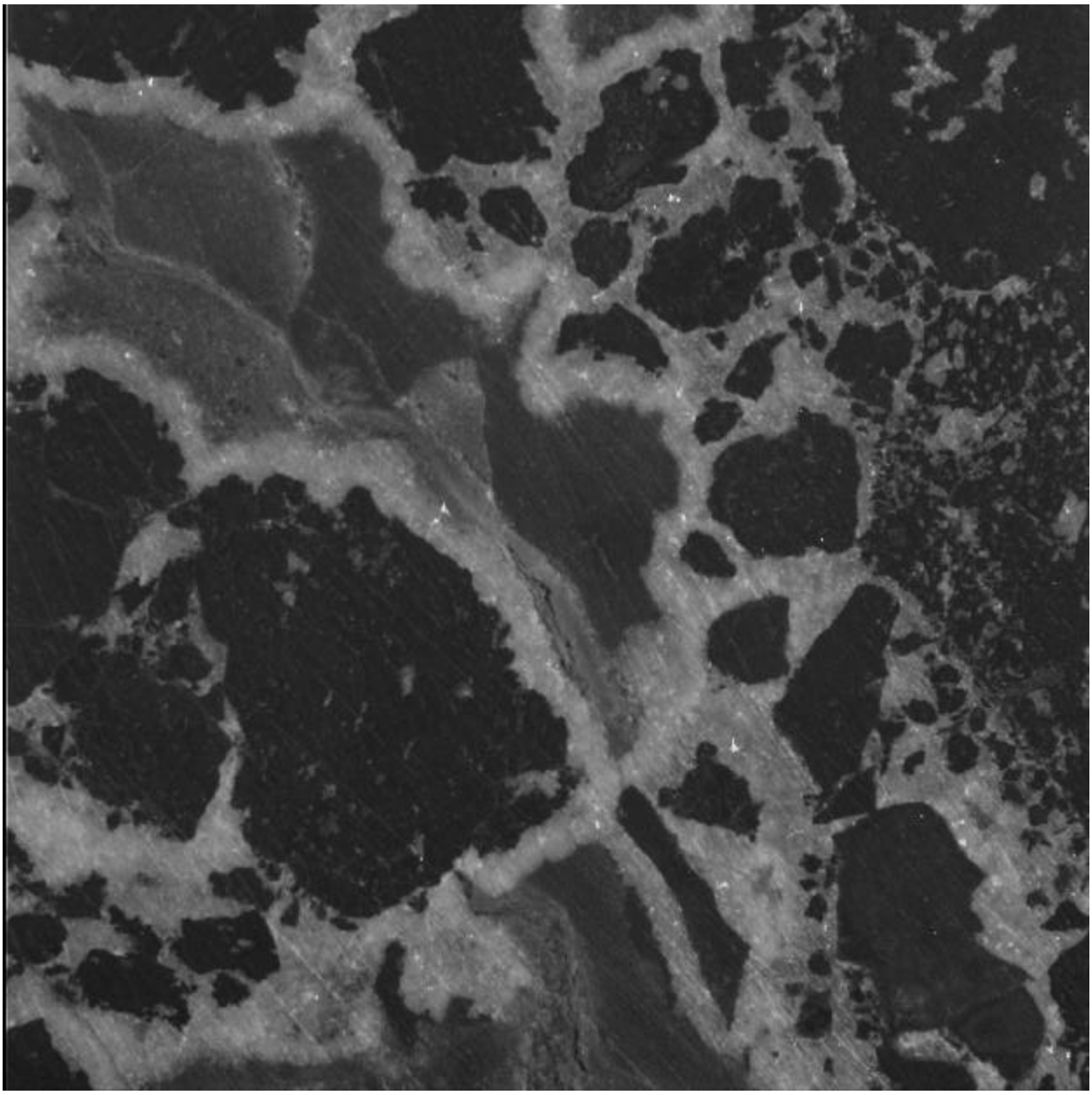

Figure 3.2.5b. Raw MI image of smooth (abraded) side of rock target AREF146, taken under room lighting.

3.2.5.5 Accuracy and Relationship to Requirements

The target distances are accurate to ±1 mm. These data are consistent with Level 3 requirement #49 (depth of field).

3.2.6 CCD Electronic Shutter Effect (Transfer Smear)

3.2.6.1 Purpose and Description

To determine the integration times at which frame transfer of the image of a bright spot from imaging to storage areas on the CCD will leave a significant "readout smear" or shutter effect. This was done with the final flight electronics, which govern the frame transfer speed.

3.2.6.2 Test Procedure

Images of a fiber optic were taken at several integration times including the minimum integration time (5.12 msec). An example image is shown in Figure 3.2.6a. Integration times were increased until the fiber image was nearly saturated.

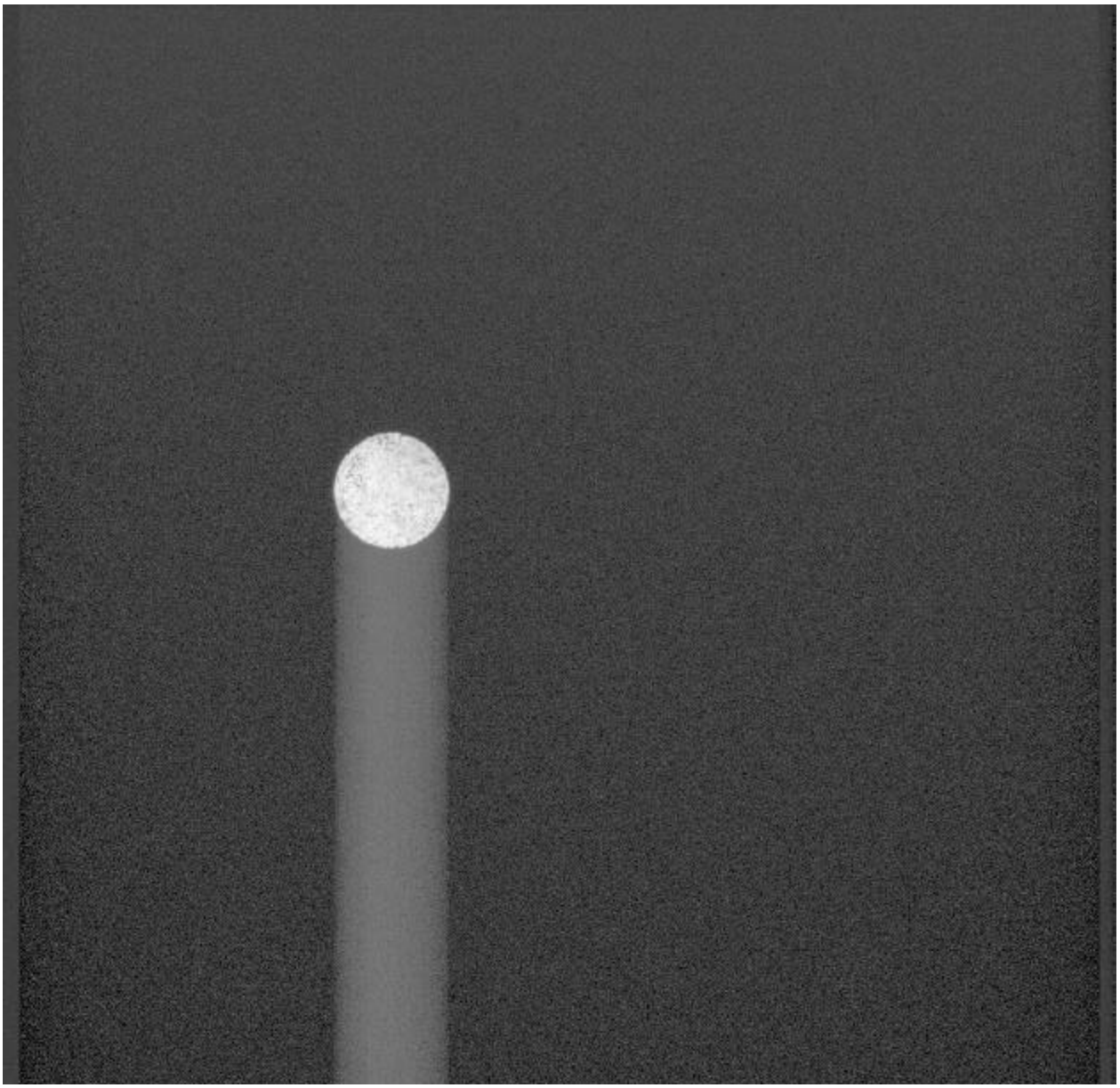

Figure 3.2.6a. MI serial # 105 image of fiber (020718092113_0000102) taken under ambient conditions with exposure time = 10.24 msec. Average zero-second dark frame has been subtracted to remove dark current accumulated during readout. Image transfer direction is toward top; note transfer smear below fiber image.

3.2.6.3 Environmental Conditions

Ambient temperature and pressure.

3.2.6.4 Data Processing and Products

An average of zero-second dark frames taken near the time of the fiber images was subtracted from each image of the fiber. Statistics were gathered in rectangular regions centered on the fiber image and on either side of the fiber image, and in the smeared region and on either side of the smeared region. The average of the background levels on either side of the fiber and smeared regions were subtracted from the averages of the signal in the fiber and smear regions. Analysis of this data showed that the magnitude of the transfer smear was twice as large as expected from the following model:

$$T(r) = \frac{t_{tr}}{t_{ex}N}[S(r) - T(r-1)] + T(r-1),$$

where $T(r)$ is the transfer smear at row r, $S(r)$ is the signal at row r, with transfer time t_{tr} = 5.12 msec, exposure time t_{ex}, and number of rows N = 1024. The discrepancy was also noted in analysis of test data taken with the MER EDL cameras. The reason for this discrepancy was that the charge accumulation during pre-integration flushing was not included in the model. When the CCD is fast flushed, charge is clocked away from the storage area at the same rate as a regular frame transfer. For the fiber optic imaging setup this means that at the end of the fast flush (and at the start of the integration period) there is a trail of charge leading away from the storage area that looks identical to the frame transfer smear image. Integration is followed by a frame transfer into the storage area that effectively doubles the amount of charge in the smear. Therefore, the model above was corrected to account for the flush smear by doubling the transfer time t_{tr} to 10.24 msec. An example of accuracy of the revised model is shown in Figure 3.2.6b. This model can be used to remove transfer smear from images for which "shutter frames" (zero-second exposures of the same scene) are not available. Otherwise, the typical correction for transfer smear involves subtraction of the "shutter frame" from each image. This method was used extensively in the reduction of the MI calibration data, and can be used onboard the rovers during flight. However, shutter frames were not acquired for some of the MI calibration data, so the model must be used to remove transfer smear in some cases (see section 3.2.3).

The relative magnitude of the transfer smear depends on the exposure time. For the MER cameras, the minimum effect on SNR due to transfer smear (for the last pixels transferred) is

$$SNR = \frac{t_{ex}}{10.24}$$

where the exposure time t_{ex} is in msec and 10.24 is the sum of the flush duration (5.12 msec) and the transfer time (5.12 msec). For example, the minimum SNR of a 1.024 second image is 100:1, if transfer smear is the only noise source.

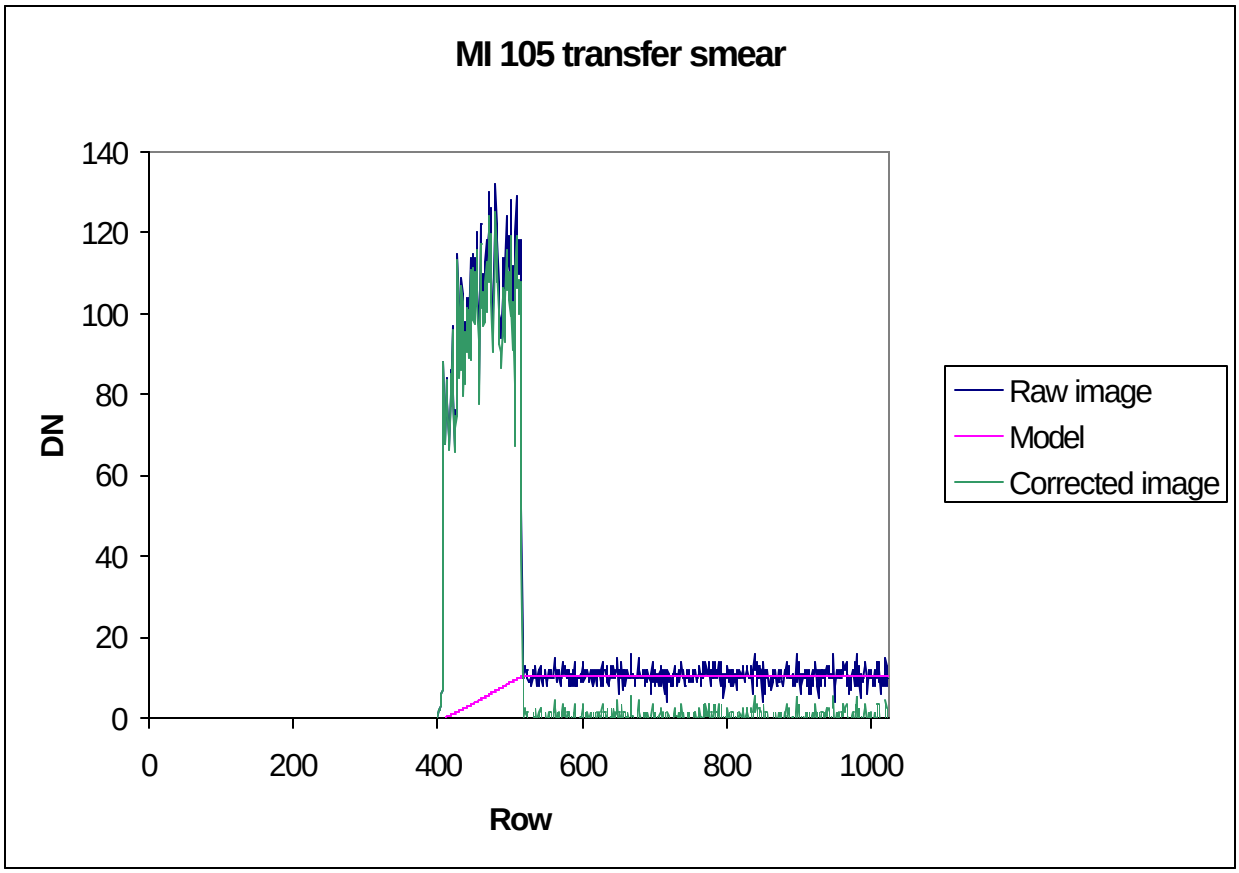

Figure 3.2.6b. Comparison of transfer smear data (from image in Fig. 3.2.6a) and model for 10.24 msec exposure.

3.2.6.5 Accuracy and Relationship to Requirements

As shown in Fig. 3.2.6b, the transfer smear model removes the shutter effect to within the noise level of the test images, ±2 DN in this case. For a well exposed (half well) image at room temperature, this corresponds to ±0.1%. Subtraction of shutter frames during flight (at lower temperatures) will even more accurately correct for transfer smear. As shown above, SNR > 100 for exposures longer than 1 second considering noise contributions only from transfer smear. Correction of the shutter effect, either by subtracting a zero-exposure frame of the same scene, or using the model described above, is therefore required for images taken with exposure times less than 1 second in order to meet the 100:1 SNR requirement (Level 3 requirement #1192). Similarly, the shutter effect must be corrected for images taken with exposure times less than 205 msec to remain in compliance with Level 3 requirement #1191 (relative radiometric accuracy better than 5%).

3.2.7 Grid Target Imaging

3.2.7.1 Purpose and Description

Imaged a well-known grid target at best focus and at various distances inside and outside of best focus. Characterized the geometric distortion introduced by the MI into its images. Measured the effective focal length and field of view by measuring the dimensions of the target image. These data were used to construct the MI camera models, as described below.

3.2.7.2 Test Procedure

The following camera alignment procedure was used for both grid and bar target imaging:

1. A flat mirror with crosshairs was mounted to the camera bracket (Fig. 3.1.1) so that the crosshairs were centered on the nominal MI optical axis. An alignment telescope was used to adjust the location and orientation of the crosshairs so that they were centered and perpendicular to telescope axis to within 0.5 mrad. The mirror was then removed from the mounting bracket.
2. A pinhole target was placed in the target holder and viewed with the alignment telescope. The 3-axis stage tip-tilt screws (red in Fig. 3.1.1) were used to align the target holder perpendicular to the telescope boresight to within 0.5 mrad. The horizontal (x) and vertical (y) actuators of the stage were used to center the pinhole on the alignment telescope boresight.
3. A custom aluminum bracket (shown at bottom of Fig. 3.1.1, below camera mounting bracket) was mounted along with a micrometer to set the distance of the target from the camera. The z-axis of the stage was used to position the target at the nominal best focus position (62.9 mm from the first principal plane). The nominal best focus position was based on the mechanical design of the MI optics, which included a scribe mark on the optics barrel that was machined to a tolerance of 25 micrometers with respect to the datum (barrel mounting surfaces). The stage z-axis controller was set to zero at this location.
4. An MI flight unit was mounted to the bracket using the same holes used to mount the alignment mirror.

The intent of this procedure was to align the base of the camera parallel to the target to within the machining tolerances (probably better than 1 mrad). Before target imaging, a “central pixel” test was performed: A fiber illuminator was used to feed light through the alignment telescope to the camera. The resulting spot in MI test images was in a slightly different location from camera to camera and before and after vibration/thermal testing. These results indicate that there were errors of about 2 mrad in the alignment and mounting of the cameras.

The integrating sphere was then moved (to the right in Fig. 3.1.1) into position to illuminate the targets from behind. Images of the sphere without any target in the holder were also taken to enable flat-field correction of the images. Geometric calibration of the Microscopic Imagers was accomplished by imaging a target having 1.2 mm diameter circular spots arranged in a square grid on 3.5 mm centers. The spots consist of holes in an opaque aluminum layer deposited on a glass slide. For each flight model camera, images were obtained before vibration and thermal vacuum testing ("Initial" in Table 3.2.7a) with the camera at a number of positions

spanning ±12 mm relative to the expected best-focus distance of 100 mm from the camera focal plane. A smaller number of images were obtained after vibration ("MOD") and thermal vacuum tests ("MOD2"). As described below, a few images and some individual spot measurements were examined but excluded from our final fits.

Table 3.2.7a. Images Acquired for Microscopic Imager Geometric Calibration

Camera	Phase	Camera Position (mm)	No. of Images	Spots/ Image
105	Initial	-12	3	81
		-8	3	72
		-4	3	56
		-2	3	49
		0	3	49
		2	3	49
		4	3	49
		8	3	49
		12	3	36
	MOD	-5	1	56
		-4	1	56
		-3	1	56
		-2	1	49
		-1	1	49
		0	1	49
	MOD2	-5	3	56
		-4	3	49
		-3	3	49
		-2	3	49
		-1	3	49
		0	2	49
110	Initial	-12	3	81
		-8	3	56
		-6	3	56
		-4	3	56
		-3	3	56
			5	49
		-2	3	49
		0	3	49
		2	3	49
		4	3	49
		8	3	49
		12	3	30
	MOD	-4	2	49
		-3	3	49
		-2	2	49
	MOD2	-4	3	56
		-3	3	56
		-2	3	56

Multiple images were acquired to allow reduction of errors in image location precision by averaging images together.

3.2.7.3 Environmental Conditions

Ambient temperature and pressure.

3.2.7.4 Data Processing and Products

Examination of the images revealed artifacts caused by reflected light that could adversely influence the geometric calibration (Fig. 3.2.7a). Diffuse reflections visible in the

space between the spots are presumably out-of-focus images of the calibration setup, including a view of the spot target reflected in the MI optics. Such reflections would contribute primarily to random residuals in the calibration solution. Within the spots, a brighter crescent is visible on the side farther from the center of the image. The size of these crescents increases systematically with distance from the center of the image. The cause of the crescents is double reflection of light from the back of the aluminized film on the front of the target, off the back of the target, and thence through the hole in the film to the camera. The brightness of the spots is increased from ~2900 DN (data numbers) outside the crescents to ~2940 within them. The farther the spot from the optical axis, the greater the area of the illuminated back of the film that is visible through the hole. The contribution of light in the crescent can thus influence the estimated centroid position of each spot in a systematic way, potentially biasing our estimates of both image scale and distortion. This effect is therefore a more serious concern than the irregular reflections.

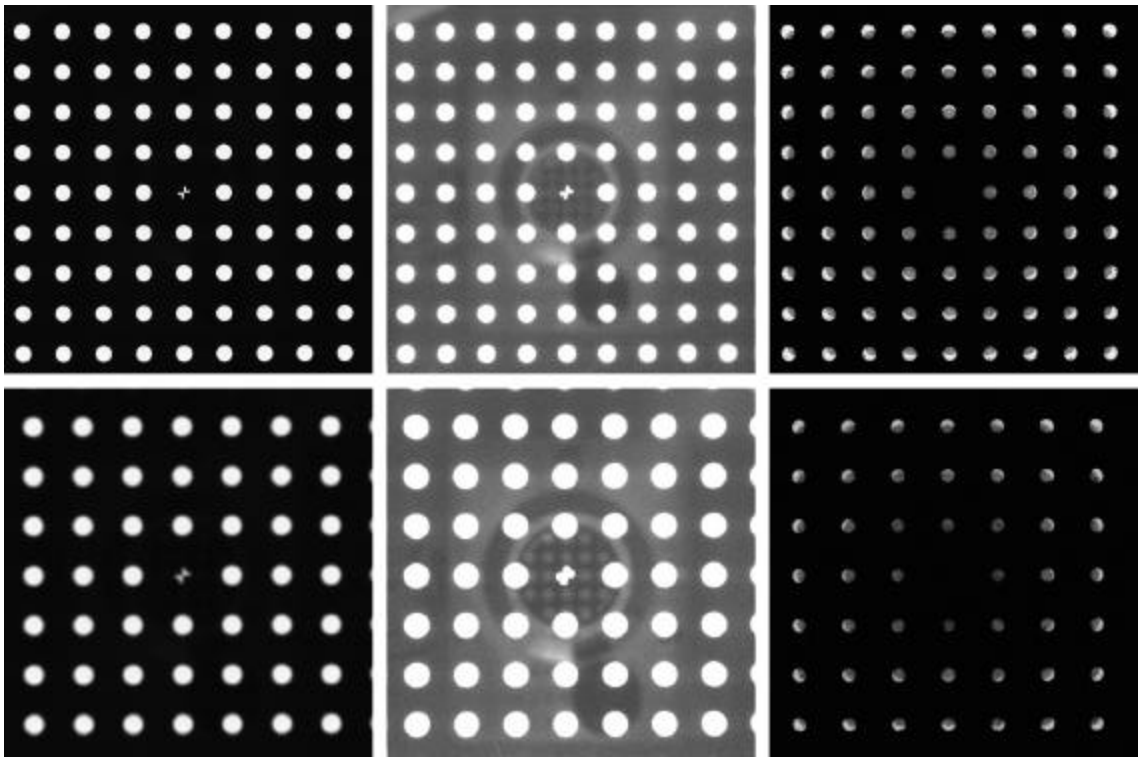

Figure 3.2.7a. Examples of spot target images used for MI geometric calibration. Top row, in-focus image shown with three contrast stretches, from left to right, 0–3000 DN, 0–100 DN to emphasize diffuse reflections seen between spots, and 2850–2950 DN to emphasize crescents formed by internal reflection within the spot target. Bottom row: maximally out-of-focus image, same stretches.

To minimize the influence of the reflections, we thresholded the images before measuring the spots, setting DN less than 100 to zero and those greater than 1000 to 1000. This thresholding eliminates the diffuse reflections outside the images and the cores of the crescents but cannot entirely eliminate the influence of the reflections on the brightness of the spots near the edges where the data numbers were between 80 and 1000. The residual effects will be greatest for the out-of-focus images, in which the spots have a wider annulus of non-thresholded pixels. We can place an upper limit on the apparent shift in the spot center of mass by assuming that the entire unclipped annulus on the outer side of the spot is brightened by 40 DN. The

annulus widths vary from 2 pixels at best focus to 3 pixels at the greatest distance from the target to 5 pixels at the closest setting. The corresponding spot radii at these positions are approximately 24, 21, and 30 pixels, giving maximum spot shifts of 0.0033, 0.0056, and 0.0066 pixels respectively. The largest of these values is still only ~1% of the peak-to-peak radial distortion. Because the brightened annuli, unlike the crescents visible in the unclipped images, do not become wider with distance from the image center, the systematic variation of the spot shift with radial position is expected to be weak.

Automatic measurement of the spot locations proceeded in three steps. Initial estimates, accurate only to several pixels, were determined by forming row and column sums of the images and locating the maxima of these sums. Each intersection of a maximum-sum row and maximum-sum column was then used as a starting point for the second measurement pass. The **CNTRD** IDL routine that is based upon the **DAOPHOT "FIND"** algorithm was modified to read the calibration images and used to automatically estimate the centroids of the spots, which were recorded with a precision of 0.001 pixel. This software, available from the *IDL Astronomy User's Library*, is designed to find the centroid coordinates of stellar objects by locating the position where line and sample derivatives go to zero. Spots within 100 pixels of the image edge were not measured because of the limitations of the software. It was found in practice that this algorithm, which is optimized for star images, is not well suited to finding broad, flat-topped features such as the spots in the MI calibration target. Locations recovered with **CNTRD** were accurate to the nearest pixel but displayed large systematic errors in their fractional-pixel part. These locations were therefore not used directly but were taken as the center of a search box for each spot in which the two-dimensional center of mass of thresholded image data was computed.

Fitting Approach: The observed spot centroids obtained as just described were fitted in a least-squares sense with an imaging model. This model was implemented as a spreadsheet, providing great flexibility in selecting subsets of the data, adding parameters, and displaying the behavior of residuals. The three sets of observations (Initial, MOD, and MOD2) for each camera were included in a single fit. As discussed below, a small subset of data for each camera (both whole images and individual spots) were subsequently excluded from the fits based on their large residuals. Finally, separate fits to the Initial, MOD, and MOD2 data were made and compared. The parameters fitted were as follows:

- An in-plane rotation of the target for each camera and calibration phase (Initial, MOD, and MOD2). The use of separate rotations for each camera-target distance was investigated and found not to reduce the residuals.
- An in-plane translation of the target for each set of images (typically 3) taken at a single camera-target distance without moving the calibration apparatus.
- Two parameters describing the variation of image scale with camera position. These can be expressed in more than one way. We report the (on-axis) coordinates of the front and rear principal points. For convenience, the fits were performed in terms of front principal point position and magnification at camera station 0 mm.
- A radial optical distortion coefficient corresponding to a deviation of the observed spot location from its ideal distance from the optical axis that is cubic in that ideal distance.
- A center for this radial optical distortion within the image frame. The residuals depend relatively weakly on the optical distortion center, so the grid search for these parameters was carried out only to the nearest 5 pixels.

- A fixed correction to the camera position (i.e., to the distance from front principal point to the target) applied to all "MOD" images and a separate such correction applied to all "MOD2" images.
- For a few sets of images, the recorded target position appeared to be in error and was adjusted to bring the results for these images into concordance with the remainder of the data. Specifically, the camera 105 data at nominal position –12 mm appear to have been obtained at –11.944 mm, and those for camera 110 at nominal position +12 mm at +12.017 mm. These discrepancies are well outside the normal uncertainties in determination of image scale and may result from "blunders" in setting or recording the camera position, but these very out-of-focus images are subject to the largest reflection effects and, as described below, also departed significantly from the distortion model for the other images. They were therefore excluded from the fits reported here.

The location where the camera axis intersects the focal plane was not estimated but was set at line and sample 512.5. This position can be estimated when targets of known angular coordinates are imaged, but not when, as in this case, targets of known Cartesian position are used and no independent survey of the camera position and orientation is available. Finally, the target was assumed to be parallel to the focal plane of the camera because the pattern of residuals showed no sign of the type of perspective distortion that would result from a nonparallel configuration.

Selection of Data for Final Fitting and Systematic Patterns of Residuals: An interactive adjustment of the parameters just listed yielded minimum root-mean-square (RMS) two-dimensional residuals of 0.02–0.03 pixel (0.015–0.02 pixel each in sample and line) for the two cameras (Table 3.2.7b). This is an order of magnitude less than the 0.2 pixel one-dimensional RMS error that we have documented for stereomatching of various planetary images (Kirk *et al.*, 1999; 2003a; 2003b), as would be expected given that the calibration spots have much higher contrast and simpler shape than natural features.

A handful of individual spot measurements were excluded from the fits because they displayed residuals on the order of 0.1 pixel, substantially larger than those for all other spots. These excluded spots fell into two categories, for each of which the cause of the large residuals was apparent. First, the center spot on the target (row and column 0) is unique in being a small cross rather than a 1.2-mm circle. Useful measurements were obtained for this spot in the out-of-focus images but not in those obtained near best focus. Second, several spots at or near the corners of the images on occasion had high residuals that could be traced to stronger than average reflections in the vicinity of the spot.

We examined the spatial pattern of the residuals to the camera model for individual images, as a function of position (line and sample) in the images, and as a function of position (row and column) on the target. Results for individual images were generally similar, and the displacement of corresponding spots between images taken at different distances is relatively small, so that a useful summary of the patterns could be obtained by averaging together all observations for a given camera and test phase (excluding the individual bad measurements described above) as a function of row and column. The results are shown in Figure 3.2.7b. Several generalizations about the residual patterns are immediately apparent. The spatial distribution of the residuals is not random, but neither is it simple; the simplest patterns that would result from rotation, translation, and scale errors have been eliminated by the fits. As

noted above, no evidence for non-perpendicularity of the target and camera axis, which would take the form of a systematic change in scale across the field of view, is visible.

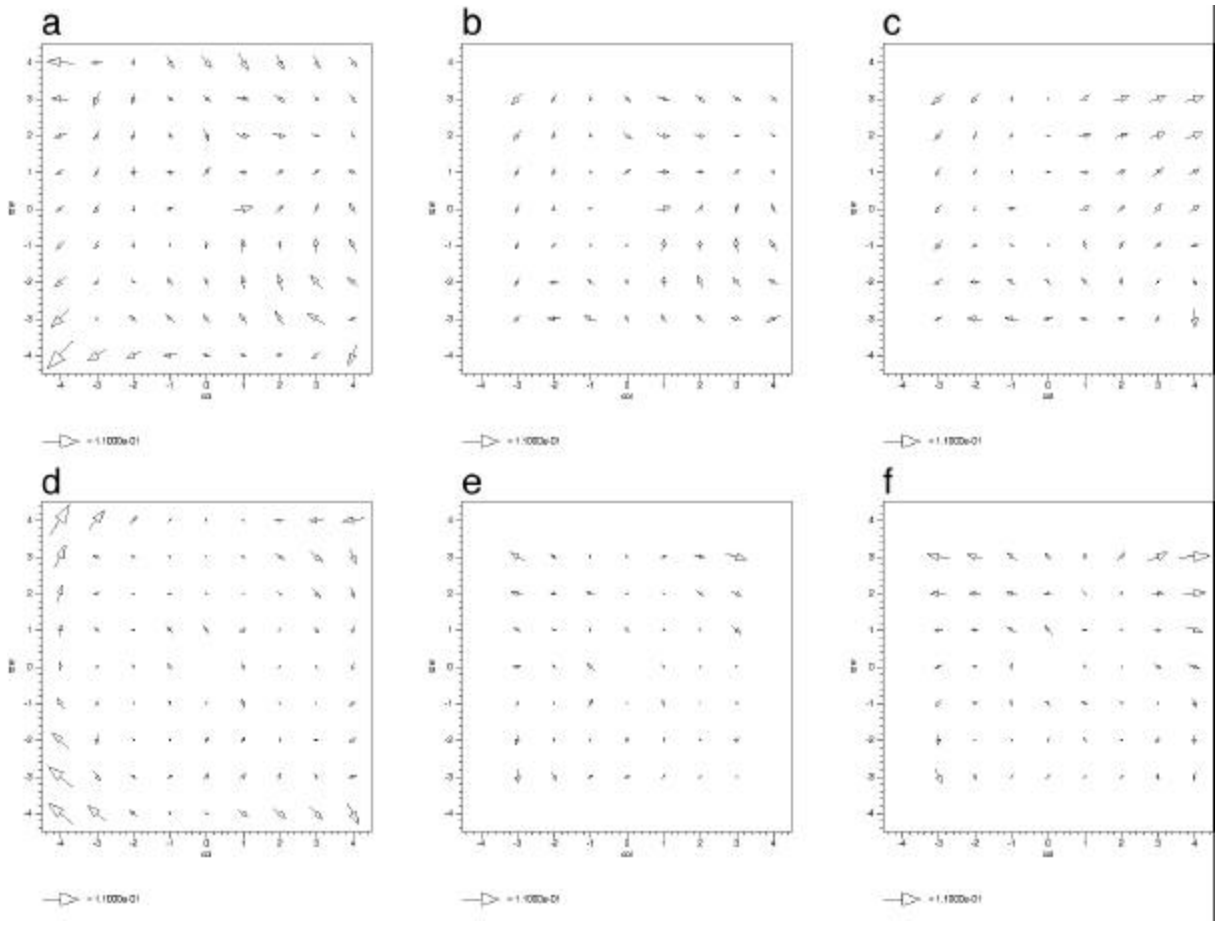

Figure 3.2.7.b. Vector plots showing spatial distribution of residuals to the MI camera model fits. Data for each camera and test phase have been averaged and plotted as a function of spot location (row and column) on the target; not all spots are observed in all image sets. (a) Camera MI 105 initial observations; (b) MI 105 MOD (post-vibration) observations; (c) MI 105 MOD2 (post-thermal-vacuum) observations; (d) MI 110 initial; (e) MI 110 MOD; (f) MI 110 MOD2.

The maximum residuals are on the order of 0.1 pixel, but the residuals tend to increase towards the edges of the images and values closer to the center are typically 0.03 pixel or less. The target rows and columns observed depend on the camera position. In particular, column –4 and rows ±4 are visible only at the most negative camera station. They are therefore not observed in the MOD and MOD2 datasets and are constrained by only 3 images in each initial set. As discussed above, these images, which are severely out of focus, are among the most susceptible to systematic errors due to reflections, and they fit the overall model least well as noted below. We therefore elected to use only the spots in rows and columns –3 to 3 in our final fits. These spots are visible in all images, so fitting only to them avoids potential biases caused either by actual imperfections in the target or by the limited, poor, and unequally distributed observations of the outermost spots.

A final observation about Fig. 3.2.7b is that the patterns are qualitatively similar but not identical in detail between the cameras and test phases. The "swirling" pattern is consistent with the tangential distortion that can occur when elements of a multi-element lens design are not

perfectly aligned. Such distortions can in principle be modeled but in general photogrammetric practice are not (Wolff *et al*., 1983, p. 36).

The radial component of the residuals also displays some regular variation with camera position. We fit a polynomial with linear and cubic terms in radial position to the radial residuals for each camera position, subsequent to the overall model fit. These fits reveal the departures from the average scale and optical distortion that has been determined by looking at the full dataset. The residual cubic term for different positions was found to vary by roughly ±0.003 pixel at the image edge (~1% of the mean cubic distortion term found in the overall fit), with positive and negative values often alternating from one position to the next. The cause of these departures is not known; they may simply represent the effects of random measurement errors. The fitted trends in radial residuals do not correlate with the maximum or RMS distance of spots from the centers of the images, which would support their being related to the radial bias in spot position caused by internal reflections. Nor do the fit results change significantly if we exclude spots beyond a given distance from the center of the image.

The linear and in some cases cubic fits to the residuals showed roughly ten times larger departures (equivalent to ~0.03 pixel at the image edge) for the most out-of-focus images. Although larger errors would be expected for these images based on our previous discussion of the effects of internal reflections in the target, the magnitude of the effect is greater than was estimated above. In any case, the images taken at focus positions of –12, +8, and +12 mm were excluded from the fits used to determine the best estimates of parameter values.

Rear Principal Point and Distortion: The most important elements of the camera model for use in analysis of flight images are the distance between the focal plane and rear principal point PP_2, which determines the scale of any given image, and the distortion model, including the coefficient(s) of a radial distortion polynomial and a center about which that distortion applies.

The principal point distance d_2 is obtained from the (distortion-corrected) radial coordinate R of a feature and the angle θ between the ray to that feature and the optical axis according to the relation

$$R = (d_2/\delta) \tan(\theta)$$

where δ is the "pixel pitch" or linear dimension of a pixel in the same units as d_2. The distortion model used in the fits can be expressed in the form

$$R' = R \{1 + C_1 + C_3 (R/R_{ref})^2 \},$$

where R is the distance in pixels between the distortion center and the location a feature would have in a distortion-free camera, and R' is the equivalent quantity observed for the real camera with distortion. To avoid having very small values of C_3, it is convenient to use a reference value $R_{ref} = 512.5$ in the above definition; C_3 is then of the same order of magnitude as the fractional distortion at the image edge, and $C_3 R_{ref}$ is the distortion in pixels at the image edge. This normalization differs slightly from standard photogrammetric practice (Wolff *et al*., 1983, p. 103), but can easily be converted to any other required normalization of the coefficients. In performing the actual fits, the linear coefficient C_1 in the distortion model was set to zero. For purposes of reporting the results, C_1, was changed to $-3/2\ C_3$ and the resulting change in mean image scale was compensated for by adjusting the distance between the focal plane and rear principal point. The distortion model as reported is thus

$$R' = R \{1 + C_3 [-3/2 + (R/R_{ref})^2] \},$$

With this choice, the radial distortion function $\Delta R = R' - R$ has a maximum and minimum that are equal and opposite over the range of radii from 0 to v2 R_{ref}, *i.e.*, from center to edge of the image. Balancing the maximum and minimum distortions is customary for camera calibration because it minimizes the errors incurred if the distortion polynomial is not used (Wolff *et al.*, 1983, pp. 74–79). The resulting focal length (or, in the case of close-range imaging, rear principal point coordinate) describes the average scale across the entire image rather than the local scale at the image center, and is referred to as the calibrated focal length (or calibrated principal point distance).

Table 3.2.7b. Best Estimates of Microscopic Imager Geometric Calibration Parameters

Parameter	Optical Prescription	Camera 105 Initial	Camera 105 Final	Camera 105 CAHVOR	Camera 110 Initial	Camera 110 Final	Camera 110 CAHVOR
Calibrated Rear PP Distance d_2 (mm)	28.157	28.486	28.486	28.553	29.514	28.510	28.495
Focal Length f (mm)	20.111	20.631	20.631	Unknown	20.542	20.540	Unknown
Magnification M	0.400	0.381	0.381	Unknown	0.388	0.388	Unknown
IFOV (microns/pixel)	30	31.5	31.5	Unknown	30.9	30.9	Unknown
Distortion center sample	512.5	445	460	330.0	460	470	476.3
Distortion center line	512.5	405	395	383.3	500	510	606.8
Cubic Distortion Coefficient C_3		-0.00069	-0.00064	-0.00487	-0.00095	-0.00090	0.00328
Quintic Distortion Coefficient C_5		0	0	0.00137	0	0	-0.00159
Maximum radial distortion (pixels)	=3	0.25	0.23	0.60	0.34	0.33	0.45
RMS 2-dimensional residual (pixels)	—	0.031	0.027	Unknown	0.023	0.022	Unknown

Our best estimates of calibrated d_2, C_3, and the sample/line coordinates of the center of the radial distortion are shown in Table 3.2.7b. Values of d_2 are ~1% greater than the optical prescription. The negative sign of C_3 corresponds to negative or "barrel" distortion. For our models of the two MI cameras, these extremal distortions are ±0.23 pixel and ±0.33 pixel respectively; the distortion polynomials are shown in Figure 3.2.7c. The distortion centers are ~130 and ~50 pixels from the image center, respectively (Figure 3.2.7d). Given the small amount of distortion, the effect of this displacement is relatively subtle, no more than 0.2 pixel anywhere in the images.

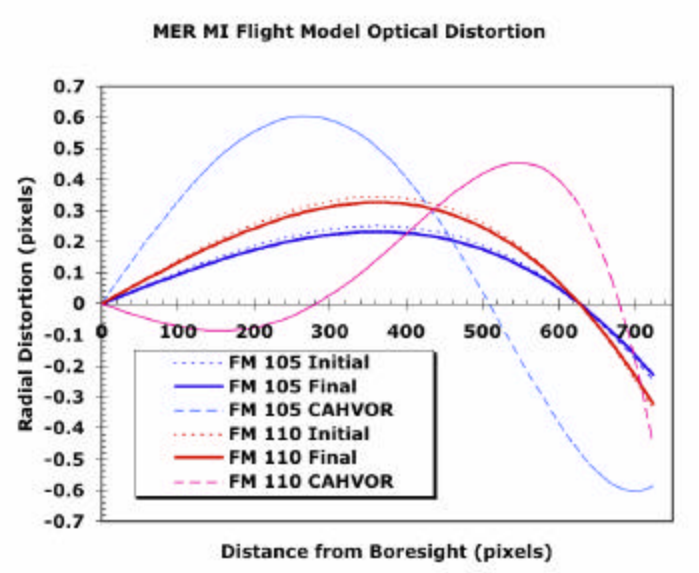

Figure 3.2.7c. Radial distortion polynomials based on a fit to spot data within a 800-pixel radius of the image center and ±3 rows/columns of the target center. Models based on final (MOD2) data, recommended for adoption, are shown as solid lines. Fits to the initial data (obtained before vibration and thermal vacuum testing) are shown as dotted lines, and differ by <0.02 pixel . Distortion models from JPL CAHVOR fits, adjusted to equal and opposite extreme values, are shown as dashed lines.

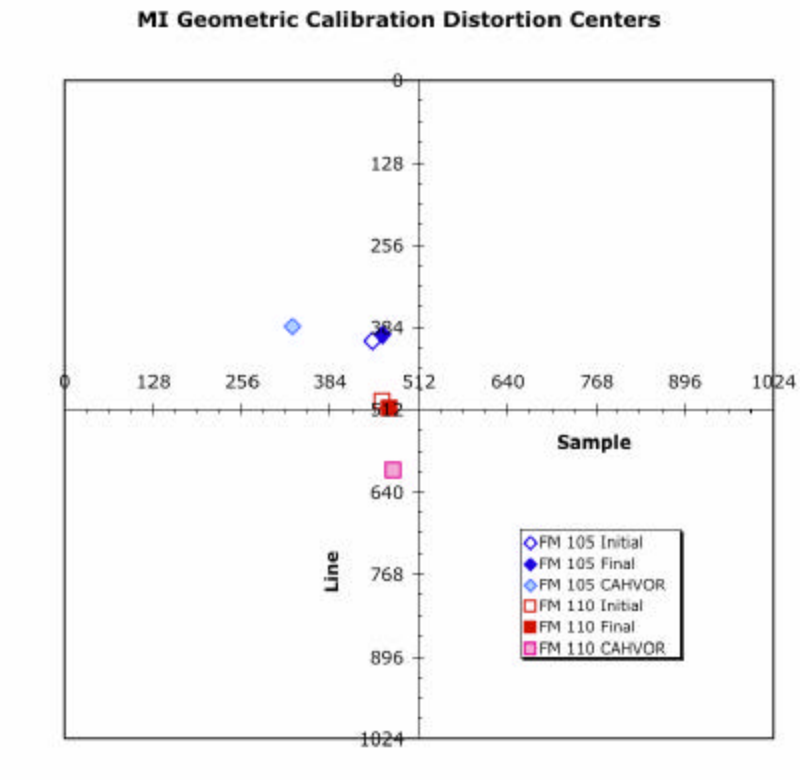

Figure 3.2.7d. Location of centers of radial distortion pattern shown in Fig. 3.2.7c.

Front Principal Point, Best Focus, Magnification, and Focal Length: The position of the front principal point (front PP, or PP_1) is estimated as part of the calibration analysis. This parameter is of somewhat less interest for operational purposes than the rear principal point (PP_2) position, but is of interest to compare with the design prescription for the camera. These values put PP_1 0.806 mm *behind* PP_2 for camera 105 and 0.520 mm in front for camera 110; the prescription value is 1.463 mm in front. These discrepancies are not alarming when it is remembered that the fitting process effectively determines the locations of the two principal points in different coordinate systems. PP_2 is located with respect to the detector plane, because its distance d_2 from this plane affects the scale of all images by an equal multiplicative factor. In contrast, PP_1 is located in the coordinate system where the camera-target separation is measured; its coordinate is the extrapolated point where the image magnification becomes infinite. The two results can thus be reconciled with one another and with the prescription separation of principal points by attributing the error instead to the location of the camera relative to the target. At the nominal camera position, the distance from detector plane to target is intended to be 100 mm. Increasing this nominal separation by 2.269 and 0.943 mm respectively for the two cameras would put the principal points at their prescription separation.

This conclusion is especially interesting in light of additional calibration results that showed the best-focus position for both cameras to be at –2.5±1 mm relative to the nominal location. This shift of best focus does not result from the apparent error in locating the camera relative to the target as described above. Instead, it must be a separate effect that works to further increase the best-focus working distance of the cameras. Combining the two effects, the estimated target-detector separation in best focus is 104.8±1 mm for MI serial # 105 and 103.4±1 mm for MI serial # 110. The fractional discrepancy between design and calibration results is much greater (4–6%) for the best-focus distance between the target and PP_1 than for the focal length (2–2.5%) or detector-PP_2 distance (1–1.2%). In summary, both cameras have longer focal lengths and smaller magnifications than the prescription, as shown in Table 3.2.7b. The parameters for the two cameras overlap within the error bars corresponding to the ±1 mm uncertainty in determining the best focus position, which are 0.075 mm in focal length, and 0.005 in magnification at best focus.

Effects of Vibration and Thermal Vacuum Testing: The MOD (post-vibration) and MOD2 (post-thermal/vac) observations were included with the initial results and the entire set of images for each camera were initially fit with a single set of parameters. As noted above, however, it was necessary to add a parameter correcting the scale of the MOD/MOD2 results in order to reconcile them with the initial results. The MOD/MOD2 images for camera 105 span a 5 mm range of camera positions compared with 24 mm for the initial images, but this was sufficient to determine whether the scale discrepancy resulted from an offset in the camera position, a change in d_2, or some combination of these effects. Changing d_2 would affect the scale of images at all positions equally, and would also affect the scale of images obtained operationally. An offset of the camera within the test apparatus, on the other hand, would have no implications for operations. It would result in greater scale changes at closer working distances (positive values of the camera position) than at longer distances, but the scatter in the residuals for individual camera positions is too large for any trend of this sort to be discerned. For MI serial # 105, adjusting the camera position gives lower residuals and more accurate image scale over the full range of camera positions. For MI serial # 110, the MOD/MOD2 camera positions were taken only over a range of 2 mm so our ability to distinguish the two effects is reduced. An adjustment of d_2 rather than camera position is required to remove the scale trend

with camera position, but this cannot be taken at face value as indicating that d_2 actually changed. The supposed scale trend (for data from only 3 camera stations) is comparable to the fluctuations in the linear fits to radial residuals from station to station seen in all the datasets. In particular, the same trend is seen in the initial data at these stations, suggesting that it is an artifact caused by small (a few micrometers) but repeatable errors in setting the camera positions. We therefore used an offset of the camera within the test apparatus to reconcile the MOD/MOD2 and initial results for both cameras.

Shifts for the MOD2 data (obtained after thermal vacuum testing) were estimated independently and found to be very similar those obtained from the post-vibration MOD data. The shift was 0.220 mm (toward the target) for serial # 105 MOD testing and 0.217 mm for MOD2. The corresponding shifts for serial # 110 are –1.019 mm and –1.028 mm (away from the target). It is not known whether errors of this magnitude in positioning the camera are plausible given the calibration apparatus, though the positional correction needed to place PP_1 in front of PP_2 suggests that they are. The shifts are considerably less than the ±3 mm depth of field or even the 1 mm spacing of camera stations, so the shift in best focus position that they would induce are too small to be observed.

Having reconciled the initial, MOD, and MOD2 data for each camera in order to combine them in a single fit, we next investigated the similarity of separate fits to the initial and final (MOD2) data. The results for these separate fits are shown in Table 3.2.7b. The primary differences are a change of <0.02 pixel in the radial distortion solution (Fig. 3.2.7c) and a 15–20 pixel shift in the distortion center (Fig. 3.2.7d). The rear principal point position (and focal length, etc.) for serial # 105 was unchanged, whereas that for serial # 110 changed by 0.004 mm, or only 0.014%. Given the possibility that the optical elements of the microscopic imagers could have been displaced slightly during vibration and thermal vacuum testing, we recommend that the final (MOD2) results be used to model the inflight data. The changes in the spatial distribution of residuals seen in Fig. 3.2.7b support this conclusion that the differences are real. It is possible that the rigors of the mission have induced additional changes in the MI optics. If so, the magnitude of these changes would be expected to be similar, with deviations from the available optical model <<0.1 pixel. The practical ability to coregister images and make stereo elevation models, which rest on matching image features with typically 0.2 pixel precision, should not be affected by such changes.

A more significant concern is raised by the inferred changes in camera position between the initial and MOD/MOD2 calibration observations. These changes have no impact per se on the camera parameters determined, but if all camera positions were to contain an absolute position error of the same magnitude (~1 mm) as the inferred shift, then the overall image scale could be in error by 1.3%. Given an absolute error as large as the 2.3 mm shift needed to reconcile the principal point separation with its prescription value, a 3% scale error could result. Although such a scale error would be frustrating to our desire to calibrate the microscopic imagers to subpixel accuracy, it must be admitted that an overall misstatement of the size of features on Mars by even 3% would have negligible scientific consequences.

Comparison with JPL CAHVOR Fits: CAHVOR (Yakimovsky and Cunningham, 1978; Gennery, 2001) models of the MI flight cameras were converted to the conventional photogrammetric notation used here (*cf.* Di and Li, 2004) and compared to our results. Because the MER camera model master list contains multiple CAHVOR models for each instrument, the highest-numbered models for each camera (ID 172/173 for serial # 105, ID 87/88 for serial # 110) were selected. In each case, the pair of fits given for the MI cover in the open and closed

position were strictly identical because calibration data were taken in only one cover position for each camera.

The parameters to be compared consist of the "focal length" (rear principal point distance), radial distortion pattern, and center of radial distortion. The CAHVOR model includes an estimate of the camera (*i.e.*, front principal point) position, but this cannot be directly compared to our results because the calibration setup is different. CAHVOR also includes parameters that describe where the perpendicular to the detector through the rear principal point (not necessarily the same as the optic axis) intersects the focal plane. The nominal position at the frame center was used for the principal point position in our models. The principal point was found to be ~19 pixels from the frame center in both CAHVOR models. Focal length and magnification values could not be derived from the CAHVOR models for comparison because the working distance at best focus was not known.

We "balanced" the CAHVOR-derived optical distortion models by adjusting the C_1 term to give equal and opposite extreme errors as described above, and made the corresponding correction to the "focal length". The resulting calibrated rear distance values are respectively 0.23% greater and 0.06% less than our best estimates. The two redundant estimates of focal length, obtained from the H and V vectors of the CAHVOR models, differed by about 0.1% for each camera, so these models are consistent with our results at about the level of their own internal consistency. An alternative explanation for the discrepancy involves small errors in the assumed camera-target distance in the JPL models, leading to proportional errors in the inferred focal length. A systematic offset of <0.2 mm in the distance between the target and front principal point could account for the difference; because the CAHVOR models are base on in-focus images that span a limited range of camera distances, an error of this magnitude would be difficult to detect.

The balanced radial distortion functions obtained from the CAHVOR models are shown in Fig. 3.2.7c. The sense of the distortion (negative or barrel) agrees with our models. The maximum distortion for serial # 105 is about 160% greater than for our model (0.6 vs 0.22 pixel) and occurs closer to the image center. The peak distortion for serial # 110 is only about 36% greater than our model but occurs closer to the image edge. The different shapes of the distortion models are not by themselves surprising, since the CAHVOR model includes a fifth-order term in the distortion model that was not included in the USGS fits. The differences between the two distortion models for each camera approach ±0.4 pixels, however, which greatly exceeds the scatter in radial residuals to our fits. Thus, if radial distortion as described by the CAHVOR models had actually been present in the images used here, our radial residuals would have shown unambiguous departures from a pure cubic distortion model. The reason for the difference in recovered distortion functions is not understood. We speculate that the CAHVOR models may be biased because of the different spot target used, which consisted of several concentric zones with different spot sizes and spacings. Even a small error in knowledge of the spot spacings for the different zones could result in an apparent radial distortion.

Given the level of discrepancy between our radial distortion functions and those from the CAHVOR models, and, more importantly, the small amount of total distortion in either type of model, the agreement for the center of radial distortion is good. The coordinates in Table 3.2.7a are plotted in Figure 3.2.7d. For each camera, our distortion center agrees with the CAHVOR results to <20 pixels in one direction but only to ~100 pixels in the orthogonal direction. Our fits to initial and final data for each camera are consistent to 15 pixels or less.

3.2.7.5 Accuracy and Relationship to Requirements

When locations of the calibration target "spots" were measured automatically and fitted with a relatively simple physical model, 2D RMS residuals of ~0.02–0.03 pixel were obtained. Radial distortion is less than ±0.33 pixel for both cameras and was estimated to 0.03 pixel or better. The distortion is negative (barrel distortion).

The calibrated rear principal point distance (which is used in place of "focal length" in close-range photogrammetric calculations) was on the order of 1% greater than the prescription value. The best-focus working distance was found to be 4–6% longer than its prescription value, resulting in slightly longer focal lengths and smaller magnifications than nominal.

The robustness of the calibration was compromised slightly by doubly reflected light visible through the calibration target spots. This effect acts to bias the apparent position of spots away from the optical axis. The calibration results reported here had the influence of reflected light minimized by clipping the images and by examining the systematic variation of fit results with the radius (in the image plane) of data included in the fits. The residual effects of the reflections on spot position are estimated to be at most 0.007 pixel and to vary weakly with radius, so that the systematic effect on the recovered camera models is believed to be <<0.01 pixel.

Changes in apparent image scale after vibration testing appear to result from 0.2–1 mm errors in positioning the cameras. The alternative explanation that they are due to changes in the rear principal point distance can be ruled out with certainty for MI serial # 105 and with somewhat less certainty for serial # 110. Nevertheless, if the *absolute* previbration camera-target distances are in error by an amount comparable to the postvibration change or the discrepancy between the prescription and estimated PP_1-PP_2 distance, the recovered rear principal point distance and hence image scale could be in error by as much as 3%.

Our calibration results agree with JPL CAHVOR models at the ~0.4 pixel level or better. The calibrated, CAHVOR-derived rear principal point distances are 0.2–0.6% greater than our values, plausibly as the result of small errors in the assumed camera-target distance. The CAHVOR-derived radial distortion models have the same sign but larger maximum distortion and differ in detailed shape (by including a higher-order term). The estimated centers of distortion differ by ~100 pixels.

Such accuracies are consistent with Level 2 requirement #921 (image coregistration) and Level 3 requirement #1184 (IFOV).

3.2.8 Bar Target Imaging

3.2.8.1 Purpose and Description

Determine the depth of field (defocus blur) and camera modulation transfer function (MTF) by imaging a bar/edge target at various distances from the camera, including best focus. The MTF evaluates the ability of imaging systems to capture spatial detail and preserve the detail. The spatial detail can be measured in line pairs per millimeter (lp/mm) and evaluating MTF includes using either bar targets with square or sine wave patterns or the use of edge images. For bar targets the wave patterns alternates between dark and light sections. The modulation is dependent upon the difference in the light intensity of the light and dark sections. The modulation transfer is dependent upon the output modulation captured by the imaging system and input modulation. For the lower frequency data the amplitude of the modulation transfer tends to be 1.0, which means that all the input modulation was preserved by the imaging system. As the frequency of the bar pattern increases the modulation transfer tends to approach zero.

3.2.8.2 Test Procedure

See section 3.2.7.2 above. The bar/edge target (Fig. 3.2.8a) was observed at distances ranging from -12 to +12 mm about best focus in 1 mm steps. MI serial # 105 images obtained prior to vibration and thermal/vacuum testing are referred to as **MI_105** images. MI 105 images obtained after vibration testing but before thermal/vacuum testing are referred to as **MI_MOD1_105** images. MI 105 images obtained after the thermal/vacuum tests are referred to as **MI_MOD2_105** images. A similar scheme is used below for the MI serial # 110 images.

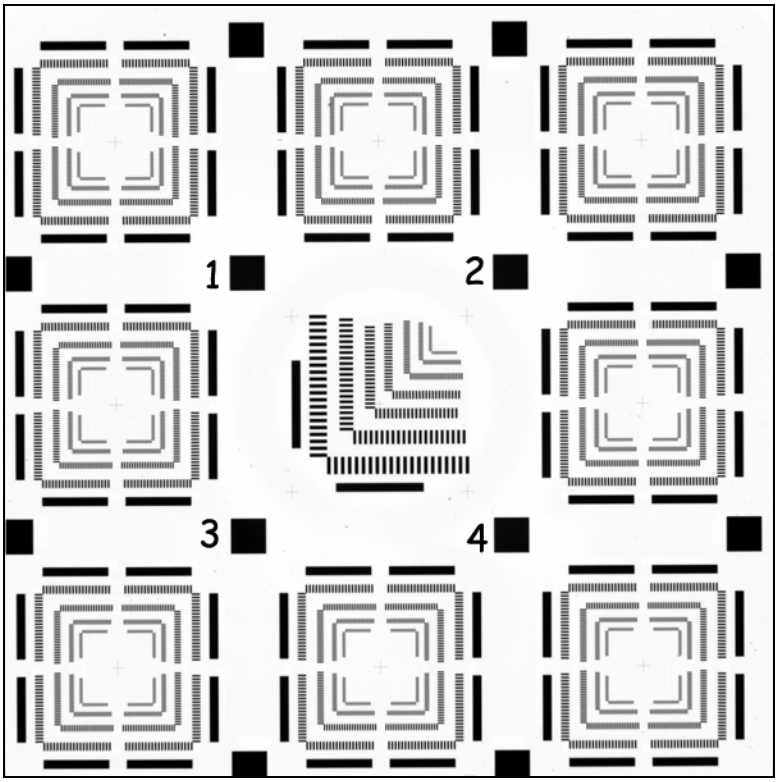

Figure 3.2.8a. Bar Target Image – numbers added to show location of sub-images (actual size is 1024 lines by 1024 samples)

Table 3.2.8a lists the distances (between target and CCD, in mm) and positions (relative to nominal best focus, in mm) at which images were obtained. MOD1 data were acquired after vibration testing, and MOD2 data were acquired after thermal/vacuum testing.

Table 3.2.8a. Images obtained at positions denoted by **X**

Dist.	Position	MI_105	MI_MOD1_105	MI_MOD2_105	MI_110	MI_MOD1_110	MI_MOD2_110
112	-12	**X**			**X**	**X**	
108	-8	**X**			**X**	**X**	
106	-6	**X**	**X**		**X**	**X**	**X**
105	-5	**X**	**X**	**X**	**X**	**X**	**X**
104	-4	**X**	**X**	**X**	**X**	**X**	**X**
103	-3	**X**	**X**	**X**	**X**	**X**	**X**
102	-2	**X**	**X**	**X**	**X**	**X**	**X**
101	-1	**X**	**X**	**X**	**X**	**X**	**X**
100	0	**X**	**X**	**X**	**X**	**X**	**X**
99	1	**X**	**X**		**X**	**X**	
98	2	**X**	**X**		**X**	**X**	
97	3	**X**			**X**		
96	4	**X**			**X**		
95	5	**X**			**X**		
94	6	**X**			**X**	**X**	
92	8	**X**			**X**		
88	12	**X**			**X**	**X**	

3.2.8.3 Environmental Conditions

Ambient temperature and pressure.

3.2.8.4 Data Processing and Products

The Vicar Application Program OTF1 determines the Modulation Transfer Function (MTF) by using one-dimensional Fast Fourier Transformations to compute the Optical Transfer Function (OTF) from degraded edges in images. The modulus of the OTF is the MTF. The program provides tabulated output of the spatial frequency in cycles/sample and the amplitude of the MTF. By providing a scaling factor the cycles/sample were converted to cycles/mm.

For input into the OTF1 program sub-images were extracted that contained the edge information needed for the program (Fig. 3.2.8b). The bar target pattern had large squares as part of the images. Sub-images of 21 lines and 64 samples were made of each of the 4 large black squares near the center of the image (see Fig. 3.2.8a).

Figure 3.2.8b. Example of a sub-image used for testing (actual size is 21 lines by 64 samples)

To obtain the scaling factor between cycles/sample and cycles/mm we need to determine the Nyquist Limit of the camera system. In sampling theory a sample should be obtained at twice the frequency of the highest waveform frequency. For a digital imaging system

the highest frequency that can be captured would be by using 2 pixels, one to capture the light part of the bar pattern and the other pixel to capture the dark pattern. For the MI the pixel pitch is 12 microns so the limit is 24 microns per cycle or 41.667 cycles/mm at the detector.

The optical system magnifies the image and changes the Nyquist Limit of the camera. To determine the magnification factor the following formula was used:

$$MAG = (PP2 – FP) / (T - PP1),$$

where MAG is the magnification factor, PP1 is the front principle point, PP2 is the rear principal point, FP is the focal plane position, and T is the distance to the target. Based on initial estimates of the camera geometry the front principal point is at 27.68 mm, the rear principal point is at 28.486 mm, and the focal plane is at 0 mm. The Nyquist limit at various distances is given by multiplying the CCD Nyquist limit by the magnification factor. Table 3.2.8b provides the magnification and Nyquist limit in cycles/mm at various distances to the target for MI serial # 105. Table 3.2.8c provides the magnification and Nyquist limit in cycles/mm at various distances to the target for MI serial # 110. In both tables, distances are given relative to the nominal best focus position, 100 mm from the CCD, with negative positions being farther from the camera, positive positions being nearer to the camera.

Table 3.2.8b. Magnification factor and Nyquist Limit for MI 105

T-PP1	Position	Magnification	Cycles/mm
84.32	-12	0.33783	14.076
80.32	-8	0.35466	14.777
78.32	-6	0.36371	15.155
77.32	-5	0.36842	15.351
76.32	-4	0.37324	15.552
75.32	-3	0.37820	15.758
74.32	-2	0.38329	15.970
73.32	-1	0.38852	16.188
72.32	0	0.39389	16.412
71.32	1	0.39941	16.642
70.32	2	0.40509	16.879
69.32	3	0.41093	17.122
68.32	4	0.41695	17.373
67.32	5	0.42314	17.631
66.32	6	0.42952	17.897
64.32	8	0.44288	18.453
60.32	12	0.47225	19.677

Table 3.2.8c. Magnification factor and Nyquist Limit for MI 110

T-PP1	Position	Magnification	Cycles/mm
82.97	-12	0.34362	14.317
78.97	-8	0.36102	15.043
76.97	-6	0.37040	15.433
75.97	-5	0.37528	15.637
74.97	-4	0.38028	15.845
73.97	-3	0.38542	16.059
72.97	-2	0.39071	16.279
71.97	-1	0.39613	16.506
70.97	0	0.40172	16.738
69.97	1	0.40746	16.977
68.97	2	0.41337	17.224
67.97	3	0.41945	17.477
66.97	4	0.42571	17.738
65.97	5	0.43216	18.007
64.97	6	0.43881	18.284
62.97	8	0.45275	18.865
58.97	12	0.48346	20.144

Images were converted from PDS to ISIS format using the ISIS program PDS2ISIS and most of the image processing was performed in ISIS. The sub-images were converted from ISIS to VICAR format using ISIS2VICAR and were used as input into the VICAR OTF1 Application program.

Flat Field Processing: Images of the integrating sphere were taken without the bar/edge target in place to allow flat field variations to be corrected. To account for the transfer smear and dark current that is present in all images captured by the MI, images of the integrating sphere were taken with zero and at a set amount of exposure time. The zero exposure time images were averaged together and saved. The names of the saved images and values for the histograms are given in Table 3.2.8d.

Table 3.2.8d Filenames and histogram values for zero exposure flat fields

Filename	Minimum	Maximum	Average	St Dev
MI105flat0nocover	45.0	3289	204.1	94.1
MI105_MOD1_flat0nocover.cub	44.5	4095	196.3	92.9
MI105_MOD2_flat0nocover.cub	45.0	4095	201.2	97.5
MI110flat0nocover.cub	35.0	4095	167.6	85.9
MI110_MOD1_ flat0nocover.cub	34.3	3947	182.2	94.7
MI110_MOD2_ flat0nocover.cub	34.8	4095	174.4	96.1

The average flat field with zero exposure time (Table 3.2.8d) was subtracted from the average of the images of the flat fields taken with a set exposure time and the image saved. The names of the saved images and the values for the images histogram are given in Table 3.2.8e. Note that in Table 3.2.8d the maximum values for MOD1 and MOD2 images are 4095 and in Table 3.2.8d the minimum values for MOD1 and MOD2 images are 0. This is due to about 20 pixels in the first and last column of the zero exposure time flat fields having values of 4095. After the subtraction the pixel values are 0. The average of the central 101 x 101 pixels was

calculated for each of the resulting images in Table 3.2.8e, then each file was divided by this average. The result was saved and used to normalize the bar targets and remove the dark current noise from the bar target images. The average and standard deviation of the central 101 x 101 pixels are given in Table 3.2.8f. Table 3.2.8g shows the resulting image filenames and their statistics.

Table 3.2.8e. Filenames and histogram values for flat field images with transfer smear removed

Filename	Minimum	Maximum	Average	Standard Deviation
MI105avgflat.cub	806.5	3936.8	2424.7	105.7
MI105_MOD1_avgflat.cub	0	3941	2483.7	108.2
MI105_MOD2_avgflat.cub	0	3931.1	2440.96	106.9
MI110avgflat.cub	0	3942.8	2161.0	101.6
MI110_MOD1_avgflat.cub	147.7	3950.7	2435.4	103.7
MI110_MOD2_avgflat.cub	0	3946.0	2161.0	102.1

Table 3.2.8f. Statistics for central 101 x 101 pixels

Filename	Average	Standard Deviation
MI105avgflat.cub	2534.6	72.1
MI105_MOD1_avgflat.cub	2597.6	74.6
MI105_MOD2_avgflat.cub	2553.4	72.8
MI110avgflat.cub	2247.4	62.5
MI110_MOD1_avgflat.cub	2534.2	70.8
MI110_MOD2_avgflat.cub	2248.1	62.8

Table 3.2.8g. Statistics for average flat field images

Filename	Minimum	Maximum	Average	Standard Deviation
MI105avgflatnocover.cub	0.318	1.533	0.957	0.042
MI105_MOD1_avgflatnocover.cub	0	1.517	0.956	0.041
MI105_MOD2_avgflatnocover.cub	0	1.540	0.956	0.042
MI110avgflatnocover.cub	0	1.754	0.962	0.045
MI110_MOD1_avgflatnocover.cub	0.058	1.559	0.961	0.041
MI110_MOD2_avgflatnocover.cub	0	1.755	0.961	0.045

The average flat field images for the MI_105, MI_MOD1_105, and MI_MOD2_105 are nearly identical. Similarly, the average flat field images for the MI_110, MI_MOD1_110, and MI_MOD2_110 are nearly identical. The only exception is the minimum values. This is caused by a few pixels in the first and last columns of some of the zero exposure flat fields images (Table 3.2.8d) having larger maximum values than the MI_105 or MI_MOD1_110 images. When these images are subtracted from the average flat fields with a nonzero exposure time the resulting images in Table 3.2.8e have lower minimum values. Since these pixels are in the first and last column, they have no effect on the MTF analysis.

Images of the bar target were obtained with zero and a finite exposure time. To correct for the transfer smear the average of the zero exposure time images was subtracted from the average of the images with a finite exposure time. Taking the average increased the signal-to-noise ratio in the images. An exception was that for the MI_MOD1_105 images there were not multiple exposures so there was no need to average the images. The transfer-smear-corrected images were divided by the appropriate flat field image in Table 3.2.8g and saved. For each resulting image 4 sub-images were obtained; one sub-image for each of the 4 central dark squares in the bar target images (Fig. 3.2.8a).

MTF Processing: The sub-images were transferred to a JPL computer so the VICAR OTF1 Application program could be used to compute the MTF. The VICAR help function provides the following description of the otf1 program:

> PURPOSE:
> OTF1 is a VICAR applications program which performs one-dimensional Fast Fourier Transformations in order to compute Optical Transfer Functions (OTF) from degraded edges in images or from either a tabulated real function, or a line spread function using parameter inputs. OTF1 is able to compute the entire optical transfer function (not just the MTF) from digital picture data with greater accuracy and ease than other methods available. This technique for computing imaging system MTF's is preferable to previously used techniques which involved the imaging of sine wave targets.

The OTF1 tabular output file for each sub-image was saved and transferred back to USGS computers in Flagstaff. For each camera position (Table 3.2.8a) at which images were obtained a plot was produced to show the MTF for each sub-image, the average of the 4 sub-image MTFs, and the standard deviation of the 4 MTFs (Appendix L). For each image sequence the averages of the 4 sub-images at each image position were plotted together (Figures 3.2.8c,d and Appendix L). Finally, plots (Figures 3.2.8e,f) were produced to show the MTF amplitude at 8 and 14 cycles/mm for each image sequence where images were obtained at common image positions. The 8 cycles/mm position was chosen because the variances in the MTF curves at this position were low and there were noticeable differences in the MTF. The 14 cycles/mm position was chosen because it was in common with all camera positions and it avoids the regions of the curves where large variances and noise can be seen.

Figure 3.2.8c shows the average of MTF curves from the 4 sub-images that were taken from each MI 105 image at the different positions. Images taken 102 and 103 mm from the target (positions -2 and -3) have the highest MTF and are shown as dashed and solid black lines respectively. The MTFs are symmetrical about these curves in that the MTF for images taken 101 and 104 mm from the target are similar (positions -1 and -4; dashed and solid orange lines). The MTF for images taken 100 and 105 mm from the target are similar (positions 0 and -5; dashed and solid yellow lines). The MTF for images taken 99 and 106 mm from the target are similar (positions +1 and -6; dashed and solid green lines). The MTF for images taken 97 and 108 mm from the target are similar (positions +3 and -8; dashed light green line and solid blue line). The MTF for images taken 94 and 112 mm from the target are similar (positions +6 and -12; double dashed yellow line and solid green line).

Figure 3.2.8d shows the average of MTF curves from the 4 sub-images that were taken from each MI 110 image at the different positions. Images taken 103 mm from the target (position -3) have the highest MTF and are shown as solid black line. The MTFs for images taken 102 and 104 mm from the target (positions -2 and -4; dashed black line and solid orange line) are quite similar to the MTF for images taken 103 mm from the target. MTFs for images taken 101 and 105 mm from the target are similar (positions -1 and -5; dashed orange line and solid yellow line). MTFs for images taken 100 and 106 mm from the target are similar (positions 0 and -6; dashed yellow line and solid green line). MTFs for images taken 98 and 108 mm from the target are similar (positions +2 and -8; dashed and solid blue lines). MTFs for images taken 94 and 112 mm from the target are similar (positions +6 and -12; double dashed yellow line and solid green line).

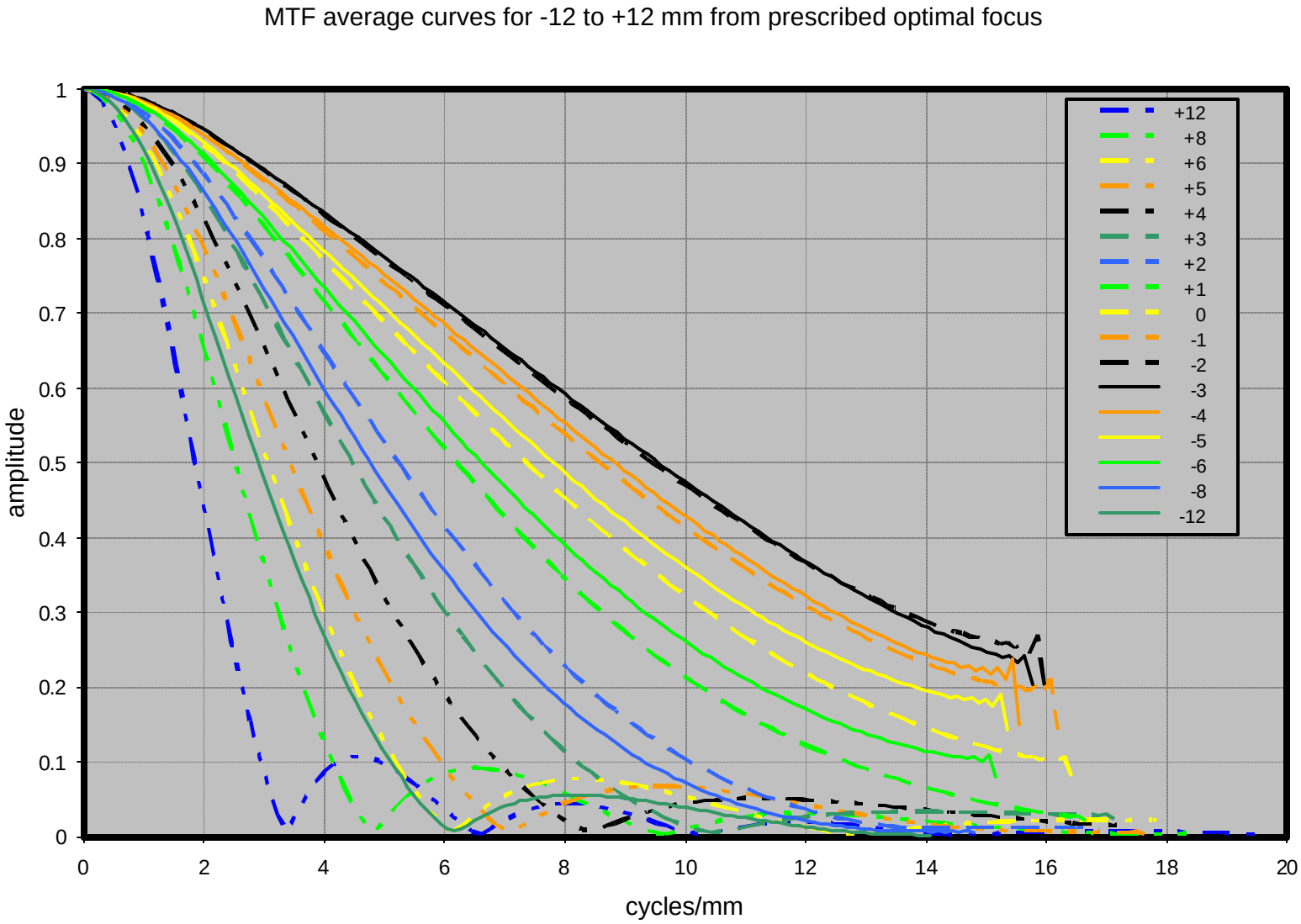

Figure 3.2.8c. Average MTF curves for MI_105 image sequence. Each curve shows data for positions (in mm) relative to target distance from CCD of 100 mm.

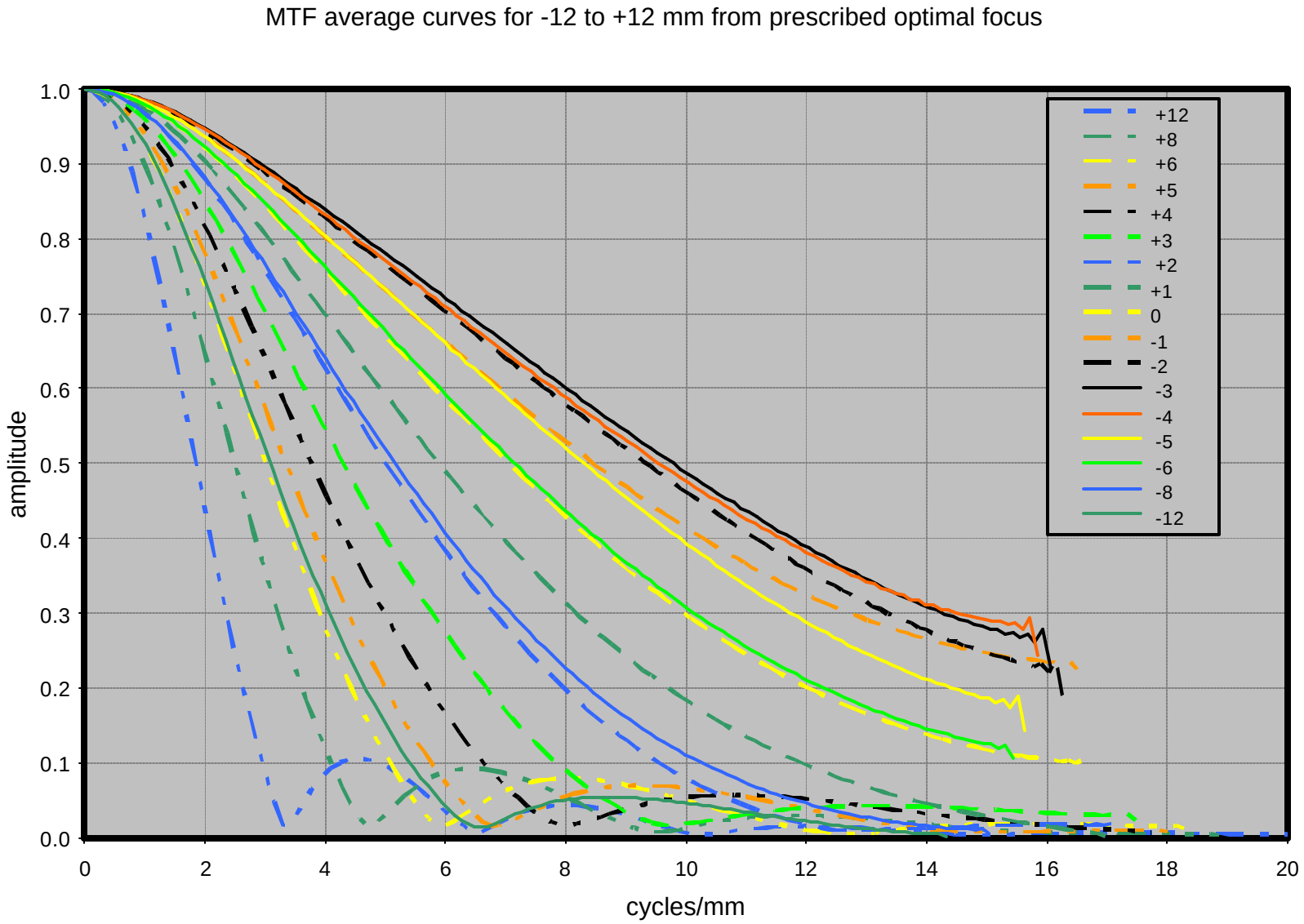

Figure 3.2.8d. MTF average curves for MI_110 image sequence. Each curve shows data for positions (in mm) relative to target distance from CCD of 100 mm.

In some of the MTF curves, at the higher frequencies, there are wiggles, a spike and then a large drop off. These artifacts are probably caused by the Fourier transform that was used to calculate the MTF.

In general the highest MTF responses were obtained when the target was 102 or 103 mm (positions -2 or -3) from the CCD. Figures 3.2.8e and 3.2.8f show the average and the standard deviation of the MTF for the 4 sub-images obtained at different positions and for the different image sequences. An average and standard deviation of the amplitude of the MTF at 8 and 14 cycles/mm in the 4 sub-images from an image obtained during the different image sequences and at different positions relative to the nominal best focus (-5, -4, -3, -2 -1, and 0). The averages are plotted as curves for 8 and 14 cycles/mm and for the different images sequences. The standard deviations are plotted as error bars. The three curves at 8 cycles/mm are consistent and are practically identical. The peak of the curve is when the target is about 102.5 mm from the CCD for MI 105, about 103 mm from the camera for MI 110. The error bars are similar at all positions. According to the optical design, the front of the optics (sapphire window) is 37.1 mm from the CCD, so the best focus target distance is about 66 mm from the front of the optics.

The three curves at 14 cycles/mm are not as consistent, do not have similar shape, and have larger error bars that vary with the image position and image sequence. The larger error bars are caused by aliasing in the images obtained at these positions. This aliasing can be seen in the individual plots for images at these positions because the plots are not near zero at the Nyquist limit and the different sub-images give different MTF plots. The error bars are generally smaller for images obtained when the target was 100, 101, and 102 mm from the CCD. Also, the error bars are smaller at these positions for images from the MI_MOD1_105 image sequence. This was the sequence that did not contain multiple exposures of the images. Taking into consideration the error bars in the curves for 14 cycles/mm, the estimates of the best MTF from the curves at 8 cycles/mm are consistent with the curves for 14 cycles/mm.
The overlap of the error bars in Figures 3.2.8e and 3.2.8f indicate that there are no significant variations in MTF due to vibration or thermal/vacuum testing.

3.2.8.5 Accuracy and Relationship to Requirements

Level 3 requirement #1188 states that the MTF of the optics must exceed 0.35 at 30 lp/mm (at the detector, equivalent to 12 cycles/mm at the target) at best focus. As shown in Appendix L, this requirement was met at the camera level.

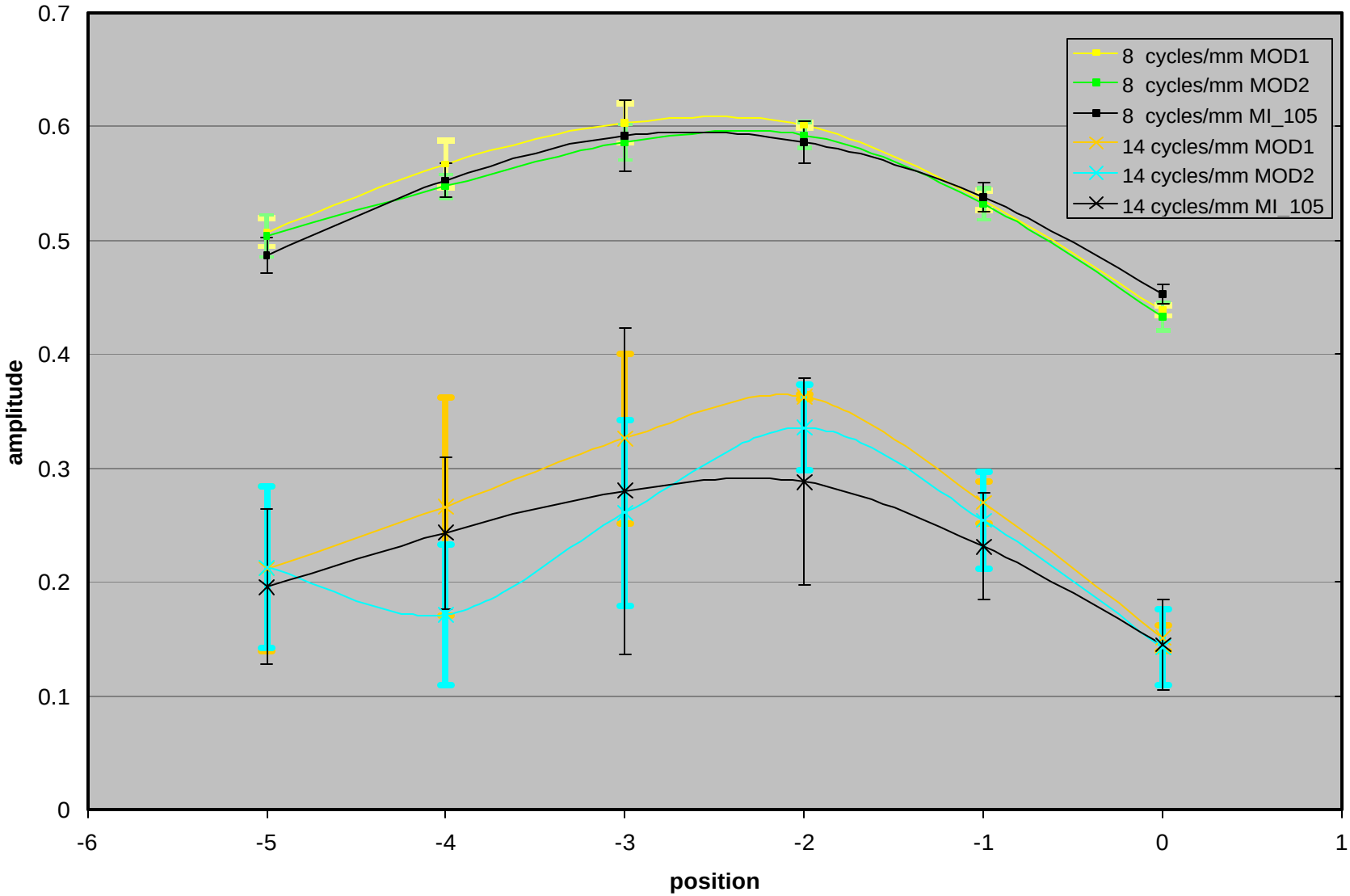

Figure 3.2.8e. Average and standard deviation of the MTF amplitude at 8 and 14 cycles/mm (selected to reduce variance) for MI serial # 105. Position is given in mm relative to the nominal best focus position, 100 mm from the CCD.

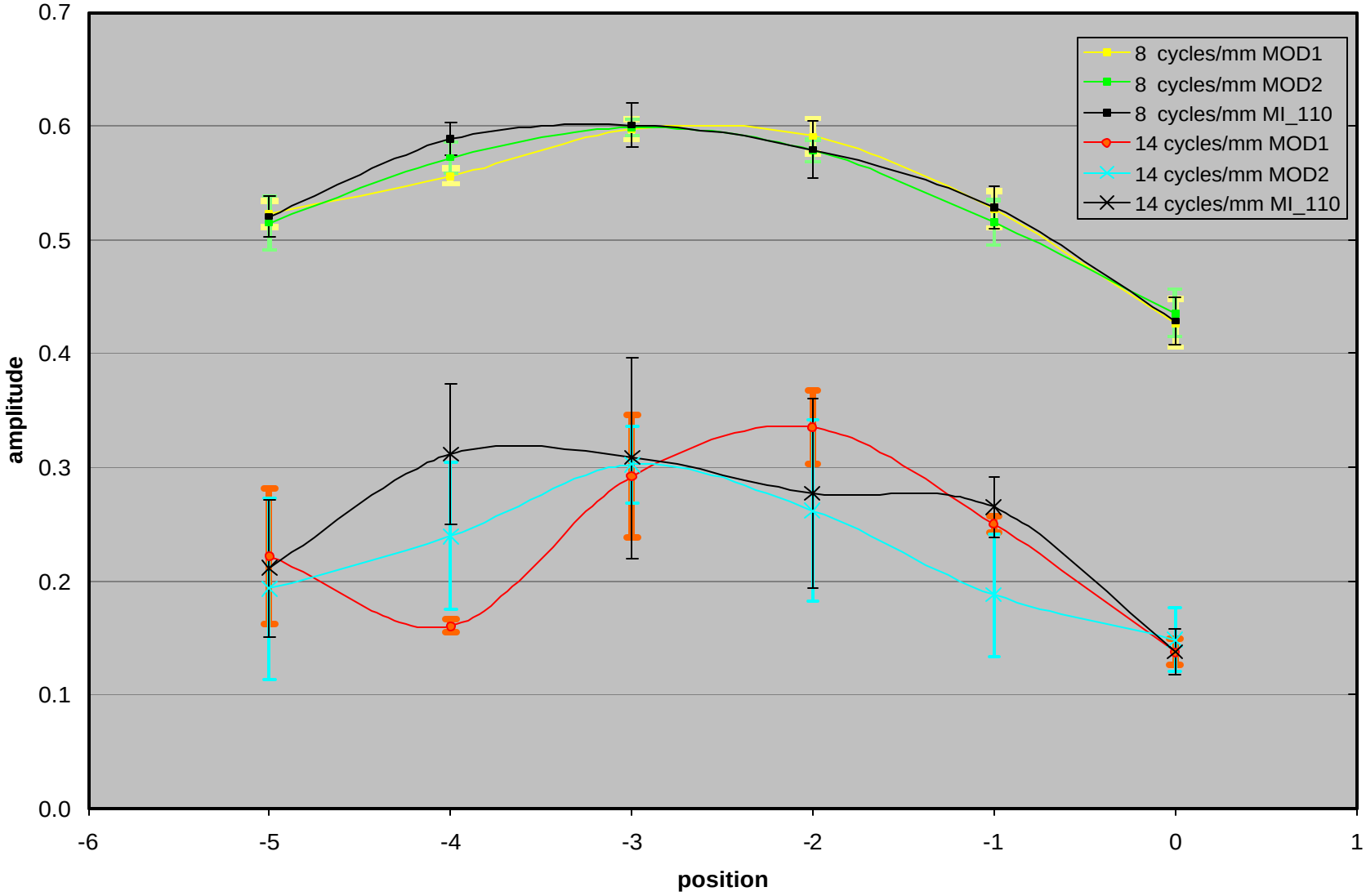

Figure 3.2.8f. Average and standard deviation of the MTF amplitude at 8 and 14 cycles/mm (selected to reduce variance) for MI serial # 110. Position is given in mm relative to the nominal best focus position, 100 mm from the CCD.

3.2.9 Scattered and Stray Light

3.2.9.1 Purpose and Description

To determine the intensity of light reaching the CCD from off-axis or internally-scattered sources (ghosts), as a function of source intensity and either distance off-axis or (for bright point-like sources) position on-axis.

3.2.9.2 Test Procedure

Images of a fiber optic were taken at exposure times that resulted in saturation when the fiber was in the field of view. The fiber was moved in 5° angular increments within and beyond the edge of field, with shutter frames taken at each location. The fiber was moved in both yaw (horizontally) and pitch (vertically) relative to the MI optical axis, in both positive and negative yaw directions but only positive pitch. The fiber was positioned near best focus for MI 105, and at a distance of ~300 mm for MI 110 testing.

3.2.9.3 Environmental Conditions

Ambient temperature and pressure.

3.2.9.4 Data Processing and Products

Zero-second images were subtracted from each image taken in the same configuration to remove transfer smear and dark current accumulated during readout. Dark current images taken on the same day at the same exposure times as the stray light images were used to subtract the dark current accumulated during the exposure of each image. The brightness of the fiber was measured at various input power levels (Appendix K), including those used for the stray light tests. These data were weighted by the MI spectral response (see section 3.2.3) in order to determine the ratio of intensities at the fiber settings used for the stray light tests. The intensity ratio was then used to determine the intensity of ghosts relative to the fiber intensity.

All MI 105 stray light images were taken with an exposure time of 71.7 msec. The maximum brightness of ghost images was measured in each image, and is expressed relative to the fiber brightness in Figure 3.2.9a for MI 105. There is no significant difference in ghost brightness between positive and negative yaw, so the absolute angle from the center of the field of view was calculated and plotted in Figure 3.2.9a. The plot also shows that there is very little difference in the intensity of ghosts between the yaw and pitch directions. When the yaw or pitch exceeds 12.3 degrees, the source is outside of the field of view of the MI. The decrease in ghost intensities with central angle does not appear to be affected by the source position being outside of the field of view. The image taken with the source closest to the center of the field of view (central angle = 1.06°) shows the greatest ghost intensity, nearly 0.1% (Fig. 3.2.9b). As shown in Figures 3.2.9c and 3.2.9d, the pattern of ghost images is rather symmetrical about the center of the field of view. When the fiber was moved outside of the MI field of view, the pattern of ghost images remained similar (Fig. 3.2.9e). Images taken with the fiber pitched upward and outside of the field of view show similar ghost patterns (Fig. 3.2.9f), indicating little dependence on the azimuth of the source.

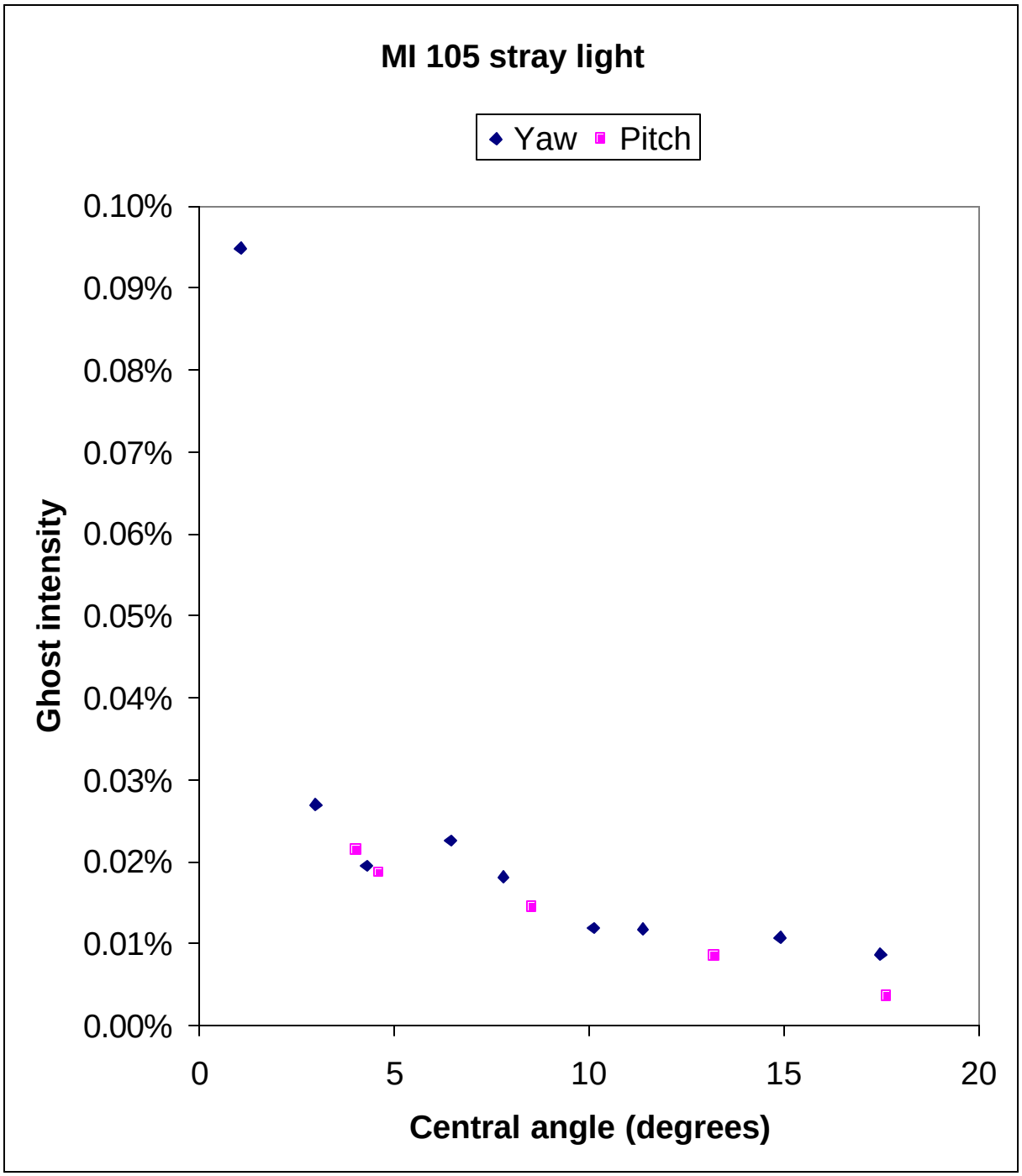

Figure 3.2.9a. Maximum intensity of ghost images in MI serial # 105, relative to intensity of fiber source.

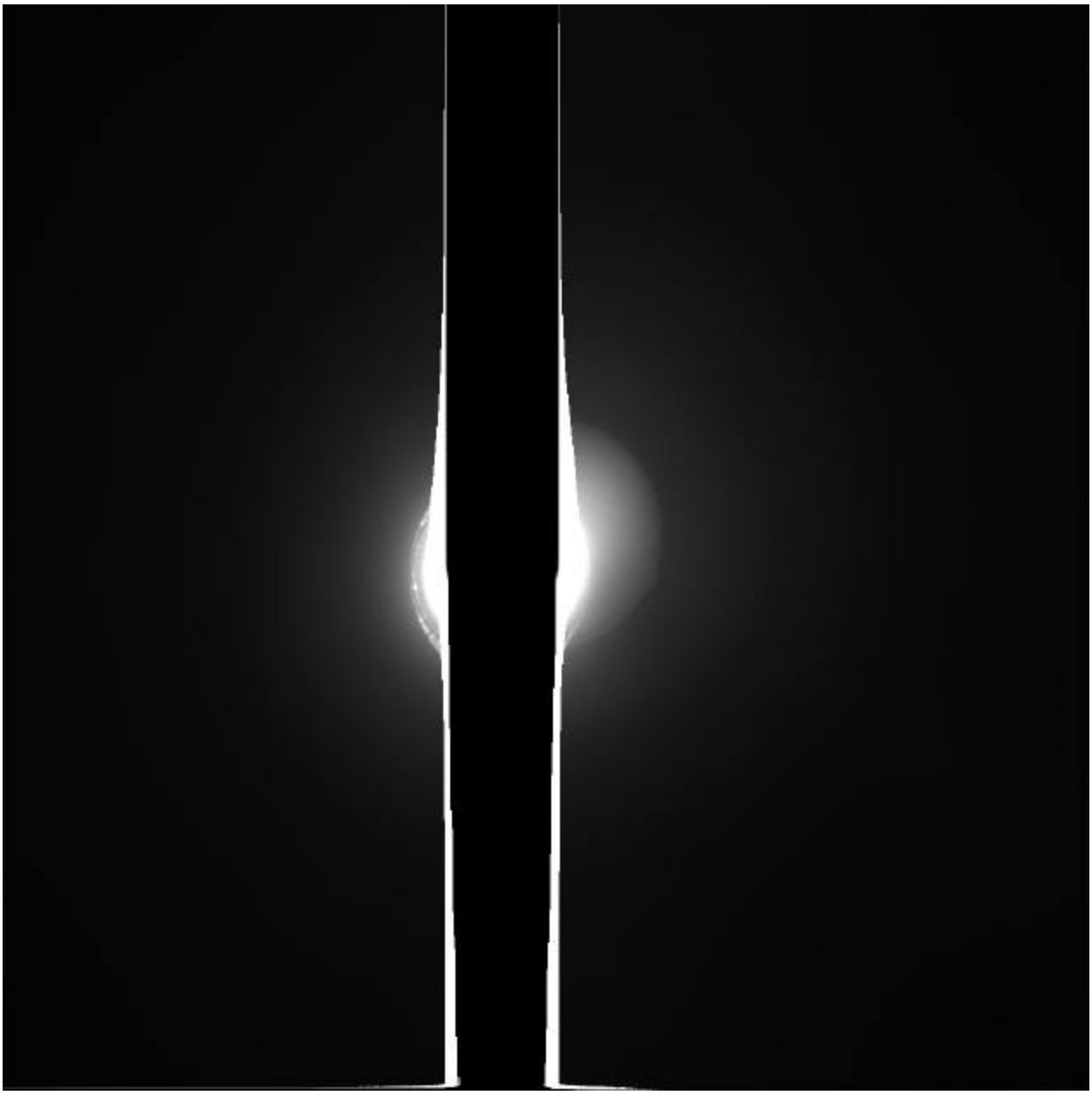

Figure 3.2.9b. Worst-case ghost image for MI serial # 105 (020718084631). Zero-exposure "shutter" frame (also saturated) was subtracted from the raw image, resulting in the column of pixels with DN = 0 at center. Hard linear stretch used to show ghost image.

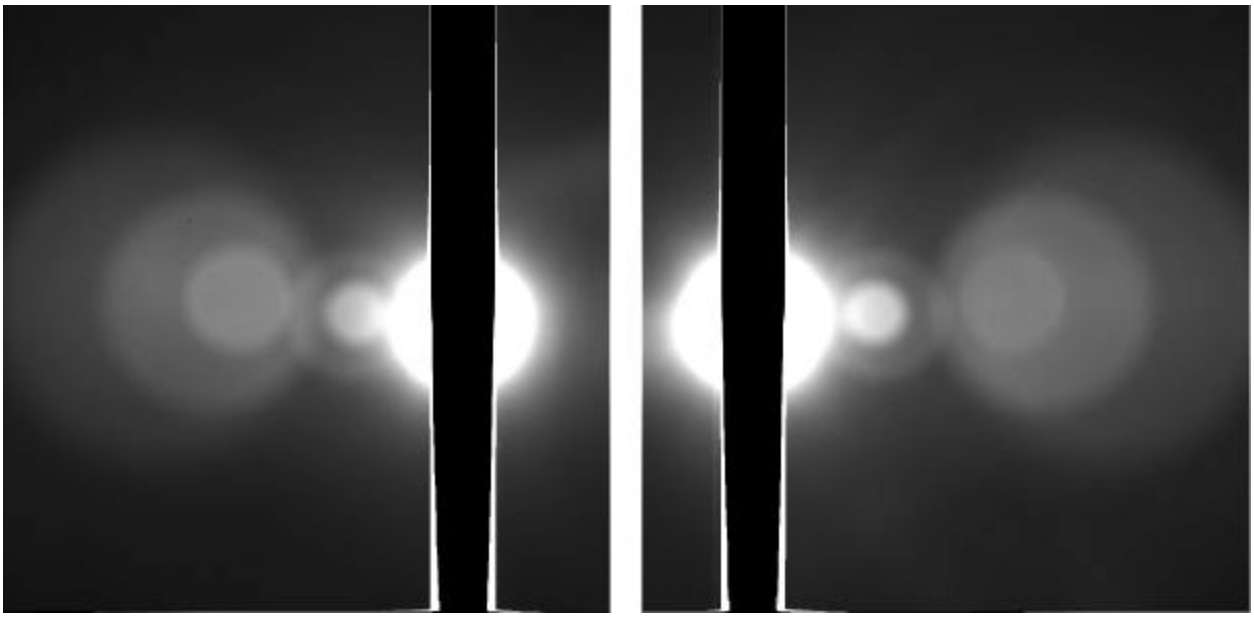

Figure 3.2.9c. Typical ghost images in MI serial # 105 images, corrected for transfer smear and stretched hard to show ghosts. Maximum ghost intensity ~0.02%. (left) Image 020718082943, yaw +6.4°. (right) Image 020718084958, yaw -7.8°.

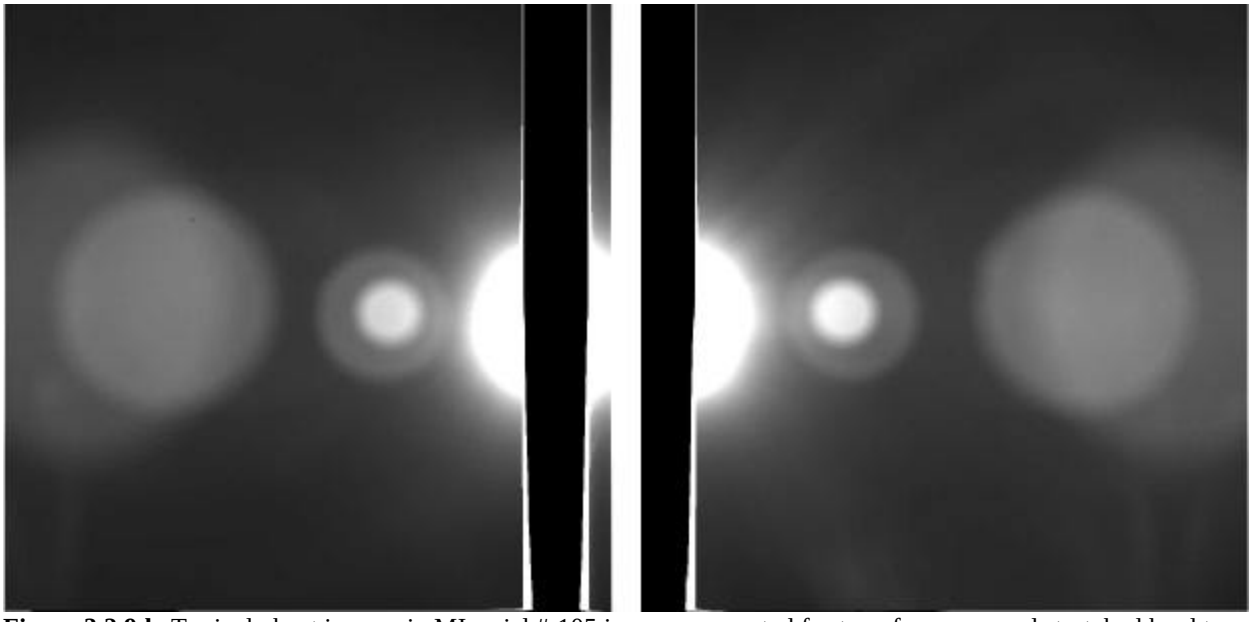

Figure 3.2.9d. Typical ghost images in MI serial # 105 images, corrected for transfer smear and stretched hard to show ghosts. Maximum ghost intensity ~0.01%. (left) Image 020718083140, yaw +10.1°. (right) Image 020718085123, yaw -11.4°.

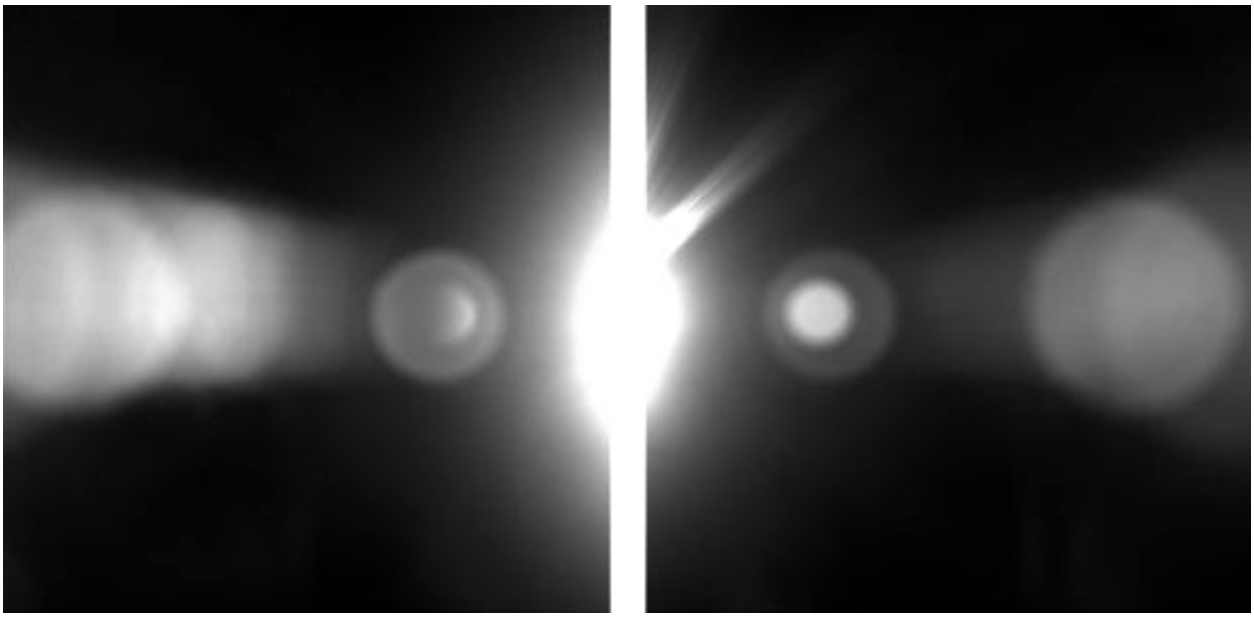

Figure 3.2.9e. Typical ghost images in MI serial # 105 images, corrected for transfer smear and stretched hard to show ghosts. Maximum ghost intensity ~0.01%. (left) Image 020718083748, yaw +17.5°. (right) Image 020718085232, yaw -14.9°.

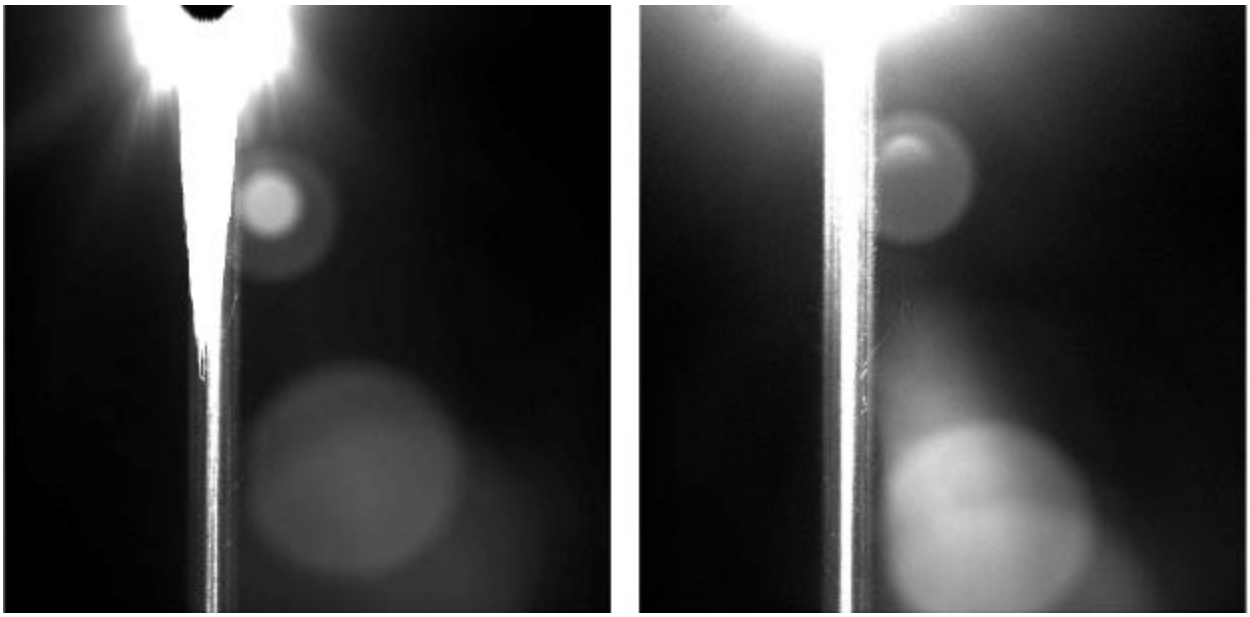

Figure 3.2.9f. Ghost images in MI serial # 105 images taken with fiber source moved upward out of frame, corrected for transfer smear and stretched hard to show ghosts. Ghost intensity less than 0.01%. (left) Image 020718090836, pitch ~12.6°. (right) Image 020718091102, pitch ~17.2°.

MI 110 stray light tests did not include any changes in the pitch of the fiber source, but extended up to 45° in yaw. All MI 110 stray light images were taken with an exposure time of 450.6 msec. As for MI 105, the intensity of the ghosts is always less than 0.1%, and typically much less. Figure 3.2.9g summarizes the results of the ghost analysis for MI 110. The ghost intensity is symmetric about the optical axis. The brightest ghost is again seen at the lowest scattering angles when the fiber is near the center of the field of view (Fig. 3.2.9h). The pattern

of ghosts is similar when the fiber is moved outside of the field of view (Fig. 3.2.9i). Overall, the results for MI 110 are very similar to the results for MI 105, with somewhat more streaks of stray light around the source in the MI 110 images.

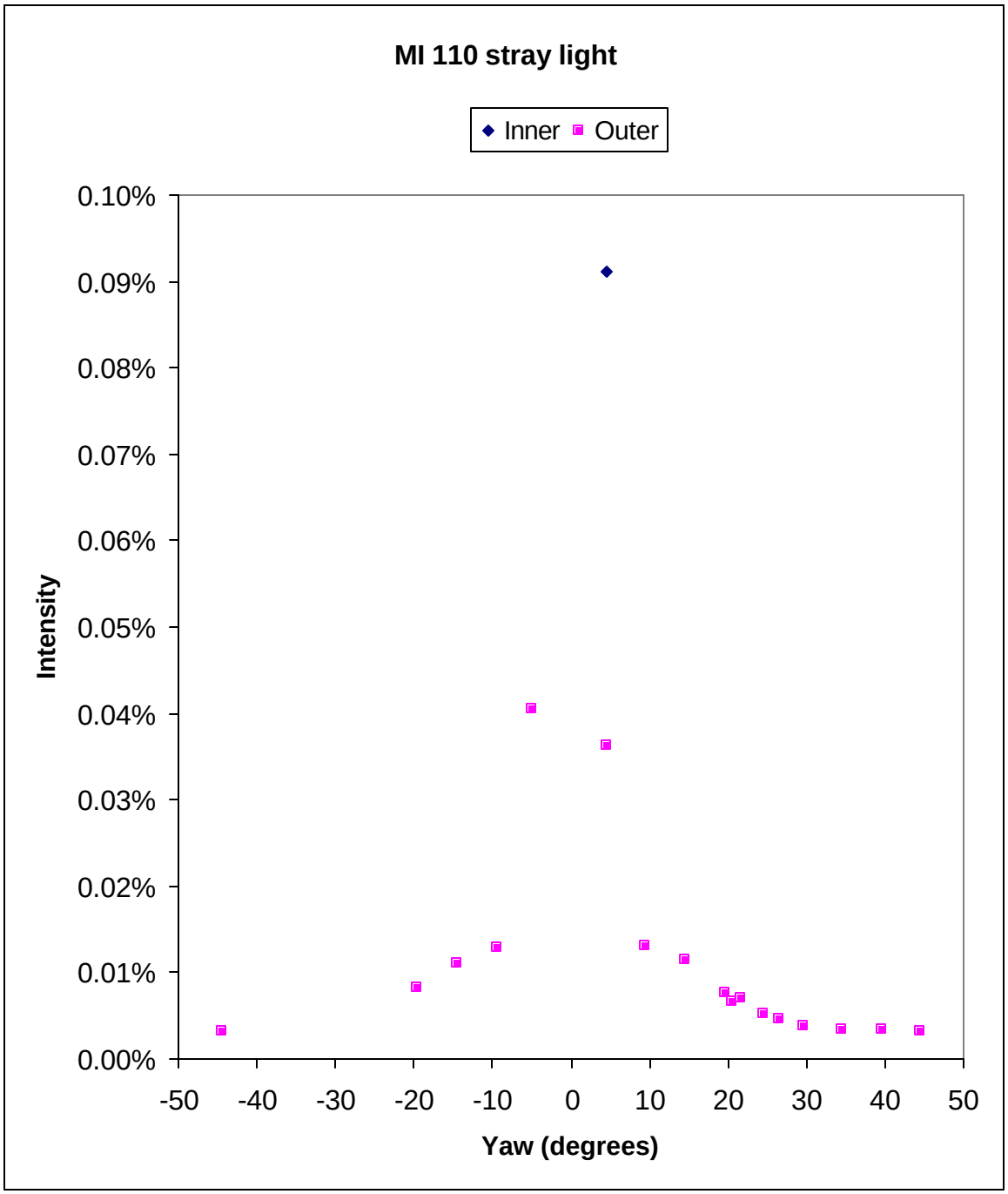

Figure 3.2.9g. Maximum intensity of ghost images in MI serial # 110, relative to intensity of fiber source. The "inner" data point is for the brightest ghost, show in the left image of Figure 3.2.9h.

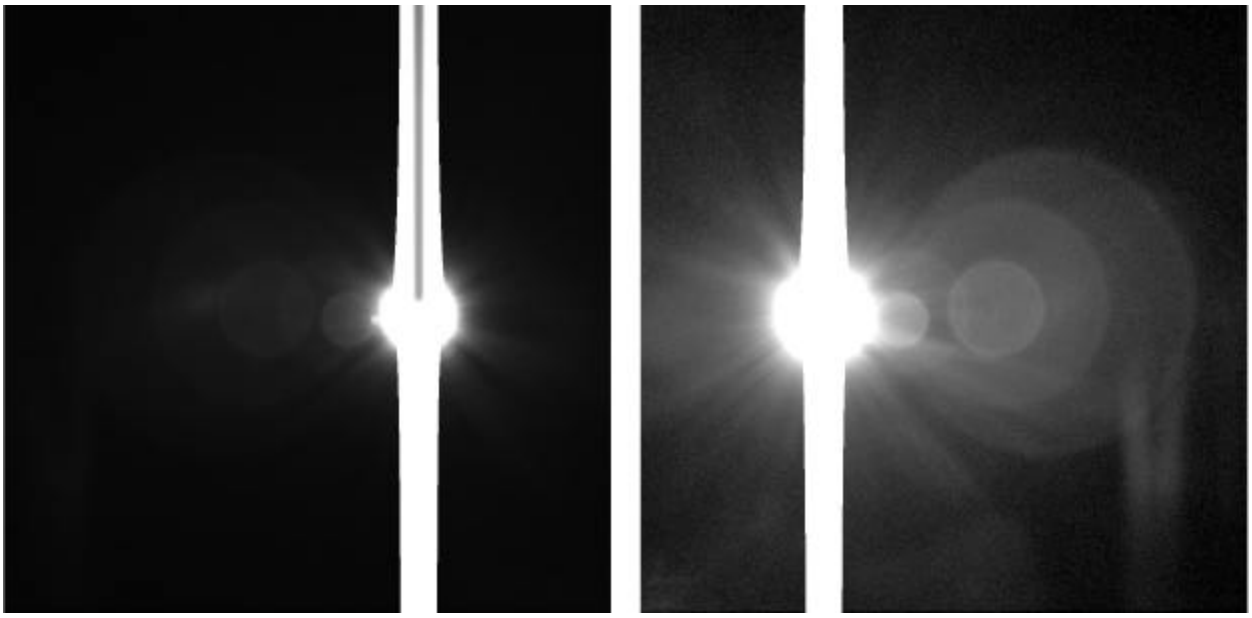

Figure 3.2.9h. Worst-case ghost images in MI serial # 110 images, corrected for transfer smear and stretched hard to show ghosts. (left) Image 020819170945, yaw +4.5°, showing maximum "inner" ghost intensity of ~0.1% just left of saturated source image. (right) Image 020819174157, yaw –4.9, contrast enhanced to show more subtle "outer" ghosts.

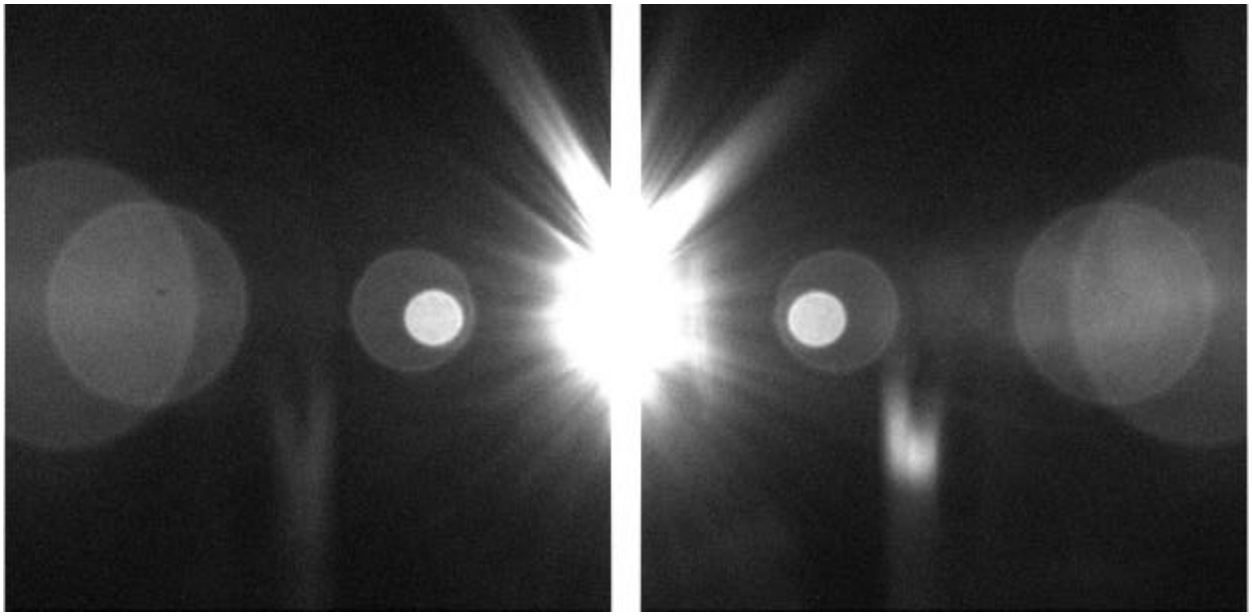

Figure 3.2.9i. Typical ghost images in MI serial # 110 images, corrected for transfer smear and stretched hard to show ghosts. (left) Image 020819171336, yaw +14.5. (right) Image 020819173811, yaw –14.5.

3.2.9.5 Accuracy and Relationship to Requirements

The intensity of ghosts observed in MI images is less than 0.1% in all cases. Scattered light around the source is more intense, but is restricted in extent and not a concern. These results verify that Level 3 requirement #1189 has been met.

4 SYSTEM LEVEL CALIBRATION AND TESTING

4.1 Overview

The Calibration and Test activities at the IDD-integrated level were primarily geometric in nature, designed to determine the physical layout of the camera relative to the IDD as well as to assess the actual IDD pointing performance compared to MI Level 3 requirements (Table 4.1.1). The tests were performed in room temperature and pressure (STP) conditions, and a subset of these tests were performed during ATLO in thermal vacuum conditions to validate performance in the flight environment. These requirements have been met, with the exception that apparent changes in Hazcam geometry during flight have caused the IPS positioning errors to exceed Level 3 requirements 1071 and 1072.

Table 4.1.1: MER Requirements relevant to MI System-Level Calibration and Testing

Level	ID #	Requirement
2	921	The Project System shall be capable of coregistering images from the Microscopic Imager with images and panoramas from the Pancam, Hazcam, Navcam observations of Mars.
2	922	The Project System shall ensure that the quality of the calibration of the science instruments be sufficient to satisfy the requirements and objectives in the Science Requirements Document and the Level 1 science requirements.
2	923	It shall be possible to produce radiometrically calibrated images from the Microscopic Imager, Hazcam, and Navcam observations on Mars, using pre-launch calibration data.
3	310	The IDD shall be capable of positioning instruments to an angular accuracy of 5 degrees in free space within the dexterous workspace of the IPS.
3	312	The IDD shall be capable of positioning instruments to a positional accuracy of 5 mm in free space within the dexterous workspace of the IPS.
3	313	The IDD shall be capable of repeatably positioning instruments to +/- 4 mm in position and +/- 3 degrees in orientation.
3	316	The IDD shall have a minimum controllable motion along a science target's surface normal vector of 2 mm +/- 1 mm RMS.
3	1071	The IPS shall be capable of positioning each in-situ payload element to within 10 mm of a science target that has not been previously contacted by another in-situ instrument.
3	1072	The IPS shall be capable of orienting each in-situ payload element to within 10 degrees of normal to a science target's local surface that has not been previously contacted by another in-situ instrument.
3	1073	After placing the MI in position for imaging, the motion of the IDD shall damp down to an amplitude of less than 30 microns within 15 seconds.
3	1195	The Microscopic Imager boresight shall be aligned to its mounting interface to within 1 degree in all 3 axes.

Table 4.2.1 provides a prioritized overview of the MI and IDD system-level calibration and testing plan. "Flight-like" environmental conditions refer to thermal/vacuum environment during integrated system tests.

Table 4.2.1. Overview of MI/IDD System-Level Calibration and Test Plan

Test	*Priority*	*Environmental Conditions*
1. Dust cover flat field	Medium	Ambient
2. Target imaging CCT Magnet array	High	Flight-like
3. IDD tests Positioning control Positioning knowledge Contact sensor position MI boresight alignment Vibration damping time	High	Flight-like
4. Stray/scattered light	Medium	Ambient
5. Coherent noise	High	Flight-like

4.2 Test Procedures and Results

4.2.1 Dust Cover Flat Field

The polycarbonate film originally selected for the MI dust cover (Roscolux) showed unacceptable outgassing under vacuum, so both MI dust covers were removed from the flight cameras for rework. By the time the Roscolux was replaced with Kapton film, the ATLO schedule did not allow flat field testing of the integrated system. Therefore, dust cover flat field measurements were not made before flight.

4.2.2 Target Imaging

Due to ATLO schedule constraints, MI images of the CCT and magnet array were not obtained using the flight cameras/IDD. However, target images were acquired using the Surface System Testbed (SSTB), using an engineering model MI and IDD. The results of these tests were used to position the flight MI cameras during landed operations.

4.2.3 Instrument Deployment Device (IDD) Tests

4.2.3.1 Purpose and Description

Take images of a precision test target and measure the position and orientation of MI relative to the rover coordinate frame. Determine IDD positioning control accuracy and repeatability (including backlash) and positioning knowledge accuracy. Determine the orientation of the MI boresight relative to the IDD coordinate frame. Measure damping of IDD vibrations immediately following various IDD motions. These tests will provide information needed to accurately command IDD to acquire MI image sequences, and to construct MI camera models.

4.2.3.2 Test Procedure

In system thermal testing (MI and IDD flight units), the MI/IDD heaters were turned on, the IDD unstowed, and the MI dust cover opened. The MI was then moved over a geometric

target and images captured while moving the MI away from the target in 3 mm increments. Images were also acquired after moving in azimuth and elevation about the target, then the dust cover was closed. These tests were performed at -95°C and 0°C. Tests were also conducted on the Surface System Testbed with the engineering model MI (see IPS V&V Test Procedure, MER IT-0246).

4.2.3.3 Environmental Conditions

Thermal/vacuum simulating landed environment and at ambient temperature/pressure.

4.2.3.4 Data Processing and Products

An example of the MI data acquired during system thermal testing is shown in Figure 4.2.3a. This type of data was used to develop camera models independently of the analysis described in section 3.2.7, and to determine the IDD positioning accuracy.

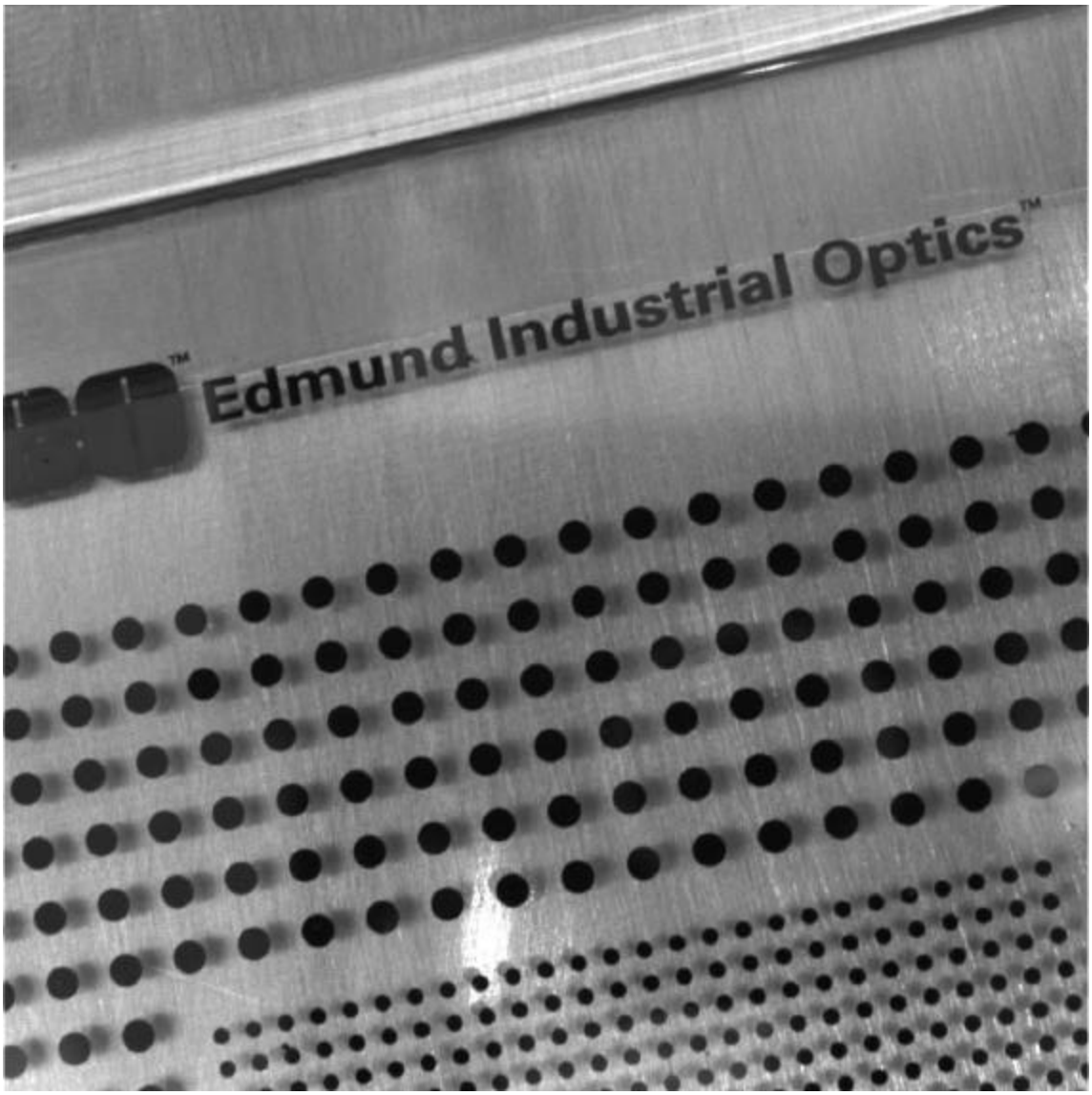

Figure 4.2.3a. MI image of geometric target taken during system thermal testing.

4.2.3.5 Accuracy and Relationship to Requirements

The IDD absolute angular positioning accuracy is 1.182° (3σ), consistent with Level 3 requirement #310.

4.2.4 Stray/scattered light test

The ATLO schedule did not allow specific stray/scattered light tests to be performed after the MI cameras were integrated with the rovers. No evidence of scattered light has been observed in images taken by the flight units during system tests or in images taken by the engineering model MI on the SSTB.

4.2.5 Coherent Noise

No evidence of coherent noise has been found in any of the images taken by the MI flight units during system testing, or in images taken by the MI engineering model on the SSTB. However, images taken by the MI flight units in ATLO showed radiation hits from the Mössbauer spectrometer reference source after it was installed, as expected.

5 MI SOFTWARE

5.1 Flight Software

Camera flight software was tested before launch to verify proper function, as summarized in Table 5.1.1 and Table 5.1.2. Because bad pixels were not detected, MI bad pixel tables were not loaded onto the spacecraft.

Table 5.1.1. Imaging flight software test summary (testbeds)

Report #	Facility	UTC Start	Prepared By	Topic/Retests
398	FSWTB	37306	maki	Tests of IMG FSW Camera Power Testing
399	FSWTB	37306	maki	Tests of IMG FSW Camera Power Testing
400	FSWTB	37306	maki	Tests of IMG FSW Camera Power Testing
410	FSWTB	37308	maki	FSW Testing of Camera Power and Image Acquisition
434	FSWTB	37314	Maki	IMG FSW Testing of Autoexposure Algorithm, Shutter Subtraction, PDS Image Generation
462	FSWTB	37322	Justin Maki	IMG FSW Development Testing
508	FSWTB	37336	Maki	IMG Services Development Testing
656	FSWTB	37376	Justin Maki	Camera Command Testing (FSW Release 4.0) R4-0_t4_0a_c4_0b_20020424
756	FSWTB	37399	Maki,Collisson	Camera Hardware Integration (Procedure IT-0011)
776	FSWTB	37405	Maki	Camera Software/Hardware Testing (with Cameras EM-005, EM-006)
778	FSWTB	37406	Maki, Litwin	Camera Software/Hardware Testing (with Cameras EM-005, EM-006)
1022	FSWTB	37467	Maki	IT-0046: Camera Functional Test
1253	FSWTB	37512	Maki	Camera Functional IT-0046 Simultaneous Testing Session (STS) Camera Functional (IT-0046) - Maki and
1337	FSWTB	37525	Maki	Mini-TES Elevation Mirror Debug - Denise/Biesiadecki
1476	FSWTB	37546	Maki	Camera FSW Functional Testing (IT-0046) MTG RS 2: Camera Functional Testing via IT-0046 1. IMG command buffering verification
1526	FSWTB	37552	Maki	2. Autoexposure Testing Image Performance Test:
1602	FSWTB	37564	Maki	Record the time required to acquire a Navcam Panorama (uncompressed, stereo).
1620	FSWTB	37566	Maki	Image Performance Testing
1623	FSWTB	37566	Maki	Camera Functional Testing, with PMA
1664	FSWTB	37573	Maki	Image Performance Testing, Procedure IT-XXXX, Rev. A.
1675	FSWTB	37574	Maki	Instrument Checkout (ICO) Dry Run

				Run the following sequences: c3400: APXS/Mossbauer c3420: Imaging c3401: Mini-TES
1715	FSWTB	37580	Maki	Image Performance Testing (IT-0095)
1840	FSWTB	37602	Maki	Camera Functional (IT-0046) (Coordinate Frame Section) LOG# Z79439 - Timeout Error During Pancam Image Acquisiton
2613	FSWTB	37721	Maki	Try to reproduce image_cct timeout error seen in ATLO, using Rear Hazcam cameras and TEST images. Retest LOG# Z79439 : Timeout Error During Image Acquisition Acquire 1000+ test images in an attempt to reproduce the Image timeout error from img_cct.
2653	FSWTB	37726	Maki	Run Sequence all night, unattended. IMG Autoexposure Testing Session #1
2716	SSTB	37732	Maki	Acquire Rear Hazcam images (with all 5 SSTB lights on) with various autoexposure parameters.
2782	SSTB	37741	Maki	Autoexposure Test Session #2 SORT 1 - Dry Run B
2887	SSTB	37756	Maki	Run as many of the 23 imaging sequences as possible.
3227	CETB	37811	Maki	Cruise Instrument Checkout Camera Dry Run in CETB
3301	FSWTB	37822	Maki	MER B Ops: Instrument Checkout IMG Autoexposure Testing Session #3 Retest LOG# Z79612 PASSED: Autoexposure - IMG autoexposure producing overly saturated images Retest LOG# Z78736 PASSED: Autoexposure - capture image autoexposure took excessive number of ite Retest LOG# Z79220 PASSED: Stow Camera Unknown Ticket Retest LOG# Z79167 PASSED: Stow Camera Unknown Ticket
3329	SSTB1	37825	Maki	Retest LOG# Z78224 : CPU Utilization during image post processing
3347	FSWTB	37827	Maki	MER B Ops: Instrument Checkout Dry Run
3380	SSTB1	37832	Maki	Testbed Fidelity Run - Imaging Performance: Pancam panorama timing test
3501	SSTB1	37851	Maki	IMG FSW Performance Testing: Panorama - Image Types, Session #1
3590	SSTB1	37861	Maki	IT-0095: IMG Performance Testing: Panorama - Image Types, Session #2 (with lights)

				IMG Compression Testing, Session #1 (of 2). Using Procedure IT-0095
				LOG# Z80744 --- Retest passed. LOG# Z80743 --- Retest passed.
3627	SSTB	37866	Maki	LOG# Z78224 --- Retest passed. IT-0046, IMG Functional Test MTG Cleanup
3663	SSTB1	37869	Maki	LOG# Z81712: Retest Passed. Image Compression Test Session #2 (Acquire data that was lost in PORT 4_5)
3861	SSTB1	37895	Maki	Retest LOG# Z81743
4119	SSTB1	37930	Lewicki/Maki	1. Wirth has a camera crew in this morning, so doing some actuations for them to film while we're getting s 2. Take tons of HAZCAM images and NAVCAM pans with different parameters to see what we like for ITE
				Retest CR 624 - Passed Retest CR 781 - Passed Retest LOG# Z81731 (retest CR 907) - Passed Retest LOG# Z82191 (retest CR 952) - Passed Retest LOG# Z81498 (retest CR 962) - Passed
4127	SSTB1	37930	Maki	Retest LOG# Z81755 - passed
4132	SSTB1	37931	Maki	MER A Instrument Checkout #2 - Ops product testing
4176	FSWTB	37937	Maki	MER DIMES/Camera ICO #2
4186	FSWTB	37938	Maki	IMG regression testing.
4191	SSTB1	37938	Maki	Image Regression Tests with "final" FSW load. - Run p0046 Camera functional sequence. V and V items regression tested: 12583 13454 13449 13458 13459 13460

				13461 13462 13451 13461 13453 13452 13456 13447
4354	CETB	12/ 3/2003	Maki	MER A Ops: IMG Parm Load Sequence Testing Image Sequence Dry Runs
4449	SSTB1	12/17/2003	Maki	p1515 (Sol 3 Navcam Panorama) p1516 (Sol 3 Navcam Panorama with deferred compression) t1517 (LUT1,LU2,LU3 testing)

Table 5.1.2. Imaging flight software test summary (flight systems)

Report No.	Procedure Name	Start	Open Date	Platform
MER2-STR-76-1	Camera mini-TES coalignment	Yes	10/02/2002, 14:38:06	MER2
MER2-STR-74-1	PMA ratation axis measurements	Yes	10/02/2002, 07:30:40	MER2
MER2-STR-72-1	Navcam mini panorama	No	09/28/2002, 14:54:11	MER2
MER2-STR-70-1	Set NAVCAM/PANCAM Models	No	09/27/2002, 18:02:24	MER2
MER2-STR-57-1	MI Software debugging	Yes	09/12/2002, 09:43:25	MER2
MER2-STR-170-1	MER 2 Therm Test Speckle Hunt	No	01/17/2003, 09:34:48	MER2
MER2-STR-169-1	Right Pancam Isolation Checks	No	01/16/2003, 15:33:42	MER2
MER2-STR-167-1	Camera TDR	No	01/15/2003, 08:49:39	MER2
MER2-STR-153-1	Pancam Speckle Troubleshoot	Yes	01/07/2003, 14:26:09	MER2
MER2-STR-147-1	Pancam Speckle Troubleshoot P-3006 sequence	No	12/23/2002, 14:00:03	MER2
MER2-STR-123-1	Navcam pan test	No	11/21/2002, 21:01:18	MER2
MER2-STR-122-1	Pancam cover motion test	No	11/21/2002, 22:31:25	MER2
MER1-STR-252-1	Pancam 360 degree panorama	Yes	04/01/2003, 16:43:54	MER1
MER1-STR-179-1	MI Geometric Calibration	No	01/28/2003, 09:11:41	MER1
MER2-STR-69-1	Mini Pancam panorama	Yes	09/28/2002, 12:11:29	MER2
MER2-STR-57-3	MI Software debugging	No	09/12/2002, 14:50:18	MER2
MER2-STR-57-2	MI Software debugging	No	09/12/2002, 11:06:39	MER2

Report No.	Procedure Name	Start	Open Date	Platform
MER2-STR-236-1	Camera alignment check	Yes	03/26/2003, 07:39:24	MER2
MER2-STR-170-2	MER 2 Therm Test Speckle Hunt	No	01/18/2003, 13:30:19	MER2
MER2-STR-169-2	Right Pancam Isolation Checks	No	01/18/2003, 13:37:21	MER2
MER2-STR-161-1	IDD/MI calibraion	No	01/10/2003, 19:04:38	MER2
MER2-STR-160-2	Hazcam wide angle sup. cal	No	01/10/2003, 17:39:38	MER2
MER2-STR-160-1	Hazcam wide angle sup. cal	Yes	01/10/2003, 17:26:56	MER2
MER2-STR-152-2	Cruise Instrument Checkout - No sequence	No	01/06/2003, 19:16:32	MER2
MER2-STR-152-1	Cruise Instrument Checkout - No sequence	Yes	01/06/2003, 14:50:13	MER2
MER2-STR-129-2	DIMES imaging	Yes	11/27/2002, 08:31:33	MER2
MER2-STR-129-1	DIMES imaging	No	11/26/2002, 15:58:02	MER2
MER2-STR-107-1	MI and Front Hazcam X-ray detection Test	Yes	11/04/2002, 20:49:59	MER2
MER1-STR-236-3	Camera alignment check	No	04/09/2003, 13:50:11	MER1
MER1-STR-236-2	Camera alignment check	No	04/09/2003, 11:19:57	MER1
MER1-STR-236-1	Camera alignment check	Yes	04/08/2003, 13:17:42	MER1
MER2-420-5-4321-4	Rover System Thermal Test Procedure	No	12/12/2002, 19:52:23	MER2
MER2-420-5-4281-2	System Test: Critical Surface Deployments	No	01/04/2003, 10:15:33	MER2
MER2-420-5-4286-1	System Test: Surface Science	Yes	01/09/2003, 12:24:54	MER2
MER1-420-5-4253-3	System Test: Deployments Through Sol #2 (ST4.1 runs 1 and 2)	No	04/04/2003, 15:57:50	MER1
MER1-420-5-4258-1	System Test: System Test 4 - Surface	Yes	04/02/2003, 04:34:17	MER1

5.1.1 Test Results

One of the first camera images taken with the MER flight software and hardware is shown in Figure 5.1.1a.

Figure 5.1.1a. MI image taken with flight hardware and software.

5.1.1.1 ICER Compression Performance

These tests are still ongoing, and results will be reported in a revised version of this document. Deviations between the original and compressed images will be used to assess the effects of various levels of ICER compression on radiometric precision and accuracy.

5.1.1.2 Auto Exposure Performance

The automatic exposure software was tested on both the flight cameras and the engineering models on the SSTB, as summarized above. The performance of this software has been excellent.

5.1.1.3 Readout Smear (Electronic Shutter) Correction

Shutter correction software was tested on both flight units and the engineering model MI. It was confirmed that FSW automatically acquires and subtracts a zero-exposure frame.

5.2 Calibration Software

An overview of MI software developed at USGS is shown in Figure 5.2.1a. Keywords in the PDS labels of the MI EDRs are used to determine which processing steps are needed for each image. Before flight, no bad pixels were found that warranted correction.

5.2.1 Processing Procedure

If no shutter correction was performed onboard the rover (by acquiring and subtracting a zero-second exposure) and the exposure time is less than 1 second, transfer smear can be corrected using the ISIS program DESMEAR. In this case, dark current must be removed from the image first. If shutter correction was performed onboard, then the zero-second and reference pixel components of the dark current are corrected in this process. In this case, only the active-area component of the dark current must be removed.

The next step is flat field correction, in which the image is divided by the 32-bit normalized flat field described in section 3.2.2.4 above. The result is calibrated in a relative radiometric sense, so that DN values in each pixel can be accurately compared to DN values in other pixels.

The conversion of DN values to I/F (radiance factor) involves correction for both the camera radiometric response and solar distance at the time of image acquisition:

$$I / F = DN\left(\frac{R^2}{t_{\exp} w_0}\right)$$

where R is the distance to the Sun in AU, $t_{\exp}$ is the exposure time in seconds, and w_0 is given by the equations in Figure 3.2.2f.

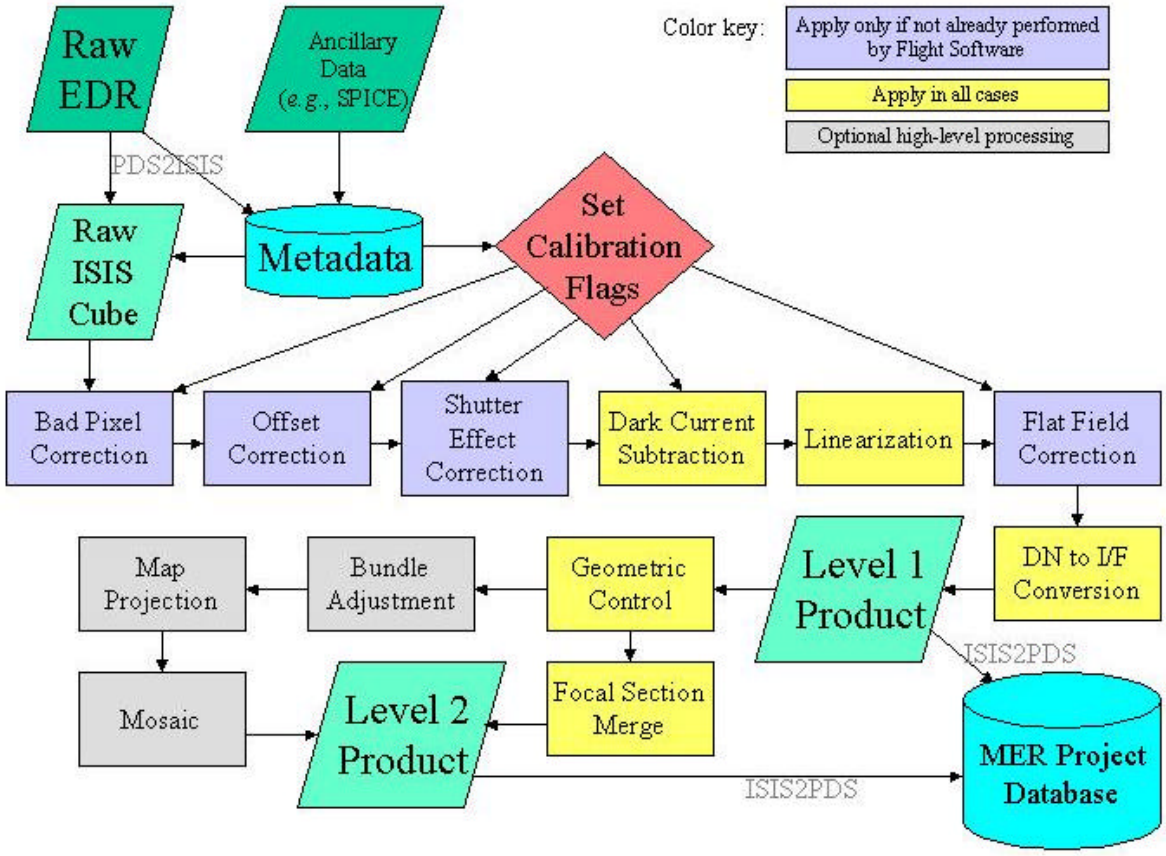

Figure 5.2.1a. MI ground processing flowchart.

6 INFLIGHT CALIBRATION

In order to verify the accuracy of preflight calibration and to identify changes in camera performance, acquisition of a limited amount of inflight calibration data is planned. Analysis of these data will enable updating of calibration parameters if necessary, perhaps improving MI calibration. Anticipated inflight calibration activities are described below. Results of these activities will be reported in a future revision of this document.

6.1 Darks

During cruise to Mars, MI dark current images and extra pixel data were acquired and returned to Earth. These dark data were acquired at different temperatures early and late in cruise and losslessly compressed. The darks served as a functional test and allowed the dark current model to be verified and updated. They showed radiations hits, as expected, from the sources in the Mössbauer spectrometer, and evidence for minor bad pixels. None of the bad pixels generate enough spurious signal that correction is required.

6.2 Target Imaging

During surface operations, in particular during the “calibration campaign” soon after landing, images of the CCT and magnet array will serve to verify IDD positioning accuracy and MI focus distance. This test will take advantage of the experience and sequences derived from the system level test 4.3.2 described above. Any changes with respect to preflight calibration data will be analyzed and may be used to modify MI/IDD command sequences.

6.3 Sky Flat Fields

MI images of the martian sky, taken with the dust cover open and closed, will be used to verify flat field calibration and perhaps update it. Sky images could be acquired while the Mössbauer or Alpha Particle X-ray spectrometers are placed against a surface target, for example.

7 CALIBRATION DATA FORMAT AND ARCHIVING

All calibration data were acquired in the PDS file format, so that it can be archived directly into the PDS without having to go through a file conversion. Calibration file labels and the details of the format itself will be defined by the Athena Data and Archives Working Group (DAWG) and are described in the MER Archive Generation, Validation, and Transfer Plan (MER 420-1-200; JPL D-19658). The data presented in this document will be delivered to the PDS for safe storage, rather than included in a formal MER archive.

8 ACKNOWLEDGEMENTS

The calibration of the Microscopic Imagers owes much to the Athena Science team and the JPL team that built and tested the MER cameras. The authors appreciate the contributions made by Jim Aragon, Ali Bakhshi, John Bousman, Paul Cate, B. J. Chippindale, Nancy Cowardin, Roberta Davis, Darryl Day, Tom Dea, Bob Deering, Don Dunn, Perry Fatehi, Carolina Flores-Helizon, Virginia Ford, Wayne Hartford, Pete Kobzeff, John Koehler, Greg Lievense, Tim McCann, Ali Pourangi, Walt Proniewicz, Don Schatzel, Alejandro Soto, Beverly Stange, Robby Stephenson, Mike Sucy, Charles Thompson, Rudy Vargas, Enrique Villegas, Marc Walch, Len Wayne, Reg Willson, and Bobbie Woo. Many of these individuals assisted with the testing and calibration of the cameras, as did Deborah Bass, Charles Budney, John Callas, Wendy Calvin, Emily Dean, Bill Farrand, Lisa Gaddis, John Grant, Ed Guinness, Jeff Johnson, Jonathan Joseph, Kjartan Kinch, Mark Lemmon, Zoe Learner, Morten Madsen, Elaina McCartney, Scott McLennan, Doug Ming, Mary Mulvanerton, Tim Parker, Jon Proton, Frank Seelos, Jason Soderblom, Rob Sullivan, Roger Tanner, Cathy Weitz, and Michael Wolff. The camera testing was well supported by the MER management staff and the IDD and ATLO teams at JPL. The MI contact sensor and dust cover were designed and built at Alliance Spacesystems, Inc., with Lori Shiraishi serving as the JPL liason. We also thank the rest of the USGS MER team: Jeff Anderson, Brent Archinal, Janet Barrett, Kris Becker, Debbie Cook, Eric Eliason, Lisa Gaddis, Annie Howington-Kraus, Chris Isbell, Jeff Johnson, and Tracie Sucharski. The review of this document by Wendy Calvin is much appreciated.

The use of trade, product, or firm names in this paper does not imply endorsement by the U.S. Government.

9 REFERENCES

Bell, J. F. III *et al*. (2003). The Mars Exploration Rover Athena Panoramic Camera (Pancam) Investigation, *J. Geophys. Res*. **108**, 8067, doi:10.1029/2003JE00207.

Bell, J. F. III et al. (2004). Mars Exploration Rover Pancam Calibration Report. MER 420-6-700 (JPL D-19826).

Di, K., and Li, R., 2004, CAHVOR camera model and its photogrammetric conversion for planetary applications, *J. Geophys. Res*., submitted.

Gennery, D. B., Least-squares camera calibration including lens distortion and automatic editing of calibration points, Workshop on Calibration and Orientation of Cameras, in *Computer Vision*, XVII Congress of the International Society of Photogrammetry and Remote Sensing, Washington, DC, August 2, 1992.

Herkenhoff, K. E. *et al*. (2003). The Athena Microscopic Imager Investigation. *J. Geophys. Res*. **108**, 8065, doi:10.1029/2003JE002076.

Janesick, J. R., K. P. Klaasen, and T. Elliott (1987). Charge-coupled-device charge-collection efficiency and the photon-transfer technique. *Opt. Eng*. **26**, 972.

Kirk, R. L., Howington-Kraus, E., Hare, T., Dorrer, E., Cook, D., Becker, K., Thomas, K., Redding, B., Blue, J., Galuszka, D., Lee, E. M., Gaddis, L. R., Johnson, J. R., Soderblom, L. A., Ward, A. W., Smith, P. H. ,and Britt D. T., 1999, Digital photogrammetric analysis of the IMP camera images: Mapping the Mars Pathfinder landing site in three dimensions, *Journal of Geophysical Research,* **v. 104 (E4),** pp. 8868–8888.

Kirk, R. L., Howington-Kraus, E., Redding, B., Galuszka, D., Hare, T. M., Archinal, B. A., Soderblom, L. A., and Barrett, J. M., 2003a, High-resolution topomapping of candidate MER landing sites with Mars Orbiter Camera Narrow-Angle images, *J. Geophys. Res*., in press.

Kirk, R. L., Howington-Kraus, E., Soderblom, L. A., Giese, B., and Oberst, J., 2003b, Comparison of USGS and DLR topographic models of Comet Borrelly and photometric applications, *Icarus*, **167**, pp. 54–69, doi:10.1016/j.icarus.2003.07.009,

Maki, J. N. *et al*. (2003). The Mars Exploration Rover Engineering Cameras, *J. Geophys. Res*. **108**, doi: 10.1029/2003JE00.

Squyres, S. W. *et al*. (1999). The Mars 2001 Athena Precursor Experiment (APEX). *Lunar Planet. Sci*. **XXX**, Abstract #1672, Lunar and Planetary Institute, Houston (CD-ROM).

Squyres, S. W., R. E. Arvidson, E. T. Baumgartner, J. F. Bell III, P. R. Christensen, S. Gorevan, K. E. Herkenhoff, G. Klingelhöfer, M. B. Madsen, R. V. Morris, R. Rieder, and R. A. Romero (2003). The Mars Exploration Rover Athena investigation, *J. Geophys. Res*. **108**, doi:10.1029/2003JE002121.

Wolf, P. R., 1983, *Elements of Photogrammetry*. 2nd Edition, McGraw-Hill Book Company, Boston, 628 pp.

Yakimovsky, Y. and R. Cunningham, 1978, A system for extracting three-dimensional measurements from a stereo pair of TV cameras, *Computer Graphics and Image Processing*, 7,195–210.

APPENDIX A: THERMAL TEST MATRIX

Table 10.1.

MER Science Cameras Thermal Flight Acceptance & Calibration Test Matrix									
STEP #	HEAT EXCHANGER PLATE C	CAMERA CCD C	CAMERA EBOX C	CHAMBER CONTROL ON/OFF	EBOX HTR ON/OFF	PRES. TORR	CAMERA FUNCTIONAL CHECKOUT	CAL TESTS	DESCRIPTION
1	22	22	22	OFF	OFF	760 AIR	X		Pre-Test Inpection & Functional Test
2	22	22	22	OFF	OFF	<1E-5	X		Functional Test in Vacuum.
3	55	55	55	ON	OFF	<1E-5			FA Non-Op Max Temp (cycle 1)
4	45	45	55	ON	ON	<1E-5	X	X	FA Op Max Temp (50 hr powered-on soak)
5	-110	-110	-110	ON	OFF	<1E-5			FA Non-OP Min Temp (cycle 1)
6	-110	-110	-60	ON	ON	<1E-5	X	X	FA Op Min Temp (24 hr powered-on soak)
7	55	55	55	ON	OFF	<1E-5			FA Non Op Max Temp (cycle 2)
8	45	45	55	ON	ON	<1E-5	X		FA Op Max Temp (cycle 2)
9	-110	-110	-110	ON	OFF	<1E-5			FA Non Op Min Temp (cycle 2)
10	-110	-110	-60	ON	ON	<1E-5	X		FA Op Min Temp (cycle 2)
11	55	55	55	ON	OFF	<1E-5			FA Non Op Max Temp (cycle 3)
12	45	45	55	ON	ON	<1E-5	X		FA Op Max Temp (cycle 3)
13	-110	-110	-110	ON	OFF	<1E-5			FA Non Op Min Temp (cycle 3)
14	-110	-110	-60	ON	ON	<1E-5	X		FA Op Min Temp (cycle 3)
15	-55	-55	-55	ON	OFF	<1E-5	X	X	Calibration Tests (setpoint #1, -55C)
16	-10	-10	-10	ON	OFF	<1E-5	X	X	Calibration Tests (Setpoint #2, -10C)
17	5	5	5	ON	OFF	<1E-5	X	X	Calibration Tests (setpoint #3, +5C)
18	22	22	22	OFF	OFF	760 AIR	X		Post Test Inspection & Functional Test

APPENDIX B: LIGHT SHIELD TEST RESULTS

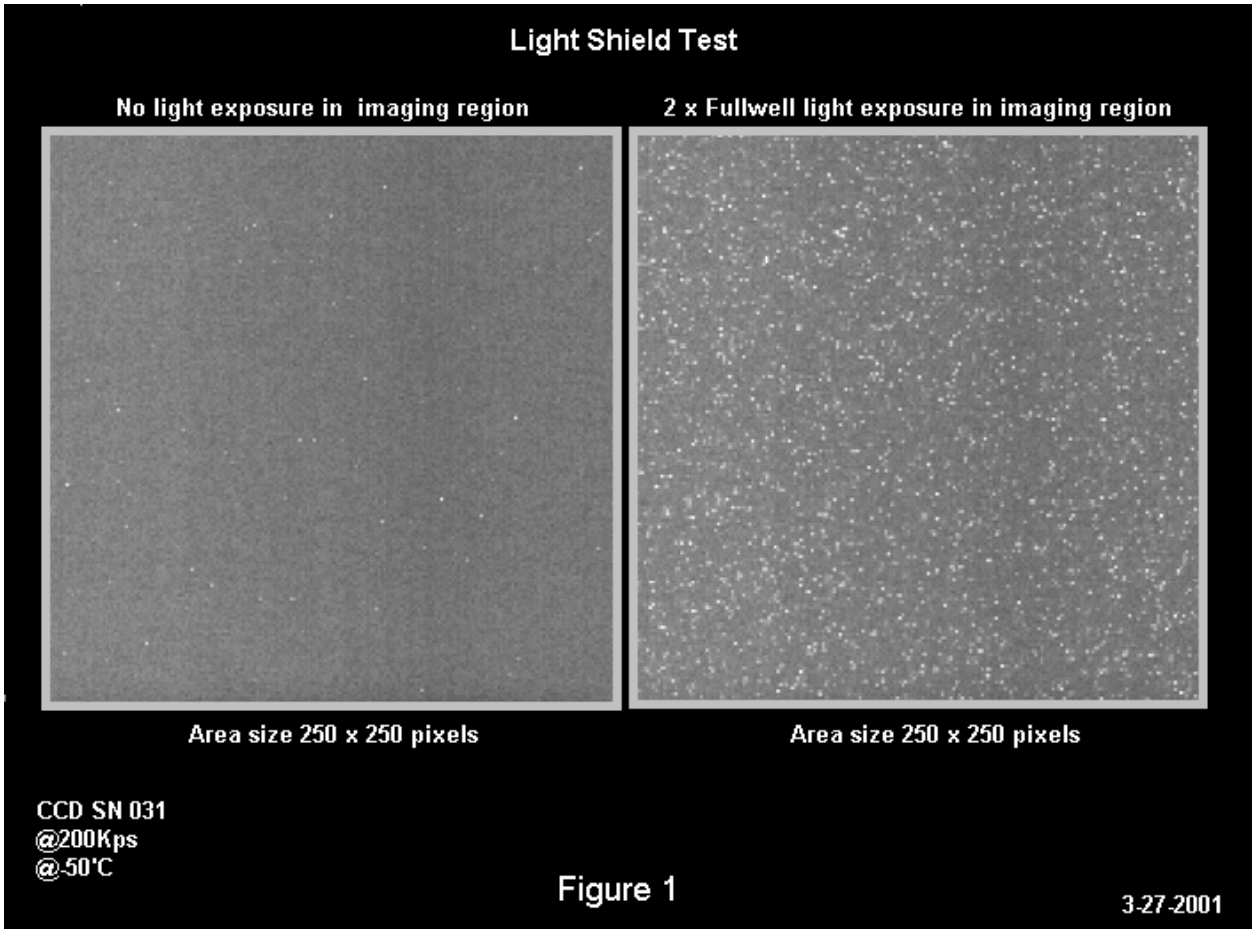

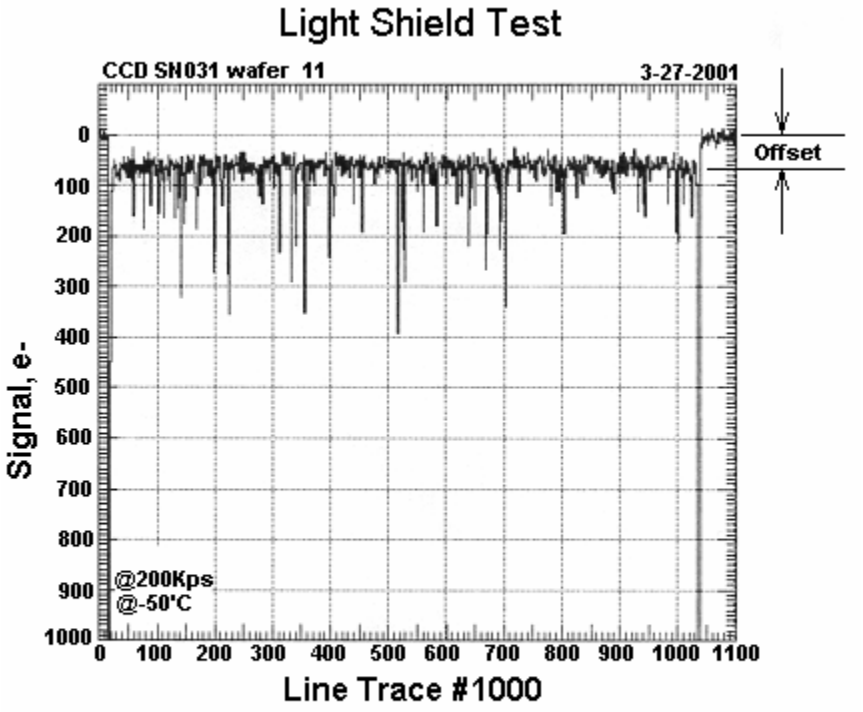
Light Shield Test
CCD SN031 wafer 11
3-27-2001
Offset
Signal, e-
0
100
200
300
400
500
600
700
800
900
1000
@200Kps
@-50°C
0 100 200 300 400 500 600 700 800 900 1000 1100
Line Trace #1000

Figure 2

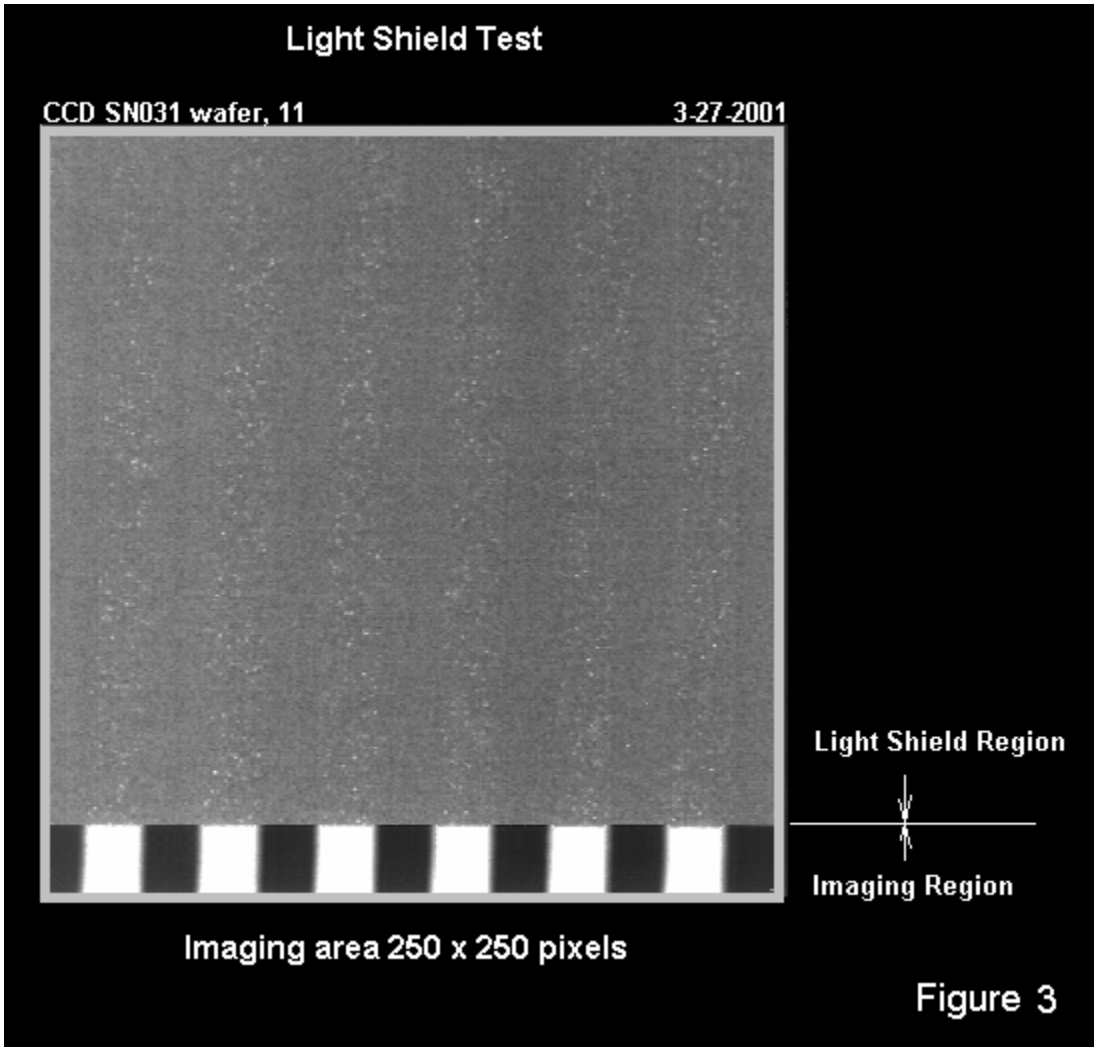
Light Shield Test
CCD SN031 wafer, 11
3-27-2001
Light Shield Region
Imaging Region
Imaging area 250 x 250 pixels

Figure 3

APPENDIX C: RESIDUAL IMAGE TEST RESULTS

JET PROPULSION LABORATORY **MEMORANDUM**

8 June 2001

To: Mark Wadsworth
Andy Collins
George Fraschetti
Mark Schwochert

Subject: Consequences of Changing MER CCD negative parallel operating voltage

From: Tom Elliott

Reference: MER Camera CCD Specification MER 420-7-495 D-20365

Background: The MER Camera CCD Specification (reference 1) documents the optimum operating voltages for the MER CCDs. It prescribes a negative parallel operating voltage of –8V. An issue has recently arisen regarding the availability of an acceptable electronic component to provide this voltage and I was asked to investigate the consequences of operating the negative parallels at a less negative potential. Several tests have been conducted, using non-optimal drive voltages, and the results are reported below.

Summary of Results: Using a negative parallel operating voltage of –7V will result in a ~20% increase in dark current, an increased vulnerability to the effects of ionizing radiation and an increase in residual image, with the residual image effect becoming pronounced as the temperature is decreased toward the lowest expected MER CCD operating temperature, ≤-100C.

Tutorial: The interface between the photosensitive epitaxial silicon layer and the overlying, insulating oxide layer has a critical effect on a CCDs performance. The uniformity of the underlying silicon crystal is disrupted at this interface, resulting in numerous open silicon bonds that serve as mid-band generators of dark current and as charge trapping sites, sites which produce a residual image as the trapped charge is gradually released . It has long been standard CCD operating technique to mitigate these effects by operating a CCD in inversion, ie. biasing the overlying gates sufficiently negatively to flood this interface with holes drawn from the channel stops. These holes suppress the generation of dark current and prevent signal charge from coming in contact with potential charge traps at the interface. For the MER CCD, -8V provides for such inverted operation with a margin of ~0.5V. Operation at –7V, of course, is non-inverted operation and results in increased dark current, vulnerability to ionizing radiation damage and increased residual image.

Tests: Dark current was measured as a function of negative parallel potential. The results, shown in Figure 1, indicate that dark current will increase in both the shielded and unshielded portions of the array by ~20% when the potential is increased to –7V. This figure shows the common characteristic that dark current is lower in the shielded region than in the unshielded region. This is due to the passivating effects of hydrogen derived from the overlying aluminum. We did not conduct a radiation test for this effort but others have observed, on occasion, that ionizing radiation damage causes the dark current to increase in the shielded region more rapidly than in the unshielded region, eventually yielding eliminating the dark current difference between the two regions.

Residual surface image (RSI) is the development of residual image due to charge trapping at the silicon-oxide interface. Figure 2 plots fullwell capacity as a function of parallel operating potentials. The conventional selection of operating potentials is to balance between achieving maximum fullwell capacity, by biasing most negatively and avoiding surface channel operation (and consequent dark current and trapping increases) by not biasing too negatively. The –8V curve, combined with a +2V positive potential on adjacent phases, achieves this, as shown in the figure. The –7V curve is translated into the surface channel regime.

Figure 3 shows the potential RSI consequences of such a shift for the more extreme conditions of +5V and –5V, -90C. In this figure, a circular image is focussed on the CCD (image A). The exposure is then increased to the point where the signal is 4x full well capacity (image B. The faint, displaced circular image is an optical artifact. The original spot is in the center of the elongated, bloomed pattern.) A mechanical shutter is then closed and a dark current is immediately read out (image C). This final image contains the unmistakable residual of the previous saturated image.

Figure 4 shows similar data for the nominal MER CCD parallel operating conditions (-8V and +2V) and shows no residual image. Figure 5 illustrates the effects of operation at –7V and +3V at –85C, revealing a residual image of ~ 80e^- under these conditions. Finally, Figure 6 is a residual image taken at –55 C, showing that residual, while present, is much less as shown in Figure 6.

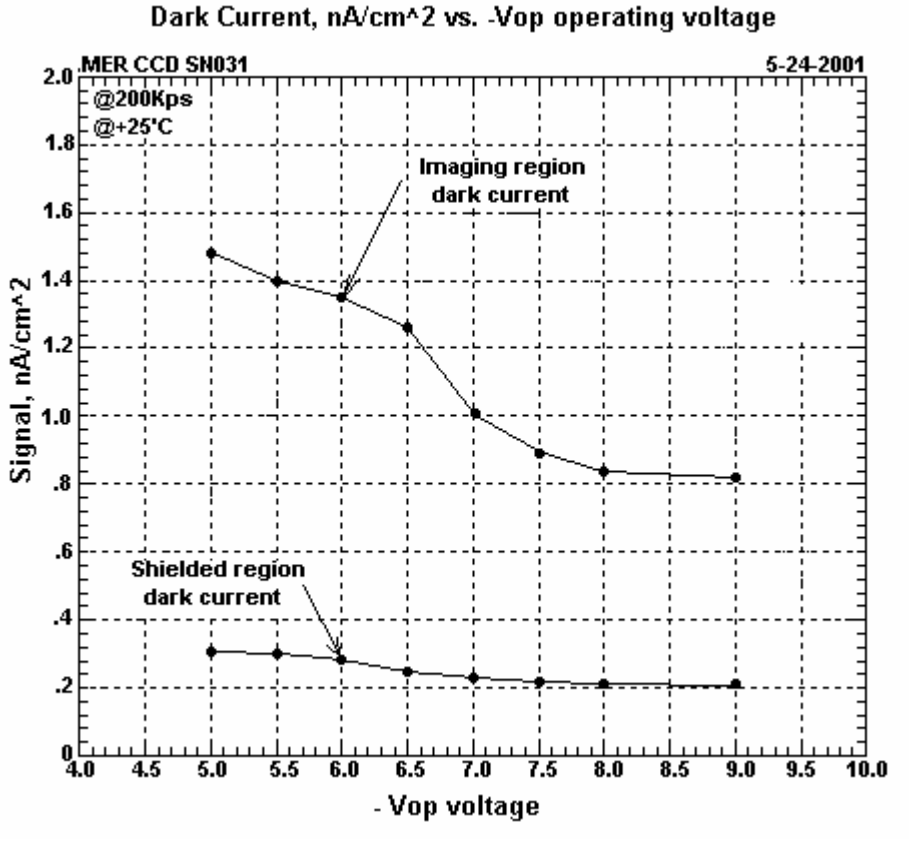
Dark Current, nA/cm^2 vs. -Vop operating voltage
MER CCD SN031
5-24-2001
@200Kps
@+25'C
Imaging region
dark current
Shielded region
dark current
Signal, nA/cm^2
- Vop voltage
2.0
1.8
1.6
1.4
1.2
1.0
.8
.6
.4
.2
0
4.0
4.5
5.0
5.5
6.0
6.5
7.0
7.5
8.0
8.5
9.0
9.5
10.0

Figure 1

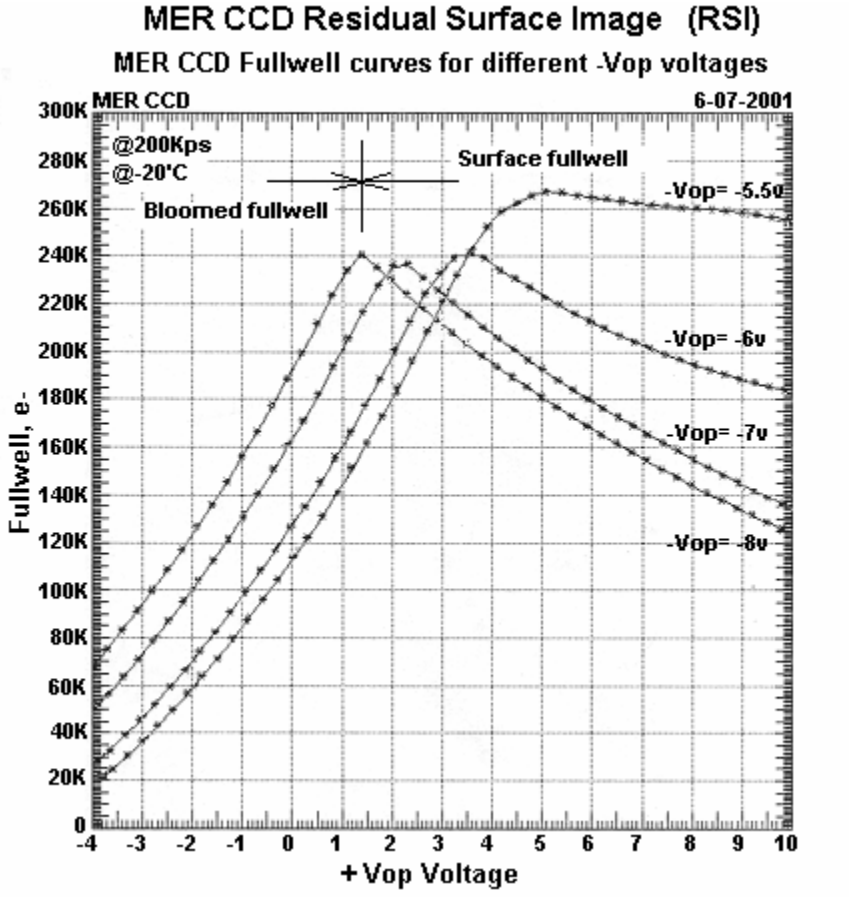
MER CCD Residual Surface Image (RSI)
MER CCD Fullwell curves for different -Vop voltages
MER CCD
6-07-2001
@200Kps
@-20'C
Surface fullwell
Bloomed fullwell
-Vop= -5.5v
-Vop= -6v
-Vop= -7v
-Vop= -8v
Fullwell, e-
300K
280K
260K
240K
220K
200K
180K
160K
140K
120K
100K
80K
60K
40K
20K
0
-4 -3 -2 -1 0 1 2 3 4 5 6 7 8 9 10
+Vop Voltage

Figure 2

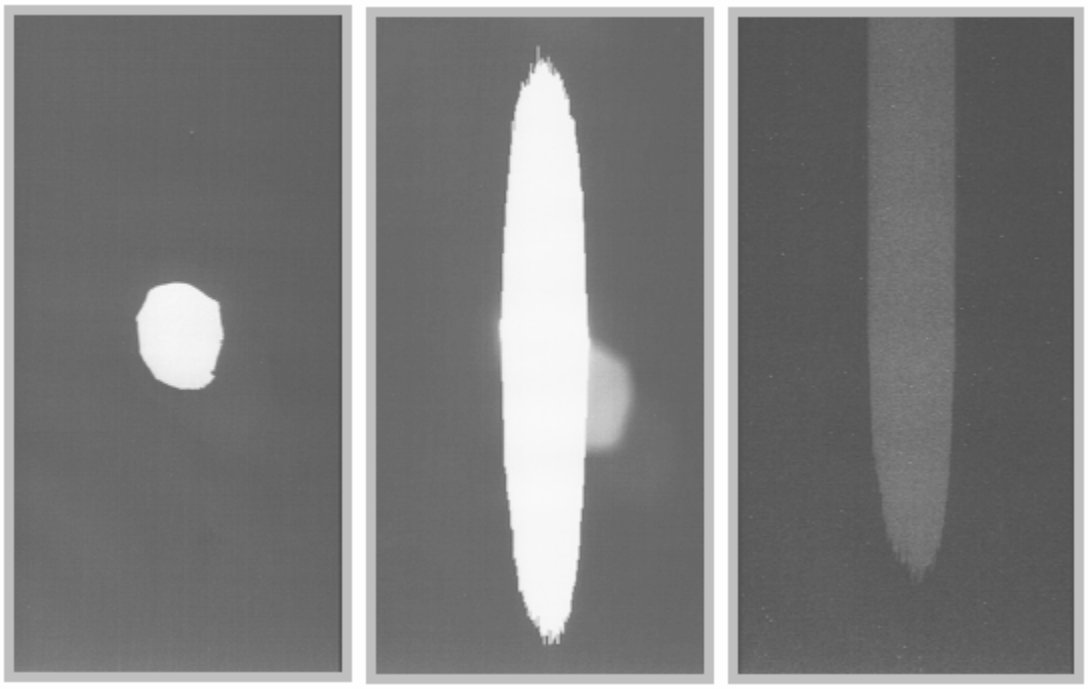

Image A. Image B. Image C.

Image A shows a focused spot of light on a 300 x 500 pixela area of the MER CCD. Image B shows the blooming that occurs after a 4X fullwell exposure. The other image in the picture is a reflection caused in the focusing of the lense. Image C shows the residual surface image the remains after a 1 minute dark integration.

Operating conditions were as follows:

Readout rate = 200Kpixels/second
CCD temperature = -90°C

Positive parallel clock voltage =+ 5 volts
Negative parallel clock voltage =- 5 volts

Remaining operating voltages nominal

Test sequence: CCD is exposed to 4 x fullwell (500nm). Then the device is readout completely in one readout cycle. The device is immediately put into integration mode under dark conditions for a integration time of 1 minute. Then the device is readout and the residual surface image that remains is measured.

Figure 3

MER CCD Residual Surface Image (RSI)

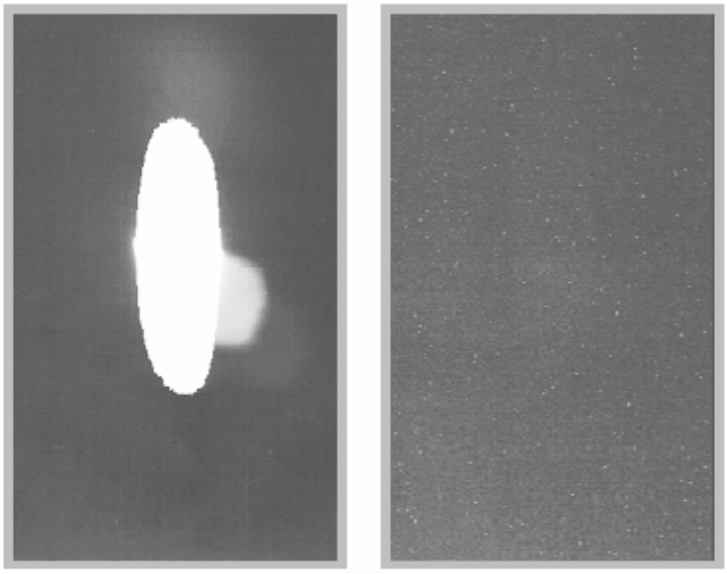

Image A. Image B.

Image A, is a 300 x 500 pixel image taken @-90'C showing the blooming of a 4x fullwell exposure. The device was completely readout and then immediately put into integration mode under dark conditions for 1 minute. Image B indicates that even at a negative parallel operating voltage of -8 volts, which is considered inverted, there is still a trace of RSI. This is due to only operating the negative parallel clocks 1/2 volt into inversion.

Parallel Clock operating voltages:
+Vop = +2
-Vop = - 8

Remaining operating voltages were nominal.

Figure 4

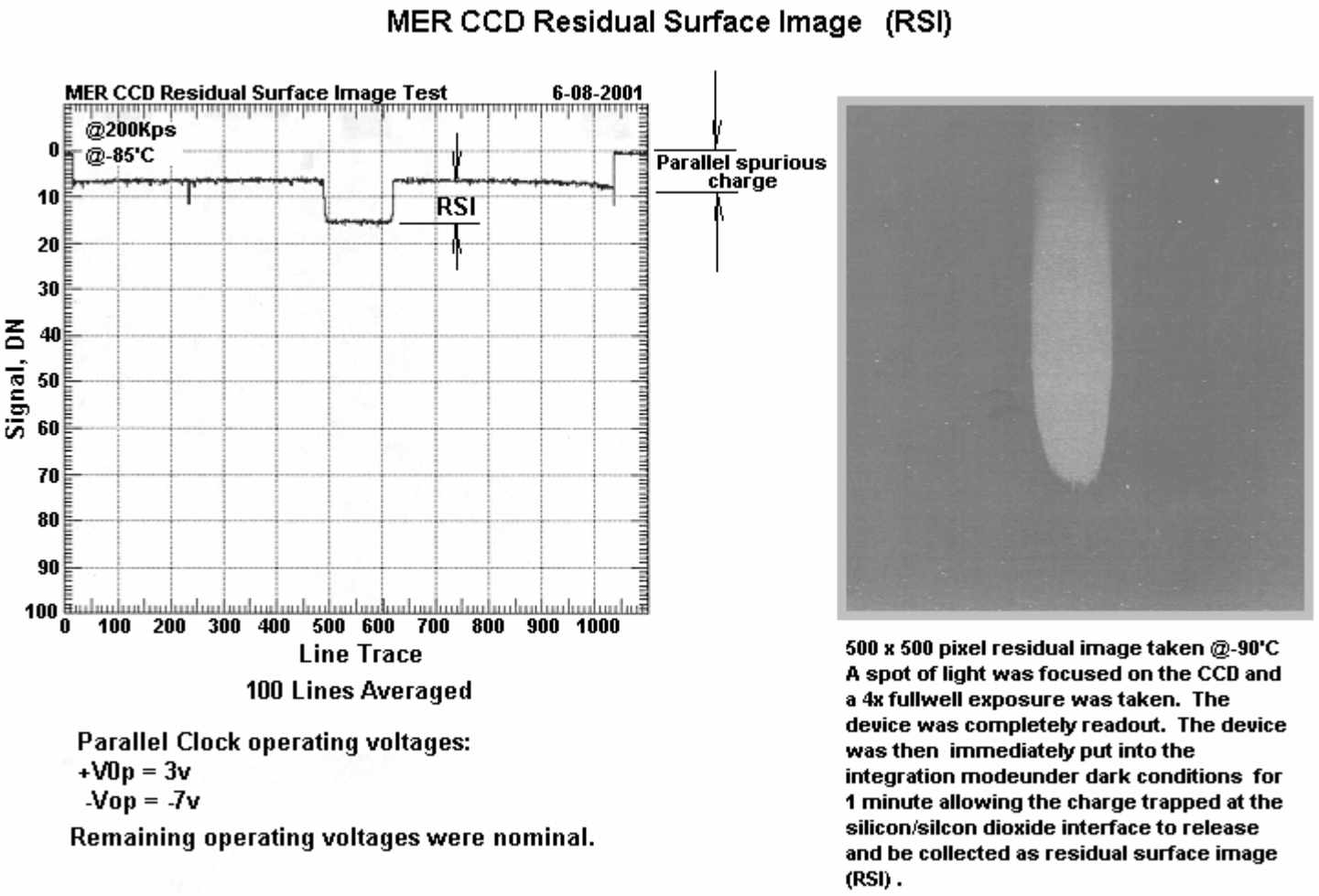

Figure 5

APPENDIX D: MI LENS ASSEMBLY TEST RESULTS

Table 13.1. Data for MER MI lenses as measured by Kaiser Electro-Optics

optics barrel	RMS DISTORTION SPEC ≤ 0.10λ RMS @ HeNe wavelength			MTF SPEC ≤ 0.35 MTF @ 30 lp/mm			MEASURED			
serial #	ON-AXIS	8.696mm	-8.696mm	ON-AXIS	8.696mm	-8.696mm	EFL (mm)	Δ EFL (mm)	FFL (mm)	Δ EFL (%)
001	0.037	0.058	0.062	--	--	--	20.218	0.088	2.282	0.44
003	0.022	0.055	0.079	0.52	0.58	0.58	20.000	-0.120	2.456	-0.6
004	0.019	0.066	0.077	0.60	0.49	0.48	20.240	0.110	2.352	0.55
005	0.025	0.074	0.044	0.60	0.46	0.38	20.54	0.41	2.267	2.04

DESIGN EFL = 20.13 MM

Δ EFL = MEASURED EFL -20.13 MM

FFL = FLANGE FOCAL LENGTH MEASURED FROM DATUM A (3 PADS) ON ASSY DRAWINGS

APPENDIX E: FILTER TRANSMISSION DATA

Table 14.1. Schott BG-40 filter average transmission data

	MER10212705-3-2	MER10212705-3-6	MER10212705-3-8
Wavelength (nm)	Transmission (%)	Transmission (%)	Transmission (%)
200	-2.32642E-05	-2.87612E-05	-3.67068E-05
201	-1.3503E-05	-3.47037E-05	-1.12907E-05
202	-2.24704E-05	-2.4721E-05	-1.24283E-05
203	-2.21017E-05	-2.5766E-05	-1.51741E-05
204	-2.60817E-05	-2.55635E-05	-1.95225E-05
205	-2.58497E-05	-2.30745E-05	-9.45581E-06
206	-2.81001E-05	-1.77636E-05	-1.97047E-05
207	-1.71679E-05	-3.0855E-05	-1.53861E-05
208	-2.20301E-05	-4.63938E-05	-1.97781E-05
209	-9.31261E-06	-2.51569E-05	-2.48272E-05
210	-1.09356E-05	-3.47941E-05	-4.1653E-05
211	-3.11678E-05	-2.85908E-05	-1.52535E-05
212	-2.11619E-05	-2.62938E-05	-3.20372E-05
213	-2.65818E-05	-3.88855E-05	-2.33231E-05
214	-2.82397E-05	-4.25387E-05	-1.36643E-05
215	-3.62289E-05	-4.15657E-05	-3.10768E-05
216	-1.79031E-05	-2.75506E-05	-2.39781E-05
217	-2.24064E-05	-3.3066E-05	-1.86012E-05
218	-2.17996E-05	-1.44531E-05	-3.01877E-05
219	-2.45432E-05	-3.07229E-05	-2.46165E-05
220	-2.10802E-05	-3.67037E-05	-3.39943E-05
221	-2.39663E-05	-4.56424E-05	-2.18664E-05
222	-3.35468E-06	-2.31282E-05	-1.11486E-05
223	-1.5755E-05	-3.45884E-05	-3.07467E-05
224	-2.09032E-05	-2.52632E-05	-1.52831E-05
225	-2.87317E-05	-3.85413E-05	-1.72769E-05
226	-1.82437E-05	-3.35248E-05	-3.14057E-05
227	-2.45233E-05	-4.61684E-05	-2.63763E-05
228	-1.89788E-05	-2.37689E-05	-2.21068E-05
229	-2.57158E-05	-3.64451E-05	-1.50364E-05
230	-1.28378E-05	-3.23765E-05	-2.61016E-05
231	-4.49429E-05	-2.68107E-05	-2.90216E-05
232	-2.85905E-05	-3.77842E-05	-2.02791E-05
233	-3.24016E-05	-2.44787E-05	-2.29121E-05
234	-1.75442E-05	-3.40625E-05	-1.59634E-05
235	-2.58717E-05	-3.57067E-05	-2.92459E-05
236	-2.06711E-05	-2.55482E-05	-2.07527E-05
237	-2.37767E-05	-2.33632E-05	-2.79392E-05
238	-2.49398E-05	-3.51054E-05	-1.56696E-05
239	-2.50093E-05	-2.42005E-05	-1.04246E-05
240	-1.4163E-05	-2.27278E-05	-2.69174E-05
241	-2.28983E-05	-2.01734E-05	-1.47825E-05
242	-1.55098E-05	-3.35014E-05	-2.97799E-05
243	-2.73416E-05	-2.61753E-05	-2.31801E-05

244	-2.61451E-05	-1.56543E-05	-2.97333E-05
245	-2.58578E-05	-3.4488E-05	-1.92814E-05
246	-3.52325E-05	-2.29323E-05	-3.01829E-05
247	-2.88649E-05	-1.71915E-05	-2.53423E-05
248	-3.09577E-05	-3.09436E-05	-2.38521E-05
249	-1.22239E-05	-3.41604E-05	-2.96552E-05
250	-2.10042E-05	-3.19525E-05	-3.28488E-05
251	-1.25547E-05	-2.76E-05	-2.13664E-05
252	-2.22483E-05	-1.94256E-05	-2.75655E-05
253	-1.95323E-05	-2.63981E-05	-2.69203E-05
254	-1.6713E-05	-2.96524E-05	-2.02124E-05
255	-3.17891E-05	-3.329E-05	-3.11137E-05
256	-2.96585E-05	-2.26362E-05	-2.27493E-05
257	-2.03694E-05	-2.19223E-05	-4.04991E-05
258	-3.3812E-05	-2.27254E-05	-2.36161E-05
259	-2.52024E-05	-3.51362E-05	-1.84587E-05
260	-2.77656E-05	-1.48164E-05	-3.06773E-05
261	-2.72074E-05	-2.5971E-05	-3.09937E-05
262	-1.57365E-05	-2.79995E-05	-1.62067E-05
263	-1.714E-05	-2.18076E-05	-1.99507E-05
264	-1.23131E-05	-2.41457E-05	-1.90959E-05
265	-2.05814E-05	-2.90244E-05	-2.38927E-05
266	-2.29397E-05	-2.74792E-05	-3.10001E-05
267	-2.96255E-05	-1.87909E-05	-2.04305E-05
268	-2.20076E-05	-2.78969E-05	-3.23424E-05
269	-2.21226E-05	-2.12982E-05	-1.77726E-05
270	-2.86819E-05	-1.76394E-05	-2.11432E-05
271	-2.35518E-05	-2.35641E-05	-3.13956E-05
272	-1.94318E-05	-3.40715E-05	-3.10007E-05
273	-1.06672E-05	-4.09576E-05	-2.81259E-05
274	-1.79598E-05	-2.29225E-05	-2.03191E-05
275	-2.19703E-05	-2.78006E-05	-3.10116E-05
276	-2.29565E-05	-2.25761E-05	-2.26345E-05
277	-2.92954E-05	-2.64537E-05	-3.35366E-05
278	-2.63264E-05	-2.20866E-05	-2.48543E-05
279	-1.96046E-05	-1.24858E-05	-3.14981E-05
280	-1.37985E-05	-2.50517E-05	-3.11827E-05
281	-2.73009E-05	-2.5262E-05	-1.2006E-05
282	-1.86841E-05	-1.66783E-05	-3.20777E-05
283	-2.37769E-05	-3.1409E-05	-3.39142E-05
284	-3.69904E-05	-3.88891E-05	-3.89907E-05
285	-1.26122E-05	-1.41704E-05	-3.42255E-05
286	-2.34857E-05	-1.02757E-05	-3.59821E-05
287	-3.02888E-05	-1.5899E-05	-2.96043E-05
288	-2.19866E-05	-2.77958E-05	-3.68379E-05
289	-2.72995E-05	-2.69202E-05	-2.34304E-05
290	-3.64044E-05	-2.71408E-05	-3.08552E-05
291	-2.69507E-05	-2.14967E-05	-3.32996E-05
292	-2.15297E-05	-1.72797E-05	-1.8123E-05
293	-2.5542E-05	-1.49043E-05	-3.11509E-05

294	-2.00527E-05	-2.44689E-05	-2.21389E-05
295	-1.94253E-05	-1.39724E-05	-2.33964E-05
296	-1.72493E-05	-1.40938E-05	-2.81199E-05
297	-1.37216E-05	-2.27481E-05	-4.2558E-05
298	-2.41918E-05	-3.57839E-05	-2.50141E-05
299	-2.15615E-05	-2.38458E-05	-2.07848E-05
300	-2.68232E-05	-2.05331E-05	-2.64469E-05
301	-1.79835E-05	-9.16054E-06	-3.0687E-05
302	-2.33401E-05	-1.64207E-05	-2.45382E-05
303	-2.46609E-05	-2.34914E-05	-2.63045E-05
304	-1.9699E-05	2.63765E-06	-2.09476E-05
305	-1.17472E-05	-2.45447E-05	-3.38003E-05
306	-1.40569E-05	-2.29998E-05	-1.41236E-05
307	-1.19343E-05	-2.9994E-05	-2.10481E-05
308	-1.59189E-05	-1.47498E-05	-2.53622E-05
309	-1.30723E-05	-8.3124E-06	-2.62474E-05
310	-9.73358E-06	3.31415E-07	-1.34328E-05
311	2.53945E-05	3.24331E-05	1.44259E-05
312	0.000114339	0.000121735	0.000118372
313	0.000360793	0.000378609	0.000375961
314	0.000921263	0.000941957	0.000928091
315	0.002035228	0.002072864	0.002071106
316	0.004055407	0.00415358	0.004115722
317	0.00735142	0.007450003	0.007406048
318	0.012169183	0.012191547	0.01211502
319	0.018925758	0.019068666	0.018972336
320	0.028007122	0.028222291	0.028087059
321	0.039456715	0.039703263	0.039555757
322	0.053477053	0.053482214	0.053237237
323	0.069359538	0.069228963	0.069017339
324	0.087508489	0.087756803	0.087082463
325	0.107130301	0.108574623	0.108201344
326	0.128347756	0.130055913	0.129875748
327	0.150288244	0.152292855	0.152116641
328	0.173170998	0.175368337	0.175144079
329	0.197320508	0.199739306	0.199564859
330	0.221656167	0.224296247	0.224061674
331	0.245944067	0.24881928	0.248569172
332	0.270312941	0.273409732	0.273208131
333	0.294799432	0.297972246	0.29781279
334	0.319748039	0.323043683	0.322947499
335	0.343493375	0.347003189	0.347010079
336	0.366959321	0.370497177	0.370626017
337	0.390634665	0.394194677	0.394337533
338	0.414588399	0.418366627	0.418584011
339	0.43664674	0.43957288	0.440443309
340	0.458343961	0.460628967	0.461042775
341	0.480345664	0.482019745	0.483020738
342	0.500750532	0.502759365	0.503653508
343	0.519920186	0.521950343	0.52286906

344	0.539431881	0.541381872	0.542401717
345	0.558909178	0.562025473	0.562076282
346	0.575938295	0.580073051	0.58055591
347	0.593000658	0.596695969	0.597386933
348	0.61052195	0.614092504	0.614522949
349	0.627583246	0.632365622	0.63304431
350	0.643052925	0.64739546	0.64847927
351	0.6571197	0.661557345	0.662310549
352	0.670499646	0.675041018	0.675797625
353	0.683960576	0.688126599	0.688960252
354	0.696499679	0.70060145	0.701607537
355	0.708014958	0.711997055	0.712743222
356	0.719785631	0.723757103	0.724742769
357	0.730262593	0.734221217	0.734971614
358	0.740653979	0.74442348	0.745283654
359	0.750088237	0.75371504	0.754487804
360	0.759175178	0.762884541	0.76357371
361	0.767913854	0.770866516	0.771494875
362	0.775762488	0.778523645	0.779242225
363	0.783598432	0.78650256	0.787109645
364	0.79143499	0.794142301	0.794774921
365	0.798109893	0.800545149	0.801145292
366	0.804585558	0.807318201	0.807588699
367	0.810231027	0.812869821	0.813430004
368	0.816370444	0.819253157	0.81958306
369	0.821659645	0.824538122	0.825212046
370	0.826373079	0.829274541	0.829895413
371	0.831790273	0.834746777	0.835062306
372	0.836076923	0.838560446	0.839146266
373	0.840502116	0.84327552	0.843592059
374	0.844746323	0.846999558	0.847381173
375	0.848674357	0.851204945	0.851357545
376	0.852309535	0.854769096	0.855129157
377	0.855610258	0.858068469	0.858258517
378	0.85880703	0.861222822	0.861377303
379	0.861953058	0.864232051	0.864324125
380	0.864822012	0.867340061	0.867125127
381	0.867530856	0.869834197	0.86998739
382	0.870408474	0.872300881	0.872277008
383	0.872735244	0.874511211	0.874598381
384	0.87467715	0.8764033	0.876541228
385	0.877193678	0.879100919	0.878996969
386	0.878893497	0.880694075	0.88068975
387	0.881434652	0.883219356	0.883049132
388	0.882976235	0.88517289	0.884651792
389	0.885002535	0.886984901	0.886912622
390	0.886491123	0.888520646	0.888261382
391	0.888435499	0.890172771	0.889963815
392	0.889754299	0.891618751	0.891253574
393	0.891197347	0.893204831	0.89271024

394	0.89300635	0.894772022	0.894305998
395	0.893960264	0.895925655	0.89539875
396	0.895689137	0.897442825	0.896986348
397	0.896976025	0.898973471	0.898340816
398	0.898241965	0.900208775	0.899655395
399	0.899610712	0.901442924	0.900873862
400	0.901121648	0.902872776	0.902173165
401	0.90198346	0.903826797	0.902951764
402	0.903818253	0.905646817	0.904956018
403	0.904723091	0.906508193	0.905770829
404	0.905835461	0.907506754	0.906891107
405	0.9072626	0.908788821	0.908258985
406	0.908259512	0.909924906	0.909213314
407	0.90964017	0.911229698	0.910438764
408	0.910581693	0.912191526	0.91166003
409	0.911565038	0.913200895	0.91248293
410	0.912805715	0.914514665	0.913771465
411	0.914282082	0.915911685	0.915182522
412	0.915344377	0.917061771	0.916171611
413	0.916152517	0.917780427	0.917027795
414	0.917449177	0.919128082	0.918338548
415	0.919069056	0.920724855	0.91972348
416	0.919801813	0.921695636	0.920787572
417	0.920833243	0.92261612	0.92170709
418	0.922049042	0.923559577	0.92269323
419	0.923118406	0.924893179	0.923998617
420	0.924221569	0.925785289	0.924768671
421	0.925881001	0.927388657	0.926449142
422	0.92655244	0.928150346	0.92730121
423	0.928078482	0.92954092	0.928694794
424	0.929028384	0.930732053	0.929917442
425	0.930267025	0.931781345	0.931041307
426	0.931514306	0.932840188	0.931998613
427	0.932545387	0.933912209	0.933054769
428	0.933554882	0.934871371	0.933863486
429	0.934566108	0.936069913	0.934963729
430	0.935959426	0.93722028	0.936172887
431	0.936887291	0.938452685	0.937471053
432	0.937922224	0.939203425	0.938399477
433	0.938788368	0.940278128	0.939256433
434	0.940162655	0.94145122	0.940543656
435	0.941182469	0.94234063	0.941480798
436	0.941989413	0.943611854	0.942372743
437	0.943188283	0.944431646	0.943642362
438	0.944168332	0.945334967	0.944482429
439	0.945116989	0.946323884	0.945437765
440	0.946335509	0.947375652	0.946625289
441	0.947040662	0.948194054	0.947128933
442	0.948766754	0.949685228	0.948796453
443	0.949173363	0.950398994	0.949538177

444	0.950391737	0.951211019	0.950570049
445	0.951405142	0.952628988	0.951551085
446	0.951606438	0.952738444	0.951954803
447	0.953549474	0.954605829	0.953650633
448	0.95387686	0.95496164	0.954089629
449	0.954464845	0.955309364	0.954450503
450	0.956048154	0.957100823	0.956093229
451	0.956252452	0.957073539	0.956360596
452	0.957352315	0.958195021	0.957459052
453	0.958271598	0.959048705	0.958329854
454	0.95897032	0.959854359	0.959001693
455	0.959542597	0.960372652	0.959657081
456	0.960492094	0.961220692	0.96067306
457	0.961282962	0.96237046	0.961568578
458	0.961445596	0.962173779	0.961222197
459	0.962839455	0.963461452	0.962737112
460	0.963204008	0.964112879	0.963489696
461	0.963951867	0.964656393	0.963881765
462	0.9648503	0.965440386	0.96453934
463	0.964872802	0.96547913	0.964923266
464	0.96596538	0.966813039	0.965981074
465	0.966708875	0.967348791	0.966703859
466	0.9672426	0.967867567	0.96706462
467	0.967710423	0.968106004	0.967455436
468	0.967976192	0.968642276	0.967989187
469	0.968777656	0.969490501	0.968777299
470	0.969413069	0.969949223	0.969398548
471	0.969810522	0.970461104	0.969851294
472	0.970473227	0.97073913	0.970178487
473	0.971162233	0.971387179	0.971005173
474	0.971203993	0.971770605	0.97125934
475	0.971496083	0.971691369	0.971546036
476	0.972118277	0.972495467	0.971928308
477	0.972356956	0.972640667	0.972181812
478	0.972646513	0.972990632	0.972547314
479	0.973329359	0.973452192	0.972928937
480	0.973671258	0.97383544	0.973429219
481	0.973947609	0.974438553	0.9737795
482	0.974039338	0.974329441	0.973873983
483	0.97445417	0.97503405	0.974341317
484	0.974880033	0.975187289	0.974485357
485	0.975095168	0.975515054	0.974864
486	0.975197185	0.975408003	0.974767919
487	0.975412556	0.975760845	0.975153399
488	0.975566966	0.975976106	0.975476583
489	0.975371197	0.975728771	0.975189639
490	0.975911152	0.976337968	0.975679651
491	0.97598664	0.976137065	0.975853149
492	0.976216795	0.976446962	0.975581987
493	0.976295869	0.97665179	0.976064506

494	0.976356744	0.976621822	0.976291823
495	0.976534373	0.976767408	0.976262621
496	0.976195554	0.976489135	0.975825868
497	0.976304843	0.976484603	0.97596676
498	0.976301813	0.9764719	0.975868291
499	0.976314136	0.976378039	0.97592619
500	0.976249507	0.976614491	0.975841062
501	0.976023697	0.975885941	0.97568762
502	0.976175953	0.976263033	0.975697798
503	0.975832861	0.97600585	0.975567605
504	0.975899769	0.975662869	0.975425614
505	0.975491262	0.975499072	0.974989633
506	0.974848514	0.975033856	0.974727216
507	0.975084943	0.975119988	0.974798993
508	0.974699625	0.974712061	0.974211152
509	0.974619761	0.974707677	0.974541258
510	0.973710475	0.97376531	0.973362931
511	0.973989176	0.973958702	0.973734474
512	0.973174806	0.973531605	0.972937313
513	0.972832634	0.972901847	0.972669162
514	0.972243221	0.972479955	0.971737205
515	0.971772254	0.972043794	0.971583444
516	0.971200521	0.971418983	0.971056194
517	0.970507166	0.970664576	0.970092441
518	0.970085565	0.970028848	0.969606864
519	0.969463199	0.969830077	0.9690183
520	0.968550068	0.968579955	0.968012569
521	0.967829172	0.968194513	0.967451291
522	0.966943308	0.966958207	0.966515899
523	0.966038865	0.966065128	0.96555644
524	0.965250273	0.965478053	0.964782218
525	0.964693912	0.964853719	0.964279121
526	0.963069503	0.963163902	0.962817917
527	0.961855754	0.961968016	0.961553293
528	0.960836303	0.961011882	0.960413159
529	0.959658123	0.959829285	0.959216281
530	0.958085252	0.958396169	0.957746062
531	0.957269644	0.957469797	0.9567694
532	0.955612489	0.955857159	0.955363699
533	0.954106546	0.954431879	0.953740546
534	0.952770563	0.953108746	0.952416067
535	0.951082005	0.951247508	0.950884765
536	0.949485185	0.949791581	0.949333934
537	0.947228341	0.947716872	0.94709947
538	0.945592902	0.945882181	0.945337802
539	0.943314831	0.943673498	0.943101558
540	0.941767468	0.941919076	0.941530724
541	0.939068124	0.939738445	0.938864574
542	0.937438604	0.937673796	0.937235743
543	0.935172815	0.935527629	0.935000572

544	0.932871505	0.933038115	0.932504251
545	0.930200271	0.930656111	0.929854753
546	0.927452091	0.927589436	0.927020368
547	0.924939049	0.925306395	0.924624282
548	0.922045341	0.922330178	0.921911748
549	0.919468344	0.91988264	0.919334656
550	0.916044625	0.916477215	0.915759172
551	0.913043897	0.913091206	0.912604307
552	0.90977473	0.910195711	0.909641478
553	0.905922656	0.906405513	0.905674793
554	0.902850374	0.903176252	0.902602392
555	0.899176286	0.899638597	0.89914025
556	0.894947876	0.895393821	0.894879408
557	0.891677421	0.892358372	0.891581847
558	0.887402957	0.888025046	0.887372406
559	0.883590326	0.88472168	0.883724171
560	0.878604502	0.879290634	0.878542276
561	0.874433974	0.87508061	0.874430107
562	0.8703084	0.870832751	0.870320053
563	0.865245972	0.865830145	0.865299071
564	0.860655066	0.861350277	0.860716298
565	0.855045773	0.85550338	0.855089666
566	0.850288994	0.850950818	0.850281668
567	0.844996294	0.845664879	0.844951851
568	0.839007271	0.83980253	0.83911139
569	0.834312807	0.834934979	0.834298708
570	0.828518088	0.829149199	0.828588486
571	0.822673951	0.823101767	0.822427493
572	0.816769734	0.817402779	0.816835999
573	0.810361819	0.81100462	0.810265348
574	0.804281708	0.805055112	0.804371873
575	0.797671017	0.798426196	0.797863273
576	0.790707154	0.791593393	0.79074027
577	0.784308831	0.785182227	0.784520582
578	0.777322638	0.778130217	0.777665584
579	0.770417014	0.771277685	0.770709131
580	0.762774612	0.763498072	0.763297532
581	0.755676751	0.756553954	0.756136264
582	0.748397269	0.749293602	0.748815193
583	0.740410937	0.741200651	0.740616593
584	0.732898771	0.733577753	0.733030923
585	0.724995933	0.725833512	0.725170052
586	0.717331765	0.718207252	0.71749903
587	0.708830832	0.709706114	0.709168001
588	0.700565902	0.701519664	0.700856958
589	0.692437935	0.693309168	0.692724801
590	0.683828747	0.684911675	0.684263725
591	0.675305125	0.67623516	0.675751502
592	0.666863473	0.66768434	0.667174129
593	0.657866154	0.658735167	0.658233673

594	0.648946583	0.649890012	0.649347079
595	0.63959788	0.640759666	0.640202991
596	0.630583171	0.631636679	0.631044495
597	0.621214446	0.622336375	0.621709106
598	0.61192857	0.612904158	0.612296335
599	0.602497986	0.603581341	0.603021004
600	0.593073856	0.594605575	0.59370166
601	0.583627018	0.585269067	0.584556328
602	0.573806597	0.575533996	0.57458507
603	0.564164664	0.565696951	0.565039
604	0.55453685	0.555476341	0.555222174
605	0.544811254	0.54591415	0.545500291
606	0.534808114	0.535984139	0.535681283
607	0.524561895	0.525717781	0.525320429
608	0.51473271	0.515908501	0.515540745
609	0.504808281	0.506011608	0.505676395
610	0.494984246	0.496188127	0.495720658
611	0.485147025	0.486208524	0.485886033
612	0.475054537	0.47623666	0.475885164
613	0.465119365	0.466248235	0.465931234
614	0.455414517	0.456621178	0.456219662
615	0.445336708	0.446402539	0.446062842
616	0.435219454	0.436414721	0.436123875
617	0.425475012	0.42675563	0.426337564
618	0.415653662	0.416844343	0.416571544
619	0.405759856	0.406959959	0.406640644
620	0.395963287	0.397149246	0.396977395
621	0.38627879	0.387559891	0.387377854
622	0.37675037	0.377961626	0.377944898
623	0.366951015	0.368092391	0.368252639
624	0.3575486	0.358795592	0.358697675
625	0.348145839	0.34933571	0.349171269
626	0.338966153	0.340160516	0.339952372
627	0.329640585	0.330781614	0.330619684
628	0.320287316	0.321522856	0.321391154
629	0.311331271	0.312469339	0.312319605
630	0.302375826	0.303487223	0.303412918
631	0.293444804	0.294663576	0.294471972
632	0.284683907	0.28582231	0.285700161
633	0.276108807	0.277231671	0.277099555
634	0.267593755	0.268722243	0.268655386
635	0.25928773	0.260346658	0.260329726
636	0.251114575	0.252175365	0.252094713
637	0.242909381	0.243981474	0.24397928
638	0.234890428	0.235961301	0.235930265
639	0.22702465	0.228093125	0.228077333
640	0.219288248	0.220324739	0.220312284
641	0.211828516	0.212874	0.212876482
642	0.204296167	0.205281835	0.205268603
643	0.19698075	0.197991577	0.198005967

644	0.190031636	0.191027782	0.191265409
645	0.183014257	0.184067511	0.184234989
646	0.176379098	0.177343585	0.177483057
647	0.169660637	0.170615026	0.170670037
648	0.163287978	0.164205723	0.164223357
649	0.15697212	0.157877658	0.157954067
650	0.150787883	0.151690531	0.151738829
651	0.144741467	0.145583022	0.14569132
652	0.138918543	0.139775419	0.139857802
653	0.133287971	0.134130977	0.134176875
654	0.127681934	0.128502901	0.128585653
655	0.122330317	0.123136823	0.123199044
656	0.117105778	0.117918718	0.117985086
657	0.112054823	0.112839235	0.112926619
658	0.107239474	0.10795232	0.10805686
659	0.102493801	0.103208198	0.103298628
660	0.097936397	0.098639154	0.09872393
661	0.093426156	0.094098772	0.094222725
662	0.089178918	0.08988036	0.089966956
663	0.085015434	0.085671711	0.085766574
664	0.081020103	0.081687333	0.081767311
665	0.077148793	0.077750418	0.077862059
666	0.073420011	0.074015603	0.074126937
667	0.069891975	0.07045779	0.07057237
668	0.066485801	0.06702503	0.067140732
669	0.06318758	0.063721164	0.063821228
670	0.060032161	0.060544578	0.060646429
671	0.056972464	0.057462839	0.057588355
672	0.054083995	0.054576307	0.054660757
673	0.051271873	0.051734818	0.05184195
674	0.048562574	0.049022754	0.049108028
675	0.045966589	0.046396563	0.046508038
676	0.043527375	0.043939373	0.04405372
677	0.041172887	0.041580401	0.041680707
678	0.038962434	0.039357202	0.039453006
679	0.036808555	0.037193846	0.037302497
680	0.034777087	0.035157948	0.035245865
681	0.032848765	0.033197765	0.033273898
682	0.030970311	0.0313069	0.031405484
683	0.029214457	0.029537406	0.029613061
684	0.027541732	0.027832901	0.027921778
685	0.02592607	0.026202767	0.02630086
686	0.024412317	0.024708687	0.024798518
687	0.022958104	0.023236259	0.023361602
688	0.02160325	0.021878098	0.021975412
689	0.020336818	0.020590085	0.020669639
690	0.019108175	0.019343643	0.019422909
691	0.01793944	0.018188974	0.018234278
692	0.016841606	0.017076591	0.01712589
693	0.015792371	0.016003425	0.016069533

694	0.014818975	0.01503545	0.015072422
695	0.013875949	0.014090651	0.014141422
696	0.013011097	0.013218344	0.01326063
697	0.012177816	0.01237963	0.012411238
698	0.011412089	0.011577322	0.01161486
699	0.010687435	0.010848439	0.010895
700	0.009996284	0.010154379	0.010204997
701	0.009369245	0.009504131	0.009553436
702	0.008745814	0.008890973	0.008928558
703	0.008156424	0.00831419	0.008354489
704	0.00762926	0.007746135	0.007808243
705	0.007120557	0.007246562	0.007278842
706	0.006641687	0.006757344	0.006782275
707	0.006191523	0.006324075	0.006332008
708	0.005785464	0.005885202	0.005923969
709	0.00538422	0.005488645	0.00550458
710	0.005017721	0.005122322	0.005147034
711	0.004691715	0.00477538	0.004817829
712	0.004364551	0.004437398	0.00447916
713	0.004075163	0.004150306	0.004171334
714	0.003783073	0.003851926	0.003892422
715	0.003512701	0.003587393	0.003610692
716	0.003282089	0.00334483	0.003373405
717	0.003050061	0.003101365	0.003116879
718	0.002838699	0.002886616	0.002912208
719	0.002620067	0.002663691	0.002701067
720	0.002450261	0.00249527	0.002531327
721	0.002272347	0.002305526	0.002341606
722	0.002108856	0.002161397	0.002173158
723	0.001959136	0.002013084	0.002030483
724	0.00182334	0.001865347	0.001872687
725	0.001691713	0.001741152	0.001747124
726	0.001567651	0.001614976	0.001611576
727	0.00145737	0.001500714	0.001502468
728	0.001357822	0.001385977	0.001401426
729	0.001251546	0.001286749	0.001294568
730	0.001168268	0.001199158	0.001199332
731	0.001097928	0.001104595	0.001111413
732	0.001012619	0.001024331	0.001043958
733	0.000925672	0.000939027	0.000949552
734	0.000871888	0.000894407	0.000892997
735	0.000818966	0.000822366	0.000836807
736	0.000754958	0.000755827	0.000760416
737	0.000701868	0.000721397	0.000728059
738	0.000630102	0.000649622	0.000656965
739	0.00060483	0.000618596	0.000613047
740	0.000561406	0.000559761	0.000559697
741	0.000507144	0.00051667	0.000518864
742	0.000475605	0.000466641	0.000482894
743	0.000439416	0.000440952	0.000443852

744	0.000403522	0.000404185	0.000425547
745	0.000384761	0.000380718	0.000391153
746	0.000365867	0.000361908	0.000359015
747	0.000314088	0.000318386	0.000327449
748	0.000317488	0.000293356	0.000319654
749	0.000284417	0.000281185	0.000289287
750	0.000256559	0.000263147	0.000256283
751	0.000246587	0.000240167	0.000254143
752	0.000235533	0.000221385	0.000225079
753	0.000214352	0.00020856	0.000216771
754	0.000200701	0.000198319	0.000199882
755	0.000178703	0.000182169	0.000186463
756	0.000154873	0.000161965	0.000163092
757	0.000156014	0.000141494	0.000156305
758	0.000146597	0.000138389	0.000142746
759	0.000139043	0.000133864	0.00013926
760	0.00012212	0.000118181	0.000131738
761	0.00010926	0.000112834	0.000112623
762	0.000107276	0.000101196	0.000116345
763	9.82698E-05	9.21004E-05	0.000100878
764	9.90785E-05	9.21051E-05	9.30271E-05
765	9.70573E-05	8.13439E-05	8.49987E-05
766	9.09441E-05	6.86321E-05	8.82824E-05
767	7.69669E-05	7.2122E-05	7.34248E-05
768	7.85639E-05	7.19944E-05	7.29061E-05
769	6.89081E-05	5.46088E-05	6.14316E-05
770	6.22847E-05	5.83284E-05	6.07716E-05
771	5.9608E-05	5.5599E-05	5.92683E-05
772	4.47001E-05	4.55113E-05	6.55115E-05
773	5.56906E-05	5.65105E-05	4.21815E-05
774	4.31619E-05	4.62746E-05	4.16333E-05
775	4.38237E-05	4.5015E-05	4.42557E-05
776	4.4879E-05	4.08644E-05	3.80762E-05
777	4.7612E-05	3.41661E-05	4.39801E-05
778	3.28971E-05	2.07148E-05	3.76101E-05
779	3.92372E-05	3.39402E-05	2.87826E-05
780	3.47647E-05	2.48473E-05	2.88187E-05
781	3.97291E-05	3.40877E-05	2.40177E-05
782	2.84867E-05	2.39922E-05	3.13624E-05
783	2.35389E-05	2.89354E-05	2.48669E-05
784	3.34778E-05	3.34758E-05	2.91852E-05
785	2.44688E-05	1.17976E-05	1.61263E-05
786	1.84124E-05	4.75245E-06	1.23575E-05
787	1.34047E-05	1.3816E-05	1.17443E-05
788	2.64515E-05	1.48697E-05	2.10534E-05
789	1.96643E-05	1.56557E-05	2.96006E-05
790	9.02669E-06	1.29964E-05	1.61475E-05
791	1.52165E-05	1.64183E-05	1.23767E-05
792	3.21858E-05	3.63984E-06	-5.80662E-06
793	2.31624E-05	1.61392E-05	-4.59309E-06

794	1.63388E-05	1.16598E-05	1.51469E-05
795	2.75857E-06	1.18561E-05	-2.83387E-06
796	1.48619E-05	1.9276E-05	1.00263E-05
797	2.08067E-05	-7.62374E-06	7.77396E-06
798	-3.55783E-06	7.14658E-06	9.99214E-06
799	7.25359E-06	1.04299E-05	1.52375E-05
800	1.65142E-05	2.01178E-05	-2.27949E-08
801	1.77291E-05	6.48947E-06	1.21835E-06
802	4.95603E-06	1.85302E-05	1.6556E-06
803	2.21476E-05	5.05135E-07	6.47019E-06
804	1.2148E-05	5.14659E-07	2.17179E-05
805	9.33334E-06	-2.71512E-06	4.85058E-06
806	1.61323E-05	5.87233E-08	-2.80804E-06
807	1.00881E-05	9.67816E-06	-3.43351E-08
808	1.77017E-05	-8.507E-07	6.76815E-06
809	2.75496E-06	3.51861E-06	6.71453E-06
810	4.31674E-06	6.26918E-07	9.1027E-06
811	3.0176E-06	7.04902E-06	-7.64963E-06
812	7.41721E-06	2.08851E-06	2.85664E-06
813	-9.41629E-06	2.40936E-06	5.64485E-06
814	-5.4497E-06	8.89613E-06	-1.42421E-06
815	-2.69121E-06	6.75957E-06	5.07647E-06
816	-1.44079E-05	5.52881E-08	3.32239E-06
817	5.37803E-06	1.32492E-05	5.31061E-06
818	6.9497E-06	-5.99389E-07	-7.33549E-06
819	4.34186E-06	9.074E-06	-6.87855E-07
820	-4.43192E-06	5.75435E-06	9.65719E-06
821	-2.21914E-06	9.60109E-06	8.79777E-06
822	7.94537E-06	4.76315E-06	-1.23778E-05
823	3.4625E-06	5.44119E-06	-8.98901E-06
824	4.53978E-06	1.31604E-06	-1.53369E-06
825	3.61877E-06	-1.63755E-06	-8.96349E-06
826	1.04798E-06	-3.84149E-06	1.03477E-05
827	7.62673E-08	-3.62387E-06	-1.02084E-05
828	6.47939E-06	1.12144E-06	2.5935E-07
829	-4.83029E-06	1.25217E-07	3.82091E-06
830	-7.97514E-06	-7.97003E-06	3.12971E-07
831	-1.1171E-05	2.67976E-06	1.14706E-07
832	-9.06613E-06	-6.71828E-06	-5.19932E-06
833	-6.2272E-06	-6.82098E-07	2.84247E-06
834	-3.33829E-06	-5.74655E-06	-5.77871E-06
835	-3.23621E-06	1.33177E-05	7.54424E-07
836	-3.571E-06	-3.15989E-06	-8.52261E-06
837	-1.34557E-05	5.16355E-06	6.77858E-06
838	-1.45587E-06	1.28303E-06	1.29872E-05
839	4.87169E-06	1.08166E-05	-7.42917E-06
840	-5.53122E-06	6.1454E-06	-1.40291E-05
841	9.88094E-06	9.47393E-06	1.19177E-05
842	4.13064E-06	-1.10495E-05	-5.61309E-06
843	2.46931E-06	-3.08655E-06	-5.09286E-06

844	-1.33409E-06	5.16765E-06	5.5676E-06
845	-8.69801E-06	4.22432E-06	-4.95059E-06
846	1.47056E-06	-8.79225E-06	-9.22287E-06
847	-1.20318E-05	1.62769E-06	-4.99644E-06
848	-1.14686E-05	3.99996E-06	2.64161E-06
849	-2.6186E-05	-3.45031E-06	1.18642E-05
850	-2.84173E-05	-1.1392E-05	-1.70966E-06
851	-2.05271E-05	-1.99552E-05	-6.7524E-06
852	-2.10235E-05	-6.05573E-06	-6.51227E-06
853	7.0329E-06	1.39213E-05	2.63542E-06
854	-1.38106E-05	1.18903E-05	2.05515E-05
855	-1.27758E-05	-4.66375E-05	-5.57728E-06
856	-3.695E-05	-4.716E-06	3.03365E-05
857	-2.82298E-05	4.94178E-06	-3.53036E-05
858	1.85042E-05	-3.62645E-05	7.02065E-07
859	-1.63135E-05	-3.13895E-05	-2.95064E-05
860	-3.44428E-05	-2.703E-05	1.2543E-05
861	-2.16933E-05	-3.42578E-05	2.65492E-06
862	2.61082E-05	9.91387E-06	-2.56645E-07
863	-3.1995E-06	1.47976E-05	5.43053E-05
864	-1.6775E-05	-1.44329E-05	-4.68201E-06
865	6.46601E-07	-2.7986E-05	-1.27526E-05
866	-4.01927E-05	-1.64386E-05	-1.81219E-05
867	5.50008E-07	7.95934E-06	-3.00816E-05
868	6.81038E-06	-2.04486E-05	1.41279E-05
869	-1.12806E-05	-7.48648E-06	1.56679E-05
870	-3.81145E-05	1.06399E-05	-2.25973E-05
871	-1.53711E-05	-2.77554E-05	3.66525E-05
872	7.95017E-07	-1.9456E-05	-3.81459E-06
873	1.57803E-05	5.3197E-06	-2.18027E-05
874	-3.51034E-05	-1.13234E-05	-5.27907E-06
875	-2.04622E-05	1.3541E-05	-2.87307E-05
876	-1.2136E-05	-1.52023E-06	1.33076E-05
877	-7.53635E-06	-2.41151E-05	-4.37715E-06
878	2.04603E-06	-2.96991E-05	-1.79832E-05
879	-5.93053E-06	-3.50739E-06	-7.84537E-06
880	4.83902E-06	-1.59073E-05	-2.79264E-05
881	-5.25867E-06	-3.64743E-05	1.91563E-05
882	-2.11659E-05	9.02807E-07	-5.24059E-06
883	-2.94236E-05	-1.24939E-05	-1.26032E-07
884	-2.20193E-05	2.57936E-05	-2.28575E-05
885	-4.99509E-05	-9.00772E-06	9.16186E-06
886	-1.93338E-05	-2.59778E-05	-1.44338E-06
887	-6.15437E-06	-3.8652E-05	-1.27915E-08
888	1.38122E-05	-1.64521E-05	3.30806E-07
889	3.01865E-05	1.31043E-05	-1.36271E-05
890	-1.32323E-05	-6.32496E-06	-1.58992E-05
891	-1.08398E-05	1.32937E-06	3.0057E-05
892	-1.89374E-05	5.11601E-06	8.8122E-06
893	2.3862E-06	-8.47898E-06	-4.86015E-06

894	2.54778E-05	-1.71214E-05	9.6498E-06
895	-7.42409E-06	-9.73384E-07	3.60151E-05
896	-1.93021E-05	-4.05961E-05	-5.9505E-06
897	-1.00818E-05	5.21282E-06	-2.02254E-05
898	-3.13789E-05	1.59878E-05	-9.19964E-06
899	-5.05032E-05	-3.15038E-06	3.68605E-06
900	-9.49462E-06	-1.37296E-06	-1.8851E-05
901	-1.88724E-05	-2.69025E-05	3.73708E-05
902	-1.38699E-05	-2.44179E-05	-5.0138E-06
903	-1.38133E-05	-2.37139E-05	1.57281E-05
904	1.86711E-06	9.77514E-06	4.369E-06
905	-4.11576E-06	-6.62165E-06	3.91137E-06
906	1.15493E-05	2.67596E-06	2.5592E-05
907	-2.0294E-06	4.45044E-05	-1.02544E-05
908	-2.67671E-05	2.10126E-05	1.3603E-05
909	-7.43775E-06	1.01455E-05	-1.98434E-05
910	-1.9088E-05	3.01081E-05	2.33532E-05
911	1.01164E-05	-1.75431E-05	4.32646E-06
912	-3.27157E-05	-1.44497E-05	1.11452E-05
913	-1.13357E-05	1.32675E-05	1.4685E-05
914	-2.49447E-05	-7.39426E-06	1.73635E-05
915	1.26853E-06	-1.39555E-05	9.67262E-06
916	-4.28084E-06	-1.9984E-05	-1.85076E-05
917	-2.15207E-05	-3.69154E-06	1.28752E-05
918	-1.52707E-05	2.84165E-06	1.64588E-05
919	-9.36795E-07	9.20857E-06	-9.7723E-06
920	-1.88093E-05	-5.29393E-06	2.68628E-05
921	-3.29218E-06	9.14077E-06	2.25947E-05
922	1.32652E-05	2.52414E-06	-8.80983E-06
923	-2.02875E-05	-3.20111E-05	3.60753E-06
924	4.79768E-06	1.37506E-05	7.0713E-06
925	-5.12935E-06	1.31222E-05	5.64994E-06
926	-2.47062E-06	-1.13695E-05	1.63625E-05
927	3.49461E-05	8.78984E-06	2.68315E-05
928	-1.95304E-05	1.64611E-05	-9.73013E-06
929	-1.9629E-05	2.88912E-05	1.09046E-05
930	1.65483E-05	1.01913E-05	1.68011E-05
931	8.81125E-06	1.90554E-05	2.04777E-06
932	2.1482E-05	-8.01437E-06	9.62575E-06
933	-2.94426E-05	2.70621E-07	5.08465E-06
934	-2.08549E-05	6.4035E-06	4.10326E-05
935	-8.06143E-06	2.56683E-05	4.16394E-05
936	-1.69202E-06	2.2141E-06	1.1201E-05
937	1.06421E-05	2.36683E-05	1.4844E-05
938	-5.34075E-08	2.89783E-05	5.97954E-06
939	-9.68323E-06	7.90631E-06	-1.46934E-05
940	-7.25734E-06	-2.57155E-05	-6.42814E-06
941	3.98456E-06	-1.18548E-05	3.66343E-06
942	-5.08569E-06	1.13442E-05	4.5549E-06
943	-1.58662E-06	2.16907E-05	5.11148E-05

944	-1.53732E-05	-6.99216E-07	1.56024E-05
945	-5.30087E-06	-7.77554E-06	1.51772E-05
946	1.53294E-05	6.52572E-06	2.15377E-05
947	1.79625E-05	4.31455E-06	1.16768E-05
948	1.71727E-05	7.07736E-06	2.14529E-05
949	1.96605E-05	3.88699E-05	3.50956E-05
950	2.29267E-05	9.10571E-06	2.73915E-05
951	3.97053E-06	-1.84915E-05	1.64716E-05
952	2.78814E-06	1.51593E-05	-1.37763E-05
953	3.30447E-05	-1.87943E-06	2.59524E-05
954	-1.54542E-05	-2.54432E-05	2.01736E-05
955	2.53095E-05	3.29221E-05	1.53628E-05
956	-1.44774E-05	2.06409E-05	-6.6312E-06
957	-6.33734E-06	1.51571E-05	1.82942E-05
958	-1.49513E-05	3.30384E-05	4.54933E-06
959	3.34906E-05	2.03832E-05	9.85401E-06
960	-1.11594E-07	2.20303E-07	1.01459E-05
961	-1.83967E-05	2.14345E-05	9.14008E-06
962	1.8343E-06	4.88455E-06	8.88622E-06
963	1.30115E-05	1.10122E-05	2.7393E-05
964	7.66601E-06	1.78493E-05	2.61149E-05
965	7.09111E-06	8.44755E-06	2.633E-05
966	6.2468E-06	2.32764E-05	1.34434E-06
967	4.42421E-06	1.58509E-05	5.25339E-06
968	4.29559E-05	5.75731E-06	4.13071E-05
969	-2.50239E-05	2.16162E-05	5.18271E-05
970	8.02499E-06	5.1228E-05	3.82291E-05
971	1.2047E-06	1.30145E-05	2.62883E-05
972	-1.87009E-05	2.05525E-05	6.29316E-06
973	5.91948E-06	2.36092E-05	2.88019E-05
974	1.60203E-05	-1.45697E-05	2.35707E-05
975	2.81776E-05	2.51058E-05	4.31488E-05
976	1.48286E-05	1.41761E-05	4.63028E-05
977	-7.68636E-07	1.9244E-05	1.62512E-05
978	7.80525E-06	2.68699E-05	2.67654E-05
979	-1.09655E-05	3.85117E-05	5.75891E-06
980	6.352E-06	1.15114E-05	5.97856E-06
981	-1.39287E-05	-8.75483E-07	7.58756E-06
982	2.26554E-05	3.60054E-05	2.00436E-06
983	-5.17997E-06	7.24122E-07	2.35401E-05
984	4.62008E-05	-2.85833E-06	3.69347E-05
985	7.94605E-06	9.36239E-06	5.02717E-05
986	2.83483E-06	6.66593E-06	1.97579E-05
987	-3.44982E-06	-1.09612E-05	1.44066E-05
988	-4.01757E-06	4.13286E-06	3.42731E-05
989	8.62993E-06	3.2593E-05	5.26827E-06
990	4.69316E-05	2.14691E-05	5.04254E-05
991	1.70792E-05	6.74718E-05	1.71469E-05
992	2.58012E-06	-8.56727E-06	1.96023E-05
993	5.23853E-05	5.79332E-05	4.63019E-05

994	-1.3955E-05	2.7575E-05	2.64751E-05
995	-1.48987E-05	7.43041E-06	-4.83414E-06
996	2.29201E-05	3.74278E-05	1.94583E-05
997	1.72428E-05	1.63923E-05	1.45948E-05
998	-1.99733E-07	2.6482E-07	2.53208E-05
999	1.54294E-05	2.21772E-05	2.92516E-05
1000	-8.56488E-06	-7.3814E-07	1.53421E-05
1001	2.08999E-05	2.10201E-05	4.9652E-05
1002	2.52639E-05	3.65646E-05	4.06405E-05
1003	3.58436E-05	1.84256E-05	2.02406E-05
1004	3.61769E-05	1.2767E-05	2.80705E-05
1005	1.0595E-05	1.11689E-05	1.93851E-05
1006	4.35245E-05	5.34306E-05	3.47108E-05
1007	-4.69874E-06	3.56407E-05	2.5247E-05
1008	3.65691E-05	2.05526E-05	1.62775E-05
1009	1.47318E-05	5.58912E-05	1.41761E-05
1010	2.27225E-05	3.65692E-05	2.09154E-05
1011	4.2696E-05	3.9587E-05	3.80303E-05
1012	2.15205E-05	7.82302E-06	4.64892E-05
1013	4.37463E-05	5.84672E-06	4.98247E-05
1014	4.17211E-05	1.26728E-06	2.77999E-06
1015	1.29075E-05	5.83997E-05	3.5032E-05
1016	9.6549E-06	5.95592E-05	4.21735E-05
1017	1.75341E-05	6.06857E-07	5.1946E-05
1018	-7.7169E-06	4.37904E-05	5.85626E-05
1019	2.14438E-05	4.50716E-05	3.8247E-05
1020	6.18724E-05	4.09227E-05	1.1257E-05
1021	2.62901E-05	2.66281E-05	2.42892E-05
1022	4.75472E-05	2.86561E-06	3.35972E-05
1023	2.84864E-05	1.8332E-05	6.04043E-05
1024	6.08622E-05	2.72456E-05	4.46686E-05
1025	2.31407E-05	5.1203E-05	4.05681E-05
1026	3.40597E-05	3.67341E-05	4.91742E-05
1027	2.99244E-05	3.67997E-05	3.57312E-05
1028	5.41028E-05	2.84014E-05	2.55721E-05
1029	2.84088E-05	3.48217E-05	5.63055E-05
1030	2.15161E-05	3.78207E-05	4.45626E-05
1031	1.2837E-05	3.28454E-06	4.69699E-05
1032	5.9458E-05	4.12262E-05	3.60337E-05
1033	2.88645E-05	1.51409E-05	6.38648E-05
1034	1.17671E-05	5.647E-05	7.55974E-05
1035	3.58985E-05	5.27586E-05	4.05429E-05
1036	2.09398E-05	5.09582E-05	2.66658E-05
1037	2.29173E-05	5.38236E-05	7.04579E-05
1038	4.01895E-05	4.46397E-05	4.56531E-05
1039	3.07806E-05	1.99458E-05	6.44466E-05
1040	4.67912E-05	4.2004E-05	4.70807E-05
1041	6.16778E-05	5.58506E-05	3.35451E-05
1042	6.51204E-05	3.06148E-05	4.73579E-05
1043	2.41331E-05	3.13495E-05	2.5254E-05

1044	2.84748E-05	7.20039E-05	7.15881E-05
1045	3.48757E-05	3.61622E-05	8.34713E-05
1046	4.90726E-05	4.58789E-05	7.51666E-05
1047	3.07082E-05	5.23053E-05	6.45388E-05
1048	3.52132E-05	3.26432E-05	7.98085E-05
1049	6.01359E-05	7.72856E-05	6.58389E-05
1050	3.1105E-05	4.94542E-05	8.6656E-05
1051	3.59245E-05	7.1434E-05	6.67951E-05
1052	5.33249E-05	8.30107E-05	7.78519E-05
1053	5.06714E-05	6.75932E-05	7.57272E-05
1054	3.3089E-05	6.5373E-05	9.66328E-05
1055	4.20961E-05	6.92691E-05	0.000109515
1056	3.61896E-05	3.83123E-05	7.49165E-05
1057	6.44995E-05	5.41588E-05	8.88241E-05
1058	4.27847E-05	6.30715E-05	5.09434E-05
1059	7.05028E-05	3.93229E-05	6.71557E-05
1060	5.21818E-05	5.18884E-05	5.34251E-05
1061	5.19322E-05	7.41E-05	0.000100763
1062	5.77721E-05	9.02009E-05	6.819E-05
1063	4.13579E-05	8.01668E-05	6.43404E-05
1064	7.63324E-05	7.02729E-05	7.16423E-05
1065	6.54001E-05	7.94797E-05	6.72162E-05
1066	6.22792E-05	9.64724E-05	8.03513E-05
1067	7.92859E-05	6.88217E-05	6.49559E-05
1068	9.49954E-05	9.92885E-05	7.79144E-05
1069	9.92801E-05	8.65484E-05	0.000122208
1070	3.54071E-05	0.000101664	7.14537E-05
1071	6.32518E-05	9.52163E-05	0.000113691
1072	7.44805E-05	7.64848E-05	9.77631E-05
1073	8.89148E-05	6.07273E-05	0.000113096
1074	8.84193E-05	0.000104306	0.000106603
1075	5.83166E-05	7.55464E-05	0.000134899
1076	0.000110386	8.41093E-05	0.000108067
1077	5.96902E-05	8.41245E-05	8.40921E-05
1078	9.85794E-05	9.8811E-05	0.000114905
1079	7.62084E-05	9.95167E-05	9.4E-05
1080	4.48272E-05	8.62195E-05	7.67247E-05
1081	0.000113272	9.178E-05	0.000107242
1082	0.000127066	0.000100242	0.000140011
1083	0.000110496	0.000108097	0.000132577
1084	9.69751E-05	0.000117608	0.000103984
1085	9.70118E-05	7.69229E-05	9.58755E-05
1086	0.00011011	0.000113991	0.000152971
1087	9.75702E-05	0.000157334	0.000112786
1088	7.70741E-05	0.000107952	9.79819E-05
1089	0.000102547	0.000113426	0.000111492
1090	9.50058E-05	0.000108287	0.000111994
1091	0.000106123	0.000121925	0.000114819
1092	0.000120173	0.000108029	0.000142726
1093	0.000124319	0.000111185	0.000141463

1094	0.000116396	0.000120244	0.00014331
1095	0.000126463	0.000117044	0.000153227
1096	0.000139142	0.000141013	0.000142613
1097	0.000100494	0.000150864	0.000194742
1098	9.88052E-05	0.000124632	0.000135743
1099	0.000149365	0.000147355	0.00015873
1100	0.000120577	0.000143775	0.000137453

APPENDIX F: DUST COVER TRANSMISSION DATA

Table 15.1. Kapton dust cover spectral transmission

Wavelength (nm)	Transmission
348	0.0029
352	0.0029
356	0.0030
360	0.0030
364	0.0030
368	0.0029
372	0.0030
376	0.0030
380	0.0030
384	0.0030
388	0.0030
392	0.0030
396	0.0029
400	0.0030
404	0.0031
408	0.0031
412	0.0031
416	0.0031
420	0.0031
424	0.0031
428	0.0031
432	0.0030
436	0.0030
440	0.0031
444	0.0031
448	0.0031
452	0.0035
456	0.0041
460	0.0046
464	0.0052
468	0.0054
472	0.0073
476	0.0107
480	0.0158
484	0.0232
488	0.0325
492	0.0456
496	0.0614
500	0.0812
504	0.1044
508	0.1308
512	0.1607
516	0.1914
520	0.2239
524	0.2582
528	0.2932

532	0.3266
536	0.3590
540	0.3897
544	0.4179
548	0.4443
552	0.4674
556	0.4883
560	0.5072
564	0.5240
568	0.5394
572	0.5528
576	0.5651
580	0.5760
584	0.5852
588	0.5944
592	0.6029
596	0.6105
600	0.6191
604	0.6268
608	0.6338
612	0.6405
616	0.6467
620	0.6525
624	0.6567
628	0.6618
632	0.6663
636	0.6707
640	0.6749
644	0.6786
648	0.6820
652	0.6853
656	0.6884
660	0.6921
664	0.6951
668	0.6984
672	0.7009
676	0.7036
680	0.7059
684	0.7079
688	0.7099
692	0.7116
696	0.7136
700	0.7159
704	0.7177
708	0.7196
712	0.7215
716	0.7235
720	0.7253
724	0.7269
728	0.7283

732	0.7299
736	0.7316
740	0.7330
744	0.7347
748	0.7362
752	0.7377
756	0.7394
760	0.7412
764	0.7424
768	0.7433
772	0.7447
776	0.7457
780	0.7464
784	0.7474
788	0.7483
792	0.7494
796	0.7505
800	0.7515
804	0.7519
808	0.7528
812	0.7537
816	0.7543
820	0.7551
824	0.7559
828	0.7574
832	0.7584
836	0.7591
840	0.7597
844	0.7602
848	0.7612
852	0.7615
856	0.7617
860	0.7622
864	0.7627
868	0.7633
872	0.7636
876	0.7645
880	0.7655
884	0.7665
888	0.7676
892	0.7680
896	0.7685
900	0.7691
904	0.7699
908	0.7700
912	0.7706
916	0.7714
920	0.7723
924	0.7732
928	0.7744

932	0.7749
936	0.7755
940	0.7761
944	0.7773
948	0.7769
952	0.7766
956	0.7766
960	0.7773
964	0.7774
968	0.7778
972	0.7788
976	0.7797
980	0.7803
984	0.7811
988	0.7813
992	0.7814
996	0.7818
1000	0.7821
1004	0.7818
1008	0.7817
1012	0.7828
1016	0.7826
1020	0.7832
1024	0.7840
1028	0.7846
1032	0.7853
1036	0.7860
1040	0.7863
1044	0.7869
1048	0.7867
1052	0.7868
1056	0.7867
1060	0.7872
1064	0.7875
1068	0.7874
1072	0.7878
1076	0.7883
1080	0.7885
1084	0.7894
1088	0.7894
1092	0.7900
1096	0.7901
1100	0.7907
1104	0.7908
1108	0.7903
1112	0.7898
1116	0.7898
1120	0.7897
1124	0.7897
1128	0.7914

1132	0.7921
1136	0.7933
1140	0.7943
1144	0.7956
1148	0.7953
1152	0.7959
1156	0.7956
1160	0.7957
1164	0.7951
1168	0.7969
1172	0.7957
1176	0.7969
1180	0.7960
1184	0.7968
1188	0.7962
1192	0.7980
1196	0.7977
1200	0.7997

APPENDIX G: MI AMBIENT CALIBRATION

PDS filenames: yymmddhhmmss_ttttttt_MI_nnn.img
where yy = year, first mm = month, dd = day, hh = hours, second mm = minutes, ss = seconds of image acquisition time; ttttttt is exposure time in units of 0.1 msec; nnn = camera serial number. Images listed below are organized by acquisition time.
NOTE: Due to changes in the GSE software during the tests, the exposure time in the filename (ttttttt) may not be correct. Similarly, the exposure time in the PDS label may not be correct. The exposure count in the PDS label *is* correct, however, and should be used to calculate true exposure times:
count * 5.12 = exposure time in msec.

Data directory structure:
Ancillary = spreadsheets containing integrating sphere calibration data, etc.
Bar target = images of focus test target, illuminated from behind by integrating sphere
Blooming = images of fiber light source to characterize CCD blooming
Central pixel = images of collimated light source in alignment telescope, centered in field of view
Dark current = camera not exposed to light, readout of thermal noise in CCD
Grid target = images of precisely machined target, illuminated from behind by integrating sphere
Light transfer = series of dark current images (really "electron transfer") at various integration times; nominally one sequence per subdirectory "Ltfnn"
Other targets = includes flat fields (images of integrating sphere)
Rock target = images of Dick Morris' rock samples
Stray light = images of fiber light source at various positions in and near field of view
Test = pre-calibration test data

PDS labels: The video offset value was automatically updated in the labels. The note field often contains useful information.
As noted above, the EXPOSURE_DURATION value may be in error, so the EXPOSURE_DURATION_COUNT keyword should be used to calculate exposure times. The only known exception to this is that, before 8 August 2002, the EXPOSURE_DURATION_COUNT keyword was being interpreted as a signed integer, so counts above 32767 are incorrect.

MI 105

17 July 2002 calibration image summary:

140136 – 141712	Electron transfer sequence
145509 – 153502	Dark current
160711 – 161029	Central pixel
164132 – 164635	Flat field without dust cover
170158 – 183046	Bar target at various distances (plus zero-exposures; no dust cover)

185121 – 202431 Bar target at various distances (plus zeros; with dust cover)
203444 – 204024 Flat field with dust cover
204413 – 205724 Flat field without dust cover
210352 – 213958 Grid target at various distances (plus zeros; no dust cover)

18 July 2002 calibration image summary:
075033 – 081737 Blooming tests using fiber
082003 – 092544 Stray light, transfer smear tests using fiber
094246 – 095617 Dark current
102720 – 123254 Rock targets

26 July 2002 post-vibration calibration image summary:
140426 – 142105 Electron transfer sequence
143123 – 143722 Central pixel
145208 – 151112 Bar target at various distances (plus zero exposures; no dust cover)
151948 – 152618 Grid target at various distances (plus zeros; no dust cover)
152832 – 153907 Flat field without dust cover

29 August 2002 post-thermal calibration image summary:
110031 – 110606 Central pixel
201309 – 202551 Bar target at various distances (plus zero exposures; no dust cover)
214112 – 205455 Grid target at various distances (plus zeros; no dust cover)
210223 – 210846 Flat field without dust cover
211500 – 212954 Stray light tests using fiber

MI 110

19 August 2002 calibration image summary:

090651 – 093026	Electron transfer sequence
103043 – 104419	Dark current
110110 – 110438	Central pixel
115104 – 115432	Flat field without dust cover
120342 – 125014	Bar target at various distances (plus zero-exposures; no dust cover)
132234 – 141101	Bar target at various distances (plus zeros; with dust cover)
142337 – 154356	Grid target at various positions (plus zeros; no dust cover)
154953 – 160413	Flat field without dust cover
162727 – 163244	Stray light tests using fiber
163541 – 164557	Transfer smear tests using fiber
165122 – 165548	Blooming tests using fiber
170220 – 174212	Stray light tests using fiber
175224 – 183058	Dark current
184934 – 200527	Rock targets, with and without dust cover

28 August 2002 post-vibration calibration image summary:

164703 – 170343	Electron transfer sequence
173406 – 173552	Central pixel
174941 – 182743	Bar target at various distances (plus zero exposures; no dust cover)
185255 – 190702	Grid target at various distances (plus zeros; no dust cover)
192600 – 193224	Flat field without dust cover

APPENDIX H: MI THERMAL/VACUUM CALIBRATION

PDS filenames: yymmddhhmmss_ttttttt_MI_nnn.img
where yy = year, first mm = month, dd = day, hh = hours, second mm = minutes, ss = seconds of image acquisition time; ttttttt is exposure time in units of 0.1 msec; nnn = camera serial number. Images listed below are organized by acquisition time.
NOTE: Due to changes in the GSE software during the tests, the exposure time in the filename (ttttttt) may not be correct. Similarly, the exposure time in the PDS label may not be correct. The exposure count in the PDS label *is* correct, however, and should be used to calculate true exposure times:
count × 5.12 = exposure time in msec.

Data directory structure:
Ancillary = spreadsheets containing monochromator, integrating sphere calibration data, etc.
Blooming = images of fiber light source to characterize CCD blooming
Cold_soak = images taken during -110°C flight acceptance testing
Dark current = camera not exposed to light, readout of thermal noise in CCD
Hot_soak = images taken during 50°C flight acceptance testing
Light transfer = series of dark current images (really "electron transfer") at various integration times; nominally one sequence per subdirectory "Ltfnn"
Other targets = includes flat fields (images of integrating sphere and diffusing plate)
Pre_test_func = pre-calibration function test images
Radiometry = images of calibrated integrating sphere
Spectral = images of calibrated monochromator
Test = miscellaneous test images

PDS labels: Instrument temperature data were typed in manually for each image or set of images, so may be incorrect. Temperatures were converted from PRT resistances using a spreadsheet. The video offset value was automatically updated in the labels. The note field often contains useful information.
As noted above, the EXPOSURE_DURATION value may be in error, so the EXPOSURE_DURATION_COUNT keyword should be used to calculate exposure times. The only known exception to this is that, before 8 August 2002, the EXPOSURE_DURATION_COUNT keyword was being interpreted as a signed integer, so counts above 32767 are incorrect.

MI 105

30 July 2002 checkout (ambient temperature and pressure) image summary:
173942 – 175543 Electron transfer sequence

31 July 2002 test (ambient temperature, vacuum) image summary:
135631 – 144949 Integrating sphere placement tests

163319 – 163425 Dark current (no useful temperature data)
163603 – 163842 Integrating sphere placement tests

3 August 2002 post-hot soak checkout image summary:
164906 – 165450 Dark current (no useful temperature data)

5 August 2002 cold soak image summary:
090812 – 091530 Dark current (no useful temperature data)
092403 – 100832 Light transfer (no useful temperature data)

8 August 2002 –110°C calibration image summary:
052833 – 054201 Dark current
063754 – 082120 Light transfer (video offset characterization)
102715 – 103752 Blooming test
113539 – 124954 Dark current (some images in test folder)
125307 – 130114 Flat fields (in "other targets" folder)

9-11 August 2002 hot soak image summary:
143150 – 135216 Dark current

11 August 2002 –110°C cold start image summary:
232833 – 234044 Light transfer

14 August 2002 –55°C spectral calibration image summary:
171833 – 191837 Monochromator images

15 August 2002 –10°C spectral calibration image summary:
014417 – 034159 Monochromator images
035116 – 035828 Dark current

16 August 2002 +5°C spectral calibration image summary:
203513 – 214525 Monochromator images
215406 – 220235 Dark current

17 August 2002 +5°C radiometric calibration image summary:
010835 – 011820 Light transfer (in Ltf2)
012316 – 013254 Light transfer (in Ltf1)
013645 – 014940 Post dust-removal images (in Ltf1)
015328 – 020448 Radiometry half-wells (in Ltf1)

21 August 2002 -10°C radiometric calibration image summary:
120744 – 121728 Light transfer #1 (in Ltf1)
122257 – 123243 Light transfer #2 (in Ltf1)
124846 Post dust-removal image
125022 – 125942 Radiometry half-wells (in Radiometry)
131206 – 134112 Dark current

22 August 2002 -55°C calibration image summary:

110047 – 113137	Dark current
115242 – 120243	Light transfer, video offset = 4095 (in Ltf11)
120936 – 121928	Light transfer, video offset = 4070 (in Ltf12)
122259 – 123252	Light transfer, video offset = 4040 (in Ltf13)
123742 – 124735	Light transfer, video offset = 4095 (in Ltf14)
130611 – 131227	Dark current
132427 – 133421	Light transfer, video offset = 4070 (in Ltf15)
133840 – 134832	Light transfer, video offset = 4040 (in Ltf16)
142731 – 144214	Radiometry half-wells
145110 – 150418	Dark current

23 August 2002 ambient calibration image summary:

194253 – 195507	Radiometry half-wells (no chamber window, no diffuser)
203249 – 204415	Radiometry half-wells (with chamber window and diffuser)
204801 – 205727	Dark current

24 August 2002 -55°C calibration image summary:

210836 – 212546	Flat fields (in “other targets” folder)

27 August 2002 calibration image summary:

013655 – 015426	Flat fields at –10°C
161954 – 163643	Light transfer at room temperature

28 August 2002 ambient calibration image summary:

124509 – 124821	Flat fields without diffuser
171859 – 1714151	Flat fields without diffuser, no chamber window

MI 110

4 September 2002 checkout (ambient temperature and pressure) image summary:
111319 – 112555 Electron transfer sequence

11 September 2002 –110°C calibration image summary:
001231 – 002627 Flat field (no diffuser) video offset characterization
003341 – 004743 Dark current
005416 – 010447 Light transfer (in Ltf02)
011743 – 012813 Light transfer (in Ltf03)
020602 – 080718 Dark current video offset characterization

11-13 September 2002 hot soak image summary:
133749 – 100931 Dark current
102057 – 102931 Hot starts

14 September 2002 -55°C spectral calibration image summary:
051758 – 052808 Light transfer at 600 nm (in Ltf04)
060030 – 075523 Dark current
081104 – 105840 Monochromator images
110359 – 111233 Dark current

16 September 2002 spectral calibration image summary:
075723 – 084141 Dark current at –10°C
085230 – 112855 Monochromator images at –10°C
120719 – 125740 Dark current at –10°C
131204 – 134284 Dark current during temperature transition
144908 – 165749 Monochromator images at +5°C
170151 – 172139 Dark current at +5°C

20 September 2002 radiometric calibration image summary:
031321 – 032337 Light transfer (in Ltf05) at +5°C
033318 – 034331 Light transfer (in Ltf06) at +5°C
034646 – 035628 Radiometry half-wells at +5°C
064647 – 065658 Light transfer (in Ltf07) at –10°C
070203 – 071215 Light transfer (in Ltf08) at –10°C
071502 – 072511 Radiometry half-wells at –10°C

24 September 2002 -55°C radiometric calibration image summary:
082441 – 083523 Light transfer (in Ltf09)
083825 – 084907 Light transfer (in Ltf10)
085922 – 091025 Radiometry half-wells
092528 – 093806 Radiometry half-wells after cleaning chamber window
094508 – 095230 Dark current
100537 – 113341 Dark current during temperature transition

24 September 2002 ambient calibration image summary:

190723 – 191920 Radiometry half-wells (no chamber window, no diffuser)
195725 – 200300 Dark current

25 September 2002 +5°C calibration image summary:

075446 – 080808 Dark current
083941 – 085148 Flat fields
093647 – 095102 Dark current

26 September 2002 calibration image summary:

080304 – 081813 Dark current at –55°C
083012 – 084353 Flat fields at –55°C
192210 – 193928 Dark current at –10°C during camera warmup
195110 – 200200 Flat fields at –10°C
200808 – 201255 Dark current at –10°C

APPENDIX I: RADIOMETRIC CALIBRATION DATA

Table 18.1.
Transmission of chamber window in room 111 building 168 1/4/02

filter (nm)	transmission
350	0.916
400	0.930
450	0.932
500	0.934
550	0.935
600	0.935
650	0.936
700	0.936
750	0.936
800	0.937
850	0.938
900	0.938
950	0.927
1000	0.938
1050	0.938
1100	0.931

Table 18.2. Spectral Irradiance Values for Lamp OL 220IR-D-P serial #: M-775, 6.5A @ 50cm

Wavelength (nm)	Irradiance W/(cm^2-nm)
250	5.818E-09
260	9.994E-09
270	1.631E-08
280	2.517E-08
290	3.744E-08
300	5.342E-08
310	7.479E-08
320	1.010E-07
330	1.342E-07
340	1.736E-07
350	2.210E-07
360	2.748E-07
370	3.380E-07
380	4.098E-07
390	4.912E-07
400	5.795E-07
410	6.771E-07
420	7.831E-07
430	8.971E-07
440	1.018E-06
450	1.146E-06
460	1.279E-06
470	1.417E-06
480	1.559E-06
490	1.706E-06
500	1.856E-06
510	2.011E-06
520	2.167E-06
530	2.325E-06
540	2.484E-06
550	2.642E-06
560	2.798E-06
570	2.951E-06
580	3.102E-06
590	3.251E-06
600	3.396E-06
610	3.538E-06
620	3.675E-06
630	3.808E-06
640	3.938E-06
650	4.062E-06
660	4.182E-06
670	4.296E-06
680	4.405E-06
690	4.509E-06
700	4.607E-06

710	4.700E-06
720	4.788E-06
730	4.871E-06
740	4.948E-06
750	5.020E-06
760	5.086E-06
770	5.148E-06
780	5.204E-06
790	5.254E-06
800	5.300E-06
810	5.339E-06
820	5.374E-06
830	5.403E-06
840	5.428E-06
850	5.448E-06
860	5.464E-06
870	5.476E-06
880	5.484E-06
890	5.489E-06
900	5.490E-06
910	5.489E-06
920	5.485E-06
930	5.479E-06
940	5.469E-06
950	5.457E-06
960	5.442E-06
970	5.425E-06
980	5.405E-06
990	5.383E-06
1000	5.359E-06
1010	5.333E-06
1020	5.306E-06
1030	5.276E-06
1040	5.244E-06
1050	5.210E-06
1060	5.173E-06
1070	5.134E-06
1080	5.093E-06
1090	5.050E-06
1100	5.006E-06

Table 18.3. Radiometer calibration data

JPL

CALIBRATION DATA **JPL STANDARDS LABORATORY 125-2**

				SHEET	
S.T. NO.	ST805			DATE	see below
DESCRIPTION	Red Radiometer	MANUFACTURER	JPL	BY:	C13
MODEL NO.	Red 1	I.D. NO.	IS022208	TEMP. C	23
SERIAL NO.		INSTRUCTION NO.		R.H. %	50

WORKING STANDARDS USED:

INSTRUMENT	MANUFACTURER	MODEL	IDENTIFICATION	SERIAL NO.	UNCERTAINTY	TEST NUMBER	Cal.Due
Irradiance Lamp	Optronic Labs	220IR-D-P	IS010723	M775			3/5/1999
Current Source	Optronic Labs	65D	1204073				7/12/1999
Diff. Refl.Panel	Labsphere	SRT-99-050				5 X 5 in.	n/a
Electrometer	Keithley	617	1049023		customer supplied		7/12/1999
TEC Controller	Alpha Omega	2-060	N/A	2-9566	customer supplied		(setpt.=15.02 C)

				(window out)	(diffuser window in)		
Wavelength Filter	Det.Signal (nA) 1/1998	Det.Signal (nA) 12/2001	Det.Signal (nA) 7/18/2002	Det.Signal (nA) 10/10/2002	Det.Signal (nA) 10/10/2002	Det.Signal (nA) 10/10/2002	(peak angle)
Dark	10.5 pA	1.7 pA	3.5 pA	0.001	0.001		
350	0.271	0.2692	0.2583	0.263	0.033		
400	0.676	0.677	0.662	0.688	0.095		
450	1.758	1.780	1.745	1.812	0.263		
500	4.910	5.012	4.936	5.097	0.773		
550	6.392	6.437	6.351	6.551	1.026		
600	9.494	9.512	9.413	9.686	1.566		
650	13.231	13.340	13.203	13.605	2.242		

700	13.081	13.172	13.015	13.405	2.319		
750	16.130	16.050	15.888	16.309	3.018		
800	18.875	18.420	18.313	18.767	3.676		
850	14.630	14.320	14.256	14.575	2.949		
900	12.395	12.050	12.025	12.276	2.546		
950	6.810	6.610	6.596	6.754	1.445		
1000	2.765	2.632	2.620	2.681	0.608		
1050	1.192	1.1020	1.0923	1.113	0.267		
1100	0.326	0.2980	0.2928	0.296	0.077		
Dark	25.3 pA	8.6pA	4.6 pA	0.001	0.001		
350		0.2709	0.2589		0.033		
800		18.415	18.311		3.702		

Notes:

No Window at input aperture
Radiometer covered with black cloth during measurements
Lamp Current=6.5 Adc @ 50cm(center of filament to panel)
Orient UUT at 800nm Maximum Response Angle (Approx. 39.5 X 39.5 cm)
Filter Shiny surface faces Out towards light source
Filters occupy middle slot, aperture @ rear slot

Table 18.4. Sphere calibration data used for MI 105 at -10°C

Date 21-Aug-02 Shutter width (mm) 15

Time 11:31 AM

Dark Current (amps) 5.00E-14 No filter diode (amps) 1.17E-04

Power Supply:

Filter	Electrometer Reading	Electrometer Units	Electrometer Reading	Radiometer Dark Current (from above)	Electrometer Reading Minus Dark Current (Ie)	Multiplicative constant (K)	Radiometry Reading (Ie * K)
(nm)	**Record Units!!**		**Amps**	Amps	Amps	(W/m^2/nm/sr)/(amps)	(W/m^2/nm/sr)
350	11.7	pa	1.17E-11	5E-14	1.165E-11	2.715E+06	3.163E-05
400	70.73	pa	7.073E-11	5E-14	7.068E-11	2.761E+06	0.0001951
450	0.224	na	2.24E-10	5E-14	2.2395E-10	2.067E+06	0.0004629
500	0.7023	na	7.023E-10	5E-14	7.0225E-10	1.184E+06	0.0008315
550	0.9496	na	9.496E-10	5E-14	9.4955E-10	1.309E+06	0.001243
600	1.406	na	1.406E-09	5E-14	1.40595E-09	1.135E+06	0.0015958
650	1.906	na	1.906E-09	5E-14	1.90595E-09	9.669E+05	0.0018429
700	1.851	na	1.851E-09	5E-14	1.85095E-09	1.112E+06	0.0020583
750	2.186	na	2.186E-09	5E-14	2.18595E-09	9.929E+05	0.0021704
800	2.419	na	2.419E-09	5E-14	2.41895E-09	9.085E+05	0.0021976
850	1.796	na	1.796E-09	5E-14	1.79595E-09	1.198E+06	0.0021515
900	1.411	na	1.411E-09	5E-14	1.41095E-09	1.435E+06	0.0020247
950	0.7212	na	7.212E-10	5E-14	7.2115E-10	2.603E+06	0.0018772
1000	0.3	na	3E-10	5E-14	2.9995E-10	6.428E+06	0.0019281
1050	124.5	pa	1.245E-10	5E-14	1.2445E-10	1.505E+07	0.001873
1100	35.41	pa	3.541E-11	5E-14	3.536E-11	5.442E+07	0.0019243

Table 18.5. Sphere calibration data used for MI 105 at -55°C

Date	22-Aug-02	Shutter width (mm)	15
Time	11:25 AM		
Dark Current (amps)	3.00E-14	No filter diode (amps)	1.22E-07
Power Supply:	110.1 V	4.86 A	

Filter (nm)	Electrometer Reading	Electrometer Units	Electrometer Reading	Radiometer Dark Current (from above)	Electrometer Reading Minus Dark Current (Ie)	Multiplicative constant (K)	Radiometry Reading (Ie * K)
	Record Units!!		**Amps**	Amps	Amps	(W/m^2/nm/sr)/(amps)	(W/m^2/nm/sr)
350	12.2	pA	1.22E-11	3E-14	1.217E-11	2.715E+06	3.304E-05
400	73.59	pA	7.359E-11	3E-14	7.356E-11	2.761E+06	0.0002031
450	0.2326	nA	2.326E-10	3E-14	2.3257E-10	2.067E+06	0.0004807
500	0.7293	nA	7.293E-10	3E-14	7.2927E-10	1.184E+06	0.0008635
550	0.9853	nA	9.853E-10	3E-14	9.8527E-10	1.309E+06	0.0012897
600	1.4593	nA	1.4593E-09	3E-14	1.45927E-09	1.135E+06	0.0016563
650	1.982	nA	1.982E-09	3E-14	1.98197E-09	9.669E+05	0.0019164
700	1.927	nA	1.927E-09	3E-14	1.92697E-09	1.112E+06	0.0021428
750	2.279	nA	2.279E-09	3E-14	2.27897E-09	9.929E+05	0.0022628
800	2.521	nA	2.521E-09	3E-14	2.52097E-09	9.085E+05	0.0022903
850	1.869	nA	1.869E-09	3E-14	1.86897E-09	1.198E+06	0.002239
900	1.4693	nA	1.4693E-09	3E-14	1.46927E-09	1.435E+06	0.0021084
950	0.7532	nA	7.532E-10	3E-14	7.5317E-10	2.603E+06	0.0019605
1000	0.313	nA	3.13E-10	3E-14	3.1297E-10	6.428E+06	0.0020118
1050	130.08	pA	1.3008E-10	3E-14	1.3005E-10	1.505E+07	0.0019573
1100	37.04	pA	3.704E-11	3E-14	3.701E-11	5.442E+07	0.0020141

Table 18.6. Sphere calibration data used for MI 110 at +5°C

NOTE: small external diffuser on sphere exit, diffuser material in front of diode

Date 9/20/2002

Time 2:40 AM

Dark Current (amps) 3.30E-14

Shutter width (mm) 15

for MI light transfer / radiometry at +5C

No filter diode (amps) 1.13E-07

Power Supply: 111.3 V
4.87 A

Filter (nm)	Electrometer Reading **Record Units!!**	Electrometer Units	Electrometer Reading **Amps**	Radiometer Dark Current (from above) Amps	Electrometer Reading Minus Dark Current (Ie) Amps	Multiplicative constant (K) (W/m^2/nm/sr)/(amps)	Radiometry Reading (Ie * K) (W/m^2/nm/sr)
350	12.21	picoa	1.221E-11	3.3E-14	1.2177E-11	2.715E+06	3.306E-05
400	73.35	picoa	7.335E-11	3.3E-14	7.3317E-11	2.761E+06	0.0002024
450	0.2273	nanoa	2.273E-10	3.3E-14	2.27267E-10	2.067E+06	0.0004698
500	0.7004	nanoa	7.004E-10	3.3E-14	7.00367E-10	1.184E+06	0.0008292
550	0.9342	nanoa	9.342E-10	3.3E-14	9.34167E-10	1.309E+06	0.0012228
600	1.371	nanoa	1.371E-09	3.3E-14	1.37097E-09	1.135E+06	0.001556
650	1.854	nanoa	1.854E-09	3.3E-14	1.85397E-09	9.669E+05	0.0017926
700	1.7906	nanoa	1.7906E-09	3.3E-14	1.79057E-09	1.112E+06	0.0019911
750	2.104	nanoa	2.104E-09	3.3E-14	2.10397E-09	9.929E+05	0.002089
800	2.32	nanoa	2.32E-09	3.3E-14	2.31997E-09	9.085E+05	0.0021077
850	1.7137	nanoa	1.7137E-09	3.3E-14	1.71367E-09	1.198E+06	0.002053
900	1.3441	nanoa	1.3441E-09	3.3E-14	1.34407E-09	1.435E+06	0.0019287
950	0.687	nanoa	6.87E-10	3.3E-14	6.86967E-10	2.603E+06	0.0017882
1000	0.2853	nanoa	2.853E-10	3.3E-14	2.85267E-10	6.428E+06	0.0018337
1050	117.62	picoa	1.1762E-10	3.3E-14	1.17587E-10	1.505E+07	0.0017697
1100	33.55	picoa	3.355E-11	3.3E-14	3.3517E-11	5.442E+07	0.001824

Table 18.7. Sphere calibration data used for MI 110 at -10°C
NOTE: small external diffuser on sphere exit, diffuser material in front of diode

Date 9/20/2002

Time 6:30 AM

Dark Current (amps) 5.00E-14

Power Supply: 111.3 V
4.87 A

Shutter width (mm) 15

for MI light transfer / radiometry at -10C

No filter diode (amps) 1.13E-07

Filter	Electrometer Reading	Electrometer Units	Electrometer Reading	Radiometer Dark Current (from above)	Electrometer Reading Minus Dark Current (Ie)	Multiplicative constant (K)	Radiometry Reading (Ie * K)
(nm)	**Record Units!!**		**Amps**	Amps	Amps	(W/m^2/nm/sr)/(amps)	(W/m^2/nm/sr)
350	12.4	picoa	1.24E-11	5E-14	1.235E-11	2.715E+06	3.353E-05
400	73.8	picoa	7.38E-11	5E-14	7.375E-11	2.761E+06	0.0002036
450	0.228	nanoa	2.28E-10	5E-14	2.2795E-10	2.067E+06	0.0004712
500	0.703	nanoa	7.03E-10	5E-14	7.0295E-10	1.184E+06	0.0008323
550	0.937	nanoa	9.37E-10	5E-14	9.3695E-10	1.309E+06	0.0012265
600	1.375	nanoa	1.375E-09	5E-14	1.37495E-09	1.135E+06	0.0015606
650	1.86	nanoa	1.86E-09	5E-14	1.85995E-09	9.669E+05	0.0017984
700	1.794	nanoa	1.794E-09	5E-14	1.79395E-09	1.112E+06	0.0019949
750	2.111	nanoa	2.111E-09	5E-14	2.11095E-09	9.929E+05	0.002096
800	2.326	nanoa	2.326E-09	5E-14	2.32595E-09	9.085E+05	0.0021131
850	1.718	nanoa	1.718E-09	5E-14	1.71795E-09	1.198E+06	0.0020581
900	1.347	nanoa	1.347E-09	5E-14	1.34695E-09	1.435E+06	0.0019329
950	0.689	nanoa	6.89E-10	5E-14	6.8895E-10	2.603E+06	0.0017933
1000	0.286	nanoa	2.86E-10	5E-14	2.8595E-10	6.428E+06	0.0018381
1050	118.5	picoa	1.185E-10	5E-14	1.1845E-10	1.505E+07	0.0017827
1100	33.8	picoa	3.38E-11	5E-14	3.375E-11	5.442E+07	0.0018367

Table 18.8. Sphere calibration data used for MI 110 at -55°C

NOTE: small external diffuser, diffuser material in front of diode

Date 9/24/2002

Time 8:02 AM

Dark Current (amps) 3.00E-14

Shutter width (mm) 15

No filter diode (amps) 1.05E-07

Power Supply: 110.5 V
4.87 A

Filter	Electrometer Reading	Electrometer Units	Electrometer Reading	Radiometer Dark Current (from above)	Electrometer Reading Minus Dark Current (Ie)	Multiplicative constant (K)	Radiometry Reading (Ie * K)
(nm)	**Record Units!!**		**Amps**	Amps	Amps	(W/m^2/nm/sr)/(amps)	(W/m^2/nm/sr)
350	11.42	picoa	1.142E-11	3E-14	1.139E-11	2.715E+06	3.092E-05
400	0.06797	nanoa	6.797E-11	3E-14	6.794E-11	2.761E+06	0.0001876
450	0.2097	nanoa	2.097E-10	3E-14	2.0967E-10	2.067E+06	0.0004334
500	0.6459	nanoa	6.459E-10	3E-14	6.4587E-10	1.184E+06	0.0007647
550	0.8621	nanoa	8.621E-10	3E-14	8.6207E-10	1.309E+06	0.0011284
600	1.266	nanoa	1.266E-09	3E-14	1.26597E-09	1.135E+06	0.0014369
650	1.712	nanoa	1.712E-09	3E-14	1.71197E-09	9.669E+05	0.0016553
700	1.653	nanoa	1.653E-09	3E-14	1.65297E-09	1.112E+06	0.0018381
750	1.943	nanoa	1.943E-09	3E-14	1.94297E-09	9.929E+05	0.0019292
800	2.144	nanoa	2.144E-09	3E-14	2.14397E-09	9.085E+05	0.0019478
850	1.584	nanoa	1.584E-09	3E-14	1.58397E-09	1.198E+06	0.0018976
900	1.244	nanoa	1.244E-09	3E-14	1.24397E-09	1.435E+06	0.0017851
950	0.638	nanoa	6.38E-10	3E-14	6.3797E-10	2.603E+06	0.0016606
1000	0.2634	nanoa	2.634E-10	3E-14	2.6337E-10	6.428E+06	0.0016929
1050	0.1088	nanoa	1.088E-10	3E-14	1.0877E-10	1.505E+07	0.001637
1100	31	picoa	3.1E-11	3E-14	3.097E-11	5.442E+07	0.0016854

Table 18.9. MI serial # 105 radiometry image filenames

-55°C	-10°C
020822143113_0010496_MI_105	020821125022_0011981_MI_105
020822143128_0010496_MI_105	020821125050_0011981_MI_105
020822143142_0010496_MI_105	020821125117_0011981_MI_105
020822143157_0010496_MI_105	020821125145_0011981_MI_105
020822143211_0010496_MI_105	020821125217_0011981_MI_105
020822143226_0010496_MI_105	020821125245_0011981_MI_105
020822143241_0010496_MI_105	020821125314_0011981_MI_105
020822143255_0010496_MI_105	020821125343_0011981_MI_105
020822143309_0010496_MI_105	020821125411_0011981_MI_105
020822143324_0010496_MI_105	020821125439_0011981_MI_105
020822143338_0010496_MI_105	020821125508_0011981_MI_105
020822143353_0010496_MI_105	020821125537_0011981_MI_105
020822143407_0010496_MI_105	020821125606_0011981_MI_105
020822143421_0010496_MI_105	020821125635_0011981_MI_105
020822143436_0010496_MI_105	020821125704_0011981_MI_105
020822143450_0010496_MI_105	020821125734_0011981_MI_105
020822143504_0010496_MI_105	020821125802_0011981_MI_105
020822143519_0010496_MI_105	020821125831_0011981_MI_105
020822143533_0010496_MI_105	020821125900_0011981_MI_105
020822143547_0010496_MI_105	020821125928_0011981_MI_105
020822143602_0010496_MI_105	
020822143616_0010496_MI_105	
020822143631_0010496_MI_105	
020822143645_0010496_MI_105	
020822143659_0010496_MI_105	
020822143714_0010496_MI_105	
020822143728_0010496_MI_105	
020822143742_0010496_MI_105	
020822143756_0010496_MI_105	
020822143811_0010496_MI_105	

Table 18.10. MI serial # 110 radiometry image filenames

-55°C	-10°C	+5°C
020924092909_0011469	020920071635_0013261	020920034759_0013824
020924092925_0011469	020920071650_0013261	020920034814_0013824
020924092941_0011469	020920071705_0013261	020920034829_0013824
020924092957_0011469	020920071720_0013261	020920034845_0013824
020924093012_0011469	020920071735_0013261	020920034900_0013824
020924093028_0011469	020920071750_0013261	020920034915_0013824
020924093043_0011469	020920071805_0013261	020920034930_0013824
020924093059_0011469	020920071820_0013261	020920034945_0013824
020924093114_0011469	020920071835_0013261	020920035000_0013824
020924093131_0011469	020920071850_0013261	020920035015_0013824
020924093147_0011469	020920071905_0013261	020920035030_0013824
020924093203_0011469	020920071920_0013261	020920035045_0013824
020924093219_0011469	020920071935_0013261	020920035100_0013824
020924093234_0011469	020920071950_0013261	020920035115_0013824
020924093250_0011469	020920072005_0013261	020920035130_0013824
020924093305_0011469	020920072020_0013261	020920035145_0013824
020924093321_0011469	020920072035_0013261	020920035200_0013824
020924093337_0011469	020920072050_0013261	020920035215_0013824
020924093352_0011469	020920072105_0013261	020920035230_0013824
020924093408_0011469	020920072120_0013261	020920035245_0013824
020924093423_0011469	020920072135_0013261	020920035300_0013824
020924093439_0011469	020920072150_0013261	020920035315_0013824
020924093455_0011469	020920072205_0013261	020920035330_0013824
020924093510_0011469	020920072220_0013261	020920035345_0013824
020924093526_0011469	020920072235_0013261	020920035400_0013824
020924093542_0011469	020920072250_0013261	020920035415_0013824
020924093557_0011469	020920072305_0013261	020920035430_0013824
020924093613_0011469	020920072320_0013261	020920035445_0013824
020924093628_0011469	020920072335_0013261	020920035500_0013824
020924093644_0011469	020920072350_0013261	020920035515_0013824

APPENDIX J: MI SPECTRAL CALIBRATION DATA

Monochromator wavelength offset files

(All wavelengths are in nanometers)

off_020814112912.prn:

Commanded Wavelength	Actual Wavelength
350	348.78
351	349.67
352	350.58
353	351.48
354	352.39
355	353.3
356	354.21
357	355.12
358	356.04
359	356.96
360	357.88
361	358.81
362	359.74
363	360.67
364	361.6
365	362.53
366	363.47
367	364.41
368	365.35
369	366.29
370	367.24
371	368.19
372	369.14
373	370.09
374	371.04
375	372
376	372.95
377	373.91
378	374.87
379	375.83
380	376.8
381	377.76
382	378.73
383	379.7
384	380.67
385	381.64
386	382.62
387	383.59
388	384.57
389	385.55
390	386.53
391	387.51
392	388.49
393	389.47
394	390.46
395	391.44
396	392.43
397	393.42
398	394.41
399	395.4
400	396.39
401	397.38
402	398.38
403	399.37
404	400.37
405	401.36
406	402.36
407	403.36
408	404.36
409	405.36
410	406.36
411	407.36
412	408.37
413	409.37
414	410.37
415	411.38
416	412.38
417	413.39
418	414.4
419	415.4
420	416.41
421	417.42
422	418.43
423	419.44
424	420.45
425	421.46
426	422.47
427	423.49
428	424.5
429	425.51
430	426.52
431	427.54
432	428.55
433	429.57
434	430.58
435	431.6
436	432.61
437	433.63
438	434.64
439	435.66
440	436.67
441	437.69
442	438.71
443	439.72
444	440.74
445	441.76
446	442.78

447	443.79
448	444.81
449	445.83
450	446.85
451	447.86
452	448.88
453	449.9
454	450.92
455	451.94
456	452.95
457	453.97
458	454.99
459	456.01
460	457.03
461	458.04
462	459.06
463	460.08
464	461.1
465	462.11
466	463.13
467	464.15
468	465.17
469	466.18
470	467.2
471	468.22
472	469.23
473	470.25
474	471.27
475	472.28
476	473.3
477	474.32
478	475.33
479	476.35
480	477.36
481	478.38
482	479.39
483	480.41
484	481.42
485	482.43
486	483.45
487	484.46
488	485.48
489	486.49
490	487.5
491	488.51
492	489.53
493	490.54
494	491.55
495	492.56
496	493.57
497	494.58
498	495.6
499	496.61
500	497.62
501	498.63
502	499.63
503	500.64
504	501.65
505	502.66
506	503.67
507	504.68
508	505.68
509	506.69
510	507.7
511	508.71
512	509.71
513	510.72
514	511.72
515	512.73
516	513.73
517	514.74
518	515.74
519	516.75
520	517.75
521	518.75
522	519.76
523	520.76
524	521.76
525	522.76
526	523.77
527	524.77
528	525.77
529	526.77
530	527.77
531	528.77
532	529.77
533	530.77
534	531.77
535	532.77
536	533.77
537	534.76
538	535.76
539	536.76
540	537.76
541	538.75
542	539.75
543	540.75
544	541.74
545	542.74
546	543.74
547	544.73
548	545.73
549	546.72
550	547.72
551	548.71
552	549.7
553	550.7
554	551.69
555	552.69
556	553.68
557	554.67
558	555.66
559	556.66
560	557.65

561	558.64
562	559.63
563	560.62
564	561.62
565	562.61
566	563.6
567	564.59
568	565.58
569	566.57
570	567.56
571	568.55
572	569.54
573	570.53
574	571.52
575	572.51
576	573.5
577	574.49
578	575.48
579	576.47
580	577.45
581	578.44
582	579.43
583	580.42
584	581.41
585	582.4
586	583.39
587	584.37
588	585.36
589	586.35
590	587.34
591	588.33
592	589.31
593	590.3
594	591.29
595	592.28
596	593.26
597	594.25
598	595.24
599	596.23
600	597.22
601	598.2
602	599.19
603	600.18
604	601.17
605	602.15
606	603.14
607	604.13
608	605.12
609	606.11
610	607.09
611	608.08
612	609.07
613	610.06
614	611.05
615	612.04
616	613.02
617	614.01
618	615
619	615.99
620	616.98
621	617.97
622	618.96
623	619.95
624	620.94
625	621.93
626	622.92
627	623.91
628	624.9
629	625.89
630	626.88
631	627.87
632	628.86
633	629.85
634	630.85
635	631.84
636	632.83
637	633.82
638	634.81
639	635.81
640	636.8
641	637.79
642	638.79
643	639.78
644	640.77
645	641.77
646	642.76
647	643.76
648	644.75
649	645.75
650	646.74
651	647.74
652	648.74
653	649.73
654	650.73
655	651.73
656	652.72
657	653.72
658	654.72
659	655.72
660	656.72
661	657.72
662	658.72
663	659.72
664	660.72
665	661.72
666	662.72
667	663.72
668	664.72
669	665.73
670	666.73
671	667.73
672	668.73
673	669.74
674	670.74

675	671.75
676	672.75
677	673.76
678	674.76
679	675.77
680	676.78
681	677.78
682	678.79
683	679.8
684	680.81
685	681.81
686	682.82
687	683.83
688	684.84
689	685.85
690	686.86
691	687.88
692	688.89
693	689.9
694	690.91
695	691.92
696	692.94
697	693.95
698	694.97
699	695.98
700	697
701	698.01
702	699.03
703	700.04
704	701.06
705	702.08
706	703.09
707	704.11
708	705.13
709	706.15
710	707.17
711	708.19
712	709.21
713	710.23
714	711.25
715	712.27
716	713.29
717	714.32
718	715.34
719	716.36
720	717.38
721	718.41
722	719.43
723	720.46
724	721.48
725	722.51
726	723.53
727	724.56
728	725.58
729	726.61
730	727.64
731	728.67
732	729.69
733	730.72
734	731.75
735	732.78
736	733.81
737	734.84
738	735.87
739	736.9
740	737.93
741	738.96
742	739.99
743	741.02
744	742.05
745	743.08
746	744.11
747	745.14
748	746.17
749	747.21
750	748.24
751	749.27
752	750.3
753	751.34
754	752.37
755	753.4
756	754.44
757	755.47
758	756.5
759	757.54
760	758.57
761	759.61
762	760.64
763	761.67
764	762.71
765	763.74
766	764.78
767	765.81
768	766.84
769	767.88
770	768.91
771	769.95
772	770.98
773	772.01
774	773.05
775	774.08
776	775.11
777	776.15
778	777.18
779	778.21
780	779.24
781	780.28
782	781.31
783	782.34
784	783.37
785	784.4
786	785.43
787	786.47
788	787.5

789	788.53
790	789.56
791	790.58
792	791.61
793	792.64
794	793.67
795	794.7
796	795.72
797	796.75
798	797.78
799	798.8
800	799.82
801	800.85
802	801.87
803	802.89
804	803.92
805	804.94
806	805.96
807	806.98
808	808
809	809.01
810	810.03
811	811.05
812	812.06
813	813.08
814	814.09
815	815.1
816	816.12
817	817.13
818	818.14
819	819.14
820	820.15
821	821.16
822	822.16
823	823.17
824	824.17
825	825.17
826	826.17
827	827.17
828	828.17
829	829.16
830	830.16
831	831.15
832	832.14
833	833.13
834	834.12
835	835.1
836	836.09
837	837.07
838	838.05
839	839.03
840	840.01
841	840.99
842	841.96
843	842.94
844	843.91
845	844.88
846	845.84
847	846.81
848	847.77
849	848.73
850	849.69
851	850.64
852	851.6
853	852.55
854	853.5
855	854.45
856	855.39
857	856.33
858	857.27
859	858.21
860	859.14
861	860.08
862	861.01
863	861.93
864	862.86
865	863.78
866	864.69
867	865.61
868	866.52
869	867.43
870	868.34
871	869.24
872	870.14
873	871.04
874	871.93
875	872.82
876	873.71
877	874.59
878	875.47
879	876.35
880	877.22
881	878.09
882	878.96
883	879.82
884	880.68
885	881.53
886	882.4
887	883.4
888	884.4
889	885.4
890	886.4
891	887.4
892	888.4
893	889.4
894	890.39
895	891.39
896	892.39
897	893.39
898	894.39
899	895.39
900	896.39
901	897.39
902	898.39

903	899.39
904	900.39
905	901.39
906	902.39
907	903.39
908	904.39
909	905.39
910	906.38
911	907.38
912	908.38
913	909.38
914	910.38
915	911.38
916	912.38
917	913.38
918	914.38
919	915.38
920	916.38
921	917.38
922	918.38
923	919.38
924	920.38
925	921.37
926	922.37
927	923.37
928	924.37
929	925.37
930	926.37
931	927.37
932	928.37
933	929.37
934	930.37
935	931.37
936	932.37
937	933.37
938	934.37
939	935.37
940	936.37
941	937.36
942	938.36
943	939.36
944	940.36
945	941.36
946	942.36
947	943.36
948	944.36
949	945.36
950	946.36
951	947.36
952	948.36
953	949.36
954	950.36
955	951.36
956	952.35
957	953.35
958	954.35
959	955.35
960	956.35
961	957.35
962	958.35
963	959.35
964	960.35
965	961.35
966	962.35
967	963.35
968	964.35
969	965.35
970	966.35
971	967.35
972	968.34
973	969.34
974	970.34
975	971.34
976	972.34
977	973.34
978	974.34
979	975.34
980	976.34
981	977.34
982	978.34
983	979.34
984	980.34
985	981.34
986	982.34
987	983.33
988	984.33
989	985.33
990	986.33
991	987.33
992	988.33
993	989.33
994	990.33
995	991.33
996	992.33
997	993.33
998	994.33
999	995.33
1000	996.33
1001	997.33
1002	998.32
1003	999.32
1004	1000.32
1005	1001.32
1006	1002.32
1007	1003.32
1008	1004.32
1009	1005.32
1010	1006.32
1011	1007.32
1012	1008.32
1013	1009.32
1014	1010.32
1015	1011.32
1016	1012.32

1017	1013.32
1018	1014.31
1019	1015.31
1020	1016.31
1021	1017.31
1022	1018.31
1023	1019.31
1024	1020.31
1025	1021.31
1026	1022.31
1027	1023.31
1028	1024.31
1029	1025.31
1030	1026.31
1031	1027.31
1032	1028.31
1033	1029.3
1034	1030.3
1035	1031.3
1036	1032.3
1037	1033.3
1038	1034.3
1039	1035.3
1040	1036.3
1041	1037.3
1042	1038.3
1043	1039.3
1044	1040.3
1045	1041.3
1046	1042.3
1047	1043.3
1048	1044.3
1049	1045.29
1050	1046.29
1051	1047.29
1052	1048.29
1053	1049.29
1054	1050.29
1055	1051.29
1056	1052.29
1057	1053.29
1058	1054.29
1059	1055.29
1060	1056.29
1061	1057.29
1062	1058.29
1063	1059.29
1064	1060.28
1065	1061.28
1066	1062.28
1067	1063.28
1068	1064.28
1069	1065.28
1070	1066.28
1071	1067.28
1072	1068.28
1073	1069.28
1074	1070.28
1075	1071.28
1076	1072.28
1077	1073.28
1078	1074.28
1079	1075.28
1080	1076.27
1081	1077.27
1082	1078.27
1083	1079.27
1084	1080.27
1085	1081.27
1086	1082.27
1087	1083.27
1088	1084.27
1089	1085.27
1090	1086.27
1091	1087.27
1092	1088.27
1093	1089.27
1094	1090.27
1095	1091.26
1096	1092.26
1097	1093.26
1098	1094.26
1099	1095.26
1100	1096.26

off_020816053000.prn:

Commanded Wavelength	Actual Wavelength
350	347.8305
350.1	347.93043
350.2	348.03036
350.3	348.13029
350.4	348.23022
350.5	348.33015
350.6	348.43008
350.7	348.53001
350.8	348.62994
350.9	348.72987
351	348.8298
351.1	348.92973
351.2	349.02966
351.3	349.12959
351.4	349.22952
351.5	349.32945
351.6	349.42938
351.7	349.52931
351.8	349.62924
351.9	349.72917
352	349.8291
352.1	349.92903
352.2	350.02896
352.3	350.12889
352.4	350.22882
352.5	350.32875
352.6	350.42868
352.7	350.52861
352.8	350.62854
352.9	350.72847
353	350.8284
353.1	350.92833
353.2	351.02826
353.3	351.12819
353.4	351.22812
353.5	351.32805
353.6	351.42798
353.7	351.52791
353.8	351.62784
353.9	351.72777
354	351.8277
354.1	351.92763
354.2	352.02756
354.3	352.12749
354.4	352.22742
354.5	352.32735
354.6	352.42728
354.7	352.52721
354.8	352.62714
354.9	352.72707
355	352.827
355.1	352.92693
355.2	353.02686
355.3	353.12679
355.4	353.22672
355.5	353.32665
355.6	353.42658
355.7	353.52651
355.8	353.62644
355.9	353.72637
356	353.8263
356.1	353.92623
356.2	354.02616
356.3	354.12609
356.4	354.22602
356.5	354.32595
356.6	354.42588
356.7	354.52581
356.8	354.62574
356.9	354.72567
357	354.8256
357.1	354.92553
357.2	355.02546
357.3	355.12539
357.4	355.22532
357.5	355.32525
357.6	355.42518
357.7	355.52511
357.8	355.62504
357.9	355.72497
358	355.8249
358.1	355.92483
358.2	356.02476
358.3	356.12469
358.4	356.22462
358.5	356.32455
358.6	356.42448
358.7	356.52441
358.8	356.62434
358.9	356.72427
359	356.8242
359.1	356.92413
359.2	357.02406
359.3	357.12399
359.4	357.22392
359.5	357.32385
359.6	357.42378
359.7	357.52371
359.8	357.62364
359.9	357.72357
360	357.8235
360.1	357.92343
360.2	358.02336
360.3	358.12329
360.4	358.22322
360.5	358.32315
360.6	358.42308
360.7	358.52301
360.8	358.62294

360.9	358.72287	366.6	364.41888
361	358.8228	366.7	364.51881
361.1	358.92273	366.8	364.61874
361.2	359.02266	366.9	364.71867
361.3	359.12259	367	364.8186
361.4	359.22252	367.1	364.91853
361.5	359.32245	367.2	365.01846
361.6	359.42238	367.3	365.11839
361.7	359.52231	367.4	365.21832
361.8	359.62224	367.5	365.31825
361.9	359.72217	367.6	365.41818
362	359.8221	367.7	365.51811
362.1	359.92203	367.8	365.61804
362.2	360.02196	367.9	365.71797
362.3	360.12189	368	365.8179
362.4	360.22182	368.1	365.91783
362.5	360.32175	368.2	366.01776
362.6	360.42168	368.3	366.11769
362.7	360.52161	368.4	366.21762
362.8	360.62154	368.5	366.31755
362.9	360.72147	368.6	366.41748
363	360.8214	368.7	366.51741
363.1	360.92133	368.8	366.61734
363.2	361.02126	368.9	366.71727
363.3	361.12119	369	366.8172
363.4	361.22112	369.1	366.91713
363.5	361.32105	369.2	367.01706
363.6	361.42098	369.3	367.11699
363.7	361.52091	369.4	367.21692
363.8	361.62084	369.5	367.31685
363.9	361.72077	369.6	367.41678
364	361.8207	369.7	367.51671
364.1	361.92063	369.8	367.61664
364.2	362.02056	369.9	367.71657
364.3	362.12049	370	367.8165
364.4	362.22042	370.1	367.91643
364.5	362.32035	370.2	368.01636
364.6	362.42028	370.3	368.11629
364.7	362.52021	370.4	368.21622
364.8	362.62014	370.5	368.31615
364.9	362.72007	370.6	368.41608
365	362.82	370.7	368.51601
365.1	362.91993	370.8	368.61594
365.2	363.01986	370.9	368.71587
365.3	363.11979	371	368.8158
365.4	363.21972	371.1	368.91573
365.5	363.31965	371.2	369.01566
365.6	363.41958	371.3	369.11559
365.7	363.51951	371.4	369.21552
365.8	363.61944	371.5	369.31545
365.9	363.71937	371.6	369.41538
366	363.8193	371.7	369.51531
366.1	363.91923	371.8	369.61524
366.2	364.01916	371.9	369.71517
366.3	364.11909	372	369.8151
366.4	364.21902	372.1	369.91503
366.5	364.31895	372.2	370.01496

372.3	370.11489	378	375.8109
372.4	370.21482	378.1	375.91083
372.5	370.31475	378.2	376.01076
372.6	370.41468	378.3	376.11069
372.7	370.51461	378.4	376.21062
372.8	370.61454	378.5	376.31055
372.9	370.71447	378.6	376.41048
373	370.8144	378.7	376.51041
373.1	370.91433	378.8	376.61034
373.2	371.01426	378.9	376.71027
373.3	371.11419	379	376.8102
373.4	371.21412	379.1	376.91013
373.5	371.31405	379.2	377.01006
373.6	371.41398	379.3	377.10999
373.7	371.51391	379.4	377.20992
373.8	371.61384	379.5	377.30985
373.9	371.71377	379.6	377.40978
374	371.8137	379.7	377.50971
374.1	371.91363	379.8	377.60964
374.2	372.01356	379.9	377.70957
374.3	372.11349	380	377.8095
374.4	372.21342	380.1	377.90943
374.5	372.31335	380.2	378.00936
374.6	372.41328	380.3	378.10929
374.7	372.51321	380.4	378.20922
374.8	372.61314	380.5	378.30915
374.9	372.71307	380.6	378.40908
375	372.813	380.7	378.50901
375.1	372.91293	380.8	378.60894
375.2	373.01286	380.9	378.70887
375.3	373.11279	381	378.8088
375.4	373.21272	381.1	378.90873
375.5	373.31265	381.2	379.00866
375.6	373.41258	381.3	379.10859
375.7	373.51251	381.4	379.20852
375.8	373.61244	381.5	379.30845
375.9	373.71237	381.6	379.40838
376	373.8123	381.7	379.50831
376.1	373.91223	381.8	379.60824
376.2	374.01216	381.9	379.70817
376.3	374.11209	382	379.8081
376.4	374.21202	382.1	379.90803
376.5	374.31195	382.2	380.00796
376.6	374.41188	382.3	380.10789
376.7	374.51181	382.4	380.20782
376.8	374.61174	382.5	380.30775
376.9	374.71167	382.6	380.40768
377	374.8116	382.7	380.50761
377.1	374.91153	382.8	380.60754
377.2	375.01146	382.9	380.70747
377.3	375.11139	383	380.8074
377.4	375.21132	383.1	380.90733
377.5	375.31125	383.2	381.00726
377.6	375.41118	383.3	381.10719
377.7	375.51111	383.4	381.20712
377.8	375.61104	383.5	381.30705
377.9	375.71097	383.6	381.40698

383.7	381.50691	389.4	387.20292
383.8	381.60684	389.5	387.30285
383.9	381.70677	389.6	387.40278
384	381.8067	389.7	387.50271
384.1	381.90663	389.8	387.60264
384.2	382.00656	389.9	387.70257
384.3	382.10649	390	387.8025
384.4	382.20642	390.1	387.90243
384.5	382.30635	390.2	388.00236
384.6	382.40628	390.3	388.10229
384.7	382.50621	390.4	388.20222
384.8	382.60614	390.5	388.30215
384.9	382.70607	390.6	388.40208
385	382.806	390.7	388.50201
385.1	382.90593	390.8	388.60194
385.2	383.00586	390.9	388.70187
385.3	383.10579	391	388.8018
385.4	383.20572	391.1	388.90173
385.5	383.30565	391.2	389.00166
385.6	383.40558	391.3	389.10159
385.7	383.50551	391.4	389.20152
385.8	383.60544	391.5	389.30145
385.9	383.70537	391.6	389.40138
386	383.8053	391.7	389.50131
386.1	383.90523	391.8	389.60124
386.2	384.00516	391.9	389.70117
386.3	384.10509	392	389.8011
386.4	384.20502	392.1	389.90103
386.5	384.30495	392.2	390.00096
386.6	384.40488	392.3	390.10089
386.7	384.50481	392.4	390.20082
386.8	384.60474	392.5	390.30075
386.9	384.70467	392.6	390.40068
387	384.8046	392.7	390.50061
387.1	384.90453	392.8	390.60054
387.2	385.00446	392.9	390.70047
387.3	385.10439	393	390.8004
387.4	385.20432	393.1	390.90033
387.5	385.30425	393.2	391.00026
387.6	385.40418	393.3	391.10019
387.7	385.50411	393.4	391.20012
387.8	385.60404	393.5	391.30005
387.9	385.70397	393.6	391.39998
388	385.8039	393.7	391.49991
388.1	385.90383	393.8	391.59984
388.2	386.00376	393.9	391.69977
388.3	386.10369	394	391.7997
388.4	386.20362	394.1	391.89963
388.5	386.30355	394.2	391.99956
388.6	386.40348	394.3	392.09949
388.7	386.50341	394.4	392.19942
388.8	386.60334	394.5	392.29935
388.9	386.70327	394.6	392.39928
389	386.8032	394.7	392.49921
389.1	386.90313	394.8	392.59914
389.2	387.00306	394.9	392.69907
389.3	387.10299	395	392.799

395.1	392.89893	400.8	398.59494
395.2	392.99886	400.9	398.69487
395.3	393.09879	401	398.7948
395.4	393.19872	401.1	398.89473
395.5	393.29865	401.2	398.99466
395.6	393.39858	401.3	399.09459
395.7	393.49851	401.4	399.19452
395.8	393.59844	401.5	399.29445
395.9	393.69837	401.6	399.39438
396	393.7983	401.7	399.49431
396.1	393.89823	401.8	399.59424
396.2	393.99816	401.9	399.69417
396.3	394.09809	402	399.7941
396.4	394.19802	402.1	399.89403
396.5	394.29795	402.2	399.99396
396.6	394.39788	402.3	400.09389
396.7	394.49781	402.4	400.19382
396.8	394.59774	402.5	400.29375
396.9	394.69767	402.6	400.39368
397	394.7976	402.7	400.49361
397.1	394.89753	402.8	400.59354
397.2	394.99746	402.9	400.69347
397.3	395.09739	403	400.7934
397.4	395.19732	403.1	400.89333
397.5	395.29725	403.2	400.99326
397.6	395.39718	403.3	401.09319
397.7	395.49711	403.4	401.19312
397.8	395.59704	403.5	401.29305
397.9	395.69697	403.6	401.39298
398	395.7969	403.7	401.49291
398.1	395.89683	403.8	401.59284
398.2	395.99676	403.9	401.69277
398.3	396.09669	404	401.7927
398.4	396.19662	404.1	401.89263
398.5	396.29655	404.2	401.99256
398.6	396.39648	404.3	402.09249
398.7	396.49641	404.4	402.19242
398.8	396.59634	404.5	402.29235
398.9	396.69627	404.6	402.39228
399	396.7962	404.7	402.49221
399.1	396.89613	404.8	402.59214
399.2	396.99606	404.9	402.69207
399.3	397.09599	405	402.792
399.4	397.19592	405.1	402.89193
399.5	397.29585	405.2	402.99186
399.6	397.39578	405.3	403.09179
399.7	397.49571	405.4	403.19172
399.8	397.59564	405.5	403.29165
399.9	397.69557	405.6	403.39158
400	397.7955	405.7	403.49151
400.1	397.89543	405.8	403.59144
400.2	397.99536	405.9	403.69137
400.3	398.09529	406	403.7913
400.4	398.19522	406.1	403.89123
400.5	398.29515	406.2	403.99116
400.6	398.39508	406.3	404.09109
400.7	398.49501	406.4	404.19102

406.5	404.29095	412.2	409.98696
406.6	404.39088	412.3	410.08689
406.7	404.49081	412.4	410.18682
406.8	404.59074	412.5	410.28675
406.9	404.69067	412.6	410.38668
407	404.7906	412.7	410.48661
407.1	404.89053	412.8	410.58654
407.2	404.99046	412.9	410.68647
407.3	405.09039	413	410.7864
407.4	405.19032	413.1	410.88633
407.5	405.29025	413.2	410.98626
407.6	405.39018	413.3	411.08619
407.7	405.49011	413.4	411.18612
407.8	405.59004	413.5	411.28605
407.9	405.68997	413.6	411.38598
408	405.7899	413.7	411.48591
408.1	405.88983	413.8	411.58584
408.2	405.98976	413.9	411.68577
408.3	406.08969	414	411.7857
408.4	406.18962	414.1	411.88563
408.5	406.28955	414.2	411.98556
408.6	406.38948	414.3	412.08549
408.7	406.48941	414.4	412.18542
408.8	406.58934	414.5	412.28535
408.9	406.68927	414.6	412.38528
409	406.7892	414.7	412.48521
409.1	406.88913	414.8	412.58514
409.2	406.98906	414.9	412.68507
409.3	407.08899	415	412.785
409.4	407.18892	415.1	412.88493
409.5	407.28885	415.2	412.98486
409.6	407.38878	415.3	413.08479
409.7	407.48871	415.4	413.18472
409.8	407.58864	415.5	413.28465
409.9	407.68857	415.6	413.38458
410	407.7885	415.7	413.48451
410.1	407.88843	415.8	413.58444
410.2	407.98836	415.9	413.68437
410.3	408.08829	416	413.7843
410.4	408.18822	416.1	413.88423
410.5	408.28815	416.2	413.98416
410.6	408.38808	416.3	414.08409
410.7	408.48801	416.4	414.18402
410.8	408.58794	416.5	414.28395
410.9	408.68787	416.6	414.38388
411	408.7878	416.7	414.48381
411.1	408.88773	416.8	414.58374
411.2	408.98766	416.9	414.68367
411.3	409.08759	417	414.7836
411.4	409.18752	417.1	414.88353
411.5	409.28745	417.2	414.98346
411.6	409.38738	417.3	415.08339
411.7	409.48731	417.4	415.18332
411.8	409.58724	417.5	415.28325
411.9	409.68717	417.6	415.38318
412	409.7871	417.7	415.48311
412.1	409.88703	417.8	415.58304

417.9	415.68297	423.6	421.37898
418	415.7829	423.7	421.47891
418.1	415.88283	423.8	421.57884
418.2	415.98276	423.9	421.67877
418.3	416.08269	424	421.7787
418.4	416.18262	424.1	421.87863
418.5	416.28255	424.2	421.97856
418.6	416.38248	424.3	422.07849
418.7	416.48241	424.4	422.17842
418.8	416.58234	424.5	422.27835
418.9	416.68227	424.6	422.37828
419	416.7822	424.7	422.47821
419.1	416.88213	424.8	422.57814
419.2	416.98206	424.9	422.67807
419.3	417.08199	425	422.778
419.4	417.18192	425.1	422.87793
419.5	417.28185	425.2	422.97786
419.6	417.38178	425.3	423.07779
419.7	417.48171	425.4	423.17772
419.8	417.58164	425.5	423.27765
419.9	417.68157	425.6	423.37758
420	417.7815	425.7	423.47751
420.1	417.88143	425.8	423.57744
420.2	417.98136	425.9	423.67737
420.3	418.08129	426	423.7773
420.4	418.18122	426.1	423.87723
420.5	418.28115	426.2	423.97716
420.6	418.38108	426.3	424.07709
420.7	418.48101	426.4	424.17702
420.8	418.58094	426.5	424.27695
420.9	418.68087	426.6	424.37688
421	418.7808	426.7	424.47681
421.1	418.88073	426.8	424.57674
421.2	418.98066	426.9	424.67667
421.3	419.08059	427	424.7766
421.4	419.18052	427.1	424.87653
421.5	419.28045	427.2	424.97646
421.6	419.38038	427.3	425.07639
421.7	419.48031	427.4	425.17632
421.8	419.58024	427.5	425.27625
421.9	419.68017	427.6	425.37618
422	419.7801	427.7	425.47611
422.1	419.88003	427.8	425.57604
422.2	419.97996	427.9	425.67597
422.3	420.07989	428	425.7759
422.4	420.17982	428.1	425.87583
422.5	420.27975	428.2	425.97576
422.6	420.37968	428.3	426.07569
422.7	420.47961	428.4	426.17562
422.8	420.57954	428.5	426.27555
422.9	420.67947	428.6	426.37548
423	420.7794	428.7	426.47541
423.1	420.87933	428.8	426.57534
423.2	420.97926	428.9	426.67527
423.3	421.07919	429	426.7752
423.4	421.17912	429.1	426.87513
423.5	421.27905	429.2	426.97506

429.3	427.07499	435	432.771
429.4	427.17492	435.1	432.87093
429.5	427.27485	435.2	432.97086
429.6	427.37478	435.3	433.07079
429.7	427.47471	435.4	433.17072
429.8	427.57464	435.5	433.27065
429.9	427.67457	435.6	433.37058
430	427.7745	435.7	433.47051
430.1	427.87443	435.8	433.57044
430.2	427.97436	435.9	433.67037
430.3	428.07429	436	433.7703
430.4	428.17422	436.1	433.87023
430.5	428.27415	436.2	433.97016
430.6	428.37408	436.3	434.07009
430.7	428.47401	436.4	434.17002
430.8	428.57394	436.5	434.26995
430.9	428.67387	436.6	434.36988
431	428.7738	436.7	434.46981
431.1	428.87373	436.8	434.56974
431.2	428.97366	436.9	434.66967
431.3	429.07359	437	434.7696
431.4	429.17352	437.1	434.86953
431.5	429.27345	437.2	434.96946
431.6	429.37338	437.3	435.06939
431.7	429.47331	437.4	435.16932
431.8	429.57324	437.5	435.26925
431.9	429.67317	437.6	435.36918
432	429.7731	437.7	435.46911
432.1	429.87303	437.8	435.56904
432.2	429.97296	437.9	435.66897
432.3	430.07289	438	435.7689
432.4	430.17282	438.1	435.86883
432.5	430.27275	438.2	435.96876
432.6	430.37268	438.3	436.06869
432.7	430.47261	438.4	436.16862
432.8	430.57254	438.5	436.26855
432.9	430.67247	438.6	436.36848
433	430.7724	438.7	436.46841
433.1	430.87233	438.8	436.56834
433.2	430.97226	438.9	436.66827
433.3	431.07219	439	436.7682
433.4	431.17212	439.1	436.86813
433.5	431.27205	439.2	436.96806
433.6	431.37198	439.3	437.06799
433.7	431.47191	439.4	437.16792
433.8	431.57184	439.5	437.26785
433.9	431.67177	439.6	437.36778
434	431.7717	439.7	437.46771
434.1	431.87163	439.8	437.56764
434.2	431.97156	439.9	437.66757
434.3	432.07149	440	437.7675
434.4	432.17142	440.1	437.86743
434.5	432.27135	440.2	437.96736
434.6	432.37128	440.3	438.06729
434.7	432.47121	440.4	438.16722
434.8	432.57114	440.5	438.26715
434.9	432.67107	440.6	438.36708

440.7	438.46701	446.4	444.16302
440.8	438.56694	446.5	444.26295
440.9	438.66687	446.6	444.36288
441	438.7668	446.7	444.46281
441.1	438.86673	446.8	444.56274
441.2	438.96666	446.9	444.66267
441.3	439.06659	447	444.7626
441.4	439.16652	447.1	444.86253
441.5	439.26645	447.2	444.96246
441.6	439.36638	447.3	445.06239
441.7	439.46631	447.4	445.16232
441.8	439.56624	447.5	445.26225
441.9	439.66617	447.6	445.36218
442	439.7661	447.7	445.46211
442.1	439.86603	447.8	445.56204
442.2	439.96596	447.9	445.66197
442.3	440.06589	448	445.7619
442.4	440.16582	448.1	445.86183
442.5	440.26575	448.2	445.96176
442.6	440.36568	448.3	446.06169
442.7	440.46561	448.4	446.16162
442.8	440.56554	448.5	446.26155
442.9	440.66547	448.6	446.36148
443	440.7654	448.7	446.46141
443.1	440.86533	448.8	446.56134
443.2	440.96526	448.9	446.66127
443.3	441.06519	449	446.7612
443.4	441.16512	449.1	446.86113
443.5	441.26505	449.2	446.96106
443.6	441.36498	449.3	447.06099
443.7	441.46491	449.4	447.16092
443.8	441.56484	449.5	447.26085
443.9	441.66477	449.6	447.36078
444	441.7647	449.7	447.46071
444.1	441.86463	449.8	447.56064
444.2	441.96456	449.9	447.66057
444.3	442.06449	450	447.7605
444.4	442.16442	450.1	447.86043
444.5	442.26435	450.2	447.96036
444.6	442.36428	450.3	448.06029
444.7	442.46421	450.4	448.16022
444.8	442.56414	450.5	448.26015
444.9	442.66407	450.6	448.36008
445	442.764	450.7	448.46001
445.1	442.86393	450.8	448.55994
445.2	442.96386	450.9	448.65987
445.3	443.06379	451	448.7598
445.4	443.16372	451.1	448.85973
445.5	443.26365	451.2	448.95966
445.6	443.36358	451.3	449.05959
445.7	443.46351	451.4	449.15952
445.8	443.56344	451.5	449.25945
445.9	443.66337	451.6	449.35938
446	443.7633	451.7	449.45931
446.1	443.86323	451.8	449.55924
446.2	443.96316	451.9	449.65917
446.3	444.06309	452	449.7591

452.1	449.85903	457.8	455.55504
452.2	449.95896	457.9	455.65497
452.3	450.05889	458	455.7549
452.4	450.15882	458.1	455.85483
452.5	450.25875	458.2	455.95476
452.6	450.35868	458.3	456.05469
452.7	450.45861	458.4	456.15462
452.8	450.55854	458.5	456.25455
452.9	450.65847	458.6	456.35448
453	450.7584	458.7	456.45441
453.1	450.85833	458.8	456.55434
453.2	450.95826	458.9	456.65427
453.3	451.05819	459	456.7542
453.4	451.15812	459.1	456.85413
453.5	451.25805	459.2	456.95406
453.6	451.35798	459.3	457.05399
453.7	451.45791	459.4	457.15392
453.8	451.55784	459.5	457.25385
453.9	451.65777	459.6	457.35378
454	451.7577	459.7	457.45371
454.1	451.85763	459.8	457.55364
454.2	451.95756	459.9	457.65357
454.3	452.05749	460	457.7535
454.4	452.15742	460.1	457.85343
454.5	452.25735	460.2	457.95336
454.6	452.35728	460.3	458.05329
454.7	452.45721	460.4	458.15322
454.8	452.55714	460.5	458.25315
454.9	452.65707	460.6	458.35308
455	452.757	460.7	458.45301
455.1	452.85693	460.8	458.55294
455.2	452.95686	460.9	458.65287
455.3	453.05679	461	458.7528
455.4	453.15672	461.1	458.85273
455.5	453.25665	461.2	458.95266
455.6	453.35658	461.3	459.05259
455.7	453.45651	461.4	459.15252
455.8	453.55644	461.5	459.25245
455.9	453.65637	461.6	459.35238
456	453.7563	461.7	459.45231
456.1	453.85623	461.8	459.55224
456.2	453.95616	461.9	459.65217
456.3	454.05609	462	459.7521
456.4	454.15602	462.1	459.85203
456.5	454.25595	462.2	459.95196
456.6	454.35588	462.3	460.05189
456.7	454.45581	462.4	460.15182
456.8	454.55574	462.5	460.25175
456.9	454.65567	462.6	460.35168
457	454.7556	462.7	460.45161
457.1	454.85553	462.8	460.55154
457.2	454.95546	462.9	460.65147
457.3	455.05539	463	460.7514
457.4	455.15532	463.1	460.85133
457.5	455.25525	463.2	460.95126
457.6	455.35518	463.3	461.05119
457.7	455.45511	463.4	461.15112

463.5	461.25105	469.2	466.94706
463.6	461.35098	469.3	467.04699
463.7	461.45091	469.4	467.14692
463.8	461.55084	469.5	467.24685
463.9	461.65077	469.6	467.34678
464	461.7507	469.7	467.44671
464.1	461.85063	469.8	467.54664
464.2	461.95056	469.9	467.64657
464.3	462.05049	470	467.7465
464.4	462.15042	470.1	467.84643
464.5	462.25035	470.2	467.94636
464.6	462.35028	470.3	468.04629
464.7	462.45021	470.4	468.14622
464.8	462.55014	470.5	468.24615
464.9	462.65007	470.6	468.34608
465	462.75	470.7	468.44601
465.1	462.84993	470.8	468.54594
465.2	462.94986	470.9	468.64587
465.3	463.04979	471	468.7458
465.4	463.14972	471.1	468.84573
465.5	463.24965	471.2	468.94566
465.6	463.34958	471.3	469.04559
465.7	463.44951	471.4	469.14552
465.8	463.54944	471.5	469.24545
465.9	463.64937	471.6	469.34538
466	463.7493	471.7	469.44531
466.1	463.84923	471.8	469.54524
466.2	463.94916	471.9	469.64517
466.3	464.04909	472	469.7451
466.4	464.14902	472.1	469.84503
466.5	464.24895	472.2	469.94496
466.6	464.34888	472.3	470.04489
466.7	464.44881	472.4	470.14482
466.8	464.54874	472.5	470.24475
466.9	464.64867	472.6	470.34468
467	464.7486	472.7	470.44461
467.1	464.84853	472.8	470.54454
467.2	464.94846	472.9	470.64447
467.3	465.04839	473	470.7444
467.4	465.14832	473.1	470.84433
467.5	465.24825	473.2	470.94426
467.6	465.34818	473.3	471.04419
467.7	465.44811	473.4	471.14412
467.8	465.54804	473.5	471.24405
467.9	465.64797	473.6	471.34398
468	465.7479	473.7	471.44391
468.1	465.84783	473.8	471.54384
468.2	465.94776	473.9	471.64377
468.3	466.04769	474	471.7437
468.4	466.14762	474.1	471.84363
468.5	466.24755	474.2	471.94356
468.6	466.34748	474.3	472.04349
468.7	466.44741	474.4	472.14342
468.8	466.54734	474.5	472.24335
468.9	466.64727	474.6	472.34328
469	466.7472	474.7	472.44321
469.1	466.84713	474.8	472.54314

474.9	472.64307	480.6	478.33908
475	472.743	480.7	478.43901
475.1	472.84293	480.8	478.53894
475.2	472.94286	480.9	478.63887
475.3	473.04279	481	478.7388
475.4	473.14272	481.1	478.83873
475.5	473.24265	481.2	478.93866
475.6	473.34258	481.3	479.03859
475.7	473.44251	481.4	479.13852
475.8	473.54244	481.5	479.23845
475.9	473.64237	481.6	479.33838
476	473.7423	481.7	479.43831
476.1	473.84223	481.8	479.53824
476.2	473.94216	481.9	479.63817
476.3	474.04209	482	479.7381
476.4	474.14202	482.1	479.83803
476.5	474.24195	482.2	479.93796
476.6	474.34188	482.3	480.03789
476.7	474.44181	482.4	480.13782
476.8	474.54174	482.5	480.23775
476.9	474.64167	482.6	480.33768
477	474.7416	482.7	480.43761
477.1	474.84153	482.8	480.53754
477.2	474.94146	482.9	480.63747
477.3	475.04139	483	480.7374
477.4	475.14132	483.1	480.83733
477.5	475.24125	483.2	480.93726
477.6	475.34118	483.3	481.03719
477.7	475.44111	483.4	481.13712
477.8	475.54104	483.5	481.23705
477.9	475.64097	483.6	481.33698
478	475.7409	483.7	481.43691
478.1	475.84083	483.8	481.53684
478.2	475.94076	483.9	481.63677
478.3	476.04069	484	481.7367
478.4	476.14062	484.1	481.83663
478.5	476.24055	484.2	481.93656
478.6	476.34048	484.3	482.03649
478.7	476.44041	484.4	482.13642
478.8	476.54034	484.5	482.23635
478.9	476.64027	484.6	482.33628
479	476.7402	484.7	482.43621
479.1	476.84013	484.8	482.53614
479.2	476.94006	484.9	482.63607
479.3	477.03999	485	482.736
479.4	477.13992	485.1	482.83593
479.5	477.23985	485.2	482.93586
479.6	477.33978	485.3	483.03579
479.7	477.43971	485.4	483.13572
479.8	477.53964	485.5	483.23565
479.9	477.63957	485.6	483.33558
480	477.7395	485.7	483.43551
480.1	477.83943	485.8	483.53544
480.2	477.93936	485.9	483.63537
480.3	478.03929	486	483.7353
480.4	478.13922	486.1	483.83523
480.5	478.23915	486.2	483.93516

486.3	484.03509	492	489.7311
486.4	484.13502	492.1	489.83103
486.5	484.23495	492.2	489.93096
486.6	484.33488	492.3	490.03089
486.7	484.43481	492.4	490.13082
486.8	484.53474	492.5	490.23075
486.9	484.63467	492.6	490.33068
487	484.7346	492.7	490.43061
487.1	484.83453	492.8	490.53054
487.2	484.93446	492.9	490.63047
487.3	485.03439	493	490.7304
487.4	485.13432	493.1	490.83033
487.5	485.23425	493.2	490.93026
487.6	485.33418	493.3	491.03019
487.7	485.43411	493.4	491.13012
487.8	485.53404	493.5	491.23005
487.9	485.63397	493.6	491.32998
488	485.7339	493.7	491.42991
488.1	485.83383	493.8	491.52984
488.2	485.93376	493.9	491.62977
488.3	486.03369	494	491.7297
488.4	486.13362	494.1	491.82963
488.5	486.23355	494.2	491.92956
488.6	486.33348	494.3	492.02949
488.7	486.43341	494.4	492.12942
488.8	486.53334	494.5	492.22935
488.9	486.63327	494.6	492.32928
489	486.7332	494.7	492.42921
489.1	486.83313	494.8	492.52914
489.2	486.93306	494.9	492.62907
489.3	487.03299	495	492.729
489.4	487.13292	495.1	492.82893
489.5	487.23285	495.2	492.92886
489.6	487.33278	495.3	493.02879
489.7	487.43271	495.4	493.12872
489.8	487.53264	495.5	493.22865
489.9	487.63257	495.6	493.32858
490	487.7325	495.7	493.42851
490.1	487.83243	495.8	493.52844
490.2	487.93236	495.9	493.62837
490.3	488.03229	496	493.7283
490.4	488.13222	496.1	493.82823
490.5	488.23215	496.2	493.92816
490.6	488.33208	496.3	494.02809
490.7	488.43201	496.4	494.12802
490.8	488.53194	496.5	494.22795
490.9	488.63187	496.6	494.32788
491	488.7318	496.7	494.42781
491.1	488.83173	496.8	494.52774
491.2	488.93166	496.9	494.62767
491.3	489.03159	497	494.7276
491.4	489.13152	497.1	494.82753
491.5	489.23145	497.2	494.92746
491.6	489.33138	497.3	495.02739
491.7	489.43131	497.4	495.12732
491.8	489.53124	497.5	495.22725
491.9	489.63117	497.6	495.32718

497.7	495.42711	503.4	501.12312
497.8	495.52704	503.5	501.22305
497.9	495.62697	503.6	501.32298
498	495.7269	503.7	501.42291
498.1	495.82683	503.8	501.52284
498.2	495.92676	503.9	501.62277
498.3	496.02669	504	501.7227
498.4	496.12662	504.1	501.82263
498.5	496.22655	504.2	501.92256
498.6	496.32648	504.3	502.02249
498.7	496.42641	504.4	502.12242
498.8	496.52634	504.5	502.22235
498.9	496.62627	504.6	502.32228
499	496.7262	504.7	502.42221
499.1	496.82613	504.8	502.52214
499.2	496.92606	504.9	502.62207
499.3	497.02599	505	502.722
499.4	497.12592	505.1	502.82193
499.5	497.22585	505.2	502.92186
499.6	497.32578	505.3	503.02179
499.7	497.42571	505.4	503.12172
499.8	497.52564	505.5	503.22165
499.9	497.62557	505.6	503.32158
500	497.7255	505.7	503.42151
500.1	497.82543	505.8	503.52144
500.2	497.92536	505.9	503.62137
500.3	498.02529	506	503.7213
500.4	498.12522	506.1	503.82123
500.5	498.22515	506.2	503.92116
500.6	498.32508	506.3	504.02109
500.7	498.42501	506.4	504.12102
500.8	498.52494	506.5	504.22095
500.9	498.62487	506.6	504.32088
501	498.7248	506.7	504.42081
501.1	498.82473	506.8	504.52074
501.2	498.92466	506.9	504.62067
501.3	499.02459	507	504.7206
501.4	499.12452	507.1	504.82053
501.5	499.22445	507.2	504.92046
501.6	499.32438	507.3	505.02039
501.7	499.42431	507.4	505.12032
501.8	499.52424	507.5	505.22025
501.9	499.62417	507.6	505.32018
502	499.7241	507.7	505.42011
502.1	499.82403	507.8	505.52004
502.2	499.92396	507.9	505.61997
502.3	500.02389	508	505.7199
502.4	500.12382	508.1	505.81983
502.5	500.22375	508.2	505.91976
502.6	500.32368	508.3	506.01969
502.7	500.42361	508.4	506.11962
502.8	500.52354	508.5	506.21955
502.9	500.62347	508.6	506.31948
503	500.7234	508.7	506.41941
503.1	500.82333	508.8	506.51934
503.2	500.92326	508.9	506.61927
503.3	501.02319	509	506.7192

509.1	506.81913	514.8	512.51514
509.2	506.91906	514.9	512.61507
509.3	507.01899	515	512.715
509.4	507.11892	515.1	512.81493
509.5	507.21885	515.2	512.91486
509.6	507.31878	515.3	513.01479
509.7	507.41871	515.4	513.11472
509.8	507.51864	515.5	513.21465
509.9	507.61857	515.6	513.31458
510	507.7185	515.7	513.41451
510.1	507.81843	515.8	513.51444
510.2	507.91836	515.9	513.61437
510.3	508.01829	516	513.7143
510.4	508.11822	516.1	513.81423
510.5	508.21815	516.2	513.91416
510.6	508.31808	516.3	514.01409
510.7	508.41801	516.4	514.11402
510.8	508.51794	516.5	514.21395
510.9	508.61787	516.6	514.31388
511	508.7178	516.7	514.41381
511.1	508.81773	516.8	514.51374
511.2	508.91766	516.9	514.61367
511.3	509.01759	517	514.7136
511.4	509.11752	517.1	514.81353
511.5	509.21745	517.2	514.91346
511.6	509.31738	517.3	515.01339
511.7	509.41731	517.4	515.11332
511.8	509.51724	517.5	515.21325
511.9	509.61717	517.6	515.31318
512	509.7171	517.7	515.41311
512.1	509.81703	517.8	515.51304
512.2	509.91696	517.9	515.61297
512.3	510.01689	518	515.7129
512.4	510.11682	518.1	515.81283
512.5	510.21675	518.2	515.91276
512.6	510.31668	518.3	516.01269
512.7	510.41661	518.4	516.11262
512.8	510.51654	518.5	516.21255
512.9	510.61647	518.6	516.31248
513	510.7164	518.7	516.41241
513.1	510.81633	518.8	516.51234
513.2	510.91626	518.9	516.61227
513.3	511.01619	519	516.7122
513.4	511.11612	519.1	516.81213
513.5	511.21605	519.2	516.91206
513.6	511.31598	519.3	517.01199
513.7	511.41591	519.4	517.11192
513.8	511.51584	519.5	517.21185
513.9	511.61577	519.6	517.31178
514	511.7157	519.7	517.41171
514.1	511.81563	519.8	517.51164
514.2	511.91556	519.9	517.61157
514.3	512.01549	520	517.7115
514.4	512.11542	520.1	517.81143
514.5	512.21535	520.2	517.91136
514.6	512.31528	520.3	518.01129
514.7	512.41521	520.4	518.11122

520.5	518.21115	526.2	523.90716
520.6	518.31108	526.3	524.00709
520.7	518.41101	526.4	524.10702
520.8	518.51094	526.5	524.20695
520.9	518.61087	526.6	524.30688
521	518.7108	526.7	524.40681
521.1	518.81073	526.8	524.50674
521.2	518.91066	526.9	524.60667
521.3	519.01059	527	524.7066
521.4	519.11052	527.1	524.80653
521.5	519.21045	527.2	524.90646
521.6	519.31038	527.3	525.00639
521.7	519.41031	527.4	525.10632
521.8	519.51024	527.5	525.20625
521.9	519.61017	527.6	525.30618
522	519.7101	527.7	525.40611
522.1	519.81003	527.8	525.50604
522.2	519.90996	527.9	525.60597
522.3	520.00989	528	525.7059
522.4	520.10982	528.1	525.80583
522.5	520.20975	528.2	525.90576
522.6	520.30968	528.3	526.00569
522.7	520.40961	528.4	526.10562
522.8	520.50954	528.5	526.20555
522.9	520.60947	528.6	526.30548
523	520.7094	528.7	526.40541
523.1	520.80933	528.8	526.50534
523.2	520.90926	528.9	526.60527
523.3	521.00919	529	526.7052
523.4	521.10912	529.1	526.80513
523.5	521.20905	529.2	526.90506
523.6	521.30898	529.3	527.00499
523.7	521.40891	529.4	527.10492
523.8	521.50884	529.5	527.20485
523.9	521.60877	529.6	527.30478
524	521.7087	529.7	527.40471
524.1	521.80863	529.8	527.50464
524.2	521.90856	529.9	527.60457
524.3	522.00849	530	527.7045
524.4	522.10842	530.1	527.80443
524.5	522.20835	530.2	527.90436
524.6	522.30828	530.3	528.00429
524.7	522.40821	530.4	528.10422
524.8	522.50814	530.5	528.20415
524.9	522.60807	530.6	528.30408
525	522.708	530.7	528.40401
525.1	522.80793	530.8	528.50394
525.2	522.90786	530.9	528.60387
525.3	523.00779	531	528.7038
525.4	523.10772	531.1	528.80373
525.5	523.20765	531.2	528.90366
525.6	523.30758	531.3	529.00359
525.7	523.40751	531.4	529.10352
525.8	523.50744	531.5	529.20345
525.9	523.60737	531.6	529.30338
526	523.7073	531.7	529.40331
526.1	523.80723	531.8	529.50324

531.9	529.60317	537.6	535.29918
532	529.7031	537.7	535.39911
532.1	529.80303	537.8	535.49904
532.2	529.90296	537.9	535.59897
532.3	530.00289	538	535.6989
532.4	530.10282	538.1	535.79883
532.5	530.20275	538.2	535.89876
532.6	530.30268	538.3	535.99869
532.7	530.40261	538.4	536.09862
532.8	530.50254	538.5	536.19855
532.9	530.60247	538.6	536.29848
533	530.7024	538.7	536.39841
533.1	530.80233	538.8	536.49834
533.2	530.90226	538.9	536.59827
533.3	531.00219	539	536.6982
533.4	531.10212	539.1	536.79813
533.5	531.20205	539.2	536.89806
533.6	531.30198	539.3	536.99799
533.7	531.40191	539.4	537.09792
533.8	531.50184	539.5	537.19785
533.9	531.60177	539.6	537.29778
534	531.7017	539.7	537.39771
534.1	531.80163	539.8	537.49764
534.2	531.90156	539.9	537.59757
534.3	532.00149	540	537.6975
534.4	532.10142	540.1	537.79743
534.5	532.20135	540.2	537.89736
534.6	532.30128	540.3	537.99729
534.7	532.40121	540.4	538.09722
534.8	532.50114	540.5	538.19715
534.9	532.60107	540.6	538.29708
535	532.701	540.7	538.39701
535.1	532.80093	540.8	538.49694
535.2	532.90086	540.9	538.59687
535.3	533.00079	541	538.6968
535.4	533.10072	541.1	538.79673
535.5	533.20065	541.2	538.89666
535.6	533.30058	541.3	538.99659
535.7	533.40051	541.4	539.09652
535.8	533.50044	541.5	539.19645
535.9	533.60037	541.6	539.29638
536	533.7003	541.7	539.39631
536.1	533.80023	541.8	539.49624
536.2	533.90016	541.9	539.59617
536.3	534.00009	542	539.6961
536.4	534.10002	542.1	539.79603
536.5	534.19995	542.2	539.89596
536.6	534.29988	542.3	539.99589
536.7	534.39981	542.4	540.09582
536.8	534.49974	542.5	540.19575
536.9	534.59967	542.6	540.29568
537	534.6996	542.7	540.39561
537.1	534.79953	542.8	540.49554
537.2	534.89946	542.9	540.59547
537.3	534.99939	543	540.6954
537.4	535.09932	543.1	540.79533
537.5	535.19925	543.2	540.89526

543.3	540.99519	549	546.6912
543.4	541.09512	549.1	546.79113
543.5	541.19505	549.2	546.89106
543.6	541.29498	549.3	546.99099
543.7	541.39491	549.4	547.09092
543.8	541.49484	549.5	547.19085
543.9	541.59477	549.6	547.29078
544	541.6947	549.7	547.39071
544.1	541.79463	549.8	547.49064
544.2	541.89456	549.9	547.59057
544.3	541.99449	550	547.6905
544.4	542.09442	550.1	547.79043
544.5	542.19435	550.2	547.89036
544.6	542.29428	550.3	547.99029
544.7	542.39421	550.4	548.09022
544.8	542.49414	550.5	548.19015
544.9	542.59407	550.6	548.29008
545	542.694	550.7	548.39001
545.1	542.79393	550.8	548.48994
545.2	542.89386	550.9	548.58987
545.3	542.99379	551	548.6898
545.4	543.09372	551.1	548.78973
545.5	543.19365	551.2	548.88966
545.6	543.29358	551.3	548.98959
545.7	543.39351	551.4	549.08952
545.8	543.49344	551.5	549.18945
545.9	543.59337	551.6	549.28938
546	543.6933	551.7	549.38931
546.1	543.79323	551.8	549.48924
546.2	543.89316	551.9	549.58917
546.3	543.99309	552	549.6891
546.4	544.09302	552.1	549.78903
546.5	544.19295	552.2	549.88896
546.6	544.29288	552.3	549.98889
546.7	544.39281	552.4	550.08882
546.8	544.49274	552.5	550.18875
546.9	544.59267	552.6	550.28868
547	544.6926	552.7	550.38861
547.1	544.79253	552.8	550.48854
547.2	544.89246	552.9	550.58847
547.3	544.99239	553	550.6884
547.4	545.09232	553.1	550.78833
547.5	545.19225	553.2	550.88826
547.6	545.29218	553.3	550.98819
547.7	545.39211	553.4	551.08812
547.8	545.49204	553.5	551.18805
547.9	545.59197	553.6	551.28798
548	545.6919	553.7	551.38791
548.1	545.79183	553.8	551.48784
548.2	545.89176	553.9	551.58777
548.3	545.99169	554	551.6877
548.4	546.09162	554.1	551.78763
548.5	546.19155	554.2	551.88756
548.6	546.29148	554.3	551.98749
548.7	546.39141	554.4	552.08742
548.8	546.49134	554.5	552.18735
548.9	546.59127	554.6	552.28728

554.7	552.38721	560.4	558.08322
554.8	552.48714	560.5	558.18315
554.9	552.58707	560.6	558.28308
555	552.687	560.7	558.38301
555.1	552.78693	560.8	558.48294
555.2	552.88686	560.9	558.58287
555.3	552.98679	561	558.6828
555.4	553.08672	561.1	558.78273
555.5	553.18665	561.2	558.88266
555.6	553.28658	561.3	558.98259
555.7	553.38651	561.4	559.08252
555.8	553.48644	561.5	559.18245
555.9	553.58637	561.6	559.28238
556	553.6863	561.7	559.38231
556.1	553.78623	561.8	559.48224
556.2	553.88616	561.9	559.58217
556.3	553.98609	562	559.6821
556.4	554.08602	562.1	559.78203
556.5	554.18595	562.2	559.88196
556.6	554.28588	562.3	559.98189
556.7	554.38581	562.4	560.08182
556.8	554.48574	562.5	560.18175
556.9	554.58567	562.6	560.28168
557	554.6856	562.7	560.38161
557.1	554.78553	562.8	560.48154
557.2	554.88546	562.9	560.58147
557.3	554.98539	563	560.6814
557.4	555.08532	563.1	560.78133
557.5	555.18525	563.2	560.88126
557.6	555.28518	563.3	560.98119
557.7	555.38511	563.4	561.08112
557.8	555.48504	563.5	561.18105
557.9	555.58497	563.6	561.28098
558	555.6849	563.7	561.38091
558.1	555.78483	563.8	561.48084
558.2	555.88476	563.9	561.58077
558.3	555.98469	564	561.6807
558.4	556.08462	564.1	561.78063
558.5	556.18455	564.2	561.88056
558.6	556.28448	564.3	561.98049
558.7	556.38441	564.4	562.08042
558.8	556.48434	564.5	562.18035
558.9	556.58427	564.6	562.28028
559	556.6842	564.7	562.38021
559.1	556.78413	564.8	562.48014
559.2	556.88406	564.9	562.58007
559.3	556.98399	565	562.68
559.4	557.08392	565.1	562.77993
559.5	557.18385	565.2	562.87986
559.6	557.28378	565.3	562.97979
559.7	557.38371	565.4	563.07972
559.8	557.48364	565.5	563.17965
559.9	557.58357	565.6	563.27958
560	557.6835	565.7	563.37951
560.1	557.78343	565.8	563.47944
560.2	557.88336	565.9	563.57937
560.3	557.98329	566	563.6793

566.1	563.77923	571.8	569.47524
566.2	563.87916	571.9	569.57517
566.3	563.97909	572	569.6751
566.4	564.07902	572.1	569.77503
566.5	564.17895	572.2	569.87496
566.6	564.27888	572.3	569.97489
566.7	564.37881	572.4	570.07482
566.8	564.47874	572.5	570.17475
566.9	564.57867	572.6	570.27468
567	564.6786	572.7	570.37461
567.1	564.77853	572.8	570.47454
567.2	564.87846	572.9	570.57447
567.3	564.97839	573	570.6744
567.4	565.07832	573.1	570.77433
567.5	565.17825	573.2	570.87426
567.6	565.27818	573.3	570.97419
567.7	565.37811	573.4	571.07412
567.8	565.47804	573.5	571.17405
567.9	565.57797	573.6	571.27398
568	565.6779	573.7	571.37391
568.1	565.77783	573.8	571.47384
568.2	565.87776	573.9	571.57377
568.3	565.97769	574	571.6737
568.4	566.07762	574.1	571.77363
568.5	566.17755	574.2	571.87356
568.6	566.27748	574.3	571.97349
568.7	566.37741	574.4	572.07342
568.8	566.47734	574.5	572.17335
568.9	566.57727	574.6	572.27328
569	566.6772	574.7	572.37321
569.1	566.77713	574.8	572.47314
569.2	566.87706	574.9	572.57307
569.3	566.97699	575	572.673
569.4	567.07692	575.1	572.77293
569.5	567.17685	575.2	572.87286
569.6	567.27678	575.3	572.97279
569.7	567.37671	575.4	573.07272
569.8	567.47664	575.5	573.17265
569.9	567.57657	575.6	573.27258
570	567.6765	575.7	573.37251
570.1	567.77643	575.8	573.47244
570.2	567.87636	575.9	573.57237
570.3	567.97629	576	573.6723
570.4	568.07622	576.1	573.77223
570.5	568.17615	576.2	573.87216
570.6	568.27608	576.3	573.97209
570.7	568.37601	576.4	574.07202
570.8	568.47594	576.5	574.17195
570.9	568.57587	576.6	574.27188
571	568.6758	576.7	574.37181
571.1	568.77573	576.8	574.47174
571.2	568.87566	576.9	574.57167
571.3	568.97559	577	574.6716
571.4	569.07552	577.1	574.77153
571.5	569.17545	577.2	574.87146
571.6	569.27538	577.3	574.97139
571.7	569.37531	577.4	575.07132

577.5	575.17125	583.2	580.86726
577.6	575.27118	583.3	580.96719
577.7	575.37111	583.4	581.06712
577.8	575.47104	583.5	581.16705
577.9	575.57097	583.6	581.26698
578	575.6709	583.7	581.36691
578.1	575.77083	583.8	581.46684
578.2	575.87076	583.9	581.56677
578.3	575.97069	584	581.6667
578.4	576.07062	584.1	581.76663
578.5	576.17055	584.2	581.86656
578.6	576.27048	584.3	581.96649
578.7	576.37041	584.4	582.06642
578.8	576.47034	584.5	582.16635
578.9	576.57027	584.6	582.26628
579	576.6702	584.7	582.36621
579.1	576.77013	584.8	582.46614
579.2	576.87006	584.9	582.56607
579.3	576.96999	585	582.666
579.4	577.06992	585.1	582.76593
579.5	577.16985	585.2	582.86586
579.6	577.26978	585.3	582.96579
579.7	577.36971	585.4	583.06572
579.8	577.46964	585.5	583.16565
579.9	577.56957	585.6	583.26558
580	577.6695	585.7	583.36551
580.1	577.76943	585.8	583.46544
580.2	577.86936	585.9	583.56537
580.3	577.96929	586	583.6653
580.4	578.06922	586.1	583.76523
580.5	578.16915	586.2	583.86516
580.6	578.26908	586.3	583.96509
580.7	578.36901	586.4	584.06502
580.8	578.46894	586.5	584.16495
580.9	578.56887	586.6	584.26488
581	578.6688	586.7	584.36481
581.1	578.76873	586.8	584.46474
581.2	578.86866	586.9	584.56467
581.3	578.96859	587	584.6646
581.4	579.06852	587.1	584.76453
581.5	579.16845	587.2	584.86446
581.6	579.26838	587.3	584.96439
581.7	579.36831	587.4	585.06432
581.8	579.46824	587.5	585.16425
581.9	579.56817	587.6	585.26418
582	579.6681	587.7	585.36411
582.1	579.76803	587.8	585.46404
582.2	579.86796	587.9	585.56397
582.3	579.96789	588	585.6639
582.4	580.06782	588.1	585.76383
582.5	580.16775	588.2	585.86376
582.6	580.26768	588.3	585.96369
582.7	580.36761	588.4	586.06362
582.8	580.46754	588.5	586.16355
582.9	580.56747	588.6	586.26348
583	580.6674	588.7	586.36341
583.1	580.76733	588.8	586.46334

588.9	586.56327	594.6	592.25928
589	586.6632	594.7	592.35921
589.1	586.76313	594.8	592.45914
589.2	586.86306	594.9	592.55907
589.3	586.96299	595	592.659
589.4	587.06292	595.1	592.75893
589.5	587.16285	595.2	592.85886
589.6	587.26278	595.3	592.95879
589.7	587.36271	595.4	593.05872
589.8	587.46264	595.5	593.15865
589.9	587.56257	595.6	593.25858
590	587.6625	595.7	593.35851
590.1	587.76243	595.8	593.45844
590.2	587.86236	595.9	593.55837
590.3	587.96229	596	593.6583
590.4	588.06222	596.1	593.75823
590.5	588.16215	596.2	593.85816
590.6	588.26208	596.3	593.95809
590.7	588.36201	596.4	594.05802
590.8	588.46194	596.5	594.15795
590.9	588.56187	596.6	594.25788
591	588.6618	596.7	594.35781
591.1	588.76173	596.8	594.45774
591.2	588.86166	596.9	594.55767
591.3	588.96159	597	594.6576
591.4	589.06152	597.1	594.75753
591.5	589.16145	597.2	594.85746
591.6	589.26138	597.3	594.95739
591.7	589.36131	597.4	595.05732
591.8	589.46124	597.5	595.15725
591.9	589.56117	597.6	595.25718
592	589.6611	597.7	595.35711
592.1	589.76103	597.8	595.45704
592.2	589.86096	597.9	595.55697
592.3	589.96089	598	595.6569
592.4	590.06082	598.1	595.75683
592.5	590.16075	598.2	595.85676
592.6	590.26068	598.3	595.95669
592.7	590.36061	598.4	596.05662
592.8	590.46054	598.5	596.15655
592.9	590.56047	598.6	596.25648
593	590.6604	598.7	596.35641
593.1	590.76033	598.8	596.45634
593.2	590.86026	598.9	596.55627
593.3	590.96019	599	596.6562
593.4	591.06012	599.1	596.75613
593.5	591.16005	599.2	596.85606
593.6	591.25998	599.3	596.95599
593.7	591.35991	599.4	597.05592
593.8	591.45984	599.5	597.15585
593.9	591.55977	599.6	597.25578
594	591.6597	599.7	597.35571
594.1	591.75963	599.8	597.45564
594.2	591.85956	599.9	597.55557
594.3	591.95949	600	597.6555
594.4	592.05942	600.1	597.75543
594.5	592.15935	600.2	597.85536

600.3	597.95529	606	603.6513
600.4	598.05522	606.1	603.75123
600.5	598.15515	606.2	603.85116
600.6	598.25508	606.3	603.95109
600.7	598.35501	606.4	604.05102
600.8	598.45494	606.5	604.15095
600.9	598.55487	606.6	604.25088
601	598.6548	606.7	604.35081
601.1	598.75473	606.8	604.45074
601.2	598.85466	606.9	604.55067
601.3	598.95459	607	604.6506
601.4	599.05452	607.1	604.75053
601.5	599.15445	607.2	604.85046
601.6	599.25438	607.3	604.95039
601.7	599.35431	607.4	605.05032
601.8	599.45424	607.5	605.15025
601.9	599.55417	607.6	605.25018
602	599.6541	607.7	605.35011
602.1	599.75403	607.8	605.45004
602.2	599.85396	607.9	605.54997
602.3	599.95389	608	605.6499
602.4	600.05382	608.1	605.74983
602.5	600.15375	608.2	605.84976
602.6	600.25368	608.3	605.94969
602.7	600.35361	608.4	606.04962
602.8	600.45354	608.5	606.14955
602.9	600.55347	608.6	606.24948
603	600.6534	608.7	606.34941
603.1	600.75333	608.8	606.44934
603.2	600.85326	608.9	606.54927
603.3	600.95319	609	606.6492
603.4	601.05312	609.1	606.74913
603.5	601.15305	609.2	606.84906
603.6	601.25298	609.3	606.94899
603.7	601.35291	609.4	607.04892
603.8	601.45284	609.5	607.14885
603.9	601.55277	609.6	607.24878
604	601.6527	609.7	607.34871
604.1	601.75263	609.8	607.44864
604.2	601.85256	609.9	607.54857
604.3	601.95249	610	607.6485
604.4	602.05242	610.1	607.74843
604.5	602.15235	610.2	607.84836
604.6	602.25228	610.3	607.94829
604.7	602.35221	610.4	608.04822
604.8	602.45214	610.5	608.14815
604.9	602.55207	610.6	608.24808
605	602.652	610.7	608.34801
605.1	602.75193	610.8	608.44794
605.2	602.85186	610.9	608.54787
605.3	602.95179	611	608.6478
605.4	603.05172	611.1	608.74773
605.5	603.15165	611.2	608.84766
605.6	603.25158	611.3	608.94759
605.7	603.35151	611.4	609.04752
605.8	603.45144	611.5	609.14745
605.9	603.55137	611.6	609.24738

611.7	609.34731	617.4	615.04332
611.8	609.44724	617.5	615.14325
611.9	609.54717	617.6	615.24318
612	609.6471	617.7	615.34311
612.1	609.74703	617.8	615.44304
612.2	609.84696	617.9	615.54297
612.3	609.94689	618	615.6429
612.4	610.04682	618.1	615.74283
612.5	610.14675	618.2	615.84276
612.6	610.24668	618.3	615.94269
612.7	610.34661	618.4	616.04262
612.8	610.44654	618.5	616.14255
612.9	610.54647	618.6	616.24248
613	610.6464	618.7	616.34241
613.1	610.74633	618.8	616.44234
613.2	610.84626	618.9	616.54227
613.3	610.94619	619	616.6422
613.4	611.04612	619.1	616.74213
613.5	611.14605	619.2	616.84206
613.6	611.24598	619.3	616.94199
613.7	611.34591	619.4	617.04192
613.8	611.44584	619.5	617.14185
613.9	611.54577	619.6	617.24178
614	611.6457	619.7	617.34171
614.1	611.74563	619.8	617.44164
614.2	611.84556	619.9	617.54157
614.3	611.94549	620	617.6415
614.4	612.04542	620.1	617.74143
614.5	612.14535	620.2	617.84136
614.6	612.24528	620.3	617.94129
614.7	612.34521	620.4	618.04122
614.8	612.44514	620.5	618.14115
614.9	612.54507	620.6	618.24108
615	612.645	620.7	618.34101
615.1	612.74493	620.8	618.44094
615.2	612.84486	620.9	618.54087
615.3	612.94479	621	618.6408
615.4	613.04472	621.1	618.74073
615.5	613.14465	621.2	618.84066
615.6	613.24458	621.3	618.94059
615.7	613.34451	621.4	619.04052
615.8	613.44444	621.5	619.14045
615.9	613.54437	621.6	619.24038
616	613.6443	621.7	619.34031
616.1	613.74423	621.8	619.44024
616.2	613.84416	621.9	619.54017
616.3	613.94409	622	619.6401
616.4	614.04402	622.1	619.74003
616.5	614.14395	622.2	619.83996
616.6	614.24388	622.3	619.93989
616.7	614.34381	622.4	620.03982
616.8	614.44374	622.5	620.13975
616.9	614.54367	622.6	620.23968
617	614.6436	622.7	620.33961
617.1	614.74353	622.8	620.43954
617.2	614.84346	622.9	620.53947
617.3	614.94339	623	620.6394

623.1	620.73933	628.8	626.43534
623.2	620.83926	628.9	626.53527
623.3	620.93919	629	626.6352
623.4	621.03912	629.1	626.73513
623.5	621.13905	629.2	626.83506
623.6	621.23898	629.3	626.93499
623.7	621.33891	629.4	627.03492
623.8	621.43884	629.5	627.13485
623.9	621.53877	629.6	627.23478
624	621.6387	629.7	627.33471
624.1	621.73863	629.8	627.43464
624.2	621.83856	629.9	627.53457
624.3	621.93849	630	627.6345
624.4	622.03842	630.1	627.73443
624.5	622.13835	630.2	627.83436
624.6	622.23828	630.3	627.93429
624.7	622.33821	630.4	628.03422
624.8	622.43814	630.5	628.13415
624.9	622.53807	630.6	628.23408
625	622.638	630.7	628.33401
625.1	622.73793	630.8	628.43394
625.2	622.83786	630.9	628.53387
625.3	622.93779	631	628.6338
625.4	623.03772	631.1	628.73373
625.5	623.13765	631.2	628.83366
625.6	623.23758	631.3	628.93359
625.7	623.33751	631.4	629.03352
625.8	623.43744	631.5	629.13345
625.9	623.53737	631.6	629.23338
626	623.6373	631.7	629.33331
626.1	623.73723	631.8	629.43324
626.2	623.83716	631.9	629.53317
626.3	623.93709	632	629.6331
626.4	624.03702	632.1	629.73303
626.5	624.13695	632.2	629.83296
626.6	624.23688	632.3	629.93289
626.7	624.33681	632.4	630.03282
626.8	624.43674	632.5	630.13275
626.9	624.53667	632.6	630.23268
627	624.6366	632.7	630.33261
627.1	624.73653	632.8	630.43254
627.2	624.83646	632.9	630.53247
627.3	624.93639	633	630.6324
627.4	625.03632	633.1	630.73233
627.5	625.13625	633.2	630.83226
627.6	625.23618	633.3	630.93219
627.7	625.33611	633.4	631.03212
627.8	625.43604	633.5	631.13205
627.9	625.53597	633.6	631.23198
628	625.6359	633.7	631.33191
628.1	625.73583	633.8	631.43184
628.2	625.83576	633.9	631.53177
628.3	625.93569	634	631.6317
628.4	626.03562	634.1	631.73163
628.5	626.13555	634.2	631.83156
628.6	626.23548	634.3	631.93149
628.7	626.33541	634.4	632.03142

634.5	632.13135	640.2	637.82736
634.6	632.23128	640.3	637.92729
634.7	632.33121	640.4	638.02722
634.8	632.43114	640.5	638.12715
634.9	632.53107	640.6	638.22708
635	632.631	640.7	638.32701
635.1	632.73093	640.8	638.42694
635.2	632.83086	640.9	638.52687
635.3	632.93079	641	638.6268
635.4	633.03072	641.1	638.72673
635.5	633.13065	641.2	638.82666
635.6	633.23058	641.3	638.92659
635.7	633.33051	641.4	639.02652
635.8	633.43044	641.5	639.12645
635.9	633.53037	641.6	639.22638
636	633.6303	641.7	639.32631
636.1	633.73023	641.8	639.42624
636.2	633.83016	641.9	639.52617
636.3	633.93009	642	639.6261
636.4	634.03002	642.1	639.72603
636.5	634.12995	642.2	639.82596
636.6	634.22988	642.3	639.92589
636.7	634.32981	642.4	640.02582
636.8	634.42974	642.5	640.12575
636.9	634.52967	642.6	640.22568
637	634.6296	642.7	640.32561
637.1	634.72953	642.8	640.42554
637.2	634.82946	642.9	640.52547
637.3	634.92939	643	640.6254
637.4	635.02932	643.1	640.72533
637.5	635.12925	643.2	640.82526
637.6	635.22918	643.3	640.92519
637.7	635.32911	643.4	641.02512
637.8	635.42904	643.5	641.12505
637.9	635.52897	643.6	641.22498
638	635.6289	643.7	641.32491
638.1	635.72883	643.8	641.42484
638.2	635.82876	643.9	641.52477
638.3	635.92869	644	641.6247
638.4	636.02862	644.1	641.72463
638.5	636.12855	644.2	641.82456
638.6	636.22848	644.3	641.92449
638.7	636.32841	644.4	642.02442
638.8	636.42834	644.5	642.12435
638.9	636.52827	644.6	642.22428
639	636.6282	644.7	642.32421
639.1	636.72813	644.8	642.42414
639.2	636.82806	644.9	642.52407
639.3	636.92799	645	642.624
639.4	637.02792	645.1	642.72393
639.5	637.12785	645.2	642.82386
639.6	637.22778	645.3	642.92379
639.7	637.32771	645.4	643.02372
639.8	637.42764	645.5	643.12365
639.9	637.52757	645.6	643.22358
640	637.6275	645.7	643.32351
640.1	637.72743	645.8	643.42344

645.9	643.52337	651.6	649.21938
646	643.6233	651.7	649.31931
646.1	643.72323	651.8	649.41924
646.2	643.82316	651.9	649.51917
646.3	643.92309	652	649.6191
646.4	644.02302	652.1	649.71903
646.5	644.12295	652.2	649.81896
646.6	644.22288	652.3	649.91889
646.7	644.32281	652.4	650.01882
646.8	644.42274	652.5	650.11875
646.9	644.52267	652.6	650.21868
647	644.6226	652.7	650.31861
647.1	644.72253	652.8	650.41854
647.2	644.82246	652.9	650.51847
647.3	644.92239	653	650.6184
647.4	645.02232	653.1	650.71833
647.5	645.12225	653.2	650.81826
647.6	645.22218	653.3	650.91819
647.7	645.32211	653.4	651.01812
647.8	645.42204	653.5	651.11805
647.9	645.52197	653.6	651.21798
648	645.6219	653.7	651.31791
648.1	645.72183	653.8	651.41784
648.2	645.82176	653.9	651.51777
648.3	645.92169	654	651.6177
648.4	646.02162	654.1	651.71763
648.5	646.12155	654.2	651.81756
648.6	646.22148	654.3	651.91749
648.7	646.32141	654.4	652.01742
648.8	646.42134	654.5	652.11735
648.9	646.52127	654.6	652.21728
649	646.6212	654.7	652.31721
649.1	646.72113	654.8	652.41714
649.2	646.82106	654.9	652.51707
649.3	646.92099	655	652.617
649.4	647.02092	655.1	652.71693
649.5	647.12085	655.2	652.81686
649.6	647.22078	655.3	652.91679
649.7	647.32071	655.4	653.01672
649.8	647.42064	655.5	653.11665
649.9	647.52057	655.6	653.21658
650	647.6205	655.7	653.31651
650.1	647.72043	655.8	653.41644
650.2	647.82036	655.9	653.51637
650.3	647.92029	656	653.6163
650.4	648.02022	656.1	653.71623
650.5	648.12015	656.2	653.81616
650.6	648.22008	656.3	653.91609
650.7	648.32001	656.4	654.01602
650.8	648.41994	656.5	654.11595
650.9	648.51987	656.6	654.21588
651	648.6198	656.7	654.31581
651.1	648.71973	656.8	654.41574
651.2	648.81966	656.9	654.51567
651.3	648.91959	657	654.6156
651.4	649.01952	657.1	654.71553
651.5	649.11945	657.2	654.81546

657.3	654.91539	663	660.6114
657.4	655.01532	663.1	660.71133
657.5	655.11525	663.2	660.81126
657.6	655.21518	663.3	660.91119
657.7	655.31511	663.4	661.01112
657.8	655.41504	663.5	661.11105
657.9	655.51497	663.6	661.21098
658	655.6149	663.7	661.31091
658.1	655.71483	663.8	661.41084
658.2	655.81476	663.9	661.51077
658.3	655.91469	664	661.6107
658.4	656.01462	664.1	661.71063
658.5	656.11455	664.2	661.81056
658.6	656.21448	664.3	661.91049
658.7	656.31441	664.4	662.01042
658.8	656.41434	664.5	662.11035
658.9	656.51427	664.6	662.21028
659	656.6142	664.7	662.31021
659.1	656.71413	664.8	662.41014
659.2	656.81406	664.9	662.51007
659.3	656.91399	665	662.61
659.4	657.01392	665.1	662.70993
659.5	657.11385	665.2	662.80986
659.6	657.21378	665.3	662.90979
659.7	657.31371	665.4	663.00972
659.8	657.41364	665.5	663.10965
659.9	657.51357	665.6	663.20958
660	657.6135	665.7	663.30951
660.1	657.71343	665.8	663.40944
660.2	657.81336	665.9	663.50937
660.3	657.91329	666	663.6093
660.4	658.01322	666.1	663.70923
660.5	658.11315	666.2	663.80916
660.6	658.21308	666.3	663.90909
660.7	658.31301	666.4	664.00902
660.8	658.41294	666.5	664.10895
660.9	658.51287	666.6	664.20888
661	658.6128	666.7	664.30881
661.1	658.71273	666.8	664.40874
661.2	658.81266	666.9	664.50867
661.3	658.91259	667	664.6086
661.4	659.01252	667.1	664.70853
661.5	659.11245	667.2	664.80846
661.6	659.21238	667.3	664.90839
661.7	659.31231	667.4	665.00832
661.8	659.41224	667.5	665.10825
661.9	659.51217	667.6	665.20818
662	659.6121	667.7	665.30811
662.1	659.71203	667.8	665.40804
662.2	659.81196	667.9	665.50797
662.3	659.91189	668	665.6079
662.4	660.01182	668.1	665.70783
662.5	660.11175	668.2	665.80776
662.6	660.21168	668.3	665.90769
662.7	660.31161	668.4	666.00762
662.8	660.41154	668.5	666.10755
662.9	660.51147	668.6	666.20748

668.7	666.30741	674.4	672.00342
668.8	666.40734	674.5	672.10335
668.9	666.50727	674.6	672.20328
669	666.6072	674.7	672.30321
669.1	666.70713	674.8	672.40314
669.2	666.80706	674.9	672.50307
669.3	666.90699	675	672.603
669.4	667.00692	675.1	672.70293
669.5	667.10685	675.2	672.80286
669.6	667.20678	675.3	672.90279
669.7	667.30671	675.4	673.00272
669.8	667.40664	675.5	673.10265
669.9	667.50657	675.6	673.20258
670	667.6065	675.7	673.30251
670.1	667.70643	675.8	673.40244
670.2	667.80636	675.9	673.50237
670.3	667.90629	676	673.6023
670.4	668.00622	676.1	673.70223
670.5	668.10615	676.2	673.80216
670.6	668.20608	676.3	673.90209
670.7	668.30601	676.4	674.00202
670.8	668.40594	676.5	674.10195
670.9	668.50587	676.6	674.20188
671	668.6058	676.7	674.30181
671.1	668.70573	676.8	674.40174
671.2	668.80566	676.9	674.50167
671.3	668.90559	677	674.6016
671.4	669.00552	677.1	674.70153
671.5	669.10545	677.2	674.80146
671.6	669.20538	677.3	674.90139
671.7	669.30531	677.4	675.00132
671.8	669.40524	677.5	675.10125
671.9	669.50517	677.6	675.20118
672	669.6051	677.7	675.30111
672.1	669.70503	677.8	675.40104
672.2	669.80496	677.9	675.50097
672.3	669.90489	678	675.6009
672.4	670.00482	678.1	675.70083
672.5	670.10475	678.2	675.80076
672.6	670.20468	678.3	675.90069
672.7	670.30461	678.4	676.00062
672.8	670.40454	678.5	676.10055
672.9	670.50447	678.6	676.20048
673	670.6044	678.7	676.30041
673.1	670.70433	678.8	676.40034
673.2	670.80426	678.9	676.50027
673.3	670.90419	679	676.6002
673.4	671.00412	679.1	676.70013
673.5	671.10405	679.2	676.80006
673.6	671.20398	679.3	676.89999
673.7	671.30391	679.4	676.99992
673.8	671.40384	679.5	677.09985
673.9	671.50377	679.6	677.19978
674	671.6037	679.7	677.29971
674.1	671.70363	679.8	677.39964
674.2	671.80356	679.9	677.49957
674.3	671.90349	680	677.5995

680.1	677.69943	685.8	683.39544
680.2	677.79936	685.9	683.49537
680.3	677.89929	686	683.5953
680.4	677.99922	686.1	683.69523
680.5	678.09915	686.2	683.79516
680.6	678.19908	686.3	683.89509
680.7	678.29901	686.4	683.99502
680.8	678.39894	686.5	684.09495
680.9	678.49887	686.6	684.19488
681	678.5988	686.7	684.29481
681.1	678.69873	686.8	684.39474
681.2	678.79866	686.9	684.49467
681.3	678.89859	687	684.5946
681.4	678.99852	687.1	684.69453
681.5	679.09845	687.2	684.79446
681.6	679.19838	687.3	684.89439
681.7	679.29831	687.4	684.99432
681.8	679.39824	687.5	685.09425
681.9	679.49817	687.6	685.19418
682	679.5981	687.7	685.29411
682.1	679.69803	687.8	685.39404
682.2	679.79796	687.9	685.49397
682.3	679.89789	688	685.5939
682.4	679.99782	688.1	685.69383
682.5	680.09775	688.2	685.79376
682.6	680.19768	688.3	685.89369
682.7	680.29761	688.4	685.99362
682.8	680.39754	688.5	686.09355
682.9	680.49747	688.6	686.19348
683	680.5974	688.7	686.29341
683.1	680.69733	688.8	686.39334
683.2	680.79726	688.9	686.49327
683.3	680.89719	689	686.5932
683.4	680.99712	689.1	686.69313
683.5	681.09705	689.2	686.79306
683.6	681.19698	689.3	686.89299
683.7	681.29691	689.4	686.99292
683.8	681.39684	689.5	687.09285
683.9	681.49677	689.6	687.19278
684	681.5967	689.7	687.29271
684.1	681.69663	689.8	687.39264
684.2	681.79656	689.9	687.49257
684.3	681.89649	690	687.5925
684.4	681.99642	690.1	687.69243
684.5	682.09635	690.2	687.79236
684.6	682.19628	690.3	687.89229
684.7	682.29621	690.4	687.99222
684.8	682.39614	690.5	688.09215
684.9	682.49607	690.6	688.19208
685	682.596	690.7	688.29201
685.1	682.69593	690.8	688.39194
685.2	682.79586	690.9	688.49187
685.3	682.89579	691	688.5918
685.4	682.99572	691.1	688.69173
685.5	683.09565	691.2	688.79166
685.6	683.19558	691.3	688.89159
685.7	683.29551	691.4	688.99152

691.5	689.09145	697.2	694.78746
691.6	689.19138	697.3	694.88739
691.7	689.29131	697.4	694.98732
691.8	689.39124	697.5	695.08725
691.9	689.49117	697.6	695.18718
692	689.5911	697.7	695.28711
692.1	689.69103	697.8	695.38704
692.2	689.79096	697.9	695.48697
692.3	689.89089	698	695.5869
692.4	689.99082	698.1	695.68683
692.5	690.09075	698.2	695.78676
692.6	690.19068	698.3	695.88669
692.7	690.29061	698.4	695.98662
692.8	690.39054	698.5	696.08655
692.9	690.49047	698.6	696.18648
693	690.5904	698.7	696.28641
693.1	690.69033	698.8	696.38634
693.2	690.79026	698.9	696.48627
693.3	690.89019	699	696.5862
693.4	690.99012	699.1	696.68613
693.5	691.09005	699.2	696.78606
693.6	691.18998	699.3	696.88599
693.7	691.28991	699.4	696.98592
693.8	691.38984	699.5	697.08585
693.9	691.48977	699.6	697.18578
694	691.5897	699.7	697.28571
694.1	691.68963	699.8	697.38564
694.2	691.78956	699.9	697.48557
694.3	691.88949	700	697.5855
694.4	691.98942	700.1	697.68543
694.5	692.08935	700.2	697.78536
694.6	692.18928	700.3	697.88529
694.7	692.28921	700.4	697.98522
694.8	692.38914	700.5	698.08515
694.9	692.48907	700.6	698.18508
695	692.589	700.7	698.28501
695.1	692.68893	700.8	698.38494
695.2	692.78886	700.9	698.48487
695.3	692.88879	701	698.5848
695.4	692.98872	701.1	698.68473
695.5	693.08865	701.2	698.78466
695.6	693.18858	701.3	698.88459
695.7	693.28851	701.4	698.98452
695.8	693.38844	701.5	699.08445
695.9	693.48837	701.6	699.18438
696	693.5883	701.7	699.28431
696.1	693.68823	701.8	699.38424
696.2	693.78816	701.9	699.48417
696.3	693.88809	702	699.5841
696.4	693.98802	702.1	699.68403
696.5	694.08795	702.2	699.78396
696.6	694.18788	702.3	699.88389
696.7	694.28781	702.4	699.98382
696.8	694.38774	702.5	700.08375
696.9	694.48767	702.6	700.18368
697	694.5876	702.7	700.28361
697.1	694.68753	702.8	700.38354

702.9	700.48347	708.6	706.17948
703	700.5834	708.7	706.27941
703.1	700.68333	708.8	706.37934
703.2	700.78326	708.9	706.47927
703.3	700.88319	709	706.5792
703.4	700.98312	709.1	706.67913
703.5	701.08305	709.2	706.77906
703.6	701.18298	709.3	706.87899
703.7	701.28291	709.4	706.97892
703.8	701.38284	709.5	707.07885
703.9	701.48277	709.6	707.17878
704	701.5827	709.7	707.27871
704.1	701.68263	709.8	707.37864
704.2	701.78256	709.9	707.47857
704.3	701.88249	710	707.5785
704.4	701.98242	710.1	707.67843
704.5	702.08235	710.2	707.77836
704.6	702.18228	710.3	707.87829
704.7	702.28221	710.4	707.97822
704.8	702.38214	710.5	708.07815
704.9	702.48207	710.6	708.17808
705	702.582	710.7	708.27801
705.1	702.68193	710.8	708.37794
705.2	702.78186	710.9	708.47787
705.3	702.88179	711	708.5778
705.4	702.98172	711.1	708.67773
705.5	703.08165	711.2	708.77766
705.6	703.18158	711.3	708.87759
705.7	703.28151	711.4	708.97752
705.8	703.38144	711.5	709.07745
705.9	703.48137	711.6	709.17738
706	703.5813	711.7	709.27731
706.1	703.68123	711.8	709.37724
706.2	703.78116	711.9	709.47717
706.3	703.88109	712	709.5771
706.4	703.98102	712.1	709.67703
706.5	704.08095	712.2	709.77696
706.6	704.18088	712.3	709.87689
706.7	704.28081	712.4	709.97682
706.8	704.38074	712.5	710.07675
706.9	704.48067	712.6	710.17668
707	704.5806	712.7	710.27661
707.1	704.68053	712.8	710.37654
707.2	704.78046	712.9	710.47647
707.3	704.88039	713	710.5764
707.4	704.98032	713.1	710.67633
707.5	705.08025	713.2	710.77626
707.6	705.18018	713.3	710.87619
707.7	705.28011	713.4	710.97612
707.8	705.38004	713.5	711.07605
707.9	705.47997	713.6	711.17598
708	705.5799	713.7	711.27591
708.1	705.67983	713.8	711.37584
708.2	705.77976	713.9	711.47577
708.3	705.87969	714	711.5757
708.4	705.97962	714.1	711.67563
708.5	706.07955	714.2	711.77556

714.3	711.87549	720	717.5715
714.4	711.97542	720.1	717.67143
714.5	712.07535	720.2	717.77136
714.6	712.17528	720.3	717.87129
714.7	712.27521	720.4	717.97122
714.8	712.37514	720.5	718.07115
714.9	712.47507	720.6	718.17108
715	712.575	720.7	718.27101
715.1	712.67493	720.8	718.37094
715.2	712.77486	720.9	718.47087
715.3	712.87479	721	718.5708
715.4	712.97472	721.1	718.67073
715.5	713.07465	721.2	718.77066
715.6	713.17458	721.3	718.87059
715.7	713.27451	721.4	718.97052
715.8	713.37444	721.5	719.07045
715.9	713.47437	721.6	719.17038
716	713.5743	721.7	719.27031
716.1	713.67423	721.8	719.37024
716.2	713.77416	721.9	719.47017
716.3	713.87409	722	719.5701
716.4	713.97402	722.1	719.67003
716.5	714.07395	722.2	719.76996
716.6	714.17388	722.3	719.86989
716.7	714.27381	722.4	719.96982
716.8	714.37374	722.5	720.06975
716.9	714.47367	722.6	720.16968
717	714.5736	722.7	720.26961
717.1	714.67353	722.8	720.36954
717.2	714.77346	722.9	720.46947
717.3	714.87339	723	720.5694
717.4	714.97332	723.1	720.66933
717.5	715.07325	723.2	720.76926
717.6	715.17318	723.3	720.86919
717.7	715.27311	723.4	720.96912
717.8	715.37304	723.5	721.06905
717.9	715.47297	723.6	721.16898
718	715.5729	723.7	721.26891
718.1	715.67283	723.8	721.36884
718.2	715.77276	723.9	721.46877
718.3	715.87269	724	721.5687
718.4	715.97262	724.1	721.66863
718.5	716.07255	724.2	721.76856
718.6	716.17248	724.3	721.86849
718.7	716.27241	724.4	721.96842
718.8	716.37234	724.5	722.06835
718.9	716.47227	724.6	722.16828
719	716.5722	724.7	722.26821
719.1	716.67213	724.8	722.36814
719.2	716.77206	724.9	722.46807
719.3	716.87199	725	722.568
719.4	716.97192	725.1	722.66793
719.5	717.07185	725.2	722.76786
719.6	717.17178	725.3	722.86779
719.7	717.27171	725.4	722.96772
719.8	717.37164	725.5	723.06765
719.9	717.47157	725.6	723.16758

725.7	723.26751	731.4	728.96352
725.8	723.36744	731.5	729.06345
725.9	723.46737	731.6	729.16338
726	723.5673	731.7	729.26331
726.1	723.66723	731.8	729.36324
726.2	723.76716	731.9	729.46317
726.3	723.86709	732	729.5631
726.4	723.96702	732.1	729.66303
726.5	724.06695	732.2	729.76296
726.6	724.16688	732.3	729.86289
726.7	724.26681	732.4	729.96282
726.8	724.36674	732.5	730.06275
726.9	724.46667	732.6	730.16268
727	724.5666	732.7	730.26261
727.1	724.66653	732.8	730.36254
727.2	724.76646	732.9	730.46247
727.3	724.86639	733	730.5624
727.4	724.96632	733.1	730.66233
727.5	725.06625	733.2	730.76226
727.6	725.16618	733.3	730.86219
727.7	725.26611	733.4	730.96212
727.8	725.36604	733.5	731.06205
727.9	725.46597	733.6	731.16198
728	725.5659	733.7	731.26191
728.1	725.66583	733.8	731.36184
728.2	725.76576	733.9	731.46177
728.3	725.86569	734	731.5617
728.4	725.96562	734.1	731.66163
728.5	726.06555	734.2	731.76156
728.6	726.16548	734.3	731.86149
728.7	726.26541	734.4	731.96142
728.8	726.36534	734.5	732.06135
728.9	726.46527	734.6	732.16128
729	726.5652	734.7	732.26121
729.1	726.66513	734.8	732.36114
729.2	726.76506	734.9	732.46107
729.3	726.86499	735	732.561
729.4	726.96492	735.1	732.66093
729.5	727.06485	735.2	732.76086
729.6	727.16478	735.3	732.86079
729.7	727.26471	735.4	732.96072
729.8	727.36464	735.5	733.06065
729.9	727.46457	735.6	733.16058
730	727.5645	735.7	733.26051
730.1	727.66443	735.8	733.36044
730.2	727.76436	735.9	733.46037
730.3	727.86429	736	733.5603
730.4	727.96422	736.1	733.66023
730.5	728.06415	736.2	733.76016
730.6	728.16408	736.3	733.86009
730.7	728.26401	736.4	733.96002
730.8	728.36394	736.5	734.05995
730.9	728.46387	736.6	734.15988
731	728.5638	736.7	734.25981
731.1	728.66373	736.8	734.35974
731.2	728.76366	736.9	734.45967
731.3	728.86359	737	734.5596

737.1	734.65953	742.8	740.35554
737.2	734.75946	742.9	740.45547
737.3	734.85939	743	740.5554
737.4	734.95932	743.1	740.65533
737.5	735.05925	743.2	740.75526
737.6	735.15918	743.3	740.85519
737.7	735.25911	743.4	740.95512
737.8	735.35904	743.5	741.05505
737.9	735.45897	743.6	741.15498
738	735.5589	743.7	741.25491
738.1	735.65883	743.8	741.35484
738.2	735.75876	743.9	741.45477
738.3	735.85869	744	741.5547
738.4	735.95862	744.1	741.65463
738.5	736.05855	744.2	741.75456
738.6	736.15848	744.3	741.85449
738.7	736.25841	744.4	741.95442
738.8	736.35834	744.5	742.05435
738.9	736.45827	744.6	742.15428
739	736.5582	744.7	742.25421
739.1	736.65813	744.8	742.35414
739.2	736.75806	744.9	742.45407
739.3	736.85799	745	742.554
739.4	736.95792	745.1	742.65393
739.5	737.05785	745.2	742.75386
739.6	737.15778	745.3	742.85379
739.7	737.25771	745.4	742.95372
739.8	737.35764	745.5	743.05365
739.9	737.45757	745.6	743.15358
740	737.5575	745.7	743.25351
740.1	737.65743	745.8	743.35344
740.2	737.75736	745.9	743.45337
740.3	737.85729	746	743.5533
740.4	737.95722	746.1	743.65323
740.5	738.05715	746.2	743.75316
740.6	738.15708	746.3	743.85309
740.7	738.25701	746.4	743.95302
740.8	738.35694	746.5	744.05295
740.9	738.45687	746.6	744.15288
741	738.5568	746.7	744.25281
741.1	738.65673	746.8	744.35274
741.2	738.75666	746.9	744.45267
741.3	738.85659	747	744.5526
741.4	738.95652	747.1	744.65253
741.5	739.05645	747.2	744.75246
741.6	739.15638	747.3	744.85239
741.7	739.25631	747.4	744.95232
741.8	739.35624	747.5	745.05225
741.9	739.45617	747.6	745.15218
742	739.5561	747.7	745.25211
742.1	739.65603	747.8	745.35204
742.2	739.75596	747.9	745.45197
742.3	739.85589	748	745.5519
742.4	739.95582	748.1	745.65183
742.5	740.05575	748.2	745.75176
742.6	740.15568	748.3	745.85169
742.7	740.25561	748.4	745.95162

748.5	746.05155	754.2	751.74756
748.6	746.15148	754.3	751.84749
748.7	746.25141	754.4	751.94742
748.8	746.35134	754.5	752.04735
748.9	746.45127	754.6	752.14728
749	746.5512	754.7	752.24721
749.1	746.65113	754.8	752.34714
749.2	746.75106	754.9	752.44707
749.3	746.85099	755	752.547
749.4	746.95092	755.1	752.64693
749.5	747.05085	755.2	752.74686
749.6	747.15078	755.3	752.84679
749.7	747.25071	755.4	752.94672
749.8	747.35064	755.5	753.04665
749.9	747.45057	755.6	753.14658
750	747.5505	755.7	753.24651
750.1	747.65043	755.8	753.34644
750.2	747.75036	755.9	753.44637
750.3	747.85029	756	753.5463
750.4	747.95022	756.1	753.64623
750.5	748.05015	756.2	753.74616
750.6	748.15008	756.3	753.84609
750.7	748.25001	756.4	753.94602
750.8	748.34994	756.5	754.04595
750.9	748.44987	756.6	754.14588
751	748.5498	756.7	754.24581
751.1	748.64973	756.8	754.34574
751.2	748.74966	756.9	754.44567
751.3	748.84959	757	754.5456
751.4	748.94952	757.1	754.64553
751.5	749.04945	757.2	754.74546
751.6	749.14938	757.3	754.84539
751.7	749.24931	757.4	754.94532
751.8	749.34924	757.5	755.04525
751.9	749.44917	757.6	755.14518
752	749.5491	757.7	755.24511
752.1	749.64903	757.8	755.34504
752.2	749.74896	757.9	755.44497
752.3	749.84889	758	755.5449
752.4	749.94882	758.1	755.64483
752.5	750.04875	758.2	755.74476
752.6	750.14868	758.3	755.84469
752.7	750.24861	758.4	755.94462
752.8	750.34854	758.5	756.04455
752.9	750.44847	758.6	756.14448
753	750.5484	758.7	756.24441
753.1	750.64833	758.8	756.34434
753.2	750.74826	758.9	756.44427
753.3	750.84819	759	756.5442
753.4	750.94812	759.1	756.64413
753.5	751.04805	759.2	756.74406
753.6	751.14798	759.3	756.84399
753.7	751.24791	759.4	756.94392
753.8	751.34784	759.5	757.04385
753.9	751.44777	759.6	757.14378
754	751.5477	759.7	757.24371
754.1	751.64763	759.8	757.34364

759.9	757.44357	765.6	763.13958
760	757.5435	765.7	763.23951
760.1	757.64343	765.8	763.33944
760.2	757.74336	765.9	763.43937
760.3	757.84329	766	763.5393
760.4	757.94322	766.1	763.63923
760.5	758.04315	766.2	763.73916
760.6	758.14308	766.3	763.83909
760.7	758.24301	766.4	763.93902
760.8	758.34294	766.5	764.03895
760.9	758.44287	766.6	764.13888
761	758.5428	766.7	764.23881
761.1	758.64273	766.8	764.33874
761.2	758.74266	766.9	764.43867
761.3	758.84259	767	764.5386
761.4	758.94252	767.1	764.63853
761.5	759.04245	767.2	764.73846
761.6	759.14238	767.3	764.83839
761.7	759.24231	767.4	764.93832
761.8	759.34224	767.5	765.03825
761.9	759.44217	767.6	765.13818
762	759.5421	767.7	765.23811
762.1	759.64203	767.8	765.33804
762.2	759.74196	767.9	765.43797
762.3	759.84189	768	765.5379
762.4	759.94182	768.1	765.63783
762.5	760.04175	768.2	765.73776
762.6	760.14168	768.3	765.83769
762.7	760.24161	768.4	765.93762
762.8	760.34154	768.5	766.03755
762.9	760.44147	768.6	766.13748
763	760.5414	768.7	766.23741
763.1	760.64133	768.8	766.33734
763.2	760.74126	768.9	766.43727
763.3	760.84119	769	766.5372
763.4	760.94112	769.1	766.63713
763.5	761.04105	769.2	766.73706
763.6	761.14098	769.3	766.83699
763.7	761.24091	769.4	766.93692
763.8	761.34084	769.5	767.03685
763.9	761.44077	769.6	767.13678
764	761.5407	769.7	767.23671
764.1	761.64063	769.8	767.33664
764.2	761.74056	769.9	767.43657
764.3	761.84049	770	767.5365
764.4	761.94042	770.1	767.63643
764.5	762.04035	770.2	767.73636
764.6	762.14028	770.3	767.83629
764.7	762.24021	770.4	767.93622
764.8	762.34014	770.5	768.03615
764.9	762.44007	770.6	768.13608
765	762.54	770.7	768.23601
765.1	762.63993	770.8	768.33594
765.2	762.73986	770.9	768.43587
765.3	762.83979	771	768.5358
765.4	762.93972	771.1	768.63573
765.5	763.03965	771.2	768.73566

771.3	768.83559	777	774.5316
771.4	768.93552	777.1	774.63153
771.5	769.03545	777.2	774.73146
771.6	769.13538	777.3	774.83139
771.7	769.23531	777.4	774.93132
771.8	769.33524	777.5	775.03125
771.9	769.43517	777.6	775.13118
772	769.5351	777.7	775.23111
772.1	769.63503	777.8	775.33104
772.2	769.73496	777.9	775.43097
772.3	769.83489	778	775.5309
772.4	769.93482	778.1	775.63083
772.5	770.03475	778.2	775.73076
772.6	770.13468	778.3	775.83069
772.7	770.23461	778.4	775.93062
772.8	770.33454	778.5	776.03055
772.9	770.43447	778.6	776.13048
773	770.5344	778.7	776.23041
773.1	770.63433	778.8	776.33034
773.2	770.73426	778.9	776.43027
773.3	770.83419	779	776.5302
773.4	770.93412	779.1	776.63013
773.5	771.03405	779.2	776.73006
773.6	771.13398	779.3	776.82999
773.7	771.23391	779.4	776.92992
773.8	771.33384	779.5	777.02985
773.9	771.43377	779.6	777.12978
774	771.5337	779.7	777.22971
774.1	771.63363	779.8	777.32964
774.2	771.73356	779.9	777.42957
774.3	771.83349	780	777.5295
774.4	771.93342	780.1	777.62943
774.5	772.03335	780.2	777.72936
774.6	772.13328	780.3	777.82929
774.7	772.23321	780.4	777.92922
774.8	772.33314	780.5	778.02915
774.9	772.43307	780.6	778.12908
775	772.533	780.7	778.22901
775.1	772.63293	780.8	778.32894
775.2	772.73286	780.9	778.42887
775.3	772.83279	781	778.5288
775.4	772.93272	781.1	778.62873
775.5	773.03265	781.2	778.72866
775.6	773.13258	781.3	778.82859
775.7	773.23251	781.4	778.92852
775.8	773.33244	781.5	779.02845
775.9	773.43237	781.6	779.12838
776	773.5323	781.7	779.22831
776.1	773.63223	781.8	779.32824
776.2	773.73216	781.9	779.42817
776.3	773.83209	782	779.5281
776.4	773.93202	782.1	779.62803
776.5	774.03195	782.2	779.72796
776.6	774.13188	782.3	779.82789
776.7	774.23181	782.4	779.92782
776.8	774.33174	782.5	780.02775
776.9	774.43167	782.6	780.12768

782.7	780.22761	788.4	785.92362
782.8	780.32754	788.5	786.02355
782.9	780.42747	788.6	786.12348
783	780.5274	788.7	786.22341
783.1	780.62733	788.8	786.32334
783.2	780.72726	788.9	786.42327
783.3	780.82719	789	786.5232
783.4	780.92712	789.1	786.62313
783.5	781.02705	789.2	786.72306
783.6	781.12698	789.3	786.82299
783.7	781.22691	789.4	786.92292
783.8	781.32684	789.5	787.02285
783.9	781.42677	789.6	787.12278
784	781.5267	789.7	787.22271
784.1	781.62663	789.8	787.32264
784.2	781.72656	789.9	787.42257
784.3	781.82649	790	787.5225
784.4	781.92642	790.1	787.62243
784.5	782.02635	790.2	787.72236
784.6	782.12628	790.3	787.82229
784.7	782.22621	790.4	787.92222
784.8	782.32614	790.5	788.02215
784.9	782.42607	790.6	788.12208
785	782.526	790.7	788.22201
785.1	782.62593	790.8	788.32194
785.2	782.72586	790.9	788.42187
785.3	782.82579	791	788.5218
785.4	782.92572	791.1	788.62173
785.5	783.02565	791.2	788.72166
785.6	783.12558	791.3	788.82159
785.7	783.22551	791.4	788.92152
785.8	783.32544	791.5	789.02145
785.9	783.42537	791.6	789.12138
786	783.5253	791.7	789.22131
786.1	783.62523	791.8	789.32124
786.2	783.72516	791.9	789.42117
786.3	783.82509	792	789.5211
786.4	783.92502	792.1	789.62103
786.5	784.02495	792.2	789.72096
786.6	784.12488	792.3	789.82089
786.7	784.22481	792.4	789.92082
786.8	784.32474	792.5	790.02075
786.9	784.42467	792.6	790.12068
787	784.5246	792.7	790.22061
787.1	784.62453	792.8	790.32054
787.2	784.72446	792.9	790.42047
787.3	784.82439	793	790.5204
787.4	784.92432	793.1	790.62033
787.5	785.02425	793.2	790.72026
787.6	785.12418	793.3	790.82019
787.7	785.22411	793.4	790.92012
787.8	785.32404	793.5	791.02005
787.9	785.42397	793.6	791.11998
788	785.5239	793.7	791.21991
788.1	785.62383	793.8	791.31984
788.2	785.72376	793.9	791.41977
788.3	785.82369	794	791.5197

794.1	791.61963	799.8	797.31564
794.2	791.71956	799.9	797.41557
794.3	791.81949	800	797.5155
794.4	791.91942	800.1	797.61543
794.5	792.01935	800.2	797.71536
794.6	792.11928	800.3	797.81529
794.7	792.21921	800.4	797.91522
794.8	792.31914	800.5	798.01515
794.9	792.41907	800.6	798.11508
795	792.519	800.7	798.21501
795.1	792.61893	800.8	798.31494
795.2	792.71886	800.9	798.41487
795.3	792.81879	801	798.5148
795.4	792.91872	801.1	798.61473
795.5	793.01865	801.2	798.71466
795.6	793.11858	801.3	798.81459
795.7	793.21851	801.4	798.91452
795.8	793.31844	801.5	799.01445
795.9	793.41837	801.6	799.11438
796	793.5183	801.7	799.21431
796.1	793.61823	801.8	799.31424
796.2	793.71816	801.9	799.41417
796.3	793.81809	802	799.5141
796.4	793.91802	802.1	799.61403
796.5	794.01795	802.2	799.71396
796.6	794.11788	802.3	799.81389
796.7	794.21781	802.4	799.91382
796.8	794.31774	802.5	800.01375
796.9	794.41767	802.6	800.11368
797	794.5176	802.7	800.21361
797.1	794.61753	802.8	800.31354
797.2	794.71746	802.9	800.41347
797.3	794.81739	803	800.5134
797.4	794.91732	803.1	800.61333
797.5	795.01725	803.2	800.71326
797.6	795.11718	803.3	800.81319
797.7	795.21711	803.4	800.91312
797.8	795.31704	803.5	801.01305
797.9	795.41697	803.6	801.11298
798	795.5169	803.7	801.21291
798.1	795.61683	803.8	801.31284
798.2	795.71676	803.9	801.41277
798.3	795.81669	804	801.5127
798.4	795.91662	804.1	801.61263
798.5	796.01655	804.2	801.71256
798.6	796.11648	804.3	801.81249
798.7	796.21641	804.4	801.91242
798.8	796.31634	804.5	802.01235
798.9	796.41627	804.6	802.11228
799	796.5162	804.7	802.21221
799.1	796.61613	804.8	802.31214
799.2	796.71606	804.9	802.41207
799.3	796.81599	805	802.512
799.4	796.91592	805.1	802.61193
799.5	797.01585	805.2	802.71186
799.6	797.11578	805.3	802.81179
799.7	797.21571	805.4	802.91172

805.5	803.01165	811.2	808.70766
805.6	803.11158	811.3	808.80759
805.7	803.21151	811.4	808.90752
805.8	803.31144	811.5	809.00745
805.9	803.41137	811.6	809.10738
806	803.5113	811.7	809.20731
806.1	803.61123	811.8	809.30724
806.2	803.71116	811.9	809.40717
806.3	803.81109	812	809.5071
806.4	803.91102	812.1	809.60703
806.5	804.01095	812.2	809.70696
806.6	804.11088	812.3	809.80689
806.7	804.21081	812.4	809.90682
806.8	804.31074	812.5	810.00675
806.9	804.41067	812.6	810.10668
807	804.5106	812.7	810.20661
807.1	804.61053	812.8	810.30654
807.2	804.71046	812.9	810.40647
807.3	804.81039	813	810.5064
807.4	804.91032	813.1	810.60633
807.5	805.01025	813.2	810.70626
807.6	805.11018	813.3	810.80619
807.7	805.21011	813.4	810.90612
807.8	805.31004	813.5	811.00605
807.9	805.40997	813.6	811.10598
808	805.5099	813.7	811.20591
808.1	805.60983	813.8	811.30584
808.2	805.70976	813.9	811.40577
808.3	805.80969	814	811.5057
808.4	805.90962	814.1	811.60563
808.5	806.00955	814.2	811.70556
808.6	806.10948	814.3	811.80549
808.7	806.20941	814.4	811.90542
808.8	806.30934	814.5	812.00535
808.9	806.40927	814.6	812.10528
809	806.5092	814.7	812.20521
809.1	806.60913	814.8	812.30514
809.2	806.70906	814.9	812.40507
809.3	806.80899	815	812.505
809.4	806.90892	815.1	812.60493
809.5	807.00885	815.2	812.70486
809.6	807.10878	815.3	812.80479
809.7	807.20871	815.4	812.90472
809.8	807.30864	815.5	813.00465
809.9	807.40857	815.6	813.10458
810	807.5085	815.7	813.20451
810.1	807.60843	815.8	813.30444
810.2	807.70836	815.9	813.40437
810.3	807.80829	816	813.5043
810.4	807.90822	816.1	813.60423
810.5	808.00815	816.2	813.70416
810.6	808.10808	816.3	813.80409
810.7	808.20801	816.4	813.90402
810.8	808.30794	816.5	814.00395
810.9	808.40787	816.6	814.10388
811	808.5078	816.7	814.20381
811.1	808.60773	816.8	814.30374

816.9	814.40367	822.6	820.09968
817	814.5036	822.7	820.19961
817.1	814.60353	822.8	820.29954
817.2	814.70346	822.9	820.39947
817.3	814.80339	823	820.4994
817.4	814.90332	823.1	820.59933
817.5	815.00325	823.2	820.69926
817.6	815.10318	823.3	820.79919
817.7	815.20311	823.4	820.89912
817.8	815.30304	823.5	820.99905
817.9	815.40297	823.6	821.09898
818	815.5029	823.7	821.19891
818.1	815.60283	823.8	821.29884
818.2	815.70276	823.9	821.39877
818.3	815.80269	824	821.4987
818.4	815.90262	824.1	821.59863
818.5	816.00255	824.2	821.69856
818.6	816.10248	824.3	821.79849
818.7	816.20241	824.4	821.89842
818.8	816.30234	824.5	821.99835
818.9	816.40227	824.6	822.09828
819	816.5022	824.7	822.19821
819.1	816.60213	824.8	822.29814
819.2	816.70206	824.9	822.39807
819.3	816.80199	825	822.498
819.4	816.90192	825.1	822.59793
819.5	817.00185	825.2	822.69786
819.6	817.10178	825.3	822.79779
819.7	817.20171	825.4	822.89772
819.8	817.30164	825.5	822.99765
819.9	817.40157	825.6	823.09758
820	817.5015	825.7	823.19751
820.1	817.60143	825.8	823.29744
820.2	817.70136	825.9	823.39737
820.3	817.80129	826	823.4973
820.4	817.90122	826.1	823.59723
820.5	818.00115	826.2	823.69716
820.6	818.10108	826.3	823.79709
820.7	818.20101	826.4	823.89702
820.8	818.30094	826.5	823.99695
820.9	818.40087	826.6	824.09688
821	818.5008	826.7	824.19681
821.1	818.60073	826.8	824.29674
821.2	818.70066	826.9	824.39667
821.3	818.80059	827	824.4966
821.4	818.90052	827.1	824.59653
821.5	819.00045	827.2	824.69646
821.6	819.10038	827.3	824.79639
821.7	819.20031	827.4	824.89632
821.8	819.30024	827.5	824.99625
821.9	819.40017	827.6	825.09618
822	819.5001	827.7	825.19611
822.1	819.60003	827.8	825.29604
822.2	819.69996	827.9	825.39597
822.3	819.79989	828	825.4959
822.4	819.89982	828.1	825.59583
822.5	819.99975	828.2	825.69576

828.3	825.79569	834	831.4917
828.4	825.89562	834.1	831.59163
828.5	825.99555	834.2	831.69156
828.6	826.09548	834.3	831.79149
828.7	826.19541	834.4	831.89142
828.8	826.29534	834.5	831.99135
828.9	826.39527	834.6	832.09128
829	826.4952	834.7	832.19121
829.1	826.59513	834.8	832.29114
829.2	826.69506	834.9	832.39107
829.3	826.79499	835	832.491
829.4	826.89492	835.1	832.59093
829.5	826.99485	835.2	832.69086
829.6	827.09478	835.3	832.79079
829.7	827.19471	835.4	832.89072
829.8	827.29464	835.5	832.99065
829.9	827.39457	835.6	833.09058
830	827.4945	835.7	833.19051
830.1	827.59443	835.8	833.29044
830.2	827.69436	835.9	833.39037
830.3	827.79429	836	833.4903
830.4	827.89422	836.1	833.59023
830.5	827.99415	836.2	833.69016
830.6	828.09408	836.3	833.79009
830.7	828.19401	836.4	833.89002
830.8	828.29394	836.5	833.98995
830.9	828.39387	836.6	834.08988
831	828.4938	836.7	834.18981
831.1	828.59373	836.8	834.28974
831.2	828.69366	836.9	834.38967
831.3	828.79359	837	834.4896
831.4	828.89352	837.1	834.58953
831.5	828.99345	837.2	834.68946
831.6	829.09338	837.3	834.78939
831.7	829.19331	837.4	834.88932
831.8	829.29324	837.5	834.98925
831.9	829.39317	837.6	835.08918
832	829.4931	837.7	835.18911
832.1	829.59303	837.8	835.28904
832.2	829.69296	837.9	835.38897
832.3	829.79289	838	835.4889
832.4	829.89282	838.1	835.58883
832.5	829.99275	838.2	835.68876
832.6	830.09268	838.3	835.78869
832.7	830.19261	838.4	835.88862
832.8	830.29254	838.5	835.98855
832.9	830.39247	838.6	836.08848
833	830.4924	838.7	836.18841
833.1	830.59233	838.8	836.28834
833.2	830.69226	838.9	836.38827
833.3	830.79219	839	836.4882
833.4	830.89212	839.1	836.58813
833.5	830.99205	839.2	836.68806
833.6	831.09198	839.3	836.78799
833.7	831.19191	839.4	836.88792
833.8	831.29184	839.5	836.98785
833.9	831.39177	839.6	837.08778

839.7	837.18771	845.4	842.88372
839.8	837.28764	845.5	842.98365
839.9	837.38757	845.6	843.08358
840	837.4875	845.7	843.18351
840.1	837.58743	845.8	843.28344
840.2	837.68736	845.9	843.38337
840.3	837.78729	846	843.4833
840.4	837.88722	846.1	843.58323
840.5	837.98715	846.2	843.68316
840.6	838.08708	846.3	843.78309
840.7	838.18701	846.4	843.88302
840.8	838.28694	846.5	843.98295
840.9	838.38687	846.6	844.08288
841	838.4868	846.7	844.18281
841.1	838.58673	846.8	844.28274
841.2	838.68666	846.9	844.38267
841.3	838.78659	847	844.4826
841.4	838.88652	847.1	844.58253
841.5	838.98645	847.2	844.68246
841.6	839.08638	847.3	844.78239
841.7	839.18631	847.4	844.88232
841.8	839.28624	847.5	844.98225
841.9	839.38617	847.6	845.08218
842	839.4861	847.7	845.18211
842.1	839.58603	847.8	845.28204
842.2	839.68596	847.9	845.38197
842.3	839.78589	848	845.4819
842.4	839.88582	848.1	845.58183
842.5	839.98575	848.2	845.68176
842.6	840.08568	848.3	845.78169
842.7	840.18561	848.4	845.88162
842.8	840.28554	848.5	845.98155
842.9	840.38547	848.6	846.08148
843	840.4854	848.7	846.18141
843.1	840.58533	848.8	846.28134
843.2	840.68526	848.9	846.38127
843.3	840.78519	849	846.4812
843.4	840.88512	849.1	846.58113
843.5	840.98505	849.2	846.68106
843.6	841.08498	849.3	846.78099
843.7	841.18491	849.4	846.88092
843.8	841.28484	849.5	846.98085
843.9	841.38477	849.6	847.08078
844	841.4847	849.7	847.18071
844.1	841.58463	849.8	847.28064
844.2	841.68456	849.9	847.38057
844.3	841.78449	850	847.4805
844.4	841.88442	850.1	847.58043
844.5	841.98435	850.2	847.68036
844.6	842.08428	850.3	847.78029
844.7	842.18421	850.4	847.88022
844.8	842.28414	850.5	847.98015
844.9	842.38407	850.6	848.08008
845	842.484	850.7	848.18001
845.1	842.58393	850.8	848.27994
845.2	842.68386	850.9	848.37987
845.3	842.78379	851	848.4798

851.1	848.57973	856.8	854.27574
851.2	848.67966	856.9	854.37567
851.3	848.77959	857	854.4756
851.4	848.87952	857.1	854.57553
851.5	848.97945	857.2	854.67546
851.6	849.07938	857.3	854.77539
851.7	849.17931	857.4	854.87532
851.8	849.27924	857.5	854.97525
851.9	849.37917	857.6	855.07518
852	849.4791	857.7	855.17511
852.1	849.57903	857.8	855.27504
852.2	849.67896	857.9	855.37497
852.3	849.77889	858	855.4749
852.4	849.87882	858.1	855.57483
852.5	849.97875	858.2	855.67476
852.6	850.07868	858.3	855.77469
852.7	850.17861	858.4	855.87462
852.8	850.27854	858.5	855.97455
852.9	850.37847	858.6	856.07448
853	850.4784	858.7	856.17441
853.1	850.57833	858.8	856.27434
853.2	850.67826	858.9	856.37427
853.3	850.77819	859	856.4742
853.4	850.87812	859.1	856.57413
853.5	850.97805	859.2	856.67406
853.6	851.07798	859.3	856.77399
853.7	851.17791	859.4	856.87392
853.8	851.27784	859.5	856.97385
853.9	851.37777	859.6	857.07378
854	851.4777	859.7	857.17371
854.1	851.57763	859.8	857.27364
854.2	851.67756	859.9	857.37357
854.3	851.77749	860	857.4735
854.4	851.87742	860.1	857.57343
854.5	851.97735	860.2	857.67336
854.6	852.07728	860.3	857.77329
854.7	852.17721	860.4	857.87322
854.8	852.27714	860.5	857.97315
854.9	852.37707	860.6	858.07308
855	852.477	860.7	858.17301
855.1	852.57693	860.8	858.27294
855.2	852.67686	860.9	858.37287
855.3	852.77679	861	858.4728
855.4	852.87672	861.1	858.57273
855.5	852.97665	861.2	858.67266
855.6	853.07658	861.3	858.77259
855.7	853.17651	861.4	858.87252
855.8	853.27644	861.5	858.97245
855.9	853.37637	861.6	859.07238
856	853.4763	861.7	859.17231
856.1	853.57623	861.8	859.27224
856.2	853.67616	861.9	859.37217
856.3	853.77609	862	859.4721
856.4	853.87602	862.1	859.57203
856.5	853.97595	862.2	859.67196
856.6	854.07588	862.3	859.77189
856.7	854.17581	862.4	859.87182

862.5	859.97175	868.2	865.66776
862.6	860.07168	868.3	865.76769
862.7	860.17161	868.4	865.86762
862.8	860.27154	868.5	865.96755
862.9	860.37147	868.6	866.06748
863	860.4714	868.7	866.16741
863.1	860.57133	868.8	866.26734
863.2	860.67126	868.9	866.36727
863.3	860.77119	869	866.4672
863.4	860.87112	869.1	866.56713
863.5	860.97105	869.2	866.66706
863.6	861.07098	869.3	866.76699
863.7	861.17091	869.4	866.86692
863.8	861.27084	869.5	866.96685
863.9	861.37077	869.6	867.06678
864	861.4707	869.7	867.16671
864.1	861.57063	869.8	867.26664
864.2	861.67056	869.9	867.36657
864.3	861.77049	870	867.4665
864.4	861.87042	870.1	867.56643
864.5	861.97035	870.2	867.66636
864.6	862.07028	870.3	867.76629
864.7	862.17021	870.4	867.86622
864.8	862.27014	870.5	867.96615
864.9	862.37007	870.6	868.06608
865	862.47	870.7	868.16601
865.1	862.56993	870.8	868.26594
865.2	862.66986	870.9	868.36587
865.3	862.76979	871	868.4658
865.4	862.86972	871.1	868.56573
865.5	862.96965	871.2	868.66566
865.6	863.06958	871.3	868.76559
865.7	863.16951	871.4	868.86552
865.8	863.26944	871.5	868.96545
865.9	863.36937	871.6	869.06538
866	863.4693	871.7	869.16531
866.1	863.56923	871.8	869.26524
866.2	863.66916	871.9	869.36517
866.3	863.76909	872	869.4651
866.4	863.86902	872.1	869.56503
866.5	863.96895	872.2	869.66496
866.6	864.06888	872.3	869.76489
866.7	864.16881	872.4	869.86482
866.8	864.26874	872.5	869.96475
866.9	864.36867	872.6	870.06468
867	864.4686	872.7	870.16461
867.1	864.56853	872.8	870.26454
867.2	864.66846	872.9	870.36447
867.3	864.76839	873	870.4644
867.4	864.86832	873.1	870.56433
867.5	864.96825	873.2	870.66426
867.6	865.06818	873.3	870.76419
867.7	865.16811	873.4	870.86412
867.8	865.26804	873.5	870.96405
867.9	865.36797	873.6	871.06398
868	865.4679	873.7	871.16391
868.1	865.56783	873.8	871.26384

873.9	871.36377	879.6	877.05978
874	871.4637	879.7	877.15971
874.1	871.56363	879.8	877.25964
874.2	871.66356	879.9	877.35957
874.3	871.76349	880	877.4595
874.4	871.86342	880.1	877.55943
874.5	871.96335	880.2	877.65936
874.6	872.06328	880.3	877.75929
874.7	872.16321	880.4	877.85922
874.8	872.26314	880.5	877.95915
874.9	872.36307	880.6	878.05908
875	872.463	880.7	878.15901
875.1	872.56293	880.8	878.25894
875.2	872.66286	880.9	878.35887
875.3	872.76279	881	878.4588
875.4	872.86272	881.1	878.55873
875.5	872.96265	881.2	878.65866
875.6	873.06258	881.3	878.75859
875.7	873.16251	881.4	878.85852
875.8	873.26244	881.5	878.95845
875.9	873.36237	881.6	879.05838
876	873.4623	881.7	879.15831
876.1	873.56223	881.8	879.25824
876.2	873.66216	881.9	879.35817
876.3	873.76209	882	879.4581
876.4	873.86202	882.1	879.55803
876.5	873.96195	882.2	879.65796
876.6	874.06188	882.3	879.75789
876.7	874.16181	882.4	879.85782
876.8	874.26174	882.5	879.95775
876.9	874.36167	882.6	880.05768
877	874.4616	882.7	880.15761
877.1	874.56153	882.8	880.25754
877.2	874.66146	882.9	880.35747
877.3	874.76139	883	880.4574
877.4	874.86132	883.1	880.55733
877.5	874.96125	883.2	880.65726
877.6	875.06118	883.3	880.75719
877.7	875.16111	883.4	880.85712
877.8	875.26104	883.5	880.95705
877.9	875.36097	883.6	881.05698
878	875.4609	883.7	881.15691
878.1	875.56083	883.8	881.25684
878.2	875.66076	883.9	881.35677
878.3	875.76069	884	881.4567
878.4	875.86062	884.1	881.55663
878.5	875.96055	884.2	881.65656
878.6	876.06048	884.3	881.75649
878.7	876.16041	884.4	881.85642
878.8	876.26034	884.5	881.95635
878.9	876.36027	884.6	882.05628
879	876.4602	884.7	882.15621
879.1	876.56013	884.8	882.25614
879.2	876.66006	884.9	882.35607
879.3	876.75999	885	882.456
879.4	876.85992	885.1	882.55593
879.5	876.95985	885.2	882.65586

885.3	882.75579	891	888.4518
885.4	882.85572	891.1	888.55173
885.5	882.95565	891.2	888.65166
885.6	883.05558	891.3	888.75159
885.7	883.15551	891.4	888.85152
885.8	883.25544	891.5	888.95145
885.9	883.35537	891.6	889.05138
886	883.4553	891.7	889.15131
886.1	883.55523	891.8	889.25124
886.2	883.65516	891.9	889.35117
886.3	883.75509	892	889.4511
886.4	883.85502	892.1	889.55103
886.5	883.95495	892.2	889.65096
886.6	884.05488	892.3	889.75089
886.7	884.15481	892.4	889.85082
886.8	884.25474	892.5	889.95075
886.9	884.35467	892.6	890.05068
887	884.4546	892.7	890.15061
887.1	884.55453	892.8	890.25054
887.2	884.65446	892.9	890.35047
887.3	884.75439	893	890.4504
887.4	884.85432	893.1	890.55033
887.5	884.95425	893.2	890.65026
887.6	885.05418	893.3	890.75019
887.7	885.15411	893.4	890.85012
887.8	885.25404	893.5	890.95005
887.9	885.35397	893.6	891.04998
888	885.4539	893.7	891.14991
888.1	885.55383	893.8	891.24984
888.2	885.65376	893.9	891.34977
888.3	885.75369	894	891.4497
888.4	885.85362	894.1	891.54963
888.5	885.95355	894.2	891.64956
888.6	886.05348	894.3	891.74949
888.7	886.15341	894.4	891.84942
888.8	886.25334	894.5	891.94935
888.9	886.35327	894.6	892.04928
889	886.4532	894.7	892.14921
889.1	886.55313	894.8	892.24914
889.2	886.65306	894.9	892.34907
889.3	886.75299	895	892.449
889.4	886.85292	895.1	892.54893
889.5	886.95285	895.2	892.64886
889.6	887.05278	895.3	892.74879
889.7	887.15271	895.4	892.84872
889.8	887.25264	895.5	892.94865
889.9	887.35257	895.6	893.04858
890	887.4525	895.7	893.14851
890.1	887.55243	895.8	893.24844
890.2	887.65236	895.9	893.34837
890.3	887.75229	896	893.4483
890.4	887.85222	896.1	893.54823
890.5	887.95215	896.2	893.64816
890.6	888.05208	896.3	893.74809
890.7	888.15201	896.4	893.84802
890.8	888.25194	896.5	893.94795
890.9	888.35187	896.6	894.04788

896.7	894.14781	902.4	899.84382
896.8	894.24774	902.5	899.94375
896.9	894.34767	902.6	900.04368
897	894.4476	902.7	900.14361
897.1	894.54753	902.8	900.24354
897.2	894.64746	902.9	900.34347
897.3	894.74739	903	900.4434
897.4	894.84732	903.1	900.54333
897.5	894.94725	903.2	900.64326
897.6	895.04718	903.3	900.74319
897.7	895.14711	903.4	900.84312
897.8	895.24704	903.5	900.94305
897.9	895.34697	903.6	901.04298
898	895.4469	903.7	901.14291
898.1	895.54683	903.8	901.24284
898.2	895.64676	903.9	901.34277
898.3	895.74669	904	901.4427
898.4	895.84662	904.1	901.54263
898.5	895.94655	904.2	901.64256
898.6	896.04648	904.3	901.74249
898.7	896.14641	904.4	901.84242
898.8	896.24634	904.5	901.94235
898.9	896.34627	904.6	902.04228
899	896.4462	904.7	902.14221
899.1	896.54613	904.8	902.24214
899.2	896.64606	904.9	902.34207
899.3	896.74599	905	902.442
899.4	896.84592	905.1	902.54193
899.5	896.94585	905.2	902.64186
899.6	897.04578	905.3	902.74179
899.7	897.14571	905.4	902.84172
899.8	897.24564	905.5	902.94165
899.9	897.34557	905.6	903.04158
900	897.4455	905.7	903.14151
900.1	897.54543	905.8	903.24144
900.2	897.64536	905.9	903.34137
900.3	897.74529	906	903.4413
900.4	897.84522	906.1	903.54123
900.5	897.94515	906.2	903.64116
900.6	898.04508	906.3	903.74109
900.7	898.14501	906.4	903.84102
900.8	898.24494	906.5	903.94095
900.9	898.34487	906.6	904.04088
901	898.4448	906.7	904.14081
901.1	898.54473	906.8	904.24074
901.2	898.64466	906.9	904.34067
901.3	898.74459	907	904.4406
901.4	898.84452	907.1	904.54053
901.5	898.94445	907.2	904.64046
901.6	899.04438	907.3	904.74039
901.7	899.14431	907.4	904.84032
901.8	899.24424	907.5	904.94025
901.9	899.34417	907.6	905.04018
902	899.4441	907.7	905.14011
902.1	899.54403	907.8	905.24004
902.2	899.64396	907.9	905.33997
902.3	899.74389	908	905.4399

908.1	905.53983	913.8	911.23584
908.2	905.63976	913.9	911.33577
908.3	905.73969	914	911.4357
908.4	905.83962	914.1	911.53563
908.5	905.93955	914.2	911.63556
908.6	906.03948	914.3	911.73549
908.7	906.13941	914.4	911.83542
908.8	906.23934	914.5	911.93535
908.9	906.33927	914.6	912.03528
909	906.4392	914.7	912.13521
909.1	906.53913	914.8	912.23514
909.2	906.63906	914.9	912.33507
909.3	906.73899	915	912.435
909.4	906.83892	915.1	912.53493
909.5	906.93885	915.2	912.63486
909.6	907.03878	915.3	912.73479
909.7	907.13871	915.4	912.83472
909.8	907.23864	915.5	912.93465
909.9	907.33857	915.6	913.03458
910	907.4385	915.7	913.13451
910.1	907.53843	915.8	913.23444
910.2	907.63836	915.9	913.33437
910.3	907.73829	916	913.4343
910.4	907.83822	916.1	913.53423
910.5	907.93815	916.2	913.63416
910.6	908.03808	916.3	913.73409
910.7	908.13801	916.4	913.83402
910.8	908.23794	916.5	913.93395
910.9	908.33787	916.6	914.03388
911	908.4378	916.7	914.13381
911.1	908.53773	916.8	914.23374
911.2	908.63766	916.9	914.33367
911.3	908.73759	917	914.4336
911.4	908.83752	917.1	914.53353
911.5	908.93745	917.2	914.63346
911.6	909.03738	917.3	914.73339
911.7	909.13731	917.4	914.83332
911.8	909.23724	917.5	914.93325
911.9	909.33717	917.6	915.03318
912	909.4371	917.7	915.13311
912.1	909.53703	917.8	915.23304
912.2	909.63696	917.9	915.33297
912.3	909.73689	918	915.4329
912.4	909.83682	918.1	915.53283
912.5	909.93675	918.2	915.63276
912.6	910.03668	918.3	915.73269
912.7	910.13661	918.4	915.83262
912.8	910.23654	918.5	915.93255
912.9	910.33647	918.6	916.03248
913	910.4364	918.7	916.13241
913.1	910.53633	918.8	916.23234
913.2	910.63626	918.9	916.33227
913.3	910.73619	919	916.4322
913.4	910.83612	919.1	916.53213
913.5	910.93605	919.2	916.63206
913.6	911.03598	919.3	916.73199
913.7	911.13591	919.4	916.83192

919.5	916.93185	925.2	922.62786
919.6	917.03178	925.3	922.72779
919.7	917.13171	925.4	922.82772
919.8	917.23164	925.5	922.92765
919.9	917.33157	925.6	923.02758
920	917.4315	925.7	923.12751
920.1	917.53143	925.8	923.22744
920.2	917.63136	925.9	923.32737
920.3	917.73129	926	923.4273
920.4	917.83122	926.1	923.52723
920.5	917.93115	926.2	923.62716
920.6	918.03108	926.3	923.72709
920.7	918.13101	926.4	923.82702
920.8	918.23094	926.5	923.92695
920.9	918.33087	926.6	924.02688
921	918.4308	926.7	924.12681
921.1	918.53073	926.8	924.22674
921.2	918.63066	926.9	924.32667
921.3	918.73059	927	924.4266
921.4	918.83052	927.1	924.52653
921.5	918.93045	927.2	924.62646
921.6	919.03038	927.3	924.72639
921.7	919.13031	927.4	924.82632
921.8	919.23024	927.5	924.92625
921.9	919.33017	927.6	925.02618
922	919.4301	927.7	925.12611
922.1	919.53003	927.8	925.22604
922.2	919.62996	927.9	925.32597
922.3	919.72989	928	925.4259
922.4	919.82982	928.1	925.52583
922.5	919.92975	928.2	925.62576
922.6	920.02968	928.3	925.72569
922.7	920.12961	928.4	925.82562
922.8	920.22954	928.5	925.92555
922.9	920.32947	928.6	926.02548
923	920.4294	928.7	926.12541
923.1	920.52933	928.8	926.22534
923.2	920.62926	928.9	926.32527
923.3	920.72919	929	926.4252
923.4	920.82912	929.1	926.52513
923.5	920.92905	929.2	926.62506
923.6	921.02898	929.3	926.72499
923.7	921.12891	929.4	926.82492
923.8	921.22884	929.5	926.92485
923.9	921.32877	929.6	927.02478
924	921.4287	929.7	927.12471
924.1	921.52863	929.8	927.22464
924.2	921.62856	929.9	927.32457
924.3	921.72849	930	927.4245
924.4	921.82842	930.1	927.52443
924.5	921.92835	930.2	927.62436
924.6	922.02828	930.3	927.72429
924.7	922.12821	930.4	927.82422
924.8	922.22814	930.5	927.92415
924.9	922.32807	930.6	928.02408
925	922.428	930.7	928.12401
925.1	922.52793	930.8	928.22394

930.9	928.32387	936.6	934.01988
931	928.4238	936.7	934.11981
931.1	928.52373	936.8	934.21974
931.2	928.62366	936.9	934.31967
931.3	928.72359	937	934.4196
931.4	928.82352	937.1	934.51953
931.5	928.92345	937.2	934.61946
931.6	929.02338	937.3	934.71939
931.7	929.12331	937.4	934.81932
931.8	929.22324	937.5	934.91925
931.9	929.32317	937.6	935.01918
932	929.4231	937.7	935.11911
932.1	929.52303	937.8	935.21904
932.2	929.62296	937.9	935.31897
932.3	929.72289	938	935.4189
932.4	929.82282	938.1	935.51883
932.5	929.92275	938.2	935.61876
932.6	930.02268	938.3	935.71869
932.7	930.12261	938.4	935.81862
932.8	930.22254	938.5	935.91855
932.9	930.32247	938.6	936.01848
933	930.4224	938.7	936.11841
933.1	930.52233	938.8	936.21834
933.2	930.62226	938.9	936.31827
933.3	930.72219	939	936.4182
933.4	930.82212	939.1	936.51813
933.5	930.92205	939.2	936.61806
933.6	931.02198	939.3	936.71799
933.7	931.12191	939.4	936.81792
933.8	931.22184	939.5	936.91785
933.9	931.32177	939.6	937.01778
934	931.4217	939.7	937.11771
934.1	931.52163	939.8	937.21764
934.2	931.62156	939.9	937.31757
934.3	931.72149	940	937.4175
934.4	931.82142	940.1	937.51743
934.5	931.92135	940.2	937.61736
934.6	932.02128	940.3	937.71729
934.7	932.12121	940.4	937.81722
934.8	932.22114	940.5	937.91715
934.9	932.32107	940.6	938.01708
935	932.421	940.7	938.11701
935.1	932.52093	940.8	938.21694
935.2	932.62086	940.9	938.31687
935.3	932.72079	941	938.4168
935.4	932.82072	941.1	938.51673
935.5	932.92065	941.2	938.61666
935.6	933.02058	941.3	938.71659
935.7	933.12051	941.4	938.81652
935.8	933.22044	941.5	938.91645
935.9	933.32037	941.6	939.01638
936	933.4203	941.7	939.11631
936.1	933.52023	941.8	939.21624
936.2	933.62016	941.9	939.31617
936.3	933.72009	942	939.4161
936.4	933.82002	942.1	939.51603
936.5	933.91995	942.2	939.61596

942.3	939.71589	948	945.4119
942.4	939.81582	948.1	945.51183
942.5	939.91575	948.2	945.61176
942.6	940.01568	948.3	945.71169
942.7	940.11561	948.4	945.81162
942.8	940.21554	948.5	945.91155
942.9	940.31547	948.6	946.01148
943	940.4154	948.7	946.11141
943.1	940.51533	948.8	946.21134
943.2	940.61526	948.9	946.31127
943.3	940.71519	949	946.4112
943.4	940.81512	949.1	946.51113
943.5	940.91505	949.2	946.61106
943.6	941.01498	949.3	946.71099
943.7	941.11491	949.4	946.81092
943.8	941.21484	949.5	946.91085
943.9	941.31477	949.6	947.01078
944	941.4147	949.7	947.11071
944.1	941.51463	949.8	947.21064
944.2	941.61456	949.9	947.31057
944.3	941.71449	950	947.4105
944.4	941.81442	950.1	947.51043
944.5	941.91435	950.2	947.61036
944.6	942.01428	950.3	947.71029
944.7	942.11421	950.4	947.81022
944.8	942.21414	950.5	947.91015
944.9	942.31407	950.6	948.01008
945	942.414	950.7	948.11001
945.1	942.51393	950.8	948.20994
945.2	942.61386	950.9	948.30987
945.3	942.71379	951	948.4098
945.4	942.81372	951.1	948.50973
945.5	942.91365	951.2	948.60966
945.6	943.01358	951.3	948.70959
945.7	943.11351	951.4	948.80952
945.8	943.21344	951.5	948.90945
945.9	943.31337	951.6	949.00938
946	943.4133	951.7	949.10931
946.1	943.51323	951.8	949.20924
946.2	943.61316	951.9	949.30917
946.3	943.71309	952	949.4091
946.4	943.81302	952.1	949.50903
946.5	943.91295	952.2	949.60896
946.6	944.01288	952.3	949.70889
946.7	944.11281	952.4	949.80882
946.8	944.21274	952.5	949.90875
946.9	944.31267	952.6	950.00868
947	944.4126	952.7	950.10861
947.1	944.51253	952.8	950.20854
947.2	944.61246	952.9	950.30847
947.3	944.71239	953	950.4084
947.4	944.81232	953.1	950.50833
947.5	944.91225	953.2	950.60826
947.6	945.01218	953.3	950.70819
947.7	945.11211	953.4	950.80812
947.8	945.21204	953.5	950.90805
947.9	945.31197	953.6	951.00798

953.7	951.10791	959.4	956.80392
953.8	951.20784	959.5	956.90385
953.9	951.30777	959.6	957.00378
954	951.4077	959.7	957.10371
954.1	951.50763	959.8	957.20364
954.2	951.60756	959.9	957.30357
954.3	951.70749	960	957.4035
954.4	951.80742	960.1	957.50343
954.5	951.90735	960.2	957.60336
954.6	952.00728	960.3	957.70329
954.7	952.10721	960.4	957.80322
954.8	952.20714	960.5	957.90315
954.9	952.30707	960.6	958.00308
955	952.407	960.7	958.10301
955.1	952.50693	960.8	958.20294
955.2	952.60686	960.9	958.30287
955.3	952.70679	961	958.4028
955.4	952.80672	961.1	958.50273
955.5	952.90665	961.2	958.60266
955.6	953.00658	961.3	958.70259
955.7	953.10651	961.4	958.80252
955.8	953.20644	961.5	958.90245
955.9	953.30637	961.6	959.00238
956	953.4063	961.7	959.10231
956.1	953.50623	961.8	959.20224
956.2	953.60616	961.9	959.30217
956.3	953.70609	962	959.4021
956.4	953.80602	962.1	959.50203
956.5	953.90595	962.2	959.60196
956.6	954.00588	962.3	959.70189
956.7	954.10581	962.4	959.80182
956.8	954.20574	962.5	959.90175
956.9	954.30567	962.6	960.00168
957	954.4056	962.7	960.10161
957.1	954.50553	962.8	960.20154
957.2	954.60546	962.9	960.30147
957.3	954.70539	963	960.4014
957.4	954.80532	963.1	960.50133
957.5	954.90525	963.2	960.60126
957.6	955.00518	963.3	960.70119
957.7	955.10511	963.4	960.80112
957.8	955.20504	963.5	960.90105
957.9	955.30497	963.6	961.00098
958	955.4049	963.7	961.10091
958.1	955.50483	963.8	961.20084
958.2	955.60476	963.9	961.30077
958.3	955.70469	964	961.4007
958.4	955.80462	964.1	961.50063
958.5	955.90455	964.2	961.60056
958.6	956.00448	964.3	961.70049
958.7	956.10441	964.4	961.80042
958.8	956.20434	964.5	961.90035
958.9	956.30427	964.6	962.00028
959	956.4042	964.7	962.10021
959.1	956.50413	964.8	962.20014
959.2	956.60406	964.9	962.30007
959.3	956.70399	965	962.4

965.1	962.49993	970.8	968.19594
965.2	962.59986	970.9	968.29587
965.3	962.69979	971	968.3958
965.4	962.79972	971.1	968.49573
965.5	962.89965	971.2	968.59566
965.6	962.99958	971.3	968.69559
965.7	963.09951	971.4	968.79552
965.8	963.19944	971.5	968.89545
965.9	963.29937	971.6	968.99538
966	963.3993	971.7	969.09531
966.1	963.49923	971.8	969.19524
966.2	963.59916	971.9	969.29517
966.3	963.69909	972	969.3951
966.4	963.79902	972.1	969.49503
966.5	963.89895	972.2	969.59496
966.6	963.99888	972.3	969.69489
966.7	964.09881	972.4	969.79482
966.8	964.19874	972.5	969.89475
966.9	964.29867	972.6	969.99468
967	964.3986	972.7	970.09461
967.1	964.49853	972.8	970.19454
967.2	964.59846	972.9	970.29447
967.3	964.69839	973	970.3944
967.4	964.79832	973.1	970.49433
967.5	964.89825	973.2	970.59426
967.6	964.99818	973.3	970.69419
967.7	965.09811	973.4	970.79412
967.8	965.19804	973.5	970.89405
967.9	965.29797	973.6	970.99398
968	965.3979	973.7	971.09391
968.1	965.49783	973.8	971.19384
968.2	965.59776	973.9	971.29377
968.3	965.69769	974	971.3937
968.4	965.79762	974.1	971.49363
968.5	965.89755	974.2	971.59356
968.6	965.99748	974.3	971.69349
968.7	966.09741	974.4	971.79342
968.8	966.19734	974.5	971.89335
968.9	966.29727	974.6	971.99328
969	966.3972	974.7	972.09321
969.1	966.49713	974.8	972.19314
969.2	966.59706	974.9	972.29307
969.3	966.69699	975	972.393
969.4	966.79692	975.1	972.49293
969.5	966.89685	975.2	972.59286
969.6	966.99678	975.3	972.69279
969.7	967.09671	975.4	972.79272
969.8	967.19664	975.5	972.89265
969.9	967.29657	975.6	972.99258
970	967.3965	975.7	973.09251
970.1	967.49643	975.8	973.19244
970.2	967.59636	975.9	973.29237
970.3	967.69629	976	973.3923
970.4	967.79622	976.1	973.49223
970.5	967.89615	976.2	973.59216
970.6	967.99608	976.3	973.69209
970.7	968.09601	976.4	973.79202

976.5	973.89195	982.2	979.58796
976.6	973.99188	982.3	979.68789
976.7	974.09181	982.4	979.78782
976.8	974.19174	982.5	979.88775
976.9	974.29167	982.6	979.98768
977	974.3916	982.7	980.08761
977.1	974.49153	982.8	980.18754
977.2	974.59146	982.9	980.28747
977.3	974.69139	983	980.3874
977.4	974.79132	983.1	980.48733
977.5	974.89125	983.2	980.58726
977.6	974.99118	983.3	980.68719
977.7	975.09111	983.4	980.78712
977.8	975.19104	983.5	980.88705
977.9	975.29097	983.6	980.98698
978	975.3909	983.7	981.08691
978.1	975.49083	983.8	981.18684
978.2	975.59076	983.9	981.28677
978.3	975.69069	984	981.3867
978.4	975.79062	984.1	981.48663
978.5	975.89055	984.2	981.58656
978.6	975.99048	984.3	981.68649
978.7	976.09041	984.4	981.78642
978.8	976.19034	984.5	981.88635
978.9	976.29027	984.6	981.98628
979	976.3902	984.7	982.08621
979.1	976.49013	984.8	982.18614
979.2	976.59006	984.9	982.28607
979.3	976.68999	985	982.386
979.4	976.78992	985.1	982.48593
979.5	976.88985	985.2	982.58586
979.6	976.98978	985.3	982.68579
979.7	977.08971	985.4	982.78572
979.8	977.18964	985.5	982.88565
979.9	977.28957	985.6	982.98558
980	977.3895	985.7	983.08551
980.1	977.48943	985.8	983.18544
980.2	977.58936	985.9	983.28537
980.3	977.68929	986	983.3853
980.4	977.78922	986.1	983.48523
980.5	977.88915	986.2	983.58516
980.6	977.98908	986.3	983.68509
980.7	978.08901	986.4	983.78502
980.8	978.18894	986.5	983.88495
980.9	978.28887	986.6	983.98488
981	978.3888	986.7	984.08481
981.1	978.48873	986.8	984.18474
981.2	978.58866	986.9	984.28467
981.3	978.68859	987	984.3846
981.4	978.78852	987.1	984.48453
981.5	978.88845	987.2	984.58446
981.6	978.98838	987.3	984.68439
981.7	979.08831	987.4	984.78432
981.8	979.18824	987.5	984.88425
981.9	979.28817	987.6	984.98418
982	979.3881	987.7	985.08411
982.1	979.48803	987.8	985.18404

987.9	985.28397	993.6	990.97998
988	985.3839	993.7	991.07991
988.1	985.48383	993.8	991.17984
988.2	985.58376	993.9	991.27977
988.3	985.68369	994	991.3797
988.4	985.78362	994.1	991.47963
988.5	985.88355	994.2	991.57956
988.6	985.98348	994.3	991.67949
988.7	986.08341	994.4	991.77942
988.8	986.18334	994.5	991.87935
988.9	986.28327	994.6	991.97928
989	986.3832	994.7	992.07921
989.1	986.48313	994.8	992.17914
989.2	986.58306	994.9	992.27907
989.3	986.68299	995	992.379
989.4	986.78292	995.1	992.47893
989.5	986.88285	995.2	992.57886
989.6	986.98278	995.3	992.67879
989.7	987.08271	995.4	992.77872
989.8	987.18264	995.5	992.87865
989.9	987.28257	995.6	992.97858
990	987.3825	995.7	993.07851
990.1	987.48243	995.8	993.17844
990.2	987.58236	995.9	993.27837
990.3	987.68229	996	993.3783
990.4	987.78222	996.1	993.47823
990.5	987.88215	996.2	993.57816
990.6	987.98208	996.3	993.67809
990.7	988.08201	996.4	993.77802
990.8	988.18194	996.5	993.87795
990.9	988.28187	996.6	993.97788
991	988.3818	996.7	994.07781
991.1	988.48173	996.8	994.17774
991.2	988.58166	996.9	994.27767
991.3	988.68159	997	994.3776
991.4	988.78152	997.1	994.47753
991.5	988.88145	997.2	994.57746
991.6	988.98138	997.3	994.67739
991.7	989.08131	997.4	994.77732
991.8	989.18124	997.5	994.87725
991.9	989.28117	997.6	994.97718
992	989.3811	997.7	995.07711
992.1	989.48103	997.8	995.17704
992.2	989.58096	997.9	995.27697
992.3	989.68089	998	995.3769
992.4	989.78082	998.1	995.47683
992.5	989.88075	998.2	995.57676
992.6	989.98068	998.3	995.67669
992.7	990.08061	998.4	995.77662
992.8	990.18054	998.5	995.87655
992.9	990.28047	998.6	995.97648
993	990.3804	998.7	996.07641
993.1	990.48033	998.8	996.17634
993.2	990.58026	998.9	996.27627
993.3	990.68019	999	996.3762
993.4	990.78012	999.1	996.47613
993.5	990.88005	999.2	996.57606

999.3	996.67599	1005	1002.372
999.4	996.77592	1005.1	1002.47193
999.5	996.87585	1005.2	1002.57186
999.6	996.97578	1005.3	1002.67179
999.7	997.07571	1005.4	1002.77172
999.8	997.17564	1005.5	1002.87165
999.9	997.27557	1005.6	1002.97158
1000	997.3755	1005.7	1003.07151
1000.1	997.47543	1005.8	1003.17144
1000.2	997.57536	1005.9	1003.27137
1000.3	997.67529	1006	1003.3713
1000.4	997.77522	1006.1	1003.47123
1000.5	997.87515	1006.2	1003.57116
1000.6	997.97508	1006.3	1003.67109
1000.7	998.07501	1006.4	1003.77102
1000.8	998.17494	1006.5	1003.87095
1000.9	998.27487	1006.6	1003.97088
1001	998.3748	1006.7	1004.07081
1001.1	998.47473	1006.8	1004.17074
1001.2	998.57466	1006.9	1004.27067
1001.3	998.67459	1007	1004.3706
1001.4	998.77452	1007.1	1004.47053
1001.5	998.87445	1007.2	1004.57046
1001.6	998.97438	1007.3	1004.67039
1001.7	999.07431	1007.4	1004.77032
1001.8	999.17424	1007.5	1004.87025
1001.9	999.27417	1007.6	1004.97018
1002	999.3741	1007.7	1005.07011
1002.1	999.47403	1007.8	1005.17004
1002.2	999.57396	1007.9	1005.26997
1002.3	999.67389	1008	1005.3699
1002.4	999.77382	1008.1	1005.46983
1002.5	999.87375	1008.2	1005.56976
1002.6	999.97368	1008.3	1005.66969
1002.7	1000.07361	1008.4	1005.76962
1002.8	1000.17354	1008.5	1005.86955
1002.9	1000.27347	1008.6	1005.96948
1003	1000.3734	1008.7	1006.06941
1003.1	1000.47333	1008.8	1006.16934
1003.2	1000.57326	1008.9	1006.26927
1003.3	1000.67319	1009	1006.3692
1003.4	1000.77312	1009.1	1006.46913
1003.5	1000.87305	1009.2	1006.56906
1003.6	1000.97298	1009.3	1006.66899
1003.7	1001.07291	1009.4	1006.76892
1003.8	1001.17284	1009.5	1006.86885
1003.9	1001.27277	1009.6	1006.96878
1004	1001.3727	1009.7	1007.06871
1004.1	1001.47263	1009.8	1007.16864
1004.2	1001.57256	1009.9	1007.26857
1004.3	1001.67249	1010	1007.3685
1004.4	1001.77242	1010.1	1007.46843
1004.5	1001.87235	1010.2	1007.56836
1004.6	1001.97228	1010.3	1007.66829
1004.7	1002.07221	1010.4	1007.76822
1004.8	1002.17214	1010.5	1007.86815
1004.9	1002.27207	1010.6	1007.96808

1010.7	1008.06801	1016.4	1013.76402
1010.8	1008.16794	1016.5	1013.86395
1010.9	1008.26787	1016.6	1013.96388
1011	1008.3678	1016.7	1014.06381
1011.1	1008.46773	1016.8	1014.16374
1011.2	1008.56766	1016.9	1014.26367
1011.3	1008.66759	1017	1014.3636
1011.4	1008.76752	1017.1	1014.46353
1011.5	1008.86745	1017.2	1014.56346
1011.6	1008.96738	1017.3	1014.66339
1011.7	1009.06731	1017.4	1014.76332
1011.8	1009.16724	1017.5	1014.86325
1011.9	1009.26717	1017.6	1014.96318
1012	1009.3671	1017.7	1015.06311
1012.1	1009.46703	1017.8	1015.16304
1012.2	1009.56696	1017.9	1015.26297
1012.3	1009.66689	1018	1015.3629
1012.4	1009.76682	1018.1	1015.46283
1012.5	1009.86675	1018.2	1015.56276
1012.6	1009.96668	1018.3	1015.66269
1012.7	1010.06661	1018.4	1015.76262
1012.8	1010.16654	1018.5	1015.86255
1012.9	1010.26647	1018.6	1015.96248
1013	1010.3664	1018.7	1016.06241
1013.1	1010.46633	1018.8	1016.16234
1013.2	1010.56626	1018.9	1016.26227
1013.3	1010.66619	1019	1016.3622
1013.4	1010.76612	1019.1	1016.46213
1013.5	1010.86605	1019.2	1016.56206
1013.6	1010.96598	1019.3	1016.66199
1013.7	1011.06591	1019.4	1016.76192
1013.8	1011.16584	1019.5	1016.86185
1013.9	1011.26577	1019.6	1016.96178
1014	1011.3657	1019.7	1017.06171
1014.1	1011.46563	1019.8	1017.16164
1014.2	1011.56556	1019.9	1017.26157
1014.3	1011.66549	1020	1017.3615
1014.4	1011.76542	1020.1	1017.46143
1014.5	1011.86535	1020.2	1017.56136
1014.6	1011.96528	1020.3	1017.66129
1014.7	1012.06521	1020.4	1017.76122
1014.8	1012.16514	1020.5	1017.86115
1014.9	1012.26507	1020.6	1017.96108
1015	1012.365	1020.7	1018.06101
1015.1	1012.46493	1020.8	1018.16094
1015.2	1012.56486	1020.9	1018.26087
1015.3	1012.66479	1021	1018.3608
1015.4	1012.76472	1021.1	1018.46073
1015.5	1012.86465	1021.2	1018.56066
1015.6	1012.96458	1021.3	1018.66059
1015.7	1013.06451	1021.4	1018.76052
1015.8	1013.16444	1021.5	1018.86045
1015.9	1013.26437	1021.6	1018.96038
1016	1013.3643	1021.7	1019.06031
1016.1	1013.46423	1021.8	1019.16024
1016.2	1013.56416	1021.9	1019.26017
1016.3	1013.66409	1022	1019.3601

1022.1	1019.46003	1027.8	1025.15604
1022.2	1019.55996	1027.9	1025.25597
1022.3	1019.65989	1028	1025.3559
1022.4	1019.75982	1028.1	1025.45583
1022.5	1019.85975	1028.2	1025.55576
1022.6	1019.95968	1028.3	1025.65569
1022.7	1020.05961	1028.4	1025.75562
1022.8	1020.15954	1028.5	1025.85555
1022.9	1020.25947	1028.6	1025.95548
1023	1020.3594	1028.7	1026.05541
1023.1	1020.45933	1028.8	1026.15534
1023.2	1020.55926	1028.9	1026.25527
1023.3	1020.65919	1029	1026.3552
1023.4	1020.75912	1029.1	1026.45513
1023.5	1020.85905	1029.2	1026.55506
1023.6	1020.95898	1029.3	1026.65499
1023.7	1021.05891	1029.4	1026.75492
1023.8	1021.15884	1029.5	1026.85485
1023.9	1021.25877	1029.6	1026.95478
1024	1021.3587	1029.7	1027.05471
1024.1	1021.45863	1029.8	1027.15464
1024.2	1021.55856	1029.9	1027.25457
1024.3	1021.65849	1030	1027.3545
1024.4	1021.75842	1030.1	1027.45443
1024.5	1021.85835	1030.2	1027.55436
1024.6	1021.95828	1030.3	1027.65429
1024.7	1022.05821	1030.4	1027.75422
1024.8	1022.15814	1030.5	1027.85415
1024.9	1022.25807	1030.6	1027.95408
1025	1022.358	1030.7	1028.05401
1025.1	1022.45793	1030.8	1028.15394
1025.2	1022.55786	1030.9	1028.25387
1025.3	1022.65779	1031	1028.3538
1025.4	1022.75772	1031.1	1028.45373
1025.5	1022.85765	1031.2	1028.55366
1025.6	1022.95758	1031.3	1028.65359
1025.7	1023.05751	1031.4	1028.75352
1025.8	1023.15744	1031.5	1028.85345
1025.9	1023.25737	1031.6	1028.95338
1026	1023.3573	1031.7	1029.05331
1026.1	1023.45723	1031.8	1029.15324
1026.2	1023.55716	1031.9	1029.25317
1026.3	1023.65709	1032	1029.3531
1026.4	1023.75702	1032.1	1029.45303
1026.5	1023.85695	1032.2	1029.55296
1026.6	1023.95688	1032.3	1029.65289
1026.7	1024.05681	1032.4	1029.75282
1026.8	1024.15674	1032.5	1029.85275
1026.9	1024.25667	1032.6	1029.95268
1027	1024.3566	1032.7	1030.05261
1027.1	1024.45653	1032.8	1030.15254
1027.2	1024.55646	1032.9	1030.25247
1027.3	1024.65639	1033	1030.3524
1027.4	1024.75632	1033.1	1030.45233
1027.5	1024.85625	1033.2	1030.55226
1027.6	1024.95618	1033.3	1030.65219
1027.7	1025.05611	1033.4	1030.75212

1033.5	1030.85205	1039.2	1036.54806
1033.6	1030.95198	1039.3	1036.64799
1033.7	1031.05191	1039.4	1036.74792
1033.8	1031.15184	1039.5	1036.84785
1033.9	1031.25177	1039.6	1036.94778
1034	1031.3517	1039.7	1037.04771
1034.1	1031.45163	1039.8	1037.14764
1034.2	1031.55156	1039.9	1037.24757
1034.3	1031.65149	1040	1037.3475
1034.4	1031.75142	1040.1	1037.44743
1034.5	1031.85135	1040.2	1037.54736
1034.6	1031.95128	1040.3	1037.64729
1034.7	1032.05121	1040.4	1037.74722
1034.8	1032.15114	1040.5	1037.84715
1034.9	1032.25107	1040.6	1037.94708
1035	1032.351	1040.7	1038.04701
1035.1	1032.45093	1040.8	1038.14694
1035.2	1032.55086	1040.9	1038.24687
1035.3	1032.65079	1041	1038.3468
1035.4	1032.75072	1041.1	1038.44673
1035.5	1032.85065	1041.2	1038.54666
1035.6	1032.95058	1041.3	1038.64659
1035.7	1033.05051	1041.4	1038.74652
1035.8	1033.15044	1041.5	1038.84645
1035.9	1033.25037	1041.6	1038.94638
1036	1033.3503	1041.7	1039.04631
1036.1	1033.45023	1041.8	1039.14624
1036.2	1033.55016	1041.9	1039.24617
1036.3	1033.65009	1042	1039.3461
1036.4	1033.75002	1042.1	1039.44603
1036.5	1033.84995	1042.2	1039.54596
1036.6	1033.94988	1042.3	1039.64589
1036.7	1034.04981	1042.4	1039.74582
1036.8	1034.14974	1042.5	1039.84575
1036.9	1034.24967	1042.6	1039.94568
1037	1034.3496	1042.7	1040.04561
1037.1	1034.44953	1042.8	1040.14554
1037.2	1034.54946	1042.9	1040.24547
1037.3	1034.64939	1043	1040.3454
1037.4	1034.74932	1043.1	1040.44533
1037.5	1034.84925	1043.2	1040.54526
1037.6	1034.94918	1043.3	1040.64519
1037.7	1035.04911	1043.4	1040.74512
1037.8	1035.14904	1043.5	1040.84505
1037.9	1035.24897	1043.6	1040.94498
1038	1035.3489	1043.7	1041.04491
1038.1	1035.44883	1043.8	1041.14484
1038.2	1035.54876	1043.9	1041.24477
1038.3	1035.64869	1044	1041.3447
1038.4	1035.74862	1044.1	1041.44463
1038.5	1035.84855	1044.2	1041.54456
1038.6	1035.94848	1044.3	1041.64449
1038.7	1036.04841	1044.4	1041.74442
1038.8	1036.14834	1044.5	1041.84435
1038.9	1036.24827	1044.6	1041.94428
1039	1036.3482	1044.7	1042.04421
1039.1	1036.44813	1044.8	1042.14414

1044.9	1042.24407	1050.6	1047.94008
1045	1042.344	1050.7	1048.04001
1045.1	1042.44393	1050.8	1048.13994
1045.2	1042.54386	1050.9	1048.23987
1045.3	1042.64379	1051	1048.3398
1045.4	1042.74372	1051.1	1048.43973
1045.5	1042.84365	1051.2	1048.53966
1045.6	1042.94358	1051.3	1048.63959
1045.7	1043.04351	1051.4	1048.73952
1045.8	1043.14344	1051.5	1048.83945
1045.9	1043.24337	1051.6	1048.93938
1046	1043.3433	1051.7	1049.03931
1046.1	1043.44323	1051.8	1049.13924
1046.2	1043.54316	1051.9	1049.23917
1046.3	1043.64309	1052	1049.3391
1046.4	1043.74302	1052.1	1049.43903
1046.5	1043.84295	1052.2	1049.53896
1046.6	1043.94288	1052.3	1049.63889
1046.7	1044.04281	1052.4	1049.73882
1046.8	1044.14274	1052.5	1049.83875
1046.9	1044.24267	1052.6	1049.93868
1047	1044.3426	1052.7	1050.03861
1047.1	1044.44253	1052.8	1050.13854
1047.2	1044.54246	1052.9	1050.23847
1047.3	1044.64239	1053	1050.3384
1047.4	1044.74232	1053.1	1050.43833
1047.5	1044.84225	1053.2	1050.53826
1047.6	1044.94218	1053.3	1050.63819
1047.7	1045.04211	1053.4	1050.73812
1047.8	1045.14204	1053.5	1050.83805
1047.9	1045.24197	1053.6	1050.93798
1048	1045.3419	1053.7	1051.03791
1048.1	1045.44183	1053.8	1051.13784
1048.2	1045.54176	1053.9	1051.23777
1048.3	1045.64169	1054	1051.3377
1048.4	1045.74162	1054.1	1051.43763
1048.5	1045.84155	1054.2	1051.53756
1048.6	1045.94148	1054.3	1051.63749
1048.7	1046.04141	1054.4	1051.73742
1048.8	1046.14134	1054.5	1051.83735
1048.9	1046.24127	1054.6	1051.93728
1049	1046.3412	1054.7	1052.03721
1049.1	1046.44113	1054.8	1052.13714
1049.2	1046.54106	1054.9	1052.23707
1049.3	1046.64099	1055	1052.337
1049.4	1046.74092	1055.1	1052.43693
1049.5	1046.84085	1055.2	1052.53686
1049.6	1046.94078	1055.3	1052.63679
1049.7	1047.04071	1055.4	1052.73672
1049.8	1047.14064	1055.5	1052.83665
1049.9	1047.24057	1055.6	1052.93658
1050	1047.3405	1055.7	1053.03651
1050.1	1047.44043	1055.8	1053.13644
1050.2	1047.54036	1055.9	1053.23637
1050.3	1047.64029	1056	1053.3363
1050.4	1047.74022	1056.1	1053.43623
1050.5	1047.84015	1056.2	1053.53616

1056.3	1053.63609	1062	1059.3321
1056.4	1053.73602	1062.1	1059.43203
1056.5	1053.83595	1062.2	1059.53196
1056.6	1053.93588	1062.3	1059.63189
1056.7	1054.03581	1062.4	1059.73182
1056.8	1054.13574	1062.5	1059.83175
1056.9	1054.23567	1062.6	1059.93168
1057	1054.3356	1062.7	1060.03161
1057.1	1054.43553	1062.8	1060.13154
1057.2	1054.53546	1062.9	1060.23147
1057.3	1054.63539	1063	1060.3314
1057.4	1054.73532	1063.1	1060.43133
1057.5	1054.83525	1063.2	1060.53126
1057.6	1054.93518	1063.3	1060.63119
1057.7	1055.03511	1063.4	1060.73112
1057.8	1055.13504	1063.5	1060.83105
1057.9	1055.23497	1063.6	1060.93098
1058	1055.3349	1063.7	1061.03091
1058.1	1055.43483	1063.8	1061.13084
1058.2	1055.53476	1063.9	1061.23077
1058.3	1055.63469	1064	1061.3307
1058.4	1055.73462	1064.1	1061.43063
1058.5	1055.83455	1064.2	1061.53056
1058.6	1055.93448	1064.3	1061.63049
1058.7	1056.03441	1064.4	1061.73042
1058.8	1056.13434	1064.5	1061.83035
1058.9	1056.23427	1064.6	1061.93028
1059	1056.3342	1064.7	1062.03021
1059.1	1056.43413	1064.8	1062.13014
1059.2	1056.53406	1064.9	1062.23007
1059.3	1056.63399	1065	1062.33
1059.4	1056.73392	1065.1	1062.42993
1059.5	1056.83385	1065.2	1062.52986
1059.6	1056.93378	1065.3	1062.62979
1059.7	1057.03371	1065.4	1062.72972
1059.8	1057.13364	1065.5	1062.82965
1059.9	1057.23357	1065.6	1062.92958
1060	1057.3335	1065.7	1063.02951
1060.1	1057.43343	1065.8	1063.12944
1060.2	1057.53336	1065.9	1063.22937
1060.3	1057.63329	1066	1063.3293
1060.4	1057.73322	1066.1	1063.42923
1060.5	1057.83315	1066.2	1063.52916
1060.6	1057.93308	1066.3	1063.62909
1060.7	1058.03301	1066.4	1063.72902
1060.8	1058.13294	1066.5	1063.82895
1060.9	1058.23287	1066.6	1063.92888
1061	1058.3328	1066.7	1064.02881
1061.1	1058.43273	1066.8	1064.12874
1061.2	1058.53266	1066.9	1064.22867
1061.3	1058.63259	1067	1064.3286
1061.4	1058.73252	1067.1	1064.42853
1061.5	1058.83245	1067.2	1064.52846
1061.6	1058.93238	1067.3	1064.62839
1061.7	1059.03231	1067.4	1064.72832
1061.8	1059.13224	1067.5	1064.82825
1061.9	1059.23217	1067.6	1064.92818

1067.7	1065.02811
1067.8	1065.12804
1067.9	1065.22797
1068	1065.3279
1068.1	1065.42783
1068.2	1065.52776
1068.3	1065.62769
1068.4	1065.72762
1068.5	1065.82755
1068.6	1065.92748
1068.7	1066.02741
1068.8	1066.12734
1068.9	1066.22727
1069	1066.3272
1069.1	1066.42713
1069.2	1066.52706
1069.3	1066.62699
1069.4	1066.72692
1069.5	1066.82685
1069.6	1066.92678
1069.7	1067.02671
1069.8	1067.12664
1069.9	1067.22657
1070	1067.3265
1070.1	1067.42643
1070.2	1067.52636
1070.3	1067.62629
1070.4	1067.72622
1070.5	1067.82615
1070.6	1067.92608
1070.7	1068.02601
1070.8	1068.12594
1070.9	1068.22587
1071	1068.3258
1071.1	1068.42573
1071.2	1068.52566
1071.3	1068.62559
1071.4	1068.72552
1071.5	1068.82545
1071.6	1068.92538
1071.7	1069.02531
1071.8	1069.12524
1071.9	1069.22517
1072	1069.3251
1072.1	1069.42503
1072.2	1069.52496
1072.3	1069.62489
1072.4	1069.72482
1072.5	1069.82475
1072.6	1069.92468
1072.7	1070.02461
1072.8	1070.12454
1072.9	1070.22447
1073	1070.3244
1073.1	1070.42433
1073.2	1070.52426
1073.3	1070.62419
1073.4	1070.72412
1073.5	1070.82405
1073.6	1070.92398
1073.7	1071.02391
1073.8	1071.12384
1073.9	1071.22377
1074	1071.3237
1074.1	1071.42363
1074.2	1071.52356
1074.3	1071.62349
1074.4	1071.72342
1074.5	1071.82335
1074.6	1071.92328
1074.7	1072.02321
1074.8	1072.12314
1074.9	1072.22307
1075	1072.323
1075.1	1072.42293
1075.2	1072.52286
1075.3	1072.62279
1075.4	1072.72272
1075.5	1072.82265
1075.6	1072.92258
1075.7	1073.02251
1075.8	1073.12244
1075.9	1073.22237
1076	1073.3223
1076.1	1073.42223
1076.2	1073.52216
1076.3	1073.62209
1076.4	1073.72202
1076.5	1073.82195
1076.6	1073.92188
1076.7	1074.02181
1076.8	1074.12174
1076.9	1074.22167
1077	1074.3216
1077.1	1074.42153
1077.2	1074.52146
1077.3	1074.62139
1077.4	1074.72132
1077.5	1074.82125
1077.6	1074.92118
1077.7	1075.02111
1077.8	1075.12104
1077.9	1075.22097
1078	1075.3209
1078.1	1075.42083
1078.2	1075.52076
1078.3	1075.62069
1078.4	1075.72062
1078.5	1075.82055
1078.6	1075.92048
1078.7	1076.02041
1078.8	1076.12034
1078.9	1076.22027
1079	1076.3202

1079.1	1076.42013	1084.8	1082.11614
1079.2	1076.52006	1084.9	1082.21607
1079.3	1076.61999	1085	1082.316
1079.4	1076.71992	1085.1	1082.41593
1079.5	1076.81985	1085.2	1082.51586
1079.6	1076.91978	1085.3	1082.61579
1079.7	1077.01971	1085.4	1082.71572
1079.8	1077.11964	1085.5	1082.81565
1079.9	1077.21957	1085.6	1082.91558
1080	1077.3195	1085.7	1083.01551
1080.1	1077.41943	1085.8	1083.11544
1080.2	1077.51936	1085.9	1083.21537
1080.3	1077.61929	1086	1083.3153
1080.4	1077.71922	1086.1	1083.41523
1080.5	1077.81915	1086.2	1083.51516
1080.6	1077.91908	1086.3	1083.61509
1080.7	1078.01901	1086.4	1083.71502
1080.8	1078.11894	1086.5	1083.81495
1080.9	1078.21887	1086.6	1083.91488
1081	1078.3188	1086.7	1084.01481
1081.1	1078.41873	1086.8	1084.11474
1081.2	1078.51866	1086.9	1084.21467
1081.3	1078.61859	1087	1084.3146
1081.4	1078.71852	1087.1	1084.41453
1081.5	1078.81845	1087.2	1084.51446
1081.6	1078.91838	1087.3	1084.61439
1081.7	1079.01831	1087.4	1084.71432
1081.8	1079.11824	1087.5	1084.81425
1081.9	1079.21817	1087.6	1084.91418
1082	1079.3181	1087.7	1085.01411
1082.1	1079.41803	1087.8	1085.11404
1082.2	1079.51796	1087.9	1085.21397
1082.3	1079.61789	1088	1085.3139
1082.4	1079.71782	1088.1	1085.41383
1082.5	1079.81775	1088.2	1085.51376
1082.6	1079.91768	1088.3	1085.61369
1082.7	1080.01761	1088.4	1085.71362
1082.8	1080.11754	1088.5	1085.81355
1082.9	1080.21747	1088.6	1085.91348
1083	1080.3174	1088.7	1086.01341
1083.1	1080.41733	1088.8	1086.11334
1083.2	1080.51726	1088.9	1086.21327
1083.3	1080.61719	1089	1086.3132
1083.4	1080.71712	1089.1	1086.41313
1083.5	1080.81705	1089.2	1086.51306
1083.6	1080.91698	1089.3	1086.61299
1083.7	1081.01691	1089.4	1086.71292
1083.8	1081.11684	1089.5	1086.81285
1083.9	1081.21677	1089.6	1086.91278
1084	1081.3167	1089.7	1087.01271
1084.1	1081.41663	1089.8	1087.11264
1084.2	1081.51656	1089.9	1087.21257
1084.3	1081.61649	1090	1087.3125
1084.4	1081.71642	1090.1	1087.41243
1084.5	1081.81635	1090.2	1087.51236
1084.6	1081.91628	1090.3	1087.61229
1084.7	1082.01621	1090.4	1087.71222

1090.5	1087.81215
1090.6	1087.91208
1090.7	1088.01201
1090.8	1088.11194
1090.9	1088.21187
1091	1088.3118
1091.1	1088.41173
1091.2	1088.51166
1091.3	1088.61159
1091.4	1088.71152
1091.5	1088.81145
1091.6	1088.91138
1091.7	1089.01131
1091.8	1089.11124
1091.9	1089.21117
1092	1089.3111
1092.1	1089.41103
1092.2	1089.51096
1092.3	1089.61089
1092.4	1089.71082
1092.5	1089.81075
1092.6	1089.91068
1092.7	1090.01061
1092.8	1090.11054
1092.9	1090.21047
1093	1090.3104
1093.1	1090.41033
1093.2	1090.51026
1093.3	1090.61019
1093.4	1090.71012
1093.5	1090.81005
1093.6	1090.90998
1093.7	1091.00991
1093.8	1091.10984
1093.9	1091.20977
1094	1091.3097
1094.1	1091.40963
1094.2	1091.50956
1094.3	1091.60949
1094.4	1091.70942
1094.5	1091.80935
1094.6	1091.90928
1094.7	1092.00921
1094.8	1092.10914
1094.9	1092.20907
1095	1092.309
1095.1	1092.40893
1095.2	1092.50886
1095.3	1092.60879
1095.4	1092.70872
1095.5	1092.80865
1095.6	1092.90858
1095.7	1093.00851
1095.8	1093.10844
1095.9	1093.20837
1096	1093.3083
1096.1	1093.40823
1096.2	1093.50816
1096.3	1093.60809
1096.4	1093.70802
1096.5	1093.80795
1096.6	1093.90788
1096.7	1094.00781
1096.8	1094.10774
1096.9	1094.20767
1097	1094.3076
1097.1	1094.40753
1097.2	1094.50746
1097.3	1094.60739
1097.4	1094.70732
1097.5	1094.80725
1097.6	1094.90718
1097.7	1095.00711
1097.8	1095.10704
1097.9	1095.20697
1098	1095.3069
1098.1	1095.40683
1098.2	1095.50676
1098.3	1095.60669
1098.4	1095.70662
1098.5	1095.80655
1098.6	1095.90648
1098.7	1096.00641
1098.8	1096.10634
1098.9	1096.20627
1099	1096.3062
1099.1	1096.40613
1099.2	1096.50606
1099.3	1096.60599
1099.4	1096.70592
1099.5	1096.80585
1099.6	1096.90578
1099.7	1097.00571
1099.8	1097.10564
1099.9	1097.20557
1100	1097.3055

off_020913000000.prn:

Commanded Wavelength	Actual Wavelength
350	348.2799
351	349.2749
352	350.2699
353	351.2649
354	352.2599
355	353.2549
356	354.2499
357	355.2449
358	356.2399
359	357.2349
360	358.2299
361	359.2249
362	360.2199
363	361.2149
364	362.2099
365	363.2049
366	364.1999
367	365.1949
368	366.1899
369	367.1849
370	368.1799
371	369.1749
372	370.1699
373	371.1649
374	372.1599
375	373.1549
376	374.1499
377	375.1449
378	376.1399
379	377.1349
380	378.1299
381	379.1249
382	380.1199
383	381.1149
384	382.1099
385	383.1049
386	384.0999
387	385.0949
388	386.0899
389	387.0849
390	388.0799
391	389.0749
392	390.0699
393	391.0649
394	392.0599
395	393.0549
396	394.0499
397	395.0449
398	396.0399
399	397.0349
400	398.0299
401	399.0249
402	400.0199
403	401.0149
404	402.0099
405	403.0049
406	403.9999
407	404.9949
408	405.9899
409	406.9849
410	407.9799
411	408.9749
412	409.9699
413	410.9649
414	411.9599
415	412.9549
416	413.9499
417	414.9449
418	415.9399
419	416.9349
420	417.9299
421	418.9249
422	419.9199
423	420.9149
424	421.9099
425	422.9049
426	423.8999
427	424.8949
428	425.8899
429	426.8849
430	427.8799
431	428.8749
432	429.8699
433	430.8649
434	431.8599
435	432.8549
436	433.8499
437	434.8449
438	435.8399
439	436.8349
440	437.8299
441	438.8249
442	439.8199
443	440.8149
444	441.8099
445	442.8049
446	443.7999
447	444.7949
448	445.7899
449	446.7849
450	447.7799
451	448.7749
452	449.7699
453	450.7649
454	451.7599
455	452.7549
456	453.7499
457	454.7449

458	455.7399
459	456.7349
460	457.7299
461	458.7249
462	459.7199
463	460.7149
464	461.7099
465	462.7049
466	463.6999
467	464.6949
468	465.6899
469	466.6849
470	467.6799
471	468.6749
472	469.6699
473	470.6649
474	471.6599
475	472.6549
476	473.6499
477	474.6449
478	475.6399
479	476.6349
480	477.6299
481	478.6249
482	479.6199
483	480.6149
484	481.6099
485	482.6049
486	483.5999
487	484.5949
488	485.5899
489	486.5849
490	487.5799
491	488.5749
492	489.5699
493	490.5649
494	491.5599
495	492.5549
496	493.5499
497	494.5449
498	495.5399
499	496.5349
500	497.5299
501	498.5249
502	499.5199
503	500.5149
504	501.5099
505	502.5049
506	503.4999
507	504.4949
508	505.4899
509	506.4849
510	507.4799
511	508.4749
512	509.4699
513	510.4649
514	511.4599
515	512.4549
516	513.4499
517	514.4449
518	515.4399
519	516.4349
520	517.4299
521	518.4249
522	519.4199
523	520.4149
524	521.4099
525	522.4049
526	523.3999
527	524.3949
528	525.3899
529	526.3849
530	527.3799
531	528.3749
532	529.3699
533	530.3649
534	531.3599
535	532.3549
536	533.3499
537	534.3449
538	535.3399
539	536.3349
540	537.3299
541	538.3249
542	539.3199
543	540.3149
544	541.3099
545	542.3049
546	543.2999
547	544.2949
548	545.2899
549	546.2849
550	547.2799
551	548.2749
552	549.2699
553	550.2649
554	551.2599
555	552.2549
556	553.2499
557	554.2449
558	555.2399
559	556.2349
560	557.2299
561	558.2249
562	559.2199
563	560.2149
564	561.2099
565	562.2049
566	563.1999
567	564.1949
568	565.1899
569	566.1849
570	567.1799
571	568.1749

572	569.1699
573	570.1649
574	571.1599
575	572.1549
576	573.1499
577	574.1449
578	575.1399
579	576.1349
580	577.1299
581	578.1249
582	579.1199
583	580.1149
584	581.1099
585	582.1049
586	583.0999
587	584.0949
588	585.0899
589	586.0849
590	587.0799
591	588.0749
592	589.0699
593	590.0649
594	591.0599
595	592.0549
596	593.0499
597	594.0449
598	595.0399
599	596.0349
600	597.0299
601	598.0249
602	599.0199
603	600.0149
604	601.0099
605	602.0049
606	602.9999
607	603.9949
608	604.9899
609	605.9849
610	606.9799
611	607.9749
612	608.9699
613	609.9649
614	610.9599
615	611.9549
616	612.9499
617	613.9449
618	614.9399
619	615.9349
620	616.9299
621	617.9249
622	618.9199
623	619.9149
624	620.9099
625	621.9049
626	622.8999
627	623.8949
628	624.8899
629	625.8849
630	626.8799
631	627.8749
632	628.8699
633	629.8649
634	630.8599
635	631.8549
636	632.8499
637	633.8449
638	634.8399
639	635.8349
640	636.8299
641	637.8249
642	638.8199
643	639.8149
644	640.8099
645	641.8049
646	642.7999
647	643.7949
648	644.7899
649	645.7849
650	646.7799
651	647.7749
652	648.7699
653	649.7649
654	650.7599
655	651.7549
656	652.7499
657	653.7449
658	654.7399
659	655.7349
660	656.7299
661	657.7249
662	658.7199
663	659.7149
664	660.7099
665	661.7049
666	662.6999
667	663.6949
668	664.6899
669	665.6849
670	666.6799
671	667.6749
672	668.6699
673	669.6649
674	670.6599
675	671.6549
676	672.6499
677	673.6449
678	674.6399
679	675.6349
680	676.6299
681	677.6249
682	678.6199
683	679.6149
684	680.6099
685	681.6049

686	682.5999
687	683.5949
688	684.5899
689	685.5849
690	686.5799
691	687.5749
692	688.5699
693	689.5649
694	690.5599
695	691.5549
696	692.5499
697	693.5449
698	694.5399
699	695.5349
700	696.5299
701	697.5249
702	698.5199
703	699.5149
704	700.5099
705	701.5049
706	702.4999
707	703.4949
708	704.4899
709	705.4849
710	706.4799
711	707.4749
712	708.4699
713	709.4649
714	710.4599
715	711.4549
716	712.4499
717	713.4449
718	714.4399
719	715.4349
720	716.4299
721	717.4249
722	718.4199
723	719.4149
724	720.4099
725	721.4049
726	722.3999
727	723.3949
728	724.3899
729	725.3849
730	726.3799
731	727.3749
732	728.3699
733	729.3649
734	730.3599
735	731.3549
736	732.3499
737	733.3449
738	734.3399
739	735.3349
740	736.3299
741	737.3249
742	738.3199
743	739.3149
744	740.3099
745	741.3049
746	742.2999
747	743.2949
748	744.2899
749	745.2849
750	746.2799
751	747.2749
752	748.2699
753	749.2649
754	750.2599
755	751.2549
756	752.2499
757	753.2449
758	754.2399
759	755.2349
760	756.2299
761	757.2249
762	758.2199
763	759.2149
764	760.2099
765	761.2049
766	762.1999
767	763.1949
768	764.1899
769	765.1849
770	766.1799
771	767.1749
772	768.1699
773	769.1649
774	770.1599
775	771.1549
776	772.1499
777	773.1449
778	774.1399
779	775.1349
780	776.1299
781	777.1249
782	778.1199
783	779.1149
784	780.1099
785	781.1049
786	782.0999
787	783.0949
788	784.0899
789	785.0849
790	786.0799
791	787.0749
792	788.0699
793	789.0649
794	790.0599
795	791.0549
796	792.0499
797	793.0449
798	794.0399
799	795.0349

800	796.0299
801	797.0249
802	798.0199
803	799.0149
804	800.0099
805	801.0049
806	801.9999
807	802.9949
808	803.9899
809	804.9849
810	805.9799
811	806.9749
812	807.9699
813	808.9649
814	809.9599
815	810.9549
816	811.9499
817	812.9449
818	813.9399
819	814.9349
820	815.9299
821	816.9249
822	817.9199
823	818.9149
824	819.9099
825	820.9049
826	821.8999
827	822.8949
828	823.8899
829	824.8849
830	825.8799
831	826.8749
832	827.8699
833	828.8649
834	829.8599
835	830.8549
836	831.8499
837	832.8449
838	833.8399
839	834.8349
840	835.8299
841	836.8249
842	837.8199
843	838.8149
844	839.8099
845	840.8049
846	841.7999
847	842.7949
848	843.7899
849	844.7849
850	845.7799
851	846.7749
852	847.7699
853	848.7649
854	849.7599
855	850.7549
856	851.7499
857	852.7449
858	853.7399
859	854.7349
860	855.7299
861	856.7249
862	857.7199
863	858.7149
864	859.7099
865	860.7049
866	861.6999
867	862.6949
868	863.6899
869	864.6849
870	865.6799
871	866.6749
872	867.6699
873	868.6649
874	869.6599
875	870.6549
876	871.6499
877	872.6449
878	873.6399
879	874.6349
880	875.6299
881	876.6249
882	877.6199
883	878.6149
884	879.6099
885	880.6049
886	881.5999
887	882.5949
888	883.5899
889	884.5849
890	885.5799
891	886.5749
892	887.5699
893	888.5649
894	889.5599
895	890.5549
896	891.5499
897	892.5449
898	893.5399
899	894.5349
900	895.5299
901	896.5249
902	897.5199
903	898.5149
904	899.5099
905	900.5049
906	901.4999
907	902.4949
908	903.4899
909	904.4849
910	905.4799
911	906.4749
912	907.4699
913	908.4649

914	909.4599
915	910.4549
916	911.4499
917	912.4449
918	913.4399
919	914.4349
920	915.4299
921	916.4249
922	917.4199
923	918.4149
924	919.4099
925	920.4049
926	921.3999
927	922.3949
928	923.3899
929	924.3849
930	925.3799
931	926.3749
932	927.3699
933	928.3649
934	929.3599
935	930.3549
936	931.3499
937	932.3449
938	933.3399
939	934.3349
940	935.3299
941	936.3249
942	937.3199
943	938.3149
944	939.3099
945	940.3049
946	941.2999
947	942.2949
948	943.2899
949	944.2849
950	945.2799
951	946.2749
952	947.2699
953	948.2649
954	949.2599
955	950.2549
956	951.2499
957	952.2449
958	953.2399
959	954.2349
960	955.2299
961	956.2249
962	957.2199
963	958.2149
964	959.2099
965	960.2049
966	961.1999
967	962.1949
968	963.1899
969	964.1849
970	965.1799
971	966.1749
972	967.1699
973	968.1649
974	969.1599
975	970.1549
976	971.1499
977	972.1449
978	973.1399
979	974.1349
980	975.1299
981	976.1249
982	977.1199
983	978.1149
984	979.1099
985	980.1049
986	981.0999
987	982.0949
988	983.0899
989	984.0849
990	985.0799
991	986.0749
992	987.0699
993	988.0649
994	989.0599
995	990.0549
996	991.0499
997	992.0449
998	993.0399
999	994.0349
1000	995.0299
1001	996.0249
1002	997.0199
1003	998.0149
1004	999.0099
1005	1000.0049
1006	1000.9999
1007	1001.9949
1008	1002.9899
1009	1003.9849
1010	1004.9799
1011	1005.9749
1012	1006.9699
1013	1007.9649
1014	1008.9599
1015	1009.9549
1016	1010.9499
1017	1011.9449
1018	1012.9399
1019	1013.9349
1020	1014.9299
1021	1015.9249
1022	1016.9199
1023	1017.9149
1024	1018.9099
1025	1019.9049
1026	1020.8999
1027	1021.8949

```
1028 1022.8899
1029 1023.8849
1030 1024.8799
1031 1025.8749
1032 1026.8699
1033 1027.8649
1034 1028.8599
1035 1029.8549
1036 1030.8499
1037 1031.8449
1038 1032.8399
1039 1033.8349
1040 1034.8299
1041 1035.8249
1042 1036.8199
1043 1037.8149
1044 1038.8099
1045 1039.8049
1046 1040.7999
1047 1041.7949
1048 1042.7899
1049 1043.7849
1050 1044.7799
1051 1045.7749
1052 1046.7699
1053 1047.7649
1054 1048.7599
1055 1049.7549
1056 1050.7499
1057 1051.7449
1058 1052.7399
1059 1053.7349
1060 1054.7299
1061 1055.7249
1062 1056.7199
1063 1057.7149
1064 1058.7099
1065 1059.7049
1066 1060.6999
1067 1061.6949
1068 1062.6899
1069 1063.6849
1070 1064.6799
1071 1065.6749
1072 1066.6699
1073 1067.6649
1074 1068.6599
1075 1069.6549
1076 1070.6499
1077 1071.6449
1078 1072.6399
1079 1073.6349
1080 1074.6299
1081 1075.6249
1082 1076.6199
1083 1077.6149
1084 1078.6099
1085 1079.6049
1086 1080.5999
1087 1081.5949
1088 1082.5899
1089 1083.5849
1090 1084.5799
1091 1085.5749
1092 1086.5699
1093 1087.5649
1094 1088.5599
1095 1089.5549
1096 1090.5499
1097 1091.5449
1098 1092.5399
1099 1093.5349
1100 1094.5299
```

Monochromator sweep calibration data:

Line Center (Å)	Acton (nm)	Diode Output (amp)
5037.751	501.32792	5.3529000e-13
5330.778	530.61364	1.4041900e-12
5341.094	531.67857	1.5021500e-12
5400.562	537.53572	2.9961000e-12
5656.659	563.09416	6.4937000e-13
5748.298	572.14611	1.2085300e-12
5764.419	573.74351	4.5701000e-12
5804.45	577.73702	9.8818000e-13
5820.156	579.33442	2.7081000e-12
5852.488	582.52922	1.9312400e-10
5872.828	584.52598	1.1670400e-12
5881.895	585.45780	1.4210200e-10
6029.997	600.10065	7.0244000e-11
6074.338	604.62663	1.8673100e-10
6096.163	606.62338	3.0243000e-10
6128.45	609.95130	1.1383400e-11
6143.063	611.41559	5.5424000e-10
6163.594	613.41234	1.5836500e-10
6217.281	618.87013	1.4166700e-10
6266.495	623.52923	2.6311000e-10
6304.789	627.52273	9.2917000e-11
6334.428	630.31819	3.3670000e-10
6382.992	635.24351	5.0462000e-10
6402.246	637.10715	1.0195100e-09
6506.528	647.49026	7.0815000e-10
6532.882	650.15260	2.7107000e-10
6598.953	656.67533	3.9629000e-10
6678.276	664.66234	7.2879000e-10
6717.043	668.52273	4.9510000e-10
6929.467	689.68832	6.3093000e-10
7024.05	699.13962	5.7429000e-11
7032.413	699.93832	1.9474000e-09
7059.107	702.60066	8.5231000e-12
7173.938	714.04871	1.1048800e-10
7943.181	790.57996	3.6686000e-12
8082.458	804.41706	6.5721000e-12
8118.549	808.00938	1.5185100e-12
8136.406	809.87207	6.9436000e-12
8259.379	822.11258	1.3126700e-12
8266.077	822.77783	2.9763000e-12
8300.326	826.23710	1.7916700e-11
8365.749	832.62345	2.5297000e-12
8377.606	833.82090	8.7920000e-11
8463.358	842.46908	1.8973200e-12
8484.444	844.46482	8.3885000e-13
8495.36	845.52921	5.2174000e-11
8544.696	850.45203	1.0719400e-12
8571.352	853.11301	1.0901000e-12
8591.259	855.10874	1.6250400e-11
8634.647	859.36631	1.9699300e-11
8647.041	860.56375	2.1763000e-12
8654.383	861.36205	3.1243000e-11
8780.621	874.00171	3.7946000e-11
8853.867	881.31940	1.4951200e-11
9148.67	910.59019	5.0311000e-12
9201.76	915.77911	3.7765000e-12
9220.06	917.77484	3.1402000e-12
9226.69	918.30704	9.6792000e-13
9275.52	923.22985	5.3676000e-13
9300.85	925.75778	3.4137000e-12
9313.97	927.08827	1.3409600e-12
9326.51	928.28571	2.7668000e-12
9373.31	932.94243	8.1450000e-13
9425.38	938.13134	2.2920000e-12
9459.21	941.45757	1.1842700e-12
9486.68	944.25160	9.9106000e-13
9534.16	948.90832	2.5604000e-12
9547.4	950.23881	1.2912800e-12
9665.42	961.94712	2.6532000e-12
10562.41	1051.3561	5.5008000e-13

Monochromator radiance calibration files

(All wavelengths are in nanometers)

diode_020814161300.prn:

Wavelength	Diode output (nA)
348.78	0.01385
372.00	0.41300
396.39	2.18000
421.46	4.21200
446.85	6.30000
472.28	8.16000
497.62	10.38000
522.76	13.41000
547.72	15.43000
572.51	16.70000
597.22	17.17000
621.93	16.46000
646.74	21.21000
671.75	25.67000
697.00	23.90000
722.51	21.16000
748.24	18.25000
774.08	15.62000
799.82	13.27400
825.17	11.66500
849.69	10.97000
872.82	10.31000
896.39	9.22500
921.37	7.72000
946.36	5.93800
971.34	4.16100
996.33	2.59500
1021.31	1.43200
1046.29	0.71100
1071.28	0.31700
1096.26	0.11200

diode_020814191800.prn:

Wavelength	Diode output (nA)
348.78	0.01385
396.39	2.20
421.46	4.26
446.85	6.37
472.28	8.26
497.62	10.52
522.76	13.59
547.72	15.64
572.51	16.92
597.22	17.40
621.93	16.68
646.74	21.49
671.75	26.01
697.00	24.21
722.51	21.45
748.24	18.50
774.08	15.85
799.82	13.48
825.17	11.82
849.69	11.09
872.82	10.40
896.39	9.28
921.37	7.75
946.36	5.95
971.34	4.16
996.33	2.59
1021.31	1.40
1046.29	0.68
1071.28	0.30
1096.26	0.10

diode_020816200000.prn:

Wavelength	Diode output (nA)
347.8305	0.019
372.813	0.520
397.7955	2.510
422.778	4.740
447.7605	7.000
472.743	8.840
497.7255	11.470
522.708	14.810
547.6905	17.100
572.673	18.550
597.6555	19.120
622.638	18.200
647.6205	24.040
672.603	28.300
697.5855	26.250
722.568	23.270
747.5505	20.170
772.533	17.350
797.5155	14.820
822.498	12.940
847.4805	12.050
872.463	11.200
897.4455	9.900
922.428	8.270
947.4105	6.170
972.393	4.290
997.3755	2.640
1022.358	1.460
1047.3405	0.725
1072.323	0.308
1097.3055	0.108

diode_020914044800.prn:

Wavelength	Diode output (nA)
348.2799	0.013
398.0299	1.871
447.7799	5.331
497.5299	8.870
547.2799	13.490
597.0299	15.420
646.7799	19.280
696.5299	22.000
746.2799	17.130
796.0299	12.870
845.7799	10.810
895.5299	9.940
945.2799	7.610
995.0299	4.700
1044.7799	1.865
1094.5299	0.318

diode_020916081200.prn:

Wavelength	Diode output (nA)
347.8305	0.019
372.813	0.520
397.7955	2.510
422.778	4.740
447.7605	7.000
472.743	8.840
497.7255	11.470
522.708	14.810
547.6905	17.100
572.673	18.550
597.6555	19.120
622.638	18.200
647.6205	24.040
672.603	28.300
697.5855	26.250
722.568	23.270
747.5505	20.170
772.533	17.350
797.5155	14.820
822.498	12.940
847.4805	12.050
872.463	11.200
897.4455	9.900
922.428	8.270
947.4105	6.170
972.393	4.290
997.3755	2.640
1022.358	1.460
1047.3405	0.725
1072.323	0.308
1097.3055	0.108

diode_0209163131000.prn:

Wavelength	Diode output (nA)
348.2796	0.013
398.0299	1.922
447.7799	5.440
497.5299	8.970
547.2799	13.570
597.0299	15.410
646.7799	19.230
696.5299	21.960
746.2799	17.165
796.0299	12.970
845.7799	10.940
895.5299	10.010
945.2799	7.670
995.0299	4.700
1044.7799	1.850
1094.5299	0.308

Spectral response files

MI 105, -55C

Wavelength	Response
350.45665	1.80E+11
359.59888	1.66E+11
369.00229	1.65E+11
378.60664	3.09E+11
388.3818	6.88E+11
398.28756	2.94E+12
408.30379	8.04E+12
418.40043	1.52E+13
428.55732	2.38E+13
438.75444	3.23E+13
448.98166	4.08E+13
459.20889	5.40E+13
469.42608	6.33E+13
479.63319	6.69E+13
489.82025	6.89E+13
499.9872	8.39E+13
510.11399	1.01E+14
520.2106	1.14E+14
530.27711	1.24E+14
540.31345	1.31E+14
550.31962	1.33E+14
560.29574	1.44E+14
570.2517	1.40E+14
580.1876	1.41E+14
590.1235	1.38E+14
600.04928	1.27E+14
609.96513	1.10E+14
619.90097	8.59E+13
629.84692	6.06E+13
639.81293	4.40E+13
649.79905	3.43E+13
659.82533	2.27E+13
669.88178	1.47E+13
679.97846	9.39E+12
690.10518	5.35E+12
700.29224	2.73E+12
710.50941	1.36E+12
720.7668	6.58E+11
731.07441	3.18E+11
741.41213	1.60E+11
751.76996	7.72E+10
762.14791	3.43E+10
772.53585	1.65E+10
782.91379	6.71E+09
793.28168	6.31E+09
803.58929	5.72E+09
829.05688	-9.20E+08
853.69066	-1.83E+09
876.92798	5.52E+09
900.60734	5.23E+09
925.70322	2.59E+09
950.80915	7.61E+09
975.90509	1.15E+09
1001.011	-8.29E+09
1026.1069	-1.33E+10
1051.2028	-9.99E+09
1076.3088	-3.82E+08
1101.4046	8.61E+09

MI 105, -10C

Wavelength	Response
350.45665	1.39E+11
359.59888	7.68E+10
369.00229	7.61E+10
378.60664	2.20E+11
388.3818	4.84E+11
398.28756	2.12E+12
408.30379	6.11E+12
418.40043	1.23E+13
428.55732	1.98E+13
438.75444	2.78E+13
448.98166	3.57E+13
459.20889	4.75E+13
469.42608	5.67E+13
479.63319	6.08E+13
489.82025	6.28E+13
499.9872	7.63E+13
510.11399	9.12E+13
520.2106	1.02E+14
530.27711	1.13E+14
540.31345	1.20E+14
550.31962	1.24E+14
560.29574	1.35E+14
570.2517	1.32E+14
580.1876	1.31E+14
590.1235	1.28E+14
600.04928	1.18E+14
609.96513	1.03E+14
619.90097	8.00E+13
629.84692	5.63E+13
639.81293	4.11E+13
649.79905	3.20E+13
659.82533	2.12E+13
669.88178	1.37E+13
679.97846	8.87E+12
690.10518	5.14E+12
700.29224	2.67E+12
710.50941	1.35E+12
720.7668	6.70E+11
731.07441	3.24E+11
741.41213	1.55E+11
751.76996	7.51E+10
762.14791	3.17E+10
772.53585	8.70E+09
782.91379	1.74E+08
793.28168	-6.63E+09
803.58929	-1.07E+10
829.05688	-6.00E+09
853.69066	-1.14E+10
876.92798	-9.99E+09
900.60734	-5.67E+09
925.70322	-1.29E+10
950.80915	-2.12E+10
975.90509	-1.31E+10
1001.011	-1.56E+10
1026.1069	-2.68E+10
1051.2028	-2.16E+10
1076.3088	-2.16E+10
1101.4046	-2.95E+10

MI 105, +5C

Wavelength	Response
349.50275	6.46E+10
359.5421	4.90E+10
369.58147	7.09E+10
379.62085	2.32E+11
389.66019	4.52E+11
399.69957	1.85E+12
409.73894	5.45E+12
419.77829	1.08E+13
429.81766	1.75E+13
439.857	2.44E+13
449.89638	3.15E+13
459.93575	4.24E+13
469.9751	5.13E+13
480.01447	5.54E+13
490.05385	5.72E+13
500.09319	6.95E+13
510.13257	8.34E+13
520.17191	9.50E+13
530.21131	1.05E+14
540.25066	1.13E+14
550.29	1.15E+14
560.32935	1.25E+14
570.36875	1.22E+14
580.4081	1.20E+14
590.44744	1.17E+14
600.48685	1.08E+14
610.52619	9.45E+13
620.56553	7.37E+13
630.60494	5.15E+13
640.64428	3.84E+13
650.68363	2.97E+13
660.72303	1.99E+13
670.76238	1.31E+13
680.80172	8.51E+12
690.84113	4.94E+12
700.88047	2.60E+12
710.91981	1.34E+12
720.95916	6.67E+11
730.99856	3.26E+11
741.03791	1.66E+11
751.07725	7.46E+10
761.11666	1.97E+10
771.156	-5.52E+09
781.19534	-1.66E+10
791.23475	-1.97E+10
801.27409	-1.47E+10
826.37248	-1.79E+10
851.47094	-2.41E+10
876.56933	-2.52E+10
901.66772	-2.02E+10
926.76611	-2.81E+10
951.86456	-4.21E+10
976.96295	-4.26E+10
1002.0613	-5.69E+10
1027.1597	-3.26E+10
1052.2581	-5.47E+10
1077.3566	-5.79E+10
1102.455	-4.53E+10

MI 110, -55C

Wavelength	Response
349.95424	1.39E+11
359.95039	1.01E+11
369.94656	1.19E+11
379.94274	3.30E+11
389.93888	8.93E+11
399.93506	3.14E+12
409.9312	7.63E+12
419.92738	1.35E+13
429.92356	2.05E+13
439.9197	2.73E+13
449.91588	3.44E+13
459.91202	4.57E+13
469.9082	5.23E+13
479.90437	5.68E+13
489.90052	5.96E+13
499.8967	7.45E+13
509.89284	8.94E+13
519.88899	9.89E+13
529.88516	1.06E+14
539.88134	1.15E+14
549.87751	1.15E+14
559.87369	1.23E+14
569.8698	1.19E+14
579.86598	1.16E+14
589.86216	1.11E+14
599.85833	1.02E+14
609.85451	8.28E+13
619.85062	6.16E+13
629.8468	4.36E+13
639.84298	3.44E+13
649.83915	2.94E+13
659.83533	2.07E+13
669.83144	1.41E+13
679.82762	9.07E+12
689.82379	4.96E+12
699.81997	2.44E+12
709.81615	1.24E+12
719.81226	6.18E+11
729.80844	3.01E+11
739.80461	1.46E+11
749.80079	6.78E+10
759.79696	2.83E+10
769.79308	1.15E+10
779.78925	2.95E+09
789.78543	7.48E+08
799.78161	1.69E+08
824.77202	66353392
849.76242	-1.01E+09
874.75283	1.01E+09
899.74324	5.74E+08
924.73365	-7.62E+08
949.72406	7.14E+08
974.71447	-2.41E+09
999.70488	-1.38E+09
1024.6953	-4.16E+09
1049.6857	1.75E+09
1074.6761	4.54E+09
1099.6665	4.30E+09

MI 110, -10C

Wavelength	Response
349.95424	1.02E+11
359.95039	6.52E+10
369.94656	9.14E+10
379.94274	3.02E+11
389.93888	7.21E+11
399.93506	2.32E+12
409.9312	5.92E+12
419.92738	1.09E+13
429.92356	1.71E+13
439.9197	2.36E+13
449.91588	2.97E+13
459.91202	3.94E+13
469.9082	4.57E+13
479.90437	4.96E+13
489.90052	5.19E+13
499.8967	6.48E+13
509.89284	7.93E+13
519.88899	9.02E+13
529.88516	9.89E+13
539.88134	1.08E+14
549.87751	1.10E+14
559.87369	1.21E+14
569.8698	1.19E+14
579.86598	1.17E+14
589.86216	1.12E+14
599.85833	1.02E+14
609.85451	8.27E+13
619.85062	6.03E+13
629.8468	4.21E+13
639.84298	3.27E+13
649.83915	2.78E+13
659.83533	1.96E+13
669.83144	1.34E+13
679.82762	8.72E+12
689.82379	4.84E+12
699.81997	2.40E+12
709.81615	1.23E+12
719.81226	6.25E+11
729.80844	3.11E+11
739.80461	1.58E+11
749.80079	7.80E+10
759.79696	3.46E+10
769.79308	1.29E+10
779.78925	4.79E+09
789.78543	9.09E+08
799.78161	8.21E+08
824.77202	-1.29E+09
849.76242	9.12E+08
874.75283	-1.26E+09
899.74324	-5.01E+09
924.73365	-4.55E+08
949.72406	7.61E+08
974.71447	-4.05E+08
999.70488	-6.91E+09
1024.6953	-7.13E+09
1049.6857	-1.04E+10
1074.6761	-5.31E+09
1099.6665	-2.03E+09

MI 110, +5C

Wavelength	Response
349.95424	8.54E+10
359.95039	5.36E+10
369.94656	8.11E+10
379.94274	2.85E+11
389.93888	6.80E+11
399.93506	2.09E+12
409.9312	5.38E+12
419.92738	1.01E+13
429.92356	1.59E+13
439.9197	2.21E+13
449.91588	2.80E+13
459.91202	3.73E+13
469.9082	4.36E+13
479.90437	4.75E+13
489.90052	4.98E+13
499.8967	6.21E+13
509.89284	7.62E+13
519.88899	8.72E+13
529.88516	9.56E+13
539.88134	1.05E+14
549.87751	1.07E+14
559.87369	1.17E+14
569.8698	1.15E+14
579.86598	1.12E+14
589.86216	1.08E+14
599.85833	9.87E+13
609.85451	7.97E+13
619.85062	5.82E+13
629.8468	4.05E+13
639.84298	3.16E+13
649.83915	2.69E+13
659.83533	1.90E+13
669.83144	1.30E+13
689.82379	4.73E+12
699.81997	2.36E+12
709.81615	1.21E+12
719.81226	6.23E+11
729.80844	3.10E+11
739.80461	1.57E+11
749.80079	7.47E+10
759.79696	3.18E+10
769.79308	1.28E+10
779.78925	-55141550
789.78543	-6.54E+09
799.78161	-3.21E+09
824.77202	-7.53E+09
849.76242	-6.30E+09
874.75283	-1.29E+10
899.74324	-1.41E+10
924.73365	-7.80E+09
949.72406	-1.54E+10
974.71447	-2.00E+10
999.70488	-1.81E+10
1024.6953	-1.72E+10
1049.6857	-4.36E+10
1074.6761	-3.36E+10
1099.6665	-3.80E+10

APPENDIX K: FIBER ILLUMINATOR CALIBRATION

Table 20.1. Litescope fiber illuminator brightness calibration 6/19/02

Red 2 radiometer

	dial setting	dial setting	dial setting	dial setting	dial setting		Offset corrected	
filter (nm)	off	2.5 down	2 down	1 down	scribe	scribe/2.5	2.5 down	1 down
350	0.26	0.12	0.64	3.97	15.30	1.3E+02	0.00	3.71
400	0.25	0.08	3.40	130.30	1780.00	2.2E+04	0.00	130.05
450	0.24	0.20	19.90	810.00	6880.00	3.4E+04	0.00	809.76
500	0.23	1.08	122.00	2950.00	21300.00	2.0E+04	0.85	2949.77
550	0.13	2.38	310.00	6700.00	31100.00	1.3E+04	2.25	6699.87
600	0.09	7.80	690.00	9700.00	45800.00	5.9E+03	7.71	9699.91
650	0.10	27.00	1440.00	14900.00	55300.00	2.0E+03	26.90	14899.90
700	0.12	36.00	1090.00	12800.00	49700.00	1.4E+03	35.88	12799.88
750	0.13	20.30	500.00	5600.00	18600.00	9.2E+02	20.17	5599.87
800	0.10	18.24	470.00	3750.00	11130.00	6.1E+02	18.14	3749.90
850	0.10	24.90	610.00	3870.00	11200.00	4.5E+02	24.80	3869.90
900	0.13	37.30	760.00	3600.00	9750.00	2.6E+02	37.17	3599.87
950	0.11	20.60	310.00	2050.00	5160.00	2.5E+02	20.49	2049.89
1000	0.29	11.50	127.20	660.00	1720.00	1.5E+02	11.21	659.71
1050	0.16	4.18	37.40	200.00	500.00	1.2E+02	4.03	199.85
1100	0.29	2.20	16.40	63.30	153.40	7.0E+01	1.91	63.01

Stray light and blooming images were taken at the “1 down” and “2.5 down” settings. The ratio of the fiber intensity at “1 down” to the intensity at “2.5 down”, weighted by the MI spectral response, is 1106.

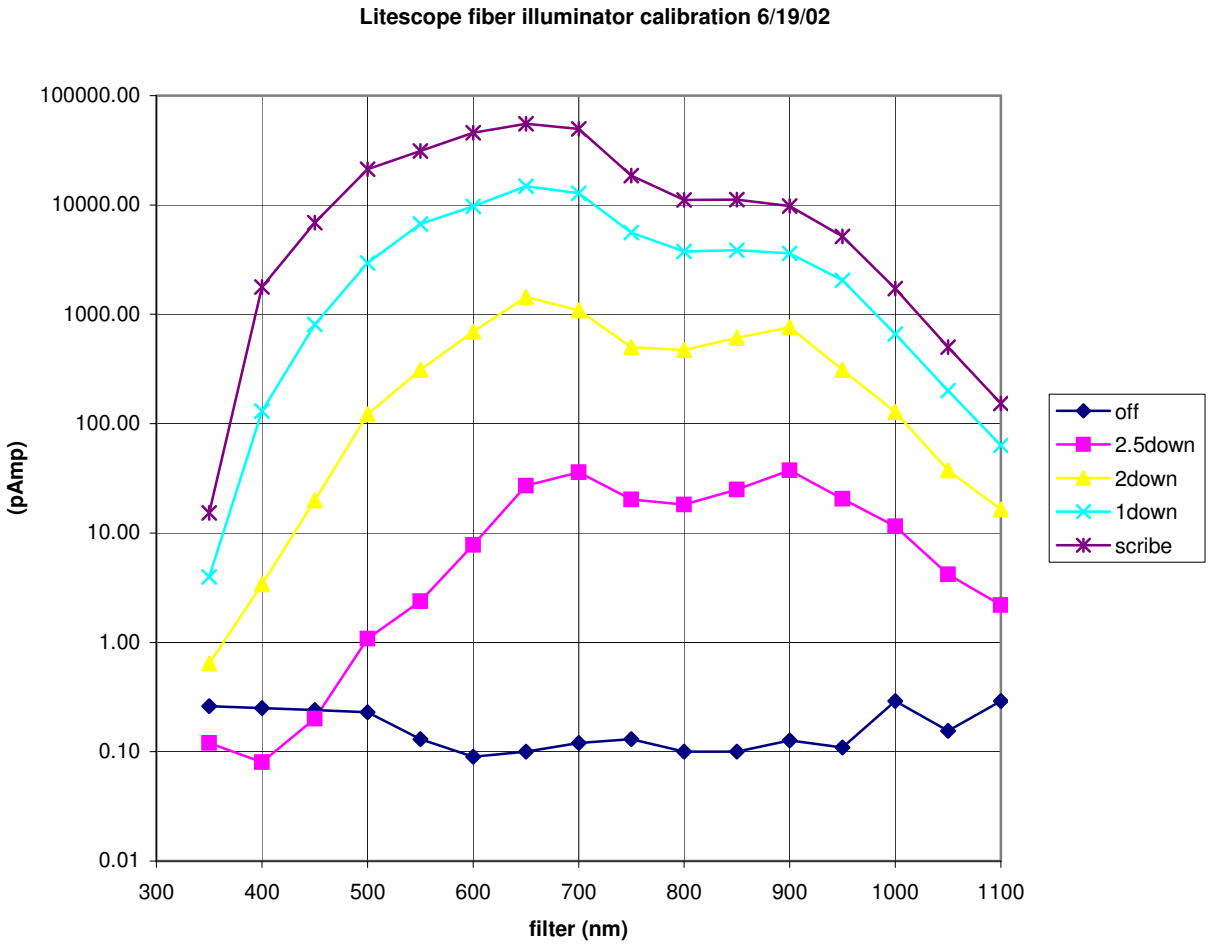

Figure 20.1. Raw data from fiber illuminator calibration.

APPENDIX L: MODULATION TRANSFER FUNCTION DATA

MTF for MI_105 Image Sequence

The Modulation Transfer Function (MTF) curves for the MI_105 image sequence, prior to vibration and thermal/vacuum testing, were calculated based on 4 sub-sampled images from 17 images of a bar target and using the VICAR application program OTF1. The 17 images were acquired with the CCD positioned 88 – 112 mm from the target. The images acquired when the CCD was 102 and 103 mm from the target have the highest MTF. The MTF curves returned by the OTF1 software indicate that there is aliasing present in the images acquired at 100 – 106 mm based on the fact that the MTF curves for the sub-samples are not consistent and the MTF curve does not approach zero at Nyquist. The aliasing can be seen in the bar targets; Figure 21.1 shows an example of aliasing. The cleanest MTF curve is from the image acquired 99 mm from the target because the sub-samples are consistent and the curve approaches zero. The MTF curves for the images acquired 112 mm, and from 96 – 88 mm from the target show multiple intersections with the zero axis indicating phase errors. Phase error can be seen in the bar target were the light and dark patterns of the bars reverse to form dark and light patterns. See Figure 21.2 for an example of phase error.

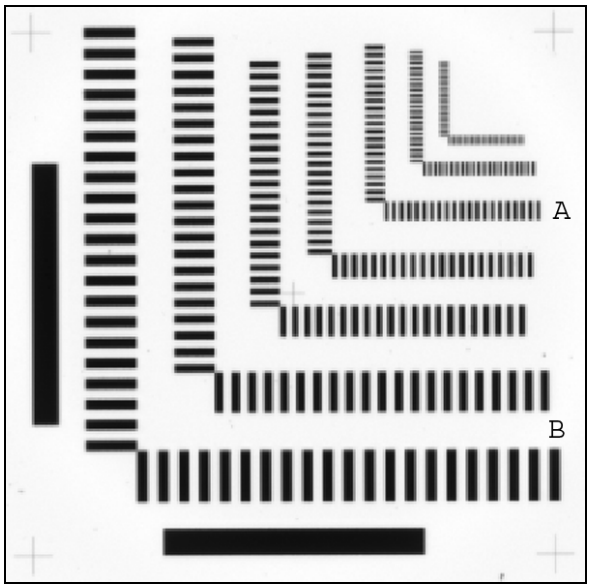

Figure 21.1 Aliasing can be seen in the bars at A, while the bars at B are clean and even.

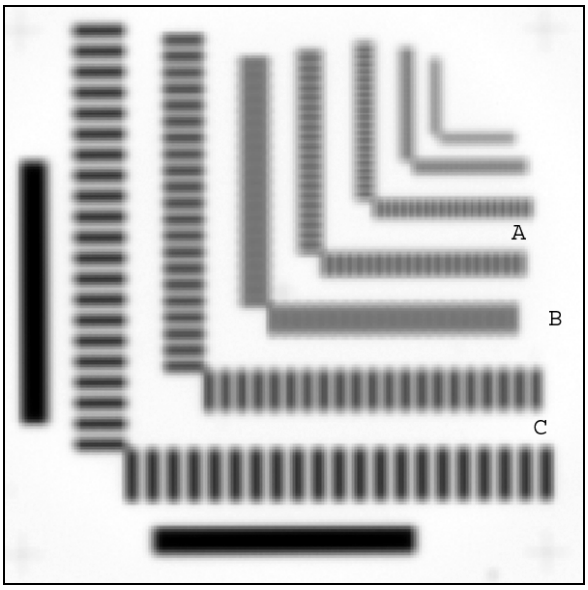

Figure 21.2. Phase errors can be seen in the bars at A, the bars at B have nearly 0 modulation, and the bars at C have no phase error.

Figures 21.3 – 21.19 show the MTF curves at the different positions (-12 to +12, see Table 3.2.8a). An MTF curve is shown for each sub-sampled image and the average of the four sub-sampled images. The standard deviations of the four sub-sampled MTF curves are plotted as error bars. Each figure lists an image number (*e.g.*, 020717173522) and the position (*e.g.*, -3, which corresponds to 103 mm from the target).

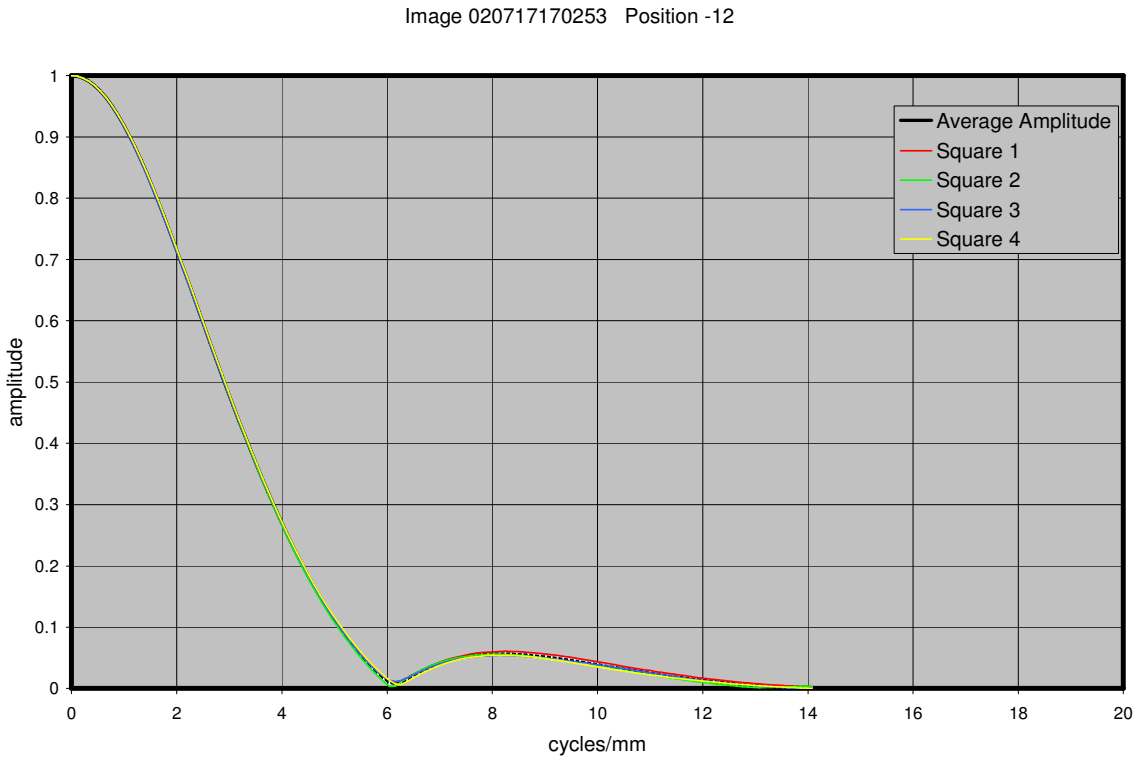

Figure 21.3. MTF curves for image with MI 105 CCD 112 mm from target

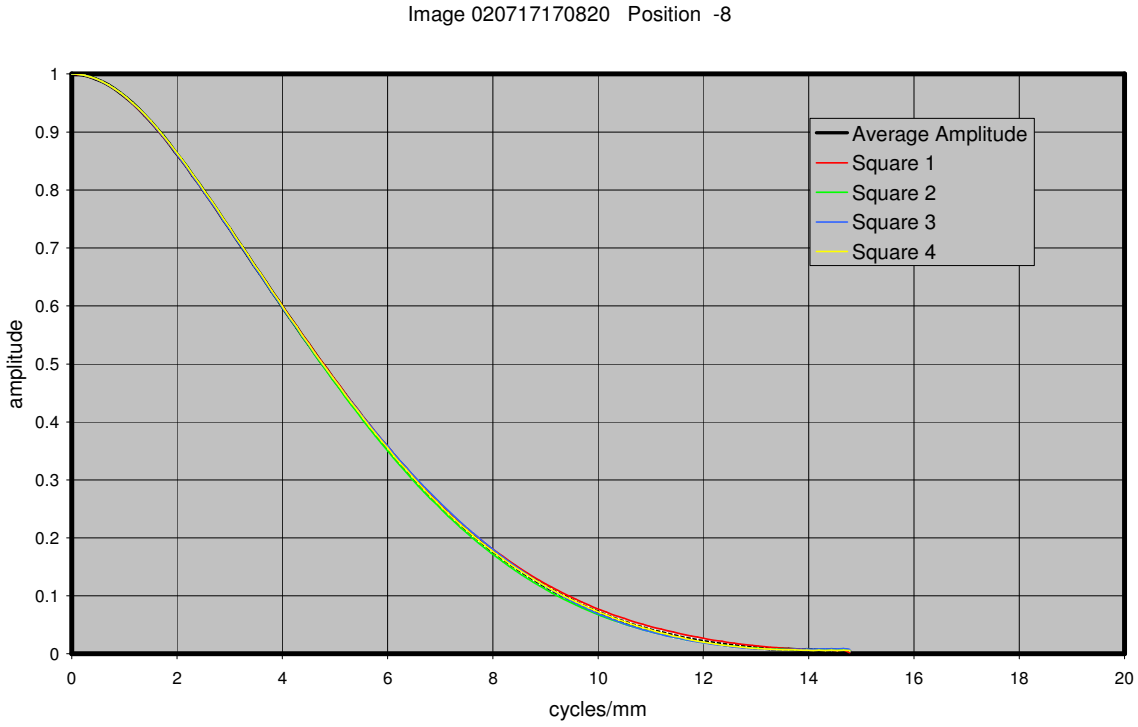

Figure 21.4. MTF curves for image with MI 105 CCD 108 mm from target

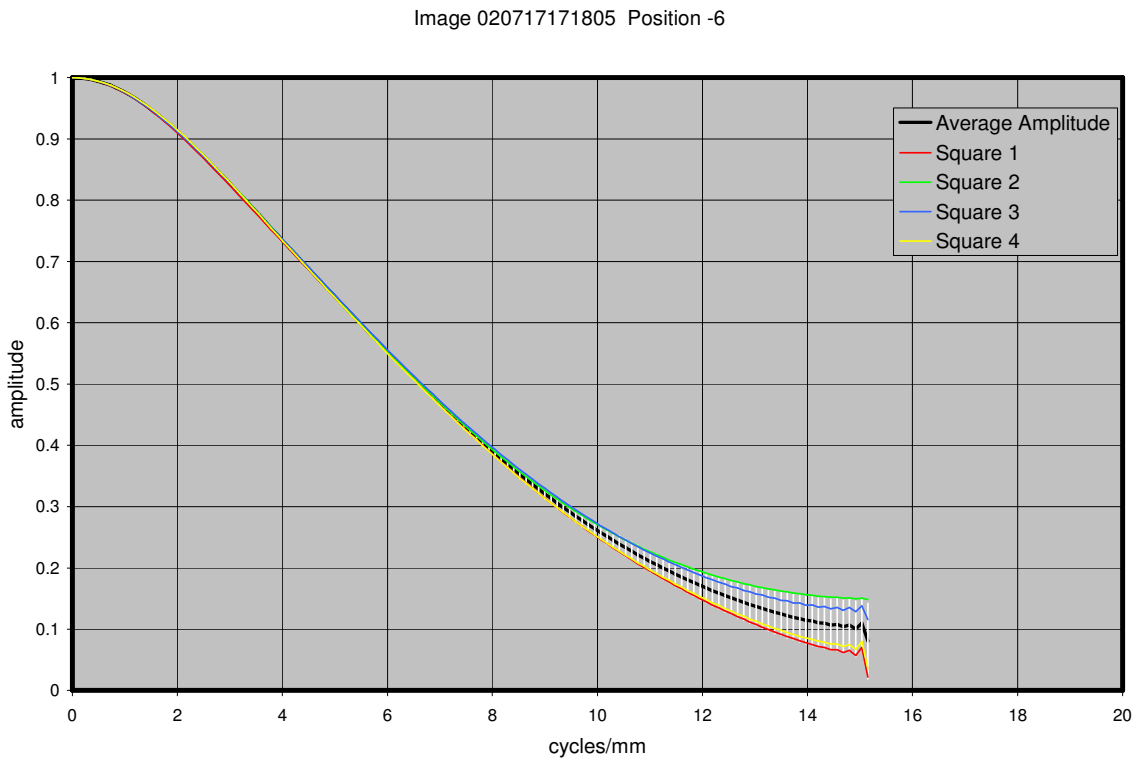

Figure 21.5. MTF curves for image with MI 105 CCD 106 mm from target

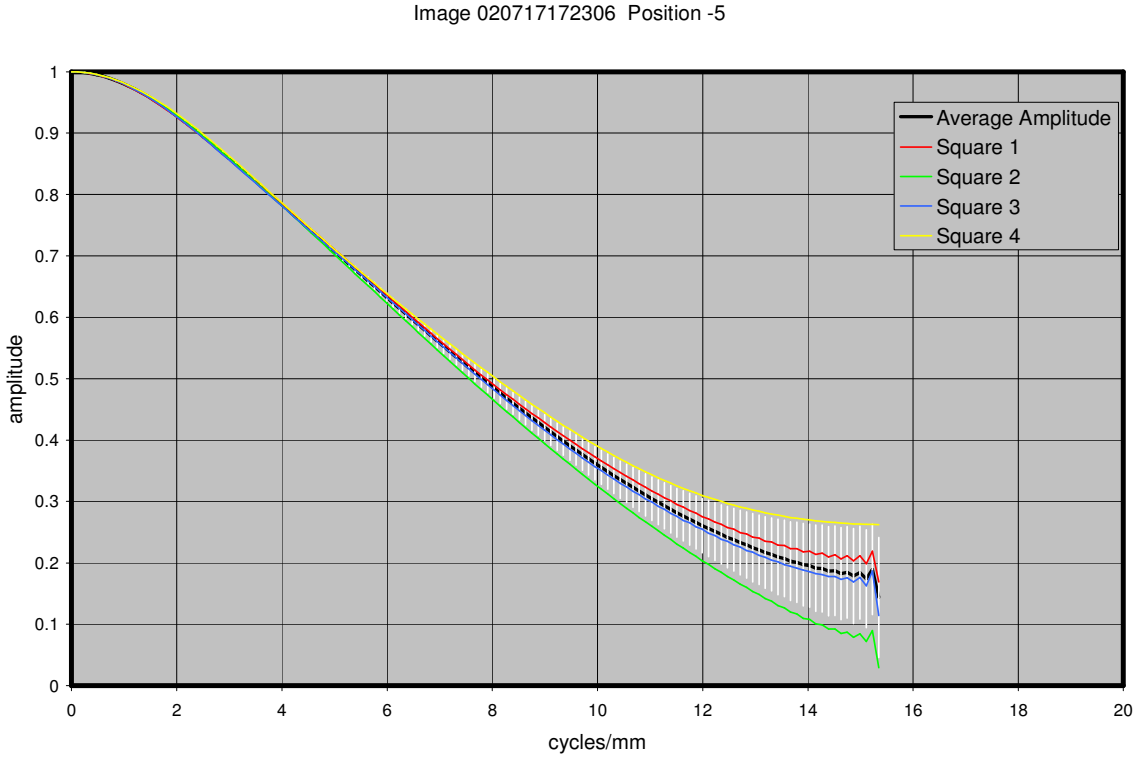

Figure 21.6. MTF curves for image with MI 105 CCD 105 mm from target

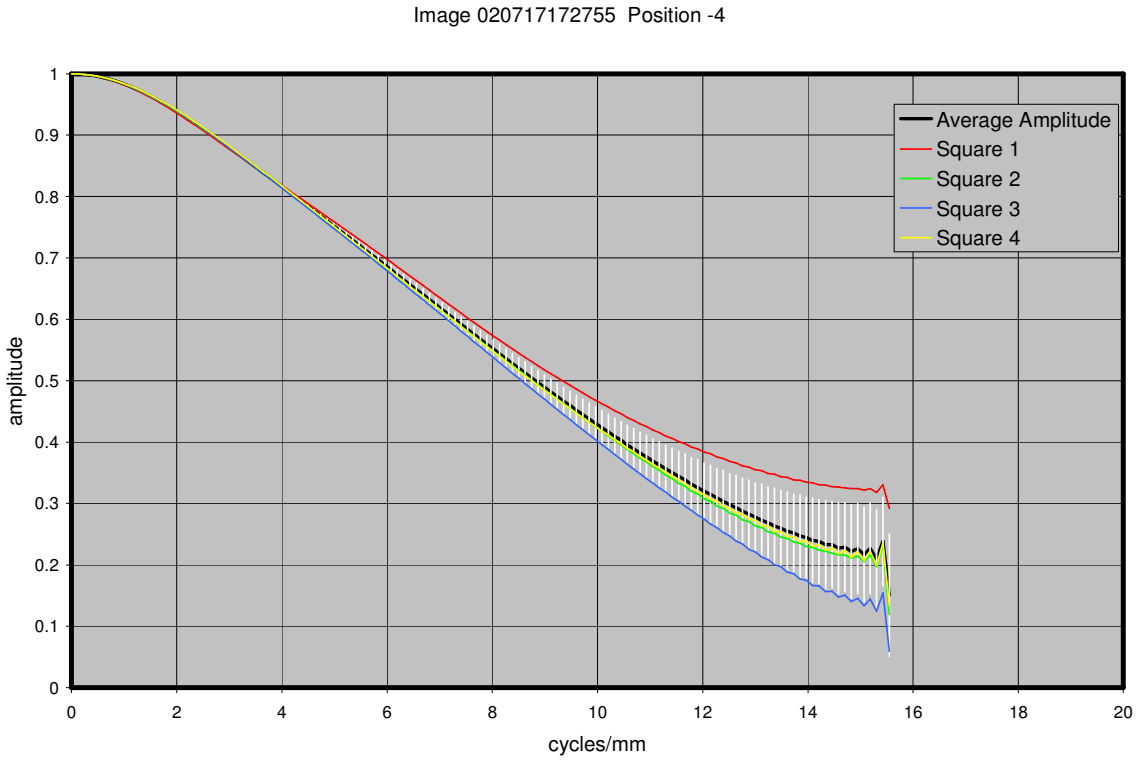

Figure 21.7. MTF curves for image with MI 105 CCD 104 mm from target

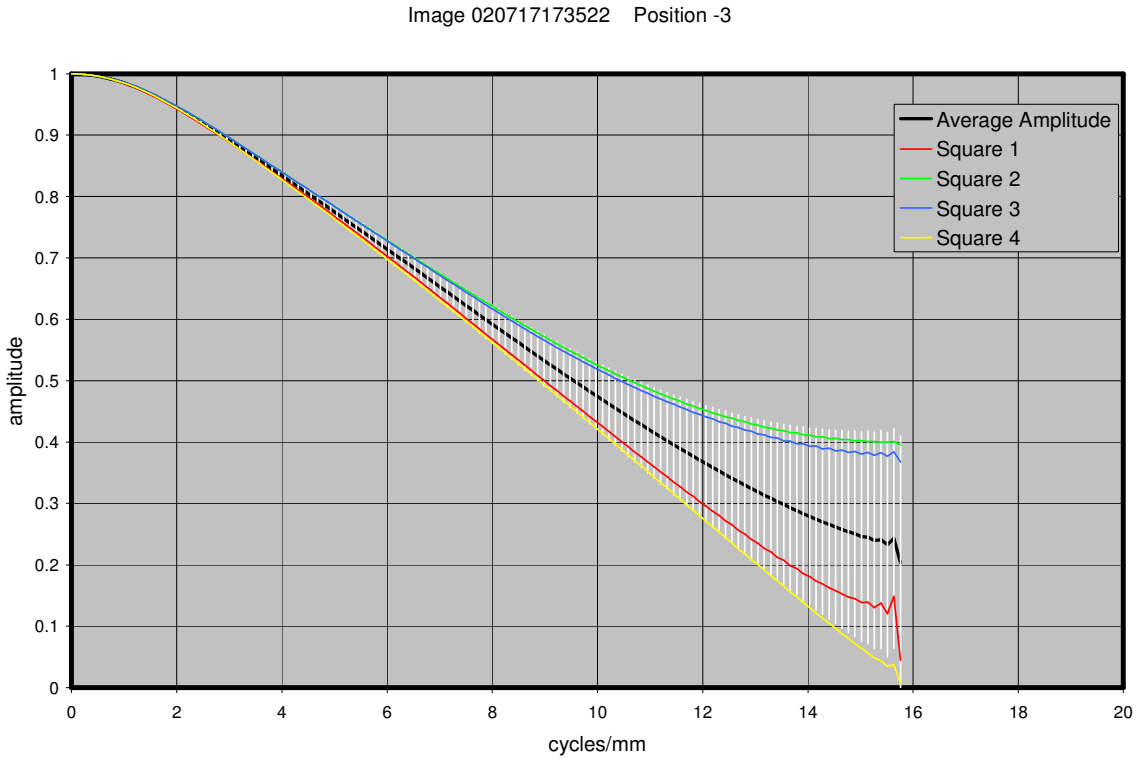

Figure 21.8. MTF curves for image with MI 105 CCD 103 mm from target

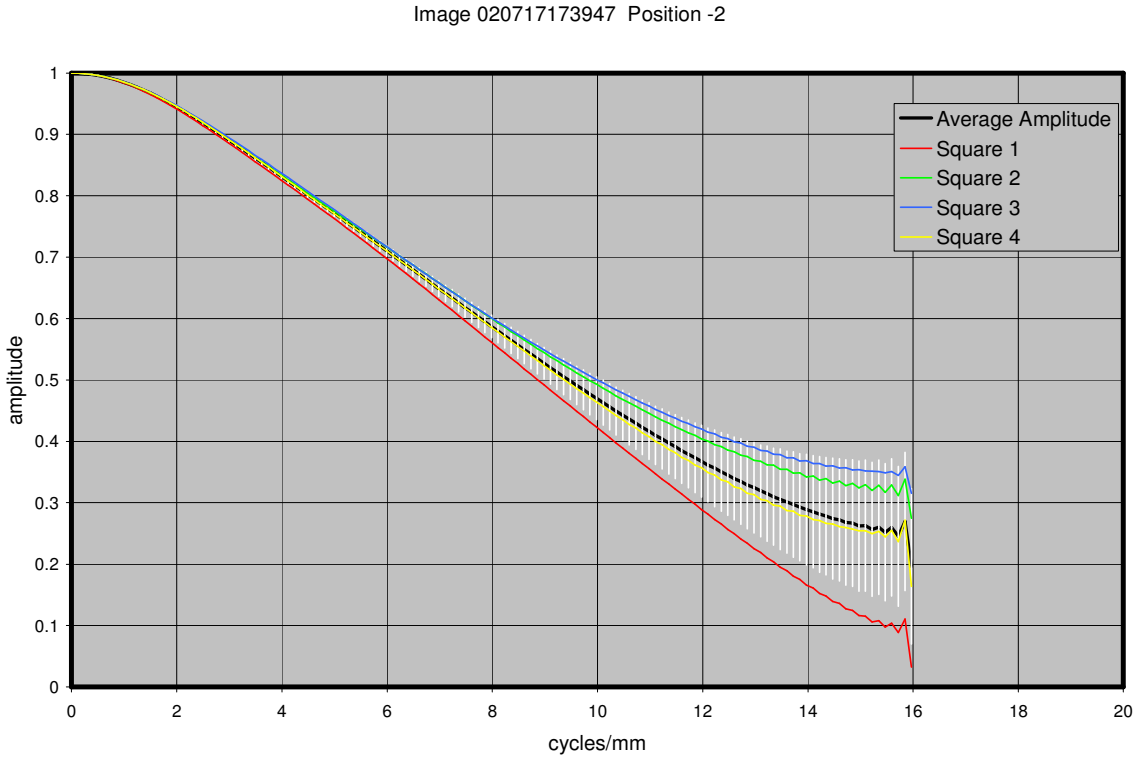

Figure 21.9. MTF curves for image with MI 105 CCD 102 mm from target

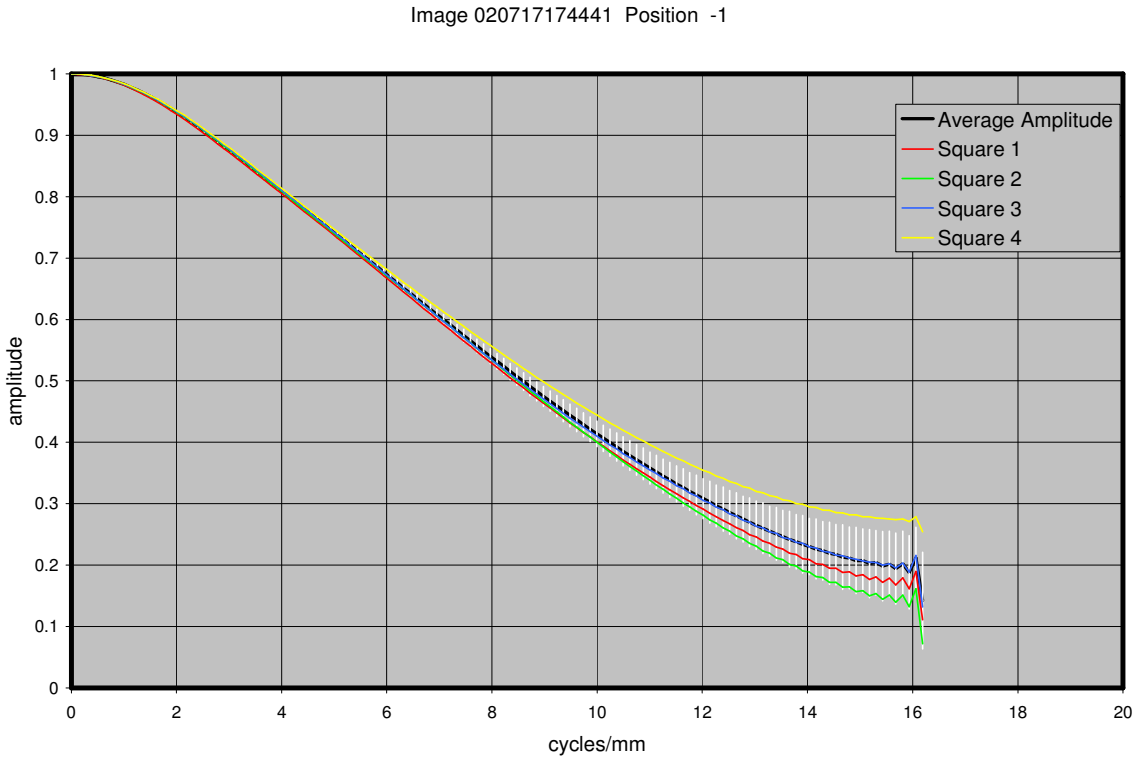

Figure 21.10 MTF curves for image with MI 105 CCD 101 mm from target

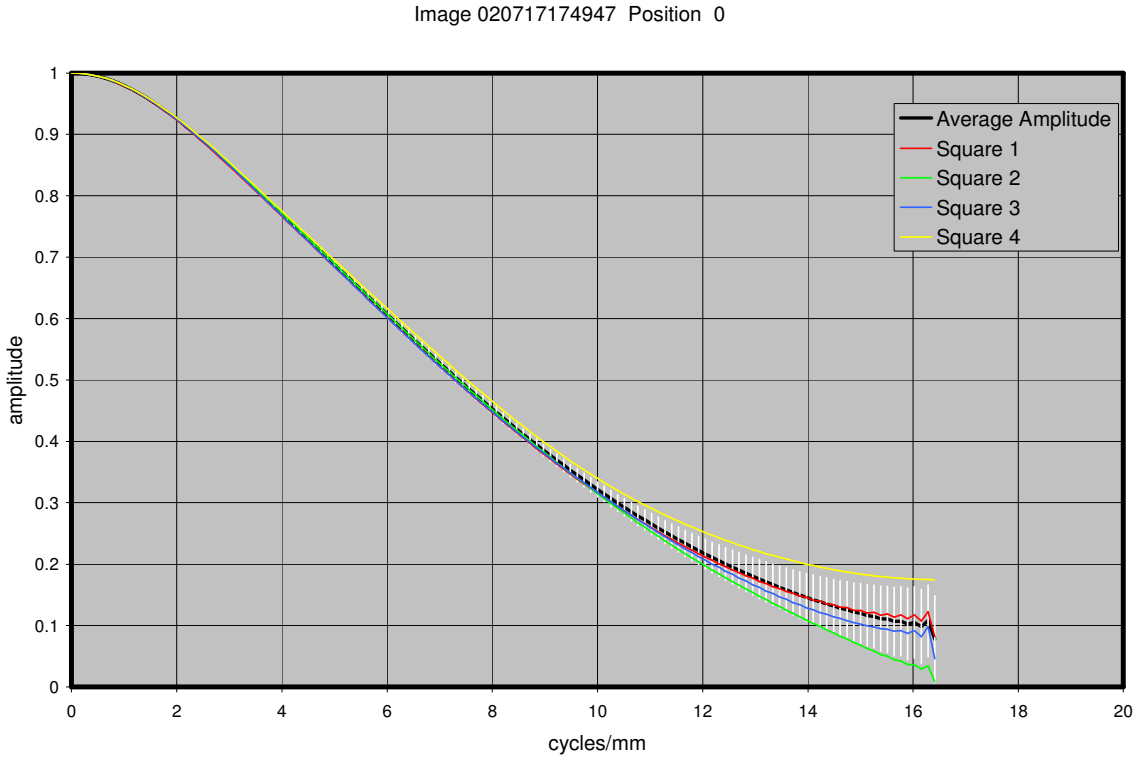

Figure 21.11. MTF curves for image with MI 105 CCD 100 mm from target

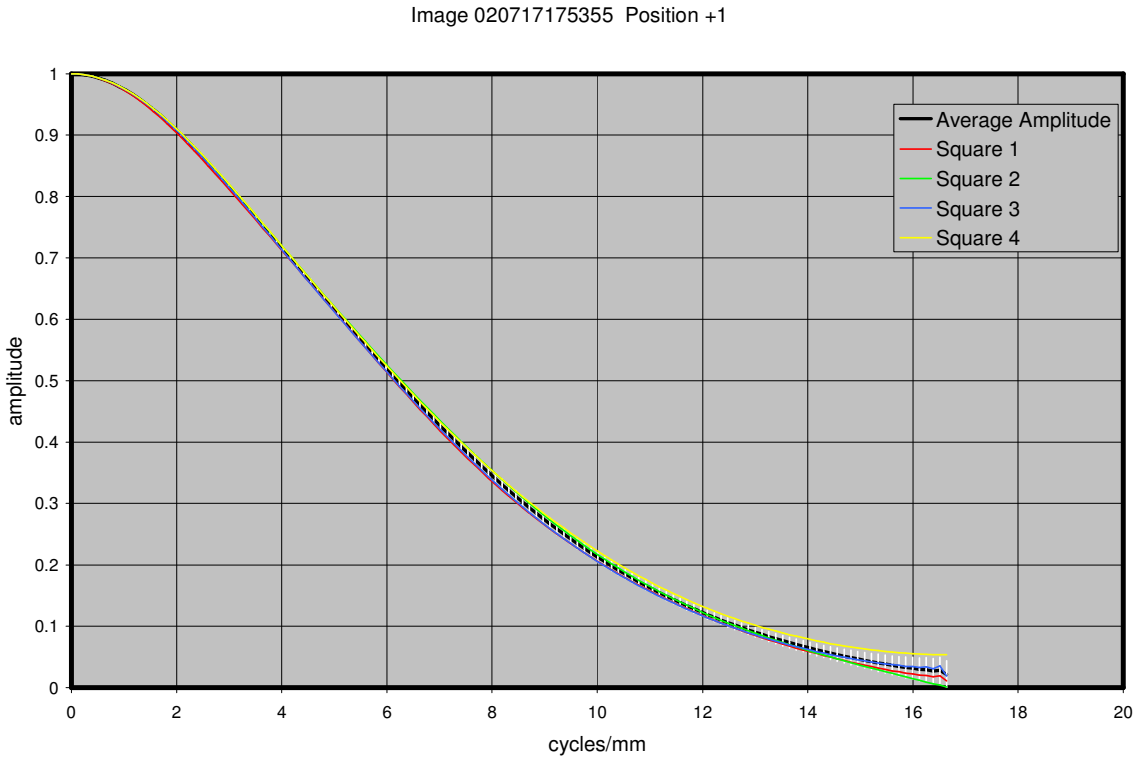

Figure 21.12. MTF curves for image with MI 105 CCD 99 mm from target

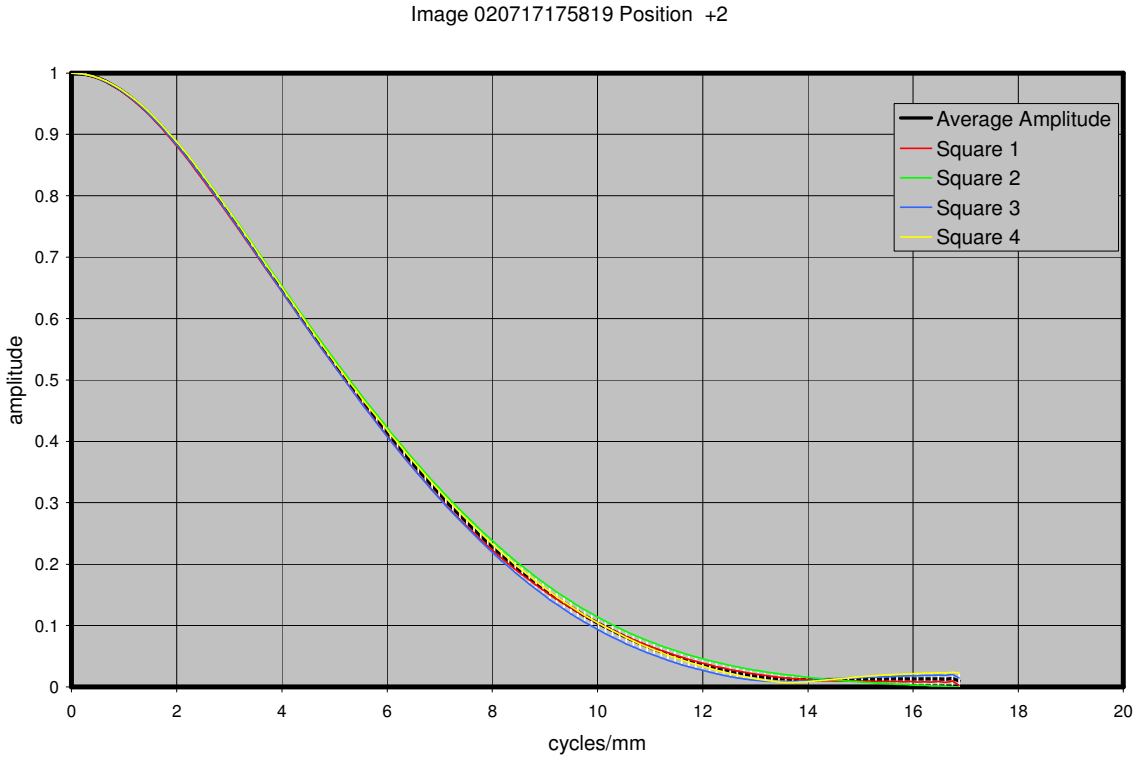

Figure 21.13. MTF curves for image with MI 105 CCD 98 mm from target

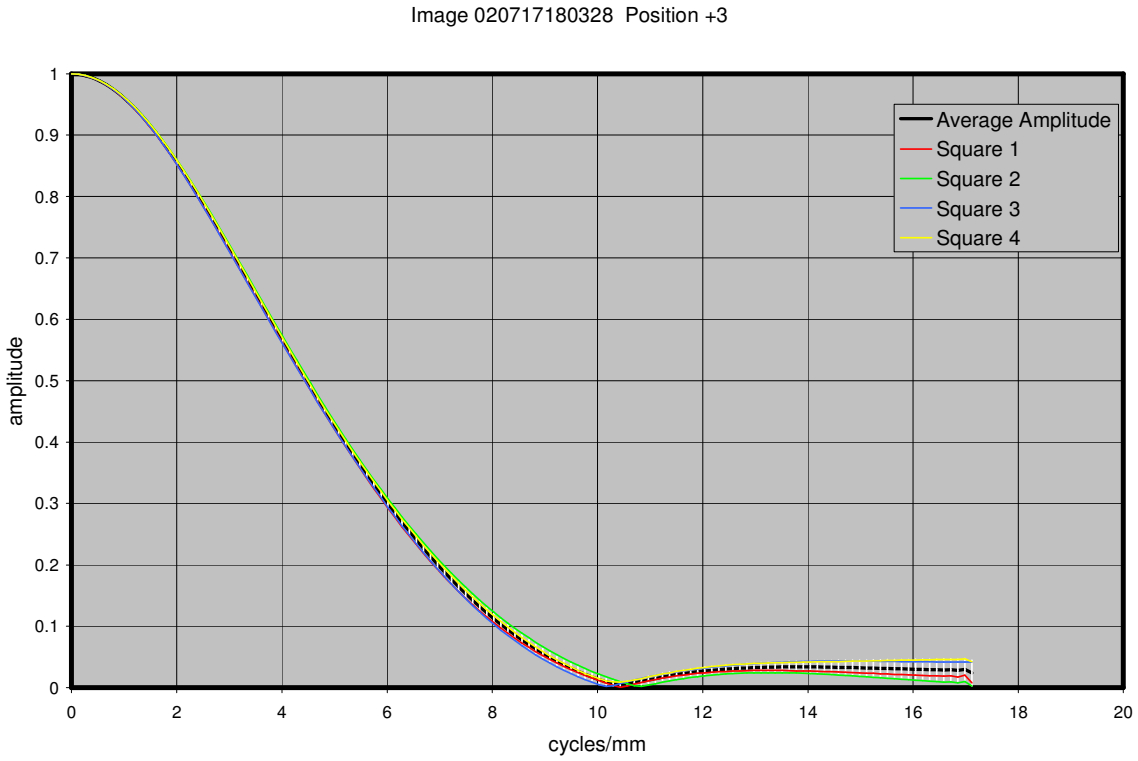

Figure 21.14. MTF curves for image with MI 105 CCD 97 mm from target

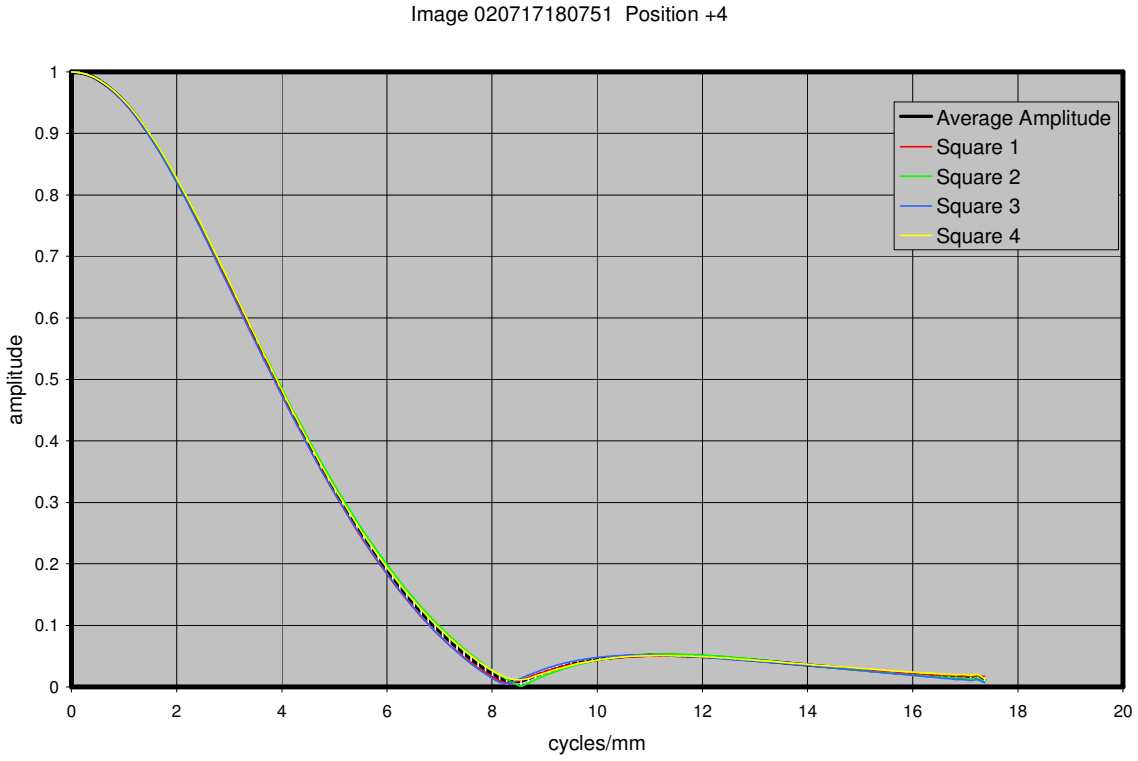

Figure 21.15. MTF curves for image with MI 105 CCD 96 mm from target

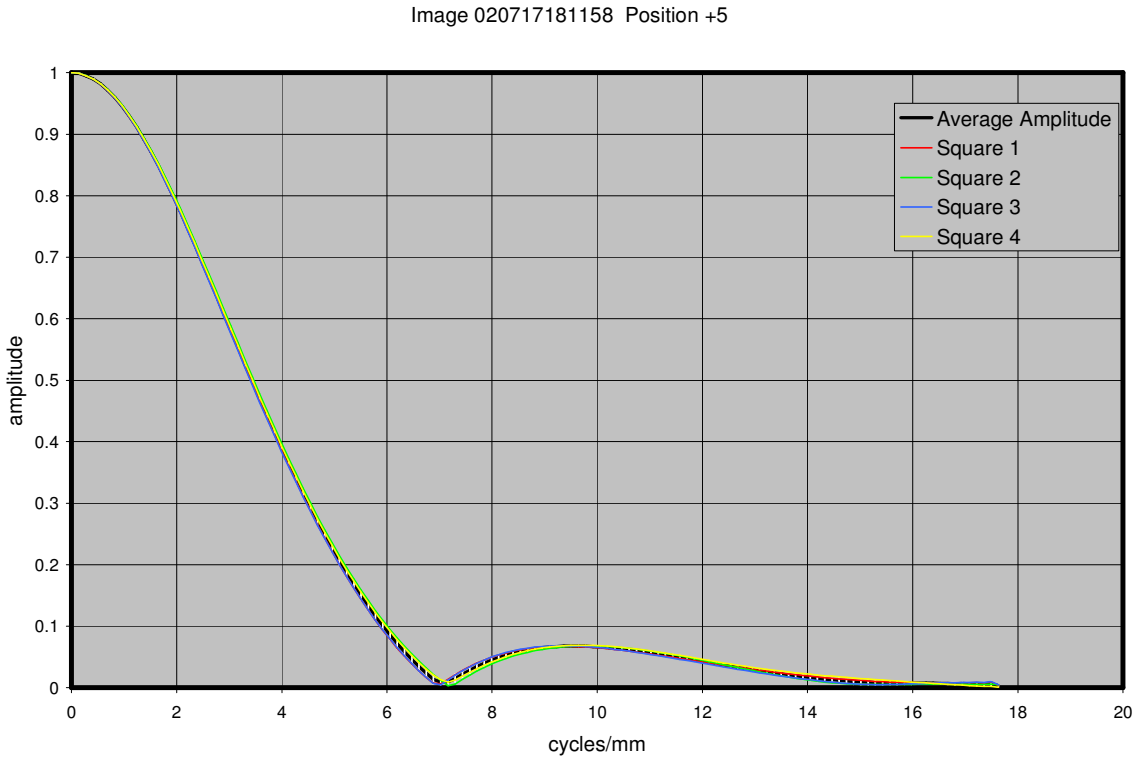

Figure 21.16. MTF curves for image with MI 105 CCD 95 mm from target

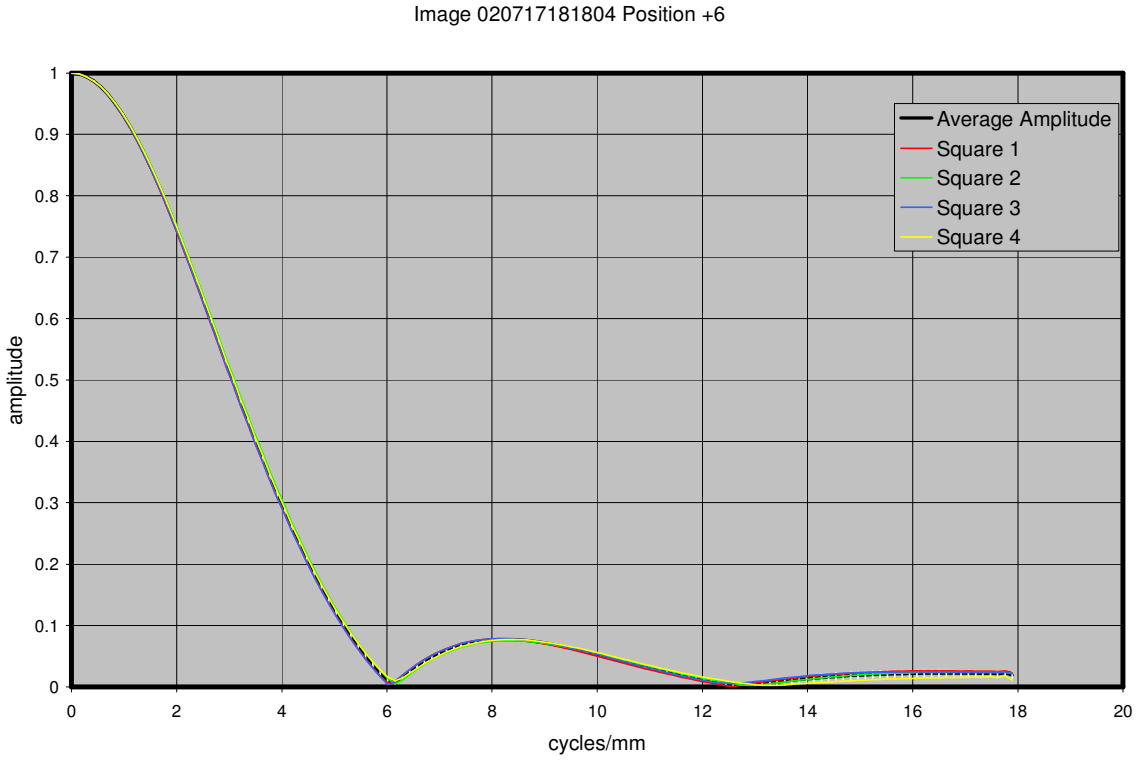

Figure 21.19. MTF curves for image with MI 105 CCD 94 mm from target

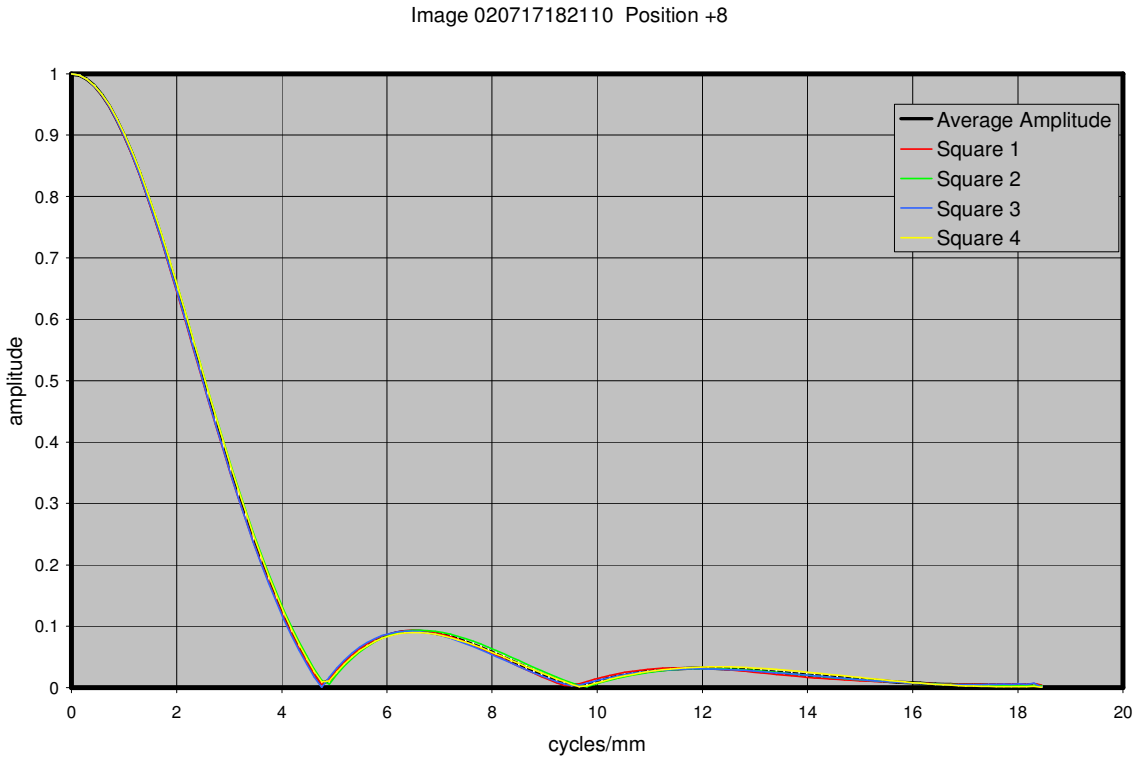

Figure 21.18. MTF curves for image with MI 105 CCD 92 mm from target

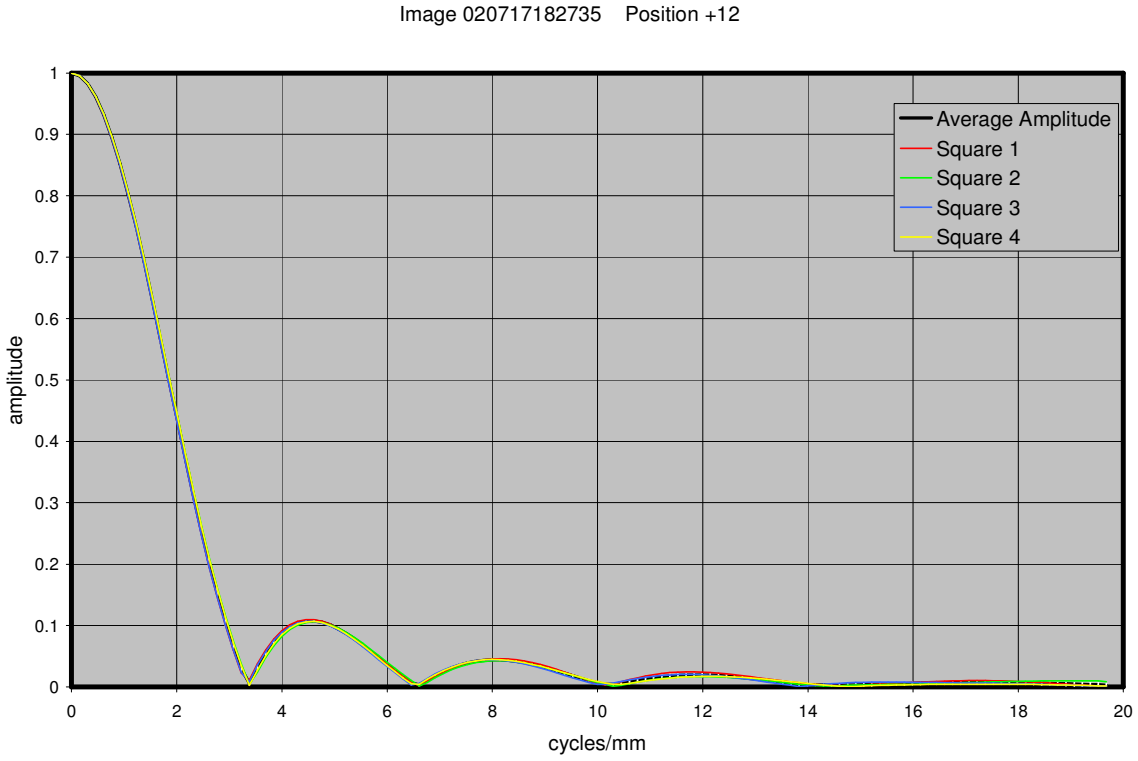

Figure 21.19. MTF curves for image with MI 105 CCD 88 mm from target

MTF for MI_Mod1_105 Image Sequence

The analysis procedure for the MI_MOD1_105 image sequence was similar to the procedure described above for the MI_105 data. The two exceptions are that (1) Not all image positions were used (See Table 3.2.8a) and (2) Multiple images were not acquired at each position, so there was no need to average the bar target images and the zero exposure images.

The MI_MOD1_105 images were acquired after vibration testing. The MTF curves for these images were calculated based on 4 sub-samples from 9 images of a bar target and using the VICAR application program OTF1. The 9 images were acquired with the camera detector positioned 98 – 106 mm from the target.

The images with the highest MTF were taken when the CCD was at 102 and 103 mm from the target. The MTF curves returned by the OTF1 software indicate that there is aliasing present in the images acquired 100 – 106 mm based on the fact that the MTF curves for the sub-samples are not consistent and/or the MTF curve does not approach zero at Nyquist. The aliasing can be seen in the bar targets. The cleanest MTF curve is from the image acquired 99 mm from the target; the sub-samples are consistent and the curve approaches zero.

The average MTF curves for the previous image sequence (Figure 3.2.8c) and this sequence (Figure 21.20), which was acquired after vibration testing, are similar. The highest MTF responses are still from the images acquired when the target was 102 and 103 mm from the CCD. Comparing the MTF curves for images acquired when the target was 106, 105 and 104 mm from the CCD (Figures 21.5, 21.6 and 21.7 against Figures 21.21, 21.22, and 21.23), the average MTF is similar and the error bars based on the standard deviation from the 4 sub-images are similar. At the next 4 positions (103, 102, 101, and 100 mm) the average MTF curves are similar, but the error bars for the MTF curves prior to vibration testing (Figures 21.8, 21.9, 21.10, and 21.11) are larger than the error bars for the MTF curves after vibration testing (Figures 21.24, 21.25, 21.26, and 21.27). The final 2 positions that are in common between the image sequences are when the target was 99 and 98 mm from the target (Figures 21.12 and 21.13 vs. Figures 21.28 and 21.29); here the average MTF curves are similar. They approach zero with very little difference between the MTF curves for the 4 sub-images, indicating an absence of aliasing.

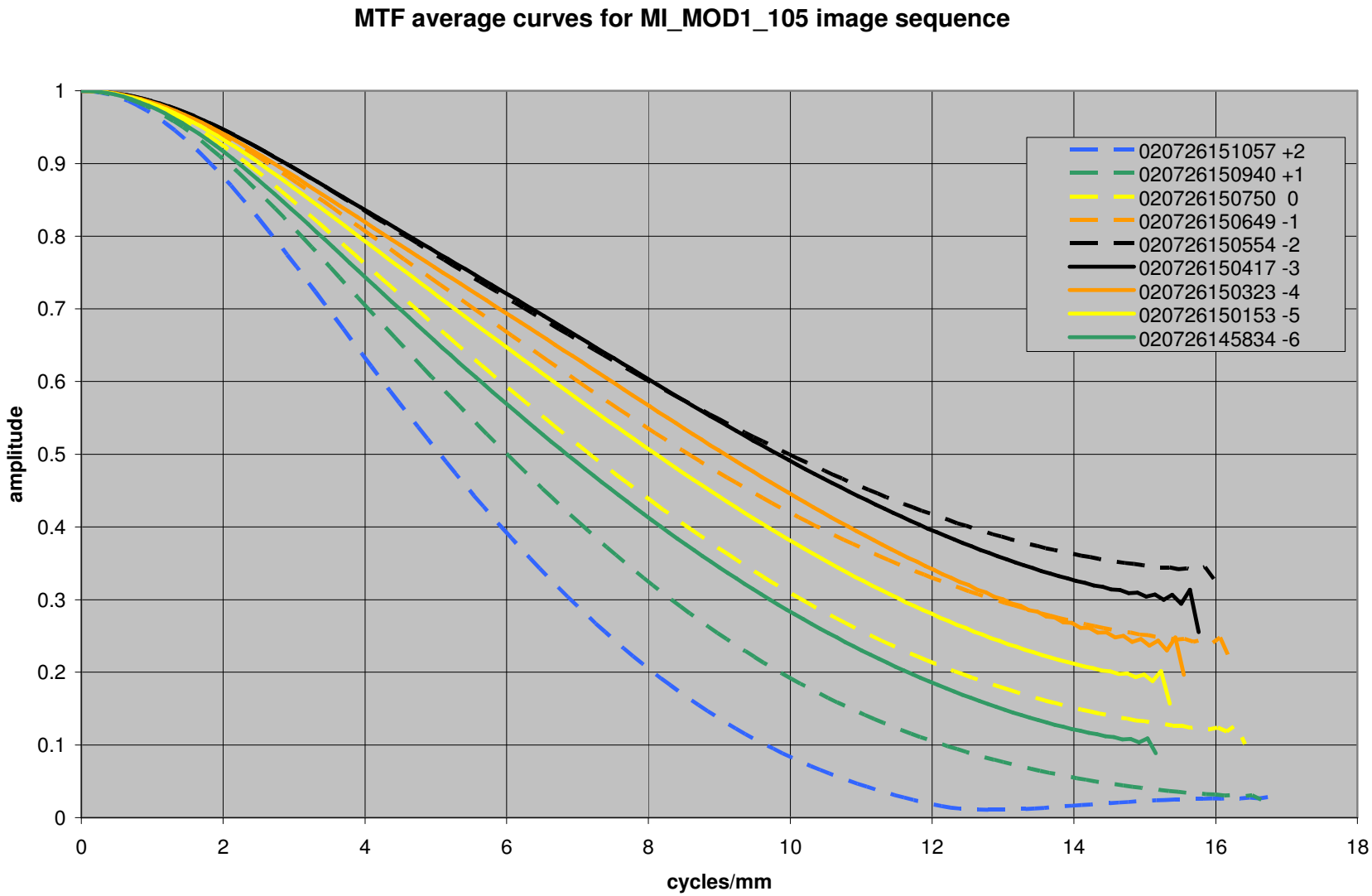

Figure 21.20. MTF average curves for MI_MOD1_105 image sequence. Each curve shows data for positions (in mm) relative to target distance from CCD of 100 mm.

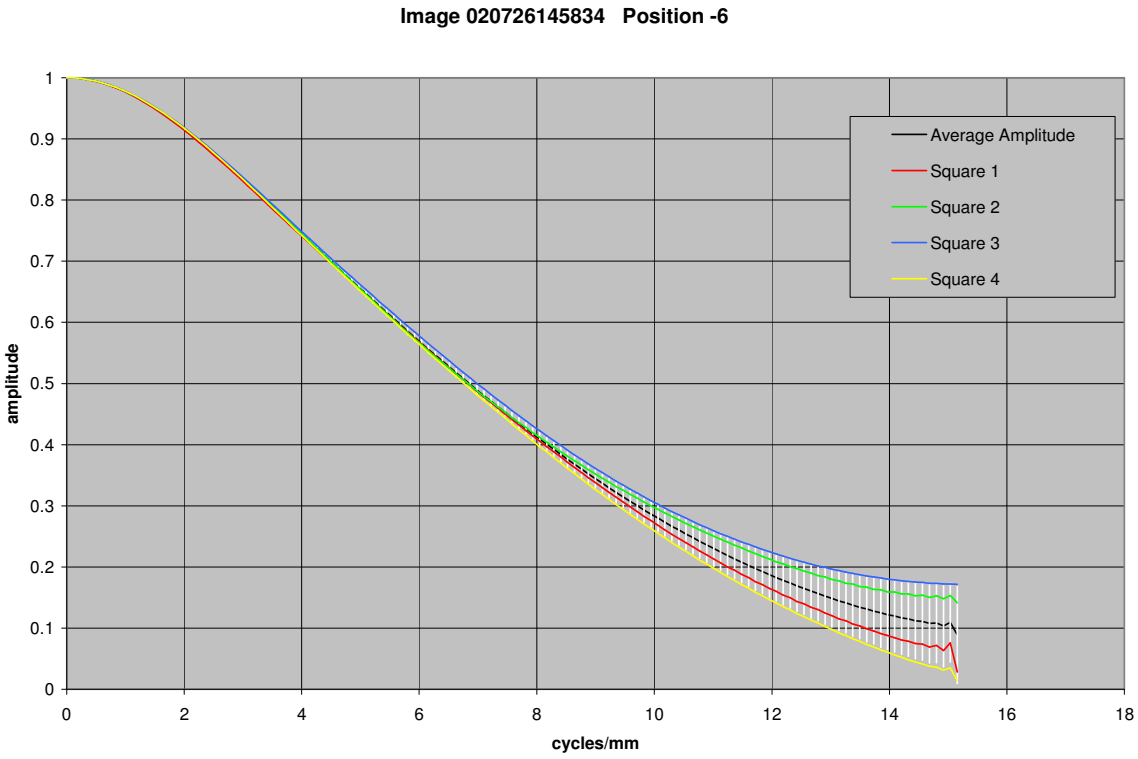

1.

Figure 21.21. MTF curves for image with MI 105 CCD 106 mm from target

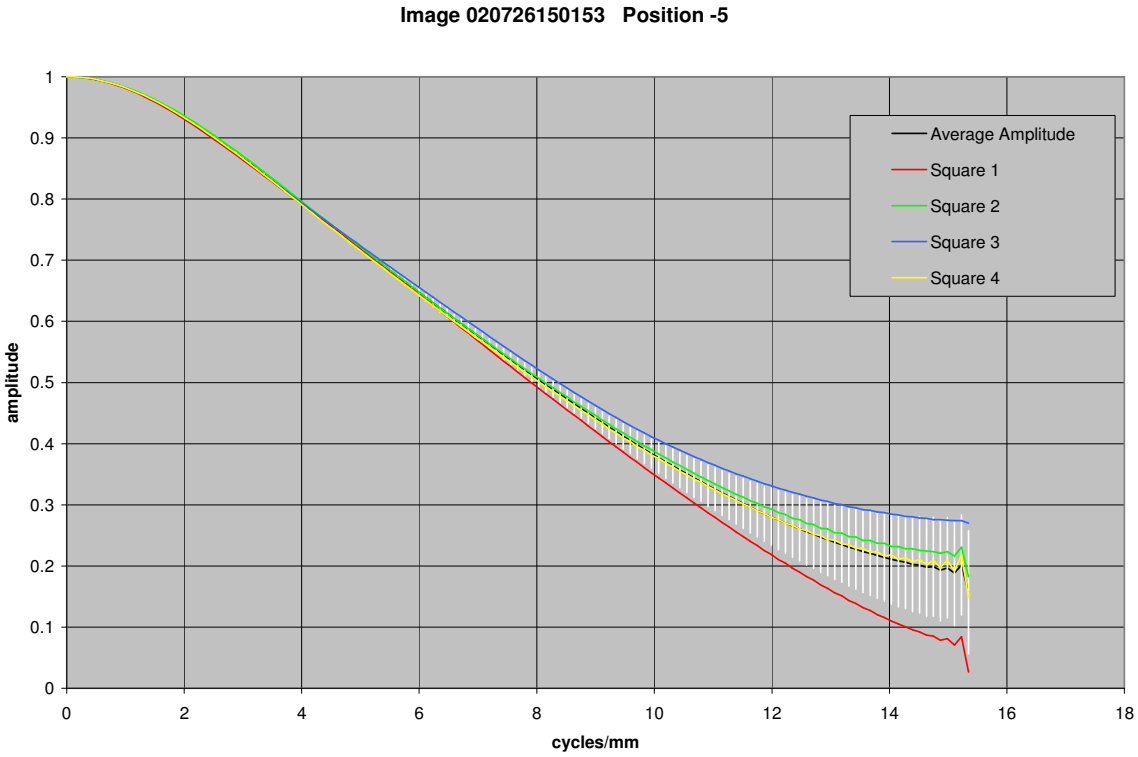

Figure 21.22. MTF curves for image with MI 105 CCD 105 mm from target

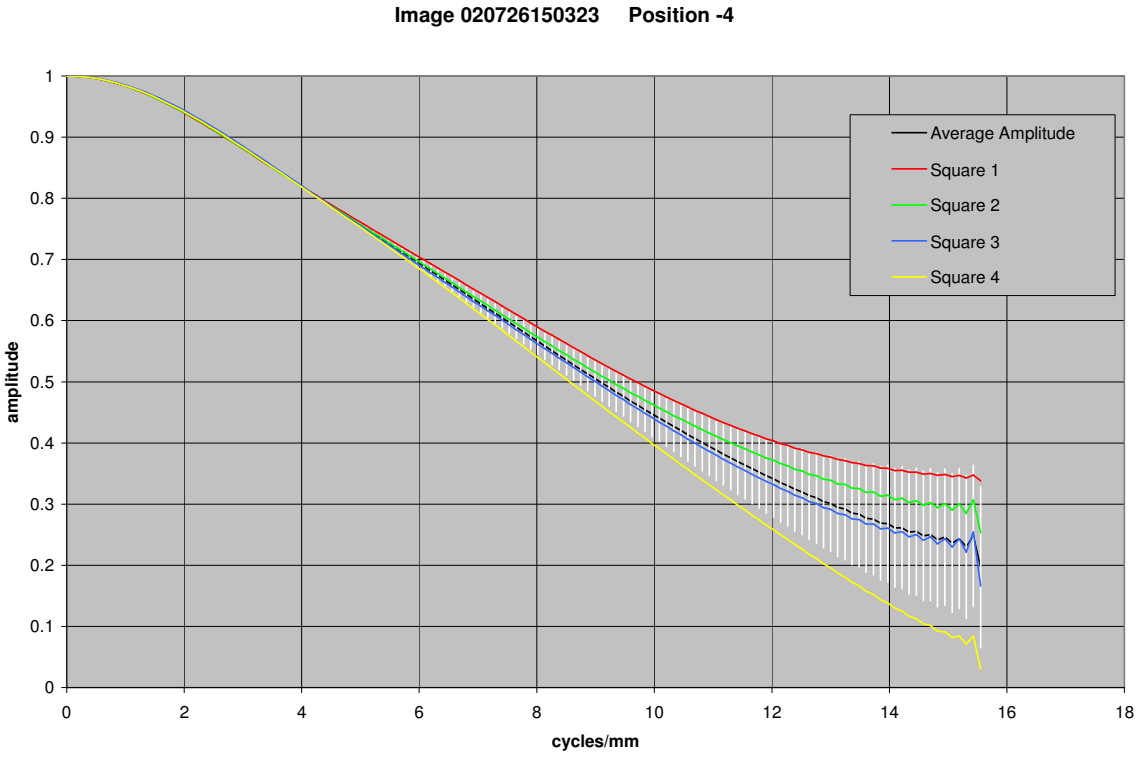

Figure 21.23. MTF curves for image with MI 105 CCD 104 mm from target

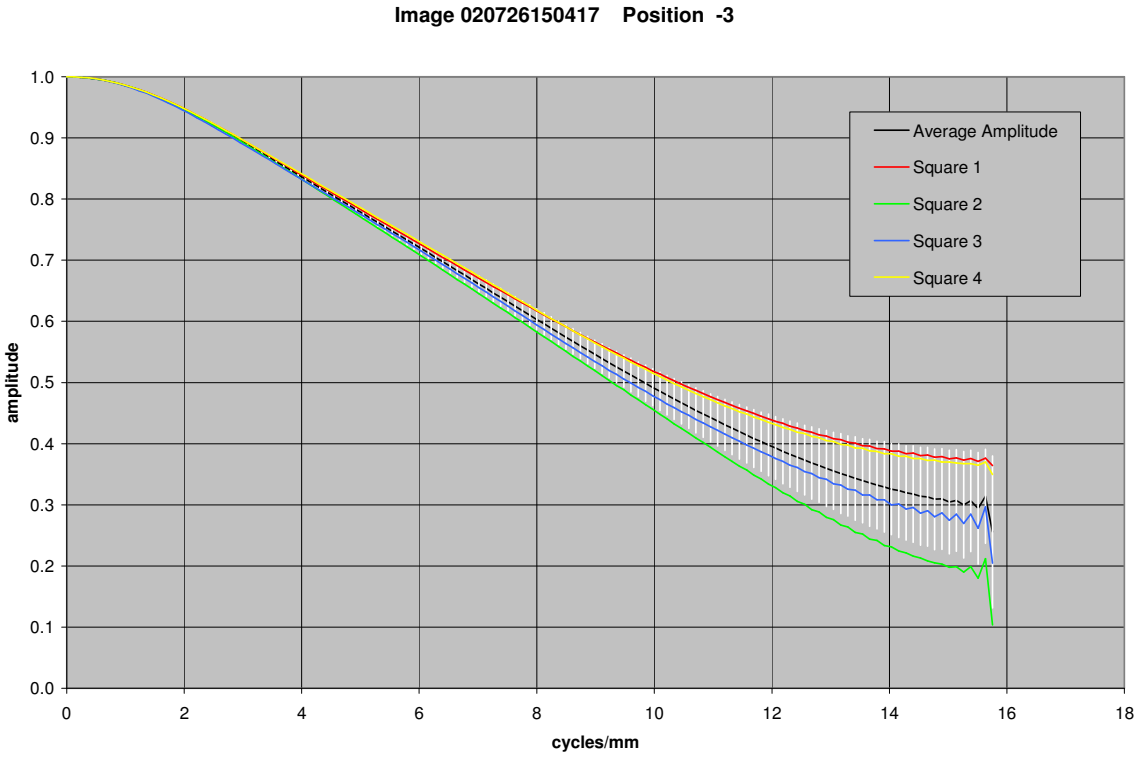

Figure 21.24. MTF curves for an image with MI 105 CCD 103 mm from target

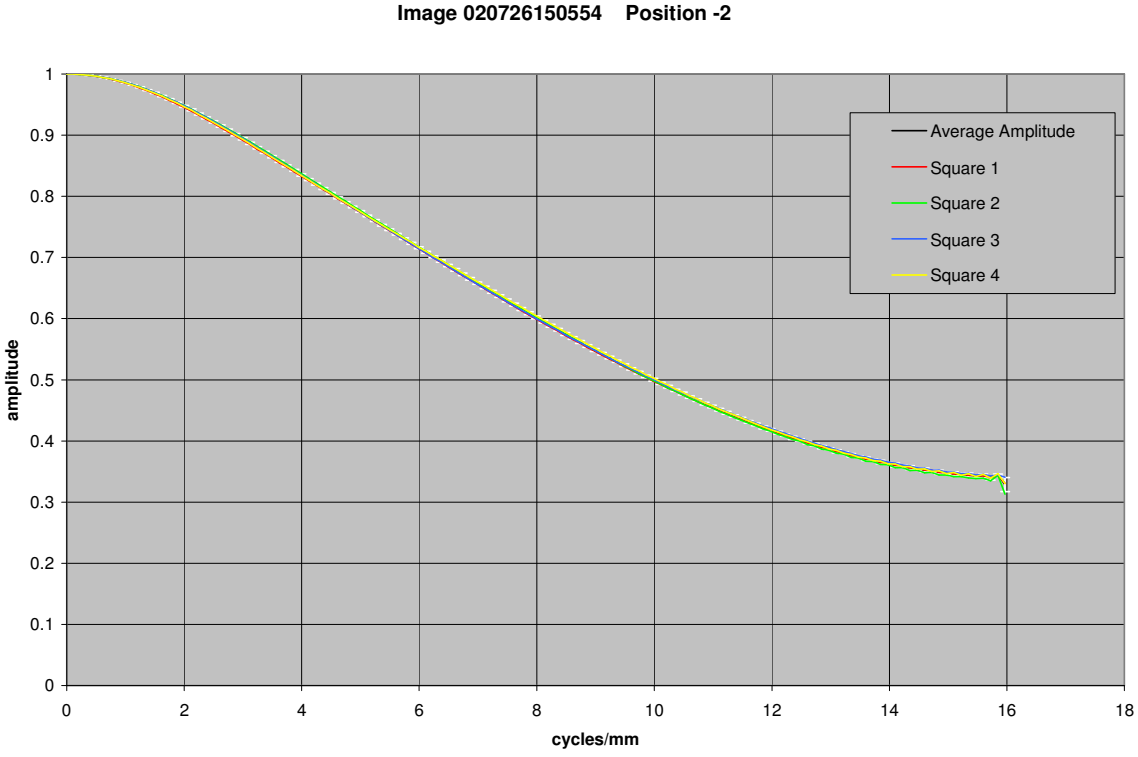

Figure 21.25. MTF curves for image with MI 105 CCD 102 mm from target

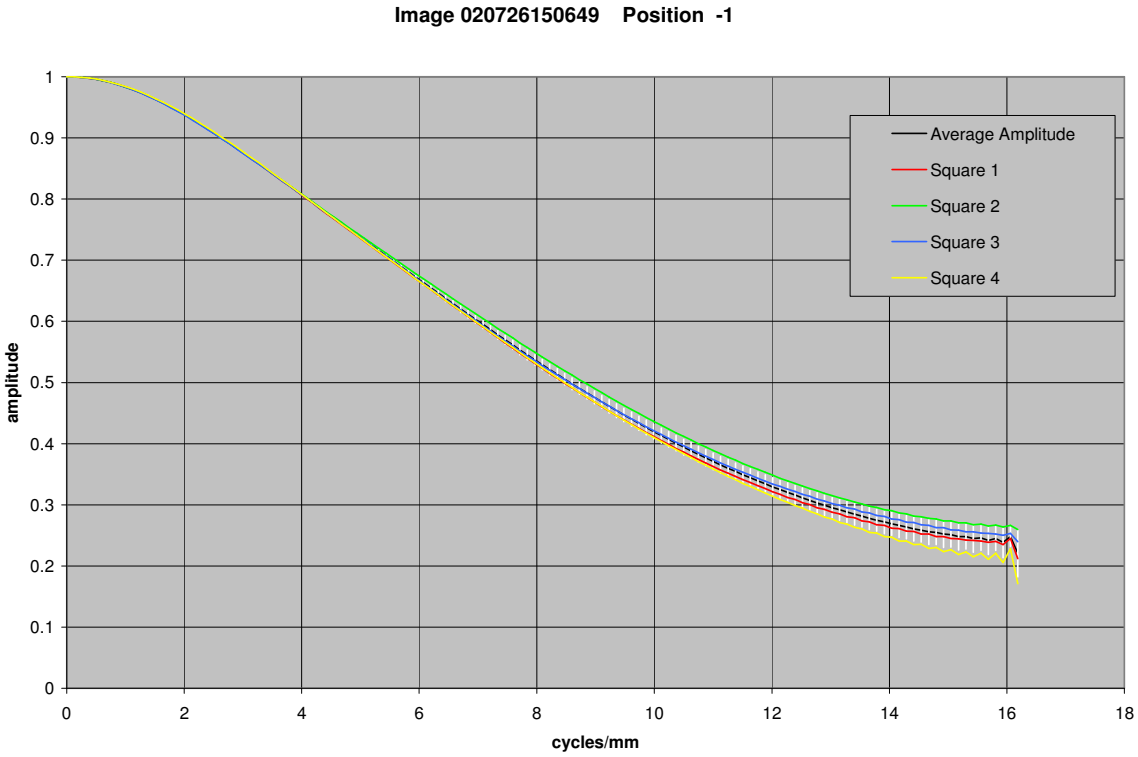

Figure 21.26. MTF curves for image with MI 105 CCD 101 mm from target

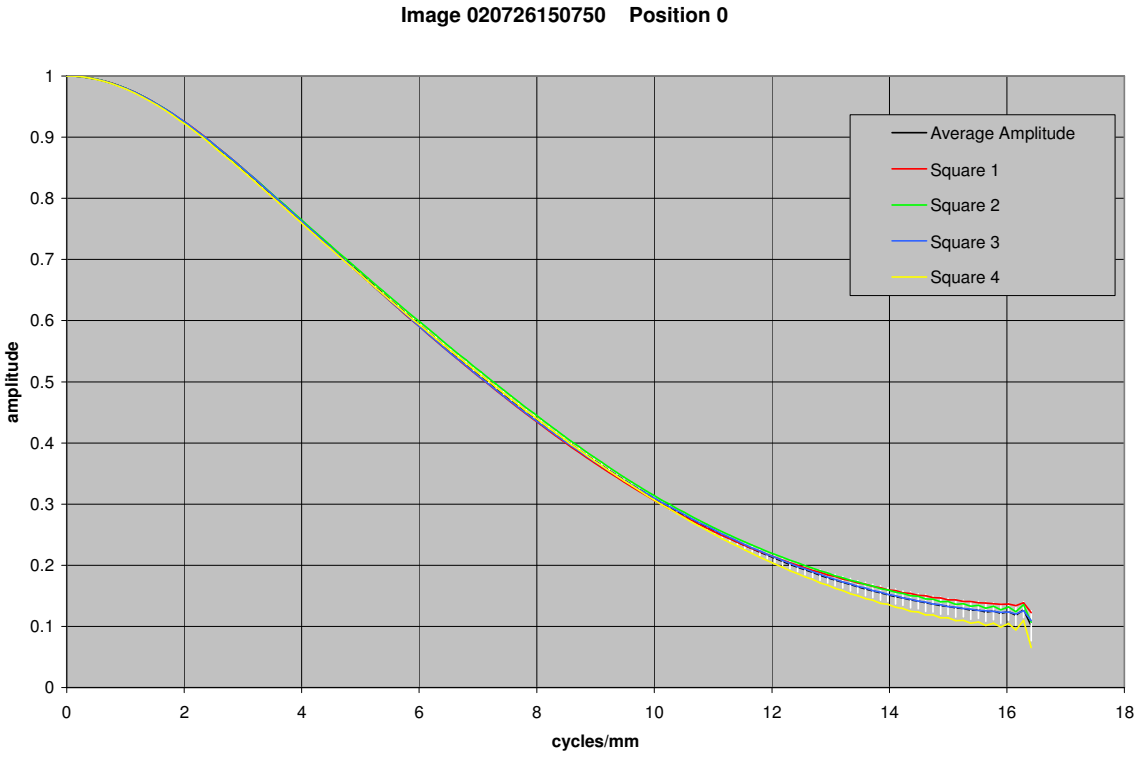

Figure 11.27. MTF curves for image with MI 105 CCD 100 mm from target

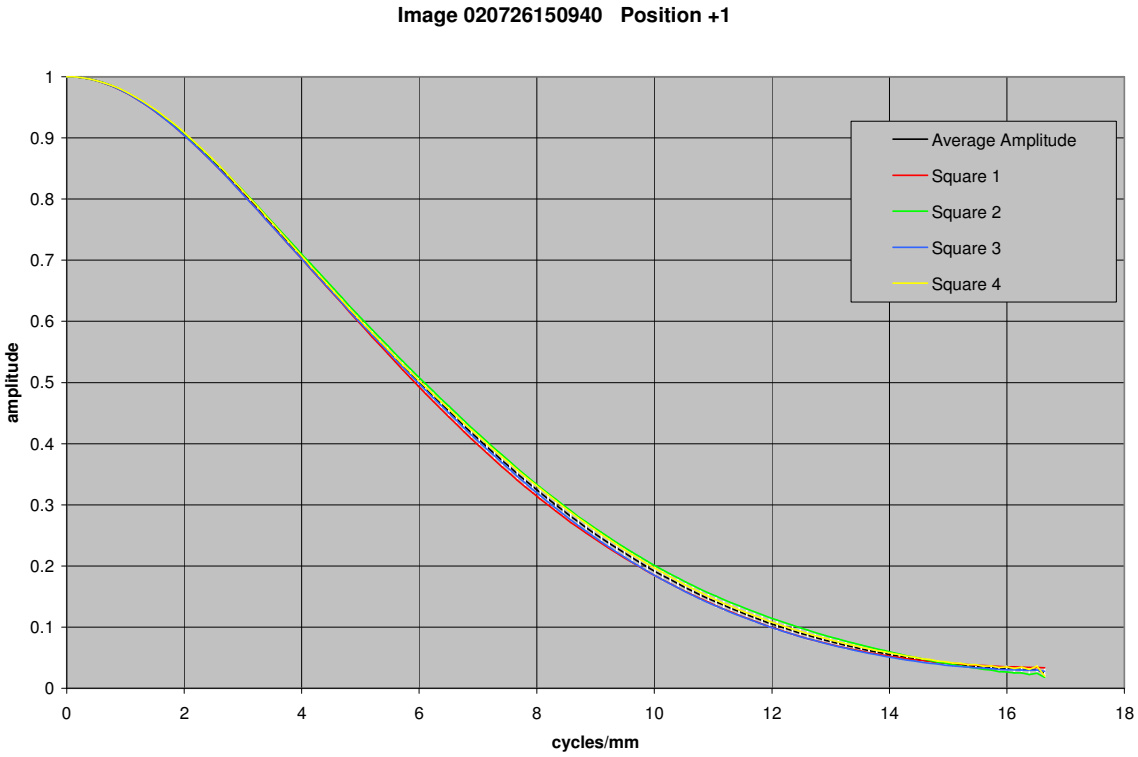

Figure 21.28. MTF curves for image with MI 105 CCD 99 mm from target

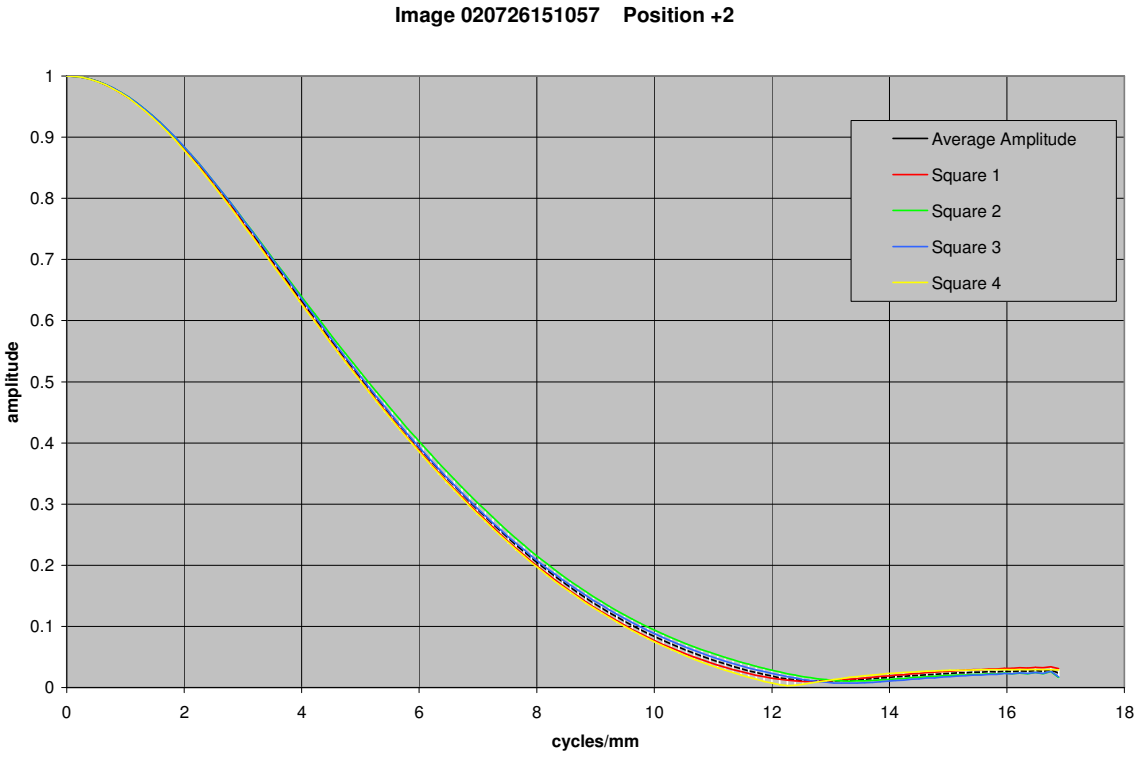

Figure 21.29. MTF curves for image with MI 105 CCD 98 mm from target

MTF for MI_MOD2_105 Image Sequence

The analysis procedure for the MI_MOD2_105 image sequence was similar to the procedure described for the MI_105 data. The one exception is that not all image positions were used (see Table 3.2.8a).

The MI_MOD2_105 images were acquired after thermal/vacuum testing. The MTF curves for these images were calculated based on 4 sub-samples from 6 images of a bar/edge target using the VICAR application program OTF1. The 6 images were acquired with the camera positioned 100 – 105 mm from the target.

The images with the highest MTF were taken when the camera was at 102 and 103 mm from the target. The MTF curves returned by the OTF1 software indicate that there is aliasing present in the images based on the fact that the MTF curves for the sub-samples are not consistent and/or the MTF curve does not approach zero at the Nyquist frequency. The aliasing can be seen in the bar targets (see Figure 21.1). The cleanest MTF curve is from the image acquired 100 mm from the target: the sub-samples are consistent and the curve approaches zero.

The MTF curves for the 4 sub-samples are plotted along with their average and standard deviation on a separate chart for each position. The average MTF curves for each position is plotted together on one chart.

The average MTF curves after thermal/vacuum testing (Figure 21.30) are similar to the average MTF curves prior to vibration and thermal/vacuum testing (Figure 3.2.8c). There are some minor differences in the noise level of the data that are probably of no practical significance. The average MTF curves and error bars are similar when the target is 105, 101 and 100 mm from the CCD (compare Figures 21.6, 21.10 and 21.11 to Figures 21.31, 21.35 and 21.36). The tail end of the average MTF curve taken when the target is 104 mm from the CCD drops for the image acquired after thermal/vacuum testing compared to the MTF curves for the image acquired prior to any testing (compare Figure 21.32 with Figure 21.7). The average MTF curves are similar for images acquired when the target is 103 mm from the target, but the error bars are smaller for the image after thermal/vacuum testing compared to the error bars for the MTF curve for image prior to testing (compare Figure 21.33 with Figure 21.8). When the target is 102 mm from the CCD, the average MTF curve is slightly higher for the image acquired after thermal/vacuum testing and the error bars are smaller compared to the error bars for the MTF curve acquired prior to testing (compare Figure 21.34 with Figure 21.9). These differences are in the noise of the data and could be caused by the Fast Fourier Transformations used to compute the MTF. Overall the MTF curves are similar for the images acquired prior to testing compared to the MTF curves for the images after vibration and thermal/vacuum testing. There was no significant change in the MTF of the camera.

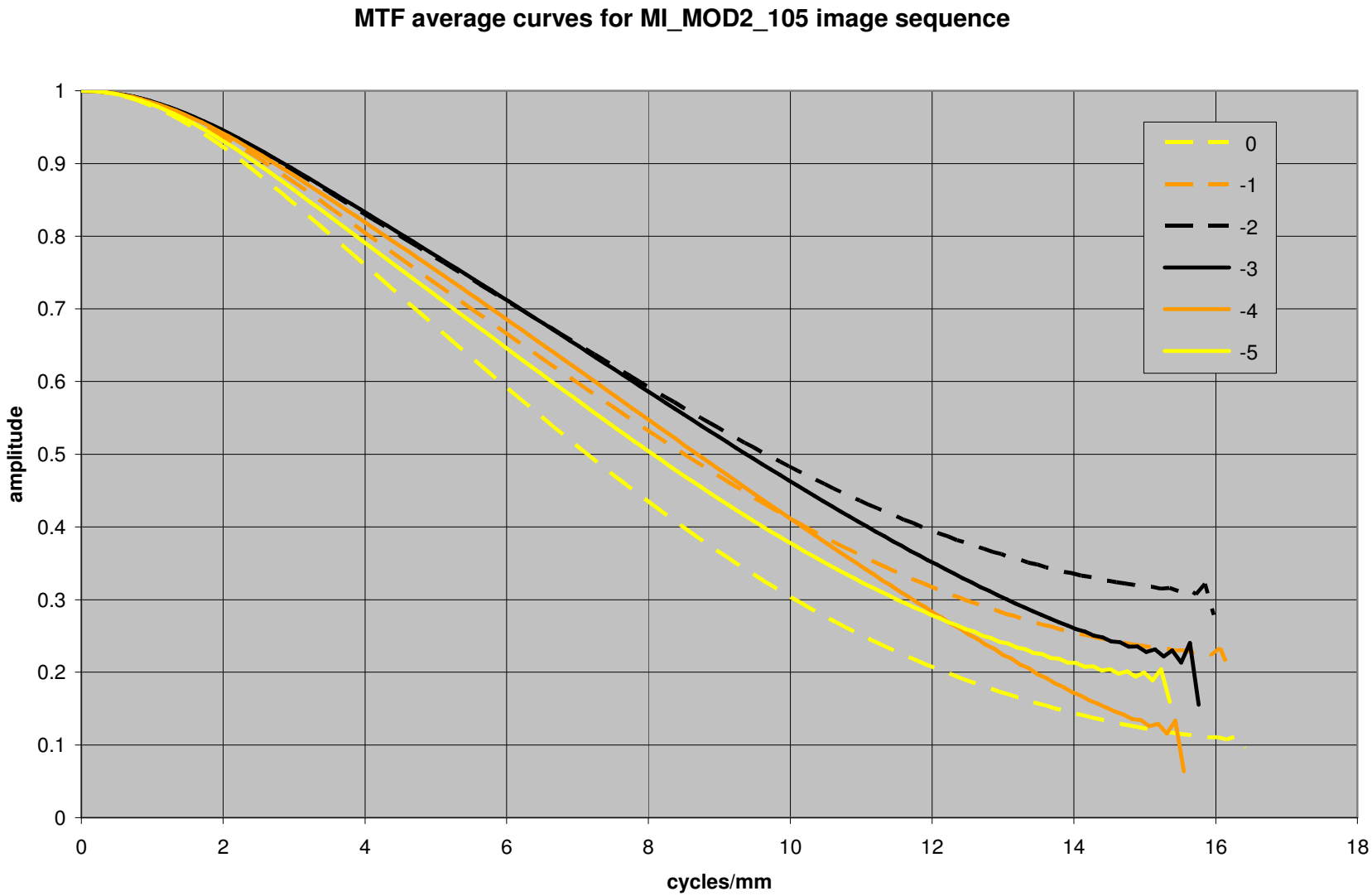

Figure 21.30. MTF average curves for MI_MOD1_105 image sequence. Each curve shows data for positions (in mm) relative to target distance from CCD of 100 mm.

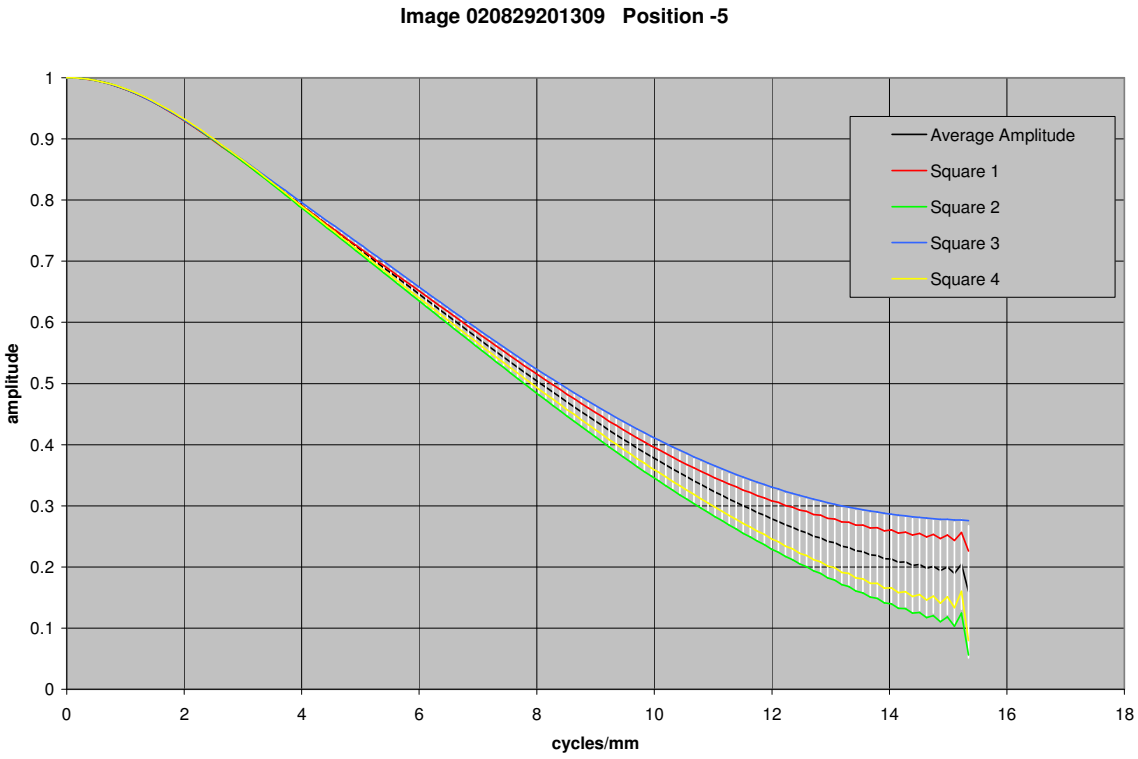

Figure 21.31. MTF curves for image with MI 105 CCD 105 mm from target

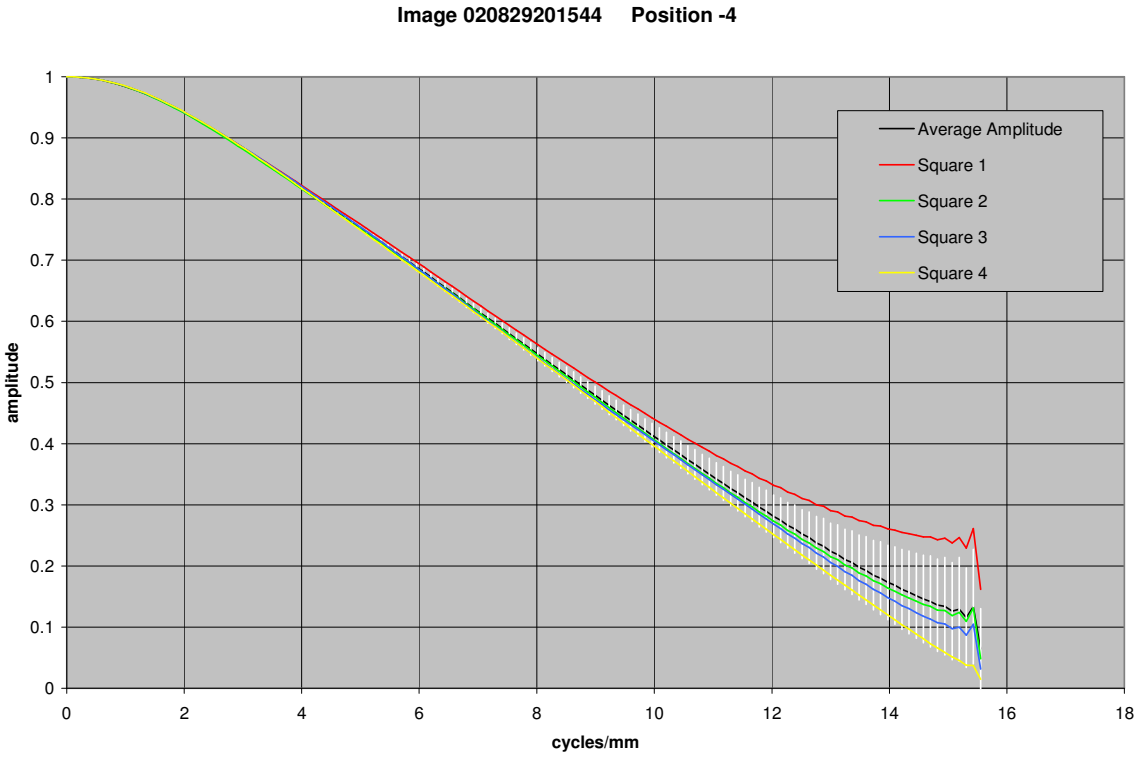

Figure 21.32. MTF curves for image with MI 105 CCD 104 mm from target

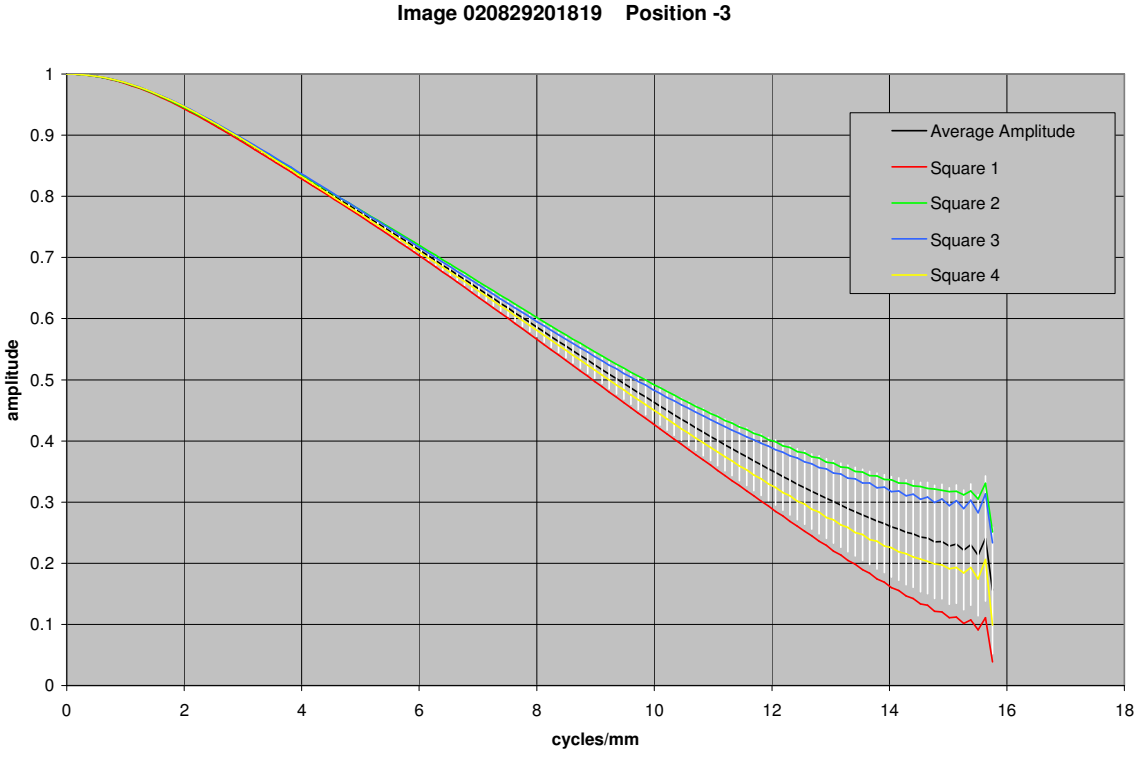

Figure 21.33. MTF curves for image with MI 105 CCD 103 mm from target

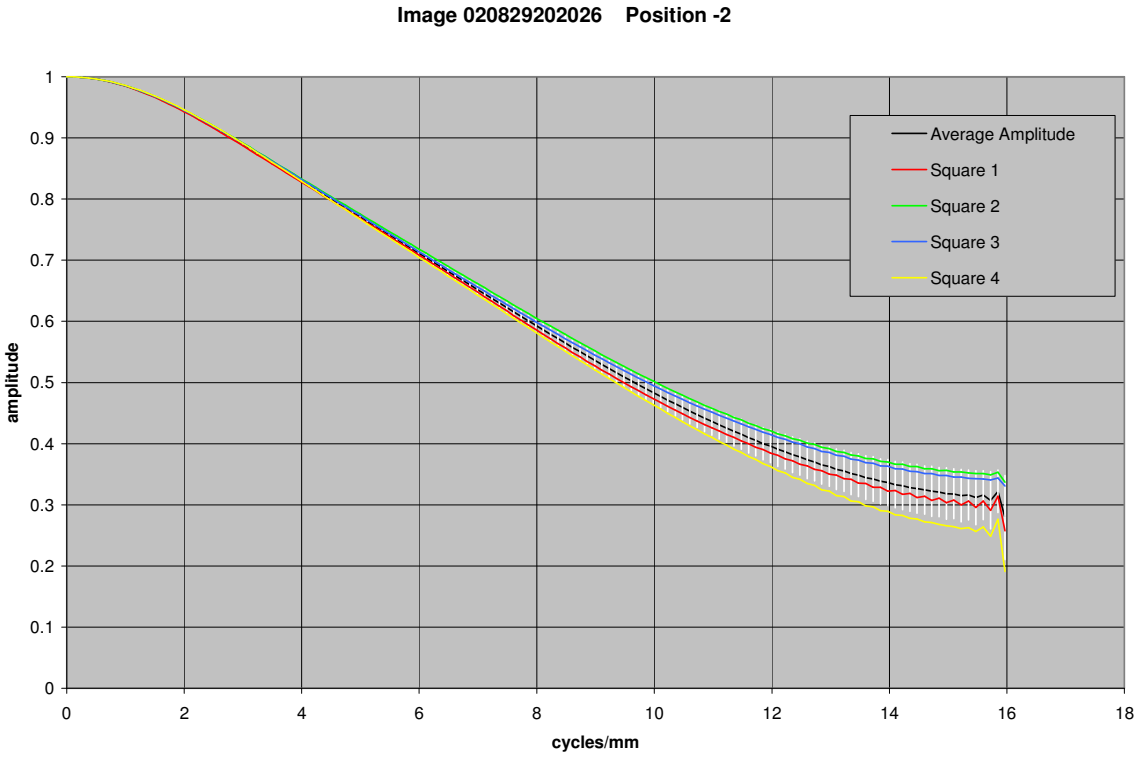

Figure 21.34. MTF curves for image with MI 105 CCD 102 mm from target

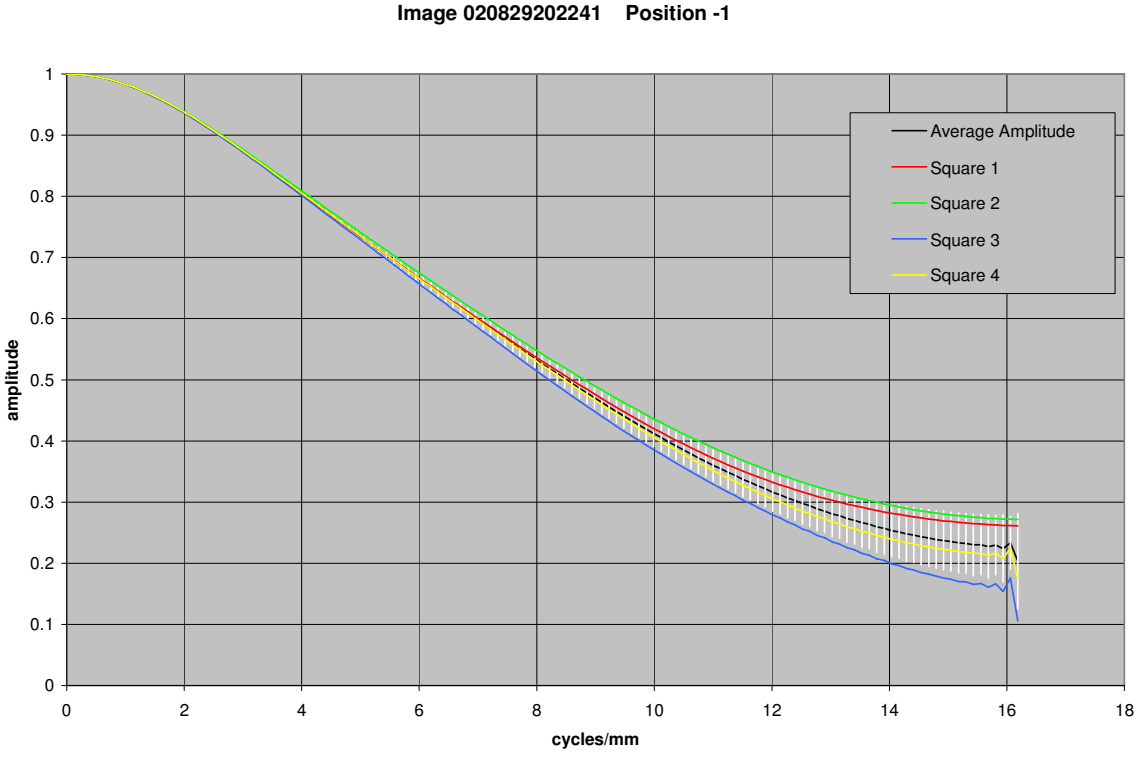

Figure 21.35. MTF curves for image with MI 105 CCD 101 mm from target

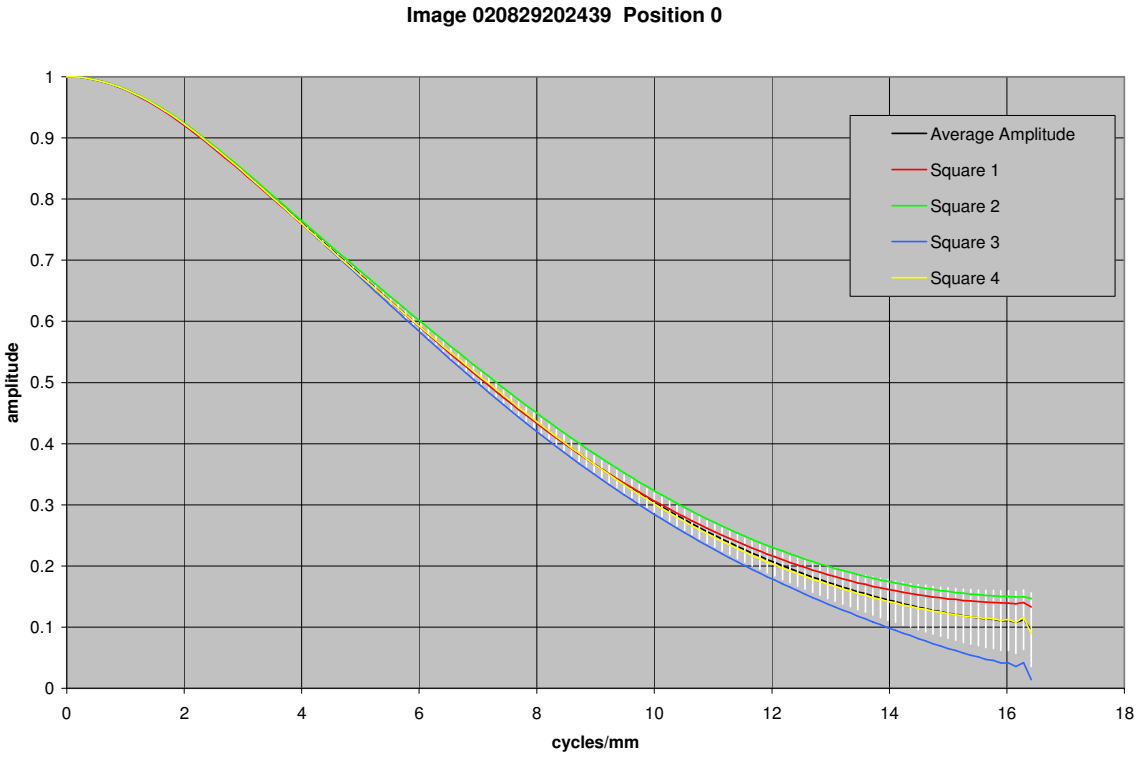

Figure 21.36. MTF curves for an image image with MI 105 CCD 101 mm from target

MTF for MI_110 Image Sequence

The Modulation Transfer Function (MTF) curves for the MI_110 image sequence, prior to vibration and thermal/vacuum testing, were calculated based on 4 sub-sampled images from 17 images of a bar target and using the VICAR application program OTF1. The 17 images were acquired with the CCD positioned 88 – 112 mm from the target. The images acquired when the CCD was 103 mm from the target have the highest MTF. The MTF curves returned by the OTF1 software indicate that there is aliasing present in the images acquired 100 – 106 mm based on the fact that the MTF curves for the sub samples are not consistent and the MTF curve does not approach zero at Nyquist. The aliasing can be seen in the bar targets: Figure 21.37 shows an example of aliasing. The cleanest MTF curve is from the image acquired 99 mm from the target: the sub-samples are consistent and the curve approaches zero. The MTF curves for the images acquired 112 mm, and from 96 – 88 mm from the target show multiple intersections with the zero axis indicating phase errors. Phase error can be seen in the bar target were the light and dark patterns of the bars reverse to form dark and light patterns. See Figure 21.38 for an example of phase error.

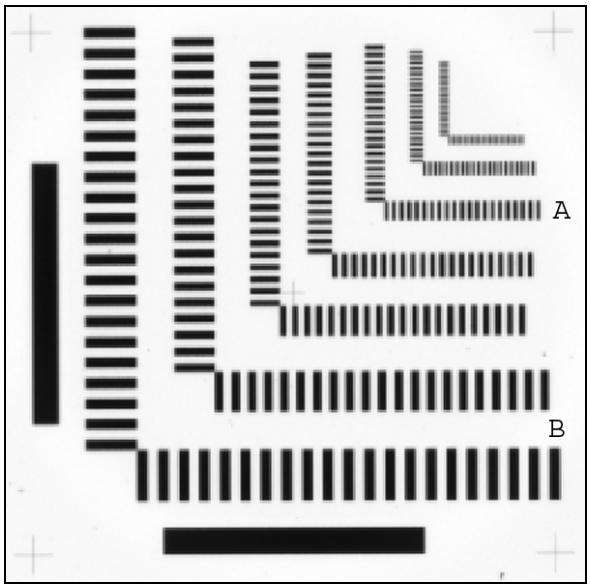

Figure 21.37. Aliasing can be seen in the bars at A, while the bars at B are clean and even.

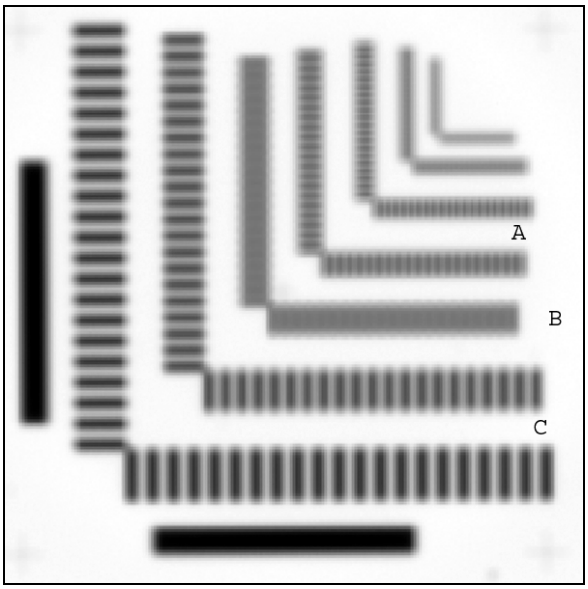

Figure 21.38. Phase errors can be seen in the bars at A, the bars at B have nearly 0 modulation, and the bars at C have no phase error.

Figures 21.39 – 21.55 are the MTF curves at the different positions (-12 to +12 mm, see Table 3.2.8a). The MTF curve is shown for each sub-sampled image and the average of the four sub-sampled images. The standard deviations of the four sub-sampled MTF curves are plotted as error bars. Each figure lists an image number (*e.g.*, 020717173522) and the position (*e.g.*, -3, which corresponds to 103 mm from the target).

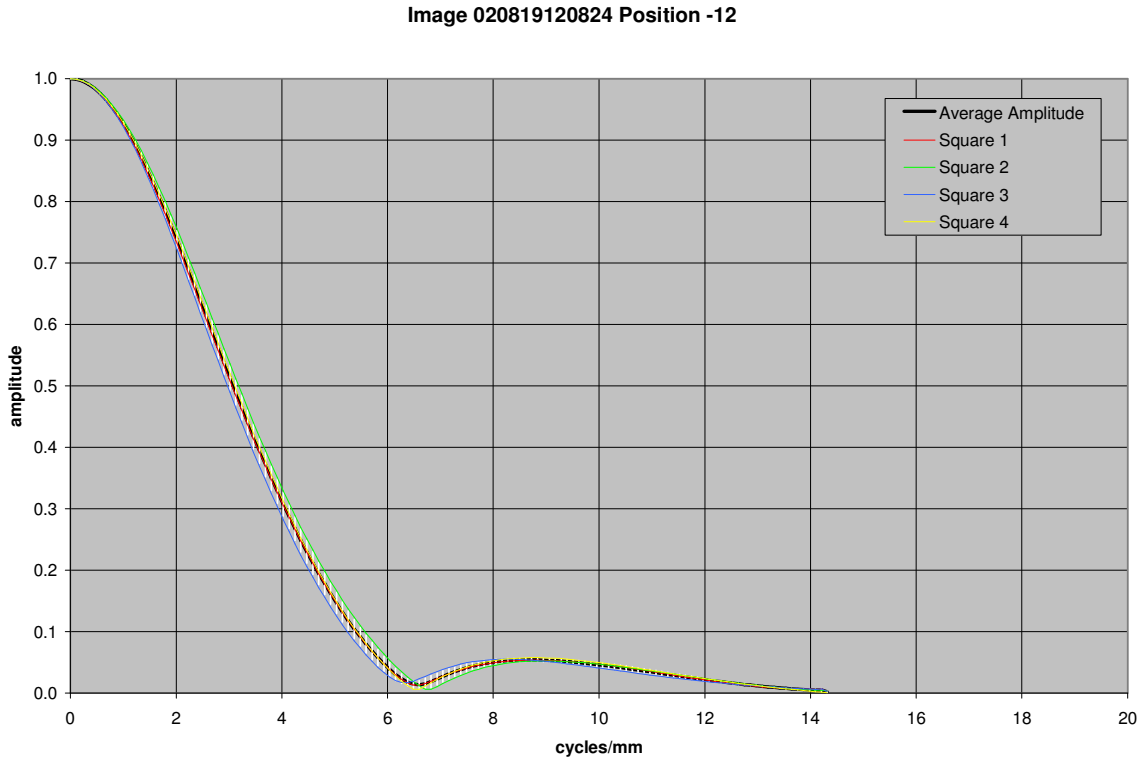

Figure 21.39. MTF curves for image taken with MI 110 CCD 112 mm from target

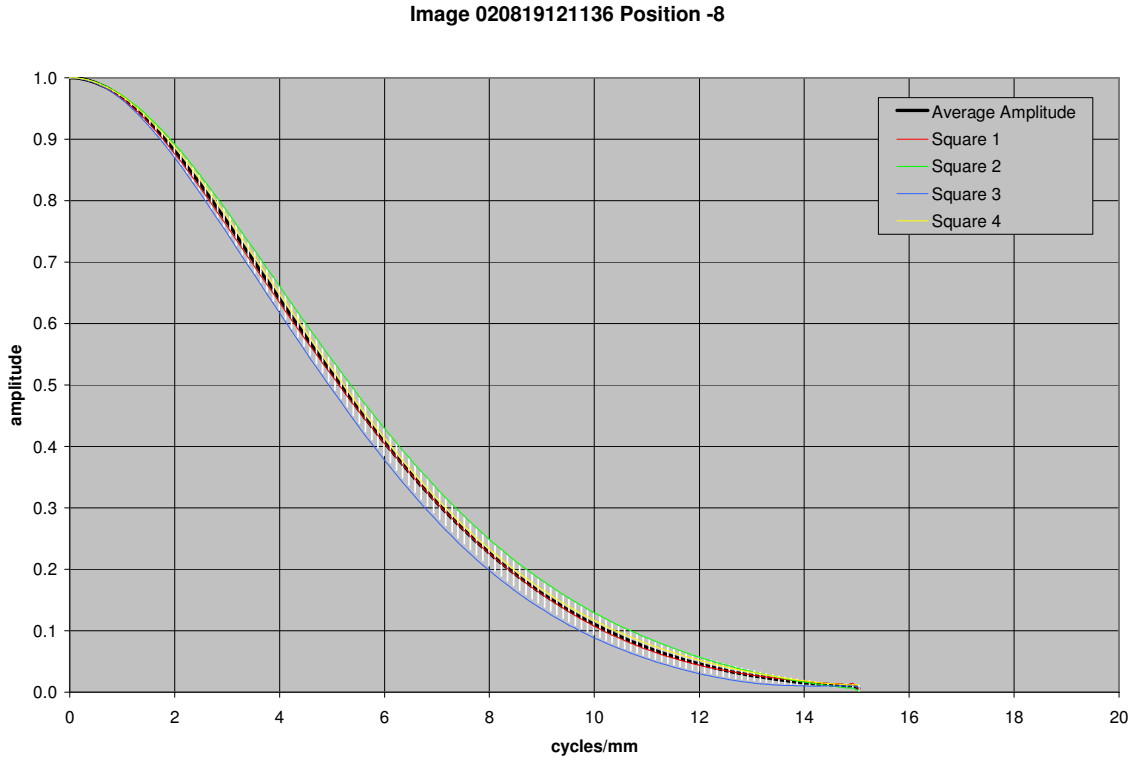

Figure 21.40. MTF curves for image taken with MI 110 CCD 108 mm from the target

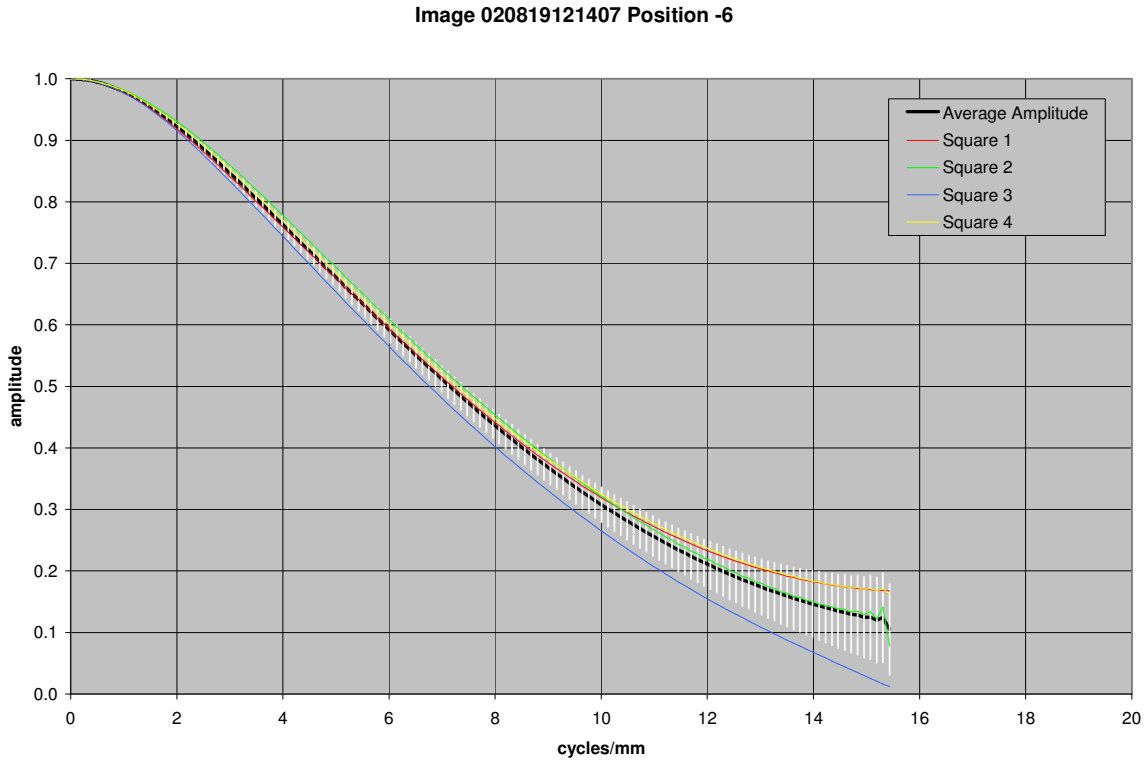

Figure 21.41. MTF curves for image taken with MI 110 CCD 106 mm from the target

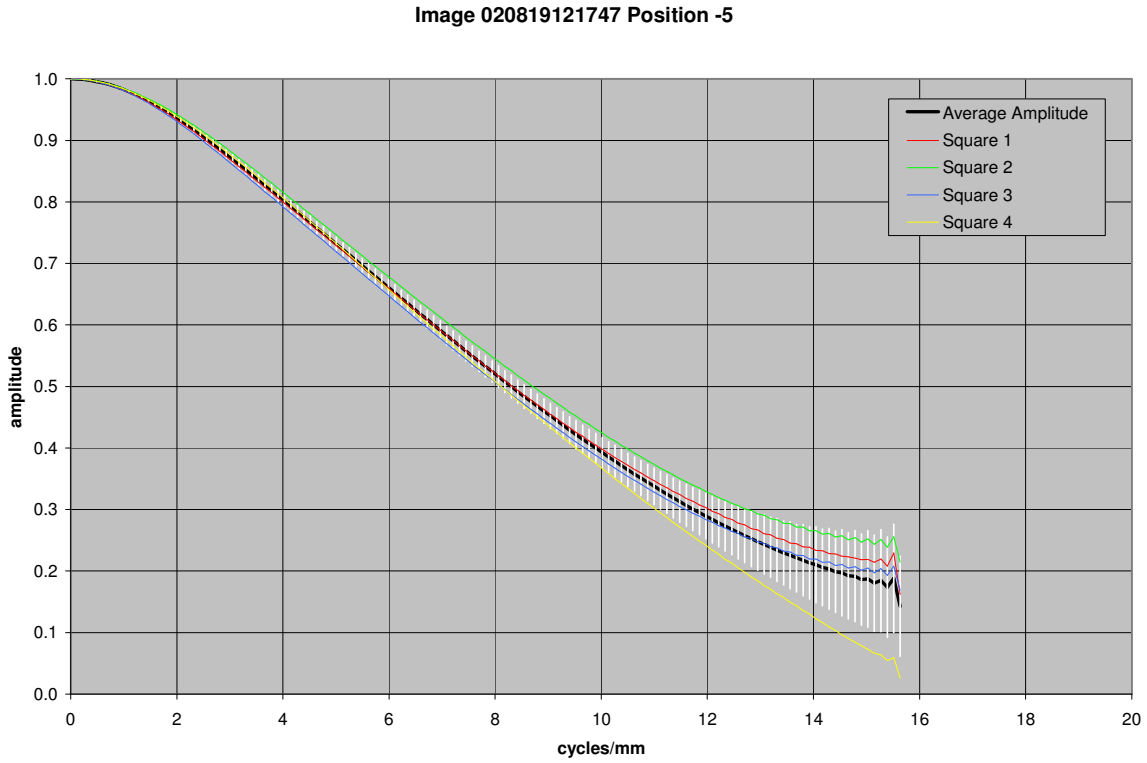

Figure 21.42. MTF curves for image taken with MI 110 CCD 105 mm from the target

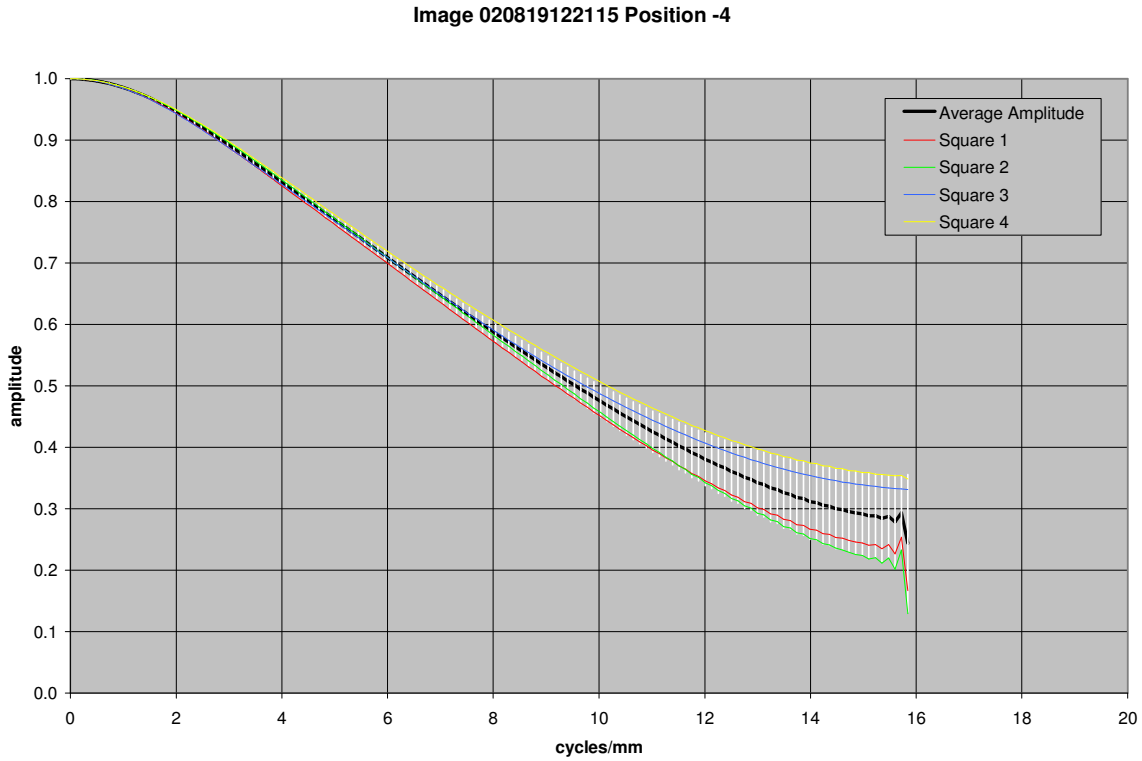

Figure 21.43. MTF curves for image taken with MI 110 CCD 104 mm from the target

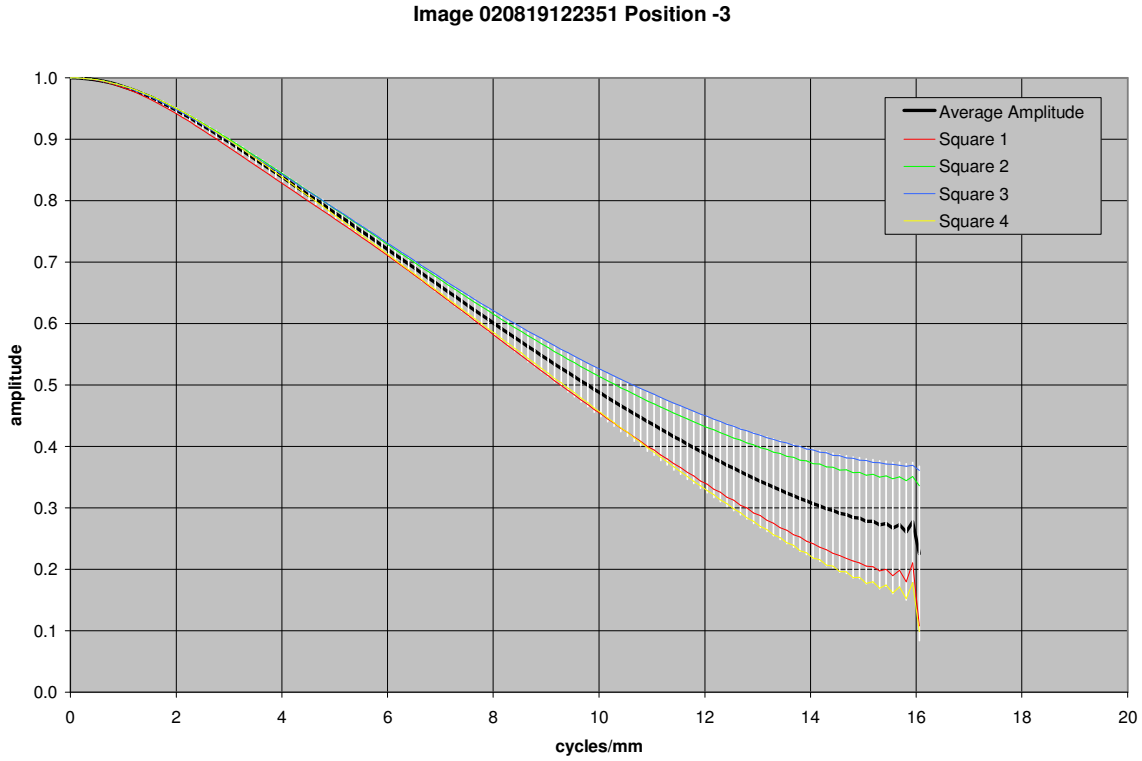

Figure 21.44. MTF curves for image taken with MI 110 CCD 103 mm from the target

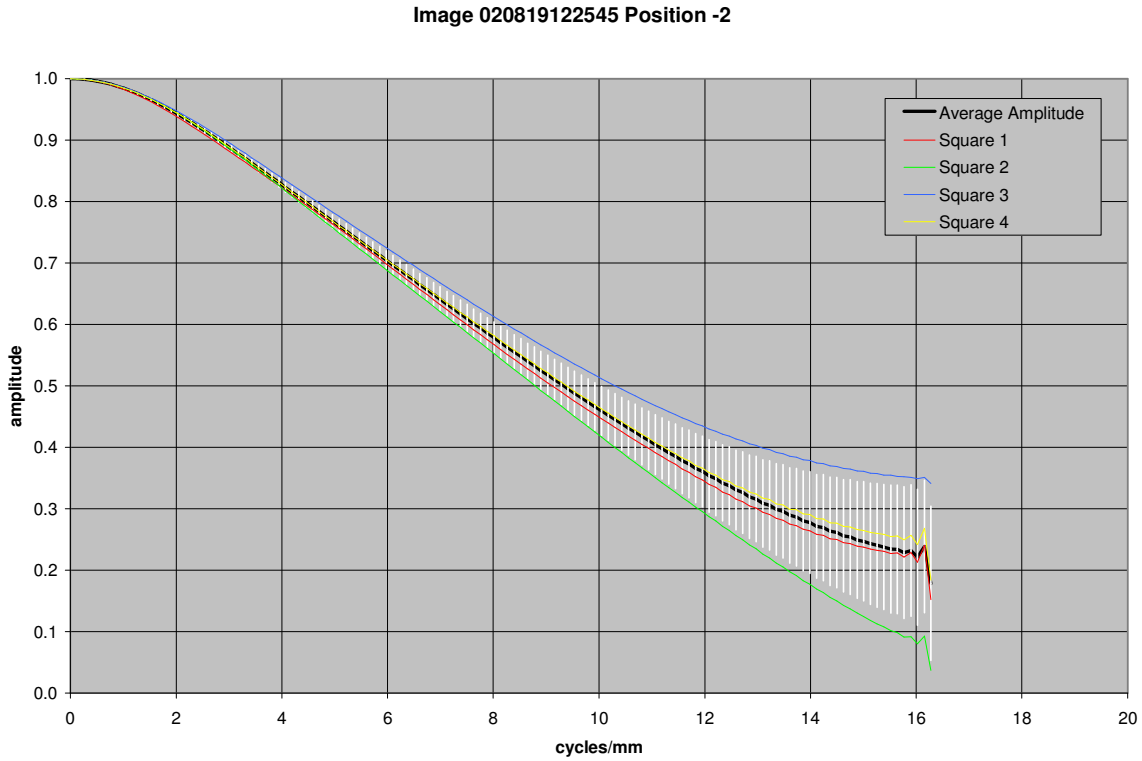

Figure 21.45 MTF curves for image taken with MI 110 CCD 102 mm from the target

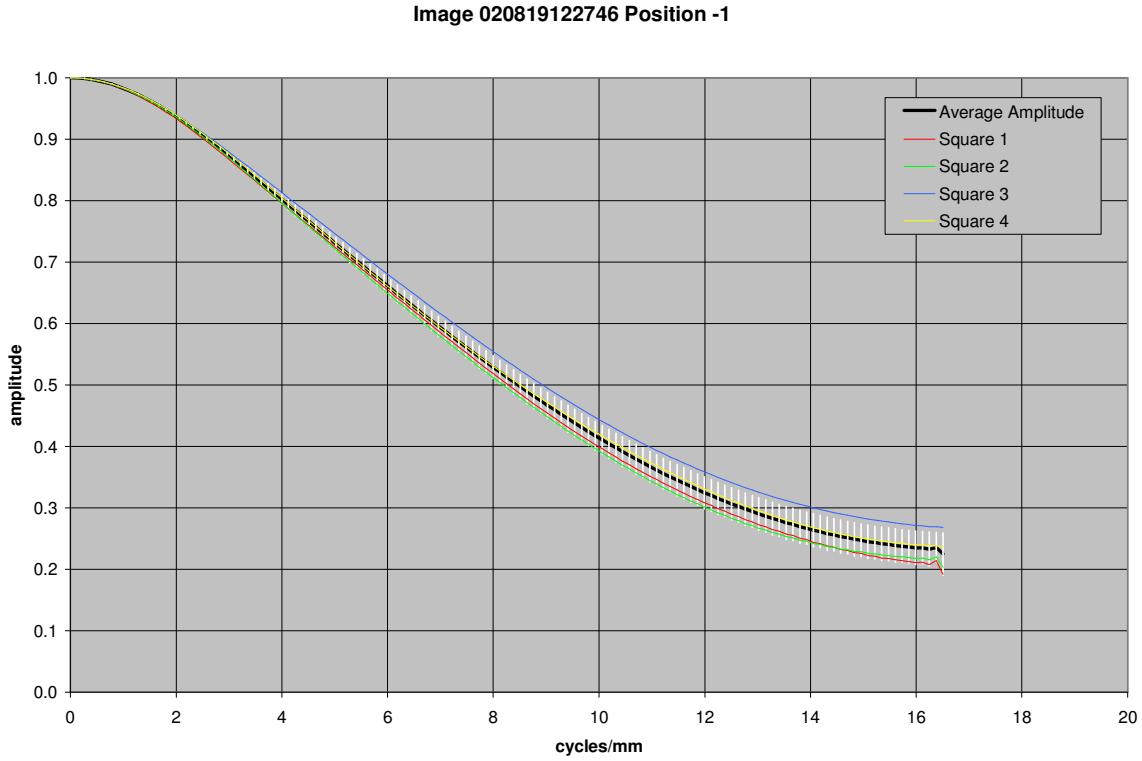

Figure 21.46. MTF curves for image taken with MI 110 CCD 101 mm from the target

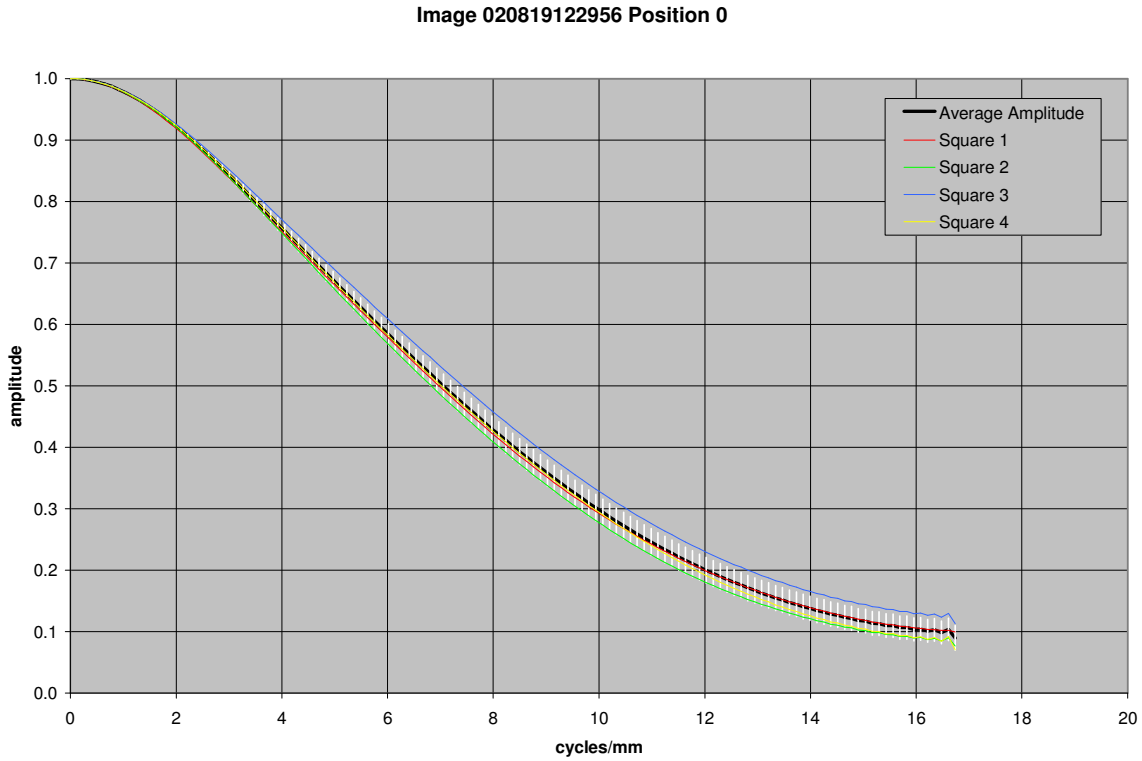

Figure 21.47. MTF curves for image taken with MI 110 CCD 100 mm from the target

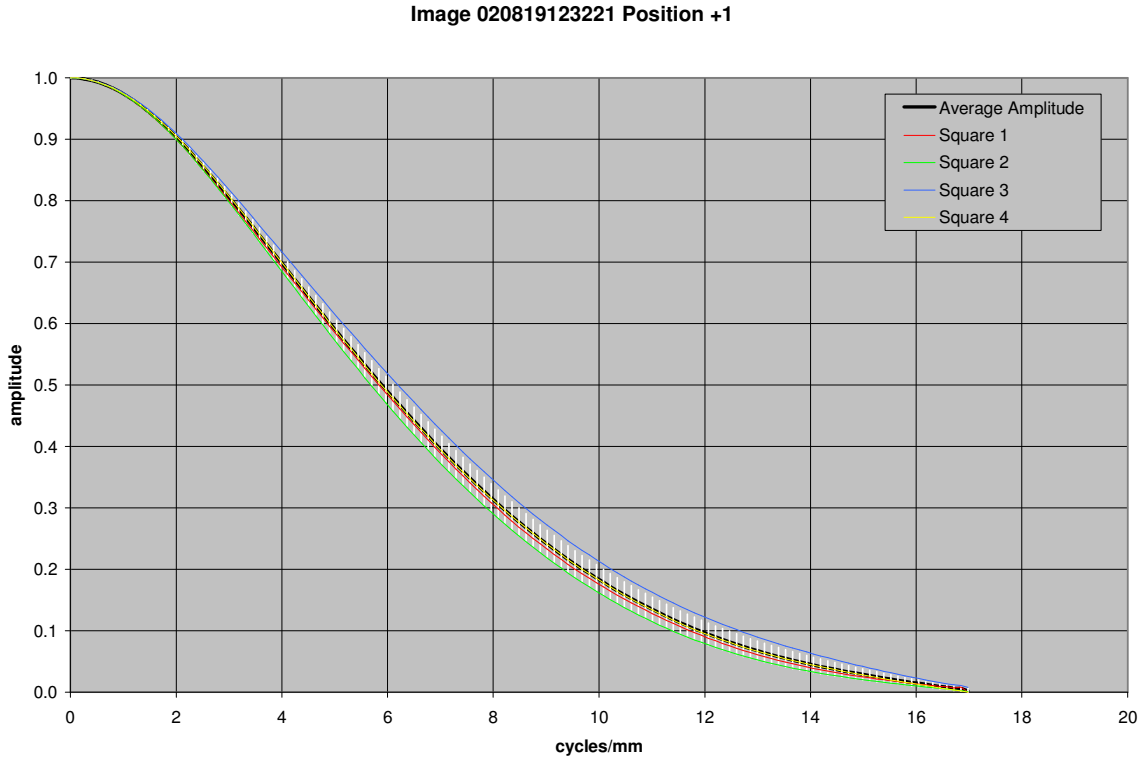

Figure 21.48. MTF curves for image taken with MI 110 CCD 99 mm from the target

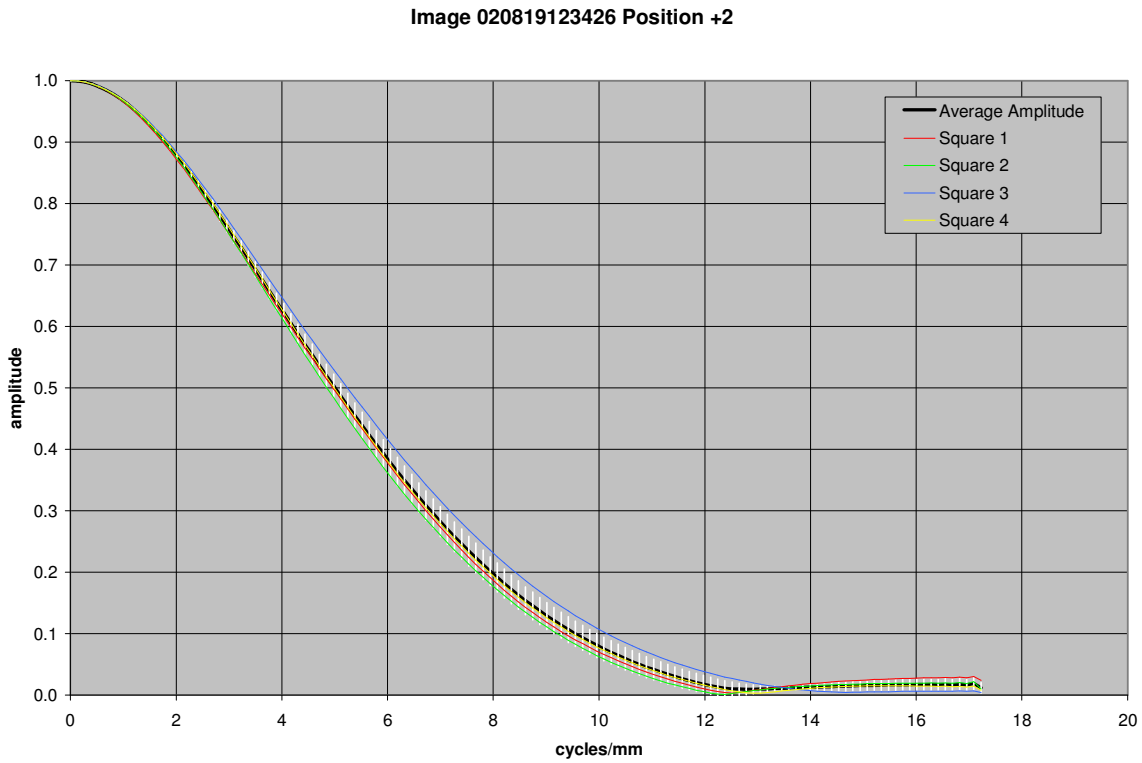

Figure 21.49. MTF curves for image taken with MI 110 CCD 98 mm from the target

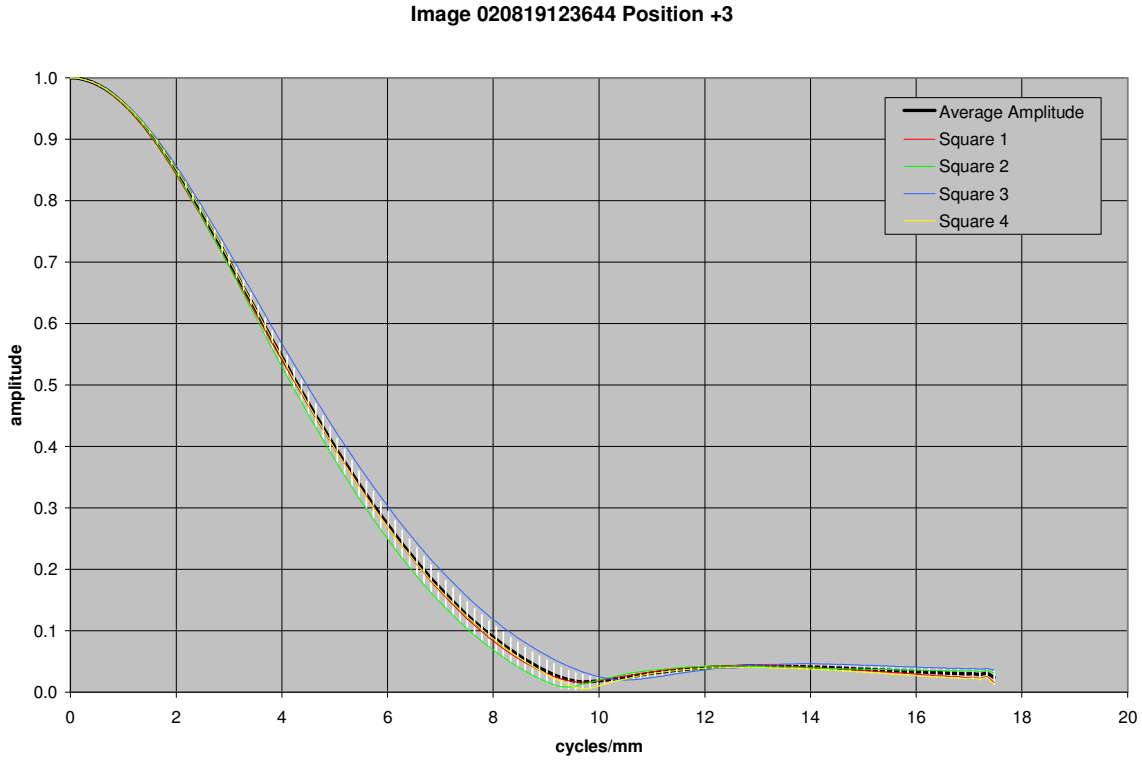

Figure 21.50. MTF curves for image taken with MI 110 CCD 97 mm from the target

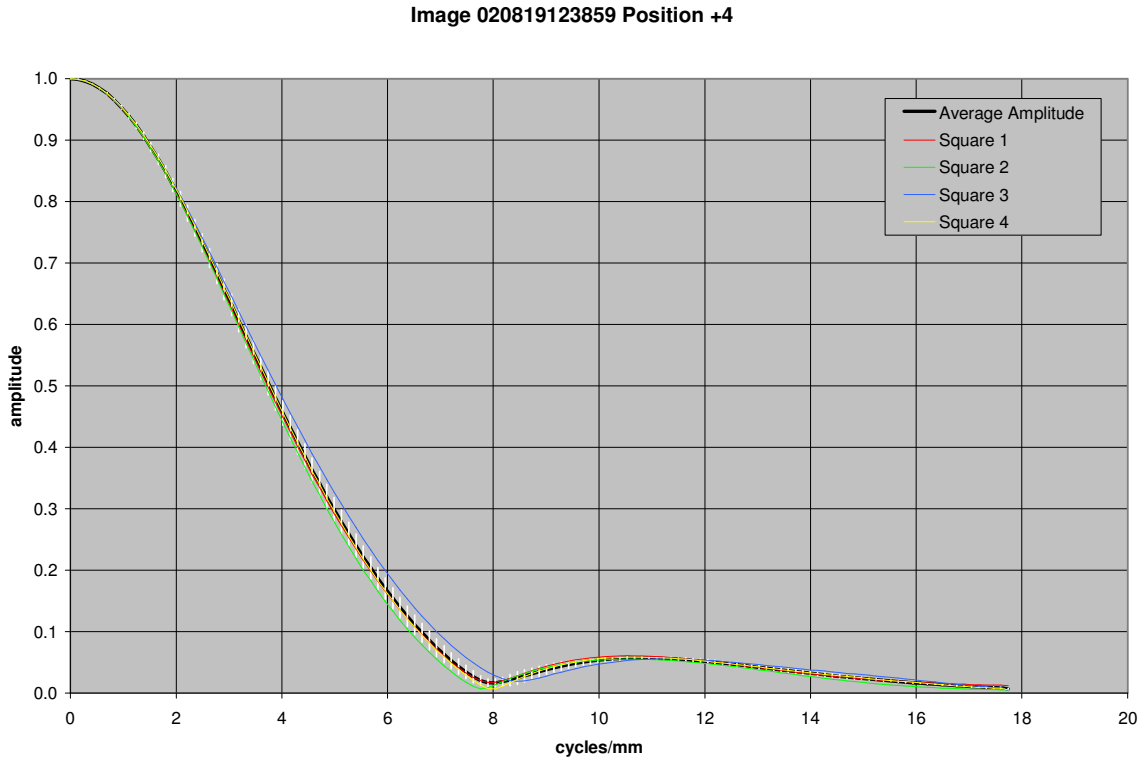

Figure 21.51. MTF curves for image taken with MI 110 CCD 96 mm from the target

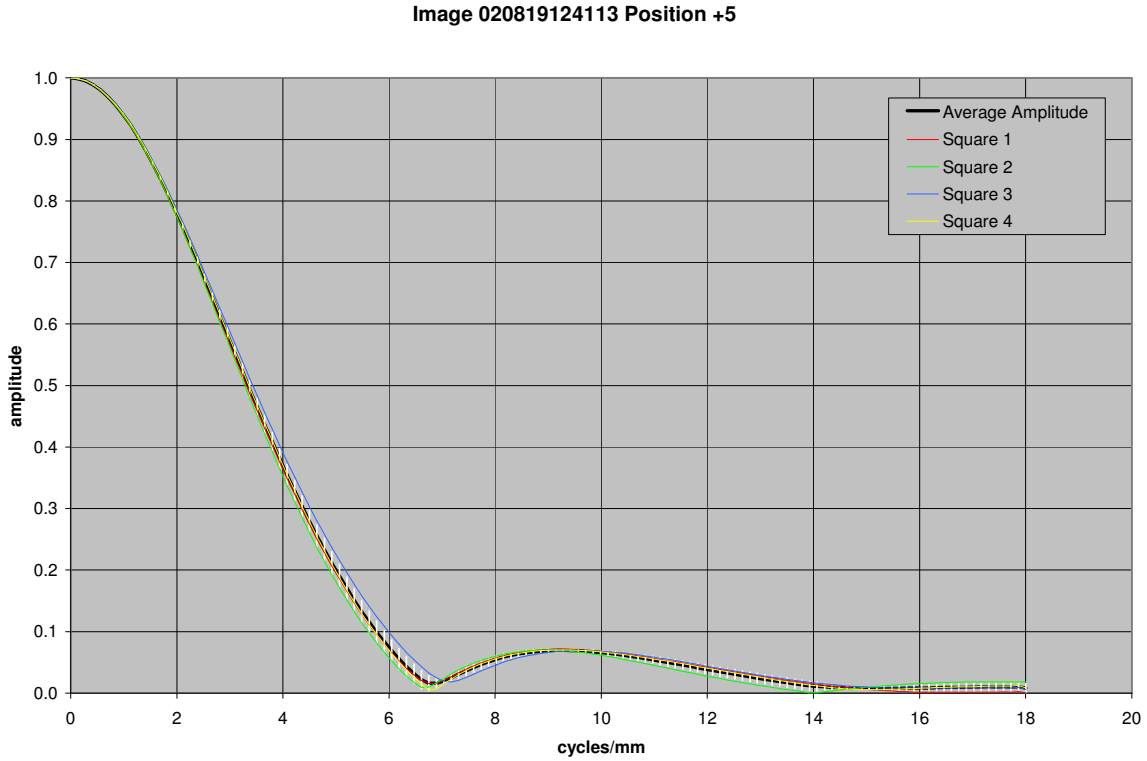

Figure 21.52. MTF curves for image taken with MI 110 CCD 95 mm from the target

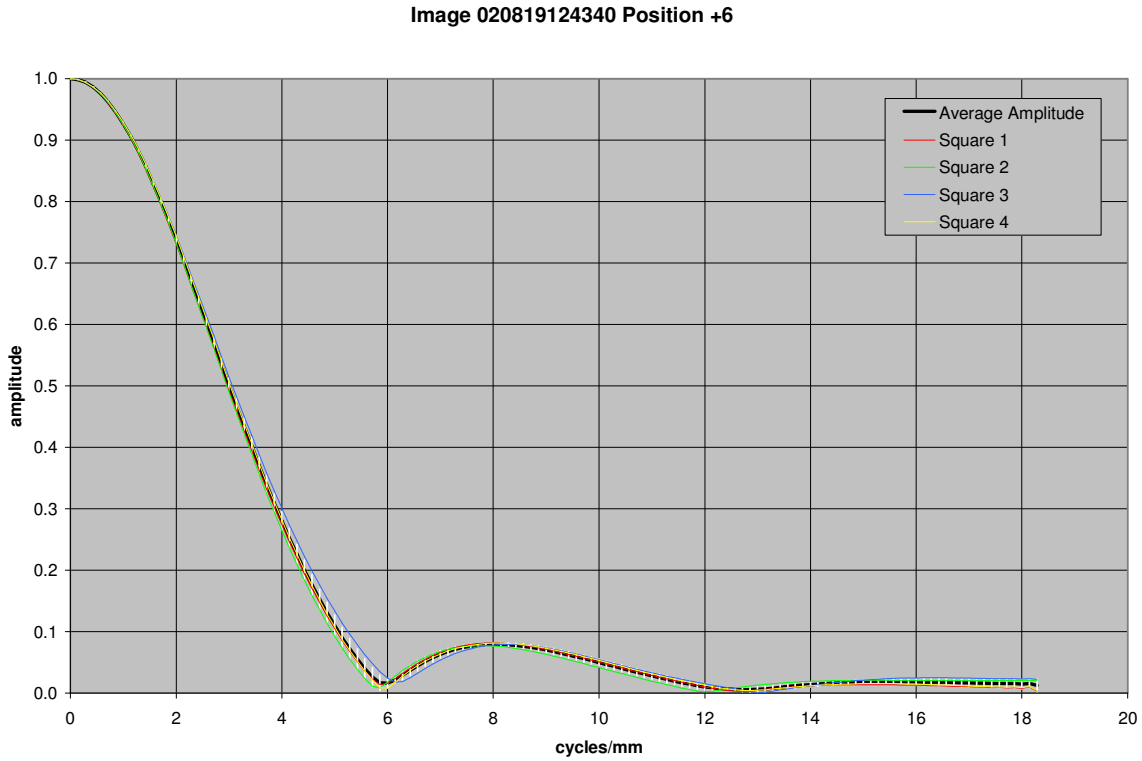

Figure 21.53. MTF curves for image taken with MI 110 CCD 94 mm from the target

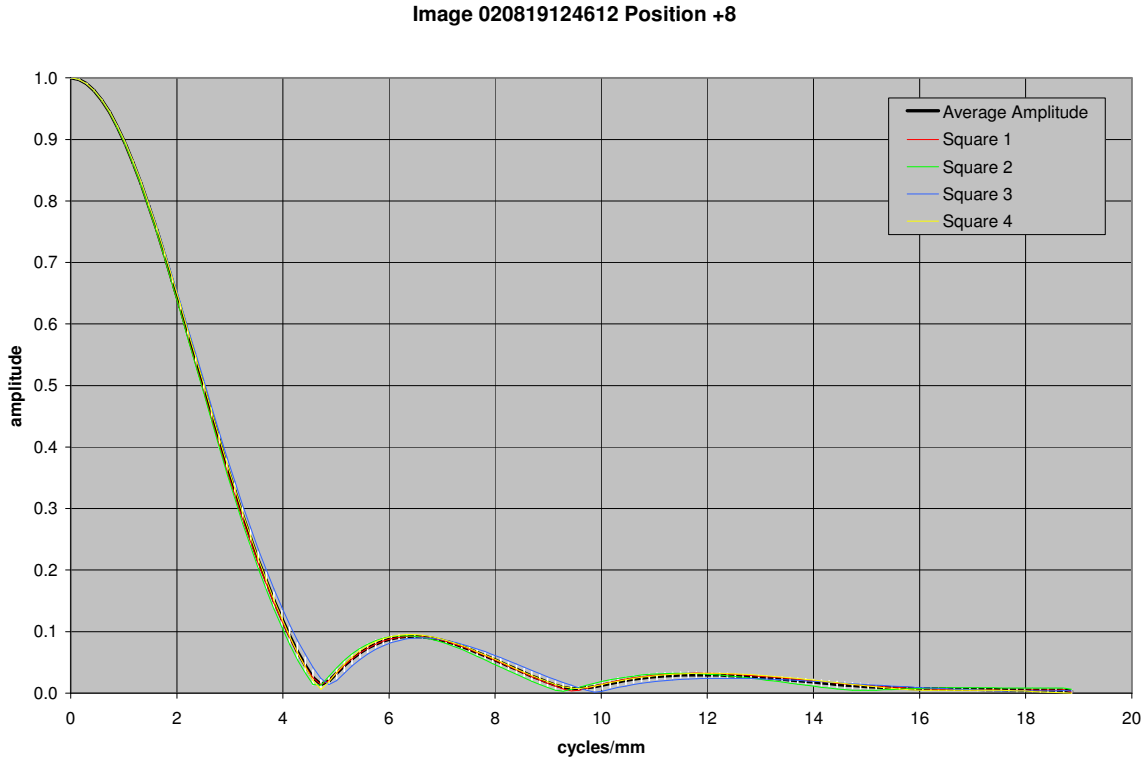

Figure 21.54. MTF curves for image taken with MI 110 CCD 92 mm from the target

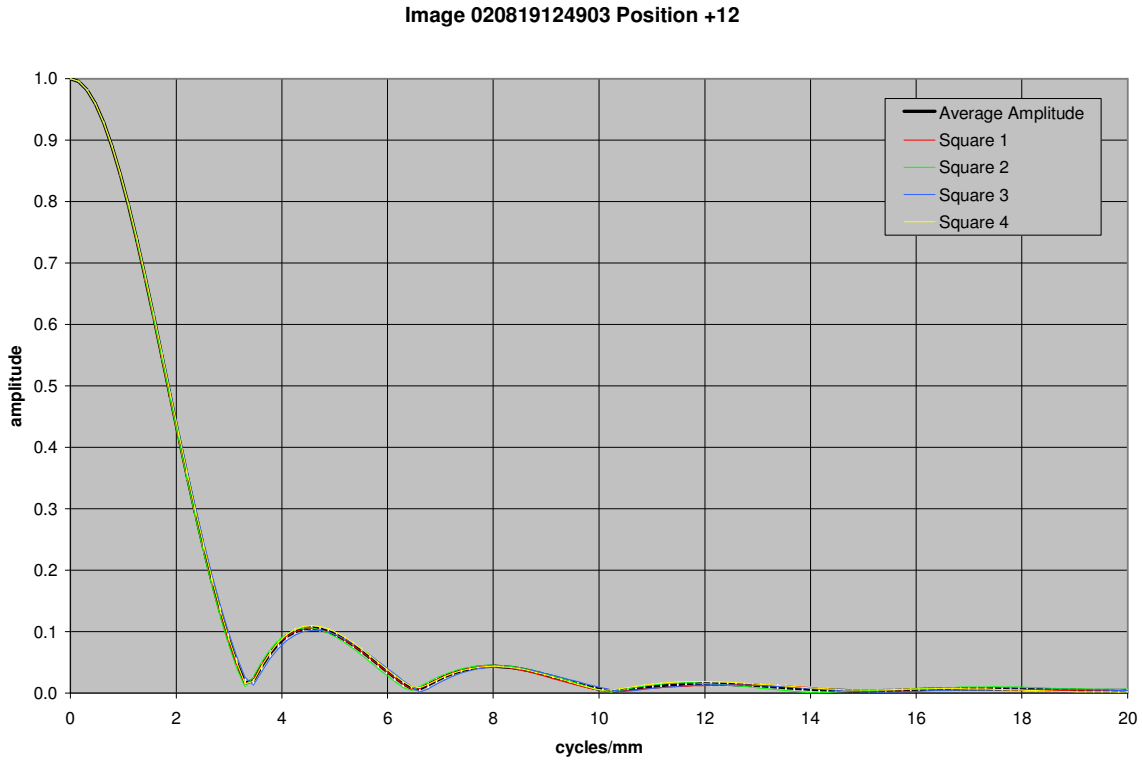

Figure 21.55. MTF curves for image taken with MI 110 CCD 88 mm from the target

MTF for MI_MOD1_110 Image Sequence

The Analysis procedure for the MI_MOD1_110 image sequence was similar to the procedure described for the MI_110 data. The one exception is that not all image positions were used.

The MI_MOD1_110 images were acquired after vibration testing. The MTF curves for these images were calculated based on 4 sub-samples from 12 images of a bar target and using the VICAR application program OTF1. The 12 images were acquired with the camera positioned 88 – 112 mm from the target.

The images acquired when the CCD was 102 and 103 mm from the target have the highest MTF. The MTF curves returned by the OTF1 software indicate that there is aliasing present in the images acquired 100 – 106 mm based on the fact that the MTF curves for the sub-samples are not consistent and/or the MTF curve does not approach zero at Nyquist. The aliasing can be seen in the bar target images. The cleanest MTF curve is from the image acquired 99 mm from the target; the sub-samples are consistent and the curve approaches zero.

The average MTF curves for the previous image sequence (Figure 3.2.8d) and this sequence (Figure 21.56) that was acquired after vibration testing are similar. However, the highest MTF responses are from the images acquired when the target was 102 and 103 mm from the CCD, while in the previous sequence the highest MTF response was at 103 mm. Considering the noise in the MTF curves and the slight differences, this is not a significant change to the MTF curves.

Comparing the MTF curves for images acquired when the target was 112, 108, 106, and 105 mm from the CCD (Figures 21.39-21.42 *vs*. Figures 21.57-21.60), the average MTFs are similar and the error bars (standard deviation of the 4 sub-images) are similar. At the next position (104, Figures 21.43 and 21.61) the shape of the curves and the error bars are different. The MTF curve for the images acquired after vibration testing (MI_MOD1_110) does not flatten out at the higher frequencies. This pattern is similar to other subimages (see Figure 21.59 MTF curve for subimage at square 3, Figure 21.41 MTF curve for subimage at square 3, and Figure 21.42 MTF curve for subimage at square 4). For the rest of the positions (103, 102, 101, 100, 99, 98, 94, and 88 mm, Figures 21.44-21.49, 21.53, and 21.55 *vs*. Figures 21.62-21.69) the curves and standard deviations are similar. Since there is only a difference at one position (104), we conclude that there was no change in the MTF due to the vibration testing.

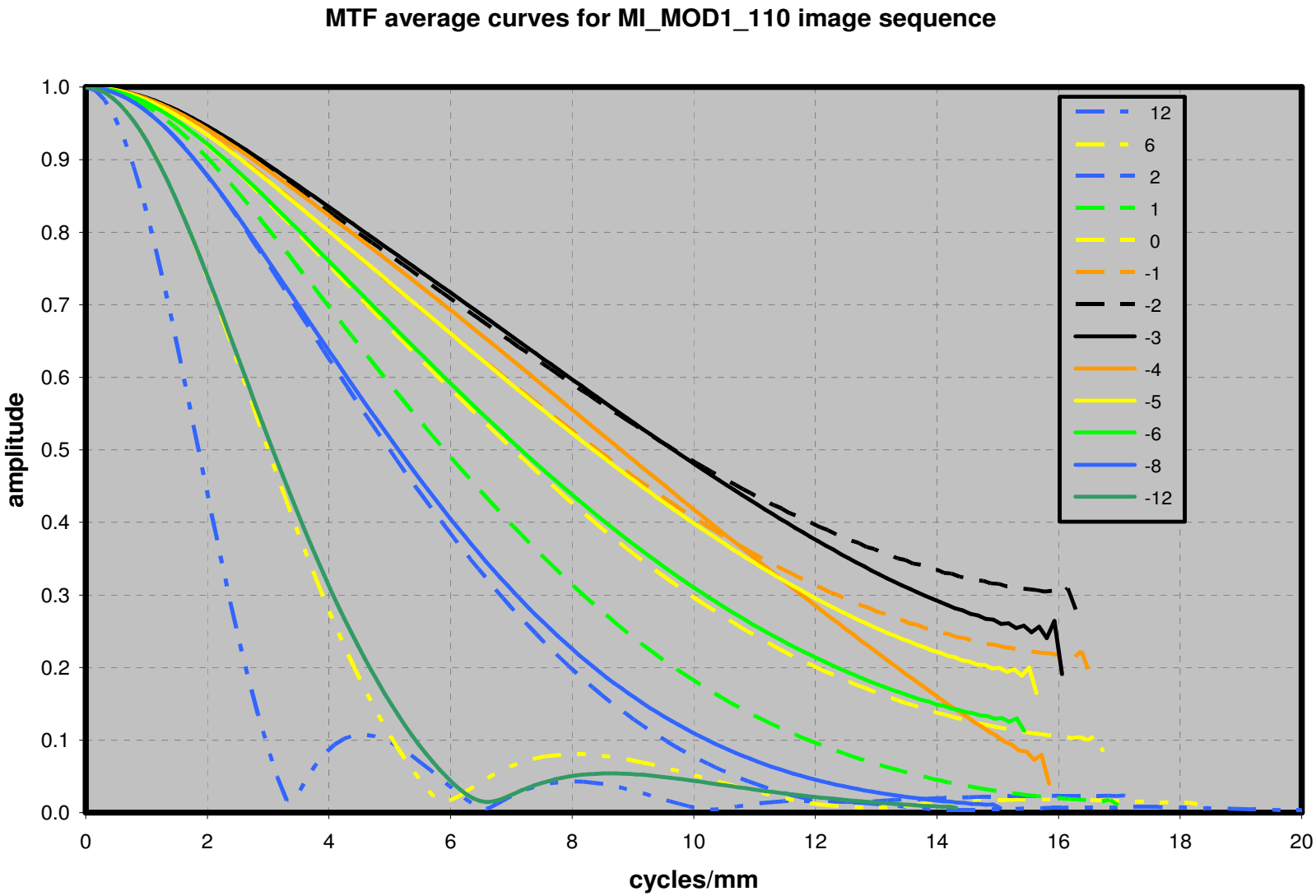

Figure 21.56. MTF average curves for MI_MOD1_110 image sequence. Each curve shows data for positions (in mm) relative to target distance from CCD of 100 mm.

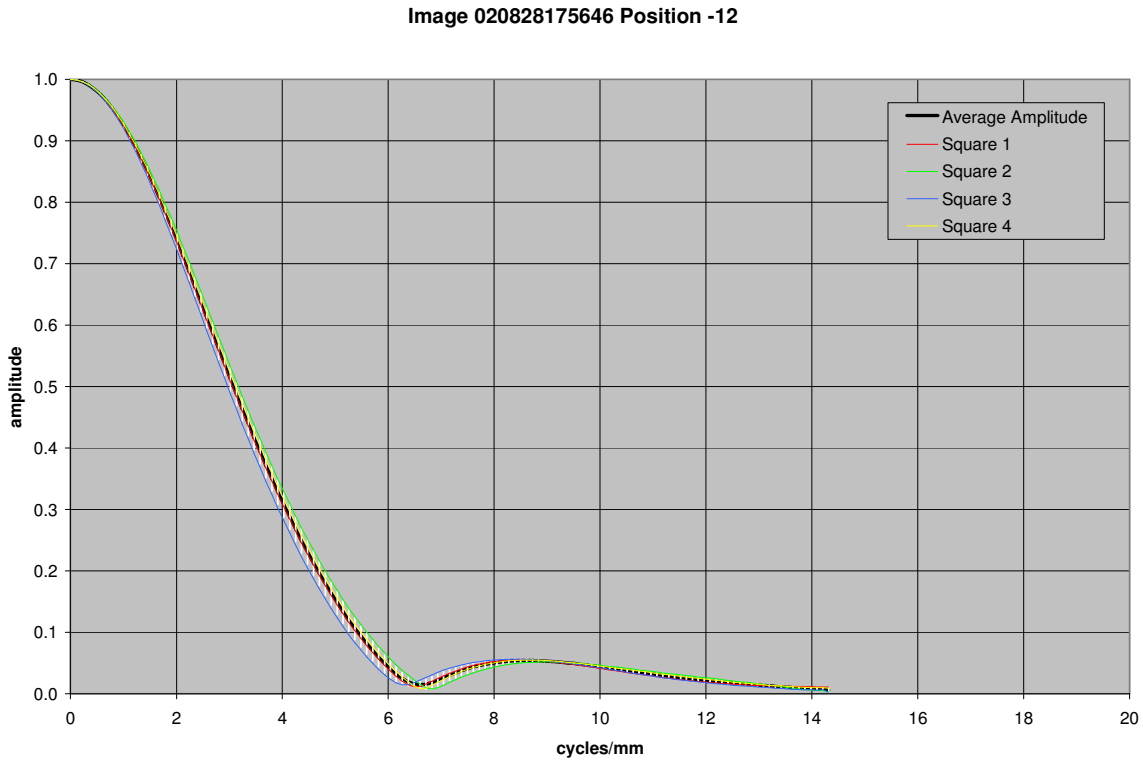

Figure 21.57. MTF curves for image taken with MI 110 CCD 112 mm from the target

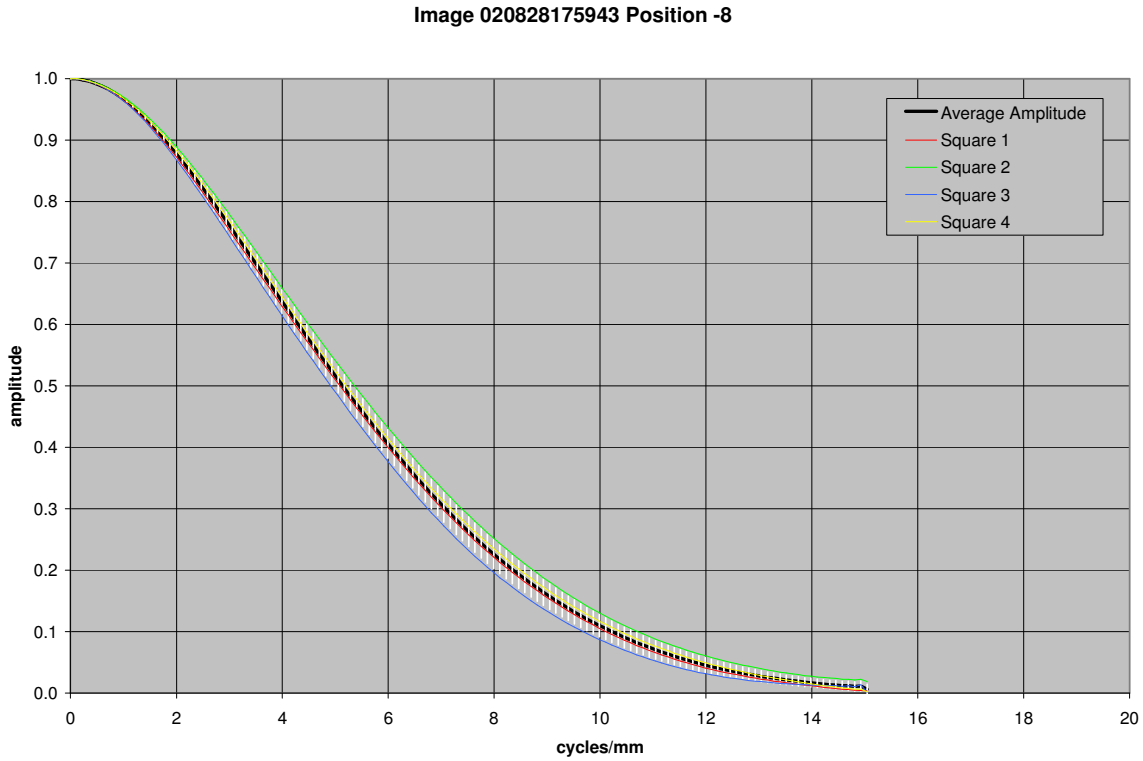

Figure 21.58. MTF curves for image taken with MI 110 CCD 108 mm from the target

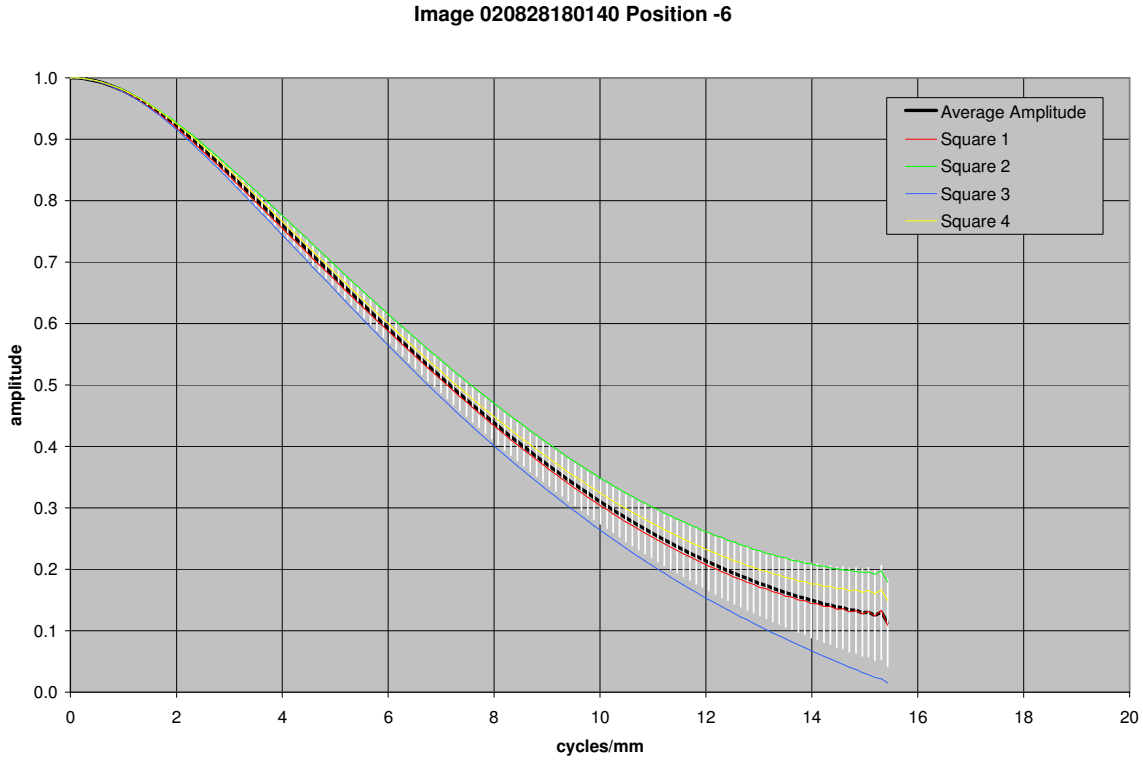

Figure 21.59. MTF curves for image taken with MI 110 CCD 106 mm from the target

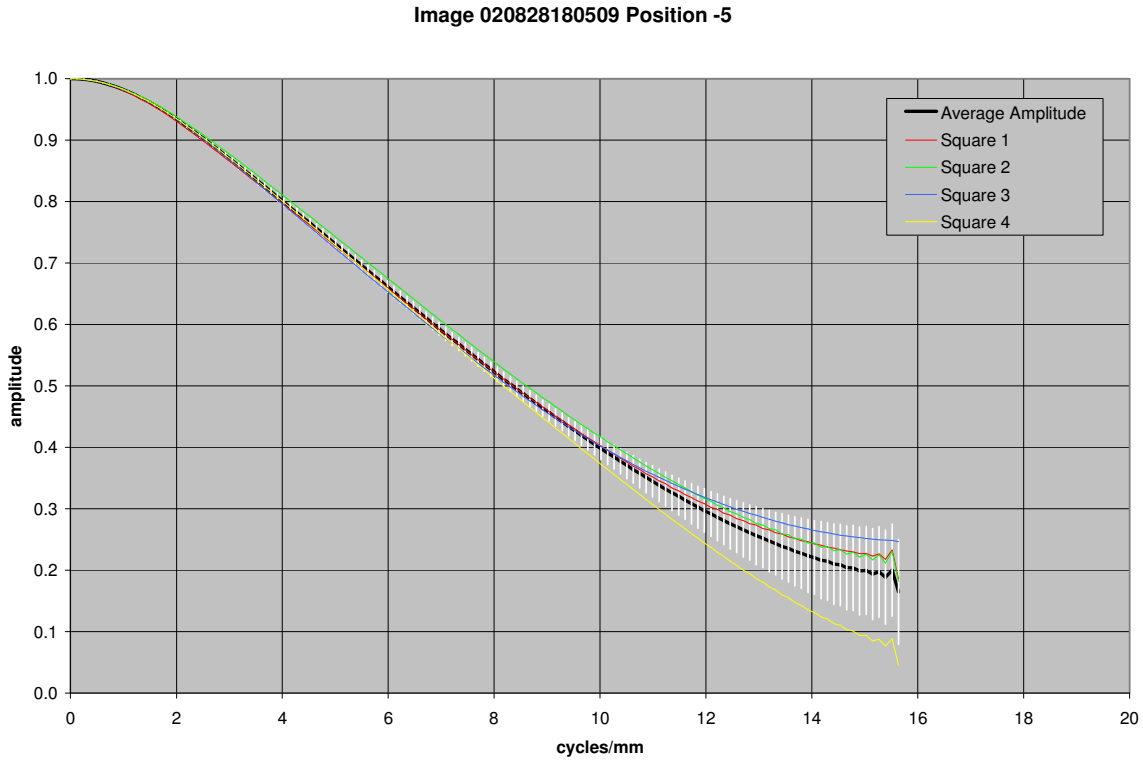

Figure 21.60. MTF curves for image taken with MI 110 CCD 105 mm from the target

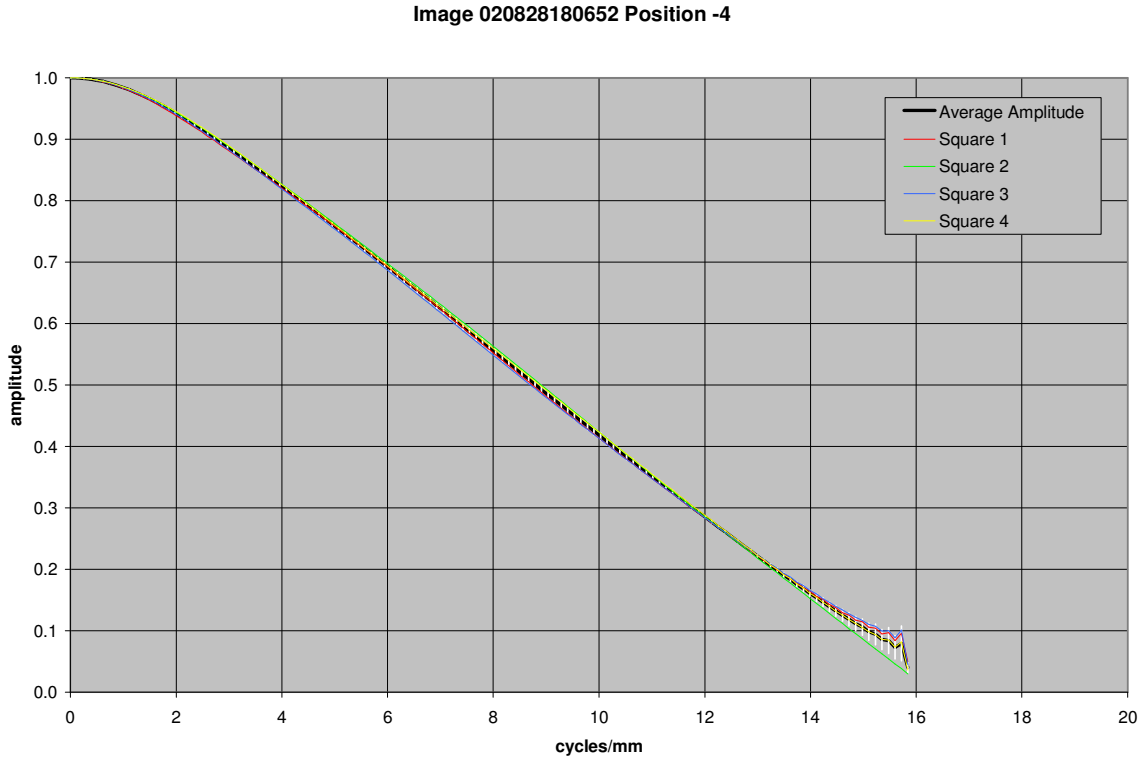

Figure 21.61. MTF curves for image taken with MI 110 CCD 104 mm from the target

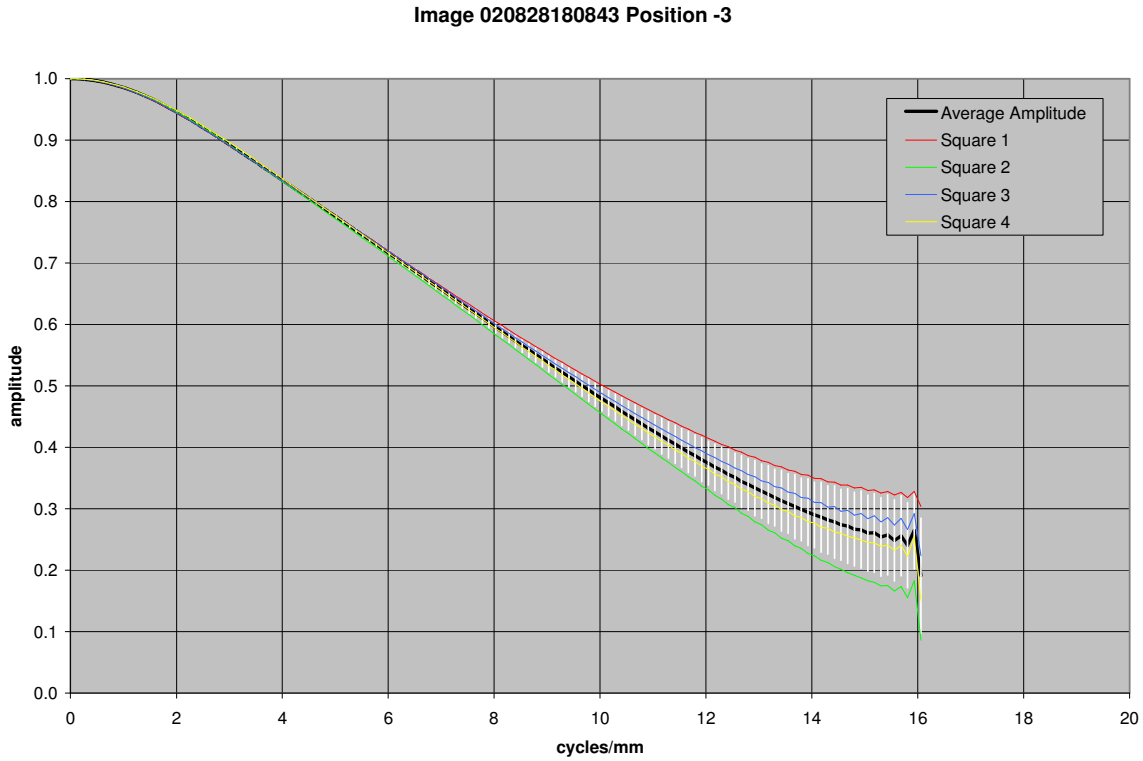

Figure 21.62. MTF curves for image taken with MI 110 CCD 103 mm from the target

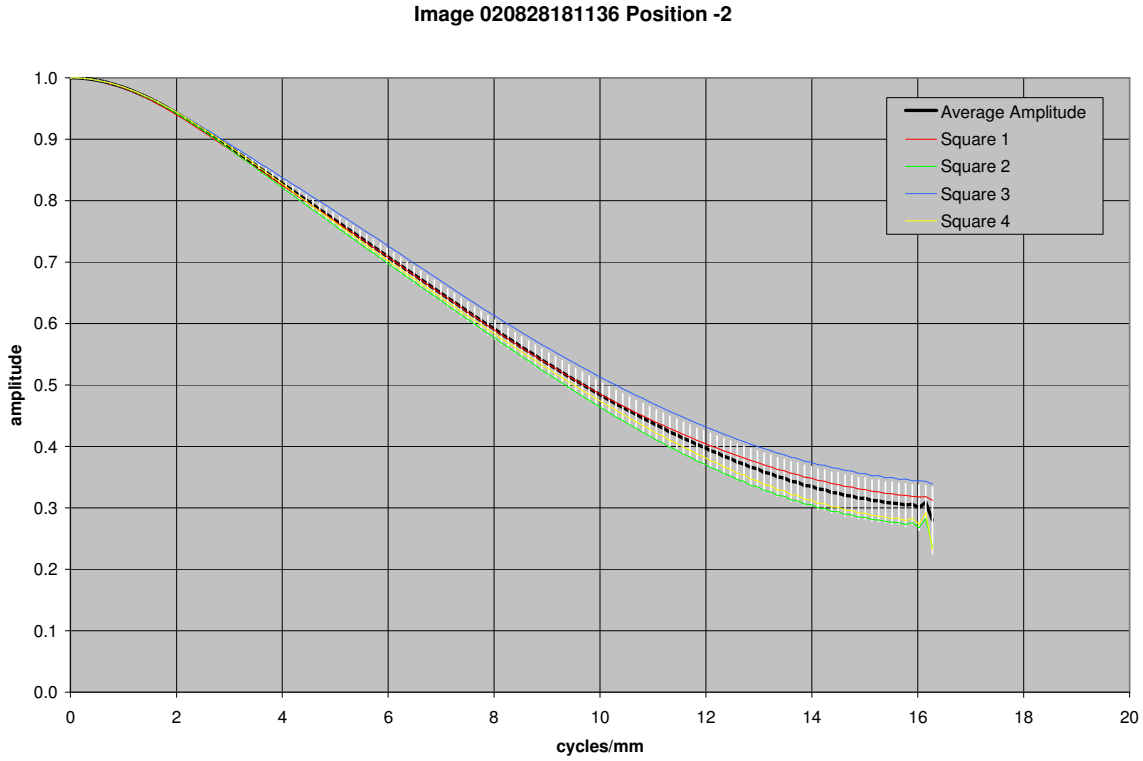

Figure 21.63. MTF curves for image taken with MI 110 CCD 102 mm from the target

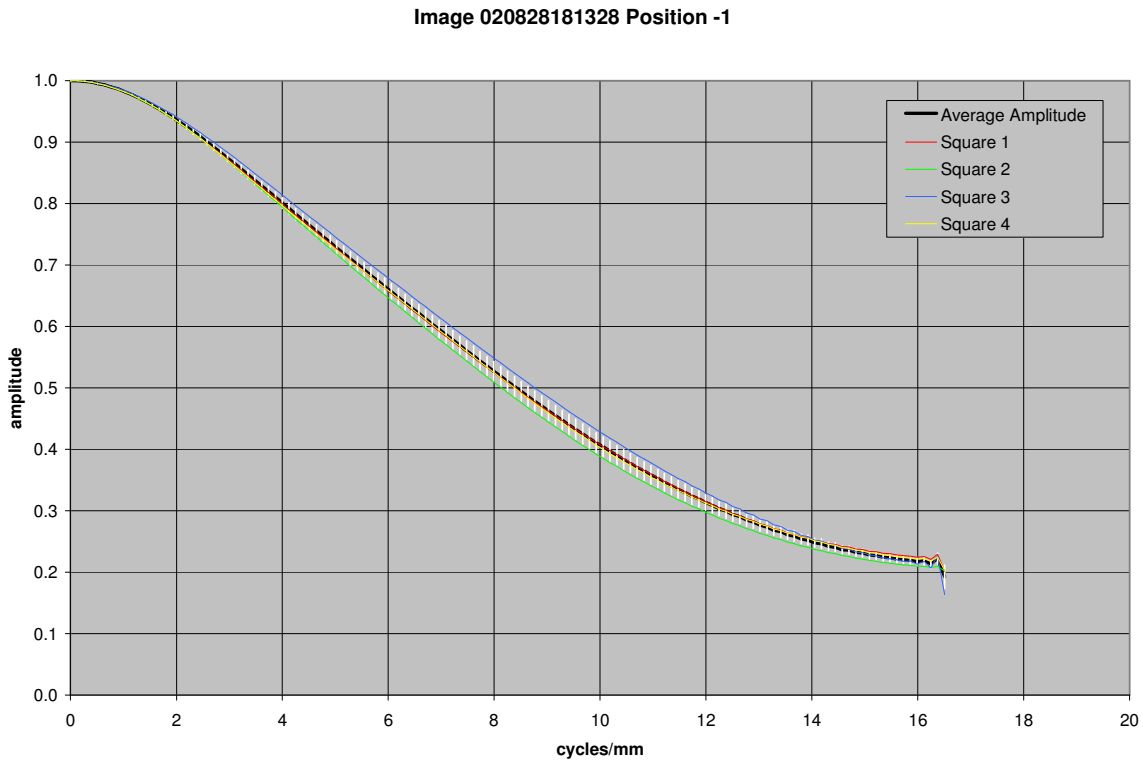

Figure 21.64. MTF curves for image taken with MI 110 CCD 101 mm from the target

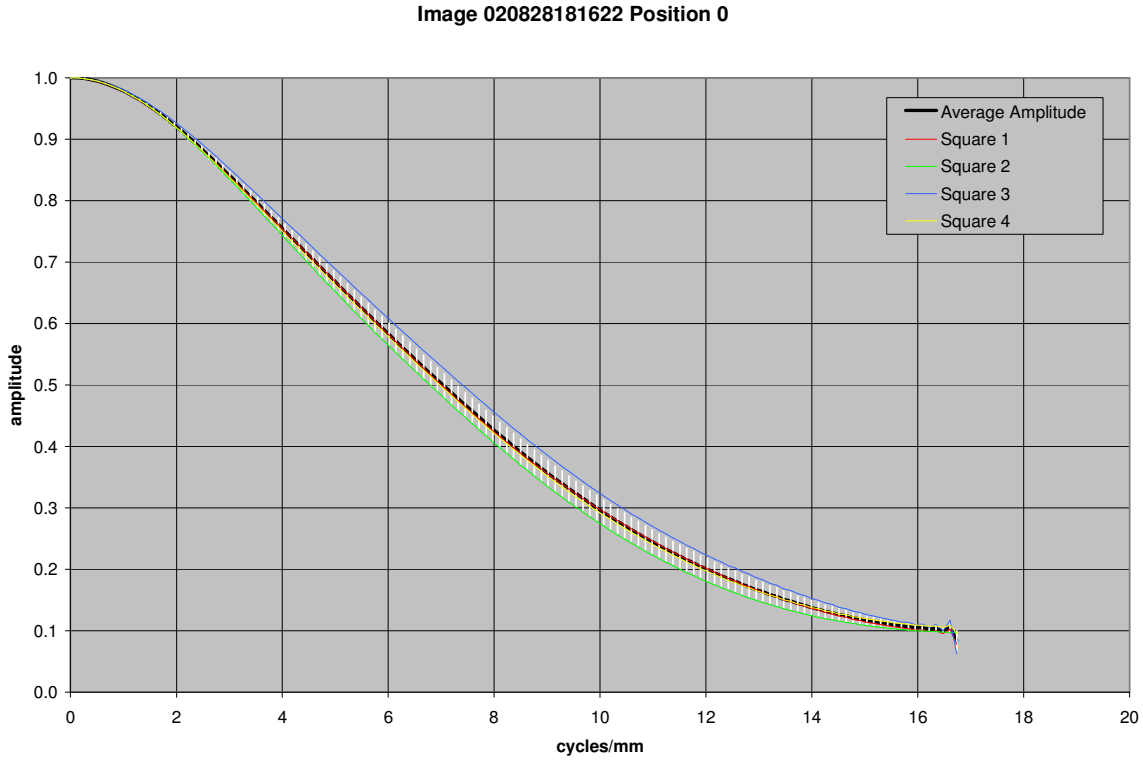

Figure 21.65. MTF curves for image taken with MI 110 CCD 100 mm from the target

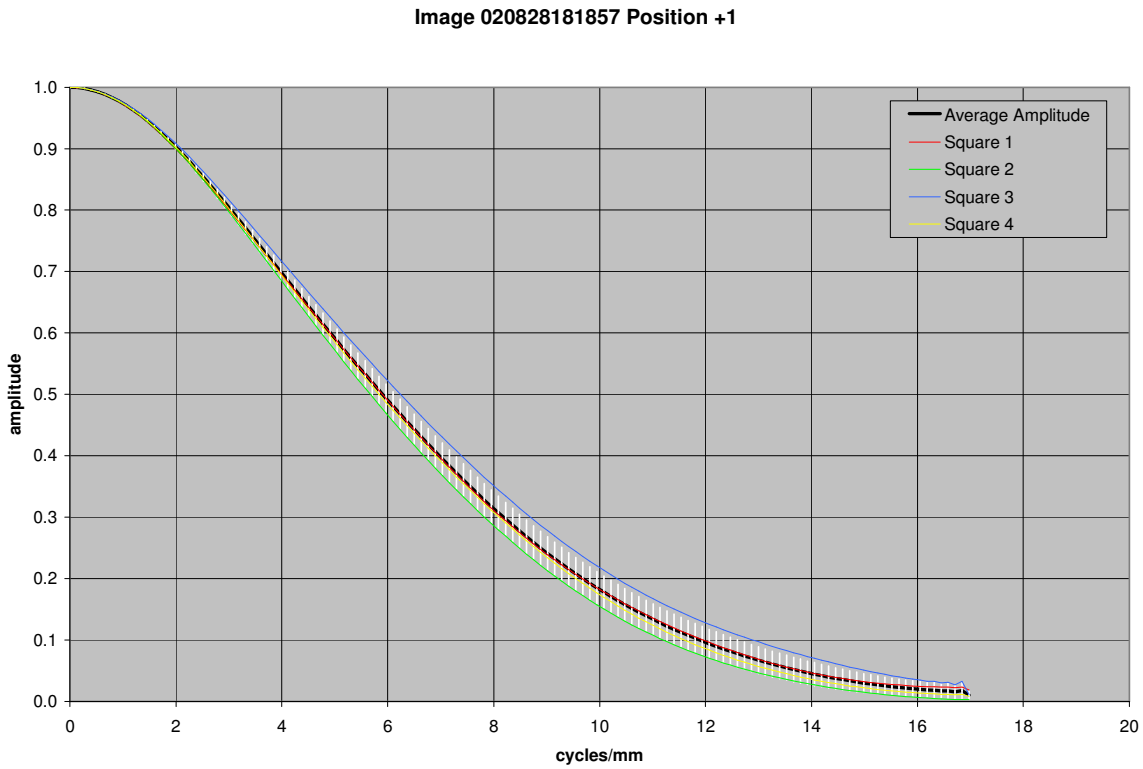

Figure 21.66. MTF curves for image taken with MI 110 CCD 99 mm from the target

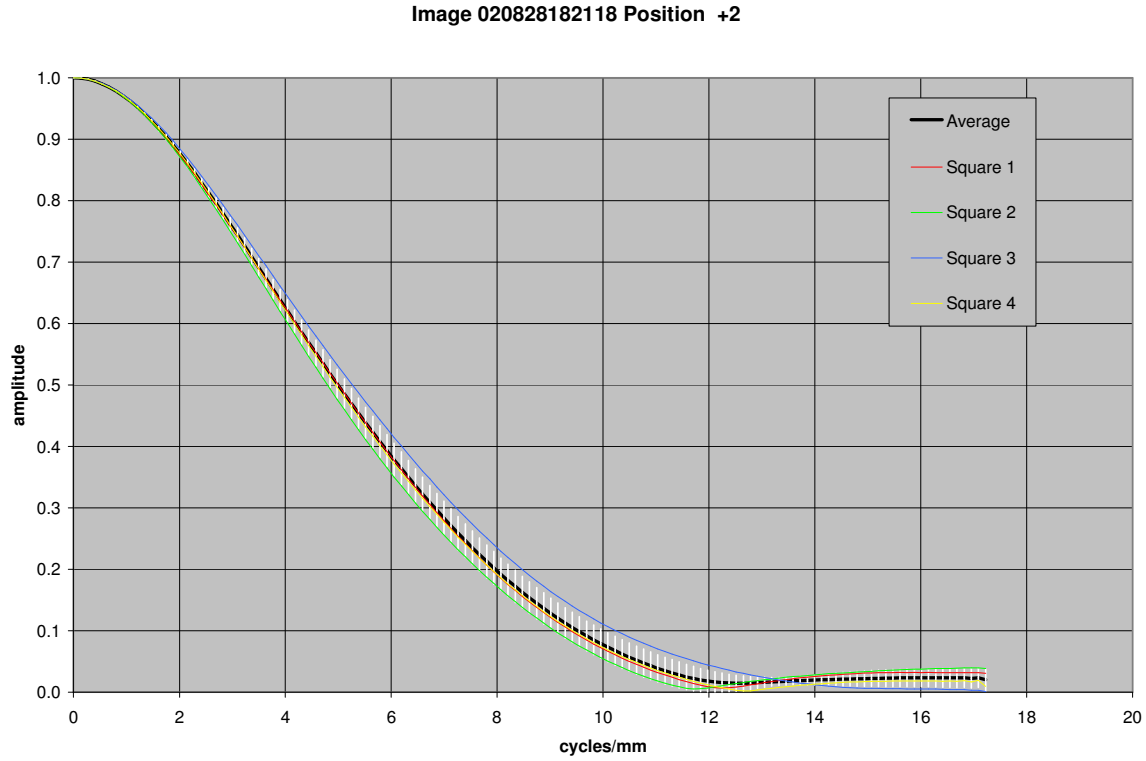

Figure 21.67. MTF curves for image taken with MI 110 CCD 98 mm from the target

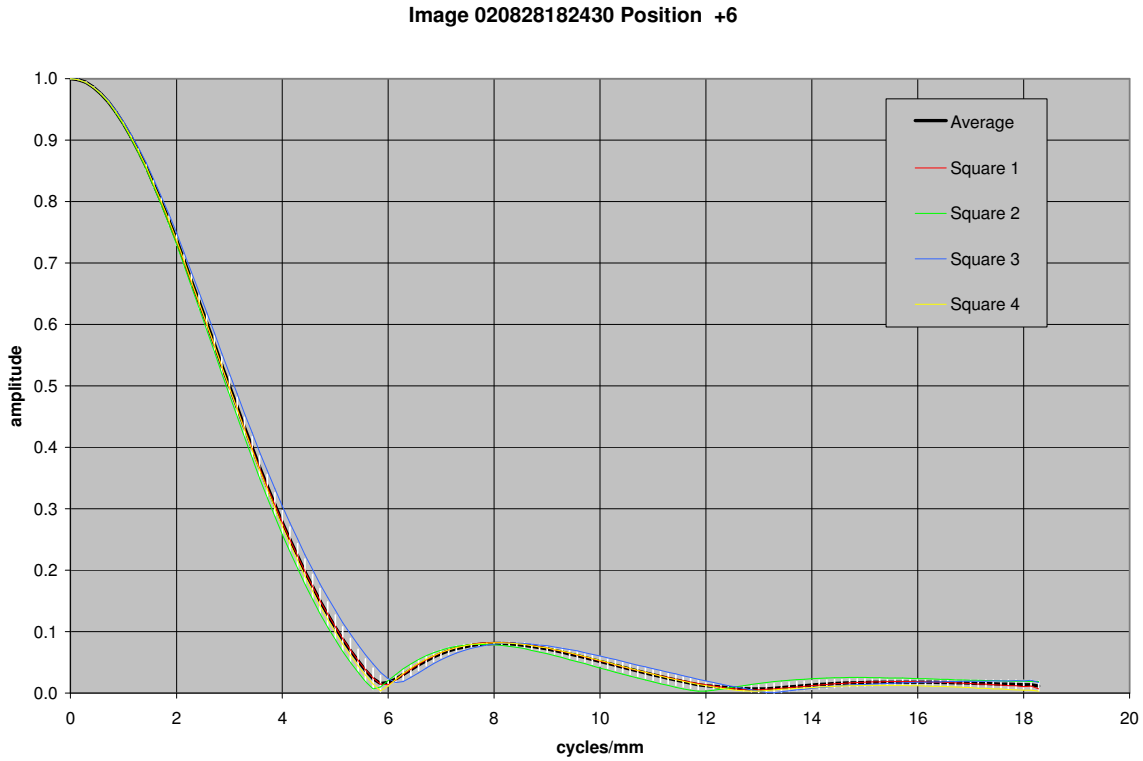

Figure 21.68. MTF curves for image taken with MI 110 CCD 94 mm from the target

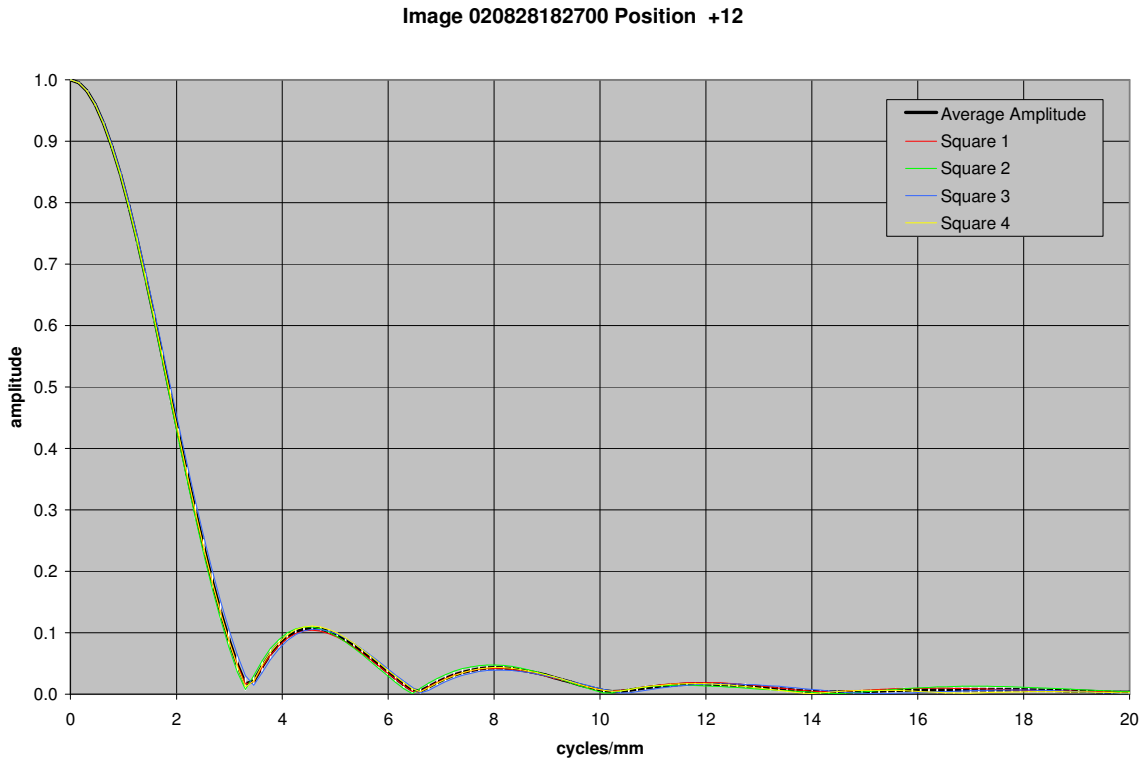

Figure 21.69. MTF curves for image taken with MI 110 CCD 88 mm from the target

MTF for MI_MOD2_110 Image Sequence

The analysis procedure for the MI_MOD2_110 image sequence was similar to the procedure described for the MI_110 data. The one exception is that not all image positions were used (see Table 3.2.8a).

The MI_MOD2_110 images were acquired after thermal/vacuum testing. The MTF curves for these images were calculated based on 4 sub-samples from 7 images of a bar/edge target and using the VICAR application program OTF1. The 7 images were acquired with the CCD detector positioned 100 – 106 mm from the target.

The image with the highest MTF was taken when the CCD was 103 mm from the target. The MTF curves returned by the OTF1 software indicate that there is aliasing present in the images based on the fact that the MTF curves for the sub-samples are not consistent and/or the MTF curve does not approach zero at the Nyquist frequency. The aliasing can be seen in the bar targets (see Figure 21.37). The cleanest MTF curves are from the images acquired 100 and 106 mm from the target: the sub-samples are the most consistent and the curve approaches zero.

The MTF curves for the 4 sub-samples are plotted along with their average and standard deviation on a separate chart for each position. The average MTF curves for each position are plotted together on one chart.

The average MTF curves after thermal/vacuum testing (Figure 21.70) are similar to the average MTF curves prior to vibration and thermal/vacuum testing (Figure 3.2.8d). There are some minor differences in the noise level of the data that are probably of no practical significance. The average MTF curves and error bars are similar when the target is 105, 101, and 100 mm from the CCD (Figures 21.42, 21.46 and 21.47 *vs*. Figures 21.72, 21.76 and 21.77). The tail end of the average MTF curve when the target is 104 mm from the CCD drops for an image acquired after thermal/vacuum testing compared to the MTF curves for the image acquired prior to any testing (Figure 21.73 *vs*. Figure 21.43). The average MTF curves are similar for images acquired when the CCD is 103 mm from the target, but the error bars are smaller for the image taken after thermal/vacuum testing compared to the error bars for the image taken prior to testing (Figure 21.74 *vs*. Figure 21.44). When the target is 102 mm from the CCD, the average MTF curve is slightly higher for the image acquired after thermal/vacuum testing and the error bars are smaller compared to the MTF curve and error bars prior to testing (Figure 21.75 *vs*. Figure 21.45). These differences are in the noise of the data and could be caused by the Fast Fourier Transformations used to compute the MTF. Overall, the MTF curves are similar for the images acquired prior to testing compared to the MTF curves for the images after vibration and thermal/vacuum testing. There was no significant change in the MTF curves.

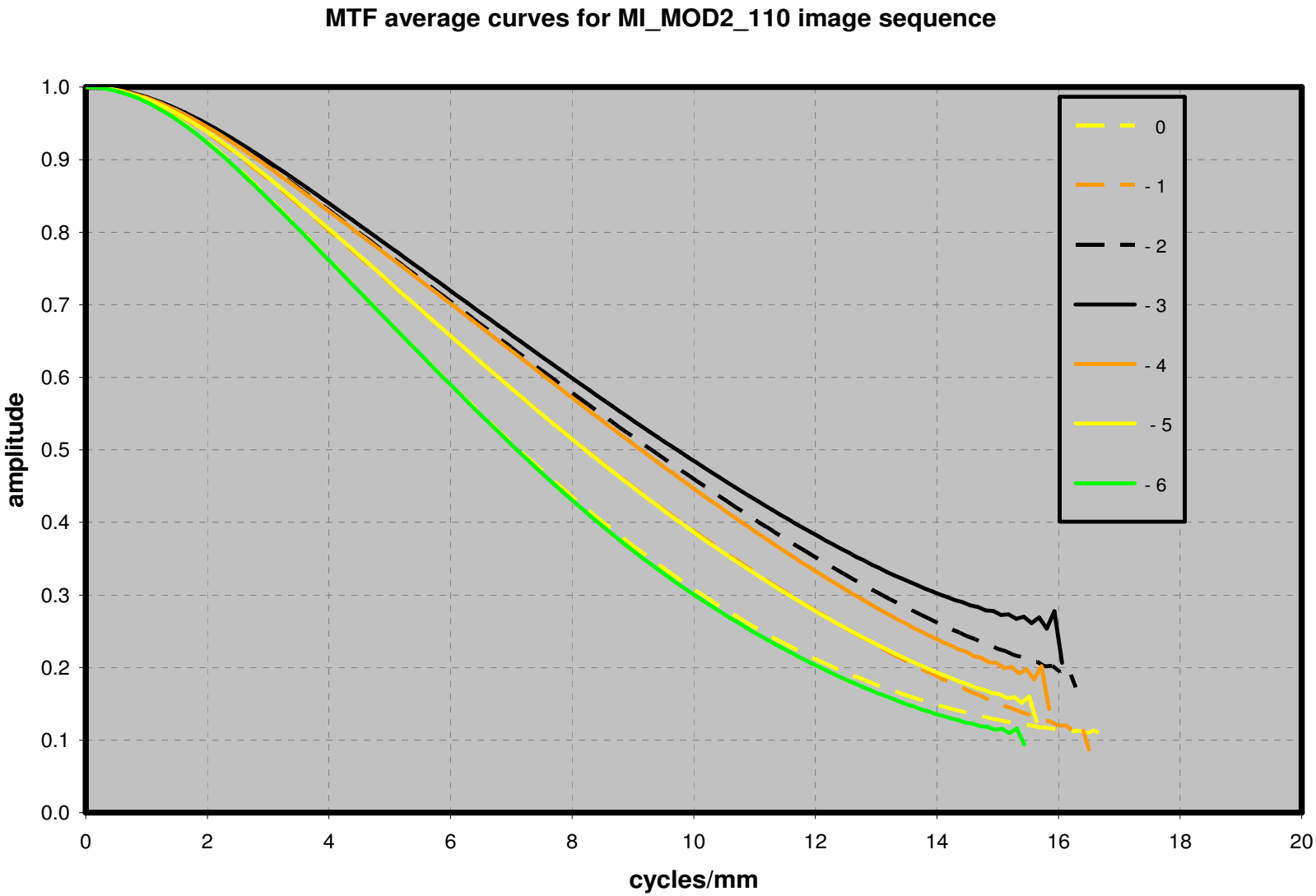

Figure 21.70. MTF average curves for MI_MOD2_110 image sequence. Each curve shows data for positions (in mm) relative to target distance from CCD of 100 mm.

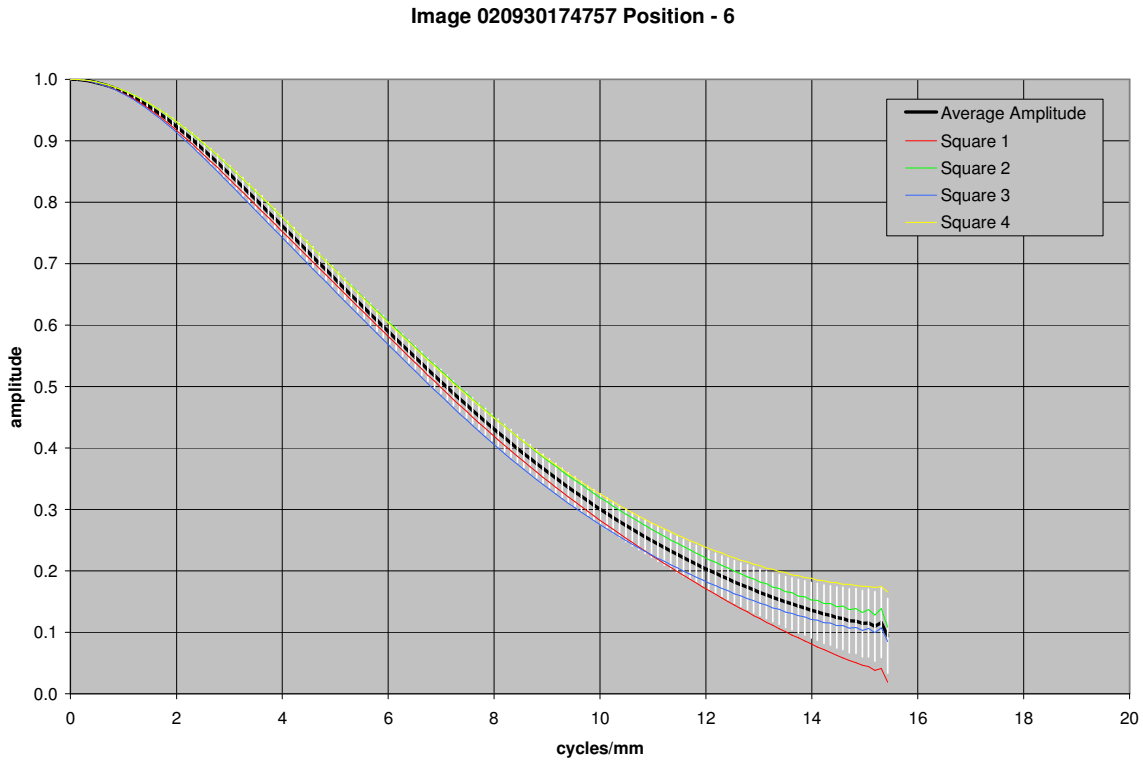

Figure 21.71. MTF curves for an image when the CCD is 106 mm from the target

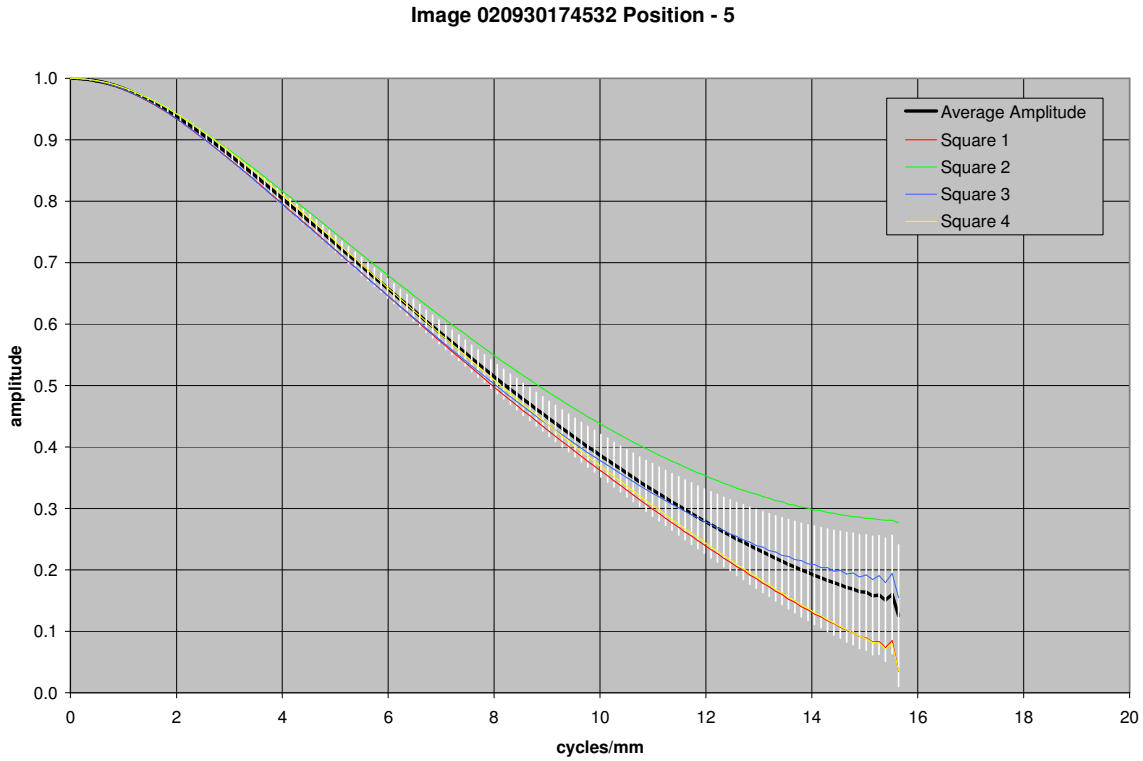

Figure 21.72. MTF curves for image taken with MI 110 CCD 105 mm from the target

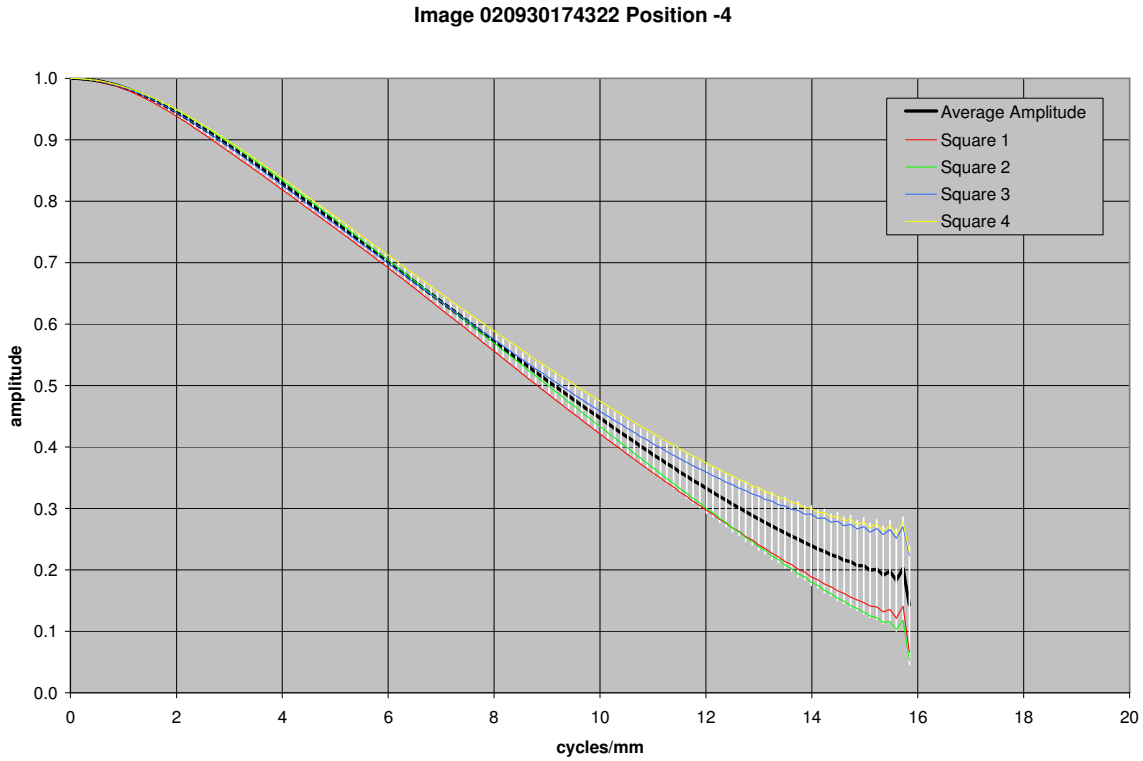

Figure 21.73. MTF curves for image taken with MI 110 CCD 104 mm from the target

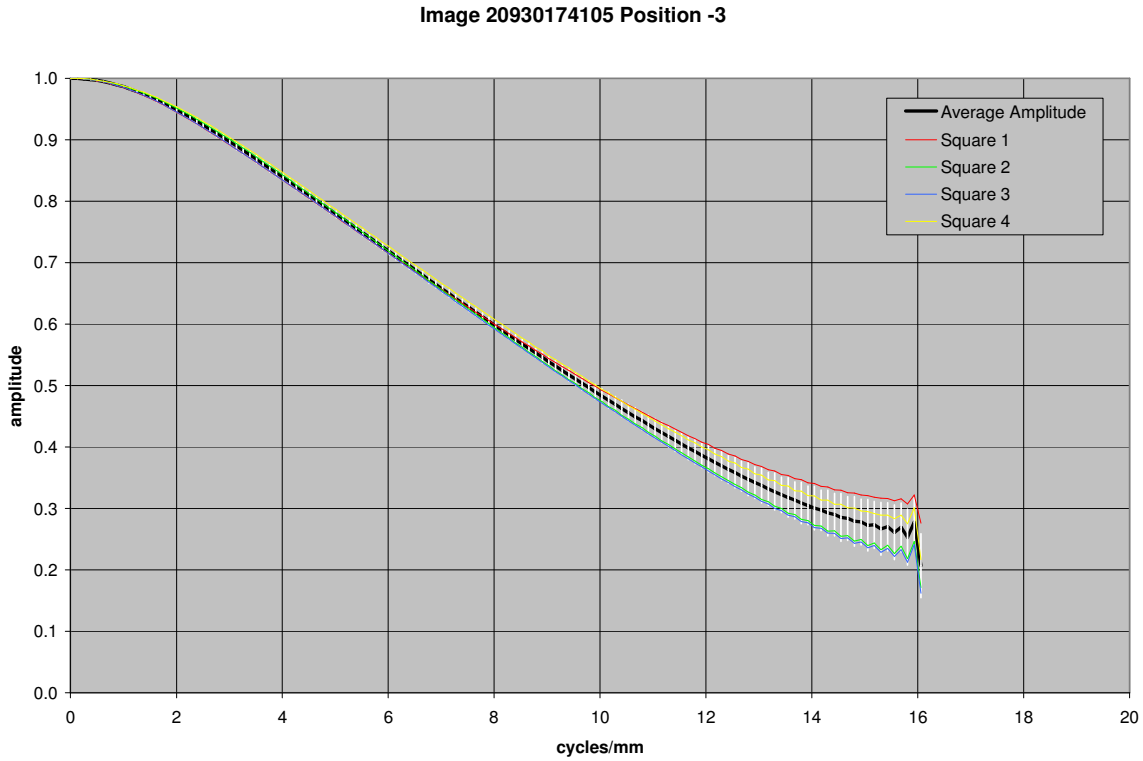

Figure 21.74. MTF curves for image taken with MI 110 CCD 103 mm from the target

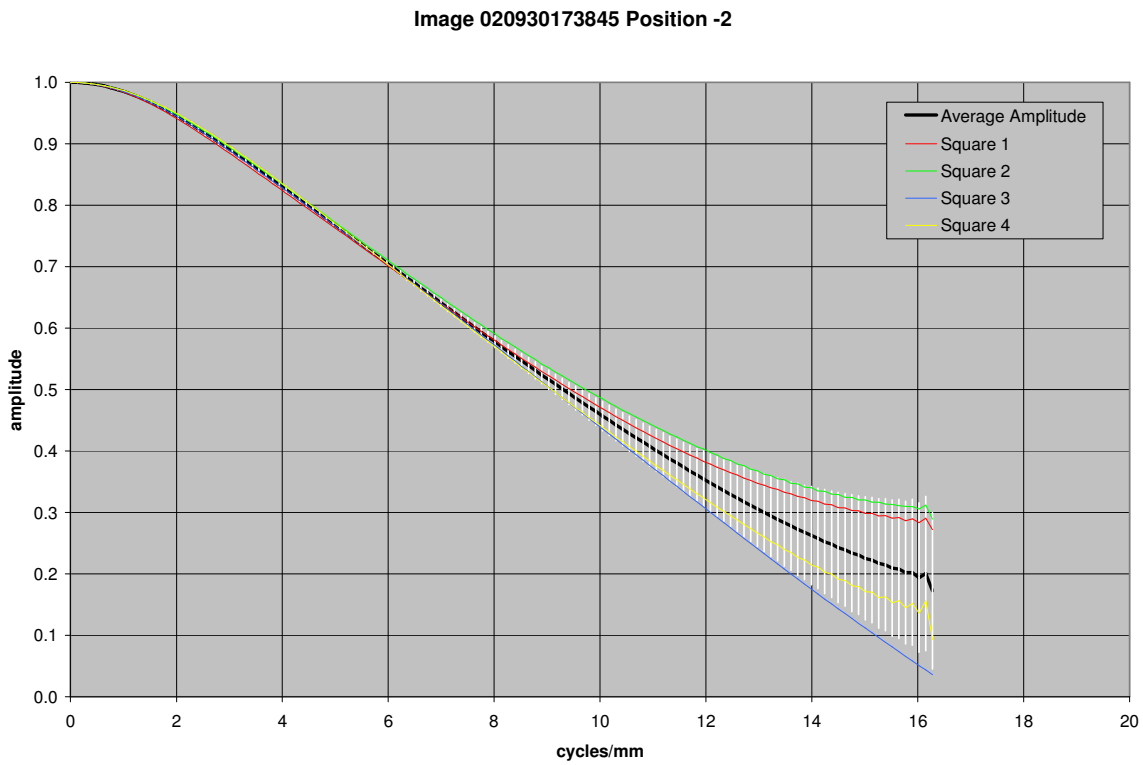

Figure 21.75. MTF curves for image taken with MI 110 CCD 102 mm from the target

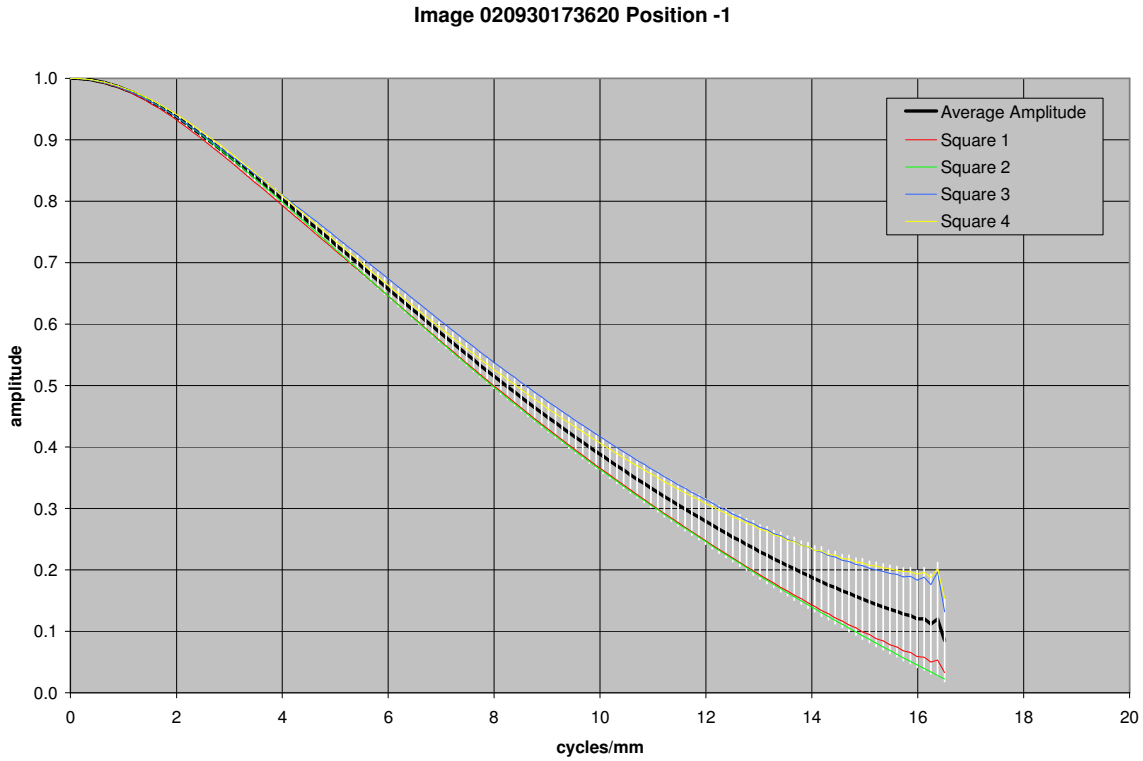

Figure 21.76. MTF curves for image taken with MI 110 CCD 101 mm from the target

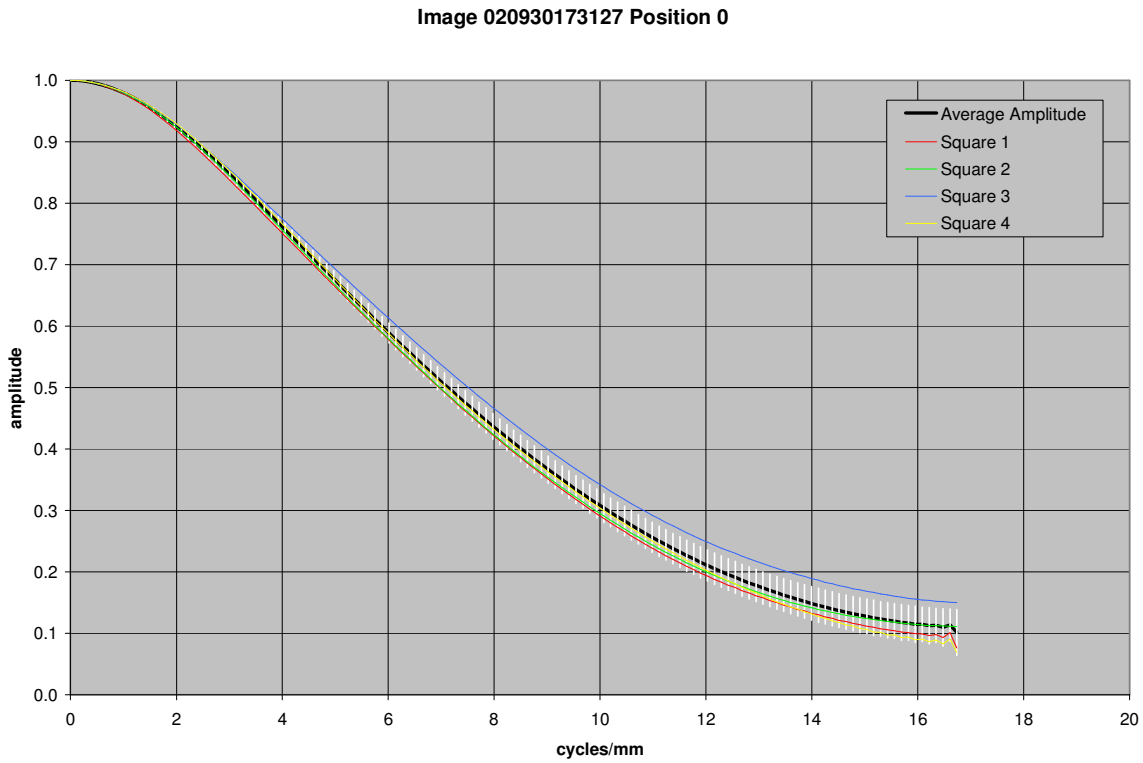

Figure 21.77. MTF curves for image taken with MI 110 CCD 100 mm from the target

Test of Image Processing Procedures for Bar Target

The number of exposures collected of the bar target varied from 1 to 3 exposures for the different test cases. A test was conducted to see if 1.) Averaging exposures together versus using a single exposure had any effect and 2.) The sub-image selection process had any effect on the results. A test case was selected that had 3 exposures. For each single exposure, an image was created by subtracting a zero exposure time image from the image of the bar target. An additional image was created by averaging the 3 zero exposure images and subtracting from the average of the 3 bar target images. The resulting 4 images were then divided by the flat field image. From each image, 4 sub-images were obtained: one sub-image for each of the 4 central dark squares in the bar target images (see Figure 3.2.8a for locations). Figure 3.2.8b shows an example of the sub-image that was obtained. To see if the selection process used for the sub-image had any effect the image was stretched to ensure that the sub-image came from the darkest part of the central squares. Figure 21.78 shows a bar target as it normally appears and stretched from 175 – 176 DN values. The stretched image was used to select the position of the sub-images.

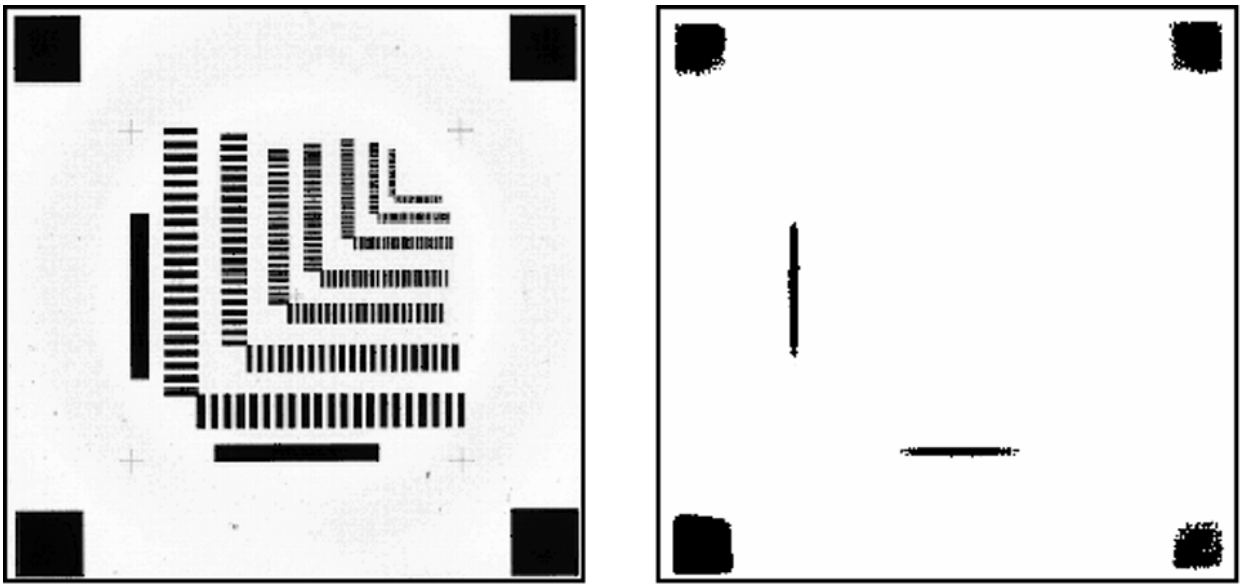

Figure 21.78. The left image is stretched normally and the right image is stretched from 175 to 176 DN

There were a total of 32 sub-images (4 images (3 images from each exposure and 1 image that was an average of the 3 single exposures), sub-images of the 4 central squares, and 2 samples from each central square). These sub-images were processed in the previously described manner for obtaining MTF curves using the VICAR OTF1 application program. Figure 21.79 shows the various MTF curves for the 32 sub-images. The largest difference is between the 2 samples collected from the central square located at position 1. There are no major differences between the MTF curves for a single exposure versus averaging the exposures together.

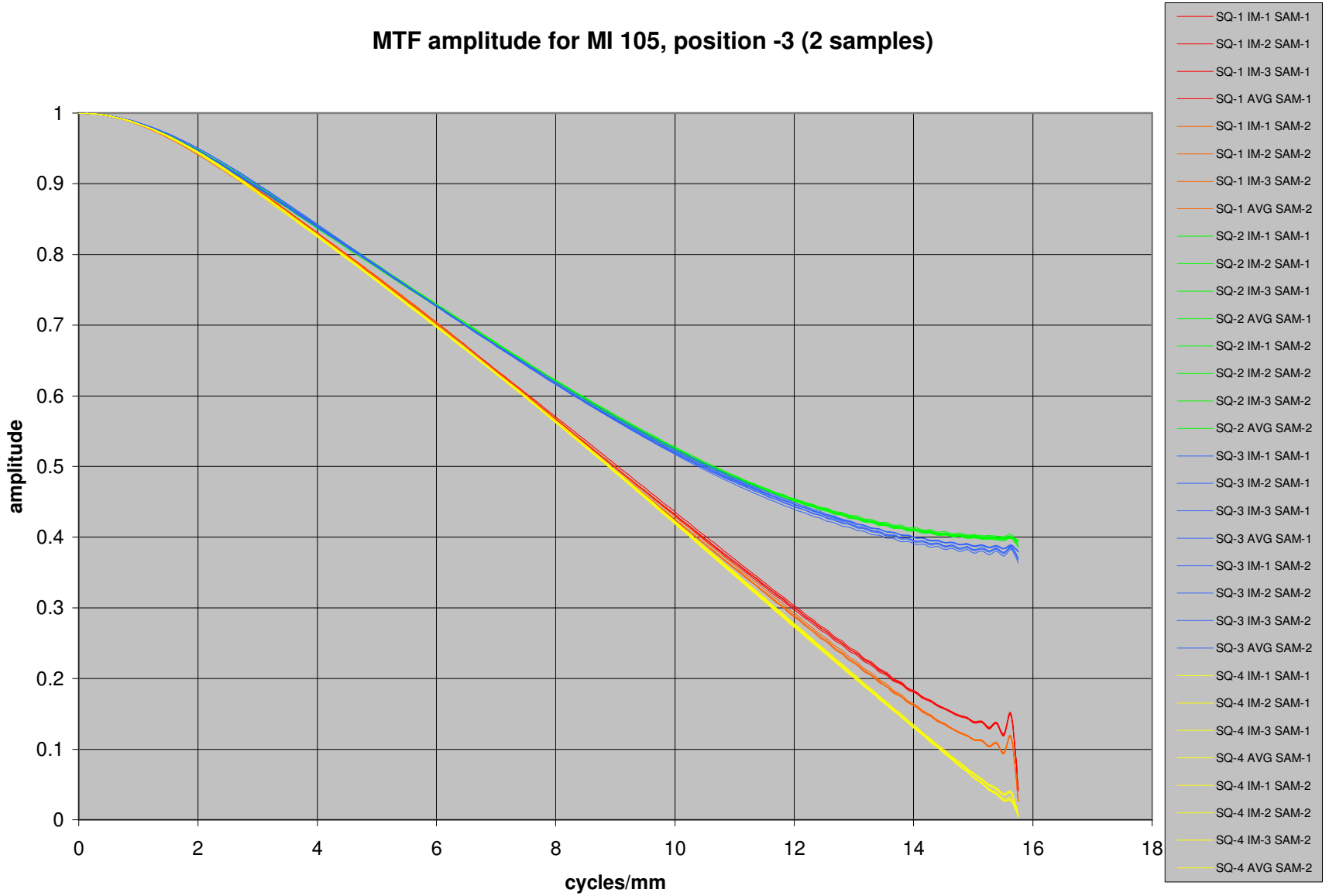

Figure 21.79. MTF curves for image taken with CCD 103 mm from target.

Figure 21.80 shows the range (maximum MTF – minimum MTF at a given cycle per mm) in the amplitude of the MTF curve when the data are grouped by either 1.) Square and sample or 2) by the square the sub-image came from. When the data are grouped by the square and the sample this shows the variation caused by the image source (using a single exposure versus using the average of the 3 exposures). The maximum range difference caused by this is about 0.008 in the amplitude of the MTF curve and is negligible. There should not be any changes in the MTF curves that were obtained from the test cases that had only a single exposure collected or when 3 exposures were collected and averaged together. When the data are grouped by square the sub-image came from this shows the variation caused by the compound effect of the image source and the sample. The maximum range difference caused by this is about 0.035 in the amplitude of the MTF curve. This is caused by the samples from square 1. Looking at the data from the other 3 squares the maximum range difference is less than 0.015 in the amplitude off the MTF curve. The maximum errors occur at the tail end of the MTF curves and do not change the overall MTF curve. The variations caused by the image source and the sample are negligible and do not effect the overall MTF curve.

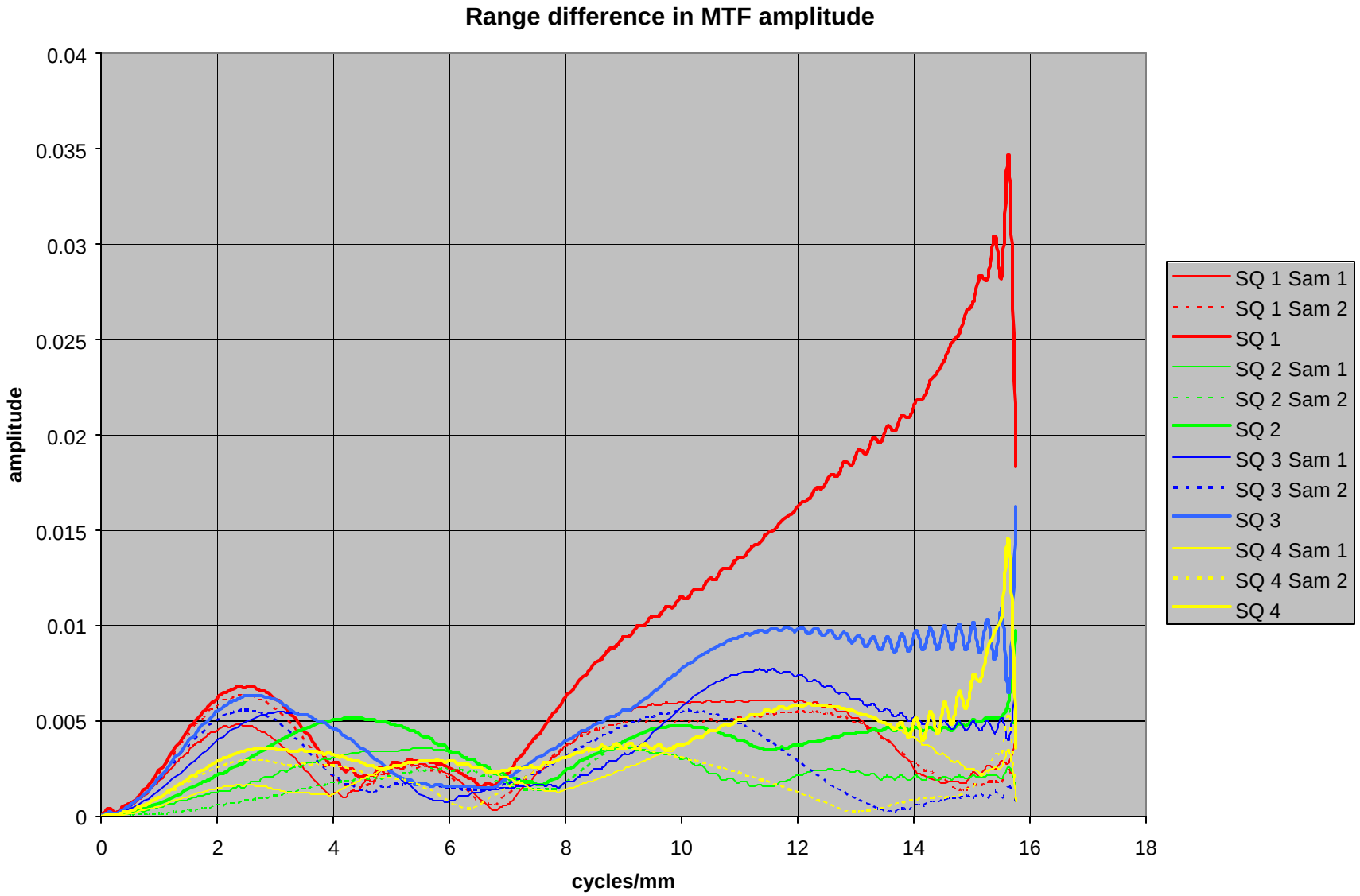

Figure 21.80. Range difference in MTF amplitude when data is grouped by image source and sub-image location.